



UNIVERSITÉ DE STRASBOURG

ÉCOLE DOCTORALE SCIENCES DE LA VIE ET LA SANTÉ (ED 414)

INSTITUTE DE BIOLOGIE MOLÉCULAIRE DES PLANTES (CNRS-UPR 2357)

THÈSE présentée par :

Juliana IGLESIAS

Pour obtenir le grade de : **Docteur de l'université de Strasbourg**

Spécialité : **Aspects moléculaires et cellulaires de la biologie**

Analyse fonctionnelle du rôle de *CYP76C2* dans les mécanismes de défense des plantes contre les agents pathogènes

Soutenue le 17 Juin 2015 à Strasbourg devant le jury composé de :

Dr. WERCK Danièle

IBMP-CNRS

Directrice de thèse

Dr. SAINDRENAN Patrick

IBP-CNRS

Rapporteur externe

Dr. FERNANDEZ Diana

IRD-CIRAD-UM2

Rapporteur externe

Dr. HUGUENEY Philippe

INRA Colmar

Examinateur interne

ANALYSE FONCTIONNELLE DU ROLE DE *CYP76C2* DANS LES MECANISMES DE DEFENSE DES PLANTES CONTRE LES AGENTS PATHOGENES

Une analyse du transcriptome d'*Arabidopsis thaliana* soumis à différents stress biotiques a révélé l'activation de certains membres de la famille *CYP76*, particulièrement celle de *CYP76C2* (≈ 50 fois). La caractérisation fonctionnelle de la famille *CYP76*, et plus particulièrement celle de *CYP76C2* a donc fait l'objet de cette thèse. Après confirmation de l'activation sélective de *CYP76C2* en réponse aux pathogènes par qRT-PCR, le phénotype de ses mutants d'insertion et de surexpression a été caractérisé sous différentes conditions d'infection par: *Pseudomonas syringae* pv. *tomato* DC3000, *P. syringae* pv. *tomato* DC3000 *avrRpm1* et par *Botrytis cinerea*. Afin d'identifier la voie métabolique faisant intervenir *CYP76C2*, un profilage métabolique ciblé et non ciblé a été entrepris, centré sur le(s) métabolite(s) différenciellement accumulés dans les différents mutants en condition d'infection. Alors que des différences subtiles de sensibilité des mutants de *CYP76C2* aux pathogènes semblent confirmer son rôle dans la réponse aux pathogènes, les lignées affectées dans son expression ne présentent pas de phénotypes clairement différents de ceux des plantes sauvages. Une analyse non-ciblée en UPLC-MS (Orbitrap) a permis d'identifier un composé absent dans le mutant *cyp76c2* qui pourrait correspondre à un dérivé conjugué en C11, sans que sa structure ne puisse pour l'instant être identifiée (formule brute $C_{17}H_{28}O_9$). *CYP76C2* ne semble pas impliqué directement dans la synthèse d'une molécule cruciale pour la mise en place du processus de défense, mais exerce plus probablement une fonction spécialisée ou partiellement redondante de défense ou de détoxification.

Mot clés: cytochrome P450, activation, defense, *Botrytis cinerea*, *Pseudomonas syringae*, metabolism.

FUNCTIONAL ANALYSIS OF *CYP76C2* IN PLANT DEFENSE MECHANISMS AGAINST PATHOGENS

A transcriptome analysis of *Arabidopsis thaliana* subjected to biotic stresses has revealed the activation of members of the *CYP76* family, especially of *CYP76C2* (≈ 50 times). The functional characterization of *CYP76C2*, has been the objective of this thesis. After confirmation of the selective activation of *CYP76C2* by pathogens, the phenotype of its insertion and overexpressor mutants was characterized under infection by *Pseudomonas syringae* pv. *tomato* DC3000, *P. syringae* pv. *tomato* DC3000 *avrRpm1* and *Botrytis cinerea*. In order to identify the metabolic pathway involving *CYP76C2*, targeted and non-targeted metabolic profiling was focused on differentially accumulated compounds in the different mutants after infection. Whereas subtle differences of response of the *CYP76C2* mutant lines in response to pathogens seemed to confirm its involvement in response to biotic stress, phenotypes strikingly different from those of wild-type plants were not observed. A non-targeted analysis by UPLC-MS (Orbitrap) identified a compound absent in the *cyp76c2* line that may correspond to an oxygenated C11 conjugate (raw formula $C_{17}H_{28}O_9$), but its structure was not identified. *CYP76C2* thus does not seem directly involved in the synthesis of a molecule crucial for defense responses, but more likely has a role in the synthesis of a potentially redundant specialized defense compound or in a detoxification process.

Keywords: cytochrome P450, activation, defense, *Botrytis cinerea*, *Pseudomonas syringae*, metabolism.

Esta tesis está dedicada a María del Carmen y Julio.

Ellos llegaron a Córdoba en busca de
sus sueños y yo llegue a Francia en
busca de los míos gracias a todos los
valores que nos supieron transmitir.

*Caminante, son tus huellas
el camino y nada más;
caminante, no hay camino,
se hace camino al andar.*

*Al andar se hace camino
y al volver la vista atrás
se ve la senda que nunca
se ha de volver a pisar.*

*Caminante no hay camino
sino estelas en la mar...*

(Extract from “Campos de Castilla, Proverbios y cantares (XXIX)”, A. Machado, 1912)

ACKNOWLEDGEMENTS

This thesis was supported by INTA (National Institute of Agricultural Technology) from Argentina and the IBMP-CNRS from France.

I wish to express my sincere thanks to Danièle Werck and Serge Kauffmann for proposing this thesis subject and providing me with all necessary facilities for the research in France. I am undoubtedly thankful and indebted to D. Werck who provided insight and expertise all along the thesis.

I want to thank the jury members for kindly accepting to review my thesis.

I would like to express my very great appreciation to B. Boachon for his valuable suggestions during the planning and development of this research work. His willingness to give his time and expertise for UPLC-MS analysis has been very much appreciated.

I take this opportunity to express my gratitude to all the former and present members of the P450 Department for their help and support, a special thank you to N. Navrot, P. Ullmann, C. Gavira, A. Alber and C. Parage, for technical guidance and proofreading of this manuscript. I am also grateful to J.F. Ginglinger, A. Lesot, B. Grausem, E. Widemann, G. Verdier, H. Renault, T. Ilc, Z. Liu and F. Pinot for helpful discussions on diverse matters. T. Heitz and H. Zuber for precious standards. M. Heinlein and E. Peña for sharing their vision of science with me.

F. Philippon, thank you for your invaluable provision of lab material. You are one of the most efficient and patient persons I know.

I am grateful to people at the different platforms of the institute for their help and assistance, especially A. Alioua, R. Lugan, M. Erhardt, J. Mutterer, V. Cognat, and F. Disdier. I thank M. Ramel for advices on plant culture. I want to recognize all the work done by people from administration and L. Monnier, who made our lives at lab easier.

I would like to thank P. Saindrenan and his team (M. Garmier, L. Didierlaurent) for his precise, concise and valuable advices on my work and assistance with *H. arabidopsidis*.

R. Baltenweck for UPLC Orbitrap analysis. Thanks a lot for your work and kindness. You saved me!!!

I would like to thank my workmates and colleagues from Argentina, for their words of encouragement, faith and support. Special thanks to my colleagues in the Maize Team and in Plant Pathology at INTA, and to F. Gándara our former Director, to C. Améndola and to I. Cattoni for insight into statistics. C. Bruno for Infostat. J.I. Fernández for photoshop assistance.

To all the authors I wrote to, thanks for your answers and insightful comments.

I would like to thank my friends and family here and in Argentina, for their support and encouragement throughout my stay in France.

To all my friends in Strasbourg: Doro and Thomas, Denise, Carolina, Andrea, Lucia and Francisco, Eduardo y Marina, Lule – I will not forget the wonderful moments spent with you.

Alexandra, Annette and Carole you know you have a huuuuuuuuuuuuuuuge place in my heart. Next stop: Argentina!

To my friends from life: Celes, Isa, Naty, gracias por todo, sin Uds no existo. No tengo palabras. Marcos! Ernes, Lore, Ale, Fer, cuanto cuanto!!!

Finally to: H.S.T, T., S.C., M.D, C.F, C.P.E, S.R, A.L, without them it would have been impossible or very boring...

LIST OF CONTENTS

Title	i
Abstract in French	ii
Abstract in English	iii
Dedication	iv
Acknowledgements	v
List of Contents	vii
List of Figures	xiii
List of Tables	xvii
Abbreviations	xviii
INTRODUCTION	1
The plant model of choice: <i>Arabidopsis thaliana</i>	2
Cytochrome P450	4
Nomenclature	8
P450 and Plant Defense	8
Secondary Metabolism	10
Phytoalexins and phytoanticipins	15
Camalexin the main phytoalexin from <i>Arabidopsis</i>	18
The camalexin pathway: work in progress	21
Specialized metabolism: application and outlook	24
Terpenoids	26
Terpenoids biosynthesis	29
DEFENSE STRATEGIES IN PLANTS	33
1- Pathogen-triggered Immunity	34
2- Effector-triggered immunity	34
a) Theory Gene-for-Gene Resistance	37
b) and c) The Guard model and The Decoy model	38
d) The Bait and Switch Model	41

Plant Immune System in motion: The Zigzag Model	42
Signaling Pathways and Downstream Responses	44
Hormones and plant defenses	44
SA Biosynthesis	46
1- The PAL pathway (PAL):	46
2- Isochorismate pathway (ICS):	47
JAs biosynthesis	50
SA pathway signaling	55
JAs pathway signaling	56
Crosstalk between SA and JA/ET	60
Crosstalk between ABA and SA/JA	60
Crosstalk between AUX and SA/JA	60
Crosstalk between GB and SA/JA	61
Programmed Cell Death	62
Hypersensitive Response (HR)	65
The role of ROS and NO in HR	67
Induction pathways of HR	73
HR: ecological cost and trade-off	75
SAR	79
The networking of small metabolites in SAR	80
Some words about MeSA and JA	83
JA and SAR	84
The role of NPR1 and SAR	85
Pathogen Lifestyle	87
The pathogens used in this thesis	89
<i>Pseudomonas syringae</i> pv <i>tomato</i> DC3000	89
Coronatine: mimicking the enemy	92
The bacterial PAMP Flagellin	94
Defense and metabolism in the interaction <i>A. thaliana</i> - <i>Pto</i> DC3000	95
<i>Botrytis cinerea</i>	99

HYPOTHESIS AND OBJECTIVES	103
HYPOTHESIS AND OBJECTIVES	104
Objectives	104
CYP76 family background information	105
MATERIALS AND METHODS	117
BIOLOGICAL MATERIAL	117
Plant Material and Growing Conditions	117
Plant Pathogens	117
1- <i>Pseudomonas syringae</i> pv <i>tomato</i> DC3000	117
2- <i>Botrytis cinerea</i>	118
METHODS	118
Construction of over-expression mutant <i>35S:CYP76C7</i> and transformation	118
<i>Escherichia coli</i> chemical transformation	119
<i>Agrobacterium tumefaciens</i> transformation using electroporation	120
RNA extraction	121
cDNA synthesis	122
Genotyping of T-DNA insertion lines	122
DNA extraction protocol	124
Genotyping of Overexpression Lines	124
Gene Expression Analysis	125
β - Glucuronidase (GUS) Activity Assay	125
qRT-PCR for Gene Expression	126
Plant Infections	129
Plant Leaves Infection with <i>Pto</i> DC3000	129
DNA extraction and qPCR quantification	130
<i>Botrytis cinerea</i> Infection	131
<i>Hyaloperonospora arabidopsidis</i>	131
<i>Hyaloperonospora arabidopsidis</i> Infection	132
Metabolomics Analysis	132
Volatile Collection	132

Metabolic Profiling in UPLC MS/MS	133
Targeted Analysis for (mono) terpenoids: UPLC MS/MS 3Q-MRM Mode	133
Hormone Profiling	135
Non-targeted analysis: UPLC MS (Orbitrap)	138
Enzymatic Activities in vitro with Microsomal Fraction of Recombinant Yeast	139
Yeast Transformation Protocol	139
P450 Quantification by Spectral Assay	142
HPLC Analysis	143
Statistical Analysis	137
WORKFLOW OF EXPERIMENTS AND DATA ACQUISITION	148
RESULTS	149
Gene Expression Analysis	149
Strategy for qRT-PCR analysis of gene expression	149
Effect of <i>B. cinerea</i> infection on the expression of <i>CYP76</i>	151
Effect of <i>Pto</i> DC3000 infection on the expression of <i>CYP76</i>	154
Effect of <i>Pto</i> DC3000 <i>avrRpm1</i> infection on the expression of <i>CYP76</i>	158
HR zone	158
LAR zone	160
SAR zone	161
Conclusion of the qRT-PCR analysis of gene expression	162
<i>CYP76C2</i> expression monitored via β -glucuronidase (GUS) activity	167
Conclusion of the <i>CYP76C2</i> expression monitored via GUS activity	172
<i>CYP76C2</i> : Phenotyping in response to pathogens	174
Virulent infection with <i>Pto</i> DC3000	174
Temporal analysis of symptoms development after <i>Pto</i> DC3000 infection	177
Infection with <i>Pto</i> DC3000 <i>avrRpm1</i> : HR LAR and SAR responses	180
HR	180
LAR and SAR responses	181
Temporal analysis of symptoms - <i>Pto</i> DC3000 <i>avrRpm1</i> infections	185
<i>Botrytis cinerea</i> Infection	186

Temporal analysis of symptoms development after <i>Botrytis cinerea</i> infections	188
Conclusion of the experiments of phenotyping of the <i>CYP76C2</i>	190
Metabolomics Analysis	191
Headspace volatile analysis in GC-MS	191
Metabolic Profiling of Soluble Metabolites in UPLC-3Q-MS/MS	197
Targeted Analysis of Monoterpenoids: UPLC-3Q-MS/MS in MRM Mode	197
Hormone profiling	201
Profiling of benzoates and derivatives at 24 HPI	201
UPLC-3Q-MS/MS analysis	201
UPLC-ORBITRAP-MS/MS analysis	207
Hormone Profiling: kinetics of accumulation in a timeline from 0 to 72 HPI	212
Two compounds of relevance: Camalexin and Linalool timeline	219
Conclusions on hormone profiling and camalexin accumulation in a time line	227
β -glycosidase/ β -xylosidase treatments	229
Enzymatic Activities in vitro with Microsomal Fraction of Recombinant Yeast	235
Non-targeted analysis: Orbitrap UPLC-MS	236
In the search for conjugate	238
Conclusion on Non-Targeted Profiling	240
CONCLUSIONS AND PERSPECTIVES	241
REFERENCES	250
APPENDIX	292
List of P450 used in transcriptomic analysis	292
Genotyping of T-DNA insertion lines and overexpression lines	296
Melting curve analysis of primers used in qRT-PCR	300
qPCR quantification of <i>Pseudomonas syringae</i> growth in planta	302
Temporal analysis of symptoms development after <i>Pto</i> DC3000 infections	304
Temporal analysis of symptoms development after <i>B. cinerea</i> infections	305
<i>Hyaloperonospora arabidopsidis</i> infection with strain <i>Noco2</i>	306
Targeted analysis for (mono) terpenoids in UPLC-3Q-MS/MS	307

Hormone Profiling in a timeline	309
Microsomes CYP76C2	314
Extended abstract in french	315
Publication in a journal	

LIST OF FIGURES

	Page
Figure 1 : <i>Arabidopsis thaliana</i>	2
Figure 2 : Ribbon representation of P450 CYP74A structure	4
Figure 3 : The P450 catalytic cycle	6
Figure 4 : Main pathways for secondary metabolites precursors	11
Figure 5 : Phytoalexins from different plant families	17
Figure 6 : The puzzling biosynthetic pathway of camalexin	23
Figure 7 : Some examples of terpenoid classes and diversity	28
Figure 8 : Schematic and summarized representation of terpene biosynthesis and classes	31
Figure 9 : Terpene biosynthesis Mav and Mep pathways and their subcellular localization	32
Figure 10 : Schematic representation of plant defenses	33
Figure 11 : PAMPS and BAK1	35
Figure 12 : Schematic representation of the gene-for-gene theory	37
Figure 13 : The guard model vs the decoy model	40
Figure 14 : The bait and switch model	41
Figure 15 : The zigzag model of plant immune system	43
Figure 16 : Structure of plant hormones relevant to plant-pathogen interactions	45
Figure 17 : SA biosynthesis and modifications	48
Figure 18 : JAs precursors and derivatives	50
Figure 19 : Cellular compartmentalization of JA biosynthesis and signaling	52
Figure 20 : JA synthesis and further transformations	54
Figure 21 : SA signaling cascade after (hemi)biotroph pathogen attack	55
Figure 22 : JA signaling cascade after necrotroph pathogen attack	56
Figure 23 : Schematic representation of hormonal crosstalk	59
Figure 24 : Col-0 plants with <i>Pto</i> DC3000 <i>avrpm1</i> showing the HR lesion	66
Figure 25 : Generation of ROS	67
Figure 26 : Enzymatic scavenging of ROS	69
Figure 27 : Biology of the oxidative burst	71
Figure 28 : Cross-talk between ROS and NO in plant cell death	72
Figure 29 : The induction pathway of HR	73
Figure 30 : The zigzag model and the threshold for HR under necrotrophic invasion	77

Figure 31	:	Model of SA-JA trade-off tissue spatial variation	78
Figure 32	:	Chemical structure of metabolites putatively involved in SAR in <i>A. thaliana</i>	80
Figure 33	:	Schematic representation model of SAR signaling	81
Figure 34	:	NPR3 and NPR4 regulation of NPR1 in SAR	86
Figure35:	:	Infection cycle of <i>Pseudomonas syringae</i> pv <i>tomato</i> in <i>A. thaliana</i> leaves	90
Figure 36	:	Schematic representation of RIN4	92
Figure 37	:	Molecular representation of coronatine	93
Figure 38	:	PAMP elicitors activate SA signaling and indole glucosinolate metabolism	94
Figure 39	:	<i>Botrytis cinerea</i>	99
Figure 40	:	Chronology of genes differentially expressed during <i>A. thaliana</i> - <i>B. cinerea</i>	101
Figure 41	:	Phylogenetic tree representing <i>CYP76</i> family members in <i>A. thaliana</i>	105
Figure 42	:	Gene structure and chromosome localization of the <i>CYP76</i> family	106
Figure 43	:	Schematic representation of expression patterns in <i>A. thaliana</i> organs	107
Figure 44	:	Reactions catalyzed by CYP76C1, CYP76C2, and CYP76C4 <i>in vitro</i>	109
Figure 45	:	Timeline progress and information CYP76C subfamily	111
Figure 46	:	Stress responsive matrix of selected P450 genes	113
Figure 47	:	Data from transcriptomic analyses LAR responses 6 HPI	114
Figure 48	:	Diagram of primers and T-DNA insertion	123
Figure 49	:	<i>A. thaliana</i> Col-0 plant, 96 HPI avirulent strain + virulent strain	130
Figure 50	:	The molecular structure of analyzed compounds	144
Figure 51	:	Absorption spectrum of analyzed compounds	145
Figure52:	:	Transcript level of <i>CYP76</i> family members during interaction with <i>B. cinerea</i>	153
Figure 53	:	Transcript level of <i>CYP76C2</i> at 8-24-48 HPI during interaction with <i>B. cinerea</i>	154
Figure 54	:	Transcript levels of <i>CYP76</i> family members interaction with <i>Pto</i> DC3000	157
Figure 55	:	Transcript levels of the <i>CYP76</i> family members interaction with <i>Pto avrRpm1</i>	164
Figure 56	:	Summary transcript levels of <i>CYP76C2</i>	166
Figure 57	:	GUS staining of <i>B. cinerea</i> infected leaves from <i>promCYP76C2:GUS</i>	168
Figure 58	:	Local and systemic gene expression <i>B. cinerea</i> infection <i>promCYP76C2:GUS</i>	169
Figure 59	:	GUS staining of <i>Alternaria brassicicola</i> infected leaves from <i>promCYP76C2:GUS</i>	169
Figure 60	:	GUS staining of <i>Pto</i> DC3000 infected leaves from <i>promCYP76C2:GUS</i>	170
Figure 61	:	GUS staining of <i>Pto</i> DC3000 <i>avrRpm1</i> infected leaves from <i>promCYP76C2:GUS</i>	171
Figure 62	:	GUS staining of <i>Pto</i> DC3000 infected leaves from <i>promCYP76C2:GUS</i>	172
Figure 63	:	<i>Pto</i> DC3000 infection on <i>A. thaliana</i> leaves of <i>Col-0</i> , <i>cyp76c2</i> and <i>35S:CYP76C2</i>	175
Figure 64	:	Disease symptoms 72 HPI in <i>A. thaliana</i> leaves of <i>Col-0</i> , <i>cyp76c2</i> , <i>35S:CYP76C2</i>	176

Figure 65	:	Time course quantification of <i>Pto</i> DC3000 infection in <i>Col-0, cyp76c2,35S:CYP76C2</i>	178
Figure 66	:	Time course quantification of <i>Pto</i> DC3000 infection in <i>Col-0, cyp76c2,35S:CYP76C2</i>	179
Figure 67	:	Quantification of <i>Pto</i> DC3000 <i>avrRpm1</i> infection on <i>Col-0, cyp76c2, 35S:CYP76C2</i>	180
Figure 68	:	Disease symptoms, LAR and SAR responses at 72 HPI in <i>Col-0</i> plants	182
Figure 69	:	Quantification <i>Pto</i> DC3000 infection on <i>A. thaliana</i> of <i>Col-0, cyp76c2,35S:CYP76C2</i>	183
Figure 70	:	Quantification <i>Pto</i> DC3000 infection on <i>A. thaliana</i> of <i>Col-0, cyp76c2, 35S:CYP76C2</i>	184
Figure 71	:	Time course progress <i>Pto</i> DC3000 <i>avrRpm1</i> infection in <i>Col-0, cyp76c2,35S:CYP76C2</i>	186
Figure 72	:	Visual assessment disease development in <i>A. thaliana Col-0, cyp76c2,35S:CYP76C2</i>	187
Figure 73	:	Quantification disease development in <i>A. thaliana Col-0, cyp76c2, 35S:CYP76C2</i>	189
Figure 74	:	GC-MS chromatograms of headspace volatiles from <i>Col-0, cyp76c2,35S:CYP76C2</i>	193
Figure 75	:	GC-MS chromatograms of headspace volatiles from <i>Col-0, cyp76c2,35S:CYP76C2</i>	194
Figure 76	:	GC-MS chromatograms of headspace volatiles from <i>Col-0, cyp76c2,35S:CYP76C2</i>	195
Figure 77	:	GC-MS chromatograms of headspace volatiles from <i>Col-0, cyp76c2,35S:CYP76C2</i>	196
Figure 78	:	Targeted UPLC-3Q-MS/MS profiling <i>Col-0, cyp76c2, 35S:CYP76C2</i>	198
Figure 79	:	Bi-plot of PCA of the metabolic profiling of <i>Col-0, cyp76c2, 35S:CYP76C2</i>	200
Figure 80	:	UPLC-3Q-MS/MS chromatograms of <i>Col-0, cyp76c2, 35S:CYP76C2</i>	202
Figure 81	:	UPLC-3Q-MS/MS chromatograms of 2,5 DHBA standard and <i>35S:CYP76C2</i>	203
Figure 82	:	Four potential compounds related to 2,5 DHBA in <i>Col-0, cyp76c2, 35S:CYP76C2</i>	204
Figure 83	:	Profiling SA, SAG, JA-Ile, JA-Ile-OH, JA-Ile-COOH in <i>Col-0, cyp76c2, 35S:CYP76C2</i>	205
Figure 84	:	Bi-plot of PCA of the hormone profiling of <i>Col-0, cyp76c2, 35S:CYP76C2</i>	207
Figure 85	:	Quantification of compounds potentially related to 2,5 DHBA and conjugated forms	208
Figure 86	:	Bi-plot of PCA of the hormone profiling of <i>Col-0, cyp76c2, 35S:CYP76C2</i>	210
Figure 87	:	Profiling of BA, SA, SAG and SGE upon <i>Pto</i> DC3000 <i>avrRpm1</i> infection	213
Figure 88	:	Profiling of 2,3 , 2,5, 2,4 and 3,4 DHBA upon <i>Pto</i> DC3000 <i>avrRpm1</i> infection	215
Figure 89	:	Profiling of JAs upon <i>Pto</i> DC3000 <i>avrRpm1</i> infection	216
Figure 90	:	Profiling of TA and its sulfated/glycosylated forms upon <i>Pto</i> DC3000 <i>avrRpm1</i>	218
Figure 91	:	Profiling of ABA upon <i>Pto</i> DC3000 <i>avrRpm1</i> infection	219
Figure 92	:	Profiling of camalexin upon <i>Pto</i> DC3000 <i>avrRpm1</i> infection	220
Figure 93	:	Profiling of linalool and hydroxylated derivatives upon <i>Pto</i> DC3000 <i>avrRpm1</i>	221
Figure 94	:	Bi-plot of PCA of the hormone profiling of <i>Col-0, cyp76c2 ,35S:CYP76C2</i> 0 HPI	224
Figure 95	:	Bi-plot of PCA of the hormone profiling of <i>Col-0, cyp76c2 ,35S:CYP76C2</i> 24 HPI	225
Figure 96	:	Bi-plot of PCA of the hormone profiling of <i>Col-0, cyp76c2 ,35S:CYP76C2</i> 48 HPI	226
Figure 97	:	Bi-plot of PCA of the hormone profiling of <i>Col-0, cyp76c2 ,35S:CYP76C2</i> 72 HPI	227
Figure 98	:	MRM methods in UPLC-3Q-MS/MS for benzenoids	229

Figure 99	: Targeted UPLC profiling of BA and glycosylated forms in <i>Col-0, 35S:CYP76C2</i>	230
Figure 100	: Targeted UPLC profiling of BA and glycosylated forms <i>Col-0, 35S:CYP76C2</i>	231
Figure 101	: Targeted UPLC profiling of SA and glycosylated forms in <i>Col-0, 35S:CYP76C2</i>	232
Figure 102	: Targeted UPLC profiling of DHBAs and glycosylated forms in <i>Col-0, 35S:CYP76C2</i>	234
Figure 103	: HPLC-photodiode array chromatogram of <i>in vitro</i> conversion	235
Figure 104	: Area values of the peak corresponding to compound 1	236
Figure 105	: Area values of the peak corresponding to compound 1	238
Figure 106	: Peak area of the compounds of m/z 377 and 215 from orbitrap UPLC-MS 6 HPI	239
Figure 107	: Mass spectrum of the [M- H ₂ O] ion 215 m/z, ESI positive	240
Figure 108	: Schematic representation of T-DNA insertion in the lines used in this thesis	297
Figure 109	: Genotyping of T-DNA insertion and overexpression lines of <i>CYP76C1</i> and <i>CYP76C2</i>	297
Figure 110	: Genotyping of T-DNA insertion and overexpression lines of <i>CYP76C3</i>	298
Figure 111	: Genotyping of T-DNA insertion and overexpression lines of <i>CYP76C4</i>	298
Figure 112	: Melting curve analysis of primers used in qRT-PCR of gene expression	300
Figure 113	: Melting curve analysis of primers used in qRT-PCR of gene expression	301
Figure 114	: Standard curve <i>AtTUB4</i> gene from <i>A. thaliana</i>	302
Figure 115	: Standard curve of plasmid containing the <i>PsOpfr</i> gene from <i>Pto</i> DC3000	303
Figure 116	: qPCR quantification of time course infection <i>Pto</i> DC3000 on <i>A. thaliana -EE</i>	304
Figure 117	: Quantification of disease development in <i>A. thaliana Col-0, cyp76c2, 35S:CYP76C2</i>	305
Figure 118	: <i>Hyaloperonospora arabidopsidis</i> infection with strain <i>noco2</i>	306
Figure 119	: Bi-plot of PCA of the metabolic profiling of <i>Col-0, cyp76c2, 35S:CYP76C2</i>	307
Figure 120	: Bi-plot of PCA of the metabolic profiling of <i>Col-0, cyp76c2, 35S:CYP76C2</i>	308
Figure 121	: Profiling of BA, SA, SAG and SEG upon <i>Pto</i> DC3000 <i>avrRpm1</i> infection	309
Figure 122	: Profiling of 2,3, 2,5, 2,4 ?3,4 DHBA upon <i>Pto</i> DC3000 <i>avrRpm1</i> infection	310
Figure 123	: Profiling of JAs upon <i>Pto</i> DC3000 <i>avrRpm1</i> infection	311
Figure 124	: Profiling of TA and glycosylated form upon <i>Pto</i> DC3000 <i>avrRpm1</i>	312
Figure 125	: Profiling of ABA and camalexin upon <i>Pto</i> DC3000 <i>avrRpm1</i> infection	312
Figure 126	: Profiling of linalool and hydroxylated derivatives	313
Figure 127	: <i>CYP76C2</i> : yeast transformation, positive colonies and P450 spectro	314

LIST OF TABLES

		Page
Table 1:	Cytochrome P450 in defense and signaling in <i>Arabidopsis thaliana</i>	9
Table 2:	Classes of specialized metabolites and their role in defense in higher plants	13
Table 3:	List of factors triggering camalexin biosynthesis in <i>Arabidopsis thaliana</i>	20
Table 4:	SA modifications in <i>Arabidopsis thaliana</i>	49
Table 5:	Metabolic fate of JAs in <i>A. thaliana</i>	53
Table 6:	Morphological classification of cell death in plants	63
Table 7:	Classification of non-autolytic cell death in plants	64
Table 8:	Pathogens and lifestyle	87
Table 9:	Reported substrates of the members of the CYP76C subfamily	108
Table 10:	Primer sequence with user extensions used to amplify <i>CYP76C7</i>	119
Table 11:	Primers sequences used for colony PCR	120
Table 12:	Primer sequences used for genotyping of knock-out lines	123
Table 13:	Primer sequences of reference genes	127
Table 14:	Primer sequences used for RT-qPCR for gene expression quantification	128
Table 15:	Reference genes annotation	128
Table 16:	Gene specific primers for pathogen DNA quantification	130
Table 17:	UHPLC gradient elution linalool derivatives	134
Table 18:	m/z Fragments obtained by UPLC-MS for different linalool derivatives	135
Table 19:	UHPLC gradient elution for hormones	136
Table 20:	m/z Fragments obtained by UPLC-MS	137
Table 21:	UHPLC gradient elution Orbitrap	138
Table 22:	HPLC gradient for benzenoids derivatives	143
Table 23:	List of candidate substrates used in CYP76C2 enzymatic assays	143
Table 24:	Mean value of <i>Botrytis</i> necrotic lesion in % of col-0 plants	190
Table 25:	PCA summary fragments from 100-450 m/z	199
Table 26:	PCA summary putatives DHBA UPLC-MS/MS	206
Table 27:	PCA summary putatives DHBA Orbitrap-UPLC	209
Table 28:	Kruskal-Wallis test for mean comparison hormone profiling	222
Table 29:	PCA summary hormone profiling timeline	223
Table 30:	Information on chemical formulae calculated with the m/z of compound 1	237
Table 31:	List of genetic material available and genetic status	299

LIST OF ABBREVIATIONS

12-OH-JA-sulfate	12-Hidroxy-(+)-7-Isojasmonic Acid Sulfate	CoA	Coenzyme A
2,3 DHBA	2,3 Dihydroxybenzoic Acid	COI1	Coronatine Insensitive 1
2,4 DHBA	2,4 Dihydroxybenzoic Acid	Col-0	Columbia Ecotype
2,5 DHBA	2,5 Dihydroxybenzoic	COR	Coronatine
3,4 DHBA	3,4 Dihydroxybenzoic Acid	CT	Threshold Cycle
4CL	4-Coumarate CoA Ligase	C-terminal	Carboxy-Terminus
		CWDE	Cell Wall Degrading Enzyme
		CYP	Cytochrome P450
		Cys(IAN)	Ian Cysteine Conjugate
A		D	
AAO	Aldehyde Oxidase	Da	Dalton
ABA	Abscisic Acid	DA	Dehydroabietal
ANOVA	Analysis of Variance	DAD1	Delayed Anther Dehiscence 1
AOC	Allene Oxide Cyclase	DAMP	Danger-Associated Molecular Pattern
AOS	Allene Oxide Synthase	DGL	Dongle
AP2/ERF	Apetala 2/Ethylene Response Factor	DHCA	Dihydrocamalexidic Acid.
Atrboh	Respiratory Burst Oxidase Homologues	DIR1	Defective In Induced Resistance 1
AtST2 α	A. Thaliana Sulfotransferase 2	DMAPP	Dimethyl Allyl Diphosphate
Avr	Avirulent	DMSO	Dimethyl Sulfoxide
Aza	Azelaic Acid	DNA	Deoxyribonucleic Acid
AZI1	Azelaic Acid Induced 1	dn-OPDA	Dinor-OPDA
		dNTP	Deoxyribonucleotide Triphosphate
B		DO	Optical Density
BA	Benzoic Acid	DTT	Dithiothreitol
BA2H	Benzoic Acid-2-Hydroxylase		
	Brassinosteroid Insensitive 1	E	
BAK1	Associated Kinase	E	Efficiency
BIK1	Botrytis Induced Kinase 1	EAR	ERF -Associated Amphiphilic Repression
BLAST	Basic Local Alignment Search Tool	EDS1	Enhanced Disease Susceptibility 1
bp	Base Pair	EDTA	Ethylene Diamine Tetraacetic Acid
BR	Brassinosteroid	EFR	Elongation Factor Ef-Tu
BSA	Bovine Serum Albumin	ER	Endoplasmic Reticulum
BZL	Benzoyl CoA Ligase	ESI	Electrospray Ionization
		EST	Expressed Sequence Tag
C		ET	Ethylene
CaMV	Cauliflower Mosaic Virus	ETI	Effector-Triggered Immunity
CAT	Catalase	ETS	Effector-Triggered Susceptibility
CC-NB-LRR	Coil-Coil -NB-LRR		
cDNA	Complementary DNA	F	
CE	Collision Energy	FAA	Formalin Acetic Acid Alcohol
CFA	Coronafacic Acid	FB1	Fumonisin B1
cfu	Colony Forming Unit	FLD	Flowering Locus D
CH4	Cinnamate 4-Hydroxylase	flg22	Flagellin 22
cJA	<i>Cis</i> - Jasmonate		
CK	Cytokinines		
CMA	Coronamic Acid		

FLS2	Flagellin Sensing 2		
G		L	
G3P	Glycerol-3-Phosphate	LAR	Localized Acquired Resistance
GB	Gibberellin	LB	Left Border
GC-MS	Gas Chromatography- Mass Spectrometry	LOX	Lipoxygenase
gDNA	Genomic DNA	LOX2	Lipoxygenase 2
GFP	Green Fluorescent Protein	LRR	Leucine Rich Repeat
GGP1/GGP3	γ -Glutamylpeptidases	LSD1	Lesion Simulating Disease Resistance
GGT1/GGT3	γ -Glutamyltranspeptidases 1 and 3	M	
GRX	Glutaredoxin	M	Molar
GSH	Glutathione	m/z	Mass To Charge Ratio
GSH(IAN)	IAN Glutathionyl Derivative	MAMP	Microbe-Associated Molecular Pattern
GST	Glutathione S-Transferase	MAPK	Mitogen Activated Protein Kinase
GSTF6	Glutathione-S-Transferase	MAPK	Mitogen Activated Protein Kinases
GUS	β -Glucuronidase	MC1	Metacaspase 1
H		MEA	Malt Extract Agar
h	Hours	MeJA	Methyl Jasmonate
HPI	Hours Post Infection	MEP	Methyl Erythrol Pathway
HPLC	High Performance Liquid Chromatography	MeSA	Methyl Salicylate
HR	Hypersensitive Response	min	Minute
I		MOS	Modifier of Snc1
IAA	Indole Acetic Acid	MRM	Multiple Reaction Monitoring Mode
IAN	Indole-3-Acetonitrile	MS	Mass Spectrometry
(IAN) _{CysGly}	IAN Cysteiny-Glycine	MVA	Mevalonate Pathway
IAOx	Indole-3-Acetaldoxime	MYC	Transcription Factor
IAR3	IAA-Alanine Resistant 3	N	
ICS1/2	Isochorismate Synthase	NADPH	Nicotinamide Adenine Dinucleotide Phosphate
ILL6	IAA-Leucine Resistant (ILR)-Like Gene 6	NASC	Nottingham European Arabidopsis Stock Centre
IPL	Isochorismate Pyruvate Lyase	NB-LRR	Nucleotide Binding-Leucine Rich Repeat
IPP	Isopentenyl Diphosphate	NDR1	Non-Race Specific Disease Resistance 1
IPTG	Isopropyl-B-D-Thiogalactopyranoside	NIMIN1	Nim Interacting 1
IS	Internal Standards	NINJA	Novel Interactor of JAZ
J		NIST	National Institute of Standards and Technology
JA	Jasmonic Acid /Jasmonate	nm	Nanometer
		NO	Nitric Oxide
		NPR1, NPR3, NPR4	Non-Expressor of PR1, 3, 4
		N-terminal	Amino-Terminus
JA-ACC	JA /1-Amino-1-Cyclopropane Carboxylic Acid Conjugate	O	
JA-ILE	Jasmonoyl Isoleucine	OD	Optical Density
JA-Ile-COOH	12-Carboxyjasmonoyl Isoleucine	OG	Oligogalacturonides
JA-Ile-OH	12-Hydroxyjasmonoyl-Isoleucine	OPDA	12-Oxo-Phytodienoic Acid
JAR1	Jasmonate Resistant 1	OPDA-GSH	OPDA Glutathione Conjugate
JA-Trp	JA /Tryptophan Conjugate	OPR3	Oxophytodienoic Acid Reductase 3
JAZ	Jasmonate Zim	ORA 59	Octadecanoid Responsive Arabidopsis 59
JMT	JA Carboxyl Methyl Transferase		

P

P450	Cytochrome P450
PAD3 CYP71B15	Phytoalexin Deficient 3
PAD4	Phytoalexin Deficient 4
PAL	Phenylalanine Ammonia- Lyase
PAMP	Pathogen-Associated Molecular Pattern
PBS	Phosphate Buffered Saline
PCA	Principal Component Analysis
PCD	Programmed Cell Death
PCR	Polymerase Chain Reaction
PCS1	Phytochelatin Synthase
PDA	Potato Dextrose Agar
PDB	Potato Dextrose Broth
PDF 1.2	Plant Defensin 1.2
PEG	Polyethylene Glycol
Pip	L-Pipecolic Acid
PR	Pathogenesis-Related
PRR	Pathogen Recognition Receptor
PTI	PAMP-Triggered Innate Immunity
<i>Pto</i> DC 3000	<i>P. syringae</i> pv. <i>tomato</i> DC3000 (Vir)
pv.	Pathovar

Q

qPCR	Real Time PCR
qRT-PCR	Real Time Reverse Transcription PCR

R

RB	Right Border
R-gene	Resistance Gene
RLK	Receptor Like Kinase
RNA	Ribonucleic Acid
ROS	Reactive Oxygen Species
R-protein	Resistance Protein
RT	Retention Time
RT-PCR	Reverse Transcription Polymerase Chain Reaction

S

SA	Salicylic Acid
SA-Asp	Salicyloyl-L-Aspartic Acid
SABP2	SA Binding Protein 2
SAG	Salicylic Acid 2-O-B-Glucoside
SAG 101	Senescence -Associated Carboxylesterase 101
SAR	Systemic Acquired Resistance

SCF-CO11 complex E3 Ubiquitin-Ligase SKP1-Cullin-F-Box Complex SCG

SDS	Sodium Dodecyl Sulphate
SE	Standard Error
sec	Seconds
SEG	Salicyloyl Glucose Ester
SM	Secondary Metabolism
SNI1	Suppressor of NPR1 Inducible 1
SOD	Superoxide Dismutase
STD	Standard Deviation

T

TA	Tuberonic Acid/ 12-Hydroxy-(+)-7-Isojasmonic Acid
TAE buffer	Buffer Tris, Acetate, EDTA
TAG	Glycosylated form of Tuberonic Acid
T-DNA	Transfer DNA
TDS	Thermal Desorber
TE	Tris-HCl EDTA
TGA	Transcription Factor
TIR-NB-LRR	Toll-Interleukin-NB-LRR
TLR	Toll Like Receptor
Tm	Melting Temperature
TMTT	4,8,12-Trimethyltrideca-1,3,7,11-Tetraene
TPL	Topless Corepressor
TPS	Terpene Synthase
Tris	2-Amino-2-Hydroxymethyl-Propane-1,3-Diol
TRX-H 3-5	Thioredoxin
TTSS	Type III Secretion System

U

UGT	UDP-Glycosyltransferase
UHPLC	Ultra High Performance Liquid Chromatography
UPLC	Ultra Performance Liquid Chromatography
UV	Ultra-Violet

V

v/v	Volume in Volume
VPE	Vacuolar Processing Enzymes
VSP2	Vegetative Storage Protein 2

W

WRKY	Transcription Factor
WS	Wassilewskija Ecotype
WT	Wild-Type

X

X-gluc	5-Bromo-4-Chloro-3-Indolyl-B-D-Glucuronic Acid
--------	--

Z

γ -GluCys(IAN)	γ -Glutamyl-Cysteine IAN
-----------------------	---------------------------------

Introduction

INTRODUCTION

INTRODUCTION

The plant model of choice: *Arabidopsis thaliana*

Arabidopsis thaliana (L.) Heynh. 1842 is a dicotyledonous species member of the *Brassicaceae* family (Figure 1). Although not of major agronomic significance, its characteristics including short life cycle (6 weeks), prolific seed production, and manageable size for cultivation has made this plant widely used as a model organism in plant biology since its full sequencing in 2000 (*The Arabidopsis Initiative*, 2000).



Figure 1: *Arabidopsis thaliana* (L.) Heynh., syn. *Crucifera thaliana* (L.) E.H. L. Krause.

From Deutschlands Flora in Abbildungen (1796) at <http://www.biolib.de>

A large number of mutant lines and genomic resources are currently available since plant transformation by *Agrobacterium tumefaciens* is highly efficient (Weigel and Glazebrook, 2002). This feature is not of minor relevance, since it allows to easily address a wide range of topics or fields that have demonstrated to be complex or problematic in more economically important plant species.

Until a few years ago, it seemed unlikely that such a small plant (and genome) would be suitable to tackle questions related to “Plant-Pathogen interaction” and “Secondary Metabolism”, but recent work have endorsed the *Arabidopsis* model for such studies (Mauch-Mani and Slusarenko, 1993; D’Auria and Gershenzon, 2005; Pieterse *et al.*, 2009; Koornneef and Meinke, 2010).

The validation of several pathosystems with useful variation in *A. thaliana* responses as a host (Mauch-Mani and Slusarenko, 1993; Katagiri *et al.*, 2002; Slusarenko and Schlaich, 2003) has in fact enlarged our understanding of plant-pathogen interactions and the underlying signaling networking. It has also increased the possibilities of applying this knowledge to solve the fundamental question in plant pathology and to improve crop development (Laluk and Mengiste, 2010; Ferrier *et al.*, 2011).

On the other hand, *A. thaliana* was also found appropriate for studies on function and evolution of plant secondary metabolism (Chapple *et al.*, 1994; D’Auria and Gershenzon, 2005) with numerous metabolites representatives of the major classes of secondary metabolites such as indole and indole-sulfur compounds, glucosinolates, terpenoids, phenylpropanoids, benzenoids, fatty acid derivatives and flavonoids (Lv *et al.*, 2014).

Displaying a striking spatial and temporal variation and distribution of secondary metabolites within the plant, but also in ecological interactions with the surrounding environment, *Arabidopsis* provides a unique opportunity to study the biosynthesis, regulation and function of secondary metabolites in some major secondary metabolic pathways (Dixon, 2001; Edda von Roepenack-Lahaye *et al.*, 2004; D’Auria and Gershenzon, 2005; Lv *et al.*, 2014).

All these general considerations made *A. thaliana* our model of choice.

Cytochrome P450

Cytochromes P450 or CYPs is a generic name for a large family of heme-thiolate proteins that use NAD(P)H as electron donor for dioxygen activation and insertion of one of its oxygen atoms into organic substrates (Mitzutani *et al.*, 1998; Schuler and Werck-Reichhart, 2003).

P450s proteins are mainly α -helical, with the heme cofactor sandwiched between a larger α -helix-rich domain and a small β -sheet-rich domain (Munro *et al.*, 2013) (Figure 2). The vast majority of the P450s are anchored into cellular membranes (usually endoplasmic reticulum) with a single N-terminal helix, with the globular part of the protein protruding into the cytoplasm (Schuler and Werck-Reichhart, 2003). The heme group is a highly conjugated ring system with four pyrrole nitrogen coordinated to iron (to form a heme b) that has as fifth ligand a conserved cysteine of the protein axially bound through a thiol bond (Munro *et al.*, 2013) (Figure 2).

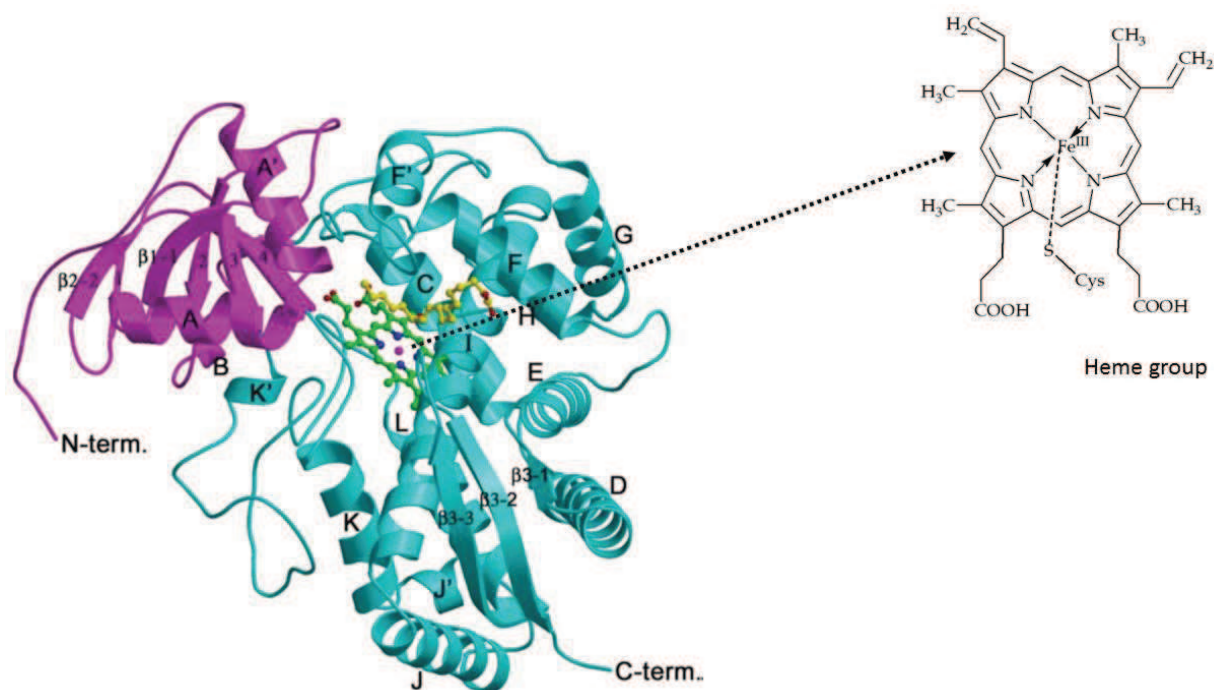


Figure 2: Ribbon representation of P450 CYP74A structure.

The α - and β -domains are shown in cyan and magenta with the secondary structures. The N- and C-termini are labeled. Heme group and substrate can be seen in the center as ball-stick model (diverse colors). From Li *et al.* (2008).

The name “P450” originates from the reduced carbon monoxide (CO)-bound versus reduced difference UV-vis spectrum displayed by the P450 proteins which has its maximum at 450 nm (Omura and Sato, 1964) (Figure 3, square in red).

P450s are probably nature’s most versatile enzymes in terms of substrate range and molecular transformations (Munro *et al.*, 2013). These enzymes can catalyse irreversible, rate-limiting steps, regio- and stereospecific oxygenations and oxidations in several branches of the plant metabolism (Morant *et al.*, 2003; Schuler and Werck-Reichhart, 2003). The current list of reactions catalyzed is extensive and probably far from complete. It includes: hydroxylation, epoxydation, dealkylation, deamination, decarboxylation, isomerization and dimerization, C-C cleavage, ring expansion, ring opening, ring migration, ring coupling, dehydration and even reduction (Schuler *et al.*, 1996; Werck-Reichhart and Feyereisen, 2000; Renault *et al.*; 2014).

In higher plants, P450s plays crucial roles in the biosynthesis and/or catabolism of fatty acids (cutins and suberins), sterols and other terpenoids, amino acid-derived compounds (glucosinolates and cyanogenic glucosides), phenylpropanoids including lignin monomers, UV protectants (flavonoids, coumarins, sinapoyl esters) and pigments (anthocyanins), defense compounds/phytoalexins (including isoflavonoids, glucosinolates, terpenes, cyanogenic glucosides), hormones (gibberellins, abscisic acid, strigolactones, cytokinins, auxin, brassinosteroids), signalling molecules (jasmonic acid) as well as herbicide, insecticide and pollutants detoxification (Schuler and Werck-Reichhart, 2003; Powles and Yu, 2010; Renault *et al.*, 2014).

Catalytically, they activate molecular oxygen (O₂) inserting one of the atoms into a substrate bound in the active site, reducing the second oxygen atom into water. Hence P450s are monooxygenases (Bak *et al.*, 2011; Meunier *et al.*, 2004; Werck-Reichhart and Feyereisen, 2000).

The reaction can be summarized as follows (hydroxylation as an example)



Where, RH: substrate, NAD(P)H: electron donor, ROH: hydroxylated product.

A more detailed explanation of the catalytic cycle can be seen in Figure 3.

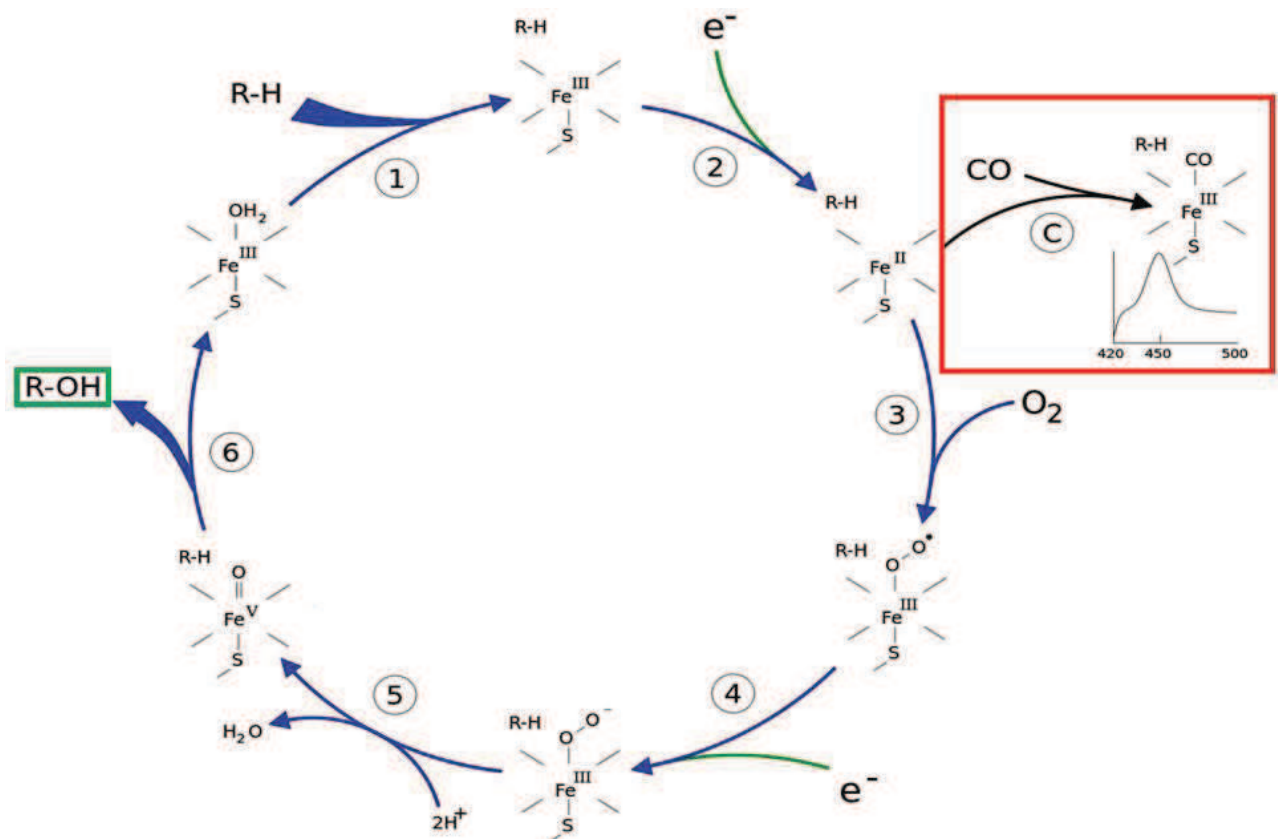


Figure 3: The P450 catalytic cycle.

See description in the text. In the red square a detail of the reduced carbon monoxide (CO) difference spectrum which has its maximum at 450 nm. (Image modified from "Medical gallery of David Richfield 2014". Wikiversity Journal of Medicine 1 (2). DOI:10.15347/wjm/2014.009. ISSN 2001-8762)

1- The substrate (R-H) binds to the active site of the P450, close to the heme group and on the opposite side of the heme-anchoring cysteine in the peptide chain.

2- The bound substrate induces a conformational change in the active site, displacing a water molecule usually bound as sixth ligand to the heme iron, and changing the state of the heme iron from low-spin to high-spin. This change favors the transfer of an electron from the electron donor NAD(P)H and the transition Fe⁺³ to Fe⁺².

3- Molecular oxygen binds covalently to the distal axial coordination position of the reduced heme iron.

4- A second electron is transferred from NAD(P)H, reducing the dioxygen adduct to a negatively charged peroxy group in short-lived intermediate state.

5: The peroxy group formed in step 4 is rapidly protonated twice by local transfer from surrounding amino-acid side chains, releasing one molecule of water, and forming a highly reactive iron-oxo species.

6: Iron-oxo is the reactive species responsible for the substrate attack. Most often a hydrogen is abstracted from a closest position on the substrate, followed by an OH rebound, resulting in substrate hydroxylation. After the product has been released from the active site (R-OH), the enzyme returns to its original state, with a water molecule occupying the distal coordination position of the heme iron.

C: If carbon monoxide (CO) binds to reduced P450, the catalytic cycle is interrupted. This reaction yields the classic CO difference spectrum with a maximum at 450 nm.

Genes encoding the cytochromes P450s have been highly duplicated and new members have diverged enormously. As quoted in Renault *et al.*, (2014), the amount of annotated plant P450s to date is 7512 which is significantly greater than seen in vertebrates (1461), insects (2137), fungi (2960), bacteria (1042), Archae (27) and viruses (2) (Nelson, 2009). Furthermore it is the third largest family of plant genes after F-box proteins (692 genes in *Arabidopsis*) and receptor-like kinases (610 genes in *Arabidopsis*). Around 300 genes grouped in 50 families compose the CYPome of Angiosperms (Nelson and Werck-Reichhart, 2011).

There are 244 P450 genes and 28 pseudogenes in the *Arabidopsis* genome (Bak *et al.*, 2011). The remarkable functional diversification showed by this enzymes in signaling, synthesis of biopolymers, formation of complex anatomical structures and in plant adaptation and defense; points to its relevance in plant metabolism (Nelson and Werck-Reichhart, 2011) and the necessity for further research to achieve full CYP exploitation (Renault *et al.*, 2014).

Nomenclature

P450 has been classified into families and subfamilies. In plants there are so far 127 families grouped in 11 clans, including single-family and multiple-family clans (Nelson and Werck-Reichhart, 2011). P450s have been classified according to their protein homology and phylogenetic criteria (Nelson *et al.*, 2006) with a 40 % of amino acid sequence identity for family membership and 55 % identity for a subfamily.

Names are assigned according to:

CYP98A3

Where:

-**CYP**: cytochrome P450

-**98**: family number

-**A**: subfamily

-**3**: specific protein

Further information can be found at <http://drnelson.uthsc.edu/CytochromeP450.html>.

P450 and Plant Defense

A worth mentioning number of P450 genes have been shown to be implicated directly or indirectly in plant defense responses against pathogens and pest, and, consequently, in disease resistance.

Their repercussion in plant defense was especially palpable when we became aware of all of the critical roles they play in pathways responsible for synthesizing hormones and signaling molecules, structural compounds and a vast array of secondary metabolites.

Their functions span through the metabolism of cutin, suberin and lignin, the metabolism of signaling molecules and hormones such as jasmonate, abscisic acid, gibberellins, auxin, strigolactones and brassinosteroids, and the metabolism of phytoalexins and phytoanticipins (*i.e* secondary metabolites) such as glucosinolates, cyanogenic glucosides, alkaloids, phenylpropanoids, terpenoids and more. For instance, in *Arabidopsis* they are essential at a metabolic branch point between auxin and indole-glucosinolate biosynthesis pathways (Glawischnig, 2006; Bak *et al.*, 2001; Dixon, 2001) that leads to the synthesis of plant defense molecules like camalexin and at the subsequent cascade of defense molecules of different sort and fortune as described and showed in Table 1. (Schuler *et al.*, 2006).

A non-exhaustive list of P450s involved in defense and signaling in *Arabidopsis thaliana* can be seen in Table 1.

Table 1: Cytochrome P450 in defense and signaling in *Arabidopsis thaliana*.

Gene	Accession number	Pathway	References
CYP707A1 CYP707A2 CYP707A3 CYP707A4	At4g19230	Abscisic acid catabolism	Kushiro <i>et al.</i> , 2004 Saito <i>et al.</i> , 2004 Okamoto <i>et al.</i> , 2006 Okamoto <i>et al.</i> , 2009/2011
CYP72C1	At1g17060	Brassinosteroids/Triterpenoids biosynthesis	Nakamura <i>et al.</i> , 2005 Tkahashi <i>et al.</i> , 2005 Turk <i>et al.</i> , 2003 Thornton <i>et al.</i> , 2010
CYP734A1	At2g26710	Brassinosteroids/Triterpenoids catabolism	Turk <i>et al.</i> , 2005 Thornton <i>et al.</i> , 2011
CYP85A1 CYP85A2	At3g30180 At5g38970	Brassinosteroids/Triterpenoids biosynthesis	Kim <i>et al.</i> , 2005
CYP90A1 CYP90B1	At3g50660 At5g05690	Brassinosteroids/Triterpenoids biosynthesis	Ohnishi <i>et al.</i> , 2012
CYP90C1 CYP90D1	At4g36380 At3g13730	Brassinosteroids/Triterpenoids biosynthesis	Kim <i>et al.</i> , 2005 Ohnishi <i>et al.</i> , 2012
CYP71A12 CYP71A13	At2g30770	Camalexin biosynthesis	Nafisi <i>et al.</i> , 2007 Millet <i>et al.</i> , 2010
CYP71B15 (PAD3)	At3g26830	Camalexin biosynthesis	Glazebrook and Ausubel, 1994 Zhou <i>et al.</i> , 1999 Schuhegger <i>et al.</i> , 2006
CYP79B2 CYP79B3	At4g39950 At2g22330	Camalexin and auxin biosynthesis	Hull <i>et al.</i> , 2000 Mikkelsen <i>et al.</i> , 2000 Glawischnig <i>et al.</i> , 2004
CYP77A4	At5g04660	Cuticle , cutin, fatty acids	Sauveplane <i>et al.</i> , 2009
CYP86A2	At4g00360	Cuticle , cutin, fatty acids	Xiao <i>et al.</i> , 2004 Duan and Schuler, 2005
CYP86A4 CYP77A6	At1g01600 At3g10570	Cuticle , cutin, fatty acids	Duan and Schuler, 2005 Li-Beisson <i>et al.</i> , 2009 Pinot and Beisson, 2011
CYP86A8	At2g45970	Cuticle , cutin, fatty acids	Wellesen <i>et al.</i> , 2001
CYP701A3	At5g25900	Gibberellins biosynthesis	Helliwell <i>et al.</i> , 1998 Davidson <i>et al.</i> , 2003/2006
CYP714A1 CYP714A2	At5g24910 At5g24900	Gibberellins biosynthesis and catabolism	Nelson <i>et al.</i> , 2004 Zhang <i>et al.</i> , 2011
CYP88A3 CYP88A4	At1g05160 At2g32440	Gibberellins biosynthesis	Helliwell <i>et al.</i> , 2001 Davidson <i>et al.</i> , 2003/2006
CYP79A2	At5g05260	Benzyl-glucosinolates biosynthesis	Wittstock and Halkier, 2000
CYP79F1 CYP79F2	At1g16400 At1g16410	Aliphatic glucosinolates biosynthesis	Hansen <i>et al.</i> , 2001 Reintanz <i>et al.</i> , 2001 Chen <i>et al.</i> , 2003
CYP81F2	At5g57220	Indole-glucosinolates processing upon attack	Bednarek <i>et al.</i> , 2009 Clay <i>et al.</i> , 2009
CYP83A1	At4g13770	Aliphatic glucosinolates biosynthesis	Bak and Feyereisen, 2001 Chen <i>et al.</i> , 2003 Hemm <i>et al.</i> , 2003 Naur <i>et al.</i> , 2003
CYP83B1	At4g31500	Indole-glucosinolates biosynthesis	Bak <i>et al.</i> , 2001 Bak and Feyereisen, 2001 Naur <i>et al.</i> , 2003
CYP74A1 CYP74B2	At5g42650	Jasmonate /Oxylipins biosynthesis	Laudert <i>et al.</i> , 1996 Bate <i>et al.</i> , 1998
CYP94B3 CYP94C1	At3g48520 At2g27690	Jasmonate conjugates catabolism	Koo <i>et al.</i> , 2011 Kitaoka <i>et al.</i> , 2011 Heitz <i>et al.</i> , 2012

Secondary Metabolism

Plants synthesize a vast array of organic compounds, referred to as secondary metabolites or natural products that are derived from plant primary metabolism and serve important adaptive functions to interact with or to adapt to the surrounding environment (Chapple *et al.*, 1994; Wink, 2011; Kroymann, 2011).

The “surroundings” suppose an everyday challenge met by the plant, starting with its sessile nature and the lack of an authentic immune system (Jones and Dangl, 2006), that can only be counteracted with their capacity of synthesize an enormous variety of chemicals (Dixon, 2001; Bednarek *et al.*, 2009; Wink, 2011).

Secondary, now more often called “specialized metabolites” possess a high structural variety. They have in common low molecular weight in a diverse array of different chemical classes of compounds such as alkaloids, amines, cyanogenic glycosides, non-protein amino acids, glucosinolates, alkalamides, peptides, lectins, terpenes, saponins, polyketides, phenolics and polyacetylenes (Winck, 2011) Illustrated in Figure 4 and Table 2.

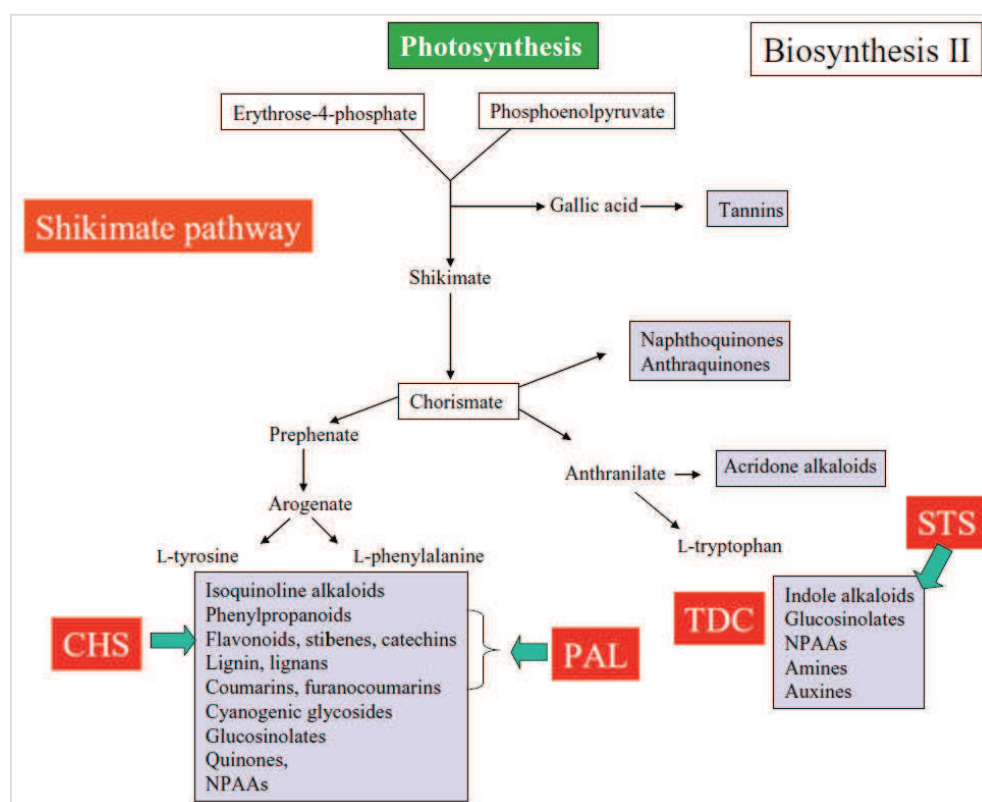
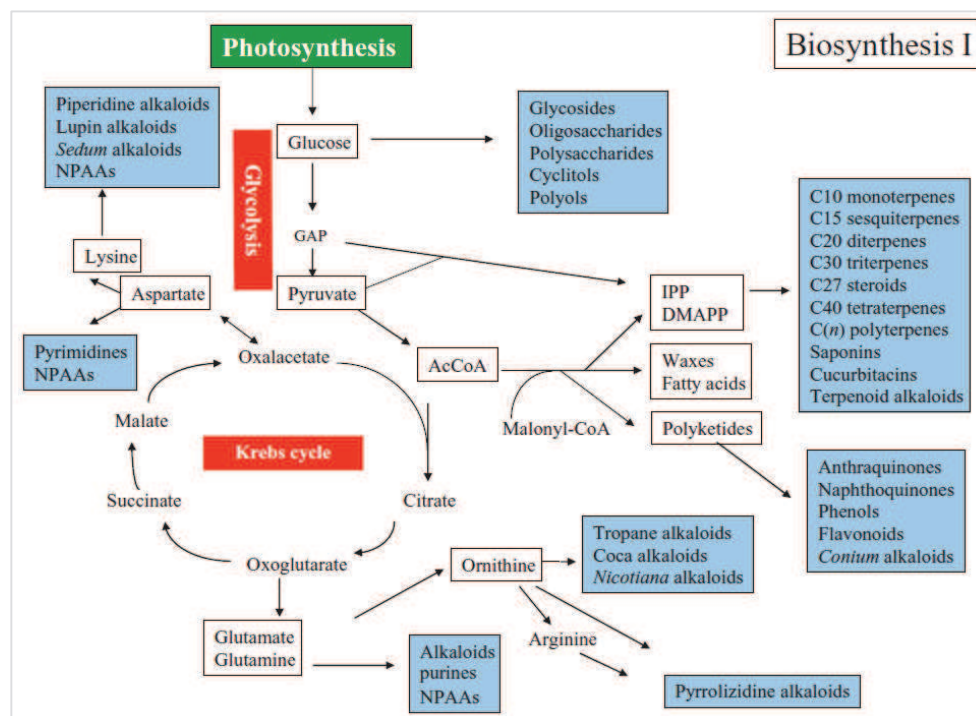


Figure 4: Main pathways leading to specialized metabolites precursors: glycolysis, the Krebs cycle or the shikimate pathway. From Wink, 2010.

They provide the plant with protection against pathogens (bacteria, fungi and viruses) and pests (insects and herbivores of all kinds, competing plants). They protect against UV light radiation and desiccation, and they can also play roles as signaling molecules: both allelochemicals and attractants for pollinators or seed dispersant (Dixon, 2001; Aharoni and Galili, 2011) (Table 2).

Specialized metabolites are often compartmentalized within vacuoles or in other specialized cellular compartments to avoid plant self-toxicity. Their modes of action include membrane disruption and pore formation (saponins, terpenoids, flavonoids), formation of physical barrier (lignin, waxes, cutin, flavonoids, amines), inhibition of DNA synthesis (cyanogenic compounds, alkaloids, flavonoids), inhibition of enzymes, nutrient and ion transport (cyanogenic glucosides, glucosinolates, alkaloids), chelation (flavonoids), generation of ROS (flavonoids), inhibition and intervention in signal transduction processes (amines, peptides, carbohydrates), inhibition of metabolism (alkaloids, tannins), growth retardation or disruption of the hormonal control of physiological processes (strigolactones, triterpenes, tetraterpenes) (several authors, see Table 2).

The mode of action can be either direct or indirect. For instance, many compounds act directly on the pathogen/herbivore/neighbor, whereas others act indirectly via the attraction of organisms from other trophic levels that, in turn, protect the plant (volatiles from terpenoids and glucosinolates)(Mithofer and Boland, 2012)

Even though, by definition, primary metabolites are essential for plant survival, it is undeniable that secondary metabolites have relevant effect on fitness and yet plant survival (Aharoni and Galili, 2011).

It has been estimated that plants produce more than 200 000 different metabolites (D'Auria and Gershenzon, 2005; Fernie, 2007), and between 5000-20 000 metabolites within one single species (Wink, 2011). This rich diversity results from an evolutionary process driven by selection, through different plant lineages, when a particular compound was able to address specific needs in a given context (Dixon, 2001; Pichersky and Gang, 2000). Since organisms never exist alone, the continuous race between plants and environmental factors is a driving force for evolution and coevolution among all the cohabitant species.

Table 2: Classes of specialized metabolites and their role in defense in higher plants. *Abundance information modified from Wink 2010, 2011, Mithöfer and Boland, 2012.

	Class Secondary metabolite	Abundance*	Some examples	Features	References
With N	Alkaloids	21000	theobromine, caffeine, nicotine atropine, solanine.	Defense mainly against herbivores and carnivores, but some cases against bacteria, fungi and viruses. Allelopathy.	-Denzel and Wink, 1993 - Katoh <i>et al.</i> , 2005 - Freeman and Beattie, 2008 - Mithofer and Boland, 2012
	Non-protein amino acids	700	<i>l</i> -canavanine, GABA, <i>l</i> -DOPA, <i>l</i> -mimosine, <i>p</i> -aminophenylalanine.	Herbivore repellent. Antimicrobial. Allelopathy.	-Janzen <i>et al.</i> , 2001 -Semar, 2011 -Huang <i>et al.</i> , 2011
	Amines	100	Several amine oxidases (copper amine oxidases and flavin-containing amine oxidases). Polyamines: spermine, putrescine.	Against pathogen, virus and nematode infection (Involvement in wall reinforcement, HR, signaling defense)	-Walters, 2003 -Cona <i>et al.</i> , 2006 -Sagor <i>et al.</i> , 2009
	Cyanogenic glycosides	60	dhurrin, linamarin, amygdalin, lotaustralin, taxiphyllin, cyanohydrin, prunasin.	Pest deterrent. Antifungal (aglycon). Allelopathy.	-Tattersall <i>et al.</i> , 2001 -Gladow and Woodrow, 2002 -Ballhorn <i>et al.</i> , 2005 -Zagrobelyny <i>et al.</i> , 2007 -Semar, 2011
	Glucosinolates and indole derivatives	150	camalexin, indole/aliphatic/glucosinolates	Anti-herbivores. Antimicrobial effect. Effect indirect: volatiles releases from glucosinolates to attract insect's enemies. Allelopathy.	-Norsworthy <i>et al.</i> , 2007 -Hopkins <i>et al.</i> , 2009 -Bednarek <i>et al.</i> , 2009 -Clay <i>et al.</i> , 2009 -Wittstock and Burow, 2010 -Semar, 2011
	Alkamides	150-200	<i>N</i> -isobutyl decanamide (affinin)	Allelochemical effect. Antimicrobial effect. (against bacteria and fungi)	-Tripathy <i>et al.</i> , 1999 -Lait <i>et al.</i> , 2003 -Mendez-bravo <i>et al.</i> , 2011
	Peptides and polypeptides (AMPs, LTPs)	2000	systemin, thionins, defensins, hevein like peptides, snakins.	Amplifying signals. Against herbivores and pathogens.	-Osborn <i>et al.</i> , 1995 -Garcia-Olmedo <i>et al.</i> , 1998 -Graham <i>et al.</i> , 2008 -Stotz <i>et al.</i> , 2013
Without N	Monoterpenes	2500	menthol, pyrethrins pinene, limonene, etc. (essential oils)	Protection against insects, fungi, bacteria. Attractant to natural enemies of insects. Allelopathy.	-Turlings <i>et al.</i> , 1990, 1995 -Davies <i>et al.</i> , 2007 -Maffei <i>et al.</i> , 2011 -Piesik <i>et al.</i> , 2011

Sesquiterpenes	5000	caryophyllene, farnesene, bergamotene, costunolide, parthenolide, artemisinin, capsidiol, polygodial (essential oils)	Anti-bacterial. Anti-insects, also by means of entomopathogenic nematodes. Allelopathy. Phytoalexins.	-Unsicker <i>et al.</i> , 2009 -Piesik <i>et al.</i> , 2011 -Huang <i>et al.</i> , 2012 -Kollner <i>et al.</i> , 2013
Diterpenes	2500	gossypol, momilactones, oryzalexin, gibberelic acid	Phytoalexin (antifungal and antibacterial).	-Cartwright <i>et al.</i> , 1981 -Akatsuka <i>et al.</i> , 1983 -Peters <i>et al.</i> , 2006 -Williams <i>et al.</i> , 2011 -Singh and Sharma, 2014
Triterpenes	5000	digitonin, saponins (avenacin, tomatine, avenacosids) citronella, brassinosteroids	Antimicrobial properties. Mimic insect hormones, mortality of larvae and adults. Anti-herbivores. Phytoalexins/Phytoanticipins.	-Papadopoulou <i>et al.</i> , 1999 -Mert-Türk, 2006 -Kreis and Müller-Uri, 2010 -Gonzalez-Coloma <i>et al.</i> , 2011
Tetraterpenes	500	carotenes, xanthophylls, strigolactone	Antioxidant, responsible of color in fruits, flowers, leaves (Pollinators and seed dispersants). Interaction with hormones.	-Ramel <i>et al.</i> , 2012 -Torres-Vera <i>et al.</i> , 2014
Flavonoids Tannins Anthocyanins	5000	catechin, lutein, flavones, rutin, kaempferol, narigenin. isoflavonoids, sakuratenin, resveratrol	Flower, fruits and leaf color, antioxidants, UV- protectant. Antimicrobial properties. Allelopathy. Toxic for insects and animals (Tannins). (Symbiosis)	-Snyder <i>et al.</i> , 1990 -Chapple <i>et al.</i> , 1995 -Skadhauge <i>et al.</i> , 1997 -Chang <i>et al.</i> , 2011 -Mierziak <i>et al.</i> , 2014
Phenylpropanoids Lignin Coumarins, Furanocoumarins	2000	lignin, phenolic esters (chlorogenic acid), phenolamides (caffeic acid) medicarpin, scopoletin, psoralen	Structure, protection, desiccation Defenses induced or preformed Antimicrobial. Allelopathy	-Rice-Evans <i>et al.</i> , 1997 -Costet <i>et al.</i> , 2002 -Dixon <i>et al.</i> , 2002 -Chong <i>et al.</i> , 2002 -Razavi, 2011
Fatty acids ,Oxylipins	1500	cutin and waxes, cuticle jasmonic acid	Prevent desiccation Signaling. Barrier against insects and microbes. Antimicrobial	-Blée, 2002 -Farmer <i>et al.</i> , 2003 -Shah <i>et al.</i> , 2005 -Kachroo and Kachroo, 2009 -Pinot and Beisson, 2011
Polyketides	750	anthraquinones (emodin)	Against herbivores	-Kim <i>et al.</i> , 2004 -Godard <i>et al.</i> , 2009
Carbohydrates	200	chitinases, glucanases, lectins	Elicitor activity	-Mauch <i>et al.</i> , 1988 -Aziz <i>et al.</i> , 2003 -Klarzynski <i>et al.</i> , 2003 -Gauthier <i>et al.</i> , 2014

Secondary metabolites can be stored as complex mixtures of inactive products that can be activated in case of “necessity” (Wink, 2011). Some are **constitutive**; others are **induced** after attack. Indeed, they can be synthesized during normal growth and development as preformed antimicrobial compounds (phytoanticipins) or accumulate *de novo* only in response to pathogen attack or stress (phytoalexins) (Papadopoulou *et al.*, 1999). Both concepts have nothing to do with their chemical structure or the implicated chemical pathway, but with the way they are produced as it is described below (Figure 5). Hence, some compounds may be phytoalexins in some species and phytoanticipins in others (Dixon, 2001).

Phytoalexins and phytoanticipins

Phytoalexins are a heterogeneous class of specialized metabolites of low molecular weight that are synthesized *de novo* in response to abiotic or biotic stress. Therefore the synthesis of phytoalexins requires transcriptional/translational changes after pathogen detection and trafficking of substances to the infection site after pathogen infection. It is a process that costs extra energy to the plant (Flors and Nonell, 2006) but still very convenient since carbon and energy sources are redirected into phytoalexin synthesis only at the beginning of infection and only at the local sites, as it will be described later (Grayer and Kokubun, 2001).

The term “Phytoalexin” was coined by Müller and Börger in 1940 and initial definition remains almost the same, except for the fact that instead of assuming *ipso facto* that they are synthesized for plant “disease resistance”, they are now rather defined as synthesized for “plant defense”, because their full mode of action and impact is not always well understood or easy to prove (Paxton, 1981, VanEtten *et al.*, 1994; Gonzalez Lamothe, *et al.*, 2009).

They serve, as many of the typical mechanisms of defense, as a protection for the plant against later situations of stress.

Phytoalexins have several interesting features, which can be summarized as follows:

- 1) They are synthesized very quickly, within hours of microbial attack.
- 2) They are generally restricted to a local area around the site of infection.
- 3) They are usually lipophilic, and therefore can cross membranes efficiently (Guest and Brown, 1997; Grayer and Kokubun, 2001). As methylation enhances its lipophilic properties, methylated phytoalexins are the most fungitoxic (Jeandet *et al.*, 2014).
- 4) Usually its synthesis is accompanied by apoptosis and HR (Dangl *et al.*, 1996; Mazid *et al.*, 2011)

- 5) Phosphorylation, defense related genes, calcium sensors, elicitors, hormone signaling, ROS, sugars (as endogenous signals), and of course the nature of the infecting pathogen are regulators of phytoalexin biosynthesis (Jeandet *et al.*, 2014).
- 6) Their toxicity is non selective, which means that they can be toxic to a broad spectrum of fungi and bacterial pathogens (prokaryotic and eukaryotic).
- 7) They have low specificity (biocide and/or biostatic effects) and are less toxic than many known fungicides. Effective doses are within 10^{-5} to 10^{-4} M (Jeandet *et al.*, 2014).
- 8) They can be detoxified by highly virulent strains (Smith *et al.*; 1996, Van Etten *et al.*, 1989; Pedras *et al.*, 2005).
- 9) They are synthesized from a redirection of primary metabolism precursors, depending on *de novo* expression of genes encoding enzymes involved in biosynthetic pathways.
- 10) They are chemically diverse and some plant families are often associated with specific chemical groups (Figure 5). For example sesquiterpenoids and polyacetylenes with solanaceae; isoflavonoids with leguminosae; sulfur-containing indoles with Cruciferae. Cereals rather produce cyclic hydroxamic acids and diterpenes, (Grayer and Kokubun, 2001; Pedra *et al.*, 2005; Mazid *et al.*, 2011; Jeandet *et al.*, 2014).
- 11) The three most characteristic pathways for phytoalexin biosynthesis are: phenylpropanoic pathway, the terpenoid pathway, the indole phytoalexin pathway (Jeandet *et al.*, 2014)
- 12) They can hinder different aspects of the host-pathogen interaction:
 - a) Propagules, causing loss of motility and deformation of hyphae, germ tubes, conidia, etc.
 - b) Cellular response, by alterations in cell shape, causing cytoplasmic granulation and leaking, membrane burst and disintegration (probably by tubulin polymerization).
 - c) Physiology, by affecting sugar intake, respiration (by disturbing electron transport and by phosphorylation events) (Jeandet *et al.*, 2014).

Phytoanticipins (VanEtten *et al.*, 1994) are low molecular weight compounds present in plants that have antimicrobial effects. Unlike phytoalexins this compounds are either pre-existent to the pathogen attack, or rapidly formed from a pre-existent compound upon attack (release from an aglycone or from a conjugate). Some of them are found at the plant surface, some others are stored in vacuoles or organelles and are activated after the plant is challenged by a pathogen attack triggering defense responses. Saponins are among the most ubiquitous phytoanticipins. Two well-studied examples are avenacin A-1 (from Oat) and tomatine (from Tomato) (Mert-Türk, 2006).

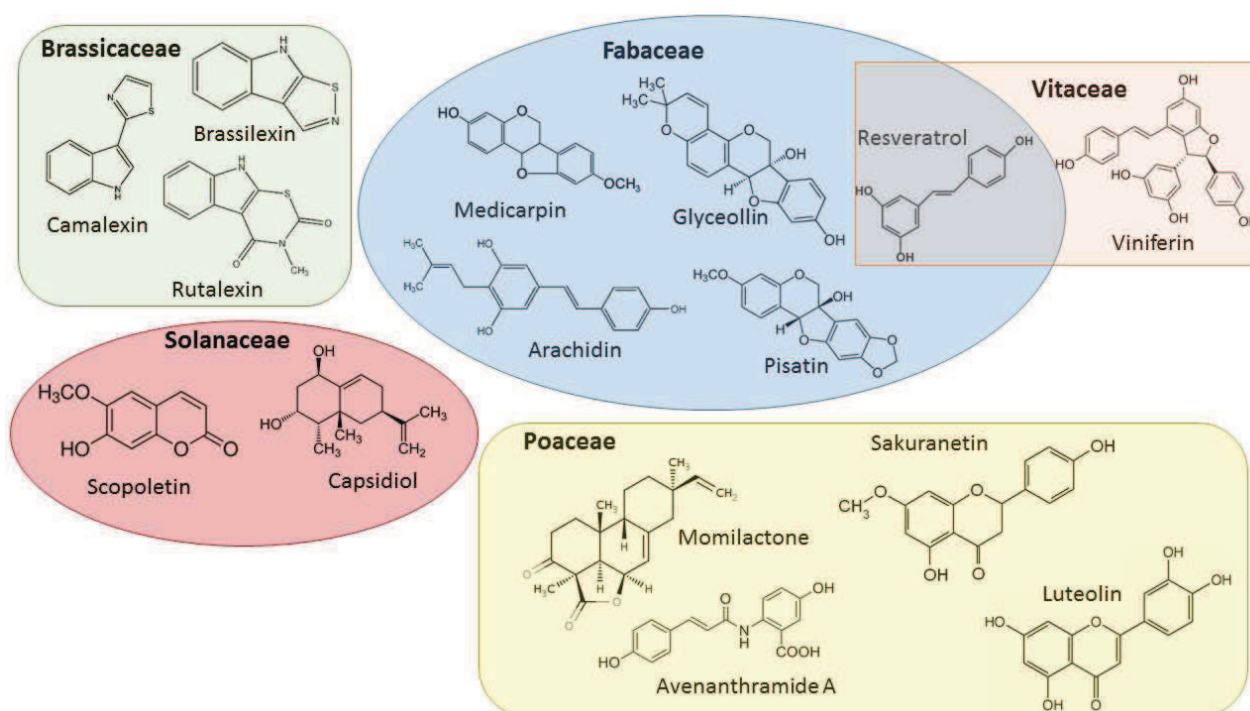
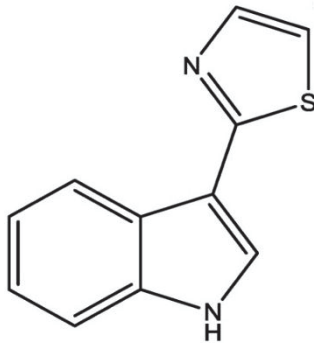


Figure 5: Phytoalexins from different plant families exemplifying structure diversity. Based in Ahuja *et al.*, 2012.

Camalexin, the main phytoalexin from *Arabidopsis*



Camalexin (3-thiazol-2'-yl-indole) is the main phytoalexin of *Arabidopsis* and some other crucifers (Glawischnig, 2007).

It can be accumulated in the infected tissues as a defense response that limits the growth of a wide range of pathogens both biotrophs and necrotrophs (Ferrari *et al.*, 2003; Glawischnig *et al.*, 2007), but can also be induced by microbe associated molecular patterns (MAMPs) and abiotic stresses (Mert-Türk *et al.*, 2003; Glawischnig *et al.*, 2004; Kishimoto *et al.*, 2006; Denoux *et al.*, 2008; Schuegger *et al.*, 2006; Böttcher *et al.*, 2009)

Camalexin acts as a part of the plant defense when pathogen triggered immunity (PTI) or effector triggered immunity (ETI) fail, *in extenso* genotypes with functional R genes has been demonstrated to accumulate less camalexin (Mert-Türk *et al.*, 2003; Narusaka *et al.*, 2004; Persson *et al.*, 2009).

In connection to abiotic stress, it has been shown that wounding *per se* cannot induce camalexin accumulation, but instead can prime the plant for a successful accumulation of the phytoalexin after being challenged with a pathogen like *Botrytis cinerea* (Kishimoto *et al.*, 2006; Chassot *et al.*, 2008).

Other inducing stimuli have been described in the literature, for example cell wall fragments, oligogalacturonides (OGs), chitosan and flagellin (flg22), which in most of cases induced the expression of camalexin biosynthetic genes, but with no obvious camalexin accumulation (Ahuja *et al.*, 2012; Ferrari *et al.*, 2013) (there are some exceptions for flg22, shown in Table 3).

A more detailed list of pathogens and elicitors triggering camalexin biosynthesis in *Arabidopsis thaliana* can be found in Table 3.

Camalexin accumulation is essentially confined to the infection site (as is expected for a phytoalexin) and this spatial distribution is associated with a strong induction of biosynthetic genes in the infection zone (Kliebenstein *et al.*, 2005; Schuegger *et al.*, 2007).

Usually camalexin accumulation is concomitant to lesion formation, however the review of Glawischnig *et al.*, (2007) mentions the work of Raacke *et al.*, (2006) in which camalexin was found in leaves challenged with an autoclaved suspension of yeast without lesion formation. Ahuja *et al.*, (2012) also quoted this example and adds the examples of fusaric acid and victorin, both fungal toxins, capable of inducing camalexin accumulation with no lesion formation.

All *Arabidopsis* accessions and ecotypes were shown to accumulate camalexin, and the observed variations in the rate of accumulation and final concentration were more related to the class of stimuli or pathogen (even strain) than to the genotype (Glawischnig *et al.*, 2007; Ahuja *et al.*, 2012).

In *Arabidopsis thaliana*, camalexin is involved in defense against *Botrytis cinerea* and *Alternaria brassicicola* (Kagan and Hammerschmidt, 2002; Denby *et al.*, 2004; Kliebenstein *et al.*, 2005; Schuhegger *et al.*, 2007), but avoidance (via ABC transporters) or active degradation was also reported for resistant fungal strains (Pedras *et al.*, 2002; 2011).

Camalexin usually accumulates in leaves, but it has also been found in root exudates (Bednarek *et al.*, 2005; Glawischnig *et al.*, 2007; Millet *et al.*, 2010).

Camalexin has all the properties of a typical phytoalexin, however, since its first isolation and description in 1991 (Browne *et al.*, 1991), it is also gaining growing attention due to its health promoting attributes such as a moderate antifungal and bacteriostatic effects, as well as its antiproliferative and cancer chemopreventive properties (Mezencev *et al.*, 2003; 2009; Smith *et al.*, 2013; 2014).

Camalexin was, for example, shown to have cytostatic and cytotoxic effects against *Trypanosoma cruzi* (Mezencev *et al.*, 2009), T-leukemia cells (Mezencev *et al.*, 2003; 2011), prostate cancer cells (Smith *et al.*, 2013; 2014) and human breast cell line in mammary tumors (Moody *et al.*, 1997) due to oxidative stress, which causes apoptosis through ROS generation.

Table 3: List of factors triggering camalexin biosynthesis in *Arabidopsis thaliana*.

		Pathogen/ elicitor	Comments	References
PATHOGEN S	BIOTROPH	<i>Blumeria graminis</i>	Non –adapted pathogen	Bednarek <i>et al.</i> , 2009
		<i>Erysiphe pisi</i>	Non –adapted pathogen	Bednarek <i>et al.</i> , 2009
		<i>Golovinomyces orontii</i>		Pandey <i>et al.</i> , 2010 Schön <i>et al.</i> , 2013
		<i>Hyaloperonospora parasitica</i>		Mert-Turk <i>et al.</i> , 2003
		<i>Puccinia triticinia</i>		Shafiei <i>et al.</i> , 2007
	HEMIBIOTROPH	<i>Colletotrichum higginsianum</i>		Narusaka <i>et al.</i> , 2009
		<i>Leptosphaeria maculans</i>		Staal <i>et al.</i> , 2006 Bohman <i>et al.</i> , 2004
		<i>Phytophthora brassicaceae/infestans</i>		Roetschi <i>et al.</i> , 2001 Qtuob <i>et al.</i> , 2006 Schlaeppli <i>et al.</i> , 2010
		<i>Pseudomonas syringae</i> pv. <i>tomato</i>		Hagemeyer <i>et al.</i> , 2001 Glazebrook <i>et al.</i> , 2005 Schuhegger <i>et al.</i> , 2007 Simon <i>et al.</i> , 2010
		<i>Pseudomonas syringae</i> pv. <i>maculicola</i>		Rogers <i>et al.</i> , 1996
	NECROTROPH	<i>Alternaria brassicicola</i>		Thomma <i>et al.</i> , 1999 Kagan and Hammerschmidt., 2002 Sellam <i>et al.</i> , 2007
		<i>Botrytis cinerea</i>		Ferrari <i>et al.</i> , 2003 Glawischnig <i>et al.</i> , 2004 Kliebenstein <i>et al.</i> , 2005 Schuhegger <i>et al.</i> , 2006 Böttcher <i>et al.</i> , 2009 Rowe <i>et al.</i> , 2010
		<i>Cochliobolus carbonum</i>		Kagan and Hammerschmidt., 2002
		<i>Plectosphaerella cucumerina</i>		Sanchez-Vallet <i>et al.</i> , 2010
		<i>Pythium sylvaticum</i> <i>Pythium</i> spp.	Root exudates	Bednarek <i>et al.</i> , 2005 Qtuob <i>et al.</i> , 2006
		<i>Sclerotinia sclerotiorum</i>		Stotz <i>et al.</i> , 2011
		VIRUS	viruses	
	ELICITORS	flagellin	Root exudates	Millet <i>et al.</i> , 2010 Schenke <i>et al.</i> , 2011
		UV radiation		Zao <i>et al.</i> , 1998 Mert-Turk <i>et al.</i> , 2003
AgNO ₃ , ions, (heavy metals)			Zao <i>et al.</i> , 1998 Glawischnig <i>et al.</i> , 2004 Böttcher <i>et al.</i> , 2009, 2014	
lipopolysaccharides			Beets <i>et al.</i> , 2012Z	
peptidoglycans			Gust <i>et al.</i> , 2007	
Victorin and Fusaric acid			Bouizgarne <i>et al.</i> , 2006	
dead yeast			Raacke <i>et al.</i> , 2006	
Chemicals: paraquat, acifluorfen , etc.			Zao <i>et al.</i> , 1998 Denby <i>et al.</i> , 2004	
volatiles (C6)		(some relation to wounding)	Kishimoto <i>et al.</i> , 2006	
wounding		(priming on <i>Botrytis</i>)	Chassot <i>et al.</i> , 2008	

The camalexin pathway: work in progress

Camalexin induction is a complex process, triggered by reactive oxygen species (ROS), partially overlapping salicylic acid (SA) and jasmonate (JA) signaling, and the glutathione status among other factors (Kliebenstein, 2004; Persson *et al.*, 2009). The biosynthetic genes involved also seems to be strongly up-regulated at the site of pathogen infection (Schuhegger *et al.*, 2007; Kliebenstein *et al.*, 2005; Glawischnig *et al.*, 2004).

In order to develop different disease protection strategies for crop development and medical applications, research has been focused on the understanding of the biosynthesis and regulation of camalexin pathway. However there is still some debate about the formation of the heterocycle and the origin of the thiazol ring which are going to be discussed later in this section.

Camalexin biosynthesis requires the activity of a number of enzymes that must be under targeted and coordinated transcriptional activation. Its biosynthesis starts from tryptophan (trp) and involves several cytochrome P450 enzymes such as *CYP79B2/CYP79B3*, *CYP71A13/CYP71A12* and *CYP71B15* (PAD3). Its location is most probably cytosolic as these P450s are located in the ER with their catalytic domain facing the cytosol (Møldrup *et al.*, 2013).

The biosynthetic pathway is represented in Figure 6 :

1- It starts with a trp, which is the donor for the indolic ring. Trp is synthesized via chorismate, and the intermediates anthranilate and indole, are the “ring” precursors (Glawischnig *et al.*, 2007).

2-The trp is converted into indole-3-acetaldoxime (IAOx) by the action of the two close paralogues *CYP79B2/CYP79B3* (Hull *et al.*, 2000; Mikkelsen *et al.*, 2000; Glawischnig *et al.*, 2004). This is an important branching point because trp can also lead to the biosynthesis of indolic compounds such as auxins (indole-3-acetic acid, IAA) and indole glucosinolates (Glawischnig, 2006; Bak *et al.*, 2001; Dixon, 2001).

3- IAOx is converted to indole-3-acetonitrile (IAN) by a non-oxidative dehydration catalyzed by the paralogues *CYP71A13/CYP71A12* (Nafisi *et al.*, 2007). An interesting feature of this two paralogues is that *in vitro* they can also convert IAOx to cys-IAN (see the plant pathway below), *CYP71A13* being more efficient than *CYP71A12* (Klein *et al.*, 2013). This finding leads to the conclusion that the *in vitro* reconstitution of the camalexin biosynthetic pathway only requires the three P450 enzymes: *CYP79B2/B3*, *CYP71A13*, *CYP71B15*, plus trp and cys, and NADPH as it was recently shown in the publication of Klein *et al.*, (2013).

4- IAN is conjugated with glutathione by the combined action of a glutathione-S-transferase (GSTF6) (Böttcher *et al.*, 2009; Su *et al.*, 2011) and probably a still unidentified P450 enzyme (Jeandet *et al.*, 2014 may be quoting Klein *et al.*, 2013), which results in an IAN glutathionyl derivative (GSH(IAN)).

5- The GSH(IAN) is then converted into two intermediates:

- IAN cysteinyl-glycine ((IAN)CysGly) via a phytochelatin synthase (PCS1) (Blum *et al.*, 2007; Böttcher *et al.*, 2009; Su *et al.*, 2011) or a carboxypeptidase (Møldrup *et al.*, 2013).

- γ -glutamyl-cysteine IAN (γ -GluCys(IAN)) through the hypothetic action of two γ -glutamyltranspeptidases called 1 and 3 (GGT1 and GGT3) (Su *et al.*, 2011) or a γ -glutamylpeptidases (GGP1/GGP3) (Geu-Flores *et al.*, 2011; Møldrup *et al.*, 2013).

Both intermediates lead to the IAN cysteine conjugate (Cys (IAN)).

There is a lot of debate going on around this step. Some authors are in support of the idea that the heterocycle comes from glutathione (Böttcher *et al.*, 2009, Geu-Flores *et al.*, 2011; Su *et al.*, 2011), while some others propose that it come from the cys (Ahuja *et al.*, 2012; Jeandet *et al.*, 2014). There is also debate around the GGT and GGP enzymes, and lack of evidence to support the role of a PCS1 or a carboxypeptidase as clearly outlined in the letter to editor of Plant Cell journal by Møldrup *et al.*, (2013) and the reply of Su *et al.*, (2013).

6- The last steps are under the control of the *CYP71B15* (*PHYTOALEXIN DEFICIENT 3*, *PAD 3*) gene encoding a multifunctional enzyme that catalyzes an oxidative decarboxylation and heterocyclization to form camalexin via dihydrocamalexin acid (DHCA) (Glazebrook and Ausubel, 1994; Zhou *et al.*, 1999; Schuhegger *et al.*, 2006). This was the first step characterized by a genetic approach.

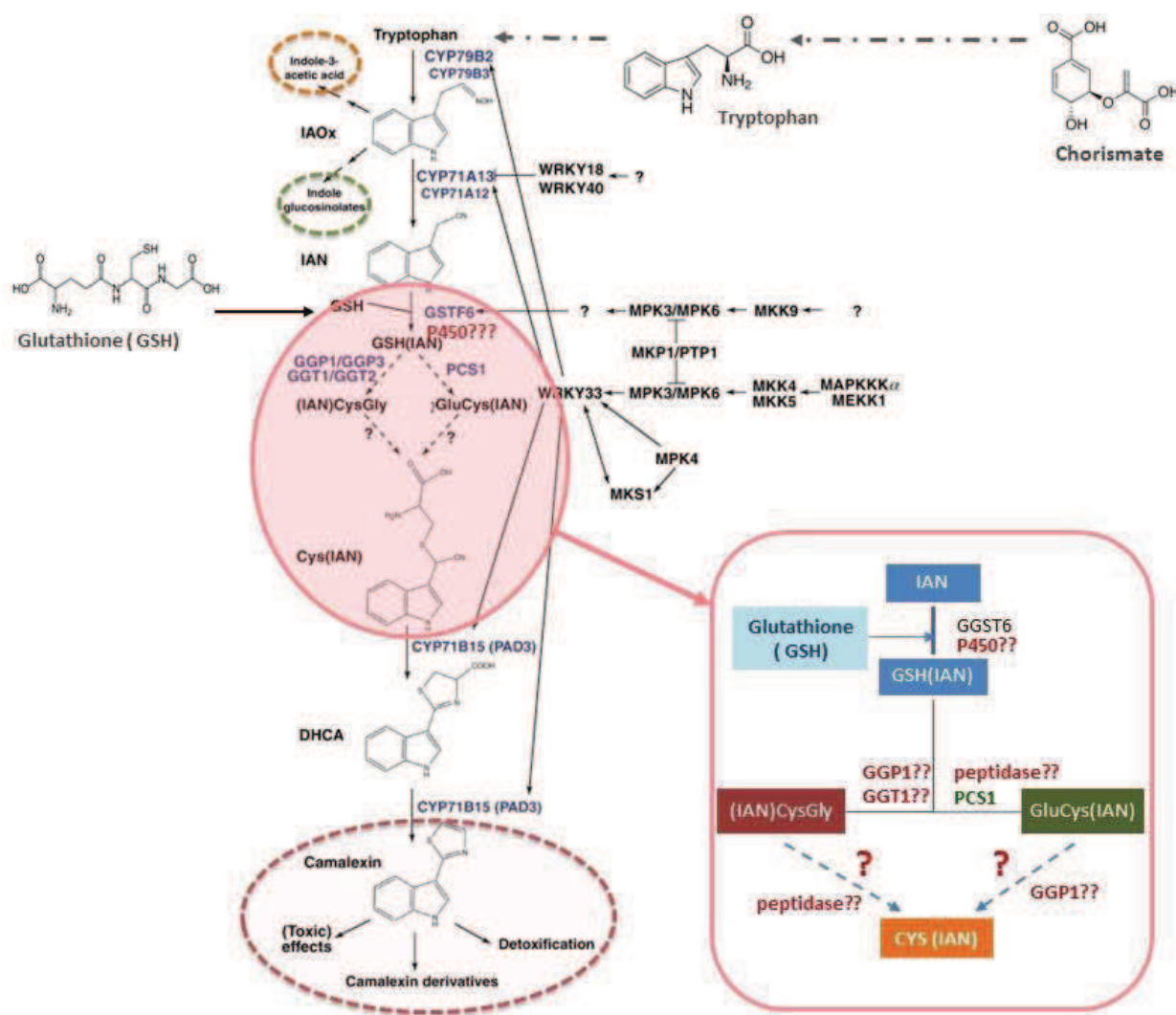


Figure 6: The puzzling biosynthetic pathway of camalexin.

In the figure, the first colored circles indicate the branching step from IAOx to **indole-3-acetic acid (auxins)** and **indoleglucosinolates**. At the **pink-magenta circle** in the center is highlighted in detail the conjugation of glutathione to the indolic ring and the generation of the thiazole ring and heterocyclation. Framed on the right side of the figure, is the hypothetical pathway to the cys-IAN end product. Some conjectural regulation steps by MAMPKs and WRKY transcription factors are displayed. **Abbreviations:** **IAOx:** indole-3-acetaldoxime; **IAN:** indole-3-acetonitrile, **GSH:** glutathione, **GSTF6:** glutathione-S-transferase, **GSH(IAN):** IAN glutathionyl derivative, **(IAN)CysGly :** IAN cysteinyl-glycine, **γ -GluCys(IAN) :** γ -glutamyl-cysteine IAN, **PCS1 :** phytochelatin synthase, **GGT1 /GGT3 :** γ -glutamyltranspeptidases 1 and 3., **GGP1/GGP3:** γ -glutamylpeptidases , **Cys(IAN):** IAN cysteine conjugate, **PAD3:** CYP71B15 PHYTOALEXIN DEFICIENT 3, **DHCA:** dihydrocamalexic acid. Modified from Ahuja *et al.*, 2012, improved with elements from Møldrup *et al.*, 2013 and Jeandet *et al.*, 2014.

Some words about the regulation of camalexin biosynthesis

As it was stated before, camalexin accumulation relies on the type of interaction. Each interaction (biotic or abiotic), especially each pathosystem, pathogen lifestyle and the resulting cascade of events, triggers the accumulation of camalexin in a specific way (Table 3).

Several studies have been published, describing regulation by JA, SA, ROS, MAPKs cascades, WRKYs among others.

For example, in the *A. thaliana-Alternaria brassicicola* interaction, camalexin accumulation was reported to be independent from JA (Thomma *et al.*, 1999; Sellam *et al.*, 2007), while in the interaction *A. thaliana-Botrytis cinerea*, it was reported to be JA-dependent (Rowe *et al.*, 2010).

In the biotrophic interaction *A. thaliana- Pseudomonas syringae*, camalexin biosynthesis, it was shown to be less important (Glazebrook and Ausubel, 1994; Glazebrook *et al.*, 2005), but for the *Pseudomonas syringae* pv *maculicola* strain ES4326, it was shown to be toxic because of cell membrane disruption and cell death (Rogers *et al.*, 1996). The work of Rogers *et al.*, (1996) also pointed out that camalexin toxicity is more important to fight sensitive fungi than gram negative bacteria.

Some others studies have also mentioned the regulation of camalexin biosynthesis in a SA-dependent or SA-independent manner (Ahuja *et al.*, 2012). Ethylene (ET) generally appears to positively regulate camalexin biosynthesis, whereas auxins and abscisic acid (ABA) have a negative effect. In response to the complex hormonal cross talk, the rewiring of the metabolic flow from **trp-->IAA** to **trp-->camalexin/glucosinolates**, helps the plant to give an accurate response to the biotroph pathogen, based on SA signaling instead of the antagonizing auxin hormone (Pieterse *et al.*, 2012).

MAMPK cascades, WRKY transcription factors (Figure 6) and ROS were described as activators of camalexin biosynthesis (Ahuja *et al.*, 2012).

Specialized metabolism and biotechnological development: application and outlook

Last decade the field has gained growing appreciation for biotechnological development in crop protection, human health and industry. Not only for the potential of the huge number of natural products that exist, but also for the high popularity and public acceptance they have (Gonzalez Lamothe *et al.*, 2009; Krings and Berger, 2010).

Secondary metabolites offer a significant potential for plant breeding and metabolic engineering of environmental friendly products in a context of highly increasing socio-economic demand.

Several compounds have proven to be suitable not only with industrial purposes but also as a treatment for various types of human diseases and disorders, from cancer and HIV to heart diseases and nosocomial and community-acquired infections with multidrug resistance (Gonzalez Lamothe *et al.*, 2009; Mierziak *et al.*, 2014; Singh and Sharma, 2014).

In crop research, such properties can be used for enhancing pest resistance or mechanical properties of crop plants (Clay *et al.*, 2009; D'Auria and Gershenzon, 2005). Relevant compounds can be produced by the crop plant or sprayed as biopesticides. Plant health and disease resistance represent major economic and societal issues and for that reason many efforts are invested for their improvement.

A major challenge for the agro-research of the next decades is to develop novel strategies to decrease the impact of pesticide treatments and to increase food production and quality (Wink, 1988; Du Fall and Solomon, 2011; FAO 2009; 2012). Ideal strategies are to exploit built-in defense and adaptation systems, but this means understanding them. However, in-plant activity and impact of these compounds have often been difficult to assess properly. Enhancing their production usually means yield reduction (due to the energy cost). Moreover, large segments of the plant defense metabolism have so far evaded characterization and, despite growing interest, only a fraction of the defense signals, antimicrobials and antioxidants have been described (Grayer and Kokubun, 2001; Du Fall and Solomon, 2011).

In order to maximize the benefits of plant specialized metabolites, it is a priority to understand in depth the way they are synthesized, the regulation mechanism, networks and cross-talks, the underlying phylogeny of genes, enzymes and different plant species, as well as the ecological roles they play.

Terpenoids

Terpenoids, also called isoprenoids, constitute the largest and most diverse class of organic compounds present in plants (but also in microorganism and animals). Generally non polar and often volatile, they usually do not contain nitrogen or sulfur in their molecule (Ashour *et al.*, 2010; Dewick, 2002).

The common building block of isoprenoids consists of units of isoprene, derived from isopentenyl diphosphate (IPP) and/or dimethyl allyl diphosphate (DMAPP). Isoprene units are assembled and modified in many different ways, but every time based on the skeleton of isopentane, usually joined head to tail (Hemmerlin *et al.*, 2012). Pyrethrins are the sole exception to the rule in *Asteracea* family (Ashour *et al.*, 2010; Hemmerlin *et al.*, 2012).

Many structural arrangements are present, forming different carbon skeletons, multicyclic structures, and decorated with a vast diversity of possible functional groups (Dewick, 2002, Ashour *et al.*, 2010) (Figure 7).

Terpenes are synthesized via two main pathways: the cytosolic mevalonate pathway (MVA) and the plastidial (and mevalonate-independent pathway) the methyl erythritol pathway (MEP).

They may be classified according to the number of isopentenyl units as:

- Monoterpenes (10-carbons terpenoids, 2 isoprenoid units) are best known as components of the volatile essences of flowers and as part of the essential oils of herbs and spices. They are part of up to 5% by weight of the dried plant. Examples are: menthol, geraniol, limonene, terpineol, myrcene, pulegone, among others.
- Sesquiterpenoids (15-carbons terpenoids, 3 isoprenoid units) can still be volatile when produced as olefins, but when further processed have important roles as phytoalexins, antibiotic compounds and as feeding inhibitors ("antifeedant") produced by plants in response to the emergence of microbes and opportunistic herbivores. Examples are: artemisinin, nootkatone, bisaborol, humulene, farnesene, polygodial.
- Diterpenoids (20-carbons terpenoids, 4 isoprenoid units) include phytol, which is the hydrophobic side of chlorophyll, gibberellin hormones, acids in conifer resins and vegetable species, phytoalexins, dehydroabietinal (important SAR metabolite) and a number of pharmacologically important metabolites, including taxol (paclitaxel), a widely used anticancer agent.

- Triterpenoids (30-carbons terpenoids, six isoprenoids units) are usually generated by head-head union of two chains of 15 carbons, each consisting of isoprene units joined head to tail. This large class of molecules includes for example brassinosteroids, phytosterols and many phytoalexins, toxins and feeding deterrents, components of surface waxes of plants. Examples are: cardiac glycosides, saponins, lupeol, oléanolic acid, lanosterol and squalene.
- Tetraterpenoids (40-carbons terpenoids, 8 isoprenoids units) include examples such as lycopene and α , β , γ -carotenes. (rubber > C40)

As mentioned above, terpenoids play roles in both primary and secondary metabolism. Their structural variety is reflected in their very diverse roles in plant growth, development, reproduction and defense.

Some terpenoids, such as phytosterols, are membrane components. Some others such as carotenoids, are photoprotective pigments. They also contribute to chlorophyll biosynthesis (C20 side-chain). Most plant hormones are isoprenoids: gibberellin, brassinosteroids, strigolactones and abscisic acid. They are also precursors of steroids and sterols too. Prenylation in addition plays a role in enhancing protein fixation to cell membranes or avoiding it (Miller *et al.*, 2011). Some important compounds such as cytokinins, and the quinone-based electron carriers (the plastoquinones and ubiquinones), have terpenoid side chains attached to a non-terpenoid nucleus (Ashour *et al.*, 2010; Tholl and Lee, 2011).

Most terpenoids however serve as allelochemicals. Some of them mediate defense against microbes, or herbivorous insects and mammals through their roles as toxins or feeding/oviposition deterrents (Wittstock and Gershenzon, 2002; Unsicker *et al.*, 2009; Vourc'h *et al.*, 2002). Volatile compounds are also signal molecules attracting pollinator insects (Pichersky and Gershenzon, 2002), fruit and seed-dispersing animals (Lomáscolo *et al.*, 2010; Rodríguez *et al.*, 2014) or predators which can destroy insect herbivores (Turlings *et al.*, 1993, Arimura *et al.*, 2004; Mithofer *et al.*, 2005; Schnee *et al.*, 2006). Some can act as inhibitors of germination and growth of neighboring plants (Nishida *et al.*, 2005). In some cases their phytoalexin-activity could be proved. It is for example the case for monilactones and oryzalexins in the interaction *Oryza sativa* - *Magnaporthe grisea* (Peters *et al.*, 2006, Hasegawa *et al.*, 2010).

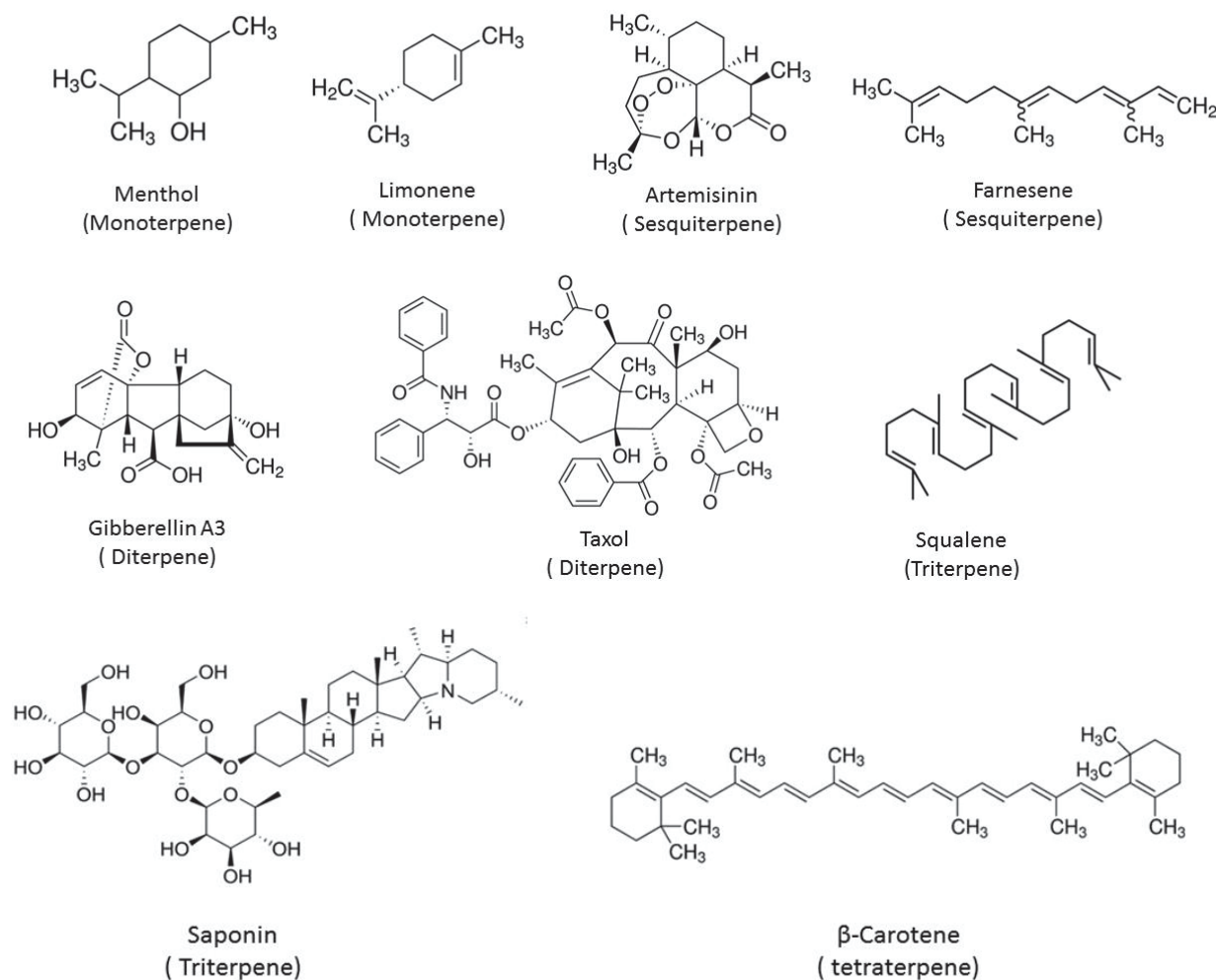


Figure 7: Some examples of terpenoid classes and diversity.

Chemical structure of the monoterpenes (C₁₀) menthol and limonene, the sesquiterpenoids (C₁₅) artemisinin and farnesene, the diterpenes (C₂₀) Gibberellin A3 and Taxol® (paclitaxel), the triterpenes squalene and saponin (a phytoanticipin) and the tetraterpene β -carotene.

As a consequence of their countless ecological roles, many terpenoids have prominent pharmacological activities and are therefore interesting for medicine and biotechnology (Ashour *et al.*, 2010; Singh and Sharma, 2014). For instance, monoterpenes and sesquiterpenes are flavor and fragrance agents that are used in food/beverages industry and perfumery (Krings and Berger, 2010; Caputti and Aprea, 2011). Lower terpenes also constitute tackifiers and emulsifiers, and are also intended for biofuels development (Bohlmann and Keeling, 2008). In pest protection, essential oils and pyrethrins are of increasing commercial importance as bio-insecticides and repellent because of their low toxicity to mammals and its lack of residual effect on environment (Tripathi *et al.*, 2009).

Some more complex terpenoids are currently used or essayed in clinical trials as treatment for different types of cancer, skin problems, anti-inflammatory, anti-glycemic, antiviral and antiparasitic effects. Taxol (antiproliferative) and artemisinin (antimalarial) constitute outstanding examples of terpenoids potential in medical advances and treatments (Martin *et al.*, 2003; Croteau *et al.*, 2006).

Terpenoids biosynthesis

Plants synthesize isopentenyl diphosphate (IPP) and its allylic isomer dimethyl allyl diphosphate (DMAPP), by one of two routes: the mevalonic acid pathway (MAV) or the methylerythritol phosphate (MEP) pathway.

The MAV pathway occurs in prokaryotes and eukaryotes and operates mainly in the endoplasmic reticulum, cytosol and mitochondria. Precursors for sterols, sesquiterpenes, triterpenes, brassinosteroids and ubiquinones are synthesized through this pathway (Figures 8 and 9).

Briefly, the pathway starts with the condensation of 3 molecules of acetyl-CoA to form a C₆ compound, the 3-hydroxy-3-methylglutaryl-CoA (HMG-CoA) (See Figure 8 and 9) that is converted to mevalonate. This step is crucial for triterpene (*i.e.* sterols) synthesis and irreversible too. Subsequently, mevalonate is phosphorylated into isopentenyl diphosphate (IPP), the “isoprenoid” building block.

The non-mevalonic acid pathway (MEP pathway) (Lichtenthaler, 2000) takes place and IPP and DMAPP are synthesized in the plastids (therefore this pathway is absent in archae, animal and fungi). This pathway forms the C₅ precursor for hemi-, mono-, sesqui-, and diterpenes, along with carotenoids (tetraterpenes), chlorophyll (phytyl tail of chlorophyll to be more precise) and gibberellins.

The pathway starts with a key regulatory step for isoprenoids/terpenoids biosynthesis, the condensation of a molecule of pyruvate and a molecule of glyceraldehyde-3-phosphate (GAP) into 1-deoxy-D-xylulose 5-phosphate (DXS). After several steps (see Figure 8 and 9 for more details), the IPP and DMAPP building blocks are produced at a ratio 5:1 (Tholl and Lee, 2011) and subsequently IPP is isomerized to DAMMP by a IPP isomerase for condensation and synthesis of higher terpenoids.

At this point, IPP and DAMMP precursors are ready, and condensations “head to tail” starts producing the linear precursors of isoprenoids for higher terpenoids biosynthesis.

The synthesis of monoterpenes is initiated by dephosphorylation and ionization of geranyl diphosphate (GPP). The synthesis of sesquiterpenes starts with the ionization of farnesyl diphosphate (FPP). FPP has a central role in the synthesis of sesquiterpenoids, triterpenoids and tetraterpenoids (sterols, brassinosteroids, ubiquinones), and in addition is needed for protein prenylation too. The

acyclic skeletons of C₅ to C₂₀ are further converted into different classes of terpenes by terpene synthases (TPS) and modified into a wide arrange of structures in subsequent reactions that give rise to the terpenoid structural and functional diversity observed.

Diterpenes are synthesized by diterpene synthases in two different pathways: 1) via the ionization of diphosphate, as catalyzed by class I enzymes, and 2) via the substrate protonation at the 14,15-double bond of *trans*-geranyl geranyl diphosphate (GGPP) catalyzed by class II enzymes. Thus GGPP is a key component in the pathway to chlorophyll, carotenoids, tocopherol, ABA, strigolactones, plastoquinones, diterpenes and polyterpenes in general. Finally, tri- and tetraterpenoids precursors will be formed by dimerization of FPP and GGPP in a head to head manner.

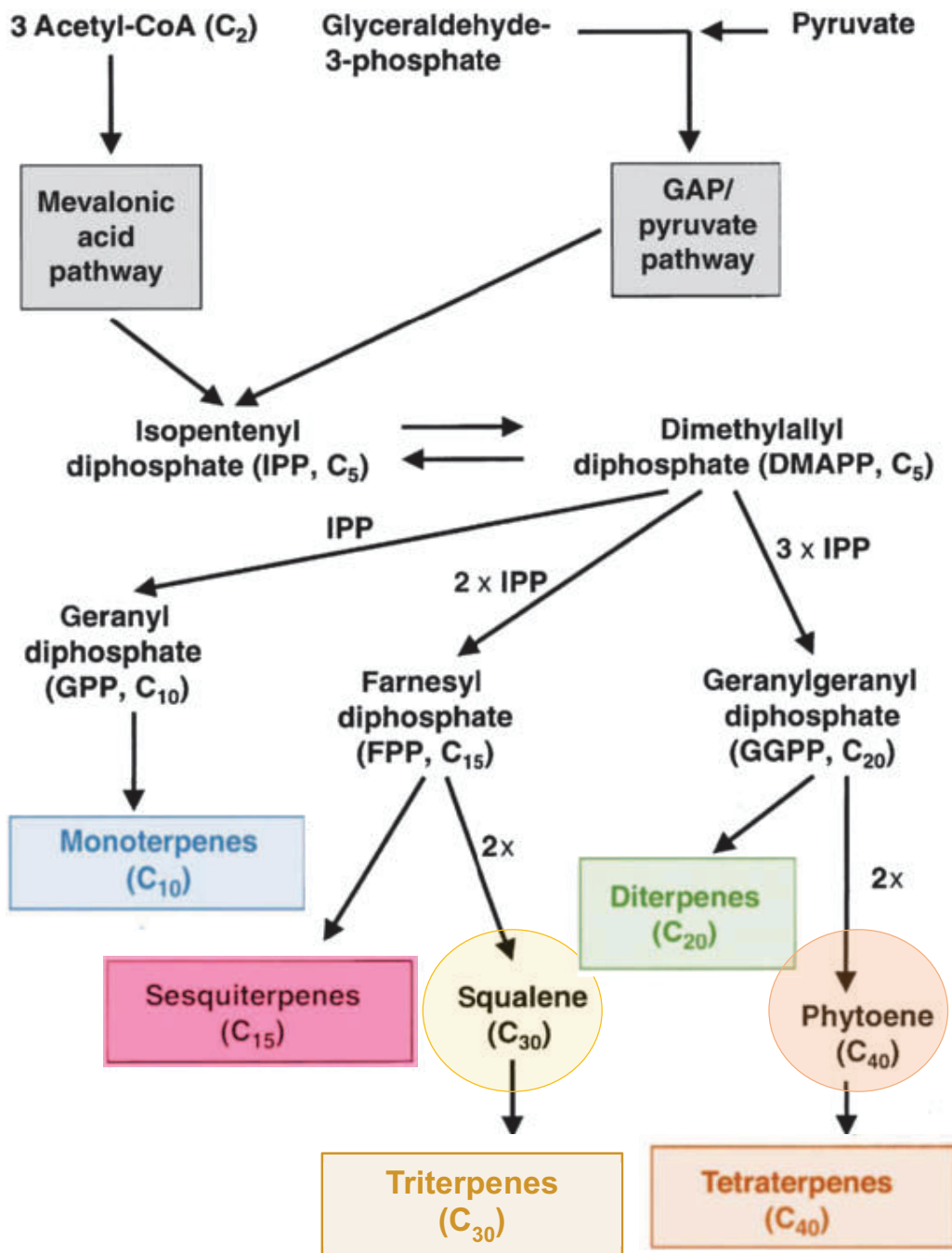


Figure 8: Schematic and summarized representation of terpene biosynthesis and classes.

Modified from Ashour *et al.*, 2010.

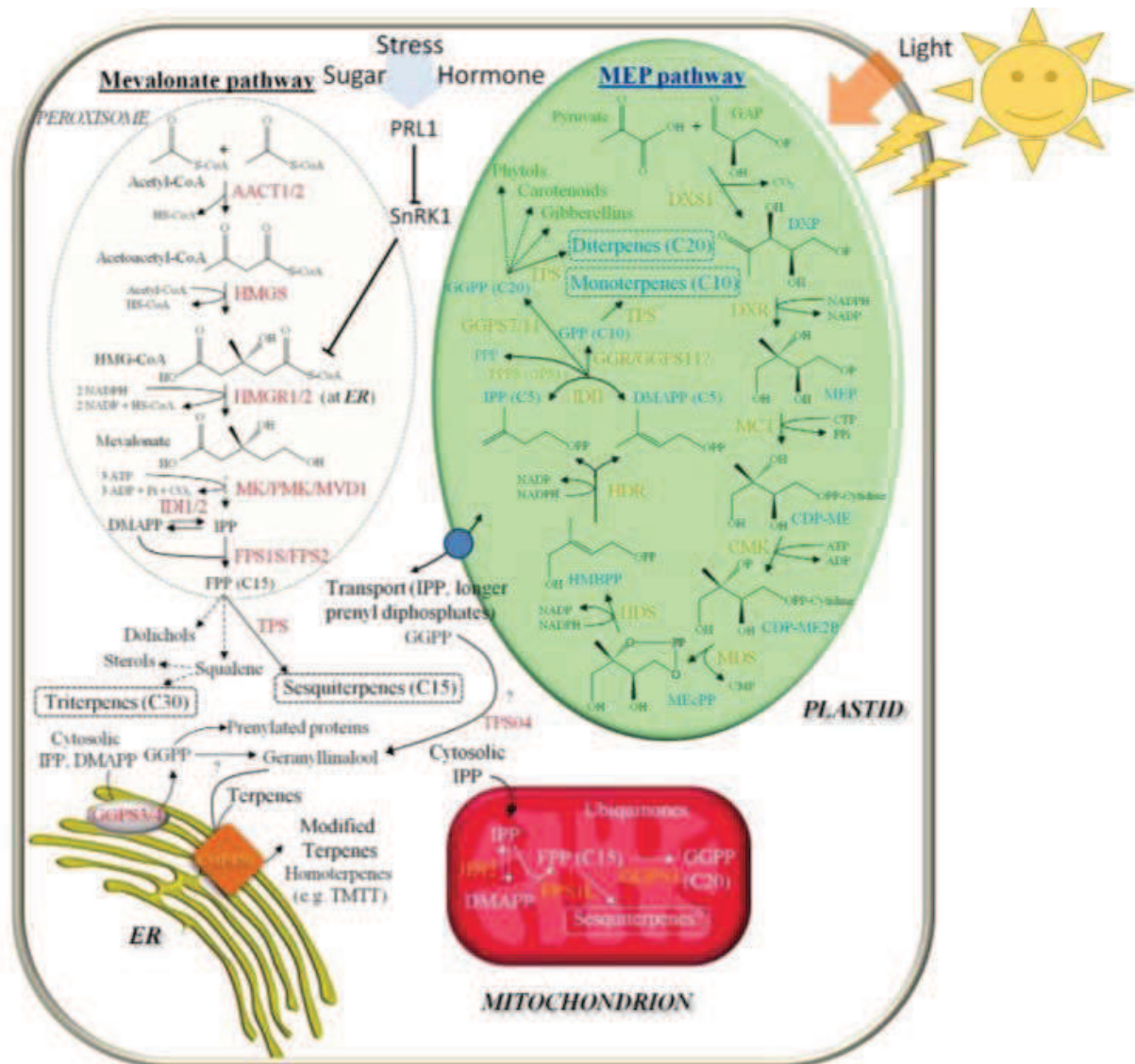


Figure 9: Terpene biosynthesis. MAV and MEP pathways and their subcellular localization.

A detailed description can be read in the text. Enzymes are depicted in different colors according to their subcellular localization: **red** (cytosol/peroxisome), **orange** (chloroplast), **yellow** (mitochondria).

Figure from Tholl and Lee, 2011.

Defense strategies in plants

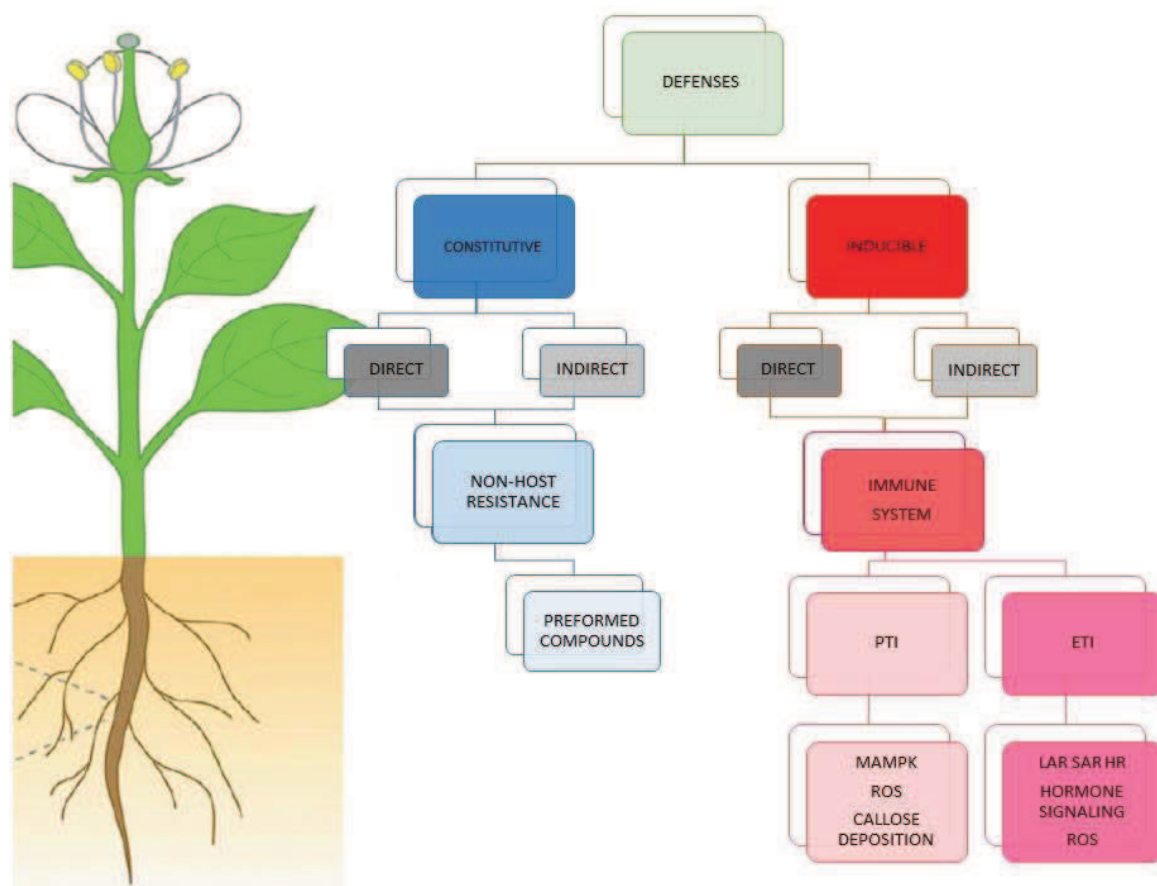


Figure 10: Schematic representation of plant defenses.

Defenses can be **Constitutive** or **Inducible**, direct and indirect (Figure 10).

Constitutive defenses comprise the preformed barriers: cell walls, waxy epidermal cuticles, bark, trichomes, idioblast, pigmented cells, crystalliferous and silica cells, as well as preformed antimicrobial compounds; chemical constituents, already present in the plant. They are available all the time and do not demand an extra quote of energy to be synthetized. These defenses constitute the first contact and first line of defense against biotic and abiotic factors.

On the other hand, **Inducible** defenses, constitute an active process in which the host recognize a pathogen/pest and acts in consequence. It implies the “active” production of chemicals (secondary metabolites), pathogen degrading enzymes, and cell death (HR). This costs a lot of energy to the plant and will vary according to the pathogen/pest implicated. Recognition is the key step.

At the same time, these defenses could be divided into **Direct responses**, (the plant itself acts on the pathogen/pest), or **Indirect responses** by means of an intermediary (the classical example of the natural enemies of pest).

The Plant Immune System

Plants lack an adaptive immune systems as we know for animals, but instead they have a remarkable capacity to recognize pathogens and to respond accordingly in a cell–autonomous way (Dodds and Rathjen, 2010). Each cell is not only capable of responding to a given pathogen locally but it is capable of sending a systemic alert to the rest of the cells. As a consequence of this recognition spectrum, most plants are resistant to most microbes and disease is more an exception than a rule (Zipfel, 2008).

In addition to preformed physical and chemical barriers in plants, there are two branches of immune responses, at membrane and intracellular level respectively (Bent and Mackey, 2007; Jones and Dangl, 2006; Dodds and Rahjten, 2010)

1- Pathogen-triggered Immunity

2- Effector-triggered immunity

1- Pathogen Triggered Immunity (PTI): It operates through transmembrane Pattern Recognition Receptors (PRRs) that recognize Pathogen Associated Molecular Patterns (PAMPs) or also called Microbe associated Molecular Patterns (MAMPs) and/or Danger/Damage Associate Molecular Patterns (DAMPs). It is a quantitative resistance regardless of pathogen lifestyle, that is conserved among species and that is also effective against non-adapted pathogens (non-host resistance).

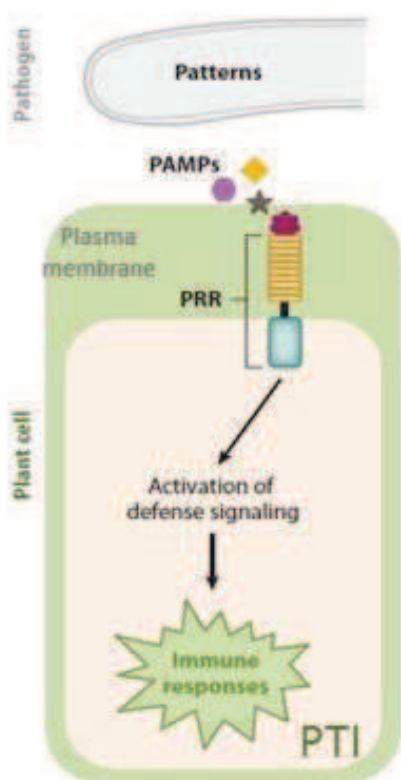


(Figure extracted and adapted from Mengiste, 2012).

- BAK1: The brassinosteroid insensitive 1- associated kinase 1 interacts with many PRR to initiate PTI. Its role is relevant for PTI and it is target of many pathogen effectors (Figure 11).

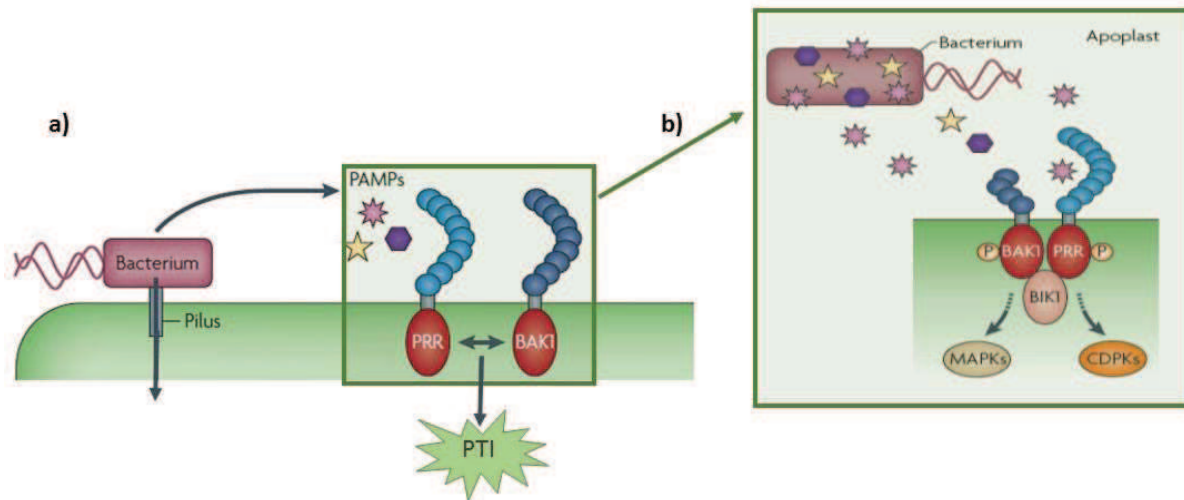
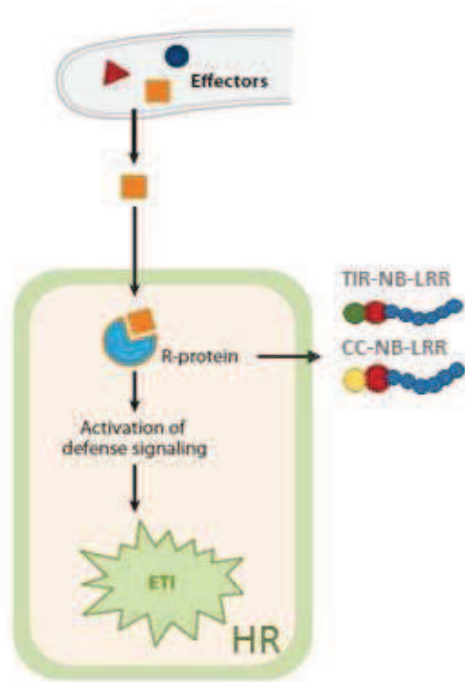


Figure 11: a) PAMPs from bacteria growing in the extracellular space are released and recognized by PRR triggering the basal immune response, PTI. b) In detail, many PRR interact with BAK1 triggering PTI. What happens is that PRR form an active complex with BAK1 that results in sequential phosphorylation events (P bubbles in the figure) that will lead to cascade signaling mediated by BIK1 (*Botrytis*-induced kinase 1), MAMPK or CDPKs . Modified from Dodds and Rathjen, 2010.

- PAMPs (also called MAPs): are conserved pathogen components of all types. Examples are: flagellin, chitin, EF-Tu (elongation factor), Ax21 (from *Xanthomonas* spp.), protein, carbohydrates, lipids, lipopolysaccharides, heptagluconides and several small molecules.

- DAMPs: endogenous molecules released as a consequence of pathogen activities. Examples: cell wall fragments, cuticle fragments, endogenous peptides, oligogalacturonides (OGs).



2- Effector triggered immunity (ETI): It operates through polymorphic nucleotide binding /leucine rich repeat domain (**NB-LRR**) proteins encoded by R genes that recognize pathogen effectors.

It is a response against adapted pathogen, effective only for pathogens holding a (hemi)biotrophic lifestyle. ETI receptor and effectors are diversified and in constant co-evolution. ETI is qualitatively stronger and faster than PTI (Jones and Dangl, 2006; Dodds and Rathjen, 2010). It produces hypersensitive response (HR).

- Effectors: proteins secreted by the pathogens into the host cells. They can suppress PTI and ETI. Some

effectors will have structural roles, while some others will have roles in nutrition or dispersion, and some others will mimic plant hormones. Effectors are variable, in some cases redundant and dispensable. They are secreted into the host cytoplasm. Examples: AvrPto, AvrPtoB, AvrRPM1, (bacteria) or RXLR (oomycetes) (figure extracted and adapted from Mengiste, 2012).

- NB-LRR: are plant intracellular receptors containing nucleotide binding and leucine-rich repeat domains that can recognize specific pathogen effectors of all kind. The recognition event can be via direct interaction or through an auxiliary protein (see different [model theories](#) below). The NB-LRR receptors can be coil-coil–NB-LRR receptor (CC-NB-LRR) or Toll-interleukin-1 receptor (TIR-NB-LRR) according to their N-terminal domain (Chisholm *et al.*, 2006). Examples of CC-NB-LRR are RPS2, RPM1, RPS5; example of TIR-NB-LRR is RPS4.

- HR: involves localized and fast cell death at the site of infection. The plant sacrifices some cells in order to stop pathogen nutrition and further expansion. HR is pathogen-specific. It is a typical defense against (hemi)biotroph pathogens (more details below in [HR](#) section).

Several models have been proposed with the aim of explaining the way that the NB-LRR receptors interact with pathogen effectors.

- a) The Gene-for-Gene Model (Flor, 1971)
- b) The Guard Model (van der Beizen and Jones, 1998)
- c) The Decoy Model (van der Hoorn and Kamoun, 2008)
- d) The Bait and Switch Model (Collier and Moffett, 2009)

a) Theory Gene-for-Gene Resistance

Around the 1950's and following the segregation studies of G. Mendel and the microbial evolution studies of J.B.S. Haldane, H.H. Flor (1956, 1971) proposed a theory that helped to explain the interaction of plants with their pathogens in an evolutionary context of *gene-for-gene* interaction among resistance (*R* genes) from the host and virulence factors (*Avr* genes) from the pathogen.

Since 1956, with the classical example of the interaction between Flax (*Linum usitatissimum*) and its fungal rust *Melampsora lini*, Flor not only studied the segregation of plant resistance genes, but also pathogen virulence. Later on, the model was enriched with the works of C. O. Person (1959) and validated in several pathogenic interactions caused by fungi, bacteria, nematodes and parasitic plants; most of them holding biotrophic lifestyles (Dangl and Jones, 2001, Dangl and McDowell, 2006).

The model proposes that plant-pathogen interaction can be interpreted as mediated by the presence of an *R* gene from the plant and the corresponding *Avr* gene in the pathogen, the also called **Receptor-Ligand model** (Figure 12).

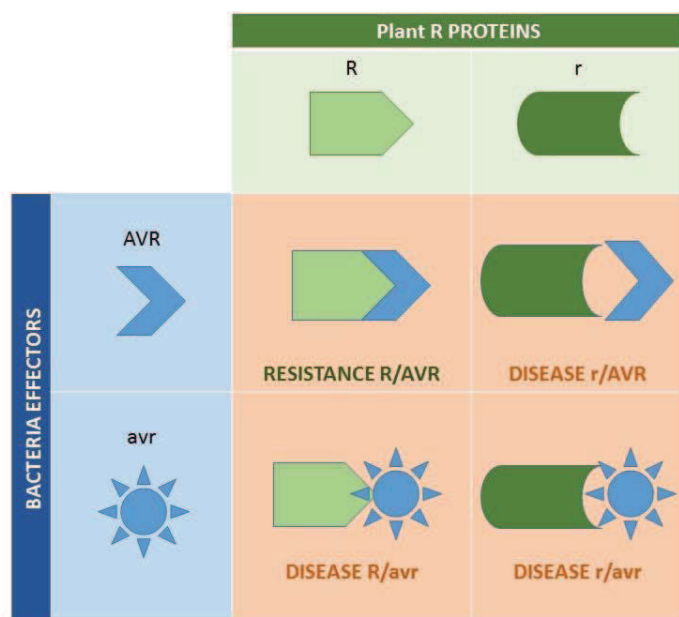


Figure 12: Schematic representation of the Gene-for-Gene theory coined by Flor in 1971, in a biotrophic interaction.

A dominant *R* gene from the plant recognizes the corresponding dominant *Avr* gene from the pathogen, the interaction is compatible and the plant turns into resistance. On the contrary, if the *R* gene is recessive (*r*) or the recognition *R-Avr* fails, the interaction is called incompatible, the plant turns to be susceptible and it becomes diseased.

In the context of this model, the interaction can be considered as **Compatible** or **Incompatible** where:

-Incompatible interaction (no disease, Resistance): In the presence of a gene-for-gene recognition, the product of the *R* dominant or partially dominant gene from the host, recognizes the product of the

Avr gene from the pathogen. Under these circumstances the host becomes **Resistant** and the pathogen is considered **Avirulent**.

The R protein participates in the recognition of the AVR effectors, initiates the signal cascade to activate defense responses and subsequently has the capacity of evolving new R specificities (Hammond-Kosack and Jones, 1997). Thus the **Resistance** will only be triggered if an *R* gene product in the plant recognizes specifically an avirulence gene (*Avr*) product from the pathogen (Figure 12). Any loss of alteration in this complementarity of dominant gene-to-gene combination will lead to **DISEASE**.

-Compatible interaction: In the absence of gene-for-gene recognition, due to absence of the avirulence gene in the pathogen and/or the *R* gene in the host, the pathogen is virulent and the host is susceptible. The plant becomes diseased.

Pathogen *Avr* proteins can be considered as **effectors** that promote pathogen virulence as a consequence of a fail in the system of recognition by the plant. Whatever the system of effector delivery the pathogen has, the goal is to take command on the host to survive. On the other hand plants will evolve different types of R proteins to detect and counteract their enemies as it will be shown later in [The Zigzag Model](#) (Jones and Dangl, 2006).

Many *R* and *Avr* genes have been identified in recent years. The *R* genes comprise several major groups, of which the largest is the nucleotide binding site–leucine rich repeat (NBS-LRR) class. In the case of bacterial pathogens, many of the avirulence genes encode type III effectors, and presumably they function by contributing to virulence in hosts lacking the appropriate *R* genes.

b) and c) The Guard model and The Decoy model

Although the Gene-for-Gene model was validated in several cases and fits to explain numerous examples of *R-Avr* combinations, a relentless number of *R-Avr* interactions remained poorly understood, because of a lack of physical or direct interaction, and/or because it was difficult to demonstrate (von der Hoorn and Kamoun, 2008).

The Guard model (van der Beizen and Jones, 1998) emerged as a way to explain the exceptions that escaped arguments based on the Gene-for-Gene model. The model proposed that instead of a direct interaction of an *R-Avr* genes/products, the R proteins acts as a **Guard** protein monitoring a second protein called the **Guardee** that interacts directly with the AVR product (pathogen effectors) (Figure 13, A).

The Guard Model helped to explain how (or why) multiple effectors could be perceived by one single R protein and how the *guardee* is essential for pathogen virulence in an incompatible interaction (the lack of the matching R protein) (Figure 13, B).

One example from *Arabidopsis thaliana* is the *guardee* protein called **RIN4** that is targeted by several pathogens effectors from *Pseudomonas syringae* (AVR products): AvrRpm1, AvrRpt2, AvrB and monitored by the guard proteins RPM1 and RPS2 (Kim *et al.*, 2005). The effectors target [RIN4](#) for phosphorylation and posterior degradation, suppressing basal immunity (an extended exemplification can be seen below in *Pseudomonas* section, [Figure 36](#)).

What is interesting about this example is that it could also fit in the **Decoy Model** (van der Hoorn and Kamoun, 2008). The Decoy Model states that the *guardee* proteins are not as essential for pathogen virulence as postulated before. A **Decoy** (as “distraction”, “trick”) is a pathogen effector target “guarded” for an R protein that is no needed for plant defense (resistance or susceptibility) or pathogen fitness, and here lies the difference with The Guard Model (Figure 13, C). As well stated by von der Hoorn and Kamoun (2008): “*The decoy mimics effector targets to trap the pathogen into a recognition event*”.

A *guardee* in the Guard Model, instead, is necessary and indispensable for plant defenses and, in the absence of R protein, enhances pathogen fitness. However, both models have one thing in common: in the presence of the R protein, both the decoy and the *guardee*, will trigger innate immunity (ETI) (Figure 13).

Therefore, back to the example of **RIN4**, this could also fit the decoy model since it is not clear whether or not its phosphorylation and degradation affects or not pathogen virulence and fitness (Jones and Dangl, 2006; Chisholm *et al.*, 2006; van der Hoorn and Kamoun, 2008).

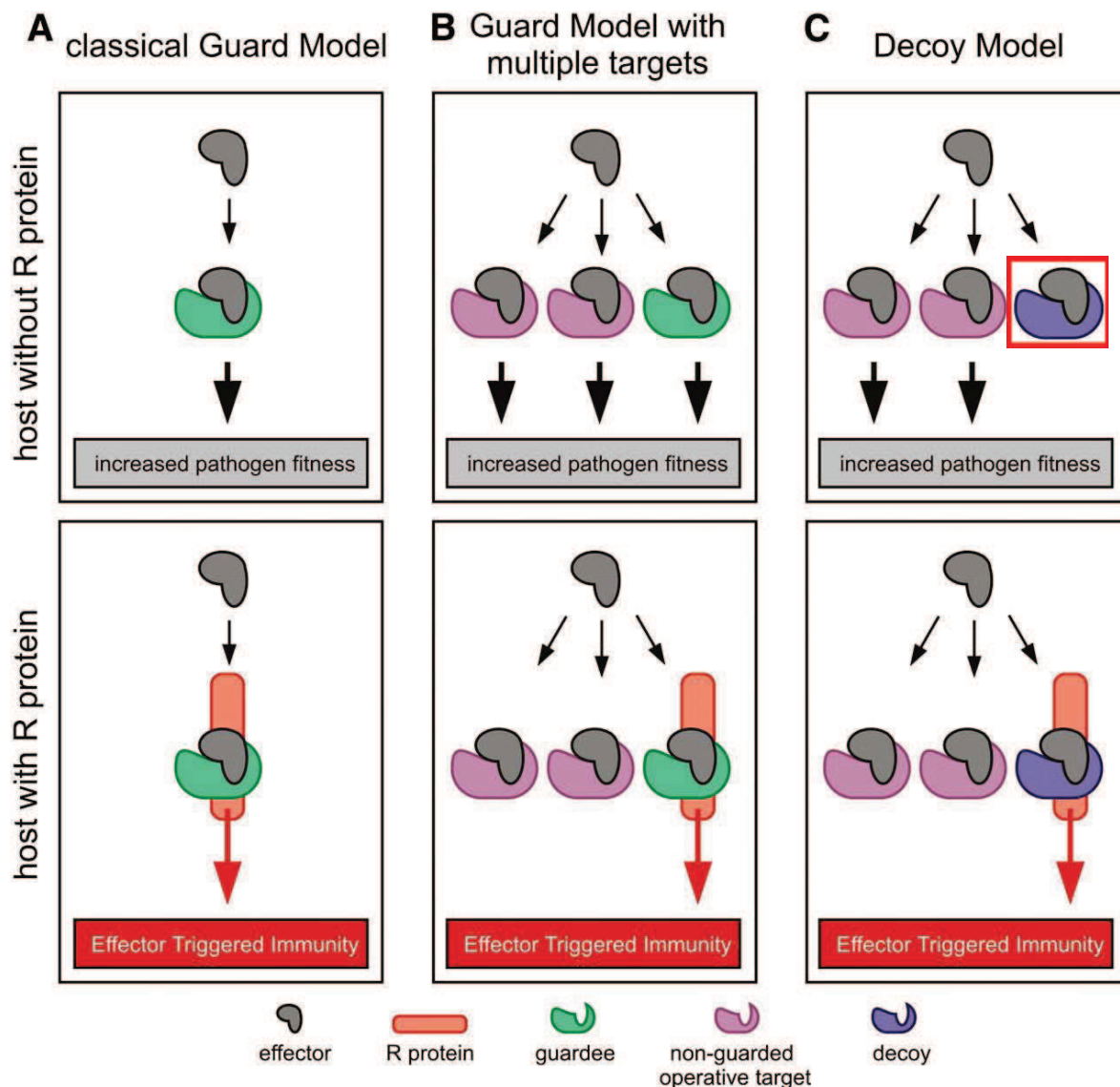


Figure 13: The Guard Model vs the Decoy model.

A) If the R protein is absent, the *guardee* protein enhances pathogen virulence and fitness, but if the corresponding R protein is present in the plant, the combination effector-*guardee*-R protein triggers ETI. B) As stated in A) but with multiple effectors. The absence of R protein causes susceptibility and enhances pathogen virulence and fitness, but if is present it triggers ETI. C) In the Decoy Model, whether the R protein is absent or present, the interaction effector-decoy does not affect pathogen virulence and fitness. Modified from van der Hoorn and Kamoun, 2008.

d) The Bait and Switch Model

This model emerged as a reconciling alternative to the Guard and Decoy Models in examples in which the assumptions of the previous models did not fulfill all the explanations required.

NB-LRR proteins are very abundant and diversified in plants (Sacco *et al.*, 2006; Maekawa *et al.*, 2011), and despite the fact of their structural similarities among some of them, they all have the incredible feature of recognizing different classes of pathogen effectors giving the similar kind of resistance response.

This model represents one of the most recent contributions in the area of plant-pathogen recognition dynamics (Figure 14). The model proposes an interaction NB-LRR/effector facilitated by two recognition steps, one indirect and the other direct in which is required:

1) **Recognition bait-effector:** The “bait” accessory protein acts as the pathogen effector target (instead of a guard or decoy) priming the second recognition step between NB-LRR and effector.

2) **Recognition NB-LRR-effector:** After the first step of recognition, NB-LRR is functional and binds the pathogen effectors triggering the immune signaling cascade.

Regardless of whether a bait protein acts as a “Guard” or “Decoy”, the interesting feature is that it facilitates the recognition process and signaling cascade through a system of cofactors which also allow, in evolutionary terms, more versatility of the *R* genes. This could also explain why plants are so efficient to detect such an infinite amount of microbes (and Avr effectors) with such a limited number of *R* genes (Zipfel, 2008; Collier and Moffett, 2009).

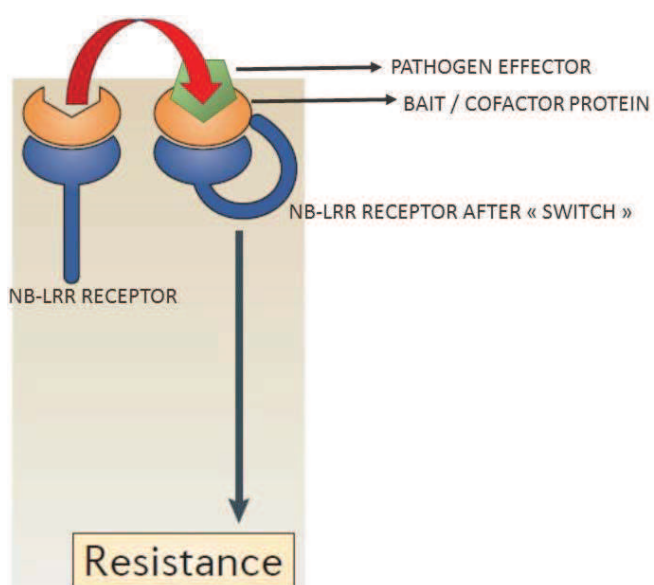


Figure 14: The Bait and Switch Model according to Collier and Moffett (2009).

The NB-LRR protein (so called *R* product) is switch to a novel conformational state after being priming by the bait-effector interaction. From Stuart *et al.*, 2013.

Plant Immune System in motion: The Zigzag Model

Putting these two branches of the plant immune system together, PTI and ETI, there is the remaining question about the dynamics underlying plant–pathogen interaction through quantitative outcome and in co-evolutionary terms. That is to say how the “molecular dialogue” between plant and pathogens could be translated into an evolutionary pathway of effective resistance.

Jones and Dangl proposed in 2006 a schematic representation of this dynamic as it is briefly explained below (Figure 15).

Once the plant comes in contact with a potential pathogen, transmembrane PRRs receptors recognize P/DAMPs and trigger PTI. This basal response will stop the pathogen from spreading and from further attacks. However, if a pathogen has the right effectors that contribute to its virulence, it can overcome PTI and succeed in the attack producing ETS. In this case the plant may deploy a second branch of immunity response: the ETI, an amplified and accelerated version of PTI (Jones and Dangl, 2006; Dodds and Rahjten, 2010). As a result, the plant will produce HR at the infection site and will become resistant. Some pathogens may diversify and acquire new capacities or whole new effectors capable of suppressing ETI, and able to produce disease again. On the other hand, natural selection will also drive R genes from the plant to diversify and acquire new specificity that can be triggered again and the cycle begins again.

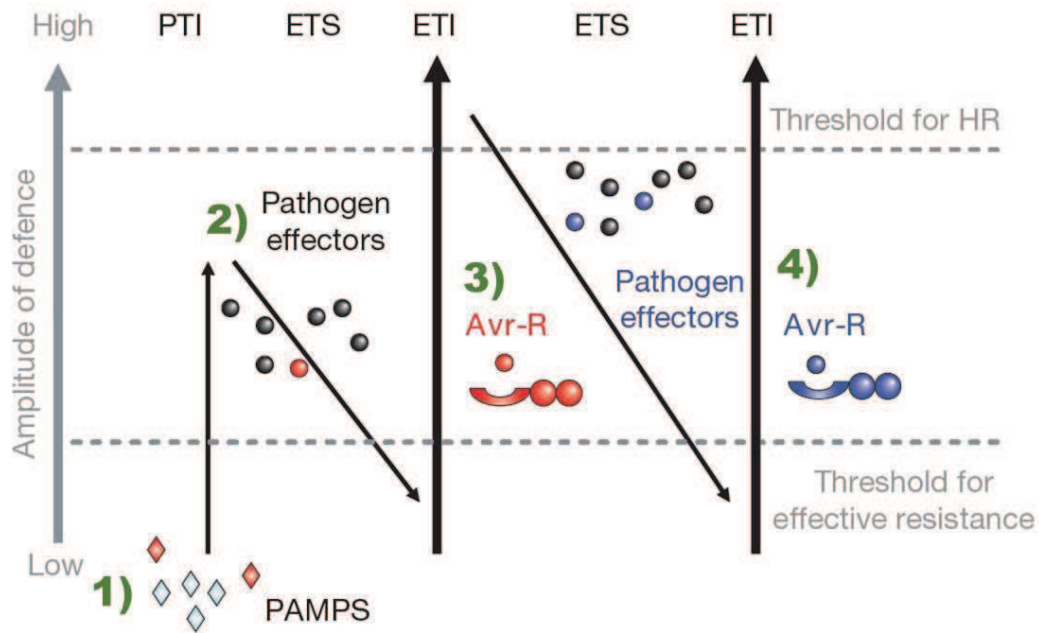


Figure 15: The Zigzag model of plant immune system from Jones and Dangl, 2006.

1) Initially the plant detects P/DAMPs and triggers PAMPs triggered immunity (PTI). **2)** In that case some pathogens would deliver some effectors to interfere with PTI or to cope with it, resulting in effector-triggered susceptibility (ETS). **3)** Effector recognition from the plant (R-Avr) would end in effector-triggered immunity (ETI) and HR. **4)** Some Pathogens would probably evolve new effectors to overcome ETI.

Signaling Pathways and Downstream Responses

The signaling flow downstream PTI or ETI includes series of events as calcium ion flux, ROS generation and MAPKs cascades, gene expression and gene reprogramming, callose/lignin deposition (cell wall fortification) , HR (as it was mentioned before and will be developed later), production of secondary metabolism and PR proteins (chitinases, glucanases, etc.)(Bari and Jones, 2009; Robert-Seilaniantz *et al.*, 2011). Additionally, diverse plant hormones play pivotal roles in the regulation of the defense network, translating the early pathogen signal (detection/recognition events) into more precise and sophisticated defense mechanism in concordance with the situation, that is to say timing, pathogen lifestyle, plant status, ecological context, etc. (Bari and Jones, 2009; Robert-Seilaniantz *et al.*, 2011 ; Pieterse *et al.*, 2009; 2012).

Hormones and plant defenses

Hormones are organic compounds from inside the plant, essential not only for plant growth, development, and reproduction, but also for defense and immunity. They are effective at low concentrations and they are interconnected in complex networks that interact with specific targets allowing plants to give accurate responses for survival in a cost efficient manner (Denancé *et al.*, 2013).

Although hormones are also responsible for interaction with pests and beneficial microbes, information in here will be focused only on pathogenic interactions.

Jasmonates and salicylic acid are the main players in plant pathogen interaction immune responses, but hormones as ethylene, abscisic acid, brassinosteroids, gibberellins, auxin, cytokinins and nitric oxide have roles as well (Bari and Jones, 2009; Pieterse *et al.*, 2009; 2012) (Figure 16).

The interplay (cross talk) and timing of hormone responses will determine the outcome of immune responses, that is to say the level of resistance of susceptibility (Robert-Seilaniantz *et al.*, 2011; Pieterse *et al.*, 2012; Lapin and Ackerveken, 2013; van Schie and Takken, 2014).

More than speaking in terms of punctual hormonal effects is dare say that there is “fine tuning” in a cost efficient manner (Spoel and Dong, 2008; Spoel *et al.*, 2007; Denancé *et al.*, 2013).

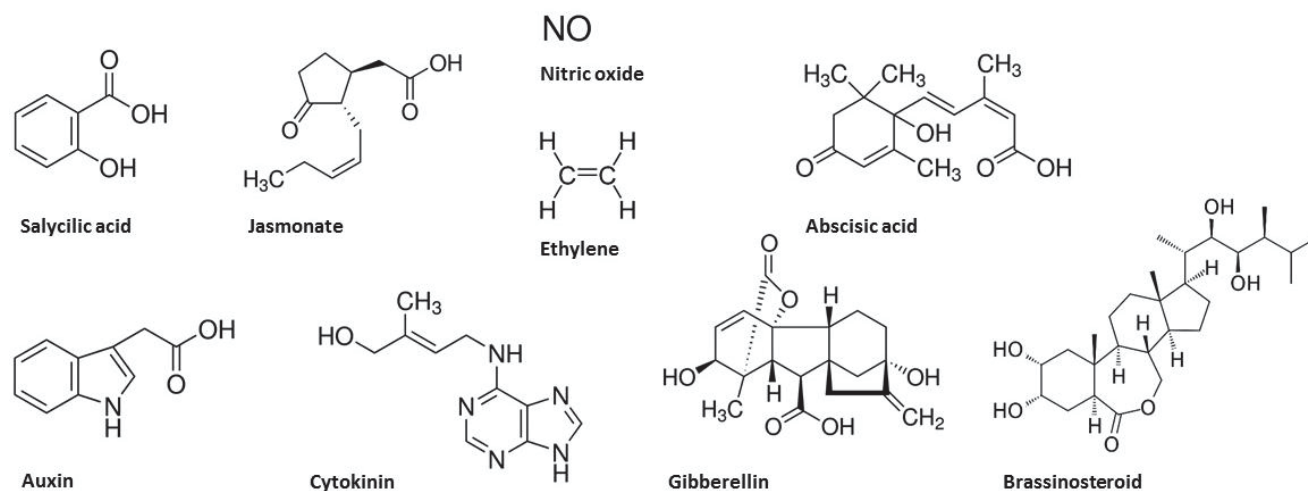


Figure 16: Structure of plant hormones relevant to plant-pathogen interactions.

Salicylic acid, jasmonate, nitric oxide, ethylene, abscisic acid, auxin (indole-3- carboxylic acid), cytokinin (zeatin), gibberellins (GA_3), brassinosteroids (brassinolide).

As it was stated before, jasmonates and salicylic acid are the main players in plant pathogen interaction immune responses hence before starting the subject of signaling pathways and downstream responses, crosstalk, fine-tuning and so on, a brief description about **Salicylic acid biosynthesis** and **Jasmonates biosynthesis** will be developed in the following paragraphs.

Salicylic Acid Biosynthesis

Salicylic acid (SA, 2-hydroxy benzoic acid) is a phenolic compound that consists in a benzoic acid bearing a hydroxyl group (Vlot *et al.*, 2009) (Figure 16 and 17). It is found in plant playing key roles in growth and development (seed germination, seedlings establishment, flowering, fruit yield), respiration, senescence, abiotic stress, stomatal and plasmodesmata closure, basal thermotolerance, nodulation (legumes) and thermogenesis (Vlot *et al.*, 2009; Bartsch *et al.*, 2010; Dempsey *et al.*, 2011; Wang *et al.*, 2013b; Zhang *et al.*, 2013). One of its most prominent roles is activation of complex mechanisms related to plant defense (PTI and ETI) in response to hemi(bio)trophs and resistance responses such as cell death and LAR/SAR in interaction with other hormones and signaling compounds (Dempsey *et al.*, 2011; Coll *et al.*, 2011; van Doorn *et al.*, 2011; Spoel and Dong, 2012; Fu *et al.*, 2012; Fu and Dong, 2013).

SA is active in response to a wide range of pathogens such as virus, bacteria and fungi (Bellés *et al.*, 2006; Vlot *et al.*, 2009, Dempsey *et al.*, 2011) and also insects (see citations in Pastor *et al.*, 2012).

SA can be synthesized via two enzymatic pathways both starting from plastidial chorismate, the end product of the shikimate pathway (Dempsey *et al.*, 2011) (Figure 17):

1- The PAL pathway (PAL): the cytoplasmic phenylalanine ammonia-lyase (PAL) converts phenylalanine (Phe) into *trans*-cinnamic acid (*t*-CA) and NH₃. Then *t*-CA can be converted to SA via two alternative routes: the *ortho*-coumaric acid route or the benzoic acid route (BA), depending on the plant species. *t*-CA is also precursor of some others phenolic compounds of relevance such as lignin, flavonoids, some volatile benzenoids ester and benzoylglucosinolates. There are four *PAL* genes described in *Arabidopsis* (Wildermuth, 2006; Dempsey *et al.*, 2011).

BA can then be produced from three different routes, according to the plant species (Figure 17):

- a) β -oxidation from cinnamoyl Co-A (CoA dependent).
- b) non-oxidative route from cinnamoyl Co-A (CoA dependent) present in *Arabidopsis*, putatively AAO₄ (*Arabidopsis* aldehyde oxidase 4) catalyzes the conversion of benzaldehyde to BA.
- c) non-oxidative route from *t*-CA.

Finally, in *Arabidopsis* conversion from BA to SA has been proposed to be catalyzed by a BA2H (BA 2-hydroxylase) (Dempsey *et al.*, 2011). BA is an active metabolite in plants and has been described as having antifungal effects (Belles *et al.*, 2006; Erb and Glauser, 2010).

2- Isochorismate pathway (ICS): chorismate is converted to SA by two enzymes, the ICS (isochorismate synthase) and the IPL (isochorismate lyase). In *Arabidopsis*, two isochorismate synthases have been described, ICS1 and ICS2, with 83% identity at amino acid level and both with a stromal location. However, only ICS1 expression was related to SA accumulation and *PR*, while ICS2 seems to have another function. ICS1 plays important roles in PTI, ETI and SAR.

This pathway also leads to the synthesis of phyloquinones.

In *Arabidopsis*, the ICS pathway prevails (80-90% of SA production), but the PAL pathway is also operative (Chen *et al.*, 2009; Dempsey *et al.*, 2011). PAL pathway seems to prevail in interaction with *Botrytis cinerea* (Ferrari *et al.*, 2003), *Pseudomonas syringae* pv. *tomato* DC3000 *AvrRpt2* (Huang *et al.*, 2010) and *Hyaloprenospora arabidopsidis* (Mauch-Mani and Slusarenko, 1996).

Once SA is synthesized, it can be subjected to several biologically relevant modifications, which convert SA into forms which are inactive (less toxic) or with attributes that might aid in the fine-tuning of SA regulation, accumulation and transport (Erb and Glauser, 2010; Dempsey *et al.*, 2011). These modifications include for example glycosylation, methylation, amino acid conjugation, sulfonation and hydroxylation (Wildermuth, 2006; Dempsey *et al.*, 2011, Zhang *et al.*, 2013) (Figure 17). A detailed list can be found in Table 4.

Figure 17: The SA biosynthesis and modifications. (Next page)

Chorismic acid, is the starting point of both PAL (in yellow) and ICS (in green) pathways. Some other branching and competing pathways are shown in different colors by laterals arrows. Different routes to BA are framed in blue (right side). Three possible pathways for BA are shown. SA glycosylation, methylation, amino acid conjugation, sulfonation and hydroxylation are shown in fuchsia circles.

Abbreviations: **ICS:** isochorismate synthase, **IPL:** isochorismate pyruvate lyase, **S3H:** SA-3-hydroxylase, **PAL:** phenylalanine ammonia-lyase, **C4H:** cinnamate 4-hydroxylase, **SAG:** salicylic acid 2-O- β -glycoside, **SGE:** salicyloyl glucose ester, **MeSA:** methyl salicylate, **SA-Asp:** salicyloyl-L-aspartic acid. In the BA frame: **4CL:** 4-coumarate CoA ligase, **AAO:** aldehyde oxidase, **BA2H:** benzoic acid-2-hydroxylase, **BZL:** benzoyl CoA ligase. Adapted from Dempsey *et al.*, 2011; Zhang *et al.*, 2013; Miura and Tada, 2014.

Table 4: SA modifications in *Arabidopsis*. Frames in orange and arrows show modifications of some SA derivatives such as MeSA and DHBA (dihydroxy benzoic acid compounds).

(Based on Dean Delaney, 2008; Wildermuth, 2006; Bellés *et al.*, 2006; Vlot *et al.*, 2009; Bartsch *et al.*, 2010; Dempsey *et al.*, 2011; Zhang *et al.*, 2013).

Modification	Triggered by	Biological function	Enzymes	Molecule
Glycosylation	Abiotic and biotic factors	Probably activated form (less toxic)	UGT74F2 (UDP-glucosyltransferase) SGT1 (salicylic acid glucosyltransferase1)	SGE: salicyloyl glucose ester
		Vacuolar storage and inactivation	UGT74F1 > UGT74F2	SGA: salicylic acid 2-O-β-glycoside
	<i>P. syringae</i> (Song <i>et al.</i> , 2008) Observed <i>in vitro</i>	Probably storage of MeSA (50% vacuolar)	SGT1	MeSAG: 2-O-β-D-glucoside
	Pathogens, senescence	Probably storage	UGT72B1	2,3 DHBA-G
			???	2,3 DHBA-X
???			2,5 DHBA-G	
???	2,5 DHBA-X			
Methylation	Abiotic and biotic factors	Increases membrane permeability and volatility Mobilization, long distance Inactivation Cues for pollinators, tritrophic interactions, neighboring plants	BSMT1 (BA/SA carboxyl methyltransferase 1) (higher expression in flowers)	MeSA: methyl salicylate
Amino acid conjugation	Abiotic and biotic stresses, influenced by the crosstalk with IAA	Probably involved in catabolism Inactivation	GH3.5 (WES1) (acyl adenylase 3.5 or WESO 1)	SA-Asp: salicyloyl-L-aspartic acid
Sulfonation	Observed <i>in vitro</i> Observed in <i>Pseudomonas</i> infection of KO mutants	Probably activation/inactivation	SOT (sulfotransferase) (still under investigation)	SA-2-sulfonate
Hydroxylation	Pathogen hemi(bio)trophs Ageing, senescence	Inactivation of SA and/or probably antioxidant protection (against ROS)	SH3 (SA-3-hydroxylase)	2,3 DHBA: 2,3 dihydroxybenzoic acid
	Pathogens, non-necrotizing (<i>i.e.</i> virus)(Bellés <i>et al.</i> , 2006)	unclear	???	2,5 DHBA: 2,5 dihydroxybenzoic acid (gentisic acid)

Jasmonates biosynthesis

Jasmonates (JAs) are oxylipins that arise from the oxygenation of tri-unsaturated fatty acids as hexadecatrienoic (16:3) and α -linolenic (18:3) acids. They play diverse and complex roles in plant growth, development and survival. They are involved in important processes such as reproduction, fruit development, senescence, defense responses, and are induced by wounding, herbivory, necrotrophic pathogens, biotrophic root pathogens and symbionts (Acosta and Farmer, 2010; Avanci *et al.*, 2010; Ballaré, 2011; Wasternack and Hause, 2013; Yan *et al.*, 2013).

As examples it can be mentioned: jasmonic acid (JA), methyl jasmonate (MeJA), jasmonoyl isoleucine (JA-Ile) among others (Figure 18).

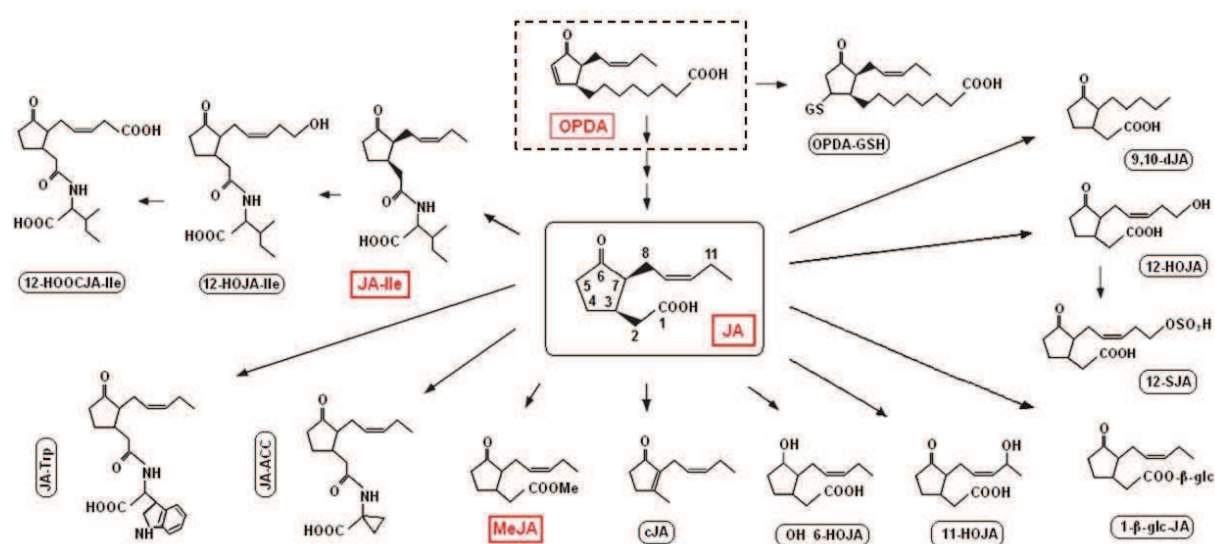


Figure 18: The jasmonates: precursors and derivatives.

Abbreviations: **OPDA**: oxo-phytodienoic acid, **OPDA-GSH**: OPDA glutathione conjugate, **JA**: jasmonic acid, **JA-ILE**: jasmonoyl isoleucine, **12-OH JA-Ile**: 12-hydroxyjasmonoyl-isoleucine, **12-HOOC JA-Ile**: 12-carboxyjasmonoyl isoleucine, **9,10 dJA**: 9,10-dihydrojasmonic acid, **12-HOJA**: tuberonic acid or 12-hydroxy-(+)-7-isojasmonic acid, **12-SJA**: 12-hydroxy-(+)-7-isojasmonic acid sulfate, **1- β -glc-JA**: JA glucosyl ester, **11-HOJA**: 11-hydroxyjasmonate, **OH 6-HOJA**: 6-hydroxyl jasmonate, **cJA**: *cis*-jasmone, **MeJA**: methyl jasmonate, **JA-ACC**: jasmonic acid /1-amino-1-cyclopropane carboxylic acid conjugate, **JA-Trp**: jasmonic acid /tryptophan conjugate. From Gfeller *et al.*, (2010) cited in Yan *et al.*, 2010.

About 67-85% of *Arabidopsis* genes related to wound/insect are regulated by JAs (Acosta and Farmer, 2010). JAs are produced from JA (pro-hormone) that later go through several metabolic conversion into JA derivatives. [JA synthesis and signaling](#) are interlinked, as it will be described later in this section.

JA biosynthesis occurs in several subcellular compartments: chloroplast, peroxisomes, nucleus, vacuoles, cytosol and probably membranes (Acosta and Farmer, 2010; Wasternack and Hause, 2013). A detailed representation can be seen in Figure 19.

1. External stimuli trigger the synthesis of 16:3 and 18:3 fatty acids from membrane lipids in the chloroplasts. The 13-LOX (lipoxygenase) oxygenates 16:3 and 18:3 fatty acids and produces 13-hydroperoxy-fatty acids. Those are further converted by the AOS (allene oxide synthase, CYP74A, Laudert *et al.*, 1996) that forms unstable allene oxides. These allene oxides (12, 13 EOT, epoxyoctadecatrienoic acid) are cyclized by an AOC (allene oxide cyclase) and converted into 12-OPDA and dn-OPDA (dinor-OPDA). OPDA and dinor-OPDA are transported to the peroxisomes, probably via the ABC transporter COMATOSE (Avanci *et al.*, 2010). There are six 13-LOX in *Arabidopsis* (Banemberg *et al.*, 2009) and four AOS (Agrawal *et al.*, 2004). AOS is fundamental in JA biosynthesis (Park *et al.*, 2002; Agrawal *et al.*, 2004; Avanci *et al.*, 2010).
2. In the peroxisomes, OPDA and dn-OPDA undergo several β -oxidations, but are first converted into cyclotanonones by OPR3 (a flavoprotein oxidoreductase called oxophytodienoic acid reductase).
3. JA undergoes several modifications. JA-Ile, JA-ACC, JA-Trp, MeJA are produced in the cytosol (Acosta and farmer, 2009). In addition, JA and JA-Ile can be further modified via glycosylation, sulfonation, hydroxylation (as shown in figure 18) (Acosta and Farmer, 2009, Avanci *et al.*, 2010; Wasternack and Hause, 2013) (more details in Table 5).
4. The signaling process occurs in the nucleus and as well as regulation of JA biosynthesis (see below in [JA signaling](#)). JA regulates its own synthesis by a feedback loop (Acosta and Farmer, 2009, Pieterse *et al.*, 2012; Wasternack and Hause 2013).
5. Finally, production and targeting of enzymes like 13-LOXs, AOS, AOC and OPR3 occur in the cytoplasm. 13-LOXs, AOS, AOC are synthesized in the cytosol and targeted to plastids. OPR3 is targeted to peroxisomes.

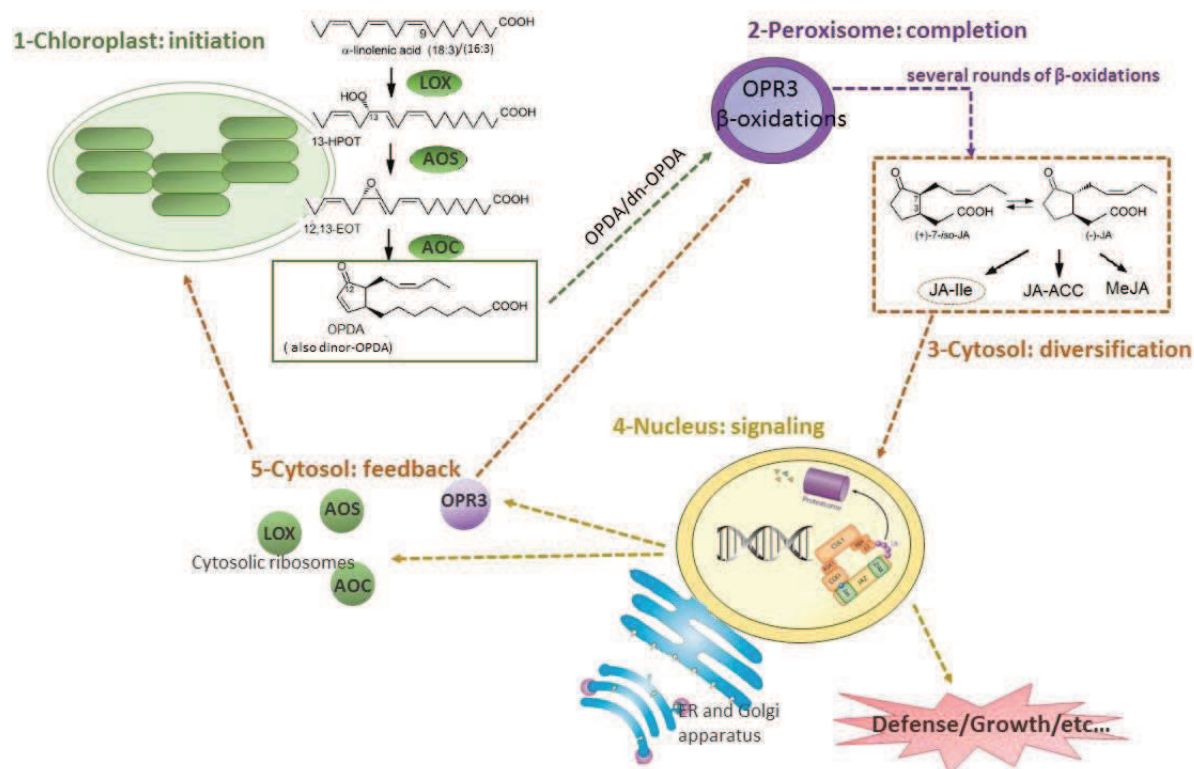


Figure 19: Cellular compartmentalization of JA biosynthesis and signaling.

Abbreviations: **LOX**: lipoxygenase, **AOS**: allene oxide synthase, **AOC**: allene oxide cyclase, **13-HPOT**: 13-hydroperoxy fatty acids, **12, 13-EOT**: 12,13-epoxyoctadecatrienoic acid, **OPDA**: oxophytodienoic acid, **dn-OPDA**: dinor-OPDA, **OPR3**: oxophytodienoic acid reductase 3, **JA-Ile**: jasmonoyl isoleucine, **JA-ACC**: jasmonic acid/1-amino-1-cyclopropane carboxylic acid conjugate, **MeJA**: methyl jasmonate. Based on Acosta and Farmer, 2009.

Modifications of JA and derivatives give rise to molecules with new functionalities for fine tuning, transportation, activation/deactivation. JA, *cis*-JA, MeJA and JA-Ile are considered as the bioactive forms of JAs while other conjugated forms and derivatives are considered as “clearance” forms of JAs. A detailed description of the molecular fate of each of the JAs known to date in *A. thaliana* can be seen Table 5.

Table 5: Metabolic fate of JAs in *A. thaliana*. Based in: Stintzi and Browse, 2001; Acosta and Farmer, 2010; Avanci *et al.*, 2010; Wasternack and Hause, 2013.

Molecule	Conversion	Biological Role
JA	Prohormone	<ul style="list-style-type: none"> – Anther filament elongation, stomium opening, dehiscence, viability and maturation of pollen – Flower opening – Growth inhibition, lateral root formation/adventitious root (crosstalk with auxin) – Senescence – ISR (induced systemic resistance) – Help in mycorrhiza colonization/nodulation – Trichome formation
<i>cis</i> -JA	Volatile	<ul style="list-style-type: none"> – Bioactive – Regulating genes in bi/tritrophic interactions (<i>CYP81D11</i>)(independent of CO1 and JAR1)
MeJA	Volatile Produced in cytoplasm by a JA carboxyl methyl transferase (Seo <i>et al.</i> , 2001).	<ul style="list-style-type: none"> – Bioactive – Intra/inter plant communication – Growth and elongation of shoot and root, flower buds – Cell division, growth – Secondary metabolism activation (terpenoids, phenylpropanoids, among others). – Defense – Systemic signaling???
11-OH-JA		<ul style="list-style-type: none"> – Clearance of JA – Wounding induces formation
12-OH-JA		<ul style="list-style-type: none"> – Clearance of JA – Root growth, seed germination
12-S-JA	AtST2 α (sulfotransferase) from 11-OH-JA and 12-OH-JA Important crosstalk	<ul style="list-style-type: none"> – Clearance of JA – Wounding induces formation
JA-Ile	Bioactive. Can be inactivated by epimerization and oxidation JAR1 (amino acid synthetase jasmonate resistant 1) (Staswick and Tiriyaki, 2004)	<ul style="list-style-type: none"> – Bioactive – Inhibition of root growth – Anthocyanin accumulation – Wounding (accumulation near wound site) – Defense, hormonal crosstalk
12-OH JA-Ile	<i>CYP94C1/B3</i>	<ul style="list-style-type: none"> – Clearance of JA – Wounding induces formation
12-COOH JA-Ile	<i>CYP94B3/C1</i>	<ul style="list-style-type: none"> – Clearance of JA – Wounding induces formation
JA-Trp		<ul style="list-style-type: none"> – Clearance of JA – Inhibition of lateral root formation (Staswick, 2009) (auxin crosstalk) also some examples on adventitious root formation inhibition (Gutierrez <i>et al.</i>, 2012 cited in Wasternack and Hause , 2013)
JA-ACC		<ul style="list-style-type: none"> – Clearance of JA? – ???
Glycosylated forms (JA, JA-Ile, 12-OH-JA, 12-OH-JA-Ile)	Fast accumulation, within minutes	<ul style="list-style-type: none"> – Clearance of JA – Wounding induces accumulation – Glycosylated TAG (tuberonic acid) in potato induce tuber formation (crosstalk with gibberellins)

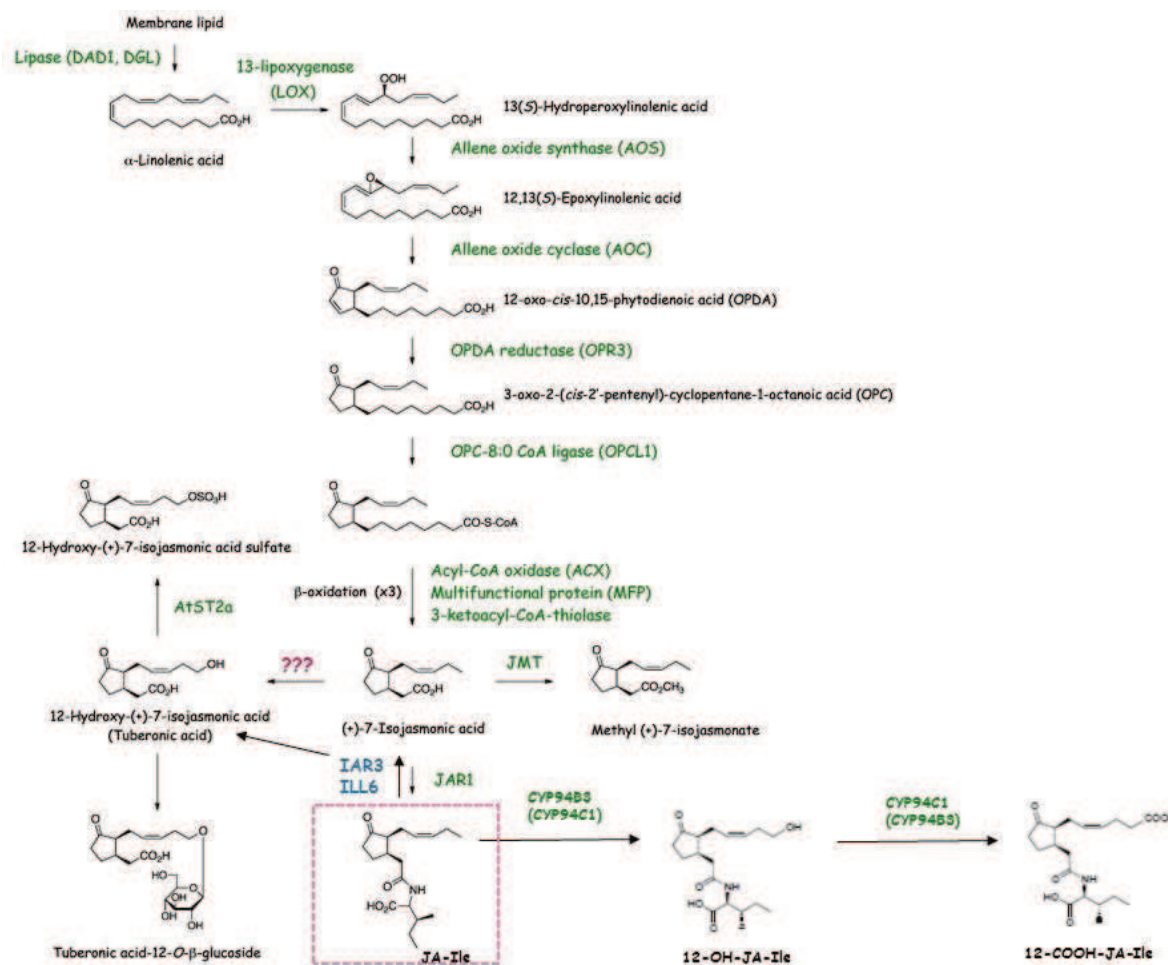


Figure 20: JA synthesis and further transformations.

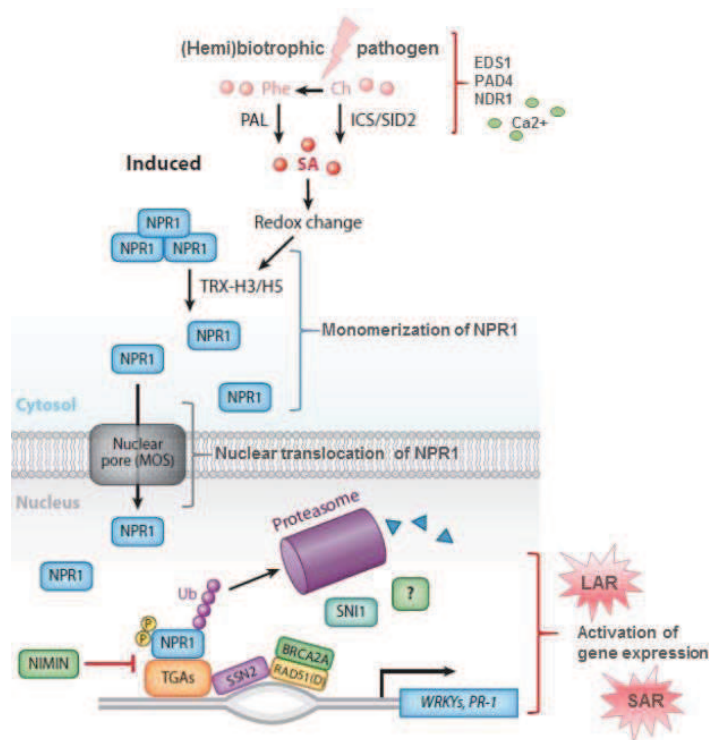
Abbreviations not explained in the figure: **DAD1**: delayed anther dehiscence 1, **DGL**: dongle, **JMT**: JA carboxyl methyl transferase, **JAR1**: jasmonate resistant 1, **AtST2α**: *A. thaliana* sulfotransferase 2, **IAR3**: IAA-alanine resistant 3, **ILL6**: IAA-leucine resistant (ILR)-like gene 6, **JA-Ile**: jasmonoyl isoleucine. Image modified from RIKEN Plant Hormone Research Network - Plant Science Center (http://hormones.psc.riken.jp/pathway_ja.shtml), Heitz *et al.*, 2012; Widemann *et al.*, 2013.

Signaling pathways

Salicylic acid pathway signaling

The SA response pathway is typical of (hemi)biotroph pathogens (with some exceptions). The cascade of events occurs as explained in Figure 21.

Figure 21: Schematic representation of SA signaling cascade after (hemi)biotroph pathogen attack. Explanations and references in the text. Modified from Pieterse *et al.*, 2012.



Plant and pathogen come in contact and PTI or ETI events are triggered. An increase in Ca²⁺ levels accompanies the onset of SA synthesis through EDS1 (enhanced disease susceptibility 1, lipase like protein) and PAD4 (phytoalexin deficient 4) (in the particular case of CC-NBS-LRR proteins receptors, it is the action of non-race-specific disease resistance 1 NDR1) (Brodersen *et al.*, 2006; Pieterse *et al.*, 2012). The downstream signaling cascade is mainly governed by the action of NPR1 (non-expressor of PR genes 1) (Spoel *et al.*, 2003). In plant basal state, NPR1 is inactivated by oligomerization. After pathogen induction, it becomes monomerized through the activity of the thioredoxins TRX-H3 and TRXH5 (Tada *et al.*, 2008) and transported to the nucleus by a nuclear pore protein MOS (modifier of *snc1*) (Cheng *et al.*, 2009). In the nucleus, it interacts with several transcription factors (bZIP and TAG families) to activate SA genes, as for example *PR1*. *PR* genes (pathogenesis related) are the best known marker for gene expression mediated by SA. WRKY transcription factors, are also, important mediators in the SA signaling pathway (Li *et al.*, 2004).

Once NPR1 is no longer necessary, it is ubiquitinated and targeted to the proteasome to avoid any further gene activation (Spoel *et al.*, 2009). Some other negative regulators as NIMIN1 (nim-interacting1), 2, and 3, and SNI1 (suppressor of NPR1 inducible1) help to avoid further untimely activations (Pieterse *et al.*, 2012).

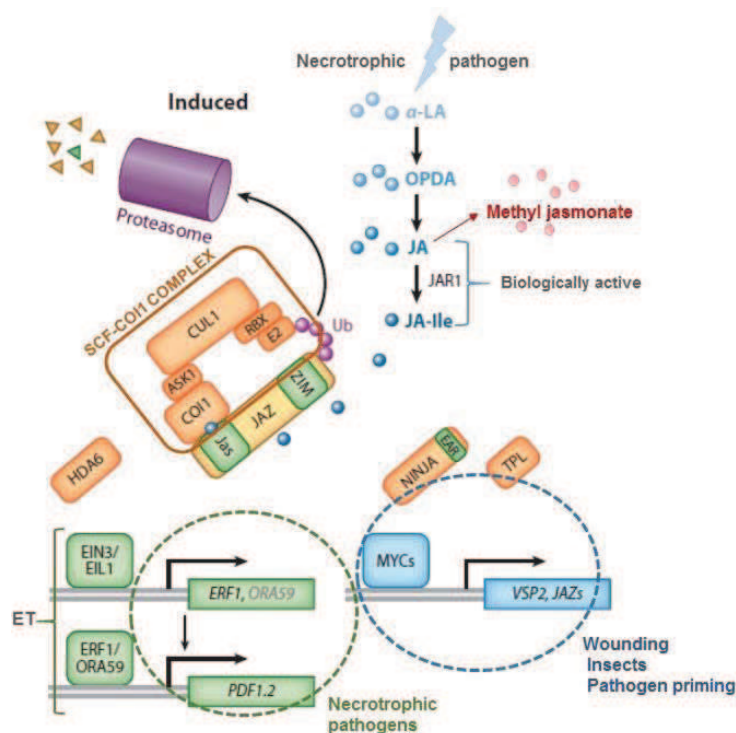
After the SA pathway is activated at the local site of infection (local acquired resistance or LAR), a similar response would be triggered in the surrounding and long-distance tissues to protect the undamaged tissue and the rest of the plant, for further attacks. This response is called **SAR** (systemic acquired resistance) (Grant and Lamb, 2006; Spoel and Dong, 2012; Shah *et al.*, 2014) and It will be developed in the following sections.

Jasmonates pathway signaling

The JAs are lipid-derived compounds synthesized after pathogen/herbivore attack or wounding through the oxylipins pathway.

The cascade of events occurs as explained in Figure 22. The example is focused in necrotroph attack with minor mention to wounding effect.

Figure 22: Schematic representation of JA signaling cascade after necrotroph pathogen attack. Explanations and references are provided in the text. Modified from Pieterse *et al* (2012).



Once the plant is attacked by a necrotroph pathogen, JA synthesis is activated. The F-box protein coronatine insensitive1 (COI1) together with jasmonate zim (JAZ) transcriptional repressor protein, both play key roles in the JA signaling pathway. COI1 is the receptor for JA-Ile and is an essential component of the SCF-CO11 complex (E3 ubiquitin-ligase SKP1-Cullin-F-box complex SCG, **orange framed box**) (Katsir *et al.*, 2008). Following the binding of JA-Ile to COI1, ubiquitinylation of the F-box to COI1, ubiquitinylation of the F-box

occurs, and the JAZ protein is also degraded (via proteasome). After repressor degradation, derepression occurs, and activation of JA responsive gene expression starts (Pauwels and Goossens, 2011). In *Arabidopsis* there are two branches of JA signaling (Lorenzo and Solano, 2005; Pré *et al.*, 2008; Pieterse *et al.*, 2009, 2012):

a) **The MYC branch** (basic helix-loop-helix leucine zipper protein): regulated by MYC transcriptional regulators. Activates the synthesis of *VSP2* (vegetative storage protein 2) gene and *LOX2*.

When the plant is not induced (basal state) JAZ proteins bind MYCs. Also the adaptor protein NINJA (novel interactor of JAZ) together with EAR (erf-associated amphiphilic repression) and TPL (corepressor topless) prevents the activation of JA signaling. This branch of JA signaling is associated with responses to wounding, insect attack and some priming by necrotrophic pathogens.

b) **The ERF branch**: regulated by the AP2/ERF (apetala2/ethylene response factor) family of transcription factors, such as ERF1 and the ORA59 (octadecanoid-responsive Arabidopsis 59). This branch requires both ET and JA to be activated, but still some details remain to be understood. Induces the expression of *PDF1.2* gen (plant defensin 1.2) and is associated with responses to necrotroph pathogens.

Hormonal networking in defense

Crosstalk between salicylic acid and jasmonic acid

In nature, plants are exposed to multiples attackers that act simultaneously or subsequently. The interplay between SA and JA is thought to help the plant to prioritize the strategy to counteract the attack from different organism, under different contexts, and to give adaptive responses to some others stresses (Ballaré, 2011). Yet spatial-temporal context of the interaction and interplay are influencing the outcome in the immune signaling responses.

In *Arabidopsis*, this crosstalk has been well studied. Interactions can be antagonistic, synergistic or neutral, even though antagonistic ones seem to prevail (Pieterse *et al.*, 2012; 2009) (Figure 23).

1) In the early activation steps of SA signaling, EDS1 and PAD4 can be modulated by MAPKs. In *Arabidopsis*, MPK4 is an example (Petersen *et al.*, 2000). It acts as negative regulator of SA signaling by interfering with this two genes and downstream responses, thereby acts as positive regulator for JA signaling.

2) SA signaling increases redox state (oxidized glutathione pool) (Dong, 2004), while JA does not. GRX (glutaredoxins) and TRXs (thioredoxins) are key regulator in SA signaling. For instance, GRX480 plays relevant roles in the SA-JA crosstalk, together with WRKYs. It encodes a protein that can suppress JA-dependent genes as *PDF1.2* (Ndamukong *et al.*, 2007). WRKY plays central roles in the modulation SA-JA.

3) NPR1 is a fundamental factor in SA signaling. As it was mentioned before, cytosolic NPR1 needs to be translocated to the nucleus to activate SA responsive genes. Interestingly, this localization is not necessary or important for JA suppression, since it was shown that cytosolic NPR1 is responsible for it (Spoel *et al.*, 2003). Nuclear NPR1 seems to be implicated in the regulation of several SA-dependent transcriptional factors as GRX480, TGAs and WRKYs (Pieterse *et al.*, 2012) and SA-responsive genes, while cytosolic NPR1 plays a role in the SA-JA crosstalk directly (Spoel *et al.*, 2007).

5) Conversely, JA signaling can also suppress SA dependent-defenses. The classical example is the interaction *P. syringae*–*A. thaliana*. *P. syringae* produces the toxin coronatine (COR) that mimics JA-Ile and suppress SA signaling defense cascades, taking command on the host and promoting susceptibility (Xin and He, 2013; Heng *et al.*, 2012; several authors see below in [Coronatine](#)).

6) For instance, JA responsive genes *PDF1.2* (necrotroph) and *VSP2* (wounding, insects) genes are highly sensitive to SA mediated suppression.

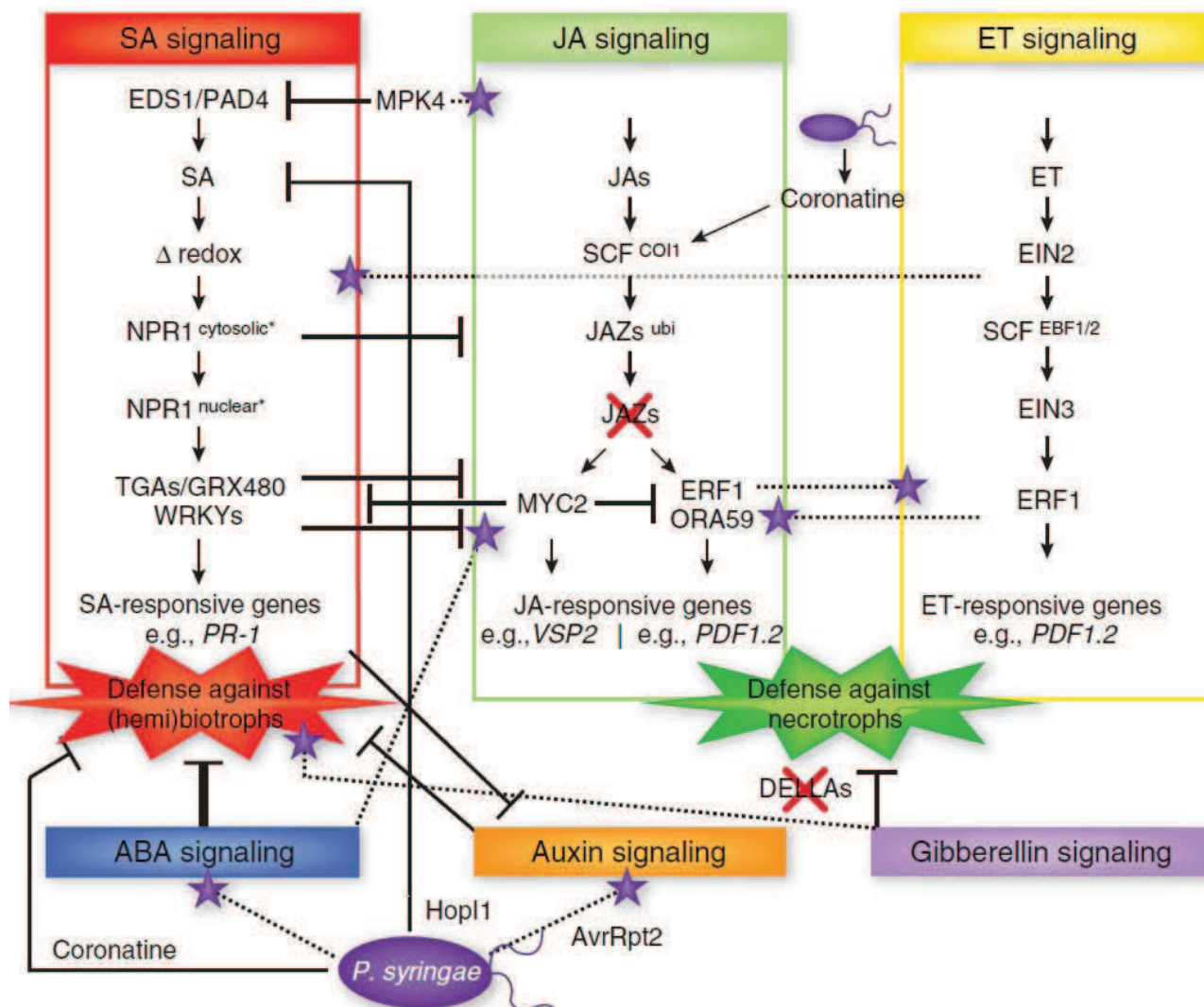


Figure 23: Schematic representation of hormonal crosstalk from Pieterse *et al.*, 2009. Description and references in the text. Each color represents an hormone: SA (red), JA (green), ET (yellow), ABA (blue), AUXIN (orange), Gas (purple).


Crosstalk between salicylic acid and jasmonic acid/ethylene

- 1) ET has a synergistic effect with the SA-dependent gene *PR1* through EIN2 and EIN3 (Glazebrook *et al.*, 2003; de Vos *et al.*, 2006). On the other hand, ET can also have an opposite effect, for instance ET transcription factors, EIN3 and EIL1, affects *ICS/SID2* affecting SA accumulation and *PR1* expression (Chen *et al.*, 2009).
- 2) ET acts synergistically with JA in the ERF branch (response to necrotroph) of JA signaling to activate defense responses, antagonizing the MYC branch (wounding, insects). For instance, activation of *PDF1.2* requires the synergistic effect of both hormones. MYC instead is a negative regulator of *PDF1.2* (Pré *et al.*, 2008).
- 3) During SA-JA interaction, ET suppresses the need for NPR1 (cytosolic) in SA repression of JA signaling pathway. This highlights the dual role of NPR1 in these cross talks (Leon Reyes *et al.*, 2009).
- 4) When the JA/ET pathways have been activated in the first place, the SA suppression of JA/ET signaling cascade is impaired (Pieterse *et al.*, 2012).


Crosstalk between abscisic acid and salicylic acid/jasmonic acid

- 1) ABA suppresses SA-dependent defenses at different levels. *In extenso* affects SAR and vice versa. ABA seems to be an important connector between biotic and abiotic stress (Yasuda *et al.*, 2008; Cutler *et al.*, 2010).
- 2) ABA lessens JA/ET-dependent genes in the ERF1 branch (Anderson *et al.*, 2004).
- 3) ABA acts on the MYC branch (herbivores, wounding) of JA signaling (when ET is absent) (Anderson *et al.*, 2004).


Crosstalk between auxin and salicylic acid/jasmonic acid

- 1) Auxin represses SA levels and signaling. Thus, repression of auxin signaling, also affects SA-JA crosstalk. Plants with auxin suppression, rewire the tryptophan-derived flux to glucosinolates, rendering the plant more resistant to biotrophs as a consequence of a reduced [camalexin biosynthesis](#) (Navarro *et al.*, 2006; Bari and Jones, 2009; Pieterse *et al.*, 2012).
- 2) Auxin affects JA biosynthesis and JA-dependent genes, but the interaction JA-Auxin is not well understood (Bari and Jones, 2009; Pieterse *et al.*, 2012).

 **Crosstalk between gibberellins and salicylic acid/jasmonic acid**

1) GBs control plant growth through the ubiquitination and degradation of DELLA proteins (repressors). DELLAs proteins interact with JA in the MYC branch, by reducing JAZ/MYC2 interaction and favoring JA signaling. Consequently, by regulating the stability of DELLAs (degradation), GBs suppress JA signaling, affecting SA-JA/ET crosstalk and enhancing, by contrast, resistance to biotrophs (Navarro *et al.*, 2008; Bari and Jones, 2009; Pieterse *et al.*, 2012).

Finally, very short word about CKs and BRs (not showed in the Figure 23).

CKs: affect SA signaling synergistically by binding to TAG transcription factor and enhancing *PR1* expression (Choi *et al.*, 2010).

BRs: have a probable connection with BAK1 (Belkhadir *et al.*, 2012). Treatment with BRs induced *PR1* expression, enhancing (hemi)biotroph resistance (Robert-Seilaniantz *et al.*, 2011). This is still a matter of debate (Pieterse *et al.*, 2012).

A word of caution

Since most of the data presented in this thesis revolves around cell death scenarios, such as HR and necrosis, precise terminology, definitions and concepts will be developed throughout the following pages in order to give accurate context for further analysis and discussions. Starting from definitions and features of programmed cell death in plants, to the definitions and induction pathways of HR in particular, closing with some remarks on the significant role of HR in a more ecological context.

Programmed Cell Death

Programmed Cell Death (PCD) is an essential part of plant development and responses to stresses.

Whereas in animals three different types of programmed cell death (PCD) exist, apoptosis, autophagy and necrosis, in plants, two classes of PCD classes can be distinguished: **Autolytic** and **Non-autolytic** cell death (van Doorn, 2011b) (Table 6).

Apoptosis, as is known for animals, seems to be absent in plants, as there is a lack of apoptotic bodies, cell protrusion and phagocytosis (van Doorn *et al.*, 2011a; Van Doorn, 2011b; Coll *et al.*, 2014).

For many years, researchers were trying to define HR as an apoptotic cell death (Morel and Dangl, 1997; Heath, 2000; van Doorn *et al.*, 2011a, Van Doorn, 2011b), and still today several publications use the term “apoptotic” to define it.

The PCD categories are based mainly on cell morphology as it can be seen in Table 6, according to the last review of van Doorn (2011b). At the moment the understanding of biochemical and genetic events underlying PCD is insufficient to develop a more precise classification.

The “key” event to define these two major classes of cell death morphologies is the tonoplast rupture followed or not by fast cytoplasm clearance. In autolytic PCD this rupture and clearance must happen before cell death, because it takes part in cell killing. Although, non-autolytic PCD shows cytoplasm clearance after the cell is dead.

In addition, abundant morphological and biochemical changes occur before PCD, but they are not exclusive or distinctive of one or another class of PCD. Among them it can be mentioned: chromatin condensation, nucleus condensation, formation of vacuole-like vesicles, autophagy-like structures (with undefined roles).

Table 6: Morphological classification of cell death in plants.

	Autolytic	Non-autolytic
Cell death scenario	<ul style="list-style-type: none"> – Developmental – Mild abiotic stress: lack of O₂ and drought 	<ul style="list-style-type: none"> – PCD caused by plant-pathogen interaction – HR – Necrosis – Endosperm of cereal seeds
Cell morphology	Fast tonoplast rupture, <u>with cytoplasm clearance before cell death</u>	Tonoplast rupture <u>without</u> cytoplasm clearance (some cases even without tonoplast rupture)
Morphological changes	<ul style="list-style-type: none"> – Chromatin condensation – Disappearance of organelles: plastids, ER membranes, ribosomes, peroxisomes – Nucleic acid degradation – Changes in cytoskeleton – Plasmodesmata closure 	<ul style="list-style-type: none"> – Swelling of organelles – Increased permeability of tonoplast
Vacuoles	<ul style="list-style-type: none"> – Several small vacuoles converge into one big vacuole – Decrease of cytoplasm volume – <u>Hydrolases</u> are released from vacuoles and degrade cytoplasm – VPE/ vacuolar processing enzymes – Several vesicles 	<ul style="list-style-type: none"> – No modification of vacuolar volume (if there is vacuolar collapse, it does not cause cell death or cytoplasm clearance)
Signaling	<ul style="list-style-type: none"> – Increase of Ca⁺² flux – MAPK induction – Serine/ Cysteine proteases (caspases) – Sphingosine: tonoplast permeabilization – ROS (oxidative reactions) 	<ul style="list-style-type: none"> – Increase of Ca⁺² flux – MAPK induction – Serine/ Cysteine proteases (caspases) – ROS (oxidative reactions)

In autolytic PCD, it is not clear how tonoplast rupture happens, but the fast clearance of cytoplasm is caused by hydrolases released from vacuoles (here the name “autolytic”), after vacuoles collapse. When a cell is about to die, vacuolization starts, and vesicles start to gather around. Cytoplasm volume decreases, while vacuolar volume increases. Complex metabolites are degraded and exported through the phloem (for example in senescent tissues, as petals, etc.).

In non-autolytic PCD, there is no hydrolase release (exception in endosperm from cereals, see below), no changes in vacuolar volume. Tonoplast rupture is important for cell death. This PCD can be divided in three main types that can be seen in Table 7. Some HR PCDs will require vacuolar collapse, while some others will not. In either case, vacuolar collapse will never cause the fast clearance of cytoplasm (as stated in the autolytic PCD). Moreover, VPE (caspase-1 activity), metacaspases and cathepsins seem to be involved in cell killing (instead of hydrolases as describe in autolytic PCD).

Table 7: Classification of non-autolytic cell death in plant

	HR	NECROSIS	CEREAL ENDOSPERMA
Signaling	<ul style="list-style-type: none"> – Calcium flux – MAPK cascade – SA – ROS/NO (oxidative burst) 	<ul style="list-style-type: none"> – Calcium flux – Oxidative burst by toxins (ROS/NO)(H₂O₂) 	
Features	<ul style="list-style-type: none"> – Tonoplast disruption after cell is dead – Cysteine proteinases Cathepsyn/VPes (vacuolar processing enzyme) (no hydrolases) – Metacaspases 	<ul style="list-style-type: none"> – Tonoplast disruption without destruction of organelles (early) 	<ul style="list-style-type: none"> – Tonoplast permeabilization, not rupture – Increase cysteine proteinases – Hydrolases released from dead cells
Cellular morphology and organelle behavior	<ul style="list-style-type: none"> – Migration of nucleus to infection site, Brownian motion of organelles, mitochondrial swelling, nucleus condensation and cessation of cytoplasm streaming, shrinkage of protoplast and collapse of cytoplasm, vacuolization and chloroplast disruption at the end 	<ul style="list-style-type: none"> – Mitochondria swelling, absence of lytic vacuoles. Protoplast shrinkage 	
Examples and exceptions	<ul style="list-style-type: none"> – Victorin toxin, from a necrotroph, causes HR to colonize host 	<ul style="list-style-type: none"> – <i>B. cinerea</i> produces oxalic acid and botrydial – FB1 toxin by <i>Fusarium verticillioides</i> 	

*Information collected from Morel and Dangl, 1997; van Doorn *et al.*, 2011a, van Doorn, 2011b; Coll *et al.*, 2011.

Hypersensitive Response (HR)

The first observation and description of HR was done in 1902 by Ward, studying the pathosystem wheat–*Puccinia glumarum*. The “**Hypersensitive**” term was coined some years later by Stakman (1915), still working on wheat-*P. graminis*, in an attempt to describe an “abnormally fast death cell” produced in the contact with the mentioned rust pathogen (Mur *et al.*, 2008).

Nevertheless HR can be largely defined as a form of cellular death (non-apoptotic) often associated with a resistance defense response. It is fast and occurs in the area immediately surrounding infection point. It can be triggered by several pathogens and/or elicitors within few hours.

So while HR is a cell death consequence of a resistance mechanism (recognition must happen). **Necrosis** instead, is a cell death consequence of the process of disease (Morel and Dangl, 1997).

As a general rule, HR is efficient against biotrophic and obligated pathogens, as a way to stop them from propagating by deprivation of water and nutrients. However, HR can also help to stop some necrotrophs, by releasing toxic content from vacuoles and producing desiccation, so creating an antimicrobial environment (Morel and Dangl, 1997; Coll *et al.*, 2011; Mengiste *et al.*, 2012; Wen, 2013).

HR seems to be an active process that requires transcriptional activation and gene expression. ROS, ion fluxes, NO (nitric oxide), SA, and sphingolipids are associated and important regulators of HR (Torres *et al.*, 2006; Mur *et al.*, 2008; Velosillo *et al.*, 2010; Berkey *et al.*, 2012; Wang *et al.*, 2013). This would explain why chloroplasts are targeted by some pathogens (Lorrain *et al.*, 2003; Jelenska *et al.*, 2007; Berkey *et al.*, 2012; Kangasjarvi *et al.*, 2012; Stael *et al.*, 2015).

In fact, there is a subtle overlapping between PTI and HR during ETI that includes SA accumulation, ROS and NO, MAPK cascades, ion fluxes, transcriptional reprogramming and synthesis of secondary metabolites (Coll *et al.*, 2011; Wen, 2013).

HR can be recognized by the presence of yellowish-brown spot that correspond to the death cells at the infection site (Figure 24). However HR can also happen without cell death. This indicates that HR represents a phenomenon of resistance beyond the cell death itself, since cell death does not seem to be necessary for resistance (Morel and Dangl, 1997; Coll *et al.*, 2011; Stael *et al.*, 2015). Moreover, the recent advances on metacaspases (see below) show how disease resistance and cell death are uncoupled processes (Coll *et al.*, 2010; 2011; 2014; Stael *et al.*, 2015).

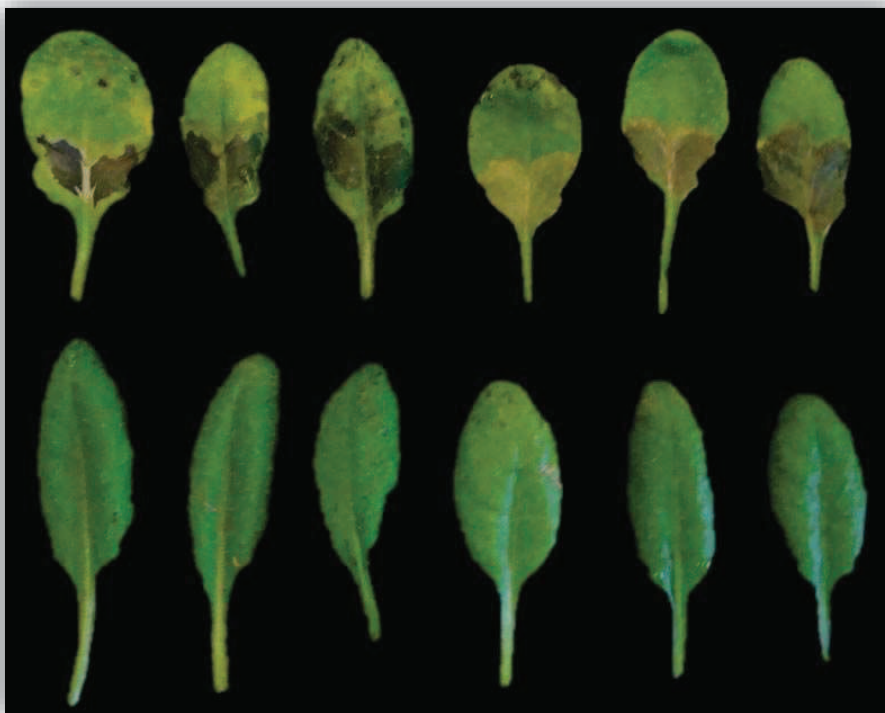


Figure 24: Picture of Col-0 plants non-infected (bottom) and infected (upper row) with *Pseudomonas syringae* pv. *tomato* DC3000 *avrRpm1* showing the HR lesion in the infected area.

The way in which regulation of HR cell death in plants occurs has not been fully elucidated. Two separate branches seem to exist (Coll *et al.*, 2011):

1- **Depending on *NDR1***: mediated by CC-NB-LRR protein receptors

2- **Depending on *EDS1* /*PAD4* /*SAG 101* (senescence)**: mediated through TIR-NB-LRR protein receptors

Both systems integrate ROS signaling and SA accumulation.

At the same time, a mechanism must exist to regulate cell death when it is enough or not needed. [ROS](#) and [NO](#) cross-talk and are important regulators, as described later in this section. In addition *Arabidopsis* zinc finger protein LSD1 (lesion simulating disease resistance) is a transcriptional regulator of cell death effectors (Dietrich *et al.*, 1997; Coll *et al.*, 2011). LSD1 can activate Cu/Zn SOD genes (superoxide dismutase) and can act negatively on some proteins to suppress cell death (Mur *et al.*, 2008; Coll *et al.*, 2010, 2011, 2014). It is hypothesized that LSD1 stops propagation of cell death by inhibiting metacaspase1 (MC1) (Coll *et al.*, 2010, 2011, 2014). For a contrasting effect, the LOL proteins (LSD one like) promote cell death (Mur *et al.*, 2008; Coll *et al.*, 2011), and other proteins have also been

mentioned has a part of the “*LSD1 Deathsome*” such as AtbZIP10, LIN1, IAA8, all of them promoting cell death. (Coll *et al.*, 2011).

For several years, intensive research was focused on caspases or analogs in plants. Caspases are a family of cysteine proteases present in animal cells, which coordinate apoptotic cell death (Coll *et al.*, 2011; Coll *et al.*, 2014). The γ -VPE (vacuolar processing enzyme) protein, has caspase-1 activity during HR in *Arabidopsis*, and has been considered one of the major effectors of HR cell death (vacuolar behavior). γ -VPE accumulates in vesicles that then are targeted to vacuole to activate hydrolytic activities (Mur *et al.*, 2008).

Metacaspases were also found in plants. While caspases from animals cleave their targets after an aspartate residue, plant metacaspases can cleave their targets after arginine or lysine residues (Vercammen *et al.*, 2004; Coll *et al.*, 2010; 2011).

AtMC1 and AtMC2 (*A. thaliana* metacaspases 1 and 2) are antagonistic metacaspases regulating HR cell death (Coll *et al.*, 2010). AtMC1 promotes cell death via interaction with LSD1 (the master switch-off regulator of cell death). AtMC2 negatively regulates AtMC1, then suppressing cell death by a still unknown mechanism (Coll *et al.*, 2010; 2011; 2014).

A holistic and integrative representation of the HR phenomenon will be shown below in Figure 29, after some consideration and details about ROS, NO and the oxidative burst, all highly relevant in the establishment of HR.

The role of ROS and NO in HR

Reactive oxygen species (ROS) and reactive oxygen intermediaries (ROI) are continuously produced in the plant as a consequence of the aerobic metabolism (Figure 25).

ROS are produced mainly at chloroplasts, peroxisomes, mitochondria (may be less studied in plant-pathogen interaction), apoplast, but also in the cytoplasm, endoplasmic reticulum, endomembrane vesicles and nucleus (Apel and Hirt, 2004; Gadjev *et al.*, 2008; Velosillo *et al.*, 2010; Stael *et al.*, 2015).

They cause oxidative damage to proteins, nucleic acids and lipids (Apel and Hirt, 2004; Gadjev *et al.*, 2008; Velosillo *et al.*, 2010).

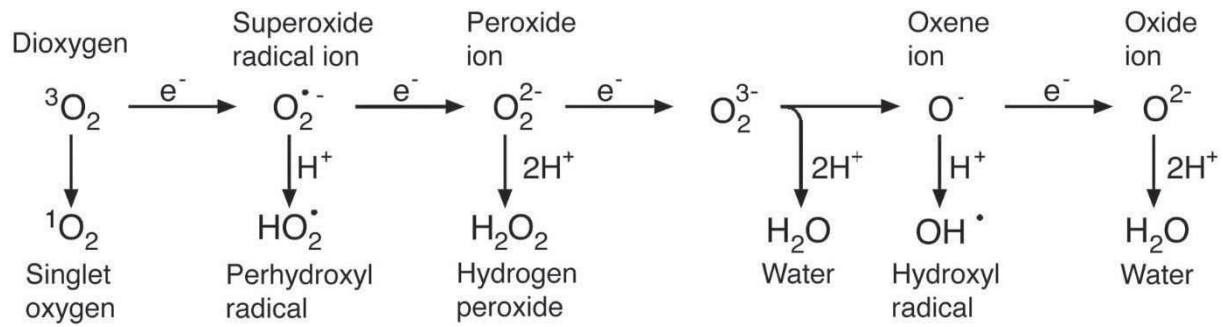


Figure 25: Generation of different ROS.

From Apel and Hirt, 2004.

In an evolutionary context of increasing levels of atmospheric oxygen and oxygen-evolving organisms, plants developed highly efficient systems to scavenge and/or detoxify ROS (Foyer and Noctor, 2005; Breusegem and Dat, 2006). Plants both produce and have enzymatic and non-enzymatic mechanisms to rapidly detoxify ROS (Torres *et al.*, 2006).

Non enzymatic systems include: ascorbate and glutathione (GSH), tocopherol, flavonoids, carotenoids and alkaloids. Enzymatic scavenging includes: superoxide dismutases (SOD), ascorbate peroxidases (APX), glutathione peroxidases (GPX) and catalases (CAT) (Apel and Hirt, 2004; Gadjev *et al.*, 2008) (Figure 26).

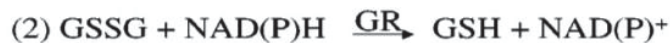
Superoxide Dismutase



Catalase



Glutathione Peroxidase Cycle



Ascorbate-Glutathione Cycle



Figure 26: Enzymatic scavenging of ROS by superoxide dismutase (SOD), catalase (CAT), the ascorbate-glutathione cycle, and the glutathione peroxidase (GPX) cycle.

From Apel and Hirt, 2004.

Additionally, ROS are used by the plant as a signal to orchestrate several processes related to development and stress response, such as defense, stomatal behavior and cell death (Apel and Hirt, 2004; Torres *et al.*, 2006; Gadjev *et al.*, 2008; Mittler *et al.*, 2011; Wang *et al.*, 2013). Rapid accumulation of ROS and NO occurs in plant cells under biotic or abiotic stress.

ROS signaling is the consequence of a dynamic between the production and scavenging, within the cell, among organelles and among cells in long distances, in a sort of “auto-propagating wave” (Mittler *et al.*, 2011).

ROS are very versatile signaling molecules, with different properties and mobility within the cells. ROS molecules (Figure 25) can be easily interconverted into less reactive forms, more mobile through membranes and water channels. For example: the radical superoxide is less diffusible than other ROIs and can be dismutated to H₂O₂ which is more diffusible. Then H₂O₂ can diffuse and activate many defense responses, including HR, SAR, or phytoalexin production (Apel and Hirt, 2004; Torres *et al.*, 2006; Gadjev *et al.*, 2008; Chaouch *et al.*, 2012).

The rapidity of ROS production and the potential of H₂O₂ to freely diffuse across membranes strongly suggest that ROS could function as an intercellular or intracellular second messenger. ROS signaling cascade can act on peptides, hormones, lipids, cell components, calcium channels, MAPK, WRKY. ROS causes strengthening of cell wall, callose deposition, lipid peroxidation and membrane and cell damage, and also mediates gene activation with SA and NO (Lamb and Dixon, 1997; Foyer and Noctor, 2005; Torres *et al.*, 2006; Gadjev *et al.*, 2008; Velosillo *et al.*, 2010; Mittler *et al.*, 2011).

Nitric oxide (NO) and intermediates (NOIs) have a key role in defense reaction against bacterial pathogens and trigger HR. Produced mainly by chloroplast and mitochondria, NO has several targets and can form diverse molecules called “reactive nitrogen species” (RNS) such as NO radicals (NO⁻), nitrosonium ions (NO⁺), peroxyxynitrite (ONOO⁻), S-nitrosothiols (SNOs), higher oxides of nitrogen (NO_x) and dinitrosyl-iron complexes (Wang *et al.*, 2013).

NO, together with H₂O₂, is an important mediator in defense response signaling (Chen *et al.*, 2014). NO upregulates genes involved in the phenylpropanoid pathway (Polverari *et al.*, 2003), SA pathway (Chen *et al.*, 2014) and SAR (together with ROS) (Wang *et al.*, 2014). NO regulation also includes MAPK and WRKY as targets (Wang *et al.*, 2014).

One of the earliest responses in plant–pathogen interactions is the **oxidative burst** caused by ROS and NO accumulation, either acting independently or synergistically (Torres *et al.*, 2006; Wang *et al.*, 2013). The oxidative burst consists in a characteristic increase and a biphasic accumulation of ROS at the site of infection (Lamb and Dixon, 1997, Torres *et al.*, 2006, Wang *et al.*, 2013). During the **phase I**, a fast and transient accumulation of ROS is produced with no regard to the type of pathogen, interaction or elicitor (*i.e* wounding can cause it too). The **phase II** is stronger and extended in duration. It will occur only under specific interactions leading to resistance and HR and is a feature of ETI (Figure 27).

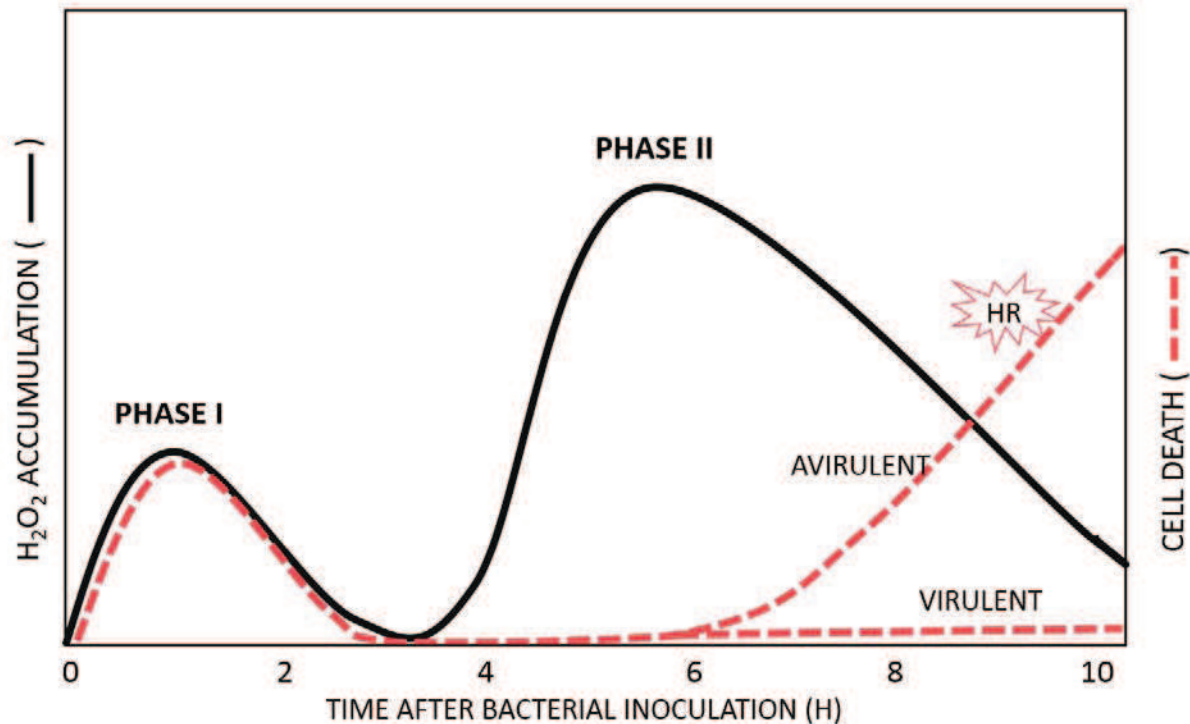


Figure 27: Biology of the oxidative burst: kinetics of H₂O₂ accumulation in HR response.

Infection with avirulent/virulent strain will cause a rapid, unspecific and transient increase of ROS accumulation within few hours (Phase I). Only in avirulent interactions, a second phase (Phase II), stronger and prolonged in time, will occur, that will lead to HR as a consequence of a specific event of recognition and resistance. From Lamb and Dixon, 1997.

In *Arabidopsis*, ten homologues of NADPH oxidases from mammalian neutrophils have been described: the *rboh* genes (respiratory burst oxidase homologues) (Torres and Dangl, 2005; Heller and Tudzynski, 2011, Suzuki *et al.*, 2011). Among them, *AtrbohD* and *AtrbohF* mainly are responsible for oxidative burst and ROS generation during avirulent interactions (Torres *et al.*, 2002; Chaouch *et al.*, 2012). Apoplastic peroxidases have also been described (Torres *et al.*, 2006).

The overall role of NO and ROS in HR and plant cell death appears as highly complex, mediated by cross-talk with several plant hormones and several targets proteins where regulation can occur in both directions. A compilation of such cross-talk can be seen in Figure 28, where this complexity is illustrated.

Induction pathways of HR

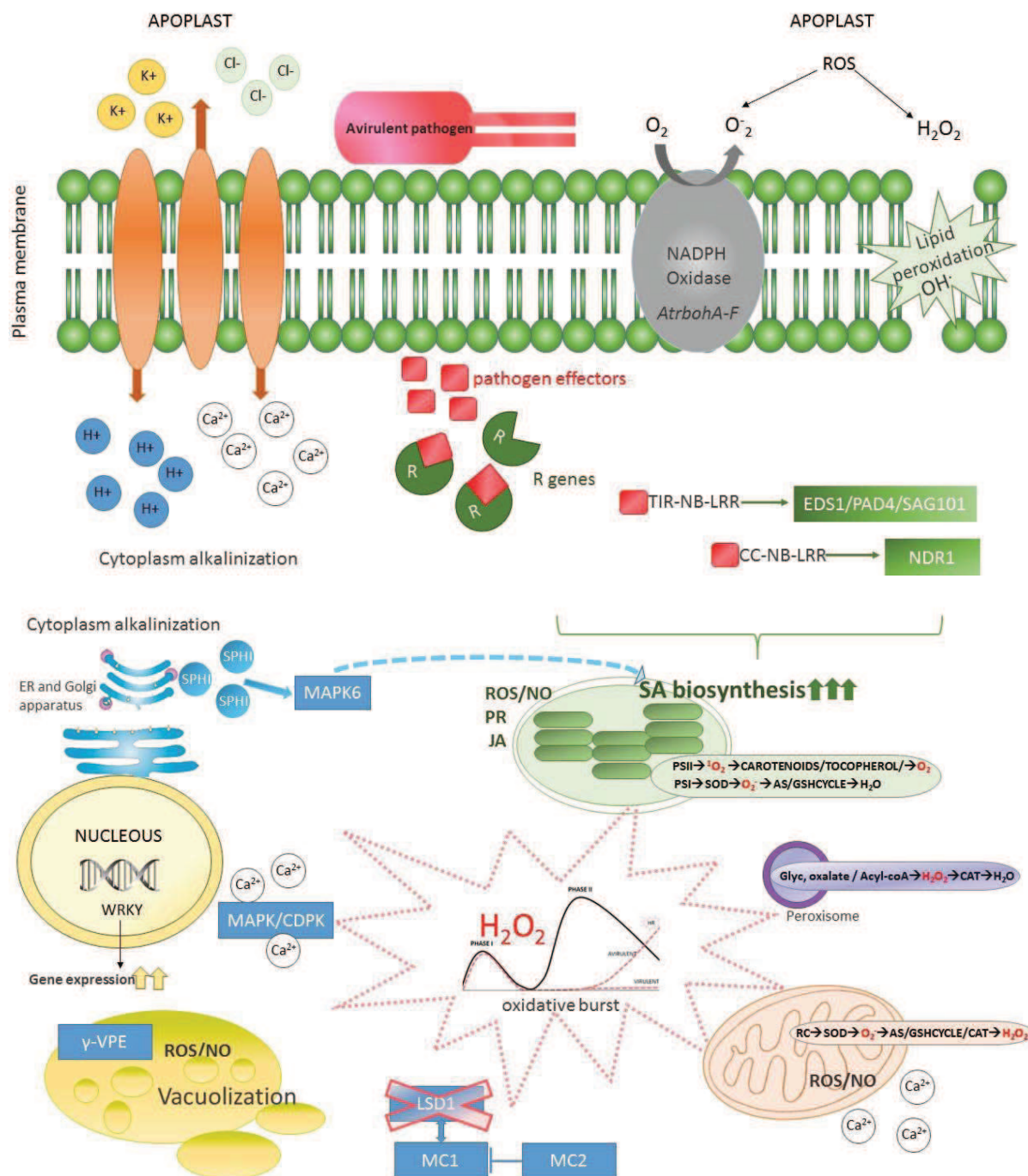


Figure 29: The induction pathway of HR.

Initial recognition of the pathogen (R-avir) triggers oxidative burst and ion fluxes. ROS, NO and Ca^{2+} are intimately connected, potentiating cell death. An uptake of Ca^{2+} , export of Cl^- , K^+ by ATPases, and H^+ cause alkalization of the cytoplasm, and activation of MAPK. MAPK6, for instance, plays an important

role in SA depending-HR, probably is a potential target of sphingolipids (then a link with SPI-CD, mechanism from necrotroph to control cell death) (Berkey *et al.*, 2012). Calcium signatures are also decoded by CDPKs. MAPK and CDPKs trigger gene expression in the nucleus, through WRKY. NADPH oxidases (AtrbohD-F) and peroxidases assist the oxidative burst, callose deposition and defense related-gene expression. ROS and Ca^{2+} waves supported by Atrboh and CDPK5 proteins, travels from cell to cell (SAR) and can activate NPR1 (master regulator of SAR) (Mittler *et al.*, 2011; Stael *et al.*, 2015). Two regulatory branches of HR are shown. The branch **NDR1** and the branch **EDS1/PAD4/SAG101**. SA accumulation increases in local cells and the signal is spread to adjacent and distant tissues (via SA, ion influxes, Ca^{2+} , ROS (Atrboh /CDPK5)), reaching NPR1. ROS (hydrogen peroxide, superoxide anion radical, singlet oxygen) are produced in different cellular compartments (chloroplast, mitochondria, peroxisomes). Major enzymes and non-enzymatic components involved in ROS homeostasis are briefly indicated. In the chloroplastic ROS branch, $^1\text{O}_2$ and H_2O_2 , CAS (calcium sensing proteins) and light are shown to induce SA biosynthesis (ICS1 and ICS2). Finally, **LSD1** and **MC1** promote cell death, while **MC2** inhibits it. **MC2** plays important roles in adjacent cells by preventing cells death when it is not needed.

Abbreviations: **ROS**: reactive oxygen species, **CDPKs**: calcium-dependent protein kinases, **LSD1**: lesion stimulating death 1 protein, **MC1 and MC2**: metacaspases 1 and 2, **PSI**: photosystem I, **PSII**: photosystem II; **RC**: respiratory chain, **SOD**: superoxide dismutase, **CAT**: catalase, **As/GSH**: ascorbic acid/glutathione, **Glyc oxidase**: glycolate oxidase, **SPHI**: sphingolipids, **γ -VPE**: vacuolar processing enzyme.

HR: ecological cost and trade-off

No doubt HR is a fascinating phenomenon that has captivated researchers since the beginning of the 1900's. An open question is still whether HR has a "social role" amplifying signal for the rest of the plant, or if it is just the "consequence" of a cascade of events following plant pathogen interactions that leads to death.

In more detail, if there is a "social role", it implies that the cell in contact with the pathogen, will overreact and amplify signals to the adjacent cells before committing suicide. Then, if HR is not an adaptive response to counteract pathogen invasion, at least it makes sense in a context of LAR and SAR, coordinating defense at neighboring cells and in prevention of secondary infection (Coll *et al.*, 2011).

On the contrary, if it is considered just as a "consequence" of defense responses, HR will mean that the toxicity of intermediates and defense responses within the plant and against the pathogen causes death of both pathogen and host in a sort of "collateral damage effect" scenario.

Whether it is a cause or a consequence or both, to develop HR supposes a cost for the plant because, if HR implies to sacrifice a few cells to stop the progress of a biotrophic pathogen, at the same time it implies the risk of having an entry door for necrotroph pathogens (even though it was mentioned before that it can stop some necrotrophs).

As in any situation of resistance, the cost of allocating resources to stop one type of pathogen also implies the cost of increased sensitivity against a second type of pathogen (Kliebenstein and Rowe, 2008).

In this context, necrotroph pathogens may suppose an ecological cost for plants developing HR as a strategy to counteract biotrophic invasions. How does the plant cope with such contrasting lifestyles giving precise and accurate responses in an ecological context of cost, fitness and trade-offs?

Kliebenstein and Rowe (2008) and Spoel *et al.*, (2007) analyzed the ecological cost of such contrasting mechanism through a three way model:

- Local cost of having HR: activation of HR increases sensitivity to necrotroph in the HR area because creates an entry point, but at the same time, when the signaling cascade has been activated, impairs necrotroph colonization in adjacent areas (LAR-SAR). Thus local HR implies an ecological risk that will rely in space and time restraints.

- Organismal cost of having HR: [The zigzag model](#) of plant disease resistance stated a threshold for effective resistance and HR. The threshold for HR is defined as a “*potential ecological cost of biotroph resistance prompted by sensitivity to necrotroph pathogens*”. In this sense, plants in environment with mainly biotroph pathogens will have lower threshold for HR, while in environments with high necrotroph pressure the threshold will be higher. In this matter, necrotroph pathogens have virulence factors that they can use to manipulate host cell death mechanism and activate HR generating another potential ecological cost (Figure 30). Then plants under environment with high necrotrophic pressure will have to develop higher threshold for HR. Evidence supporting this concepts confirm that necrotroph virulence can be enhanced in environment where the threshold for HR is lower. ROS can also influence the threshold (Govrin and Levine, 2000). R genes can be targeted by necrotroph to manipulate HR.

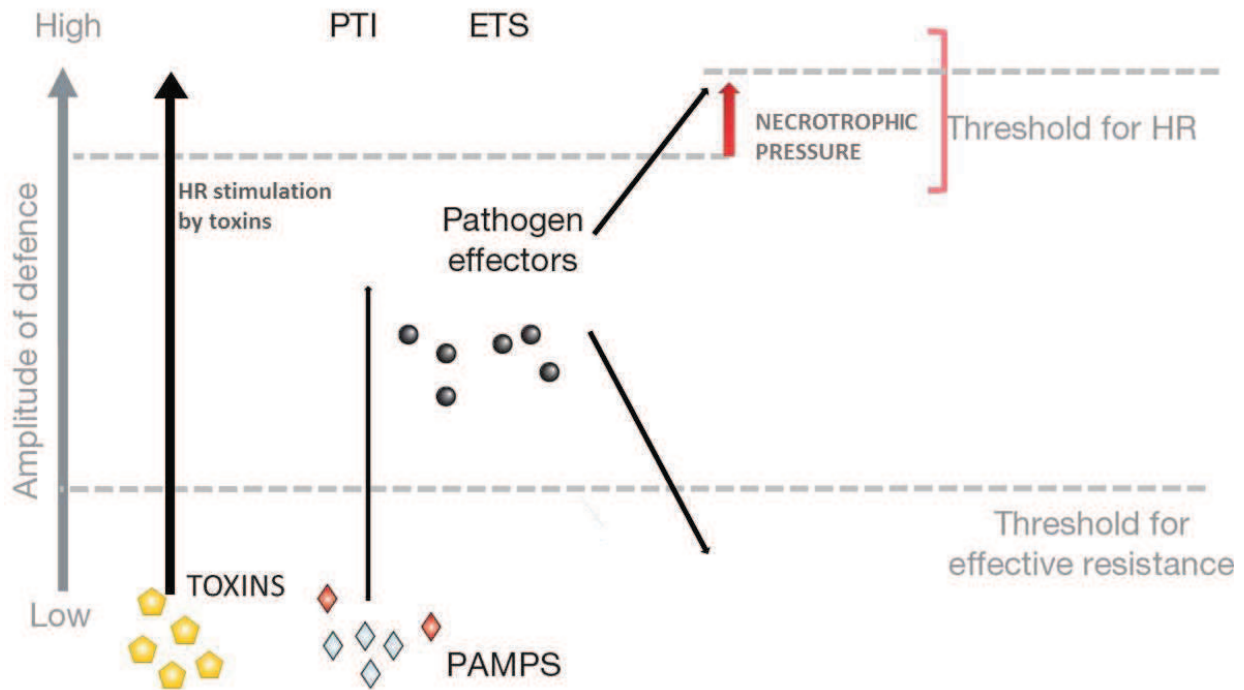


Figure 30: The zigzag model of plant disease resistance proposed by Jones and Dangl (2001) and modified by Kliebenstein and Rowe (2008) showing the threshold for HR under situation of necrotrophic invasion.

Necrotroph pathogens can stimulate HR responses by using toxins and causing cell death (examples in [Table 7](#)). The threshold for HR, as presented in the figure, would be higher or lower according to the environmental pressures and the dominant pathogen lifestyle. The ratio biotroph/necrotroph will place evolutionary pressure over the threshold for HR in a given environment or interaction. Figure modified from Kliebenstein and Rowe, 2008.

- SA/JA antagonism: As is well known, SA plays a prominent role in defense responses against hemi(bio)troph, while JA prevails against necrotroph, herbivores and wounding. In this sense, the stimulation of SA pathways leads to the repression of the JA pathway, generating an ecological cost from the trade-off between both signaling pathways. However this trade-off is tightly controlled depending on the type of pathogen and space features, as is the case for HR. When a plant is infected by a virulent biotroph, SA dependent defense responses are activated in local and adjacent tissues, creating a correlated inverse gradient of JA in systemic tissues (Figure 31, panel A). On the contrary, when the plant is infected with an avirulent biotroph (R mediated responses), the SA gradient is activated in local and adjacent tissues, but it is no

enough to suppress JA responses in distant tissues (no gradient), which suggests a mechanism to evade the cross-talk (Spoel *et al.*, 2007) (Figure 31, panel B).

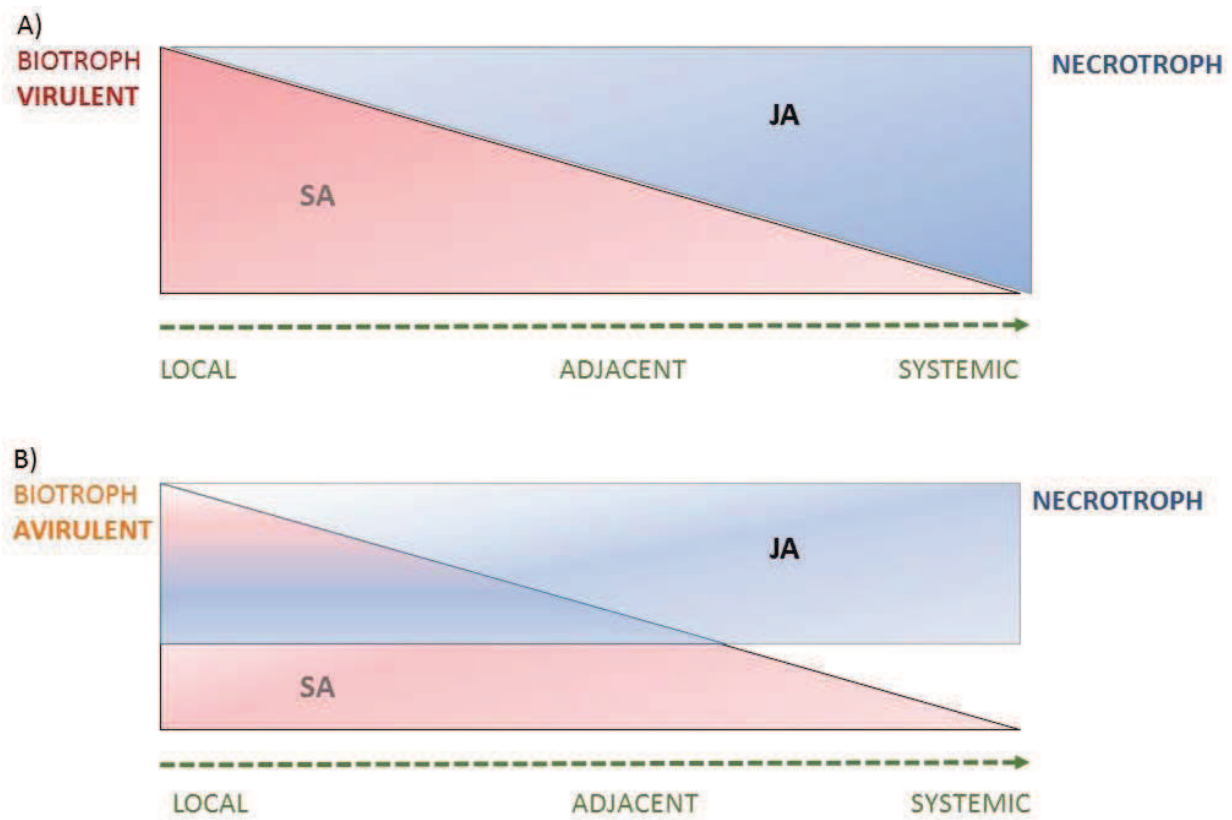


Figure 31: Model of SA-JA trade-off between plant defenses against biotrophs and necrotrophs with tissue spatial variation.

A) Model proposed for spatial regulation in a virulent interaction: SA dependent defense responses are activated in local and adjacent tissues against biotroph, creating a correlated inverse gradient of JA in systemic tissues, launched against necrotroph. In distant tissues, SA signaling is low, and biological trade-off is reduced. B) Model proposed for spatial regulation in an avirulent interaction: SA gradient is activated in local and adjacent tissues, but is not enough to suppress JA responses in distant tissues (no gradient), suggesting a mechanism to evade the cross-talk under these circumstances. Figure from Spoel *et al.*, 2007.

SAR

When a plant meets a pathogen or a pest it can retain a memory of the encounter.

Such “memory” acts as a form of an “immunological memory” allowing the plant to develop faster and stronger responses against secondary infections in distal (unaffected) tissues and against further attacks (Grant and Lamb, 2006; Spoel and Dong, 2012; Dempsey and Klessig, 2012; Fu and Dong, 2013; Shah *et al.*, 2014).

After a single locally restricted infection, the whole plant becomes resistant. The phenomenon is known as “Systemic acquired resistance” (SAR) (Ross, 1961).

Unlike the animals' immune system, this is a systemic broad-spectrum immune response with no specificity toward the initial infection agent (Fu and Dong, 2013). In fact, the induction of SAR is a process of “priming” that can last weeks or months or through the progeny (Luna *et al.*, 2012; Fu and Dong, 2013).

Besides the ability to activate SAR provides the plant with a fitness advantage (Heil, 1999) that seems to be valid not only at the present generation, but also for the subsequent ones in a phenomenon that has been called “next generation SAR” or “transgeneracional SAR” (Luna *et al.*, 2012; Luna and Ton, 2012).

SAR is triggered over the local and distal presence of SA (Dempsey *et al.*, 2011; Spoel and Dong, 2012) but also in concurrence with some other metabolites such as (Figure 32):

- azelaic acid (AzA) (a dicarboxylic acid)
- methyl salicylate (MeSA)
- dehydroabietal (DA) (an abietane diterpenoid)
- L-pipecolic acid (Pip) (a catabolite from Lys)
- glycerol-3-phosphate (G3P)

These metabolites serve as candidates for mobile signals between the infected and uninfected tissues of the plant. The phloem seems likely to be the channel used by the mobile signal(s) (Dempsey and Klessig, 2012; Shah *et al.*, 2014).

Their role in SAR helps to provide suitable adaptive responses facing diverse environmental contexts.

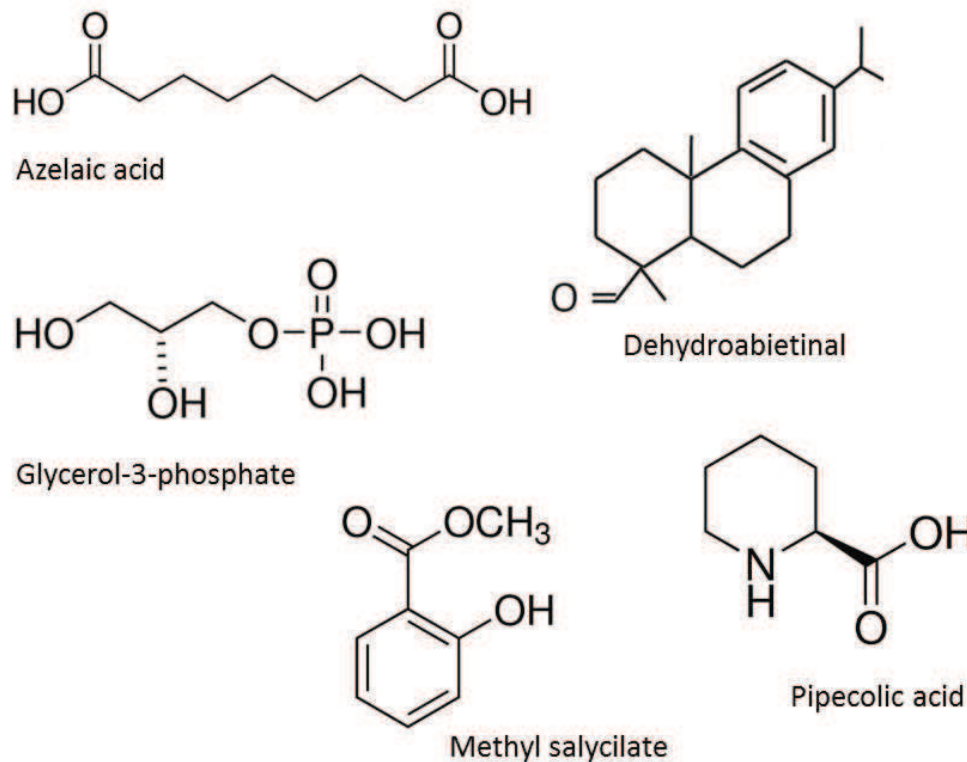


Figure 32: Chemical structure of metabolites putatively involved in systemic acquired resistance in *Arabidopsis thaliana*.

The networking of small metabolites in SAR

When the plant comes across an avirulent pathogen, ETI is triggered. HR occurs at the site of infection and SAR is activated in the secondary tissues.

In opposition to ETI, SAR is not associated with cellular death because the increase of SA promotes cell survival (Fu *et al.*, 2012; Fu and Dong, 2013).

The onset of SAR implies a considerable transcriptional reprogramming, largely dependent on NPR1 (Durrant and Dong, 2004; Spoel and Dong, 2012). The paralogs NPR3 and NPR4 regulate the stability and activity of NPR1 (Fu *et al.*, 2012)(see below).

Levels of SA, SAG/SEG ([SA-Glycosides](#)), and PR1 increase in pathogen-infected tissues, but also in the non-infected tissues (Durrant and Dong, 2004; Dempsey *et al.*, 2011; Spoel and Dong, 2012).

However it is less clear whether SA is *de novo* synthesized or whether SA or its derivatives such as glycosides or MeSA are transported in the non-infected tissue (Attaran *et al.*, 2009; Singh *et al.*, 2013).

MeSA, AzA, DA, G3P are proposed to be implicated in SAR signaling as long distance messengers through the phloem (Dempsey and Klessig, 2012; Fu and Dong, 2013; Shah *et al.*, 2014). Conversely, although Pip is highly accumulated in distant tissues and petiole exudates, its role in long-distance communication is not clear (Dempsey and Klessig, 2012; Návárová *et al.*, 2012; Shan *et al.*, 2014).

All these metabolites contribute to SAR by functioning upstream and/or by priming or increasing SA signaling (Shah *et al.*, 2014).

A schematic representation of the signal network in SAR defense responses is shown in Figure 33. A concise description is given in the text below.

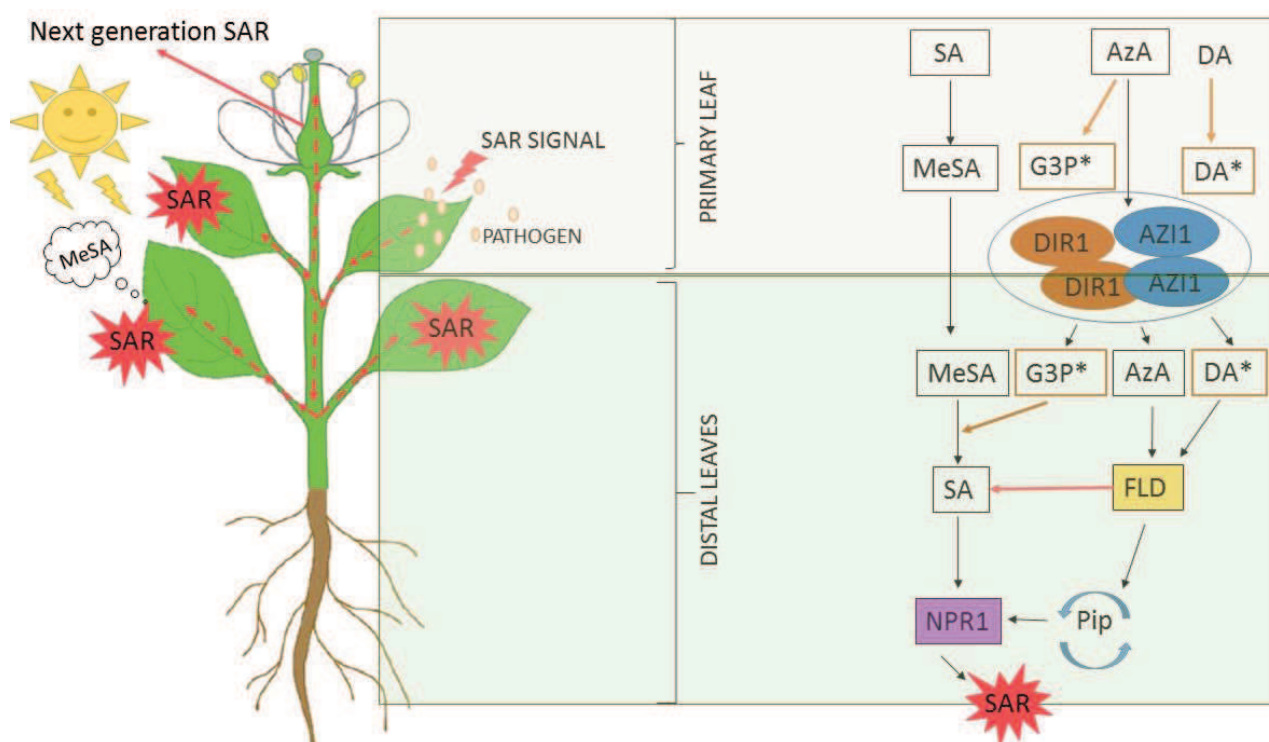


Figure 33: Schematic representation of the current model of systemic acquired resistance (SAR) signaling.

Abbreviations: **SA**: salicylic acid, **MeSA**: methyl salicylate, **AzA**: azelaic acid, **DA**: dehydroabietal, **G3P**: glycerol-3-phosphate, **Pip**: pipercolic acid, **DIR1**: defective in induced resistance 1), **AZI1**: azelaic acid-induced 1, **FLD**: flowering locus d. The activated forms G3P and DA are depicted by an asterisk (G3P* and DA*) and **framed in orange** to denote the change of status from inactive to active. **Red arrows** point to the flux of metabolite signaling from local pathogen-induced tissues to distant uninfected tissues. The sun represents the effects of light on MeSA metabolism (according to Liu *et al.*, 2011). Next-generation SAR is also represented in the germinal tissues of the flower. Illustration adapted from Shah *et al.*, 2014. Explanations in the text below.

MeSA, AzA and G3P levels increase after a tissue is challenged by an avirulent pathogen (Shah *et al.*, 2014). In addition, AzA is thought to activate G3P (G3P*) (Jung *et al.*, 2009).

DA levels remain constant. An activated form of DA (DA*) is also present. DA* is rapidly translocated under SAR scenarios and is a strong activator of SAR (Chaturvedi *et al.*, 2012).

SAR responses linked to DA* have strong effects on regulation of SA biosynthesis. In addition, DA* promotes FLD (flowering locus D), a critical component of SAR (Sigh *et al.*, 2013). What is more, some synergistic effect of DA* and AzA has also been observed (Fu and Dong, 2013).

FLD is essential for SA synthesis and accumulation, PR1 expression and related regulators in SAR at distal tissues (Sigh *et al.*, 2013). FLD is also required for AzA induction of SAR (Sigh *et al.*, 2013).

G3P* is present in local and distal tissues. The systemic increase of G3P* is probably due to *de novo* synthesis, however transport via DIR1 has also been described (Chanda *et al.*, 2011). G3P* is also a regulator of MeSA conversion into SA at local tissues (Chanda *et al.*, 2011).

Additionally, a lipid-transfer protein called DIR1 (defective in induced resistance 1) is also transported to the distal tissues (Champigny *et al.*, 2011). DIR1 interacts with another protein called AZI1 (azelaic acid induced 1), a secreted protease inhibitor /seed storage protein/lipid transfer protein. DIR1 and AZI1 are presumed to interact in a sort of "SAR signalome" that is also required for G3P*, AzA and DA*. DIR1 and AZI1 enhance the sensitivity to DA* (Shah *et al.*, 2014).

Whether DIR1 binds DA*, AzA, G3P* directly or indirectly is not clear (Dempsey and Klessig, 2012).

AZI1 seems to play a role more related to transport/production of the SAR mobile signal, than in perception itself (Jung *et al.*, 2009; Dempsey and Klessig, 2012).

AzA works through the protein FLD, with a priming effect on SAR. AzA itself cannot prime for SA signaling and SAR (Jung *et al.*, 2009). On the other hand, FLD is also suggested to work on Pip. Thus probably the role of AzA is also dependent on Pip (Shah *et al.*, 2014).

Pip increases in response to several stresses. It can accumulate in both local infected tissues and distant uninfected ones (Návarová *et al.*, 2012). However it is uncertain if it has a direct role in the long-distance communication. The assumption is that Pip may induce SAR by regulating its own synthesis and priming SA accumulation in distal tissues (Dempsey and Klessig, 2012). It seems that Pip has a pivotal role in defense amplification such as camalexin biosynthesis and accumulation, SA biosynthesis, defense-related gene expression and priming of SAR (Návarová *et al.*, 2012).

Finally, activation of NPR1 by SA signaling ends in SAR. NPR1 is a master regulator of SAR through is adapter [NPR3-NPR4](#) (see below).

In addition redox status, ROS, NO, WRKY transcription factors, ER proteins and DNA repair play significant roles in SAR. A recent Cell Reports (Wang *et al.*, 2014) proposed NO (nitric oxide) as the triggering signal upstream of ROS, Aza, and G3P during SAR.

Some words about MeSA and JA

In tobacco, it has been shown that MeSA can act as an airborne signal for SA synthesis (Park *et al.*, 2007). The authors proposed that locally synthesized SA is converted to biologically inactive MeSA by a methyltransferase, then mobilized to the distant tissues and converted into SA through a methyl salicylate esterase, the SABP2 (salicylic acid-binding protein 2). Similar results were found in potato (*Solanum tuberosum*) (Manosalva *et al.*, 2010).

Conversely, in *Arabidopsis* the function of MeSA seems to be less clear. While the work of Vlot *et al.*, (2008) proposed MeSA as a conserved SAR signal in *Arabidopsis* and tobacco, Attaran *et al.* (2009) found that MeSA was not essential for SAR in *Arabidopsis*.

MeSA strongly increases in SAR tissues but much of it, is also volatilized to the atmosphere, making it unlikely as the phloem-mobile signal.

In other contexts, MeSA acts as an airborne signal for pollinator attraction and defense against herbivore insects. Some priming effects in neighboring plants has been also reported (Zhu and Park, 2005; Attaran *et al.*, 2008; Heil, 2014). However Attaran *et al.* (2009) found that methyltransferases knock-out mutant (*bsmt1-3*) were intact showing SAR. Thus, if MeSA was critical for SAR, even as an airborne signal, mutants lacking MeSA should lack SAR, which was not the case.

They additionally stated that accumulation of SA in distal tissues was not dependent on MeSA translocation and supported the theory of *de novo* synthesis for SA.

They also indicated that JA is not involved in SAR signaling since *Pseudomonas* could be using coronatine, mimicking JA, to provoke the volatilization of SA. This could be done by a JA-mediated inter-conversion of SA to MeSA, lowering SA pool by manipulating host SA-JA crosstalk.

In this context, Liu *et al.*, (2011) observed a correlation between MeSA induction of SAR and exposure to light that might contribute to clarify the inconsistency found between tobacco, potato and *Arabidopsis*. *In extenso*, they observed that wild type primary infected plants (avirulent pathogen) showed stronger MeSA induction of SAR when inoculated during the morning than during the afternoon. However wild type plants primary infected in the afternoon showed SAR responses more dependent on MeSA. Thus, MeSA role in SAR seems to rely on the interaction with light, amplifying the

magnitude of SAR in plant inoculated under longer exposure to light but with a crucial effect in plant inoculated under light deficiencies.

Furthermore, the prospect of a less conserved SAR mechanism across species cannot be ruled out. Most studies on SAR have been conducted in a few species like tobacco, potato, tomato, *Arabidopsis*, cucumber, corn and rice. Probably there are some other ways and circumstances.

Interaction of DIR1-G3P*-MeSA and interaction DA-MeSA has been also suggested. However, more studies are required, taking in consideration how the light exerts an effect on MeSA mediated SAR.

JA and SAR

In the work of Truman *et al.*, (2007), JA was considered as the mobile signal of SAR in *Arabidopsis*. They found a rapid accumulation of JA in distal tissues at 6 HPI (hours post infection) before returning to normal levels at 11 HPI. As in responses to herbivores attack or wounding, an intense transcriptional reprogramming and *de novo* synthesis was produced. In agreement with this results, they proposed that under this scenario JA-SA were acting in phases, with a rapid and strong initial signaling of JA followed by a subsequent SA-phase as the definitive signal for SAR establishment.

Following in the same line, Chaturvedi *et al.*, (2008) found that JA did not co-purify with the SAR-inducing activity ratifying that JA was not the mobile signal in SAR. Likewise Attaran *et al.*, (2009) as it was mentioned before, endorsed the idea of no role for JA in SAR.

On the other hand, in tobacco, the hypothesis seems to be more appropriate (Grant and Lamb, 2006; Park *et al.*, 2007).

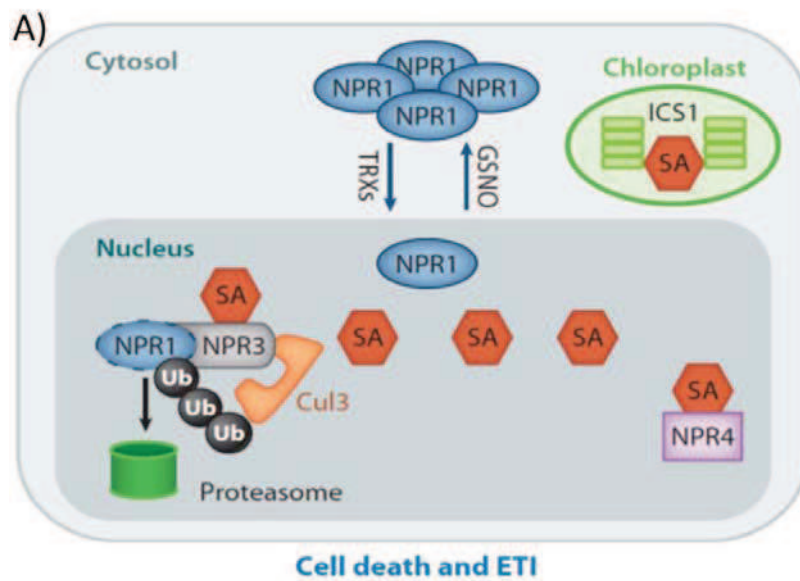
The role of JA in SAR is still under debate as for MeSA. In the latest review about SAR, presented by Dempsey and Klessig (2012) and by Fu and Dong (2013) the controversy still remains unresolved. In other reviews from Shah and Zeier (2013) and Shah *et al.*, (2014) JA has not even taken into account as a putative molecule in SAR networking.

The role of NPR1 and SAR

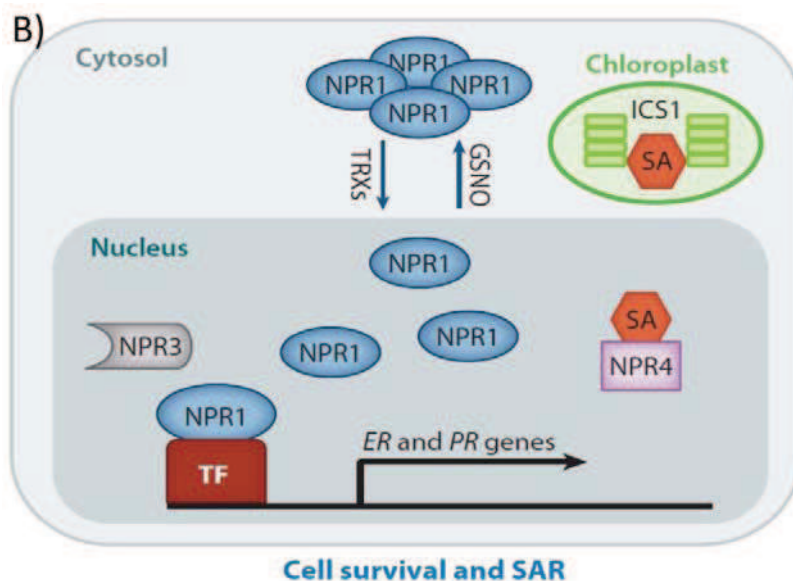
After a pathogen challenge, the oligomeric form of NPR1 is monomerized and translocated to the nucleus where it acts on TFs (transcription factors) to activate defense signaling cascades (see [hormones signaling](#))

NPR1 nuclear accumulation was shown to be essential for basal defense responses and resistance, and its turnover revealed to be essential for SAR. The paralogs of NPR1, called NPR3 and NPR4 were found to mediate NPR1 degradation by sensing SA levels (Fu *et al.*, 2012) (Figure 34).

NPR3 and NPR4 have different binding affinities to NPR1. Besides, NPR3 is SA-dependent while NPR4 seems to be constitutively induced. SA concentration at infection site is sensed by NPR3-NPR4. SA controls the accessibility to CUL3 ligase adaptor NPR3 and NPR4, consequently regulating stability and activity of NPR1. A detailed explanation can be seen at Figure 34.



a) In a cell challenged by a pathogen, SA levels increase at local and distant areas. NPR1 prevents ETI-cell death (Rate and Greenberg, 2001; Fu *et al.*, 2012). However the higher SA levels in the lesion will lead to NPR1 degradation mediated by NPR3 (CUL3-NPR3), triggering HR and resistance.



b) In the adjacent, uninfected cells, SA levels are lower and NPR1-NPR3 interaction is limited. The complex NPR4–NPR1 is disrupted. The free NPR1 (not degraded) promotes cell survival (avoiding HR) and induces SAR. NPR1 targets are NIMIN proteins (NIM-1 interacting) (NIM from NON-INDUCED PROTEIN) and several

TAGs (transcription factors). TAGs have been shown to bind PR gene promoters (Deprés *et al.*, 2003) while NIMINs were shown to inhibit defense responses (Weigel *et al.*, 2005).

Figure 34: NPR3 and NPR4 regulation of NPR1 in SAR.

Panel a) cell death and ETI, local infection and resistance without SAR. b) Cell survival and SAR.

Abbreviations: **GSNO**: glutathione, **TRXS**: thioredoxins, **SA**: salicylic acid, **Ub**: ubiquitin, **Cul3**: cullin3 E3 ligase, **TF**: transcription factor, **ICS1**: isochorismate synthase1. Extracted from Fu and Dong, 2013.

Pathogen Lifestyle

Plant pathogens have evolved different strategies to attack their host in order to get nutrients and to evade or counteract the detection and defense mechanisms activated by the plant. According to these strategies, a pathogen can be categorized as **Biotroph**, **Necrotroph** or **Hemibiotroph**. Fundamental differences exist among these classes of pathogens, including their mode of nutrition, the nature of the infection process, the disease symptoms they cause, and the nature of the resulting immune response. A detailed explanation can be seen in Table 8.

Table 8: Pathogens and lifestyle.

Based on Glazebrook, 2005; Spoel *et al.*, 2007; Kliebenstein and Rowe, 2008; Bari and Jones, 2009; Heller and Tudzynski, 2011; Lazniewska *et al.*, 2012; Mengiste, 2012; Ohm *et al.*, 2012; Wen, 2013.

Pathogen Lifestyle	Biotroph	Necrotroph	Hemibiotroph
Pathogen Strategy and "tools"	- Keep the host alive to get nutrients from living tissue	- Kill the host to get nutrients from cells and dead tissue	- They have a biotrophic period during the initial steps of colonization, followed by a necrotrophic one at the end of the cycle of disease, duration of each period varies among species
	- Cause minimal damage, they spend most of their life escaping plant defenses	- Maximal damage to death	- Minimal damage, they spend most of their life escaping plant defenses
	- Can suppress HR	- Promote cell death	
	- Secretion of low amounts of cell wall degrading enzymes (CWDE), less harmful. The intention is to weaken the cell wall, not to destroy it.	- Production of CWDE (xylanases, pectinases, endoglucanases, etc) for complete cell wall breakdown - High number of genes involved in carbohydrate degradation and secondary metabolites - Hormones : ET, auxin, ABA, GB - Polygalacturonases	
	- Generally lack of toxin production. Some examples produce toxins to promote growth and virulence	- Toxins. Specificity of toxins depends of the pathogen, some are more specific than others (broad host range vs specific host range necrotrophs)	
	- Low number of effectors	- Large number of virulence effectors that promote cell death	- Low number of virulence effectors ("stealth" pathogenesis)

	- Haustorium (in obligate biotrophs)		
Symptoms and signs	- Water soaked lesion, chlorosis, HR (non-autolytic cell death)	- Necrosis, tissue maceration and rotting of plant (non-autolytic cell death) - ROS production as a virulence factor - Plant decay	- Chlorosis followed by necrosis at the end of the stage - Depends on the pathogen
Cell death scenario	- Plant produces HR to limit pathogen access to water and nutrients, and spread	- Pathogen causes cell death to obtain nutrient from cell content	- Plant produces HR to limit some hemibiotrophs
Plant defense	- Programmed cell death and PR proteins, HR		- HR against some hemibiotroph
	- PR proteins	- PR proteins (induced by JA)	
	- SAR		
	- Gene-for-gene resistance (R genes)	- No gene-for-gene resistance (exception in <i>Arabidopsis-Leptospaheria maculans</i> interaction)	
	- ROS (signal or antimicrobial effect)	- Tolerance to ROS	- ROS
	- ETI, PTI	- PTI, OG-PTI - Some host-specific necrotrophs mirror ETI	- ETI, PTI
Metabolites	-callose deposition	- Phytoalexin/Phytoanticipin production: camalexin, α -tomatine, indole derivatives, glucosinolates, phenylpropanoids, fatty acids - Callose deposition - Chromatin modifications	
Hormones signaling	SA	JA /ET	
	ABA, GBs, BRs	ABA, Auxin, CKs, BRs	
Some examples	<i>Hyaloperonospora arabidopsidis</i> <i>Blumeria graminis</i> <i>Xanthomonas oryzae</i> <i>Peronospora parasitica</i> <i>Erysiphe spp.</i> <i>Puccinia graminis</i> <i>Ustilago maydis</i>	<i>Botrytis cinerea</i> <i>Erwinia carotovora</i> <i>Alternaria brassicola</i> <i>Stagonospora nodorum</i> <i>Phyllosticta spp.</i> <i>Magnaporthe orizea</i> <i>Sclerotinia sclerotum</i> <i>Plectosphaerella cucumerina</i>	<i>Pseudomona syringae</i> <i>Fusarium graminearum</i> <i>Magnaporthe grisea</i> <i>Colletotrichum lindemuthianum</i> <i>Leptosphaeria maculans</i> <i>Septoria tritici</i> <i>Phytophthora infestans</i>



CROSSTALK

The pathogens used in this thesis

- *Pseudomonas syringae* pv. *tomato* DC3000
- *Botrytis cinerea*

***Pseudomonas syringae* pv. *tomato* DC3000**

Pseudomonas syringae is a gram negative bacterium with flagellum. It affects a wide range of plant hosts causing diseases, which makes it race-specific and then classified into pathovars.

The pathovar (pv.) **tomato** causes bacterial speck on tomato (*Solanum lycopersicum* L.) (Goode and Sasser, 1980; Preston 2000) and the **strain DC3000** (*Pto* DC3000) is the rifampicin resistant form of DC52 (Xin and He, 2013), that can also infect *Arabidopsis* (Whalen *et al.*, 1991; Katagiri *et al.*, 2002), and is the most studied model in molecular plant pathology.

Its genome of 6.5 Mb, constituted by a circular chromosome and two plasmids (pDC3000A and pDC3000B), has been fully sequenced (Buell *et al.*, 2003; Reinhardt *et al.*, 2009).

P. syringae can be defined as a hemibiotrophic pathogen. As shown in Figure 35, its cycle of infection starts in the aerial parts of the plant, predominantly leaves (but also in fruits). The infection occurs through natural openings, as stomata, and wounds when the conditions are favorable to grow because *P. syringae* is a very weak epiphyte, and cannot survive longer periods exposed on the surface (Katagiri *et al.*, 2002; Xin and He, 2013). This makes infiltration the best method of choice for artificial infections.

After the penetration, the bacteria multiply in the apoplastic space, giving rise to the infection process and symptoms appearance, in the case of susceptibility. Symptoms consist in water soaked lesions which eventually become necrotic, and necrotic lesions at the site of infection surrounded by a chlorotic halo (Katagiri *et al.*, 2002). In resistant plants there will be HR, LAR, production of antimicrobial compounds, induction of defense-related genes and SAR (Freeman and Beatie, 2009).

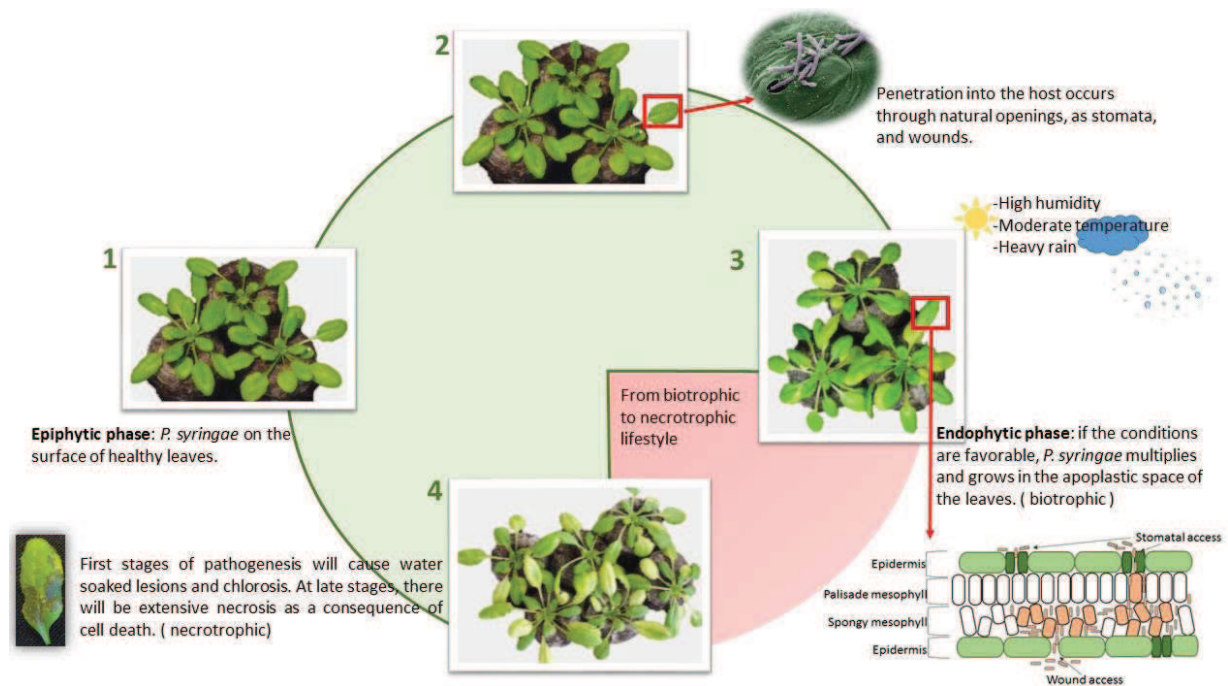


Figure35: Schematic representation of the infection cycle of *Pseudomonas syringae* pv. *tomato* in *A. thaliana* leaves.

1) On healthy plants, *P. syringae* behaves as weak epiphytic organism. 2) *P. syringae* uses natural openings or wounds to enter the plant. 3) When the conditions are favorable (high humidity, moderate temperature, heavy rain causing wounds), it colonizes very aggressively the apoplastic space causing the disease to the plant (chlorosis first). At this point, the interaction with the plant is biotrophic. This stage is apoplastic, the bacteria grow and reproduce in the intercellular space. 4) At the final stages of the cycle, the bacteria kill the host cells causing extensive necrosis, for scavenging water and nutrients. The **green area** of the circle represents the biotrophic phase, while the **red area** highlights the beginning of the necrotrophic phase. Pictures were taken from artificially infected plants. Stomata penetration image courtesy of Dr. Sheng Yang He, Michigan state university. (Note: In stage 3 *Pseudomonas* has been represented without flagella)

Pto DC3000 produces several virulence factors, as proteins secretion systems and effectors, CWDE, toxins (coronatine), plant hormones (IAA), genes related to UV and ROS tolerance, siderophores (iron chelation) (Feil *et al.*, 2005; Xin and He, 2013). Moreover it contains attachment factors (helping in biofilm aggregation, virulence), two flagella (for motility), and ABC transporters (sugars, amino acids) (Xin and He, 2013).

It encodes for several protein secretion systems, but the most important for virulence is type III secretion system (TTSS) codified by *hrp* (hypersensitive response and pathogenicity) and *hrc* (*hrc* conserved) genes (Alfano *et al.*, 2000). The system delivers into the host a mixture of effectors, a total of 28 have been reckoned with high functional redundancy (Alfano *et al.*, 2000; Kvitko *et al.*, 2009; Lindenberg *et al.*, 2012; Xin and He, 2013).

Through its TTSS, *Pto* DC3000 can activate both branches of immune system, PTI and ETI. TTSS and effectors (named Hop and Avr) are constantly targeting the plant immune system at every step of the interaction and recognition.

Briefly:

- PTI: PAPMPS from the bacteria are recognized by the plant, activating PTI. Two examples of PRR receptors are FLS2 (for [flagellin](#), a peptide flg22) and EFR (for elongation factor Ef-tu). The receptors can sometimes form a complex with BAK1. The consequent cascade of events consist in: binding to BIK1, phosphorylation events, MAPK cascade, ROS production, activation of defense-related gene expression, callose deposition, and production of antimicrobial compounds. However PTI is constantly targeted by TTSS at each of the mentioned steps.

- ETI: effectors from *Pto* DC3000 (as Avr Rpm1, AvrB, etc.) are recognized by the plant (*R* genes) and ETI is triggered. An important regulator in this dynamic is RIN4, which interacts with R proteins as RPS2 and RPM1 (see [Models Plant-Pathogen interaction](#)) after being phosphorylated and/or after cleavage. RIN4 is targeted by multiple effectors to suppress basal immunity. Collectively these events lead to JA and auxin signaling (Xin and He, 2013). A more detailed explanation of the mechanism is shown in Figure 36, according to the guard model as an example, since the mode of action of RIN4 is still under intense debate.

Furthermore, effectors can also target the chloroplast (important for SA, ROS) (Rodriguez-Herva *et al.*, 2012), mitochondria (ROS) (Block *et al.*, 2010), and microtubules (callose deposition) (Lee *et al.*, 2012).

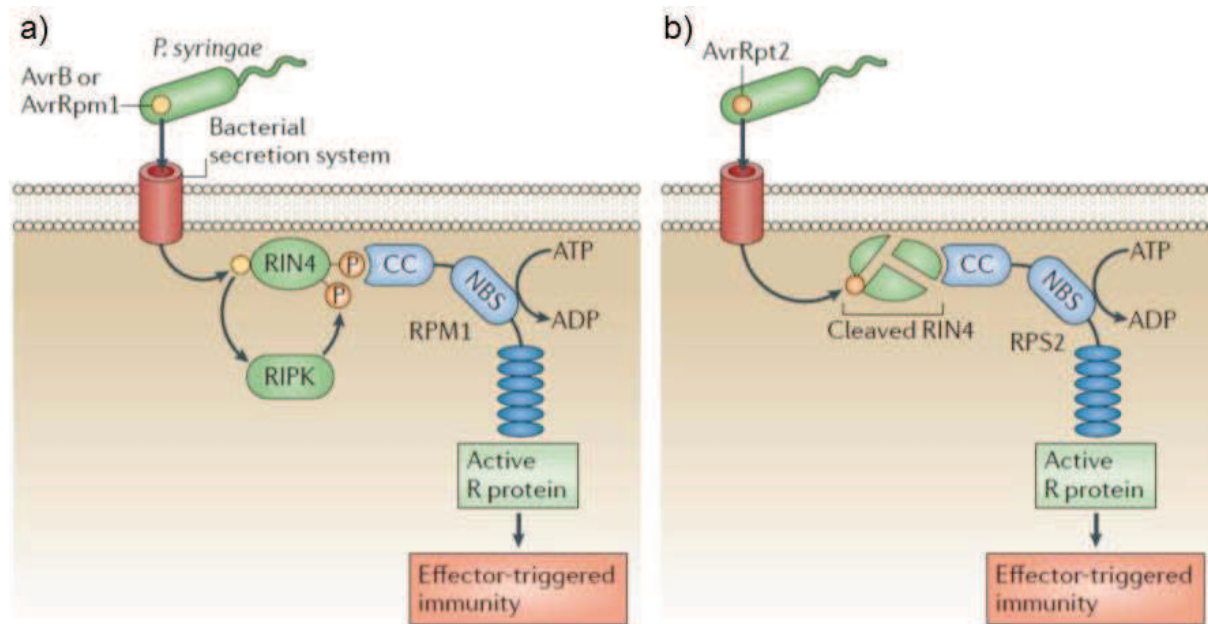


Figure 36: Schematic representation of RIN4 immune regulator being challenged by several effectors from *Pto* DC3000.

a) Effectors such as AvrB and AvrRpm1 mediate phosphorylation by RIPK, which makes RIN4 being detected by RPM1 and ETI activated. b) Effectors such as AvrRpt2 cause cleavage of RIN4, which is sensed by RPS2 activating ETI. From Spoel and Dong, 2012.

Coronatine: mimicking the enemy

Coronatine (COR) is a non-host polyketide toxin of low molecular weight that mimics JA-Ile, structurally and functionally (Katsir *et al.*, 2008; Fonseca *et al.*, 2009; Monte *et al.*, 2014). The molecule is composed by coronafacic acid (CFA) and coronamic acid (CMA) joined by an amide bond between the carboxyl of CFA and the amino group of CMA (Brooks *et al.*, 2004) (Figure 37).

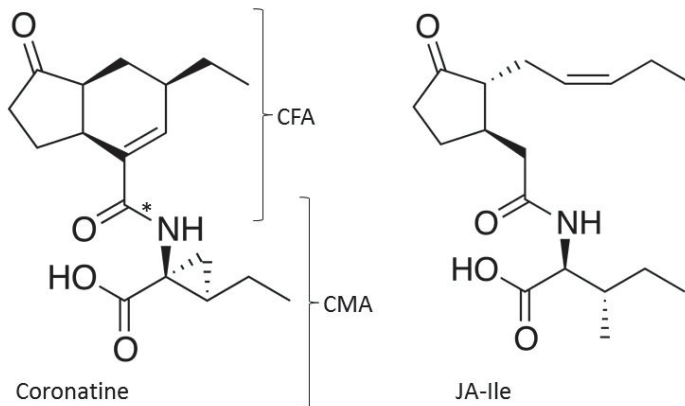


Figure 37: Molecular representation of coronatine and its moieties coronafacic acid (CFA) and coronamic acid (CMA).

On the right: (+)-7-iso-jasmonoyl-L-isoleucine (JA-Ile), showing the structural similarity between both molecules. The asterisk (*) represents the amide bond between CFA and CMA.

The toxin helps the bacteria at different steps of the cycle of pathogenesis (Geng *et al.*, 2012; Xin and He, 2013), and as stated by Geng *et al.*, (2012) is a “multifunctional defense suppressor” (Figure 38):

1- For the colonization process: by causing stomata re-opening after they are closed in response to PAMPs (for example, flagellin flg22, a peptide from the bacterium) (Melotto *et al.*, 2006; Freeman Beatie, 2009).

2- In the apoplast: by promoting bacteria multiplication and survival by intervening in SA-JA crosstalk (Katsir *et al.*, 2008; Fonseca *et al.*, 2009), callose deposition (Millet *et al.*, 2010, Lee *et al.*, 2012; Xin and He, 2013) and/or regulation of plant secondary metabolism (Trp, Met, glucosinolates) (Geng *et al.*, 2012). However COR can also suppress immunity by an independent mechanism that does not imply SA or the exploitation of SA-JA antagonism (Geng *et al.*, 2012) (more in detail in Figure 38).

3- At the final stages of infection: by contributing to develop susceptibility and symptoms, especially the chlorotic halo (chlorosis symptom) by targeting the chloroplast. This helps the bacterium to obtain water and nutrients (Rodriguez-Herva *et al.*, 2012; Xin and He, 2013).

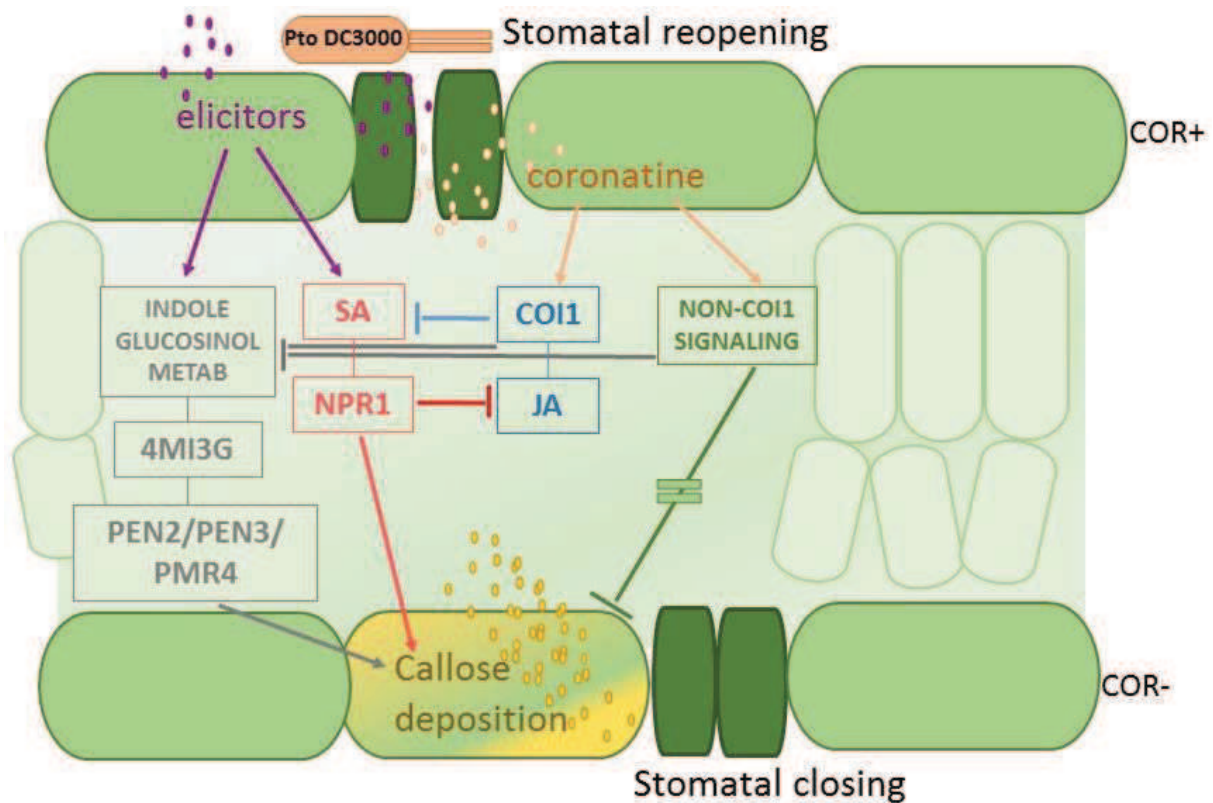


Figure 38: PAMP elicitors activate SA signaling and indole glucosinolate metabolism.

The final outcome is a signal cascade of defense responses that include ROS, MAPK, stomatal closing and callose deposition. On the other hand, COR secreted by *Pto* DC3000 mimics JA-Ile and binds COI1, antagonizing SA signaling and SA-dependent genes. It suppresses callose deposition, and causes stomatal reopening. *In extenso*, the bacterium takes advantage on the SA-JA crosstalk to overcome SA defenses by mimicking JA-Ile. SA accumulation is inhibited by the action of COR on NAC transcription factor of the MYC branch of JA signaling. COR can also suppress glucosinolate metabolism upstream of 4MI3G, and in non-COI1-dependent manner (still under debate). “COR+” (right side of the figure) represents coronatine effects, and “COR-” represents a normal defense response in the plant not challenged by COR. Based in Geng *et al.*, 2012.

The bacterial PAMP Flagellin

Flagellin is a globular protein, and the main constituent of the bacterial flagellum. Flagellin is the most popular PAMP. It triggers PTI, and is recognized by the FLAGELLIN SENSING 2 protein (FLS2), a PRR protein from the plant (Zyffel *et al.*, 2004). Flg22 is a conserved sequence of 22 amino acids residues

at the N-terminus of the protein that acts as the epitope, and can be specifically recognized by FLS2 (Chinchilla *et al.*, 2007). Flg22 can also be used as a synthetic elicitor of PTI.

Recognition of flagellin by FLS2 initiates MAPKs cascade, gene expression, ROS production, activation of defense-related gene expression, callose deposition, production of antimicrobial compounds, etc.

Defense responses and secondary metabolism in the interaction *A. thaliana*- *Pto* DC3000

As described before, *Pto* DC3000 is well equipped to manipulate host defenses. SA signaling clearly plays a relevant role in plant defenses, and HR is a strong immune response. During infection, biosynthetic pathways leading to secondary metabolites (SMs) are highly activated, because of callose deposition, signaling, ROS generation etc. (Dixon, 2001; Bednarek *et al.*, 2009; Wink, 2011). However, understanding the precise mode of action of SMs, the space-temporal dynamics of accumulation, and their roles in defense, has not been an easy task to address (Simon *et al.*, 2010; Hagemeyer *et al.*, 2001).

Accumulation of indolic metabolites seems to prevail in the *Arabidopsis-Pseudomonas* interaction (data on leaves) (Simon *et al.*, 2010; Hagemeyer *et al.*, 2001), though not always with a decisive role in disease resistance, as it seems.

In the pioneer work of Hagemeyer *et al.*, (2001), it has been described the presence of:

- a) indole-3-carboxylic acid
- b) Trp (primary metabolism)
- c) β -D-glucopyranosyl indole-3-carboxylic acid
- d) 6-hydroxyindole-3-carboxylic acid
- e) camalexin

According to this publication, the pattern of distribution/accumulation of SMs within the cells, under scenarios of compatible and incompatible interaction, varied between wall-bound (a) and free soluble forms of the compounds (from b to e). The dynamic of the accumulation studied in this work showed rapid accumulation of Trp, β -D-glucopyranosyl indole-3-carboxylic acid and 6-hydroxyindole-3-carboxylic acid in the compatible interaction (12 HPI), while camalexin and indole-3-carboxylic acid were higher in the incompatible interaction (resistance response) and delayed (24 hpi). The work also mentioned that two kaempferol glycosides remained unchanged and that sinapoyl malate decreased as Trp increased.

In the same direction, the most recent work of Simon *et al.* (2010) highlighted the importance of the differential spatial distribution of the accumulation of SMs between infected and uninfected leaf areas, under incompatible interaction (with HR present). For instance, infected tissue accumulated higher SA, camalexin and scopoletin, whereas uninfected tissues, accumulated the glycosylated form of

scopoletin. In parallel, the production of ROS was more important in infected tissues than in uninfected tissues (with cell death only in the infected tissues) which brings evidence, after well established experiments and analysis with a *cat2* (catalase deficient) mutant, of the conclusive role of redox status in the SMs differential distribution.

SA, camalexin and scopoletin were confirmed to be reactive to ROS and scavenging ROS.

In detail, we can see the list of differentially accumulated compounds as follows:

- a) adenosine: not clear role
- b) phenylalanine (Phe): early induction in infected tissues
- c) tryptophan (Trp): strong accumulation in infected tissues
- d) indole-3-carboxylic acid β -D-glucopyranosyl ester
- e) camalexin: strongly accumulated in infected tissues, but also in uninfected tissues.
- f) dihydrocamalexin: low accumulation
- g) kaempferol 3-O-[6-O-rhamnosyl]-glucoside]-7-O-rhamnoside: no role
- h) kaempferol 3-O-glucoside 7-O-rhamnoside: no role
- i) kaempferol 3-O-rhamnoside 7-O-rhamnoside: no role
- j) sinapoyl malate: slight decline in infected tissue
- k) 4-hydroxybenzoyl-choline (putative benzoic acid derivative)
- l) indole-3-carboxylic acid (conjugated to an unidentified residue)
- m) scopoletin: low accumulation in infected and uninfected tissue
- n) scopolin: in uninfected tissues

As in the work of Hagemer *et al.* (2001) there is a privileged accumulation of indolic metabolites (typical of *Brassicaceae* family).

Some other studies can also contribute to outline the SMs dynamics of the *Arabidopsis-Pseudomonas* interaction. As an example, it can be mentioned the less specific work of Hiruma *et al.*, (2013).

This work deals with non-host resistance (PTI) during post-invasive HR to non-adapted hemibiotroph pathogens. It shows that Trp and a γ -glutamylcysteine synthetase (GSH1) are essential for HR and immunity responses against hemibiotrophs (with special emphasis in fungal hemibiotrophs). In summary, GSH1 mediates glutathione synthesis, and also induces defense-related genes and HR. Since glutathione is the cysteine donor of sulfur-containing Trp-derived metabolites, it may suggest that one of these compounds is responsible of the non-host resistance observed. The role for this candidate seems to be more important than the HR itself. (Cell death is not enough to arrest hemibiotroph development. Explanations in [HR section](#)).

As a final point, some words about volatiles terpenes in *Arabidopsis-Pseudomonas* interactions.

Since they play important roles in plant-organisms interactions (pollinator attraction, direct and indirect defense against herbivores, plant-plant communication) some researchers were wondering about their roles in resistance against microbial pathogens.

Attaran *et al.*, (2008) tested the role of volatile terpenoids in *A. thaliana* plants challenged with *P. syringae* pv. *maculicola* ES4326 virulent and avirulent (*avrRpm1*) strains. Previous works showed that tobacco infected plants with *P. syringae* accumulated (E)- β -ocimene, linalool, caryophyllene, β -elemene and α -farnesene (Huang *et al.*, 2003). Attaran *et al.*, (2008) found that plants challenged with both strains of *Pseudomonas* accumulated (E,E)-4,8,12-trimethyl-1,3,7,11-tridecatetraene (TMTT), β -ionone and α -farnesene (and Me-SA).

TMTT was accumulated in early responses facing both interactions (incompatible and compatible) while β -ionone and α -farnesene accumulated in later stages of disease only under virulent infection (no related to resistance). Microarray data indicated that *TPS2*, *TPS3*, *TPS4*, *TPS10* were induced under *Pto* infections, in particular *TPS4* was highly induced. Further experiments showed that *TPS4* was responsible for TMTT synthesis, significantly activated in this interaction. However, besides the fact that TMTT has been proven to activate defense responses against herbivores (*Arabidopsis*, Lima bean, corn, tomato, cotton) and in plant-plant communication (lima bean), their role in activation or priming of defense responses as a phytoalexin or phytoanticipin in was ruled out in the context of this research. TMTT role was also excluded from mounting SAR responses. In addition, the authors suggest that it might be a byproduct of other processes denying a role for green leaf volatiles in *Arabidopsis* defense towards *Pseudomonas* strains.

In the same line of research come the publication of Huang *et al.*, (2012). The work analyzed the role of floral terpenoids in floral defense. The publication describes the antimicrobial effects of (E)- β -caryophyllene (a sesquiterpene) emitted from *A. thaliana* flowers against *Pto* DC3000 as a constitutive defense.

According to this work, caryophyllene mode of action might be related to the lipophilic nature of terpenoids acting not only at level of plant cell membrane, but also acting on bacteria membrane causing disruption, ion leakage, changes in potential and cell-cell disaggregation of bacteria.

Therefore the probable antimicrobial effects of caryophyllene could be related to the action on the bacterium itself that through SA or JA signaling, even though some alternative pathways cannot be dismissed. It has also been suggested that caryophyllene can act as a protective molecule against ROS, as reported previously for some other terpenoids.

Finally it can be mentioned the work of Barah *et al.*, (2013) concerning molecular signatures in *A. thaliana*- *Pto* DC 3000 interaction. In this work, it was found that under *Pto* DC 3000 infections, secondary metabolism was heavily affected specially regarding phenylpropanoid and glucosinolate pathways. Genes connected to terpenoids and alkaloid pathways such as *DXPS1* (1-deoxy-D-xylulose-5-phosphate synthase), *TPS10* (terpene synthase 10), *GES/TPS04* ((E,E)-geranylinalool

synthase/Terpene synthase 4), *SS2* (strictosidine synthase), *SQE6* (Squalene monooxygenase 6), and *LAS1* (lanosterol synthase) were up-regulated. It is interesting to note that *TPS4* and *TPS10*, were analyzed in the previous works of Attaran *et al.*, (2008) and were showed not to be involved in defense responses.

Botrytis cinerea

Botrytis cinerea Pers. (teleomorph *Botryotinia fuckeliana* (de Bary) Whetzel) is a generalist necrotrophic fungal pathogen of plants (Figure 39, a), b) panels). It can infect foliage, stems, flowers, and fruits, causing important economic losses in agriculture and horticulture by pre- and post-harvest damage (Muckenschnabel *et al.*, 2001; Elad *et al.*, 2007).

So far, it is considered the second most important fungal plant pathogen (Dean *et al.*, 2012) and has become an important model organism for the study of necrotrophic interactions (van Kan, 2006). To date, the genome of two strains has been fully sequenced, and several strategies for gene function analysis have been developed (van Kan, 2006; Amselem *et al.*, 2011).

The prevailing symptom of a *Botrytis* infection is the development of necrotic lesions on the leaves (Elad *et al.*, 2007) (Figure 39, c) panel). The initiation of disease involves chemical and physical interactions between the fungal propagules and the host surface (Gonzalez Collado *et al.*, 2007).

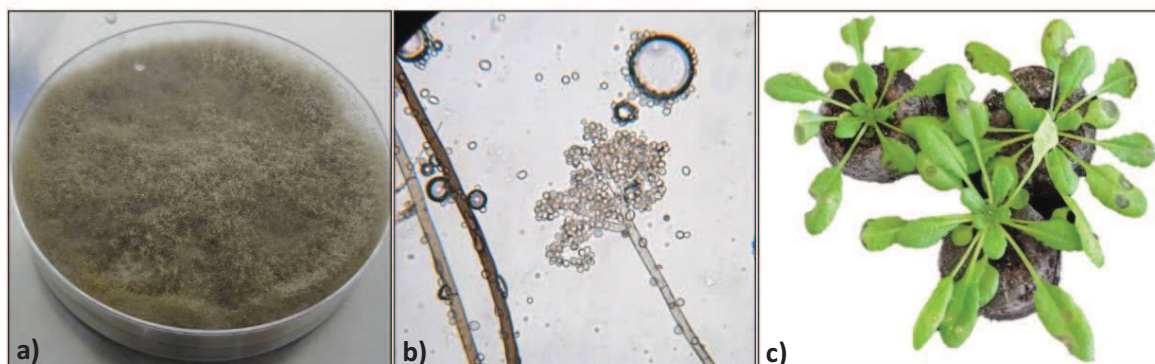


Figure 39: *Botrytis cinerea*

a) Two weeks-old mycelium on potato dextrose agar (PDA) culture, b) conidiophore and conidia under 40x magnification (picture courtesy of Steven Koike, University of California), c) necrotic lesions 72 h post infection on artificially infected leaves of *A. thaliana* Col-0 plants.

The infection, colonization and suppression of host defenses by *B. cinerea* is mediated by numerous extracellular enzymes, high levels of ROS and secondary metabolites. Cell-wall-degrading enzymes may facilitate the penetration of the host surface, while toxic molecules (such as botrydial, botcinolides), oxalate and reactive oxygen species may contribute to kill the host cells (Schouten *et al.*, 2002; van Kan, 2006; Choquer *et al.*, 2007; van Doorn, 2011b; Heller and Tudzunski, 2011; Mengiste, 2012; Wen,

2013). In addition, abscisic acid (from the host or/and the fungus) will contribute to get the plant under an important and challenging osmotic stress (Mulema and Denby, 2012).

In order to penetrate the host cuticle, *B. cinerea* develops highly specialized infection structures, called appressoria, which consist in modified hyphae with a globular tip, which helps the fungus to colonize the host and to get access to nutrients (Deising *et al.*, 2000). Appressoria are never in direct contact with the host cytoplasm, but separated by membranes from which enzymes such as oxidases, cutinases and lipases are released to the cuticle before penetration (Faulkner and Robatzek, 2012). Once the cuticle and wax layers have been weakened, appressoria secrete CWDEs, laccases, proteases, pectinases, cally- endopolygalacturanases (endo-PGs) to disrupt the epidermal cells (Mengiste, 2012).

After it has penetrated the cuticle, *B. cinerea* triggers processes indicative of programmed cell death (PCD) at a distance from the hyphae, implying that diffusible factors have a direct or indirect phytotoxic activity (Gonzalez Collado *et al.*, 2007). Epidermis cells are killed before being penetrated by hyphae. Hence the fungus exploit the hypersensitive response (HR) and the PCD of the host to advance infection (Govrin and Levine, 2000, Heller and Tudzunski, 2011).

In particular, the interaction *A. thaliana*–*B. cinerea*, involves an array of multiple differentially induced genes in space and time (Rowe *et al.*, 2010). Multiple microbe/pathogen/damage-associated molecular patterns (thereafter MAMPS, PAMPS and DAMPS) are involved in the interaction (Windram *et al.*, 2012). Fungal cell wall components, chitin, oligosaccharides and polygalacturonases are MAPS/DAMPS that activate numerous plant defenses (Windram *et al.*, 2012).

Signal transduction through plant hormones is also present. Salicylic acid, synthesized via phenylalanine ammonia lyase (PAL), appears to have a role in local resistance to *B. cinerea* and lesion development together with ethylene, jasmonate and camalexin (Ferrari *et al.*, 2007). Whereas systemic resistance only implicates the role of ethylene and jasmonate, as in any other necrotroph, in concert with auxin and abscisic acid (Thomma *et al.*, 1998). Collectively, these defenses responses can slow *B. cinerea* infection, but they do not completely block disease development (Shlezinger *et al.*, 2011, Glazebrook, 2005).

Almost one-third of the *Arabidopsis* genome is differentially expressed during the first 48 h after infection, with the majority of changes in gene expression occurring around 24 h after infection, before significant lesion development (Windram *et al.*, 2012, Mulema and Denby, 2012) (Figure 40). The spatial distribution of genes is important in this interaction, with a clear indication that gene expression related to defense is more important within the lesion or tissue close to the lesion, than away from the lesion (Kliebenstein *et al.*, 2005, Mulema and Denby, 2012). The same is valid for spatial expression of secondary metabolites, showing that, at 24 h post infection, there is an increase in the number of

genes coding for terpenoids (terpene synthases), tryptophan and metabolites downstream such as camalexin, indole glucosinolates and indole-3-acetic acid (IAA), as a possible indication of host resistance response against pathogen attack (Mulema and Denby, 2012) (Figure 40).

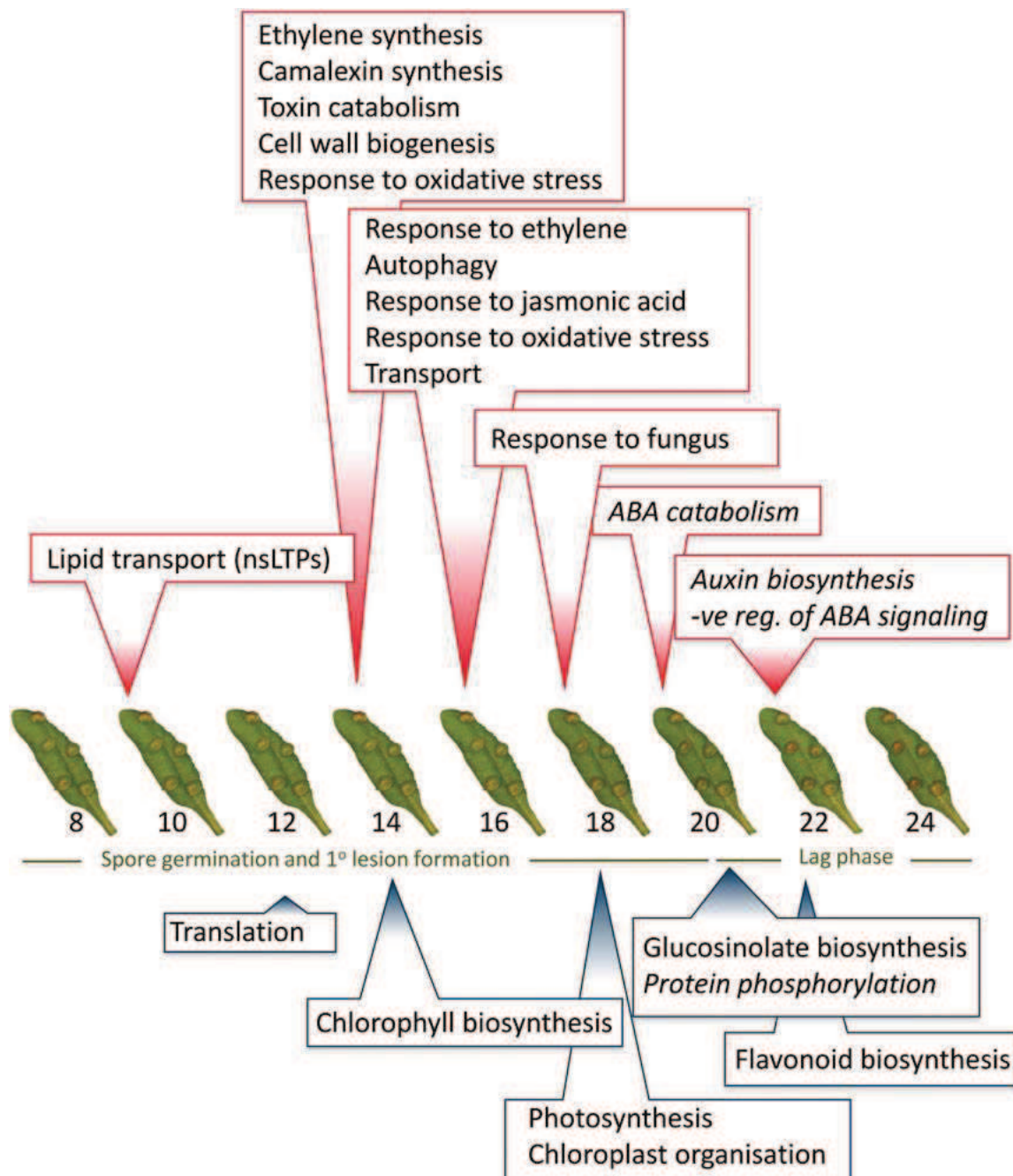


Figure 40: Schematic representation of the chronology of clusters of genes differentially expressed during *A. thaliana*-*B. cinerea* interaction (from Windram *et al.*, 2012). In red boxes up-regulated genes, in blue boxes down regulated genes. In green the timeline showing also pathogen growth phases.

HYPOTHESIS AND OBJECTIVES

Hypothesis
and objectives

HYPOTHESIS AND OBJECTIVES

Plant health and disease resistance represent major economic and societal issues and for that reason many efforts are invested to develop innovative strategies to increase food production and quality, supporting sustainable development and enhancing the environment (FAO, 2009; 2012).

[Plant immune system](#), as it was described earlier in this thesis, involves the interplay of defenses and counter-defenses between plant and pathogens (Jones and Dangl, 2006).

In order to protect our food supply and to develop highly disease-resistant plant species, it is vital to understand how plants defend themselves (Freeman and Beatie, 2008).

Disease resistance exists as a continuum of responses ranging from total immunity or resistance to total susceptibility where different kinds of defense responses such as [HR](#), [LAR](#) and [SAR](#) are taking place. In addition, the effectiveness of such defense mechanisms is related to the production of endogenous signals and metabolites that contribute to resistance or susceptibility.

Disease resistance in plants was so far mainly addressed either through screening for stress response of large mutant collections or through over-expression of candidate genes. Transcriptomic data, accumulated in the last years, and predictive biology pointed to many aspects of the plant defense strategies that remain poorly understood, even in the model *Arabidopsis*, and thus provide very useful tools for identifying novel candidate genes. This in particular applies to metabolic pathways and resulting bioactive compounds that contribute to elicitor/pathogen-inducible defenses.

Addressing this point, transcriptomic-based predictive analyses independently carried out in the host lab (France) via [CYPedia](#) (Ehltig *et al.*, 2006; 2008; <http://www-ibmp.u-strasbg.fr/~CYPedia/>) and in the group of F. Ausubel (Massachusetts General Hospital, USA) (Denoux *et al.*, 2008) under different biotic stresses concur to identify a subset of candidate P450 genes and related pathways in *A. thaliana*, showing strong activation and suggesting some roles of P450 enzymes in plant defense responses against pathogens.

Further transcriptomic analysis relative to LAR phenomenon conducted by Serge Kauffmann at host Institute ([Project SARA Trilateral Genoplante](#) “*Functional genomics of local and systemic acquired resistance in Arabidopsis*”) after infection with the bacterium *Pseudomonas syringae* pv. *tomato* DC3000 carrying the gene of avirulence *AvrRpm1* also showed that P450 genes were strongly induced, or strongly suppressed.

To date the function and substrates of several of the genes identified by these approach are still unknown or poorly characterized (Ehlting *et al.*, 2008; Denoux *et al.*, 2008; Höfer *et al.*, 2014). In particular, *CYP76C2*, a member of the *CYP76C* subfamily, showed a highly induced expression (≈ 50 fold) in response to biotic stress, especially in the context of [LAR \(Kauffman, personal communication\)](#) (shown below). [CYP76C2](#) in addition appeared differentially regulated in response to biotic and abiotic stress (Godiard *et al.*, 1998), and was alternatively predicted to be involved in the monoterpenoid (Ehlting *et al.*, 2008, Höfer *et al.*, 2014) or glucosinolate metabolism (Rowe *et al.*, 2010). Nevertheless, its function and substrate are still unknown.

Taking into account these previous results, a functional approach to identify P450 genes playing a key role in the development of defense mechanisms, was intended for this thesis with a particularly emphasis on the *CYP76* family, with special focus on *CYP76C2*.

Hypothesis

The members of the *CYP76C* family seem to be involved in defense responses, in particular *CYP76C2* is involved in LAR mediated responses and monoterpenol metabolism.

Main goal of this these

- To investigate the impact of the *A. thaliana* P450 *CYP76C* subfamily on plant defense, with particular focus on *CYP76C2*.
- To propose a mode of action of the potential bioactive *CYP76C2* enzyme products in plant defense responses.

Objectives

- To study the gene expression of the *A. thaliana* *CYP76C* subfamily in response to the infection with pathogen having contrasted lifestyles: hemibiotrophic (virulent or avirulent *P. syringae* strains) or necrotrophic (*B. cinerea*).
- To understand the impact of the *CYP76C* genes on plant defenses.
- To compare the metabolic profiles of selected mutants of the *CYP76* family with those of *A. thaliana* wild-type plants, before and after the onset of infection.
- To associate metabolic changes with already characterized metabolic pathways, or potentially new biosynthetic pathways.

- To describe/fully characterized the structure of relevant novel metabolite(s).
- To study the mode of action of these metabolites in plant defense mechanisms.

CYP76 family background information

The CYP76 P450 family is specific of *Brassicacea* spp. and in *A. thaliana* is composed of 9 members (<http://www.p450.kvl.dk/p450.shtml> and [CYPedia](#)), eight of which belong to the CYP76C subfamily (CYP76C1 to CYP76C8, CYP76C8 being a pseudogene), a single one to the subfamily CYP76G (CYP76G1) (Figure 41). The CYP76 family arose with the emergence of angiosperms and appears prone to gene duplication, loss and diversification, probably in relation of its important role in adaptation to trophic interactions in a sort of birth-and-death model of concerted evolution (Nelson and Werck-Reichert, 2011; Höfer *et al.*, 2014).

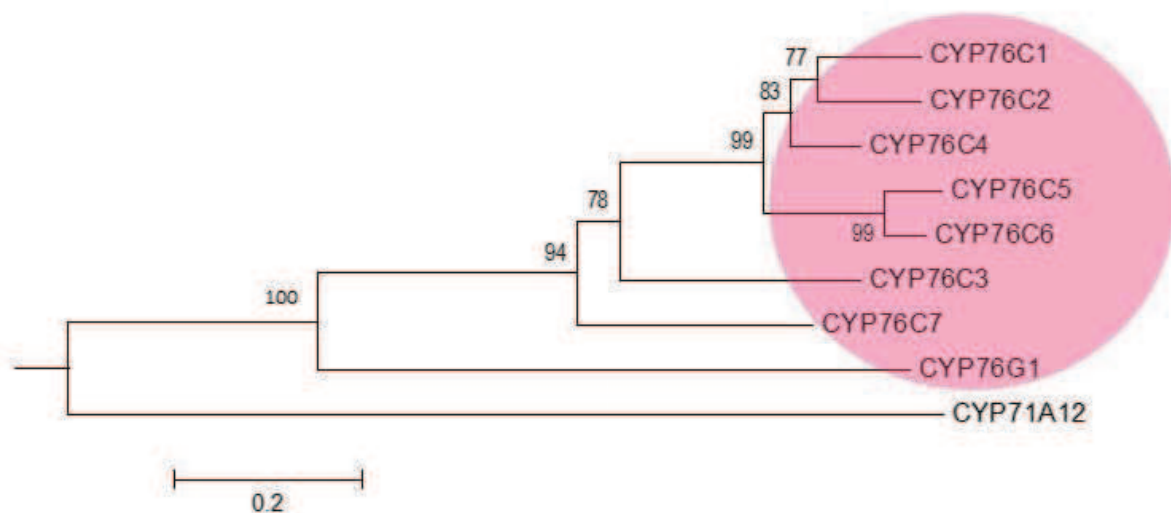


Figure 41: Phylogenetic tree representing CYP76 family members in *A. thaliana*.

The CYP76 family of *Arabidopsis* highlighted in pink color. The coding sequences were retrieved from Phytozome database (<http://www.phytozome.net/>). Coding sequences were translated into amino acid sequences and aligned with MUSCLE (Edgar, 2004) prior to determination with Gblocks (Castresana, 2000). The alignment was subsequently used for phylogeny reconstruction by maximum likelihood analysis with PhyML 3.0 software (Guindon *et al.*, 2010) using the generalized time reversible model (default settings at www.Phylogeny.fr (Deereper *et al.*, 2008). Phylogeny consistency was tested

by approximate likelihood-ratio test (aLRT). The output tree was shaped using MEGA6 software (Tamura *et al.*, 2013).

The *CYP76* family genes are distributed in several clusters on chromosomes 1, 2 and 3 as shown in Figure 42.

CYPC6 and *CYPC5* are located in chromosome 1, *CYP76C1*, *CYP76C2*, *CYP76C3*, *CYP76C4* are located in chromosome 2 and *CYP76C7* and *CYP76C8* in chromosome 3.

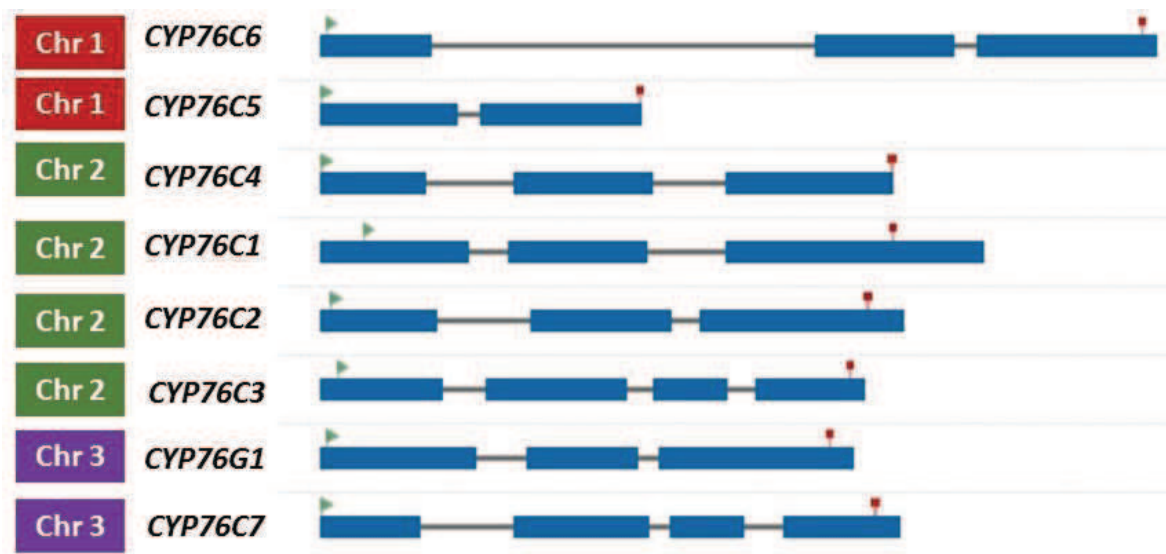


Figure 42: Gene structure and chromosome localization of the *CYP76* family in *A. thaliana*.

Exon and intron location map are presented in blue blocks and lines respectively. Chromosome localization is highlighted in the left side of the figure. Figure extracted from the synteny tool in [Phytozome](http://www.phytozome.net/) (<http://www.phytozome.net/>). *CYP76C1-C4* and *CYP76C5-C6* form clusters on chromosome 2 and chromosome 1, respectively.

qRT-PCR analysis of the constitutive expression of the different *CYP76Cs* in *A. thaliana* organs indicated low overlap in the spatial distribution of gene expression, suggesting no or limited functional redundancy (Höfer *et al.*, 2014). In some occasions, members that belonged to the same gene cluster were expressed in different organs (Figure 43). This is for example the case of *CYP76C5* (mainly siliques) and *CYP76C6* (stem). For the cluster *CYP76C1*, *C2*, *C3*, *C4*, some redundancy between *CYP76C1* and *CYP76C2* (expression in flowers and siliques) can be expected. Conversely, *CYP76C4* is expressed at very low levels only in roots.

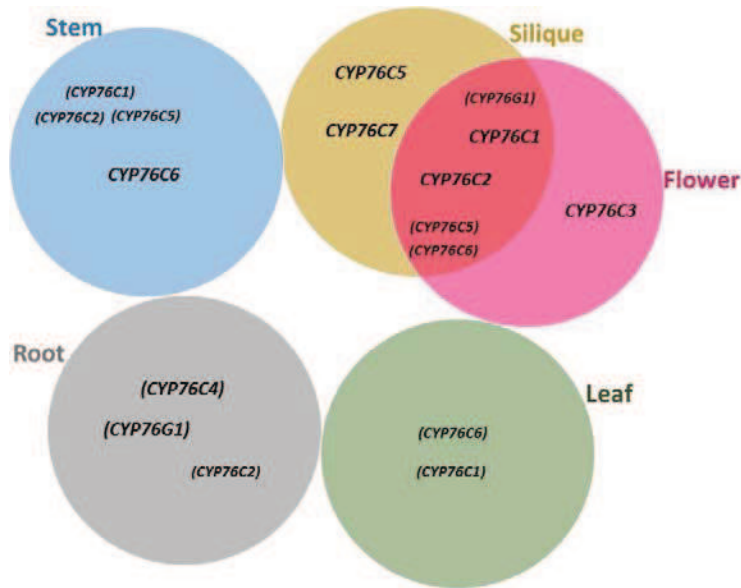


Figure 43: Schematic representation of expression patterns in *A. thaliana* organs, based on relative gene transcript levels by means of qRT-PCR.

qRT-PCR expression data from Höfer *et al.*, 2014. Large characters indicate the main expression organ for a gene, while parenthesis and small characters represent limited levels of gene expression.

Transcriptomic data and co-expression analysis of P450 with terpene synthases have suggested that several members of the CYP76C subfamily might be involved in the biosynthesis of monoterpenoids (Ehlting *et al.*, 2008). Several of them have been confirmed to be involved in the metabolism of monoterpenols (Höfer *et al.*, 2013; 2014) via heterologous expression in yeast, transient plant expression or mutant analysis (Höfer *et al.*, 2013, 2014; Ginglinger *et al.*, 2013) (Table 9). CYP76C1, CYP76C2 and CYP76C4 metabolized several monoterpenols like citronellol, linalool, geraniol and nerol *in vitro* with different efficiencies and generating different products. Besides metabolizing monoterpenols *in vitro*, CYP76C1, CYP76C2 and CYP76C4 were also shown to be able to metabolize phenylurea herbicides such as: chlortoluron, isoproturon, and linuron. CYP76C1 was the most effective (Höfer *et al.*, 2014). Ectopic expression in *A. thaliana* confirmed that all three genes conferred herbicide tolerance.

Table 9: Reported substrates of the members of the CYP76C subfamily.

Gene	Gene number	<i>in vivo</i>	<i>in planta</i>	References
<i>CYP76C1</i>	AT2G45560.1	geraniol		Otah and Mizutani, 1998
		linalool, citronellol, α -terpineol, lavandulol		Höfer <i>et al.</i> , 2014
			phenylurea	Höfer <i>et al.</i> , 2014
<i>CYP76C2</i>	AT2G45570.1	nerol, linalool, citronellol, lavandulol	phenylurea	Höfer <i>et al.</i> , 2014
<i>CYP76C3</i>	AT2G45580.1		linalool (flowers)	Ginglinger <i>et al.</i> , 2013
<i>CYP76C4</i>	AT2G45550.1	nerol, linalool, citronellol, α -terpineol, lavandulol	geraniol	Höfer <i>et al.</i> , 2013
			phenylurea	Höfer <i>et al.</i> , 2014

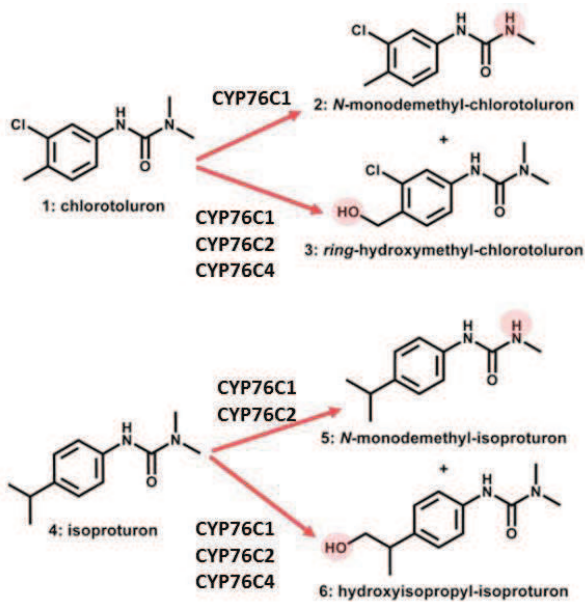
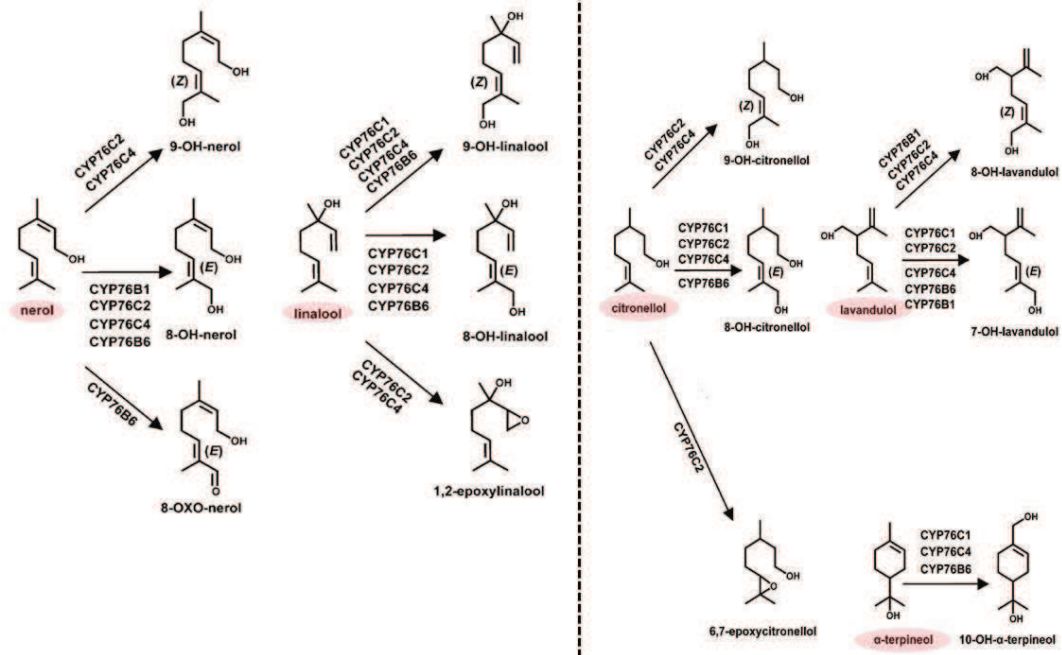


Figure 44: The reactions catalyzed by CYP76C1, CYP76C2, and CYP76C4 *in vitro*.

In the upper panel: monoterpene metabolism. In the left panel: herbicide metabolism. Demethylation products are less toxic and hydroxylation lead to non-toxic products (Höfer *et al.*, 2014).

Guiding questions based on these data:

- If expression in leaves is almost negligible, could this family be important in plant-pathogen interaction?
- Are gene expression patterns different under/after pathogen elicitation in leaves?
- Which are the most responsive/inducible gene members?
- Is a monoterpenol involved in defense? If so, is it conjugated? To what?
- Are detoxifying mechanism observed for herbicides related in some way to their possible role in defense responses?
- Is it the adaptation to pathogens a cause of the duplication/diversification observed in the CYP76C subfamily in *Brassicaceae*?

The CYP76 family and stress responses

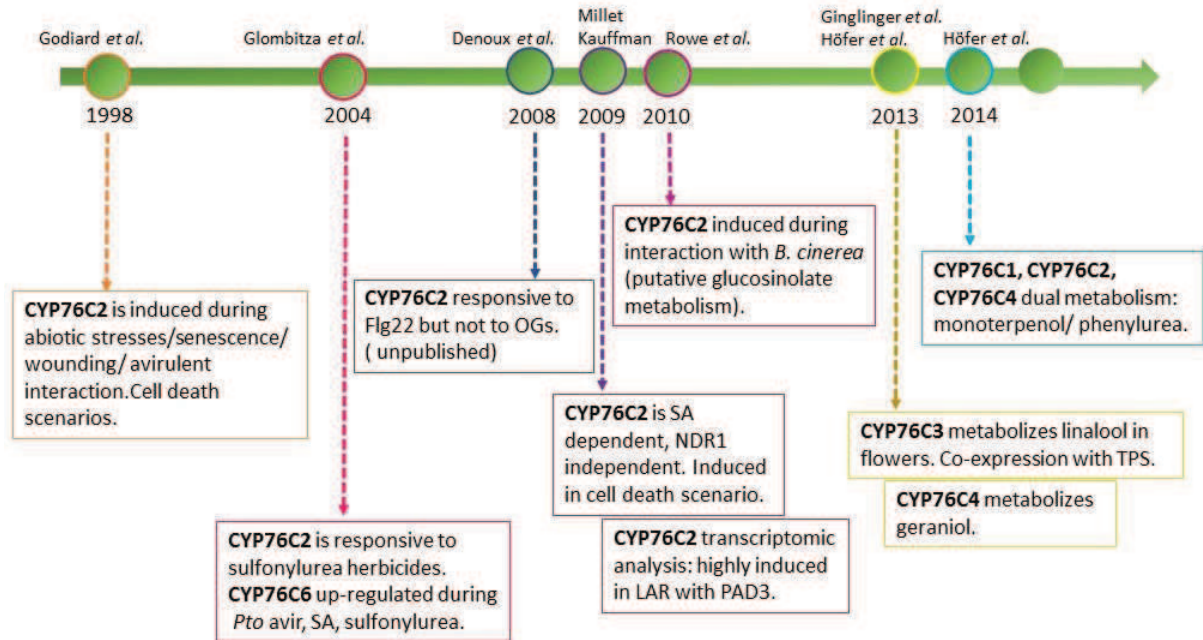


Figure 45: Timeline showing progress and information accumulated in the last years in relation to the CYP76C subfamily, with special emphasis on stress responses.

- In 1998 Godiard *et al.*, reported that the expression of *CYP76C2* was associated with processes leading to cell death such as HR, leaf senescence, ageing of cell cultures, as well as wounding and treatment with heavy metal, salts and nitrates.

The pathogen tested was *Pseudomonas syringae* pv. *maculicola* *avrRpm1* (*Pm. avrRpm1*) and p.v *tomato* (*Pto.*) carrying the avirulence genes *avrB*, *avrRpm1*, *avrRpt2*. The induction of *CYP76C2* was observed 6 HPI (*Pm. avrRpm1*), 2-4 HPI (*Pto. avrB*), 4-7 HPI (*Pto. avrRpm1*, *avrRpt2*), before HR and symptoms development (10-12 HPI). The induction was maximal before HR. After wounding, *CYP76C2* accumulated from 1 HPI to 8 HPI. ABA (50µM) also induced *CYP76C2* expression in leaves. This work also indicated very low expression in compatible interactions leading to diseases, no response to elicitors, and no expression during plant development, but activation upon senescence (correlated to ABA).

- Ten years later in 2008, Ehling *et al.*, presented a complete *in vitro* transcriptome analysis of stress response with a group of nine probe sets representing eleven P450 including *CYP76C2*, which was shown to be rapidly induced by incompatible interactions with *P. syringae* (*avrRpm1*), some elicitors (*hrpZ*, *GST*), fungal pathogens (*B. cinerea*) and some abiotic stresses like oxidative, osmotic and UV stress (UV-B, paraquat, ozone, NaCl, Cs, norfluzone, mannitol) (Figure 46).
- The same year, Carine Denoux in the lab of Pr. F. Ausubel found that *CYP76C2*, among other P450 genes, appeared to be highly up-regulated by the elicitor Flg22 after 3 h but not for oligogalacturonides (OG). Results can be seen in the PhD thesis of Yves Millet (2009).
- In the PhD thesis of Yves Millet in 2009, *CYP76C2* was shown strongly activated upon pathogen infection and various cell death elicitation scenarios (*Pto* DC3000, *Pto avrRpt2*, *Pto hrp/hrc* deletion mutant, *Pm. ES4326*, *Pm. avrRpt2*, *B. cinerea*, Flg22, FB1, senescence), paraquat and herbicide detoxification. It was observed that *CYP76C2* activation was locally restricted to the infection zone. This work also demonstrated that *CYP76C2* was partially dependent on SA and NPR1 independent. Millet also worked with *CYP76C4* because of its close sequence homology with *CYP76C2*. The author found *cyp76c4* line was more affected than *cyp76c2* line under *Pseudomonas* infections. However no differential phenotype was found for any kind of infection. Additionally it was shown that *CYP76C2* has a weak antioxidant effect (paraquat experiments).

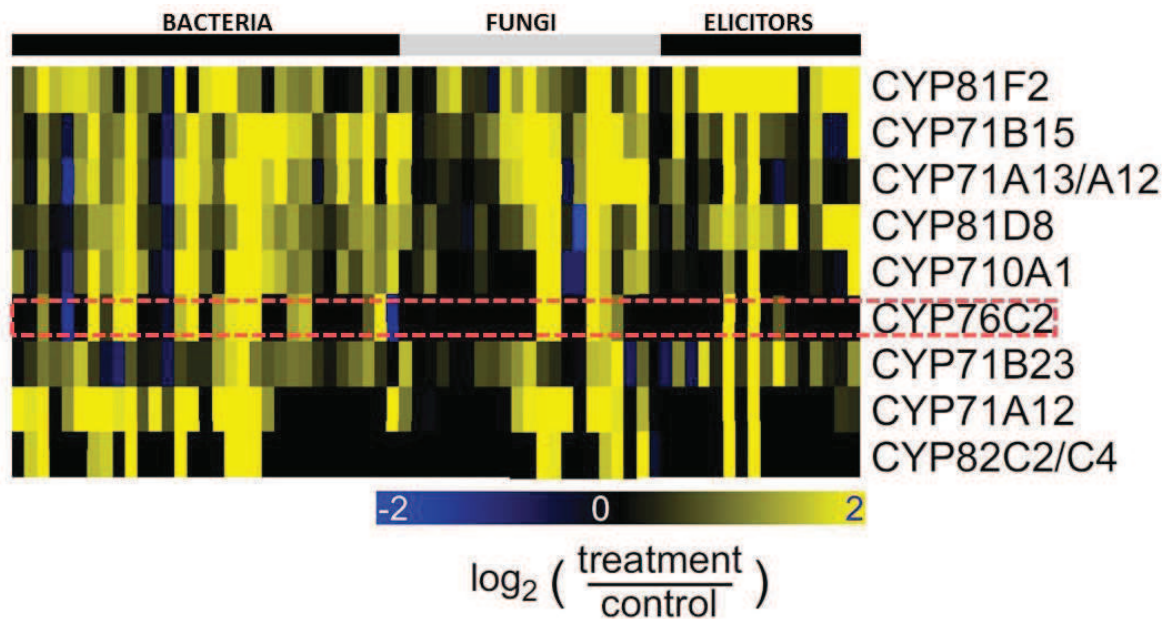


Figure 46: Stress responsive matrix of selected P450 genes. *CYP76C2* is marked in red accompanied by genes implicated in camalexin metabolism (*CYP71B15*, *CYP71A13/12*), indole-glucosinolates (*CYP81F2*), and stigmaterol biosynthesis (*CYP710A1*). Extracted from Ehltng *et al.*, (2008).

- In agreement, with previous results, Serge Kauffmann at the host Lab conducted a transcriptomic analysis, focusing the analysis on the LAR responses at 6 hours post infection (Figure 47). It was shown that *CYP76C2* was dependent of SA, *NDR1* independent, and that its expression was compromised in the mutant *dth9* (detached 9). DTH9 is a regulator of disease resistance upstream of SA that affects SAR (Mayda *et al.*, 2000). The results point to a role of some others P450 genes never mentioned before in early LAR responses, with very low induction for the others members of the *CYP76* family. Results are presented in Figure 47.

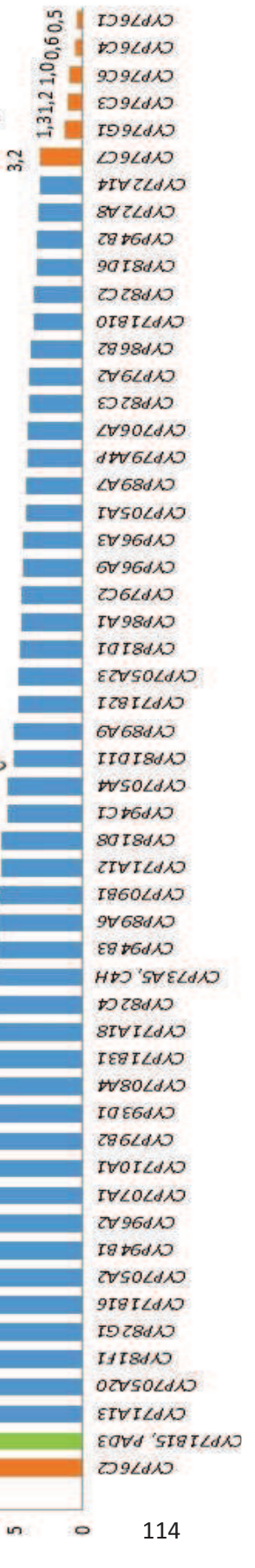
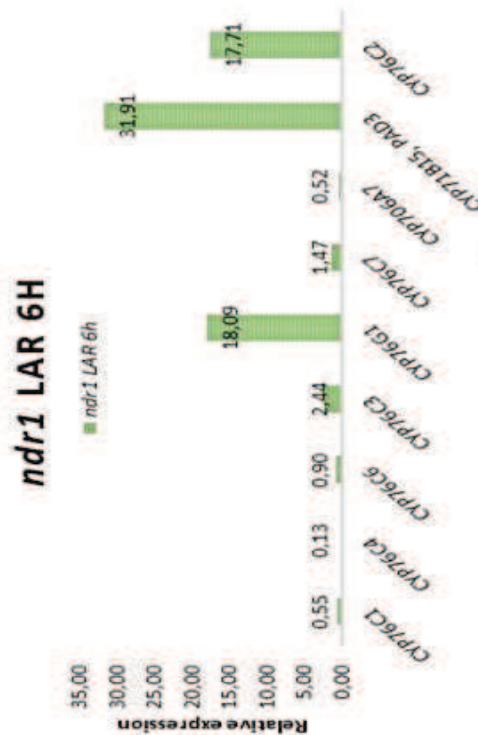
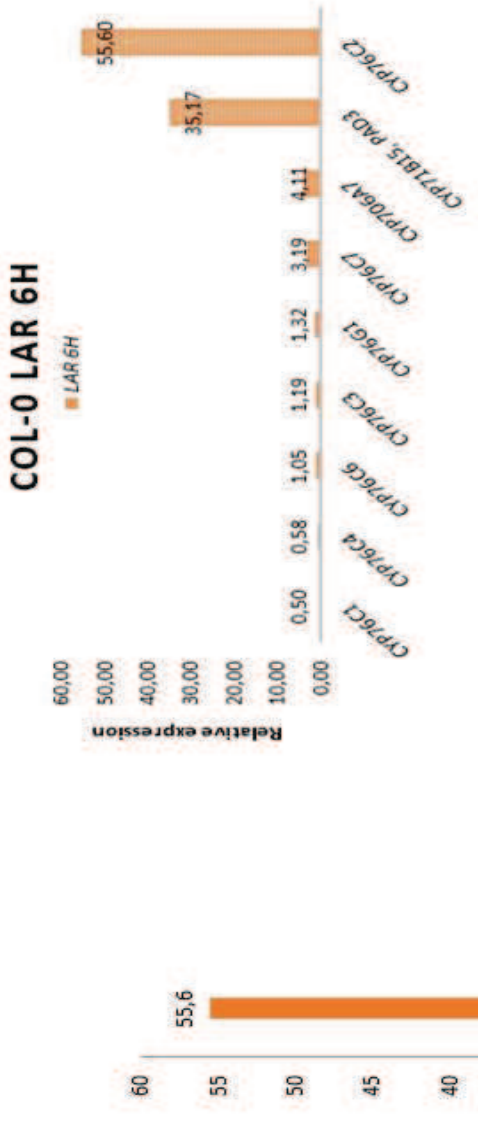
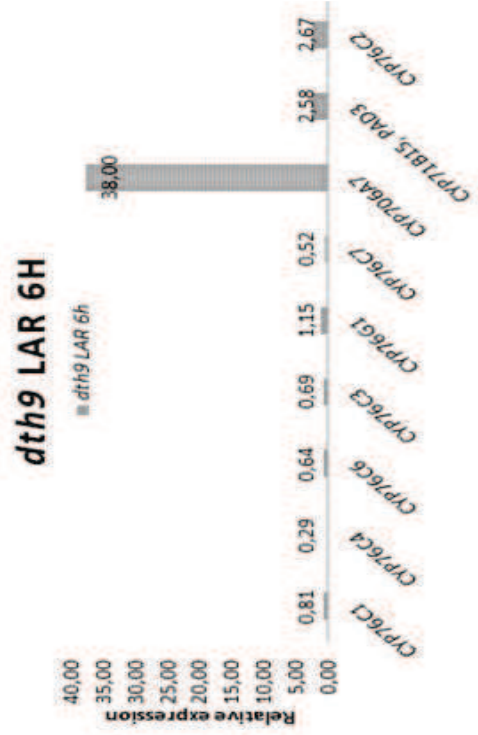


Figure 47: Data from transcriptomic analyses based on LAR responses 6 HPI observed in *A. thaliana* Col-0, *nahG/sid2*, *ndth9* and *ndr1* mutants challenged with *PTo*. DC3000 *avrRpm1*.

Each value corresponds to the mean of three replicates. The big chart represents all the P450 analysed (complete list can be seen in Appendix). All the *CYP76* family members are shown in orange (*CYP76C5* is missing from this analysis). *CYP76C2* is the gene with the highest expression level with *PAD3* (camalexin)(≈50 fold). In the upper panel are depicted in detail family members of *CYP76*, *PAD3* and *CYP706A7* (both with highest values among all P450 tested) for each mutant line.

Col-0 plants showed highest induction of *CYP76C2* and *PAD3* in response to infection in the LAR zone. This is indicative that *CYP76C2* is likely to be important in LAR, but also that it could be implicated in camalexin biosynthesis. This was also observed on the co-expression analysis presented by Ehltig *et al.*, (2008) (Figure 46). In addition, *nahG/sid2* double mutant plants (catechol hydroxylase/ SA induction-deficient mutant 2), showed that *CYP76C2* expression was SA-dependent (as shown by Millet, 2009). The double mutant is unable of synthesizing SA and in consequence is more susceptible to biotrophic infections, but still is capable of exhibiting normal HR. In this mutant, camalexin accumulation is normal and *PR1* expression is abolished, while *PR2* and *PR5* are active (Nawrath and Métraux, 1999). *PAD3* expression levels were extremely high while *CYP76C2* was almost abolished. *PAD3* and *CYP76C2* are thus unlikely to be acting in the same pathway.

dth9 (detachment 9) mutant plants showed enhanced expression of *CYP706A7* (putatively biosynthesis of sesquiterpenes). On the contrary, expression of *PAD3* and *CYP76C2* (and of the rest of the *CYP76* family) was insignificant. This mutant is not affected in SA and camalexin accumulation, and *PR* expression is normal. However, it is susceptible to biotrophic pathogens and incapable of mounting SAR. Thus the highly reduced levels of *CYP76C2* expression observed in this mutant is indicating that *CYP76C2* is somehow related to SAR response.

Finally *ndr1* mutant indicates that *CYP76C2* is *NDR1* independent together with *PAD3*. *CYP76G1* (low constitutive expression in roots, flowers, siliques) showed the same levels of inductions as *CYP76C2*.

MATERIALS AND METHODS

Materials and
Methods

MATERIALS AND METHODS

BIOLOGICAL MATERIAL

Plant Material and Growing Conditions

Arabidopsis thaliana ecotype Columbia wild-type plants (Col-0) and mutants from *CYP76* family were mainly available at the laboratory. Overexpression lines for *CYP76C1*, *CYP76C2*, *CYP76C3*, *CYP76C4* and *PromCYP76C2:GUS* were obtained by Millet Y. and Höfer R., *CYP76C7* was obtained during this work.

Lines *cyp76c1* (SALK 010566), *cyp76c2* (SALK 037019), *cyp76c3* (SALK 077330), *cyp76c4* (SALK 093179), *cyp76c7* (GK-213C08-014134), *cyp76g1* (SALK 065047C) were obtained from the Nottingham European Arabidopsis Stock Centre (NASC, Alonso *et al.*, 2003) and GABI KAT (Kleinboelting *et al.*, 2012).

All lines were checked before use, by means of PCR and qPCR with specific primers (see below).

Plants intended for infections and/or metabolite analysis on leaves were grown on 7 cm Jiffy® peat tablets (Ryomgaard, Denmark) during 4-5 weeks under 12 h daylight and maintained at 20°C day/18°C night temperature with 60% of relative humidity. Light intensity was approximately 60–90 µmol/m².sec, provided by cool-white fluorescent tubes.

Seeds were stratified at 4°C three days before sowing.

Plants intended for other purposes were grown in a standard soil compost mixture, under the same conditions. In all the cases one plant per pot was used.

Plant Pathogens

1. *Pseudomonas syringae* pv. *tomato* DC3000

Pseudomonas syringae pv. *tomato* DC3000 (virulent strain) (**Pto DC3000**) and *Pseudomonas syringae* pv. *tomato* DC3000 *avrRpm1* (avirulent strain) (**Pto DC3000 *avrRpm1***) were used for infections. Both strains were grown in King agar B (Fluka, Sigma-Aldrich, USA) Petri dishes at 28°C during 48 hours prior to liquid culture intended for plant infections. The selection media contained 50 µg/ml of rifampicin for the virulent strain of *P. syringae* and 50 µg/ml of rifampicin and 25 µg/ml of kanamycin for the avirulent one. Strains were conserved in 80% glycerol stock at -80°C.

The avirulent strain was already available at host lab and the virulent one was kindly provided by P. Saindrenan from the Institut de Biologie des Plantes (IBP), Orsay, France.

2. *Botrytis cinerea*

Botrytis cinerea Pers. (teleomorph *Botryotinia fuckeliana* (de Bary) Whetzel) strain BMM1 was kindly provided by B. Mauch Manny, from the NCCR, University of Neuchâtel, Switzerland. Small plugs of monosporic strains were kept in cryovials containing glycerol 80% at -20°C for future use.

The strain was grown in potato dextrose agar (PDA, Fluka, Sigma-Aldrich, USA) or malt extract agar medium (MEA) plates at 23°C during 2 weeks in darkness.

MEA (Malt extract agar) (for 1000 ml)

- 30 g of malt extract (Oxoid, Basingstoke, UK)
- 5 g of bactopectone
- 15 g of agar

The medium was adjusted to 1000 ml with tap water and autoclaved 20 min at 120°C. Petri dishes were conserved at 4°C.

METHODS

Construction of over-expression mutant *35S:CYP76C7* and transformation of *Arabidopsis*

Fully opened flowers of Col-0 plants were harvested, quickly frozen in liquid nitrogen, and ground to fine powder using the TissueLyser II bead grinder (Qiagen, Venlo, Limburg, Netherlands). Total RNA* was isolated (protocol modified from De Vries *et al.*, 1988) cDNA was obtained by reverse transcription of 2 µg total RNA with Superscript III (Invitrogen, Carlsbad, CA, USA). The coding sequence of the candidate gene (*CYP76C7*) was amplified by PCR from the cDNA, using primers with “USER extensions” (for details on User’s cloning compare Nour-Eldin *et al.*, 2006) (Table 10) and Pfu Turbo Cx Hotstart DNA polymerase (Stratagene, La Jolla, Ca, USA).

* Detailed protocols for RNA, and cDNA synthesis can be seen below.

Table 10: Primer sequence with USER extensions used to amplify *CYP76C7*.

Accession	Forward (5'--3')	Reverse (5--3')	T _m (°C)
At3g61040	ggcttaau ATGGATATTGTAGCAATAGTATTGTCTCTGC	ggtttaau TCAAACACGTTTCTTGATAGGCAC	71 /71

PCR was performed in a final volume of 20 µl, in an Eppendorf Mastercycler thermocycler (Hamburg, Germany) and the following amplification program was used:

95°C 2 min
 95°C 30 sec
 55°C 20 sec 45 cycles
 72°C 1.30 min
 72°C 10 min

The PCR product were separated by gel electrophoresis using buffer TAE 1X on a 1% agarose gel. Band of the right size were excised from the gel and cleaned up using Gene Elute Agarose Spin Columns (Sigma, St Louis, USA) according to the manufacturer manual. 8 µL of the cleaned PCR product was mixed with 2 µL of previously linearized vector (molar ratio 1/10), pCAMBIA 3300U (*CaMV-35S* promoter) (Cambia, Canberra, Australia) containing a USER cassette, 1 µL Taq polymerase buffer (Invitrogen, Carlsbad, USA), and 1 µL USER enzyme mix (NEB, Ipswich, USA). The reaction mix was incubated at 37°C for 20 min, followed by 25°C for 20 min, and dialyzed against MilliQ water on a 0.05 µm-pore nitrocellulose membrane (Millipore, Billerica, USA) for 45 min.

Bacterial transformation was performed using 2 µL of ligation product. Bacteria were cultured on Luria-Bertani (LB) plates with kanamycin at 37°C overnight. One positive colony was grown in 40 ml liquid LB medium at 37°C overnight. Plasmids DNA were isolated using NucleoBond Xtra Midi kit (Machery Nagel, Duren, Germany) according to manufacturer instructions. The overexpression construct was then validated by the sequencing platform of the institute. After confirming that the sequence was identical to the one available in online databases, the overexpression constructs were introduced into the *A. tumefaciens* strain GV3101 and *A. thaliana* Col-0 flowering plants were transformed by floral dip (Clough and Bent, 1998). The T1 Transgenic lines transformed with the construct were selected on soil using the

herbicide BASTA (5-10 mg/l glufosinate ammonium) and confirmed later by PCR. The T2 seeds (T3 plants) were used for experiments. The transcript level of gene of interest was quantified by qRT-PCR.

Escherichia coli chemical transformation

2 µl volume of linearized plasmid was mixed with 50 µl DH5α *E. coli* competent cells and left on ice for 20 min. A heat shock at 42°C in a thermal bath was done for 80 sec followed for a new incubation on ice for 10 min. Then 200 µl of LB medium was added and incubated at 37°C under agitation during 20 min. Culture was plated onto LB medium with kanamycin 50 µg/ml and incubated at 37°C during 12-16 hours. The presence of the construct of interest was checked by colony PCR (Table 11).

Table 11: Primers sequences used for colony PCR.

Accession	Gene	Forward (5'--3')	Reverse (5--3')	Tm (°C)
At3g61040	CYP76C7	TTGTCTCTGCTCTTTATCTTC	ACGTTTCTTGATAGGCACGA	54/55

PCR was performed in a final volume of 20 µl, in a Mastercycler Eppendorf (Hamburg, Germany) and the following amplification program was used:

95°C 2 min
 95°C 20 sec
 57°C 20 sec 30 cycles
 72°C 1.30 min
 72°C 10 min

Agrobacterium tumefaciens transformation using electroporation

A volume of 0.5-1 µl of an *E. coli* miniprep was added to 80 µl of *Agrobacterium tumefaciens* (strain GV3101). DNA and cells were mixed on ice and transferred to a prechilled electroporation cuvette (2 mm gap, Molecular Bioproducts, Thermofisher, Waltham, Ma, USA). The electroporation was carried out with a Bio-Rad electroporator Gene pulser II (Hercules, CA, USA) under the following conditions: capacitance 25 µF, voltage 2500 V, resistance 200 Ω, pulse length 5 msec. Immediately after, 1 ml of LB medium was added to the cuvette and transferred to a 15 ml LB containing falcon tube for incubation under agitation at 28°C, during 3-4 hours. Then cells were collected by brief centrifugation and a volume of 40 µl was

spread on a LB agar plate containing kanamycin 50 µg/ml, rifampicin 25 µg/ml, gentamicin 25 µg/ml for selection. Plates were grown at 28°C during 2-3 days. After that period some colonies were streaked again onto LB plates and checked by colony PCR for the presence of the plasmid (same as before). One positive colony was selected for growing in liquid LB medium intended for floral dip (Clough and Bent, 1998).

Luria-Bertani (LB) medium (for 1000 ml)

Bacto-tryptone	10 g
Yeast extract	5 g
NaCl	10 g
Agar	15 g (optional)

Adjusted to pH to 7.5 with NaOH. Autoclaved 20 min.

RNA extraction (modified from De Vries *et al.*, 1988)

Samples were harvested and frozen in screw cap tubes with 3-5 iron beads and ground during 1 min at 30 Hz. After that, 500 µl of RNA extraction buffer (10M LiCl, 1M Tris-HCl pH 8, 0.5 M EDTA pH 8, 10% (v/v) SDS, Phenol) pre-warmed at 80°C was added and vortexed during 30 sec. Next 250 µL of Chloroform/Isoamylalcohol (24:1) solution was added and vortexed for 30 sec. A centrifugation step at 12000 rpm at room temperature during 10 minutes followed. The organic phase was kept in a new 1.5 mL tube. One volume of LiCl 4 M was added, vortexed 30 sec and let it to precipitate on ice and at 4°C overnight. Subsequently samples were centrifuged 20 min at 12000 rpm at 4°C and supernatant was discarded. RNA was subjected to DNase treatment and precipitation as follows:

DNase treatment (60 µl final volume)

Components were added to the tubes containing the obtained RNA as follows: 50.5 µL ultrapure water, 5 µL DNase I/RNase-free (Thermo scientific, Waltham, MA, USA), 6 µL DNase Buffer 10X, 0.5 µL Ribolock Rnase Inhibitor (Thermo scientific). After being mixed gently, incubation was done during 30 min at 37 °C. The reaction was stopped by adding 6 µL EDTA 50 mM (Thermo Scientific) and incubation during 10 min at 65°C.

RNA cleaning and precipitation

To the previous mix, 0.1 vol of 3M CH₃COONa and 0.2 vol of 100% ethanol were added. Precipitation was allowed on ice (or -20°C) during 2 hours. After that period of time a pellet was obtained by centrifugation at 12000 rpm during 10 min at 4 °C. The pellet was washed twice with 70% and 100% ethanol. After a new

centrifugation step at 12000 rpm during 10 min at 4 °C, the pellet was dried and resuspended with 25 µL ultrapure water. RNA quantity and purity were determined in a NanoDrop® spectrophotometer (Thermo Scientific). Absorbance ratios 260/280 nm and 260/230 nm were used as a measure of RNA preparation quality.

cDNA synthesis

Aliquots of 1-2 µg/µl of total RNA were prepared in ultrapure water and incubated with 1 µl of oligo(dT)₂₃, anchored primers 70 µM (Sigma) and 1 µl of dNTP (dNTP set 100 mM Fermentas, Thermo Scientific, Vilnius, Lithuania). Incubation was done in a thermal cycler at 70°C for 10 minutes, and then immediately placed on ice for at least 1 minute. Next, 7 µl of following mix was added to each sample (on ice): 1 µl of SuperScript III, 4 µl of 5X buffer, 1 µl RNaseOUT enzyme Mix and 1 µl of 0.1M DTT (Invitrogen, Carlsbad, CA, USA).

RT-PCR program used was:

25°C 15 min
50°C 60 min
70°C 15 min

cDNA was diluted to a final volume of 200 µl with ultrapure water and stored at -20°C.

Genotyping of T-DNA insertion lines

Homozygous T-DNA insertion lines were selected and confirmed by PCR on genomic DNA extracted from young leaves according to Edwards *et al.* (1991). Specific left border primers of the T-DNA insertion (LBP) were used to check T-DNA insertion in combination with the specific primers of the target gene (LP and RP: Left, Right genomic primer). Therefore, PCR reaction was set up as LBP+RP or LP+RP for the detection of the recombinant or the wild-type allele, respectively (Figure 48).

The resulting PCR products were separated in 1 % agarose gel (Sigma) running in 1X TAE buffer at 100 V.

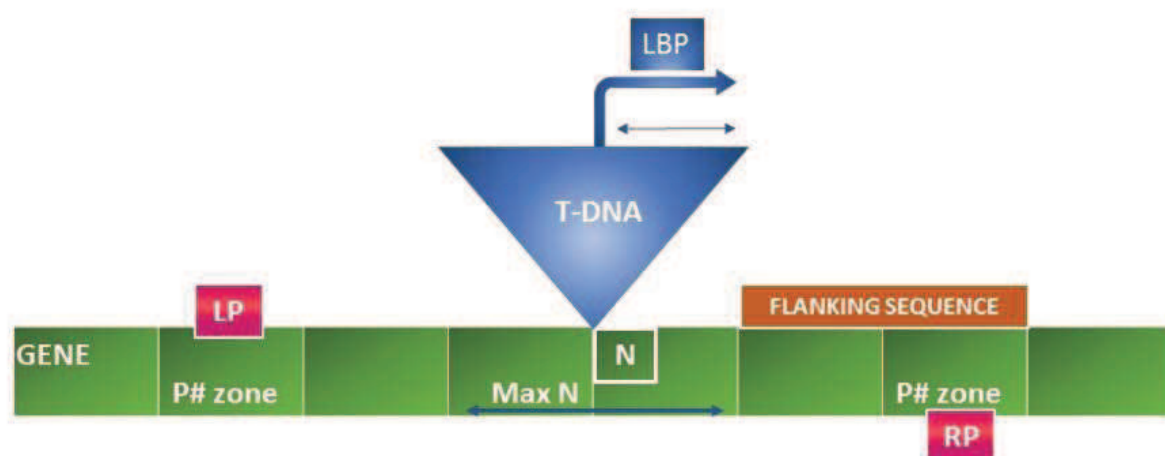


Figure 48: Diagram of primers and T-DNA insertion (from www.signal.salk.edu).

The figure shows the spatial representation of left and right genomic primers, flanking the T-DNA insertion site, as well as the LBP that anneals to T-DNA insertion. Abbreviations: **LP**: Left genomic primer, **RP**: Right genomic primer, **LBP**: left T-DNA border primer. P# zone: represents the zone allowed for genomic primers selection, up to 100 bp, N: interval of bp between insertion site and flanking sequence (300 bp), Max N is the maximum difference of N.

Table 12: Primer sequences used for genotyping of knock-out lines

Accession	Gene	Forward (5'--3')	Reverse (5--3')	T _m (°C)
SALK010566	<i>cyp76c1</i>	TGGACATAATCTCAGGGCAAG	ATTAATATTGGCGCTTTCTT	60/57
SALK037019	<i>cyp76c2</i>	ATGGATATCATCTTTGAACAAGC	AATTACGGCCACGTTTCTTG	57/60
SALK077330	<i>cyp76c3</i>	TGGACCTCTACTAATTCAAGG	GAAGACGATATTGTAGGTTTCTTGAC	60/62
SALK093179	<i>cyp76c4</i>	GGACATCATCTCAGGGCAAG	AATTAATGGTCTGTTTCTTTACGG	60/58
GK213C08-014134	<i>cyp76c7</i>	TCGATCGTTTGAAAAGCTAAAG	GAGCTAGAAAAGAAGCGAGGC	55/59
	T-DNA (LBP) 08409	ATATTGACCATCATACTCATTGC	-	55
	<i>Lb1.3</i>	ATTTTGCCGATTTTCGGAAC	-	52
SALK065047C	<i>cyp76g1</i>	GGCCAAAACGGTACAAAAAC	TCTCGAGAACATGAGGTTTCC	57/57

The resulting PCR products were separated in 1 % agarose gel (Sigma) running in 1X TAE buffer at 100 V. The transcript level of gene of interest was quantified by qRT-PCR.

PCR program for SALK lines

94 °C 2 min
94 °C 1 min
55 °C 1 min 30 cycles
72 °C 30 sec
72 °C 10 min

PCR program for GABI KAT lines

94 °C 2 min
94 °C 30 sec
59 °C 30 sec 37 cycles
72 °C 90 sec
72 °C 5 min

DNA extraction protocol (adapted from Edwards *et al.*, 1991)

Small leaves were collected, frozen and grinded in a 2 ml polypropylene tube with screw cap containing 3-5 iron beads, using the TissueLyser II (Qiagen, Venlo, Limburg, Netherlands) during 1 min at 30 Hz. After that 1.6 ml of extraction buffer (0.2 M Tris HCl pH 7.5, 0.25 M NaCl, 25 mM EDTA, 0.5% SDS) was added to the samples and vortexed for 5 seconds. Then extracts were centrifuged at 13.000 rpm for 10 min. Subsequently 300 µl of the supernatant was transferred to a fresh 1.5 ml tube and this supernatant (approx. 400 µl) was mixed with an equal volume of isopropanol and left at room temperature during 2 minutes followed by centrifugation at 13.000 rpm for 10 min. The pellet was washed twice with 500 µl ethanol 70% and vacuum dried. Next, the pellet was dissolved and resuspended in 500 µl ultrapure water and kept at -20°C or 4°C for future use.

Genotyping of Overexpression Lines

Previously selected overexpression lines were confirmed by PCR on genomic DNA extracted from young leaves according to Edwards *et al.* (1991). Specific primers of the target gene were used (Table 12). The resulting PCR products were separated in 1 % agarose gel (Sigma) running in 1X TAE buffer at 100 V. The transcript level of gene of interest was further quantified by qRT-PCR (See below).

Gene Expression Analysis

β - Glucuronidase (GUS) Activity Assay (Jefferson *et al.*, 1987)

Gus activity was assayed qualitatively by staining with the substrate X-Gluc (5-bromo-4 chloro-3 indolyl β -D-glucuronide (cyclohexamine salt)) (Euromedex, France) to determine the localization of gene expression (Weigel and Glazebrook, 2002).

Briefly, tissues were collected in 10 ml round bottom polypropylene tubes and kept in cold 90% acetone on ice until the end of the harvesting process. Once the collection of samples was done, samples were incubated 20 min at room temperature, then acetone was eliminated and washed off and fresh X-Gluc buffer was added keeping samples on ice. Immediately after, samples were infiltrated under vacuum during 20 min. After that time, vacuum was slowly released and samples were taken to overnight incubation at 37°C. The day after, buffer staining was removed and samples were subjected to an ethanol washing series of 20%- 35%- 5% ethanol at room temperature during 30 min each. Fixative FAA incubation was done during 45 min at room temperature. After that step, fixative was removed and samples were washed and kept in ethanol 70% at 4°C for subsequent analysis.

Staining buffer (100ml)

- Buffer phosphate solution (PBS) 0.1M pH 7 50 ml
- EDTA 0.5 M pH 8 2 ml
- Potassium ferricyanide 0.5 M 2 μ l
- Potassium ferrocyanide 0.5 M 2 μ l
- Triton X-100 100 μ l
- X-Gluc in DMF at 20 mg/ml 1 ml
- Distilled water qsp 100 ml

(Ferri- and Ferrocyanide, X-Gluc were kept in the dark at -20°C)

Fixation buffer FAA (room temperature)

- 50% Ethanol
- 10% glacial acetic acid
- 5% Formaldehyde

qRT-PCR for Gene Expression

The transcript level of gene of interest was quantified by qRT-PCR in 384 well plates using a LightCycler® 480 Instrument II Real-Time PCR instrument (Roche, Bale, Switzerland).

Each reaction was performed in a total volume of 10 µl (5 µl of 2x SYBR Green I Master Mix (Roche), 0.1 µl of each primer (100 µM) 250 nM, 2 µl of cDNA (50 ng/µl) and ultrapure water). Positive and negative control samples were included to validate the reactions. Reaction volumes and cDNA were delivered into the 384-plates by using the Biomek® 3000 Laboratory Automation Workstation (Beckman Coulter, Pasadena, CA, USA). Thermal cycling conditions were 95°C for 10 min, followed by 45 cycles at 95°C for 10 sec, 60°C for 15 sec and 72°C for 20 sec, followed by a melting curve analysis from 55°C to 95°C to check the specificity of each gene primer.

All results were normalized using three previously validated stable reference genes: *SAND*, *TIP41* and *EXP* (Czechowski *et al.*, 2005, Boachon *et al.*, 2014) (Table 13). Primers were designed with Primer3© software (<http://frodo.wi.mit.edu>) and checked by BLAST for gene specificity. Primer sequences, T_m, efficiencies and annotations are listed in Tables 14 and 15.

The stability was tested using the comprehensive tool RefFinder at <http://www.leonxie.com/referencegene.php?type=reference#> (integrates geNorm, Normfinder, Bestkeeper, etc).

CT threshold cycle was calculated by the 2nd derivative maximum. Primers efficiency was calculated with LinRegPCR software (Ruijter *et al.*, 2009).

Three to five biological replicates and three technical replicates were analyzed by genotype or treatment. Error calculations were done by means of Taylor series calculation and comparison between mock vs infected plants were done by Wilcoxon's signed-rank test (Mann Whitney U) (Lehman, 1975, cited in Balzarini *et al.*, 2008) with a significance level of 5%.

- Quantitative/relative gene expression of knock-out and overexpression lines were calculated by the $2^{-\Delta\Delta CT}$ method (Livak and Schmittgen, 2001) according to the equation:

$$\Delta\Delta CT = (CT_{\text{target gene}} - CT_{\text{reference gene}})_{\text{mutant}} - (CT_{\text{target gene}} - CT_{\text{reference gene}})_{\text{wild-type}}$$

Where:

CT: PCR cycle at which the fluorescence detected in the well crosses the fluorescence threshold (background level).

The fold change in expression of the target gene is related to the reference gene by assuming that both target and reference gene are amplified with similar efficiencies near 100% (Efficiency=2). The result then will correspond to fold change in gene expression of the target gene normalized not only to a reference gene but also to an untreated control.

- Quantitative/relative gene expression of *CYP76C* family members after pathogen infections were calculated by the Pfaffl method (Pfaffl, 2001) according to the equation:

$$\text{Ratio} = (E_{\text{target}})^{\Delta \text{CT}_{\text{target}} (\text{calibrator- sample})} / (E_{\text{reference}})^{\Delta \text{CT}_{\text{reference}} (\text{calibrator- sample})}$$

Where:

-E: efficiency of target /reference gene

- Calibrator: the untreated control (*i.e.* Col-0 non infected plants at Time 0)

- $\Delta \text{CT}_{\text{target}}$: is the CT of the target gene in the calibrator minus the CT of the target gene in the test sample (treatment).

- $\Delta \text{CT}_{\text{reference}}$: is the CT of the reference gene (arithmetic mean of the 3 chosen reference genes) in the calibrator minus the CT of the reference gene in the test sample.

This calculation assumes that each gene, reference and target, has the same efficiency in test and calibrator, but not necessarily the same efficiency between them.

Table 13: Primer sequences of validated reference genes used for RT-qPCR for gene expression quantification

Accession	Gene	Forward (5'--3')	Reverse (5--3')	T _m (°C)	PCR Efficiency	STD
AT2G28390	<i>SAND</i>	GGATTTTCAGCTACTCTTCAAGCTA	CTGCCTTGACTAAGTTGACACG	59/59	1.9	0.068
AT4G34270	<i>TIP41</i>	GAAGTGGCTGACAATGGAGTG	ATCAACTCTCAGCCAAAATCG	60/59	1.9	0.091
AT4G26410	<i>EXP</i>	GAGCTGAAGTGGCTTCCATGA	GAGCTGAAGTGGCTTCCATGA	61/61	1.9	0.067

Table 14: Primer sequences used for RT-qPCR for gene expression quantification

Accession	Gene	Forward (5'--3')	Reverse (5--3')	Tm (°C)	PCR Efficiency	STD
At2g45560	<i>Cyp76c1</i>	TTTCGTTGACAACCTTCTCG	TGTATCCGTGCCTGCTGTAA	59/59	1.9	0.05
At2g45570	<i>CYP76C2</i>	CGATATTGTACACCTTCTCTGGAC	ACCATTGTTTCAGGGTTTCG	60/59	1.9	0.09
At2g45580	<i>CYP76C3</i>	CCTCTGCTCGTTGGAGGTT	CGCGAAATTCATTTACTAACTCAC	60/60	1.9	0.05
At2g45550	<i>CYP76C4</i>	AGTTTCCGTCATCTGGCTTC	TGCGGTGAGAACATGAGAGT	59/59	1.9	0.05
At1g33730	<i>CYP76C5</i>	AAGAGTACTCGGGTAAATTGCTTC	TAGTGCATCCAAGAAGTCTCTGC	59/61	1.9	0.05
At1g33720	<i>CYP76C6</i>	GTCGGTTCAGAGGATTTGGA	ATGGCTCGTTTCTTCAGAGG	60/59	2	0.07
At3g61040	<i>CYP76C7</i>	CGAACCATATGTATCGTGCCTA	ATACCGGCCGAGAACTACAG	59/59	1.9	0.07
At3g52970	<i>CYP76G1</i>	GGCCAAAACGGTACAAAAC	TCTCGAGAACATGAGGTTTCC	59/59	1.9	0.05
AT2g14610	<i>PR1</i>	AAAACCTAGCCTGGGGTAGCGG	CCACCATTGTTACACCTCACTTTG	60/60	2	0.09
AT5g44420	<i>PDF1.2</i>	CTGTTACGTCCATGTAAATCTACC	CAACGGGAAAATAAACATTAACAG	60/60	1.9	0.05
AT1G17420	<i>LOX3</i>	GTGGCCGGAGTTATCAACC	GGGACGTAGCCACCGTAAG	60/60	1.9	0.10
AT2G06050	<i>OPR3</i>	GGCTCAAAGCTCGTTACC	ACTCCCTTGCCTTCCAGACT	60/60	1.9	0.05
AT5G13220	<i>JAZ10</i>	CATCGGCTAAATCTCGTTCG	CGGTACTAGACCTGGCGAGA	60/60	1.9	0.06
AT3G14440	<i>NCED</i>	CGTCTTCTCAAAGCTCCGAC	TGAATCTTCGGCGTATTTGTCT	60/60	1.9	0.05
AT5G24780	<i>VSP1</i>	CCGTCAATGTTTGGATCTTTG	GCTGTGTTCTCGGTCCATA	56/59	1.9	0.07

Table 15: Reference genes annotation

Accession	Gene	Pathway/Function/Annotation	Reference
AT2G28390	<i>SAND</i>	unknown	Czechowski <i>et al.</i> , 2005, Boachon <i>et al.</i> , 2014
AT4G34270	<i>TIP41</i>	unknown	Czechowski <i>et al.</i> , 2005, Boachon <i>et al.</i> , 2014
AT4G26410	<i>EXP</i>	unknown	Czechowski <i>et al.</i> , 2005, Boachon <i>et al.</i> , 2014
AT2g14610	<i>PR1</i>	Salicylic acid/ SAR marker	Disponible IBMP; Boachon <i>et al.</i> , 2014
AT5g44420	<i>PDF1.2</i>	Jasmonate/Ethylene / Defensine	Langlois-Meurinne <i>et al.</i> , 2005
AT1G17420	<i>LOX3</i>	Jasmonate	Didierlaurent, 2012
AT2G06050	<i>OPR3</i>	Jasmonate	Didierlaurent, 2012
AT5G13220	<i>JAZ10</i>	Jasmonate	Didierlaurent, 2012
AT3G14440	<i>NCED</i>	Abscisic acid biosynthesis	De Torres-Zabala <i>et al.</i> , 2007
AT5G24780	<i>VSP1</i>	Jasmonate / wounding	Heitz <i>et al.</i> , 2012

Plant Infections

Plant Leaves Infection with *Pto* DC3000

One single colony of each one of the *P. syringae* strains was picked from a plate to inoculate 50 ml of King B liquid medium containing the right antibiotic for selection. Cultures were grown under agitation (180 rpm) during 14-16 hours at 28°C.

King B medium (for 1000 ml)

- Bacto Peptone 20 g
- Glycerol 10 ml
- K₂HPO₄ .3H₂O 1.5 g
- MgSO₄ .7H₂O 1.5 g
- Rifampicin (100 µg/ml)
- Kanamycin (100 µg/ml)

Adjusted to pH to 7.2 ± 0.2 and autoclaved 20 min at 120°C.

For the virulent infections with *Pto* DC3000, 4-5 week old plants were infiltrated (gene expression) or inoculated by dipping the leaves (phenotype/volatile collection) in a suspension containing 5 x 10⁷ CFU/ml (abs=0.2, λ=600 nm correspond to 2x 10⁸ CFU/ml) in 10 mM MgCl₂ and 0.03% (v/v) Silwet L-77 (Lehle Seeds, Round Rock, TX, USA). Quantification of pathogen growth (biomass) was conducted four days after infection by means of qRT-PCR.

For avirulent infections, there were two types of infection. When the plants were intended for gene expression or metabolic profiling, whole leaves were syringe infiltrated. Concentration used for gene expression was 5 x 10⁶ CFU/ml and concentration used for metabolomics analysis was 5x 10⁷ CFU/ml. When plants were infected for disease assessment, bacteria were first syringe infiltrated into 3 complete leaves and 3 half-leaves using a suspension containing 5 x 10⁶ CFU/ml in 10 mM MgCl₂ and 0.03% (v/v) Silwet L-77 and then 24 h later inoculated by dipping the whole plant in a suspension with the virulent strain as explained before for virulent infections.

qPCR quantification of pathogen growth was done at zero and four days after infection by collecting the LAR and SAR area of the leaves. LAR area corresponds to the non-infiltrated part of the half-infiltrated leaves and SAR area corresponds to all the other leaves that were not infiltrated with the avirulent strain but dipped with the virulent one (Figure 49).

Plant material from both type of infections, were frozen in liquid nitrogen for total genomic DNA extraction. Five replicates were used for each treatment. One plant was considered one experimental unit.

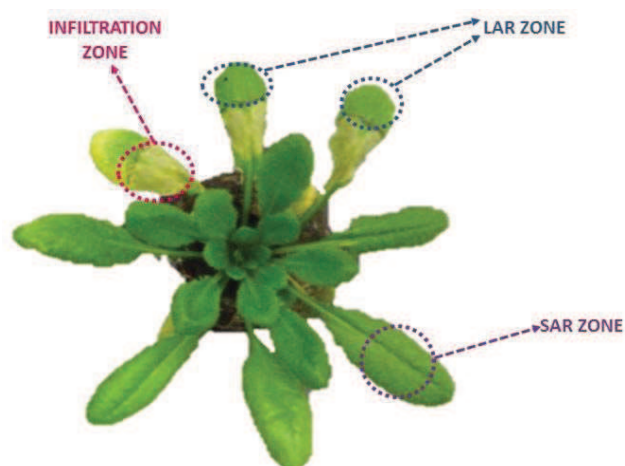


Figure 49: *Arabidopsis thaliana* Col-0 plant, four days after being syringe infiltrated with the avirulent strain of *Pseudomonas syringae* followed by dipping with the virulent strain.

In magenta the infiltration zone showing the HR response, in blue the LAR zone induced after dipping and in violet the SAR zone.

DNA extraction and qPCR quantification

Colonization of plant tissues by bacterial pathogens was quantified in each sample by measuring the amount of genomic DNA from plant and pathogen by qPCR (Boachon *et al.*, 2014)

Serial dilutions of pGEM-T Easy plasmid containing a PCR product cloned from a genomic region of *P. syringae* (*Opfr* gen) and *A. thaliana* (*Tubuline 4*) were used to relate their qPCR signal to constructed calibration curves.

Primers for the cloning of the specific regions were based on Brouwer *et al.* (2003) and Boachon *et al.* (2014) and designed with Primer 3© software (Table 16). PCR results for the pathogen quantification were expressed as logarithm of the ratio copy numbers of the pathogen gene per copy numbers of the plant gene.

Table 16: Gene specific primers for pathogen DNA quantification

Accession	Gene	Forward (5'--3')	Reverse (5--3')	T _m (°C)
At5g44340	<i>TUB4</i>	CTTGTCGCAGAGTACCAGCA	GAGGGAGCCATTGACAACAT	59/58
NC_004578	<i>Opfr</i>	GCTTCGCCAAGAAAGAAATG	GTCGTCGGTCAGGAAGTAGC	56/61

DNA extraction was conducted according to Brouwer *et al.* (2003). Briefly, 80 mg of frozen plant material were grinded with Qiagen® Tissuelyzer II using glass beads during 30 sec at maximum speed.

300 µl of lysis buffer (2.5 M LiCl, 50 mM Tris-HCl, 62.5 mM, 4.0% Triton X-100, pH 8) was added to each sample followed by an equal volume of phenol:chloroform:isoamyl alcohol (25:24:1 v/v) and grinded for 30 sec at maximum speed again. A centrifugation step at 10 000 rpm during 5 min was done to collect supernatant. DNA was precipitated by adding of 2 volumes of absolute ethanol and incubated for 15 min at -20°C. Then samples were centrifuged at 10 000 rpm during 5 min and the pellet obtained was washed with 70% ethanol and air-dried. Then it was resuspended in ultrapure water.

Quantification of pathogen and plant genomic DNA were performed by real-time qRT-PCR in a Roche Lightcycler 480 (Roche, Switzerland). Amplification was done using 2 µL of genomic DNA, 5 µl SYBR Green I Master Mix (Roche), with 100 µM primers in a final volume of 10 µl adjusted with sterile ultrapure water. Cycling conditions were 95 °C for 10 min, followed by 40 cycles at 95°C for 10 s; 60°C for 15 s and 72° C for 20 s, followed by a melting curve analysis from 55° C to 95° C.

Technical triplicates were done and all the experiments were repeated twice.

***Botrytis cinerea* Infection**

For *B. cinerea* infections 8-10 plants per treatment were used and 5-7 leaves of each plant were inoculated with a 5 µL droplet containing 1×10^5 conidia/ml in potato dextrose broth (PDB 12 g/l) (Duchefa Biochimie, Haarlem, The Netherlands).

To produce the inoculum, conidia were washed off in liquid PDB from Petri dishes cultures and filtered using cheesecloth. The conidial concentration was determined by counting twice the number of conidia in a Neubauer-improved counting chamber (Marienfeld, Lauda-Königshofen, Germany).

After infection, plants were kept immediately at 100% relative humidity in enclosed crystal clear polystyrene boxes, for the rest of the experiment to ensure fungus penetration. The macroscopic evaluation of *B. cinerea* growth was done by measuring the diameter of the lesions from 5 leaves on 8-10 individual plants 72 HPI. One plant was considered one experimental unit or replicate. Measurements were taken by using a precision magnifier Achromat 7X (23.5 mm lenses, Eschenbach, Nurnberg, Germany) or Image J (Abramoff *et al.*, 2004). Results were expressed as necrosis size in square millimeters.

Hyaloperonospora arabidopsidis

Hyaloperonospora arabidopsidis isolates Noco2 and Emwa1 were kindly provided by P. Saindrenan, IBP-Paris. Infections on healthy seedling of Col-0 (Noco2) and Wassilewskija-0 (Emwa1) ecotypes were done in order to keep the strains alive. A back-up aliquot of infected seedlings was kept at -80°C.

***Hyaloperonospora arabidopsidis* Infection (Massoud *et al.*, 2012 with some modifications)**

Small pots were prepared with around 2.5-5 mg of seeds of Col-0 and *CYP76C2* mutants. Seven days later, small plants with cotyledons were infected by pulverization with 1.5 ml of a conidial suspensions at a concentration of $5 \cdot 10^4$ conidia/ml diluted in sterile water. Plants were kept at 100% humidity (saturation) inside crystal boxes during 48 hours. After that period of time, the lid was slightly opened to regulate humidity and to allow the sporulation of the fungus, and then closed again until the end.

Seven days after infection the number of conidia developed on the leave surface was assessed by cutting the sprouts (only aerial part). Samples were weighted and diluted in 5-10 ml of sterile water followed by vortexing during 10 minutes. The liquid suspension was filtrated and conidial concentration estimated by using a Nageotte chamber (Marienfeld, Lauda-Königshofen, Germany) expressing the values as number of conidial/ mg fresh weighted leaves under a binocular microscope (x 40 magnification).

Metabolomics Analysis**Volatile Collection**

A. thaliana wild-type and mutant plants of the *CYP76C* family were tested for volatile emission after pathogen infection with *Pto* DC3000, *Pto* DC3000 *avrRpm1* and *B. cinerea*.

Infections were done as described before for each pathogen and 24 hours later plants were enclosed in 1-l glass jars closed with a lid and equipped with an inlet and an outlet for volatile collection (Ginglinger *et al.*, 2013).

The experimental unit was composed of 3 plants/jar. Triplicates were made for each treatment (mock and infected) and the experiment was repeated twice.

The jiffy pots were covered with aluminum foil to reduce the detection of soil volatiles.

A vacuum pump was used to draw air through the glass jar at a rate of 100 ml/min with the incoming air being purified through a 140 x 4 mm cartridge containing 200 mg Tenax TA (20/35, Grace Scientific, India). The same type of cartridge was used for trapping the volatiles at the outlet.

Volatiles were sampled during 24 hours. Room conditions were suitable for pathogen and plant development with a light intensity of 60–90 $\mu\text{mol}/\text{m}^2 \cdot \text{sec}$ and a temperature of 23°C.

The subsequent GC-MS analyses were performed by Dr. B. Boachon. Tenax cartridges were analyzed in a Perkin Elmer Clarus 680 gas chromatographer equipped with a Perkin Elmer Clarus 600T quadrupole mass spectrometer and a TurboMatrix 100 thermal desorber (TDS) (PerkinElmer, Waltham, USA). The procedure was done as follows: first cartridges were dry-purged with helium (He) at 100 ml/min for 10 min at room temperature to remove any water in the TDS. Volatiles were released from the Tenax traps using a thermal desorption at 250°C for 5 min under a He flow of 50 ml /min. Desorbed volatiles were then transferred to an electronically-cooled focusing trap at -30 °C and injected in 1/6 split mode into the a HP-5MS (30 m x 0.50 mm x 0.5 mm) analytical column (Agilent Technologies, Santa Clara , CA, USA) by heating the cold trap to 280°C and under a constant pressure of 15 Psi.

The temperature program was 0.5 min at 50 °C, followed by a 10 °C/min ramp to reach 320 °C, and a subsequent 10 min period at 320 °C. Fragment acquisition was done at 0.25, 50, 500 m/z electronic flux 70 eV.

The product identification was done by comparison of retention times and mass spectra with authentic standards (when available) and database NIST MS Search v2.0 (Linstrom and Mallard, 2014).

Metabolic Profiling in UPLC MS/MS

Targeted Analysis for (mono) terpenoids: UPLC MS/MS Triple Quad in MRM Mode

A. thaliana wild-type and *CYP76C2* mutant plants were syringe-infiltrated with *Pto* DC3000 *avrRpm1* and analyzed 6 hours post infection for the accumulation of (soluble) free and conjugated monoterpenoids and derivatives. The experimental unit consisted in a bulk of same size infected and non-infected leaves coming from 3-5 plants. Triplicates were made for each treatment (mock and infected) and the experiment was repeated twice.

Detached leaves were pooled together and weighted to 500 mg in order to prepare methanol extracts. Samples were grinded in a mortar at room temperature and extracted with 2 ml of HPLC grade methanol and 10 µl L-citronellol 20 µg/ml as internal standard. Extracts were placed in a 1.5 ml glass vials and stored at -20°C overnight. The following morning, extracts were subjected to sonication at room temperature during 10 min followed by a double step of centrifugation at 5000 rpm during 10 min. Clean supernatant were then transferred to a UPLC vial (Agilent technologies, Santa Clara, CA, USA) and concentrated under argon flow to 200-300 µl. Extracts were stored at -80°C and centrifuged again, prior to analysis, to obtain clearer extracts.

All analyses were performed at the Metabolomic Platform of IBMP-CNRS by Dr. B. Boachon, using a Waters Quattro Premier XE (Waters, Milford, USA) mass spectrometer equipped with an electrospray ionization (ESI) source and coupled to an Acquity UPLC system (Waters). Chromatographic separation was achieved using an Acquity UPLC BEH C18 column (100 x2.1mm, 1.7 μ m; Waters), coupled to an Acquity UPLC BEH C18 pre-column (2.1 x 5 mm, 1.7 μ m; Waters) (Table 17).

Confirmation of this information was done in UPLC MS (Orbitrap) by Dr. Raymonde Baltenweck at Laboratoire Métabolisme Secondaire de la Vigne, INRA, University of Strasbourg, Colmar

Table 17: UHPLC gradient elution.

The mobile phase consisted of (A) water and (B) methanol, both containing 0.1% formic acid. The total run time was 17 min. The column was operated at 35°C with a flow-rate of 0.5ml/min (sample injection volume 3 μ l).

Time (min)	Flow (ml/min)	%A	%B
-	0.25	95	5
2	0.25		100
12	0.25		100
14	0.25		100
15	0.25	95	5
17	0.25	95	5

Nitrogen generated from pressurized air in a N2G nitrogen generator (Mistral, Schmidlin, Switzerland) was used as the drying and nebulizing gas. The nebulizer gas flow was set to approximately 50 l/h, and the desolvation gas flow to 900 l/h. The interface temperature was set at 400°C and the source temperature at 135°C. The capillary voltage was set at 3.4 kV and the cone voltage at 25 V, the ionization was in positive and negative mode. Data acquisition and analysis were performed with the MassLynx 4.1 software. Low mass and high mass resolution was 15 for both mass analyzers, ion energies 1 and 2 were 0.5 V, entrance and exit potential were 50 V, and detector (multiplier) gain was 650 V.

MRM mode was used for quantitative analyses (Table 18).

Table 18: m/z fragments obtained by UPLC-MS for different linalool derivatives and mode (ESI + or ESI -).

	Nomenclature	Parent	Daughter	ESI
	Linalool	137	80.7	ES+
	8-hydroxylinalool	135	106.8	ES+
	8-oxo-linalool	151.2	92.8	ES+
	Carboxylinalool	167.2	92.8	ES+
	1.2-epoxylinalool	153	43.1	ES+
	Lilac alcohol	-	-	ES+
	Lilac aldehyde	-	-	ES+
	Dihydroxy linalool	139	82.8	ES+
	Geranyl linalool	273	84.8	ES+
IS	Citronellol	-	-	ES+

Hormone Profiling

A. thaliana wild-type and *CYP76C2* mutant plants were syringe-infiltrated with *Pto* DC3000 *avrRpm1* or MgCl₂ 10mM, harvested and frozen in liquid nitrogen for hormone analyses according to Heitz *et al.*, (2012). Samples were collected at the following time points: 0, 24, 48 and 72 hours post infection. The experimental unit consisted in a bulk of same size infected leaves coming from 3-5 plants. For each time point and treatment (mock vs infected) triplicates were collected.

Aliquots of 150 mg were prepared in screw cap polypropylene tubes containing from 3-5 iron beads. Frozen powder was extracted with five volumes of ice-cold 90% methanol containing Dihydro-JA (10 µM), Dihydro-JA-Ile (10 µM) and d-ABA (500 µM) as internal standards. Material was ground twice under liquid nitrogen with the TissueLyser II (Qiagen) for 30 sec at maximum speed. Subsequently the samples were placed in a rotator (axis 90°, 15-20 rpm) during 20 minutes at 4°C to maximize extraction. Two successive centrifugations steps at 14000 rpm were then performed. Samples volume was reduced to 250 µl under argon flux and kept overnight at -20°C for debris precipitation. Next morning cleared supernatants were recovered after centrifugation for UPLC-MS analysis.

All analyses were performed at the Metabolic Platform-IBMP-CNRS by Dr. R. Lugan and Dr. B. Boachon, using a Waters Quattro Premier XE (Waters, USA) equipped with an electrospray ionization (ESI) source and coupled to an Acquity UPLC system (Waters). Chromatographic separation was achieved using an Acquity UPLC BEH C18 column (100 x2.1mm, 1.7µm; Waters), coupled to an Acquity UPLC BEH C18 pre-column (2.1 x 5 mm, 1.7µm; Waters) (Table 19).

More analyses were done in UPLC MS (Orbitrap) by Dr. Raymonde Baltenweck at Laboratoire Métabolisme Secondaire de la Vigne, INRA, University of Strasbourg, Colmar

Table 19: UHPLC gradient elution.

The mobile phase consisted of (A) water and (B) methanol both containing 0.1% formic acid. The total run time was 17 min. The column was operated at 35°C with a flow-rate of 0.35 ml/min (sample injection volume 3 µl).

Time (min)	Flow (ml/min)	%A	%B
-	0.35	95	5
2	0.35	0	100
12	0.35	0	100
14	0.35	0	100
15	0.35	95	5
17	0.35	95	5

Nitrogen generated from pressurized air in a N2G nitrogen generator (Mistral) was used as the drying and nebulizing gas. The nebulizer gas flow was set to approximately 50 l/h, and the desolvation gas flow to 900 l/h. The interface temperature was set at 400°C and the source temperature at 135°C. The capillary voltage was set at 3.2 kV and the cone voltage at 25 V, the ionization was in positive and negative mode. Data acquisition and analysis were performed with the MassLynx 4.1 software. Low mass and high mass resolution was 15 for both mass analyzers, ion energies 1 and 2 were 0.6 V, entrance and exit potential were 2 V, and detector (multiplier) gain was 650 V.

The product identification was done by comparison of retention times and mass spectra with authentic standards (when available) and MassLynx software version 4.1.5 (Waters corporation).

Internal standards were kindly provided by Dr. T. Heitz and Dr. H. Zuber from IBMP-CNRS, Strasbourg, France.

Standards for product identification were purchased at Sigma-Aldrich: Abscisic acid (ABA), Benzoic acid (BA), Salicylic acid (SA), 2,3 Dihydroxybenzoic acid (2.3 DHBA), 2,5 Dihydroxybenzoic acid (2.5 DHBA), 2,4 Dihydroxybenzoic acid (2.4 DHBA), 3,4 Dihydroxybenzoic acid (3.4 DHBA), Jasmonic acid (JA).

The identity of glycosylated/xylosylated forms of SAG, SEG, DHBA were confirmed by β -glycosidase treatment (Sigma) and β -xylosidase treatment (Sigma).

MRM mode was used for quantitative analyses (Table 20).

Table 20: m/z fragments obtained by UPLC-MS, cone voltage, collision energy (CE) used, retention times (RT) and mode (Electro spray ionization + or -).

	Nomenclature	Parent	Daughter	Cone V	CE	RT	ESI
	BA	123	79.05	24	16	7.55	ES+
	SA	137/138.12	93	25	16	7.84	ES-
	2.3 DHBA	155	137	20	16	5.7	ES+
	2.4 DHBA	155	137	20	16	5.3	ES+
	2.5 DHBA (Gentisic acid)	155	137	24	16	4.7	ES+
	3.4 DHBA	155	92.9	24	16	3.5	ES+
	SAG	299	137	48	18	5.23	ES-
	SEG	299	179	20	11	6	ES-
	JA	209	59	25	23	9.16	ES-
	JA-ile	324	151	25	20	10.3	ES+
	JA-ile-OH	338	130	25	23	8.45	ES-
	JA-ile-COOH	352	130	25	23	8.33	ES-
	TA (12-OH-JA)	225	59	25	25	6.62	ES-
	TAG	387	206.8	25	20	6.2	ES-
	12-OHJA sulfate	305.2	97	30	32	5.94	ES-
	OPDA	293.4	275.3	25	15	11.4	ES+
	ABA	263	153	25	12	8.47	ES-
	Camalexin	201.05	59.1	28	32	9.2	ES+
Internal std	dh-JA	213	153	25	20	9.92	ES+
	dh-JA-ile	326	280	25	20	10.78	ES+
	D-ABA	253	191.5	25	15	8.4	ES-

List of abbreviations: **BA**: Benzoic acid, **SA**: Salicylic acid, **2.3 DHBA**: 2.3 Dihydroxybenzoic acid, **2.4 DHBA**: 2.4 Dihydroxybenzoic acid, **2.5 DHBA**: 2.5 Dihydroxybenzoic acid or Gentisic acid, **3.4 DHBA**: 3.4 Dihydroxybenzoic acid, **SAG**: Salicylic acid 2-O- β -glucoside, **SEG**: Salicyloil glucose ester, **JA**: Jasmonic acid, **JA-ILE**: Jasmonoyl isoleucine, **JA-Ile-OH**: 12-hydroxyjasmonoyl-isoleucine, **JA-Ile-COOH**: 12-carboxyjasmonoyl isoleucine, **TA**: Tuberonic acid or 12-hydroxy-(+)-7-isojasmonic acid, **TAG**: Glycosylated form of tuberonic acid called 12-O- β -glucosyl- jasmonate, **12-OH-JA-sulfate**: 12-hydroxy-(+)-7-isojasmonic acid sulfate, **OPDA**: 12-oxo-cis-10,15 phytodienoic acid, **ABA**: Abscisic acid.

Non-targeted analysis: UPLC MS (Orbitrap)

A. thaliana wild-type and *CYP76C2* mutant plants were syringe-infiltrated with *Pto* DC3000 *avrRpm1*, harvested and frozen in liquid nitrogen for non-targeted analysis.

Samples were collected in a time line at 0, 24, 48 and 72 hours after infection. The experimental unit consisted in a bulk of same size infected and non-infected leaves coming from 3-5 plants. Triplicates were made for each treatment and the experiment was repeated twice.

Analyses of leaf methanolic extracts were performed as published in Ginglinger *et al.*, (2013).

Briefly, the analyzes were done using a UHPLC system (Ultimate 3000 Dionex; Thermo Fisher Scientific, Waltham, USA) equipped with a binary pump, an online degasser, a thermostatic autosampler, and a thermostatically controlled column compartment. The chromatographic separation was performed on a C18 SB column (Rapid Resolution High Density, 2.1 x 150 mm, 1.8 μ m particle size; Agilent Technologies) maintained at 20°C (Table 21)

Table 21: UHPLC gradient elution.

The mobile phase consisted of A: water/formic acid (0.1%, v/v) and B: acetonitrile/formic acid (0.1%, v/v) at a flow rate of 0.25 mL/min. The sample volume injected was 2 μ L.

Time (min)	Flow (ml/min)	%A	%B
-	0.25	10	90
1	0.25	10	90
10	0.25	50	50
16	0.25	100	0
18	0.25	100	0

The liquid chromatography system was coupled to an Exactive Orbitrap mass spectrometer (Thermo Fischer Scientific) equipped with an electrospray ionization source operating in positive mode. Parameters were set at 300°C for ion transfer capillary temperature and -3700 V needle voltages. Nebulization with nitrogen sheath gas and auxiliary gas were maintained at 50 and 6 arbitrary units, respectively. The spectra were acquired within the m/z mass range of 90 to 800 atomic mass units, using a resolution of 50,000 at m/z 200 atomic mass units. The system was calibrated using lock mass, giving a mass accuracy <2 ppm. The instrument was operated using ExactiveTune software and data were processed using XcaliburQual software.

All analysis were done by Dr. Raymonde Baltenweck at Laboratoire Métabolisme Secondaire de la Vigne, INRA, University of Strasbourg, Colmar.

Enzymatic Activities *in vitro* with Microsomal Fraction of Recombinant Yeast

CYP76C2 was cloned into the yeast expression vector *pYeDP60U2* (Urban *et al.*, 1997; Höfer *et al.*, 2013) containing an expression cassette under the control of a *GAL10-CYC1* glucose-repressed and galactose-inducible promoter, and expressed in *Saccharomyces cerevisiae* *WAT11* strain obtained from Dr. D. Pompon (LISBP, CNRS/INSA, Toulouse) (Pompon *et al.*, 1996). The yeast microsomal fraction containing the recombinant protein was extracted and used for incubations.

Yeast Transformation Protocol (based on Gietz and Woods, 2002)

The *WAT11* strain was grown in a Petri dish on solid YPGA culture medium at 30°C during 3 days. One single colony was inoculated into 50 ml of YPGA medium and incubated at 28°C until $OD_{700} = 0.2$ (1×10^7 cells/ml). Cultures were grown during 5 more hours to allow at least 2 cell divisions. Cells were harvested by 10 min of centrifugation at 5500 rpm, washed in sterile water and aliquoted in 1.5 ml tubes to carry on transformations. In parallel, 10 mg/ml carrier DNA (Deoxyribonucleic acid Sodium Salt Type III from Salmon Testes, Sigma) was denatured during 20 min at 100°C and quickly chilled on ice.

Aliquot of yeast cells were centrifuged during 30 sec (spin down), resuspended in a solution of Lithium acetate/TE 1X (Lithium acetate 10X (1M); TE 10X (Tris-HCl 100 mM; EDTA 10 mM)) and transferred to a tube containing the chilled carrier DNA mixed with the recombinant plasmid (1-10 µg). 500 µl of PEG 40% in lithium acetate/TE 1X were added to the mix and tubes were incubated 1 hour at 30°C under rotation, then a heat shock was done by incubation 15 min at 42°C in a water bath. Cells were washed with sterile water and resuspended with 1 ml of SGI selective liquid medium and plated onto SGI agar medium. Plates were incubated during 3-4 days at 30°C until colonies appearance. Confirmation of positive transformants was done by PCR with specific primers.

YPGA medium (1000 ml)

- Bactopeptone 10 g
- Yeast extract 10 g
- Glucose 20 g
- Adenine 20 mg
- for solid preparation: 20 g/l pastagar

SGI medium (1000 ml)

- Bacto casamino acids 1 g
- Yeast nitrogen base 7 g
- Glucose 20 g
- Tryptophane 20 mg

Microsomal Fraction Extraction (based on Pompon *et al.*, 1996)

One positive recombinant colony of *WAT11* was pre-cultured on 30 ml SGI selective medium at 28°C overnight. 15 ml of the pre-culture were inoculated in 200 ml of complete medium YPGE and grown for 30 hours at 28°C until $OD_{700} = 0.7-0.9$ and a volume of 20 ml of galactose solution 200 g/l was added for induction of the promoter. The induction step was at 25°C for 16 hours. Cells were centrifuged at 7500 rpm for 10 min at 4°C, and the pellet was washed in TEK solution. All following steps were performed under cooling conditions. Cells were centrifuged at 7500 rpm for 10 min, and the pellet was washed and resuspended in 2 ml of freshly prepared TES buffer. The cells were placed in a 50 ml Falcon tube and 0.4-0.6 mm glass beads (Sartorius, Aubagne, France) were added until reaching almost the top of the mixture. Cells were broken by vigorously shaking the tubes 5 times during approximately 1 min. Beads were washed with TES buffer which was then filtered on Miracloth filter (Calbiochem, Merck Millipore, Billerica, MA, USA). After centrifugation to remove the glass beads and cell debris the supernatant was centrifuged at 100.000g for 45 min at 4°C, and the pellet (microsomal fraction) was resuspended in 1-2 ml TEG using a Potter-Elvehjem homogenizer (Sigma).

YPGE medium

Yeast extract	10 g/l
Bactopeptone	10 g/l
Glucose	15 g/l
Ethanol (added after autoclave)	3% v/v (30 ml)

YPI medium (1000 ml)

Yeast extract	10 g
Bacto peptone	10 g
Galactose	20 g

TEK buffer

Tris-HCl	50 mM pH 7.5
EDTA	1 mM
KCl	100 mM

TES buffer

Tris-HCl 50 mM pH 7.5
 EDTA 1 mM
 Sorbitol 600 mM
 (0.5 g BSA and 6 μ L β -mercapto-ethanol was added to 50mL TES before use)

TEG buffer

Tris-HCl 50 mM pH 7.5
 EDTA 1 mM
 Glycerol 30%

P450 Quantification by Spectral Assay (based on Guengerich *et al.*, 2009)

The most common method of assaying total P450 content involves the measurement of the reduced (ferrous) form of P450 that binds CO to form a complex that absorbs light at 450 nm (Klingenberg, 1958). The determinations were done in a double beam spectrophotometer Cary 300 UV-Vis (Agilent Technologies, Sta. Barbara, USA). The principle is that the reference cuvette (1) will contain only ferrous P450 (reduced artificially using the reducing salt sodium dithionite, $\text{Na}_2\text{S}_2\text{O}_4$), and the sample cuvette (2) will contain the same ferrous P450 bound to CO.

The measurement at 450 nm allows to determine the integrity and activity of P450 per unit of protein as well as the concentration of protein/mg according to the extinction coefficients developed by Omura and Sato (1964) ($91000 \text{ M}^{-1} \cdot \text{cm}^{-1}$). Hence a loss of the 450 nm spectrum will mean a conversion to a less active form with an absorbance at 420 nm.

Procedure

A 20 times diluted solution of microsome /TEG was prepared in a 2 ml tube capped with Parafilm and then invert/re-inverted several times. Hence the sample was divided into two 1 ml cuvettes (1) and (2) and invert/re-inverted again. The two cuvettes were placed in the spectrophotometer to record a baseline between 400 and 500 nm by means of baseline correction mode.

After that, the cuvette (2) was removed from the spectrophotometer and (in the fume hood) slowly bubbled with CO gas at a rate of 1 bubble/ sec, with the end of the Pasteur pipette inserted to the bottom of the cuvette during 30-60 seconds. Then both cuvettes (1) and (2) were reduced to the ferrous form by adding some milligrams of solid $\text{Na}_2\text{S}_2\text{O}_4$ in equal amounts (adding dithionite to a CO-saturated sample causes the P450 to be trapped as the reduced-CO complex as soon as reduction begins). Parafilm was placed over the tops of the two cuvettes and inverted/ re-inverted again to dissolve $\text{Na}_2\text{S}_2\text{O}_4$ and mix the contents. Cuvettes were placed back into the spectrophotometer for a

record of spectrum between 400 and 500 nm several times, over a period of a few minutes, until the size of the peak near 450 nm stopped increasing. Absorbance at 450, 490 and 420 nm was used for calculations.

Calculations were done according to the following formulae:

P450 concentration:

$$(\Delta A_{450} - \Delta A_{490}) = 0.091 \frac{1}{4} \text{ nmol of P450 per ml (a)}$$

P420 content:

$$\text{nmol of P450 / ml (a)} \times (-0.041) = (\Delta A_{420} - \Delta A_{490}) \text{ THEORETICAL}$$

Then

$$[(\Delta A_{420} - \Delta A_{490})_{\text{observed}} - (\Delta A_{420} - \Delta A_{490})_{\text{theoretical}} - (\Delta A_{420} - \Delta A_{490})_{\text{baseline}}] / 0.110 = \text{nmol of P420 per ml}$$

Degradation: calculated by the ratio P450/P420

Enzymatic assay

Purified microsomal fractions were then used for incubation with candidate substrates. Each reaction was performed in a final volume of 100 μ l according to the following reaction mix:

- PBS(20mM pH 7.4)	70 μ l
- NADPH (6mM)	10 μ l
- Microsomes	10 μ l
- Substrate (stock 100 mM in methanol) 1-2 mM	10 μ l

Incubations with candidate substrates were done at 27°C under gentle agitation, during 20 min, 60 min and 120 min. The reaction started with the addition of NADPH. Negative control, without NADPH, was included.

After incubation reaction was stopped with the addition of 10 μ l of mixture of acetic acid 50%, and methanol 40% and vortexing. After five minutes of centrifugation at 14000 rpm, supernatant was recovered and transferred to HPLC vials for HPLC and UPLC analysis.

HPLC Analysis

Analyses were performed on a HPLC Waters Alliance 2690/5 (Waters, USA) coupled to a photodiode array detector (PDA) W2996 (190-400 nm).

Compounds were separated using a Nova-Pak C18 reversed phase column (4 μ m, 4.6mm x 250 mm, Waters) at 37°C and eluted over 20 min with a gradient of 5-100% acetonitrile in 0.1% formic acid at a flow rate of 1 ml/min (Table 22). Injection volume was 50 μ l.

Table 22: HPLC gradient.

The mobile phase consisted of (A) water and (B) acetonitrile, both containing 0.2% formic acid. The column was operated at 37°C with a flow-rate of 1 ml/min with a sample injection volume of 50 μ l.

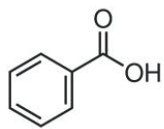
Time (min)	Flow (ml/min)	%A	%B
-	1	95	5
15	1	0	100
17	1	0	100
18	1	95	5
20	1	95	5

The run started by 15 min of 95% A, followed by isocratic run using B during 2 min. Return to initial conditions (95% A) was maintained 2 min before next injection. The total run time was 20 min.

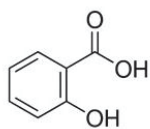
Data acquisition and analysis were performed with the Empower Pro software 2002 (built 1154) (Waters).

Table 23: List of candidate substrates used in CYP76C2 enzymatic assays.

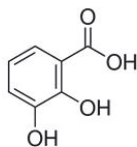
Standard Compound	λ max	Retention time	Absorption spectrum
Abscissic acid (ABA)	365.2	14.103	266.2-365.2
Benzoic acid (BA)	273.3	14.027	229.4-273.3
Salicylic acid (SA)	302	14.053	235.4-302
2.3 Dihydroxybenzoic acid (2.3 DHBA)	311.5	11.016	244.8-311.5
2.5 Dihydroxybenzoic acid (2.5 DHBA)	324.7	9.352	324.7
2.4 Dihydroxybenzoic acid (2.4 DHBA)	294.8	10.709	254.3-294.8
3.4 Dihydroxybenzoic acid (3.4 DHBA)	293.6	6.977	259.1-293.6
Linalool	272.2	14.013	272.2



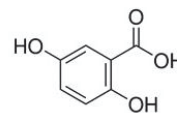
Benzoic acid



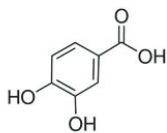
Salicylic acid



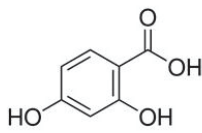
2,3 Dihydrobenzoic acid



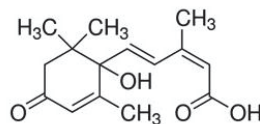
2,5 Dihydrobenzoic acid



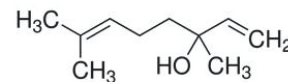
2,4 Dihydrobenzoic acid



2,5 Dihydrobenzoic acid



Abscissic acid



Linalool

Figure 50: The molecular structure of analyzed compounds.

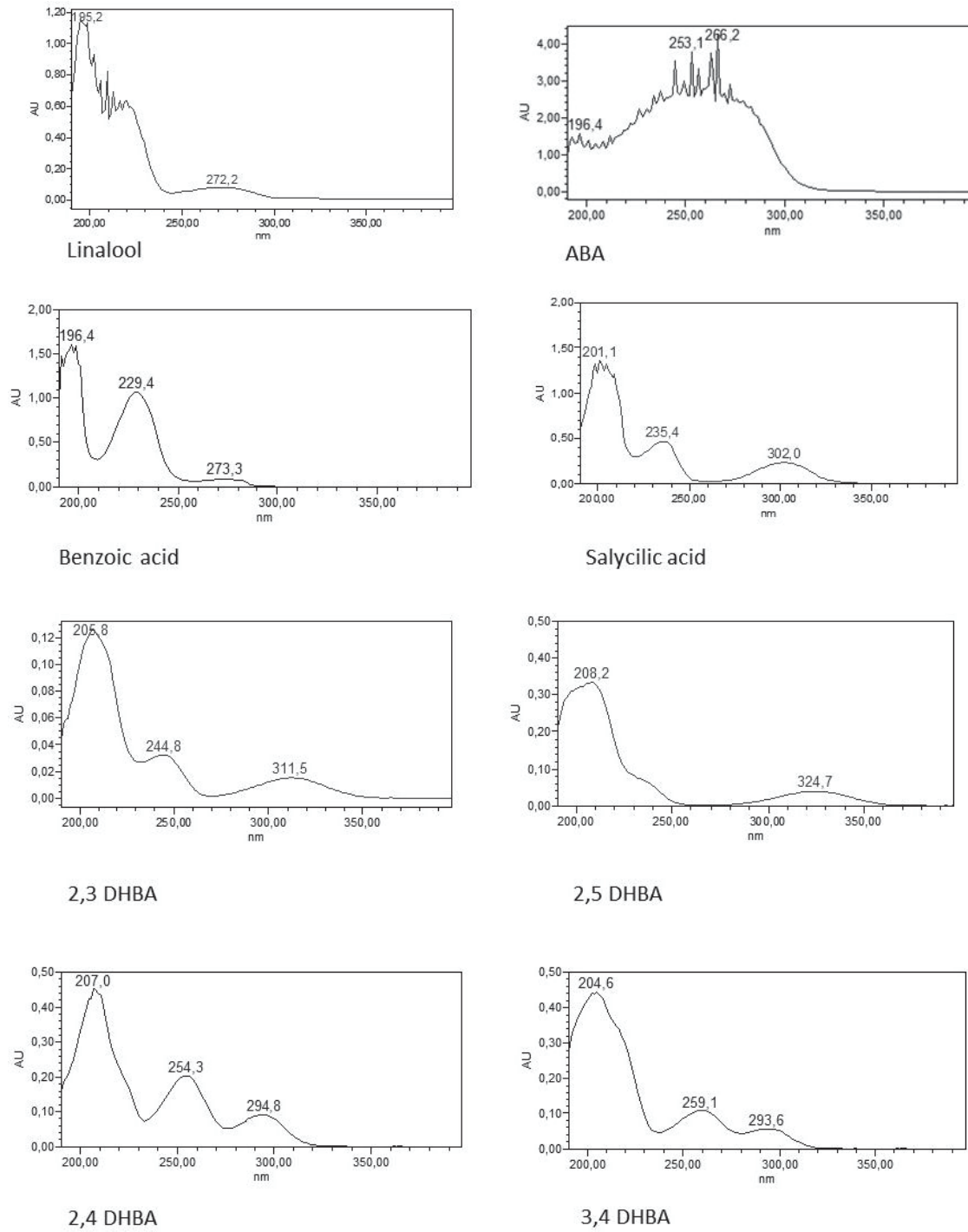


Figure 51: Absorption spectrum of analyzed compounds.

Statistical Analysis

Normal distribution of errors (plotting residues versus predicted errors) and homogeneity of variances (Shapiro-Wilks modified by Mahibbur and Govindarajulu (1997)) were tested on raw data. Transformations to reach normality were done when necessary and possible.

For each experiment, samples were classified by plant genotype, treatment (infected versus non-infected) and replicates, including the interaction term genotype x treatment and the error term to define the model. This model was also used for calculation of means, standard deviations (SD) and standard errors (SE) of each factor (genotype or treatment).

ANOVA analyses were done to assess differences between treatments and specific comparison of least square means was done for significance using Tukey's test. Non-parametric ANOVA test of Kruskal Wallis (1952) with Conover correction for t test (1999), was applied when a lack of homogeneity of variances was present or when a transformation was not possible.

Time course analyses were carried out in the same way, but using "Time" as an additional class variable or partition.

Data coming from metabolomics analyses were subjected to non-parametric methods, together with multivariate analysis of principal component (PCA), using a correlation matrix. PCA was conducted using each peak or (putative) compound as a "variable" and each combination of genotype x treatment (*i.e.* "Col-0 mock" "cyp76c2-Pst") as "classification criteria". Time points were used as a partitions as mentioned before.

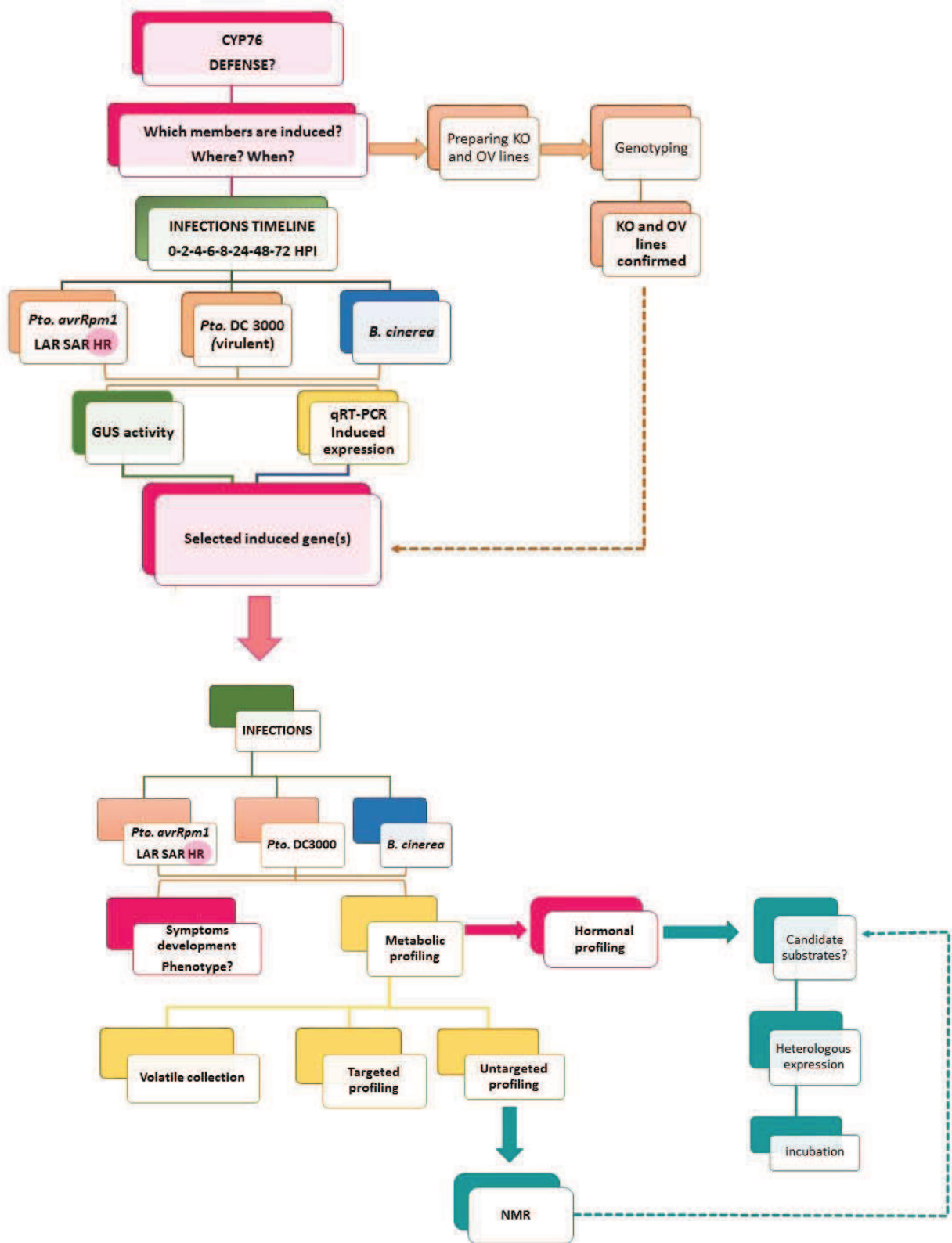
All the statistical analysis were done at a probability level of 5% ($\alpha = 0.05$) with the software INFOSTAT 2010 (Di Rienzo *et al.*, 2010).

To conclude, SE was used as a measure of the sample mean precision and variation, in the represented charts, according to: $SE = SD/\sqrt{V}$ (sample size).

RESULTS AND DISCUSSION

Results and
Discussion

WORKFLOW OF EXPERIMENTS AND DATA ACQUISITION



RESULTS

Gene Expression Analysis

Strategy for qRT-PCR analysis of gene expression

In a first step, in order to investigate the role of the genes of the *CYP76* subfamily in plant-pathogen interaction, their transcripts were quantified by qRT-PCR in *A. thaliana* Col-0 mock-treated and infected plants.

To have a clear overview about the scenarios in which *CYP76* genes could be potentially involved, three main variables were taken into consideration:

1. Pathogen lifestyle: hemibiotroph vs necrotroph.
2. Temporal scale of gene induction: 0-2-4-6-8-24-48-72 HPI.
3. Spatial distribution of gene induction: local vs systemic responses.

Briefly:

1. The pathogen tested were: *Pto* DC3000 and *B. cinerea* both holding contrasting lifestyle. *Pto.* is a hemibiotroph, while *B. cinerea* is a necrotroph. Only at the final stages of disease development (72-96 HPI) *Pto* switches to a blunt necrotrophic phase ([Figure 35](#)) which implies minimal overlapping for our analysis, since most of defense/susceptibility responses occur earlier.

In addition to pathogen lifestyle, compatible vs incompatible interactions were also tested by including in the analysis *Pto* DC 3000 carrying the avirulent gene *avrRpm1* (Whalen *et al.*, 1991). This strain will later pave the way for analyzing LAR and SAR responses. This was important for including not only a scenario of susceptible host and disease (compatible interaction with the virulent strain and ETS), but also a scenario of resistance (incompatible interaction with the avirulent strain and ETI) that later would help drawing conclusions about the role of metabolites probably implicated.

2. The temporal scale chosen includes from time zero (samples were infected and immediately frozen in liquid nitrogen) to the end of symptoms development 48-72 HPI. Evening/night period was not included in the analysis (time points 12, 36 HPI) since is known from publications and microarray databases that defenses responses in *A. thaliana* have diurnal regulation and that circadian clock regulates immune responses in a day-manner by opposition to evening/night-manner responses

(Griebel *et al.*, 2008; Bhardwaj *et al.*, 2011; Windram *et al.*, 2012; Zhang *et al.*, 2013b). Indeed, morning infection results in higher SA accumulation, *PR1* induction, callose deposition, important HR development, higher resistance to different kinds of pathogens (bacterial and fungal with different lifestyles) and secondary metabolites synthesis (*i.e* terpenoids).

3. Local and systemic responses were taken into consideration by carefully delimiting, collecting and analyzing areas separately in each interaction.

In the case of *B. cinerea* infection, merely necrotic area was collected and analyzed. As it was stated in the [introduction](#), gene expression is more relevant within the necrotic lesion than in the adjacent areas (Kliebenstein *et al.*, 2005; Mulema and Denby, 2012; Windram *et al.*, 2012). *B. cinerea* does not induces SAR (Govrin and Levine, 2002; Rowe *et al.*, 2010; De Cremer *et al.*, 2013).

Furthermore, HR, LAR and SAR areas were collected separately from Col-0 infected plants with the avirulent strain of *Pto* DC3000.

All results were normalized using three previously validated stable reference genes: *SAND*, *TIP41* and *EXP* (Czechowski *et al.*, 2005, Boachon *et al.*, 2014) that were also re-checked for this thesis. The relative expression of the *CYP76C* genes for each condition was calculated using the method of (Pfaffl, 2001). In addition, specific marker genes such as *PR1*, *PDF1.2*, *JAZ10*, *VSP1*, *OPR3* and *NCED3* were included to relate their expression to defined signaling pathways. The two terpene synthases *TPS10* and *TPS14*, were included in the analysis since they are known to generate *R*- and *S*-linalool, which are documented substrates of several *CYP76Cs* (Ginglinger *et al.*, 2013). *CYP76C3*, as well as *CYP76C4* and *CYP76G1* (*CYP76C4/CYP76G1* are constitutively mainly expressed in roots) were eliminated from the results because they were not responsive at all.

Effect of *B. cinerea* infection on the expression of *CYP76* members and defense related genes

As is shown in Figure 52, *Botrytis* infection did not significantly impact *CYP76C5*, *CYP76C6* and *CYP76C7*, *TPS10* and *TPS14* genes expression, with variation within a range of 0.5-1.5 fold between mock and infected plants at the different time points. Their gene expression however followed very similar time courses.

An interesting point of induction at 4-6 HPI appeared repeatedly in every mock-infected treatment for all the genes included in the analysis (markers included). This could be due to an initial response/perception to/of the inoculation (method of choice), since wounding had an almost negligible effect, as shown by *VSP1* induction (see below). It is surprising that this effect or “pattern” was not observed in *CYP76C2* (a detail of the first hours of infections can be seen in Figure 53).

Unexpectedly, *CYP76C1* was down-regulated in the infected plants from 48 HPI ($\approx 8/12$ fold). Conversely, *CYP76C2* was the only member of the *CYP76* subfamily significantly induced in response to *B. cinerea* infection. At time points 8-24-48 HPI the relative gene induction increased until a maximum of 35-fold the value of the calibrator control at 48 HPI (all points with statistical significance). Millet (2009) found similar responses in GUS experiments.

During the initial hours of *Botrytis* infection, conidia germination (1-3 HPI) and apleria formation (6 HPI) occur, and the early defense signals are emitted by the plant (Holz *et al.*, 2007; Shlezinger *et al.*, 2011). The number of plant genes induced increases at 24 HPI when *Botrytis* has already penetrated the epidermal leaf and secreted several CWDE, oxalic acid, botrydial (HR inducer), and several others metabolites (from 12 HPI) (Holz *et al.*, 2007; Gonzalez Collado *et al.*, 2007; Elad *et al.*, 2007; Shlezinger *et al.*, 2011; Windram *et al.*, 2012). At this point, lesion development is still incipient but the genetic and metabolic plant machinery activity is intense, and for example some *TPS* (terpene synthases) and components of the Trp metabolic pathway, including camalexin, have been shown to be specifically induced at 24 HPI (Mulema and Denby, 2011). This seems not to be the case for *TPS10* and *TPS14* analyzed here. Finally at 48 HPI, lesion development starts being visible. It reaches full development at 72 HPI, when *B. cinerea* takes the full control on host PCD to obtain nutrients and starts lesion spreading (Govrine and Levine, 2000; Shlezinger *et al.*, 2011). ROS levels and cell death are dominant in infected tissue and play decisive roles in virulence.

B. cinerea as a necrotroph pathogen, activates the ERF branch of JA signaling (JA/ET) (Glazebrook, 2005; Lorenzo and Solano, 2005; Pieterse *et al.*, 2012). As shown in Figure 52, *PDF1.2* is induced 1330-

1700 folds at 48 HPI, endorsing the method and conditions of infections (Manners *et al.*, 1998). Comparatively, *JAZ10* and *VSP1*, from the MYC branch of JA signaling associated to wounding (Pieterse *et al.*, 2012) displayed a negligible induction response, although *JAZ10* turnover appeared activated to some extent at 48 HPI.

OPR3, a marker for JA biosynthesis, showed no significant changes either. Some earlier works were trying to link OPDA (JA precursor) to defense responses using *OPR3* as a way to differentiate OPDA from JA-dependent responses. OPDA was thought to have a direct role in defense responses to *Alternaria brassicicola* (Stinzi *et al.*, 2011) and to *B. cinerea*, however its use has been recently discouraged by Wasternack and Hause (2013).

PR1 was induced as much as *CYP76C2* at 48 HPI (≈ 40 fold). *PR1* (marker of the SA cascade) has been shown to be important for the development of *Botrytis*-induced lesions (Govrin and Levine, 2002; Ferrari *et al.*, 2003; 2007; Rossi *et al.*, 2011). This accumulation is correlated with SA synthesized via the PAL pathway (Ferrari *et al.*, 2003) and associated with *B. cinerea*-dependent HR (for details see [GUS](#) experiment below).

Finally, *NCED3* encodes a rate limiting step enzyme in ABA metabolism. According to Windram *et al.*, (2012) and Ferrari *et al.*, (2007), *Botrytis* induces a strong induction of ABA catabolism at 24 and 48 HPI respectively. The result obtained here showed no induction of *NCED3* neither in mock-treated plants nor in infected plants.

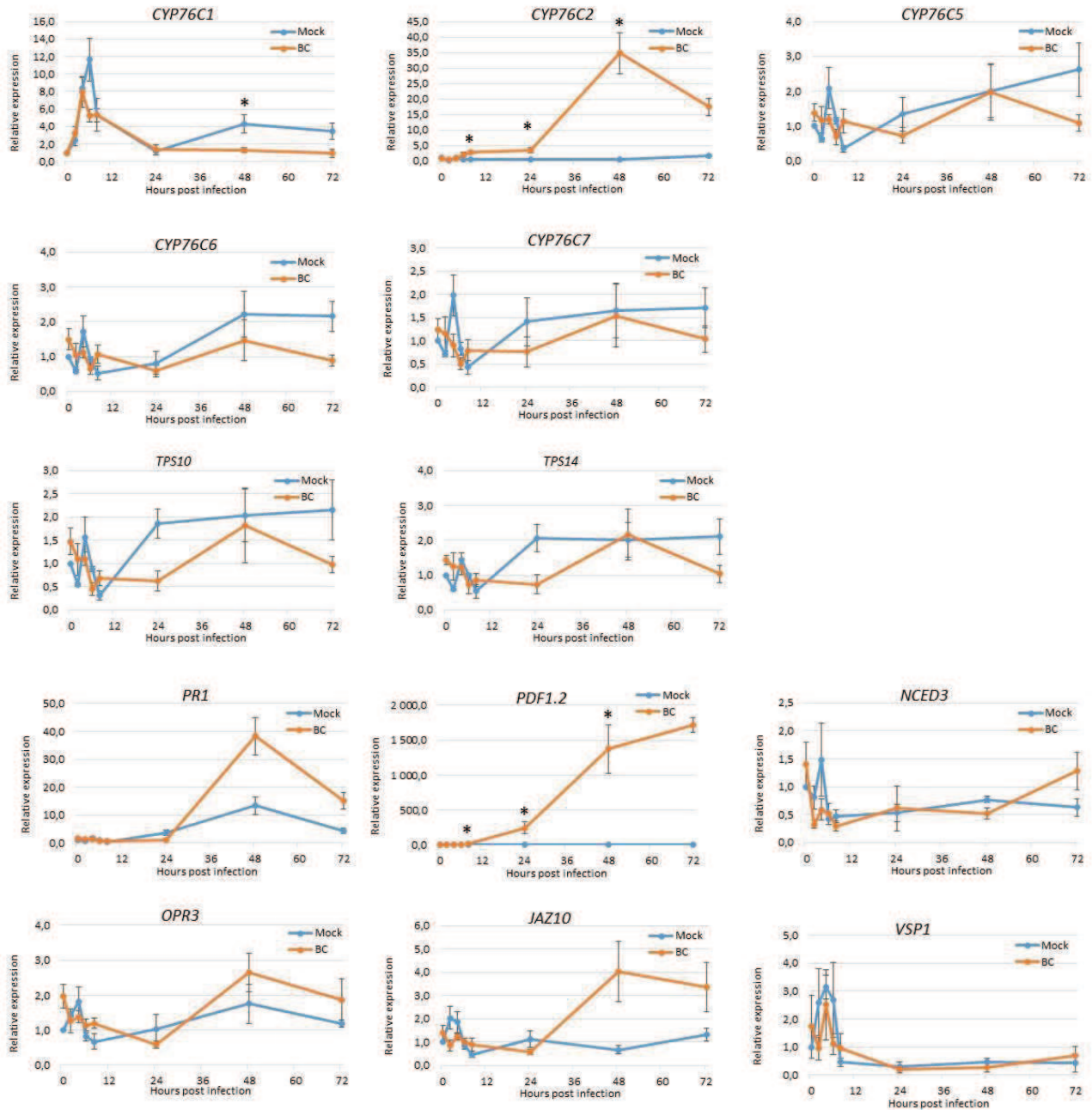


Figure 52: qRT-PCR quantification of the transcript level of *CYP76* family members and defense related genes during compatible interaction with *B. cinerea*.

Total RNA was isolated and used as template for cDNA synthesis. Mean changes in gene expression are expressed relative to the transcript level in mock-inoculated Col-0 leaves at time point 0 which was arbitrary set as 1. Bars represent errors from biological replicates (n=5). Asterisks show statistically significant effects at a 5% of probability level.

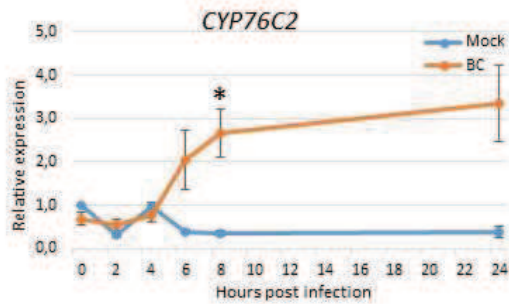


Figure 53: qRT-PCR quantification of the transcript level of *CYP76C2* at 8-24-48 HPI during compatible interaction with *B. cinerea*.

Zoom on early time-points.

Effect of *Pto* DC3000 infection on the expression of *CYP76* members and defense related genes

The interaction *A. thaliana*-*Pto* DC3000 is compatible thus we are in the presence of a diseased plant (Katagiri *et al.*, 2000; Xin and He, 2013).

Infection of *Arabidopsis* by *Pto* DC3000 naturally results in PAMP triggered defenses (PTI), which implies stomatal closure, callose deposition and SA dependent defenses to limit bacteria propagation and growth (Katagiri *et al.*, 2002; Melotto *et al.*, 2006; Freeman and Beatie, 2009; Xin and He, 2013). However in this experiment, plants were syringe-infiltrated. This implies that results should be interpreted in a context of “post-infiltration defenses” instead of PTI. Many of the usual features of *A. thaliana*-*Pto* DC3000 defense responses and signaling induction will thus probably be modified since constitutive barriers and stomatal responses are bypassed. Results can be seen in Figure 54.

In this context, *CYP76C1* showed a minor repression, but still with some statistical significance at 2-4-24-48 HPI (down-regulation as shown before for *B. cinerea* 48 HPI). This down-regulation is unique to *CYP76C1* among the genes tested and has been observed in all the experiments.

CYP76C5, *CYP76C6* and *CYP76C7* showed similar response profiles, with only quantitative differences among them. Significant effects of infection were observed at 4-8-48 HPI for *CYP76C5*, 48 HPI for *CYP76C6* and 2-4-48 HPI for *CYP76C7*. Relative gene induction was highest at 48 HPI for all three of them ranging from 20 to 125 fold. *TPS10* and *TPS14* also showed the same pattern of relative induction but with statistical significance at 4-48 HPI for *TPS10* and 4 HPI for *TPS14*, with high values of relative gene induction (80-100 fold) at 48 HPI. *TPS10* has been previously studied upon *Pto* DC3000 infection. In the work of Attaran *et al.*, (2008), it was highly induced by the virulent strain *Pto* DC3000 but showed a minor response to the avirulent strain at 24 HPI. Another study on molecular signatures has also detected up-regulation of *TPS10* in response to *Pto* DC3000, but at a later time point (72 HPI) (Barah *et*

al., 2013). Overall, it is striking that *TPS10*, *TPS14*, *CYP76C5*, *CYP76C6* and *CYP76C7* followed very similar time courses in both *B. cinerea* and *Pto* DC3000 responses, which may suggest that they contribute to the same pathway. They all showed much stronger responses after *Pto* infection compared to *B. cinerea* infection.

Additionally a significant induction at 4 HPI was observed (statistical significance for *CYP76C1*, *CYP76C2*, *CYP76C5*, *CYP76C7*, *TPS10* and *TPS14*) that does not seem to be related to wounding (see *VSP1* below) but rather to initial detection of the infection probably before the pathogen suppresses the host defenses.

CYP76C2 was the gene showing the strongest early response with an abrupt increase at 4 HPI, with an increase of 150-fold respect to the mock calibrator. Induction of gene expression remained high at 24-48 HPI, significantly higher than the response to the mock treatment that also induced a strong response 6-8h HPI. These values put again *CYP76C2* in the arena for debate, since some [previous reports](#) stated weak or not induction of this gene under compatible interactions (Godiard *et al.*, 1998; Millet (PhD thesis), 2009). It can be noted that *CYP76C1*, its closest paralogue, had a complete unrelated response.

PR1, the SA marker, was induced about 30 fold at 4 HPI, 100 fold induction at 24 HPI (both considered no significant effect) and 1500 fold at 48 HPI (significant). The stronger induction observed at 48 HPI is consistent with a compatible induction and probably correlates with SA accumulation (not measured in this experiment) as is the case for ETS in virulent interactions (Mur *et al.*, 2005; Vlot *et al.*, 2009; Spoel *et al.*, 2007; Spoel and Dong, 2008; Dempsey *et al.*, 2011; Pieterse *et al.*, 2012; Hamdoun *et al.*, 2013).

In contrast to SA signaling, *PDF1.2*, *VSP1* and *JAZ10*, the markers for JA, were significantly induced at 24 HPI. *JAZ10* activation is already significant at 6 HPI and high at 8 HPI. This would be in good agreement with the fact that [COR](#) (mimicking JA-Ile), an important virulence factor from *Pto* DC3000, was reported to bind the F-box COI1 to counteract SA mediated defense responses activated by the plant (Block *et al.*, 2005; Cui *et al.*, 2005; Geng *et al.*, 2012; Zheng *et al.*, 2012; Xin and He, 2013). *PDF1.2* decreased to minimal values at 48 HPI when maximal induction of *PR1* antagonizes JA signaling, while *JAZ10* and *VSP1* remained induced.

At this point several details are interesting to remark. First, *PDF1.2* belongs to the ER branch of JA signaling, which is induced against necrotroph infection. Second, *JAZ10* and *VSP1* belong to the MYC

branch, responsive upon wounding and insects. Third, *JAZ10* is an early responsive element of JA signaling while *VSP1* is a late one (Acosta and Farmer, 2009).

VSP1 (late signal) displayed the highest induction value of JA markers at 24 HPI (50 fold). This was observed only for infected plant and not after mock treatment, excluding wounding effect (side effect of infiltration technique).

Pto-induced-SA accumulation at 24-48 HPI was associated with JA signaling suppression, evidenced mostly by *PDF1.2* which is in agreement with the works of Spoel *et al.*, (2003; 2007, 2008; Gupta *et al.*, 2000; Pieterse *et al.*, 2009; 2012) and several authors for a while now.

On the other hand, *OPR3*, a marker of JA biosynthesis, was induced at 2 HPI with no differences between mock and infected plants. Immediately after 2 HPI, *OPR3* transcript levels sharply decreased. From 6 to 48 HPI, they however remained statistically different from mock-inoculated plants (2 fold).

Finally *NCED3* was significantly repressed in infected plants at 6 HPI.

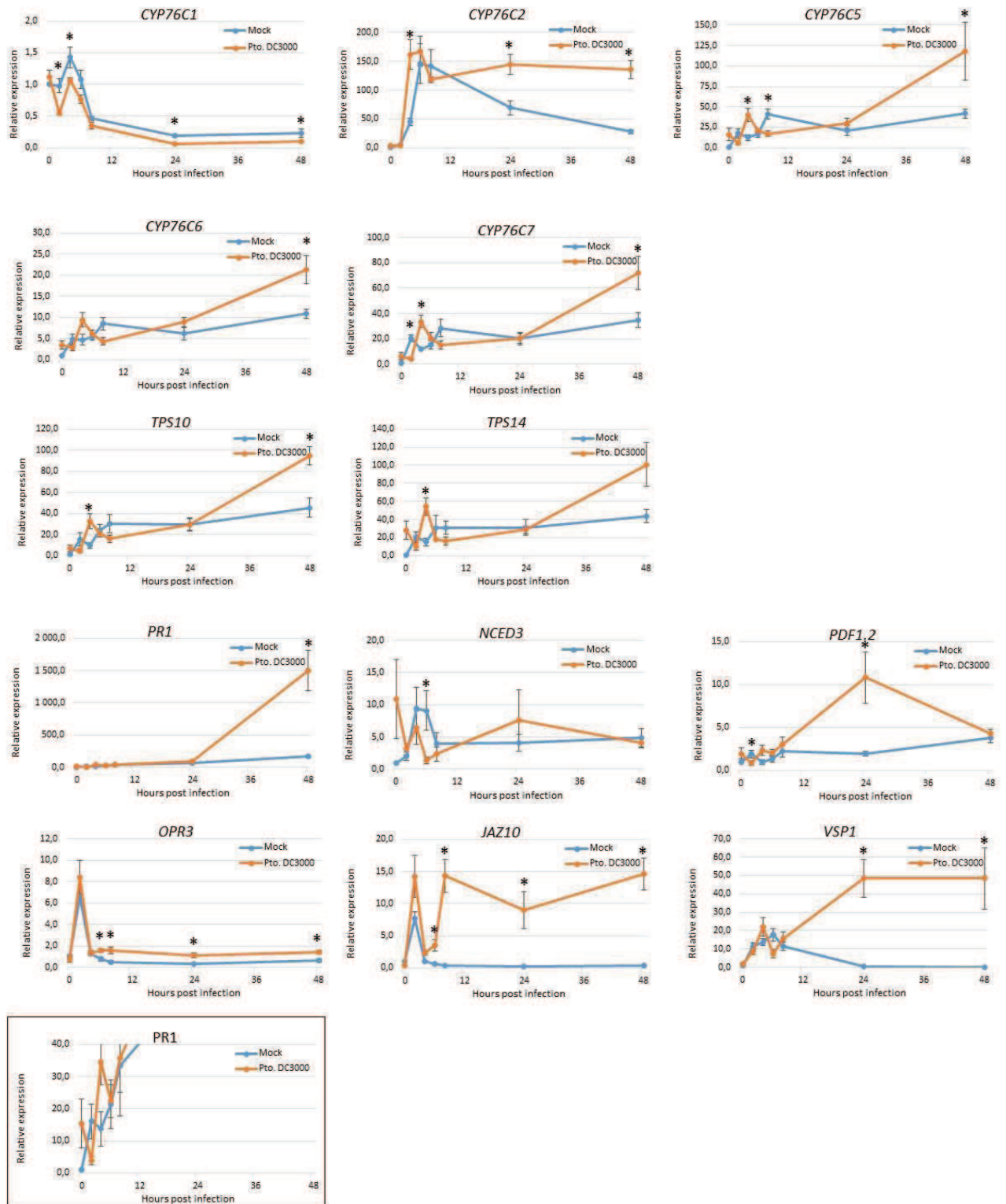


Figure 54: qRT-PCR quantification of the transcript levels of *CYP76* family members and defense related genes during compatible interaction with *Pto* DC3000.

Total RNA was isolated and used as template for cDNA synthesis. Mean changes in gene expression are expressed relative to the transcript level in mock-inoculated Col-0 leaves at time point 0 which was arbitrary set as 1. Bars represent errors from biological replicates (n=5). Asterisks show statistically significant effects at a 5% of probability level.

Effect of *Pto* DC3000 *avrRpm1* infection on the expression of *CYP76* members and defense related genes

The interaction *A. thaliana*-*Pto* DC3000 *avrRpm1* is incompatible. The plant recognizes the *avr* gene of the pathogen and initiates a cascade of defense responses including HR, LAR and SAR. Responses mediated by this type of interaction are expected to be faster, accurate and more robust than those observed in compatible interactions (Tao *et al.*, 2003; Jones and Dangl, 2006). Variations between PTI, ETS and ETI have been stated as qualitative with respect to the amplitude of defense responses (Tao *et al.*, 2003; [Jones and Dangl, 2006](#); Hamdoun *et al.*, 2013). Much overlap in the downstream signaling is observed, since signal transduction pathways are largely shared (*PR1*, SA, ROS, etc.). Accordingly, immune responses are expected to be qualitatively different and earlier than in virulent interactions.

HR zone

In the HR zone, after plant and pathogen are in contact, fast PCD occurs to limit and stop the pathogen advance (Mur *et al.*, 2008). Intense pre/post transcriptional/translational reprogramming and reallocation of metabolites to new sinks are taking place (Etalo *et al.*, 2013). In addition HR is highly interconnected to LAR and is decisive for its development (Dorey *et al.*, 1997; Costet *et al.*, 1999). Moreover, SA is a key regulator in HR by its dual function as a mediator of cell death in local infected tissues and as promotor of cell survival in adjacent tissues (Fu *et al.*, 2012; Fu and Dong, 2013).

During the initial hours, from 0 to 24 HPI, there was no substantial induction of *CYP76C1*, *CYP76C5*, *CYP76C6*, *CYPC7*, *TPS10* and *TPS14* transcription. At 48 HPI an increase of 6-8 fold induction was observed that did not reach statistical significance, but still denoted some effect in the context of overall experiment.

The absence of statistical significance in this experiment was largely due to the low level of gene expression, which caused in some extent the lack of significance at a level of 5%. Nevertheless, the problem could be fixed by increasing sample size and optimizing statistical analysis to better detect the differences between the treatments (Yuan and Reed, 2006; Suresh and Chandrashekhara, 2012).

In the choice of sample size and statistical power for this experiment, previous work and published data were considered. A priori, a power of 80% (recommended) was expected for a sample number of $n=5$ and $p\text{-values}=5\%$. However, a posteriori some changes in the variances, expected vs obtained, might have affected the power of detection of minimal differences between mock and infected plants. The idea here was that non-significance of results was more related to a lack of statistical powers in terms of sample size and variances observed, than to a lack of difference/relationship between the analyzed samples.

Another possible solution might be increasing inoculum concentration (bacterial titer). Recent work has shown that differences between ETS (vir) and ETI (avir) are not only qualitative, but also dose-dependent. For instance, higher doses of virulent and avirulent bacteria helped to accelerate ETI by comparison to ETS, while lower doses shortened the gap between ETS and ETI (Hamdoun *et al.*, 2013).

CYP76C2 showed a ≈ 10 fold induction at 4 to 6 HPI as previously observed by Godiard *et al.*, (1998), followed by a decrease to control level at 48 HPI. This was contrasting the absence of early response of *CYP76C5*, *CYP76C6*, *CYPC7*, *TPS10* and *TPS14* followed by 6 to 10 fold induction at 48 HPI when cell death in HR zone was unmistakable. The response of the latter group thus seems related to cell death and ROS environment, more than an anticipated defense response. It might be associated with the production of terpenoids as antioxidants in a tentative protection against ROS or to the production of terpene oxides as pro-oxidants. For *CYP76C2*, on the other hand, it can be mentioned that the fast and sustained induction pattern in the HR zone contrasts the pattern observed in LAR and SAR zones. This is surprising since the LAR zone is supposed to be more active than HR zone (Dorey *et al.*, 1997; Costet *et al.*, 1999). This point will be addressed in more detail below, in the [LAR](#) and [SAR](#) sections.

PR1 displayed a 16-fold induction value at 24 HPI. This induction of *PR1* was earlier than that observed for virulent infection (48 HPI), but much lower (16 fold compared to 155 fold) as would be expected for incompatible interactions (Raffaele *et al.*, 2006; Attaran *et al.*, 2008; Hamdoun *et al.*, 2013).

Surprisingly, *VSP1* was quite strongly induced (around 60 fold) at 2 HPI in infected plants and 4 HPI in mock-infiltrated plants. This was the strongest gene activation observed for the HR experiment and could result from the wounding caused by the infiltration technique. Published data on wounding effect have reported an immediate activation of *VSP1* within 1-2 HPI, together with activation of JA-signaling related markers (Utsugi *et al.*, 1998, Glauser *et al.*, 2008. Acosta and Farmer, 2009). For instance, *JAZ10* (JA early marker) was induced 10 fold at 2 HPI (as *VSP1*) in infected plants, whereas *PDF1.2* did not show an early induction but was induced at 48 HPI. Wounding was previously shown

to promote *CYP76C2* transcripts accumulation within 1-8 HPI (Godiard *et al.*, 1998). It would thus be important to clarify if *CYP76C2* activation at 6-8 HPI could be just a result of wound response. Some answer to this question will be found below ([GUS](#) experiments: *CYP76C2* was not induced upon mock-infiltration or wounds at different time points). However is clear that including a real marker for HR, such as *HSR3*, *HIN1*, *HSR203J*, *LSD1* and/or *ACD2* would have helped to answer the question (Greenberg *et al.*, 1994; Pontier *et al.*, 1999; Mur *et al.*, 2008; Coll *et al.*, 2011; Rossi *et al.*, 2011).

OPR3 and *NCED3* showed no significant activation.

LAR zone

The LAR zone constitutes a symptomless zone of living cells undergoing a distinctive and intense genetic reprogramming. LAR corresponds to a localized group of cells and tissues surrounding HR with strong defenses responses, as much abrupt and higher than SAR (Ross, 1961; Ryals *et al.*, 1994; Dorey *et al.*, 1997; Costet *et al.*, 1999). The LAR zone is a zone of intense activity and defense responses in which cell death is not activated as final outcome.

The relative levels of transcript of *CYP76C1*, *CYP76C2*, *CYP76C5*, *CYP76C6*, *CYPC7*, *TPS10* and *TPS14* genes were not substantially increased in the LAR zone.

In the LAR zone, no significant *PR1* activation occurs in the infected tissues compared to the mock-treated. It is interesting to remark that the strongest induction of *PR1* is concomitant with HR. Residual SA in LAR zone may contribute to restriction of cell death (Fu *et al.*, 2012).

PDF1.2 displayed a 20-fold induction at 24 HPI. This induction was not paralleled by a similar activation of the expression of *JAZ10*, or *VSP1*. Only a minor increase in *VSP1* expression was detected at 24 HPI. The early wounding effect is detectable much less than in the HR zone, which seems coherent since no infiltration occurred there. However it is interesting to note that the induction of *PDF1.2* was higher than the observed in HR, SAR zone (below) and in the virulent interaction (all 24 HPI), probably due to the fact that the induced synthesis of SA (evidenced by *PR1*) in local and adjacent tissues is not enough under avirulent interaction to suppress JA synthesis. The later phenomenon has been analyzed in Spoel *et al.*, (2007) and Truman *et al.*, (2007) and conclusions indicated that under R-mediated recognition the SA/JA crosstalk is not fully operating (see [HR: ecological cost and trade-off](#)).

OPR3 and *NCED3* showed no significant responses.

SAR zone

The SAR zone it is a zone of unaffected living cells, as LAR, in which defenses responses are linked to local infection. However SAR shares very few features in common to HR and LAR (Costet *et al.*, 1999) and does not depends on cell death to be initiated. [SAR](#) responses are characterized by SA and *PR1* induction (among others), and the magnitude of these responses is lower in comparison to LAR but more effective over time (Grant and Lamb, 2006; Spoel and Dong, 2012; Dempsey and Klessig, 2012; Fu and Dong, 2013; Shah *et al.*, 2014).

Responses of *CYP76C5*, *CYP76C6*, *CYP76C7*, *TPS10* and *TPS14* in the SAR zone were once more very similar, with an induction at 48 HPI. This late response at 48 HPI in systemic tissues suggests late signaling occurring as a consequence of advanced cell death established at the infection site. It suggests an increase that may continue later on (not analyzed here) and a probably sustained (long-lasting) effect, as is expected for SAR. As the levels of induction at 48 HPI are similar to those observed for the HR zone, it seems to exclude a role of this gene set in the cell death as pro-oxidants, as proposed above, *CYP76C1* however showed a different behavior with a short maximum of transcripts accumulation at 6 HPI, more similar to that of *CYP76C2*, but slightly earlier.

CYP76C2 displayed a sharp increase of relative transcript accumulation at 8 HPI and return to control at 24 HPI. The magnitude of the response is just the same as in HR, but delayed and way more relevant than in LAR tissues. This is somehow surprising since LAR implies stronger defense responses and resistance, than SAR (Dorey *et al.*, 1997). Interestingly, the transcriptomic data presented in [hypothesis](#) indicate that *CYPC2* was down regulated in a mutant impelled in its capacity of mounting SAR (*dth9* mutant).

Whereas a minor and transient induction of *PR1* seems to occur at 6 HPI, a significant and infection-dependent increase in its level of transcripts is observed later at 48 HPI, probably corresponding to a second wave of SA accumulation occurring as consequence of HR (Alvarez, 2000).

Unpredictably, *VSP1* showed the highest transcripts accumulation in the infected plants in an early response at 4 HPI, which is extremely surprising and unexpected since no infiltration occurred. The variation between samples is quite low, which means this induction was reproducible in all the n=5 and not an isolated event. An explanation is missing for this event. Visual inspection of plants at the sampling did not reveal any sign of stress.

PDF1.2 was moderately induced at 8 HPI and strongly (around 60 fold) 48 HPI. *JAZ10* and *OPR3* however did not show significant transcripts accumulation and the transient increase observed for *NCED3* in mock treated plants was suppressed in infected plants.

In conclusion, values of relative transcripts accumulation were low in the “incompatible” experiment and not significant between treatments. The less significant effects were observed at LAR zone. This was surprising since based on previous [transcriptomic analyses](#), a distinctive response of *CYP76C2* was expected in the LAR zone. The comparison of HR, LAR and SAR was thus less informative than anticipated, with not much useful information arising from the LAR zone.

One of the most consistent observation is the co-regulation of the *TPS10*, *TP14*, *CYP76C5*, *CYP76C6* and *CYP76C7* genes, suggesting a role of terpenoids in the late defense responses. *CYP76C2* is one of the most responsive genes, but more induced in HR and SAR zones, activated early but later than the JA cascade.

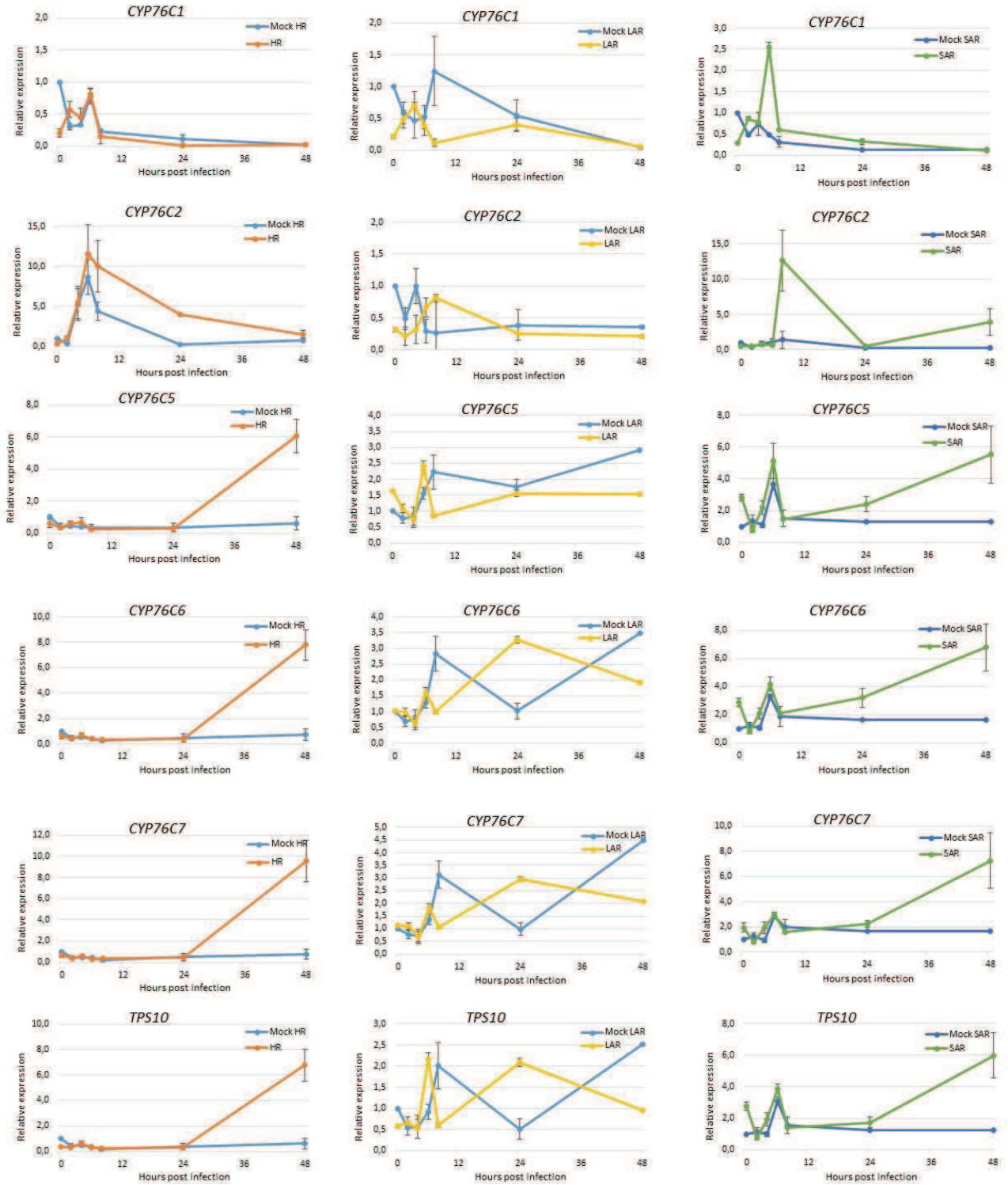
Marker genes accompanied the scarcity of information brought by this experiment and *VSP1* denoted the existence of some wounding effects.

Conclusion of the qRT-PCR analysis of gene expression

Within the *CYP76* family, *CYP76C2* displayed the most significant increases in transcript level in response to *B. cinerea* and *Pto* DC3000 infection (Figure 52, 54, 55). In addition to compatible interactions, it was also responsive to incompatible interaction with *Pto* DC3000 *avrRpm1* in HR zone and in particular at 8 HPI in the SAR zone which might suggest some function in signaling (Figure 55). Altogether these data thus seem indicative of a role of *CYP76C2* in disease resistance. None of the others members of the *CYP76* family, showed such responses of the same magnitude or relevance for the onset of defense, although they might be involved in late responses and compatible interaction.

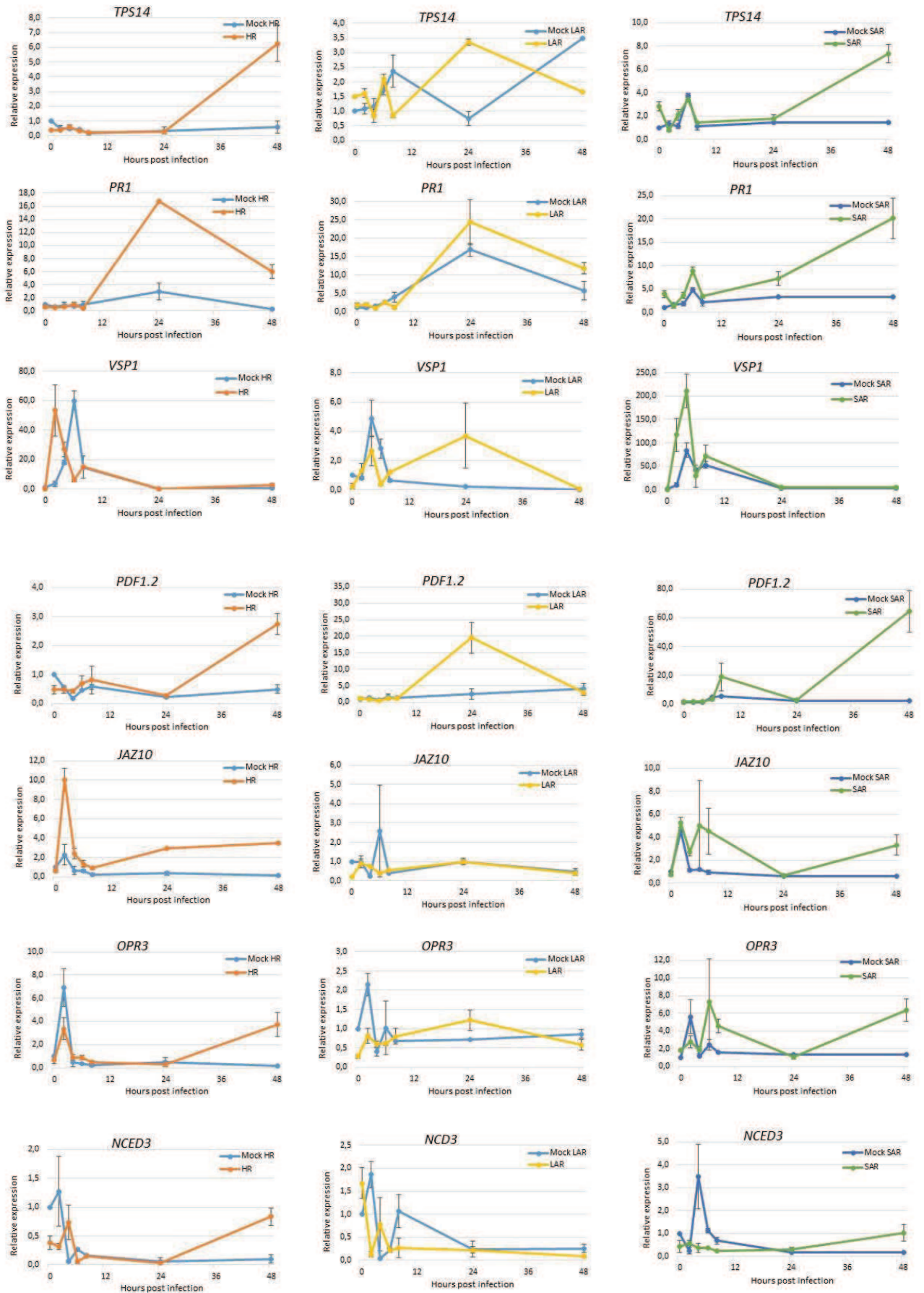
Figure 55: qRT-PCR quantification of the transcript levels of the *CYP76* family members and of defense related genes during incompatible interaction with *Pto* DC3000 *avrRpm1*.

Total RNA was isolated and used as template for cDNA synthesis. Mean changes in gene expression are expressed relative to the transcript level in mock-inoculated Col-0 leaves at time point 0 which was arbitrary set as 1. Bars represent errors from biological replicates (n=5). There were no statistical significances in this experiment.



(Continues next page)

Results and Discussion



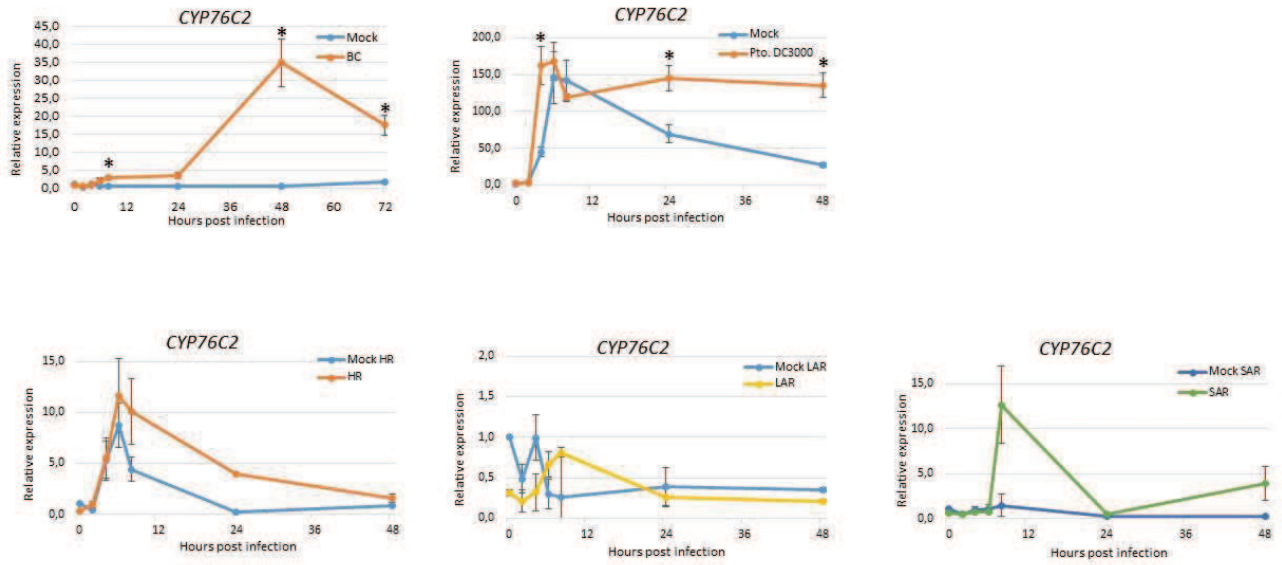


Figure 56: A summary of the transcript levels of qRT-PCR quantification of *CYP76C2* gene during *B. cinerea*, *Pto* DC3000 and *Pto* DC3000 *avrRpm1* interactions.

Bars represent errors from biological replicates (n=5). Asterisks show statistically significant effects at a 5% of probability level.

***CYP76C2* expression monitored via β -glucuronidase (GUS) activity in *Prom*_{*CYP76C2*}:*GUS* transformants**

The gene expression data obtained from qRT-PCR on *CYP76C2* was further validated and refined *in planta* by using GUS staining of *Prom*_{*CYP76C2*}:*GUS* transformed *Arabidopsis* plants. The *Prom*_{*CYP76C2*}:*GUS* line was infected with *Pto* DC3000, *Pto* DC3000 *avr* *Rpm1* and *B. cinerea*, in the same manner as it was done for qRT-PCR. In addition staining was carried out after *Alternaria brassicicola* infection (necrotroph incompatible interaction). Five biological replicates were analyzed by treatment. Experiment was repeated twice with similar results and can be seen in Figure 57, 59, 60, 61 and 62.

The results obtained after the GUS staining confirmed that, as it was previously stated (Figure 56), *CYP76C2* is responsive to the virulent infection, avirulent infection (HR) and *B. cinerea*. In addition, complementary information was obtained in relation to localization patterns of gene expression *in vivo*. Some differences in the early detection of gene induction (4-6-8 HPI) were observed, probably due to the sensitivity of the staining, since qRT-PCR sensitivity is much higher and accurate than GUS.

In addition, staining of mock-treated leaves demonstrated a lack of wounding effect in each experiment. Separate experiments were carried-out to assess the wounding effect, without visible GUS staining (not shown here).

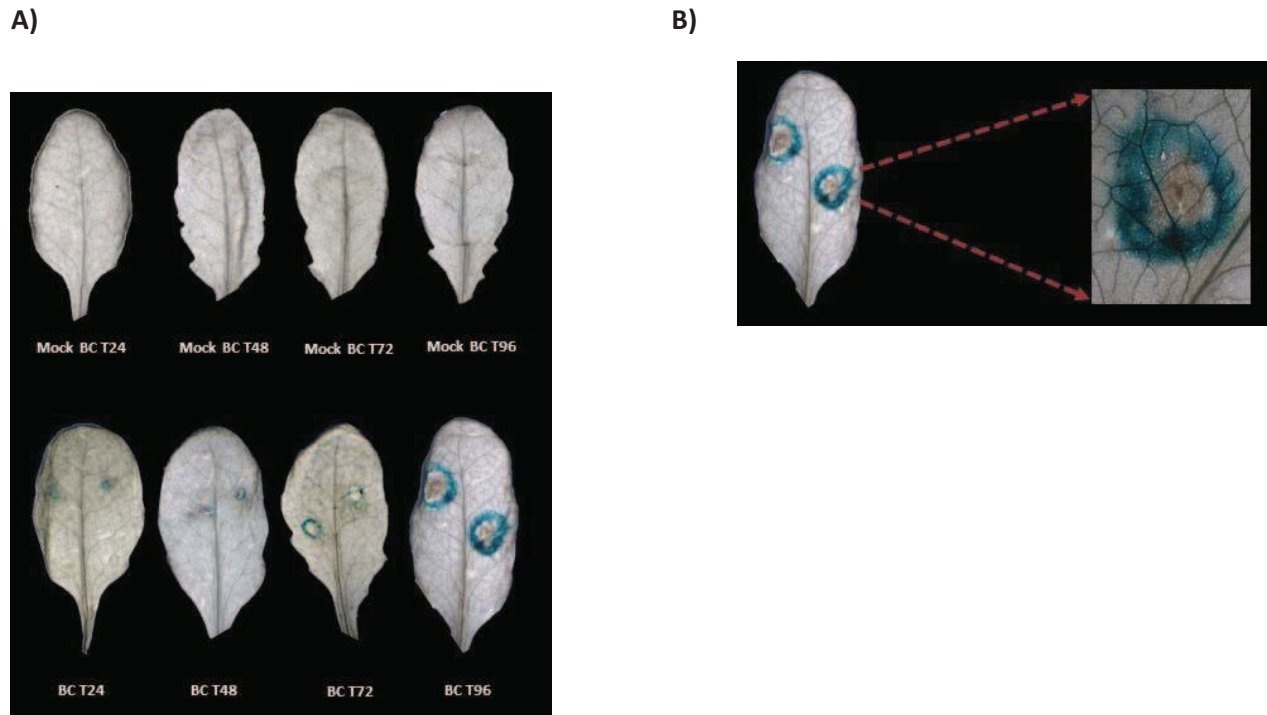


Figure 57: GUS staining of *Botrytis cinerea* infected leaves from *Prom_{CYP76C2}:GUS* transformed plants.

A) *CYP76C2* is induced upon *B. cinerea* infection in the region surrounding the local lesions (Halo). Mock-infected (upper line) and *Botrytis*-infected leaves (bottom line) were assayed at 0-2-4-6-8-24-48-72-96 HPI, results are displayed from 24 HPI. *CYP76C2* shows visible and localized induction from 24 HPI and until 96 HPI. Mock-treated leaves and infected leaves at early time points (0-2-4-6-8 HPI) did not show any coloration. No systemic responses were observed beyond the point of droplet infection. The results are in agreement with previous data obtained by Millet (2009). **B)** Detail of a lesion at 96 HPI showing what it could be a “defense halo” evidencing localized defense responses or LAR.

Abbreviations: **BC:** *Botrytis cinerea*, **T:** time.

B. cinerea causes HR on its host to kill cells and tissues and feeds on the content (Elad *et al.*, 2007; Rossi *et al.*, 2011). *Arabidopsis* local responses to *Botrytis* involves SA-mediated signaling and camalexin production to stop lesion development (Ferrari *et al.*, 2003). The pattern of expression displayed in the picture (Figure 57) resembles the one obtained by Ferrari *et al.*, (2003) in *Prom_{PR1}:GUS* lines challenged with *B. cinerea* (Figure 58, see below). This could indicate that *CYP76C2* expression is localized to the region in which SA signaling mediated responses are taking place (PAL pathway)(Millet, 2009).

Indeed, it can be assumed that the (unstained) lesion core of the lesion corresponds to an area of dead cells, full of fungal hyphae, with no activity, surrounded by a halo of necrotic cells undergoing HR in which *CYP76C2* is expressed and in which synthesis of SA via PAL is occurring. During the first 24-48 hours of contact with *Botrytis*, the plant causes PCD on the fungus to stop its advance. The only viable fungal cells (conidia, may be hyphae) are localized within the necrotic area and are protected from the host toxic molecules. These cells are those giving rise to new hyphae, which secrete molecules that induce PCD now in the host (*i.e* Botrydial), more precisely in the surrounding plant tissues and promote lesion spreading (Shlezinger *et al.*, 2011).



Figure 58: Local and systemic defense gene expression during *Botrytis cinerea* infection in *Prom_{PR1}:GUS* lines (from Ferrari *et al.*, 2003).

GUS staining of leaves of *Prom_{PR1}:GUS* lines. Plants were infected with *B. cinerea* and analyzed at 48 HPI.

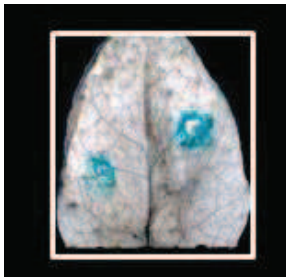


Figure 59: GUS staining of *Alternaria brassicicola* infected leaves from *Prom_{CYP76C2}:GUS* transformed plants at 72 HPI.

The interaction *A. thaliana*-*A. brassicicola* is incompatible. However, like for *B. cinerea*, *A. brassicicola* is a necrotroph but whose resistance relies on JA signaling and camalexin biosynthesis (JA-independent) (Thomma *et al.*, 1999; Glazebrook, 2005). An example of *CYP76C2* response in a situation that combines necrotrophic lifestyle with incompatibility.

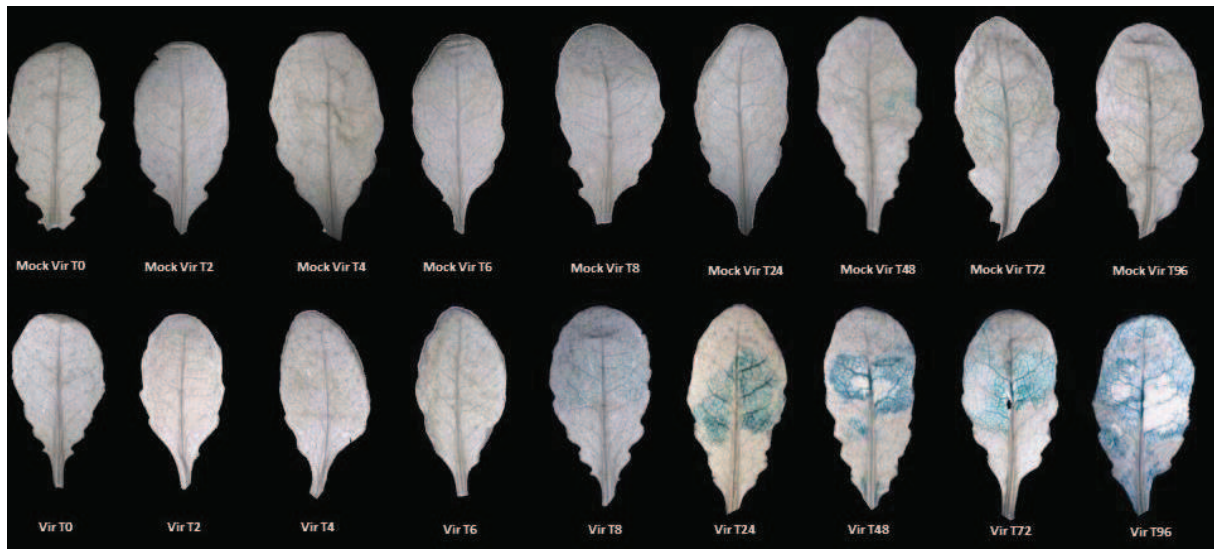


Figure 60: GUS staining of *Pto* DC3000 infected leaves from *Prom_{CYP76C2}:GUS* transformed plants.

GUS staining was carried out on mock-treated (upper row) and infected leaves (bottom) at 0-2-4-6-8-24-48-72-96 HPI. *CYP76C2* induction becomes detectable at 8 HPI and intensifies until 96 HPI. Mock-treated and infected leaves at (0-2-4-6 HPI) did not show any significant coloration. The subtle coloration observed at 48 and 72 HPI in mock-infected leaves is probably a consequence of soft-wounding effect.

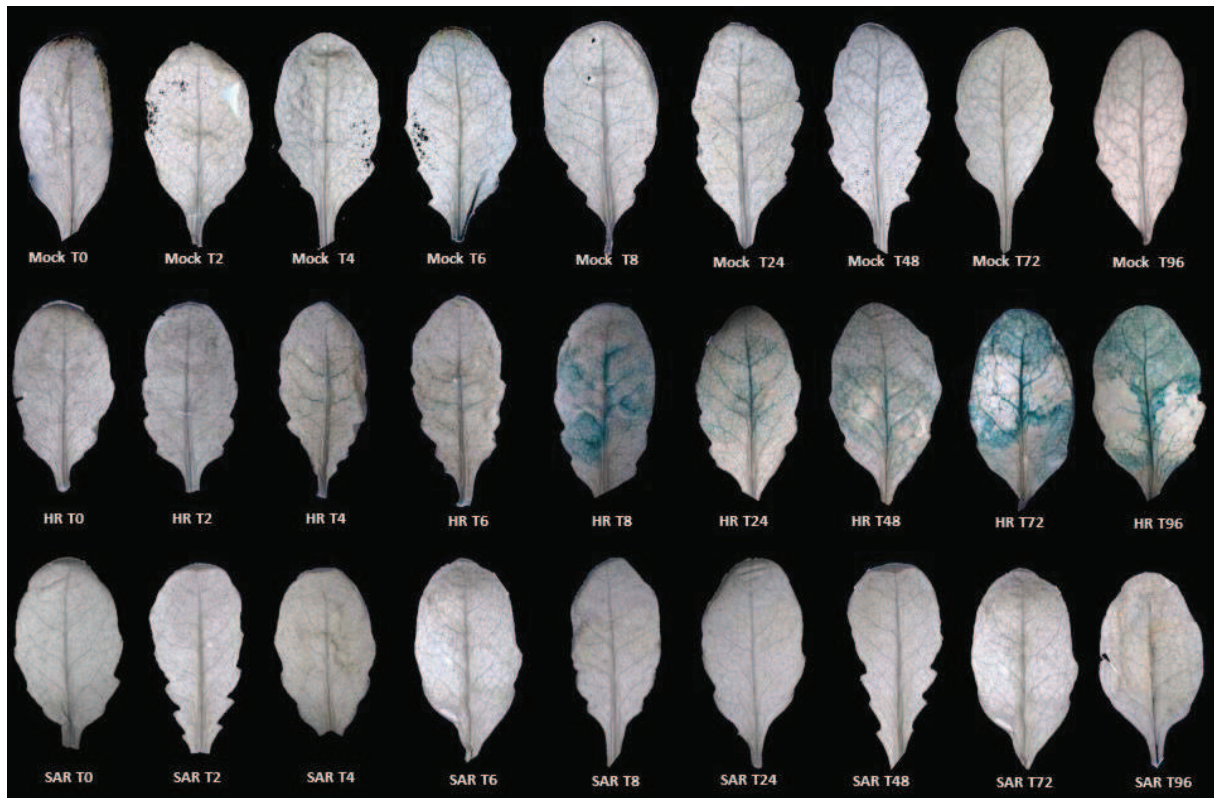


Figure 61: GUS staining of *Pto* DC3000 *avrRpm1* infected leaves from *Prom_{CYP76C2}:GUS* transformed plants.

CYP76C2 is induced upon *Pto* DC3000 *avrRpm1* infection in the HR zone, but not in the adjacent tissues (LAR) or in a systemic manner (SAR). GUS staining was carried out on mock-treated and infected leaves at 0-2-4-6-8-24-48-72-96 HPI. In the upper row mock-treated plants (treated leaves). Middle row, infected leaves. Bottom row SAR leaves. *CYP76C2* induction becomes detectable at 8 HPI in the infected leaves and staining intensifies until 96 HPI. Mock-treatment, LAR and SAR tissues did not displayed any significant coloration. Abbreviations: **T**: time, **SAR**: systemic acquired resistance zone. Not wounding effect after infiltration is noticed.

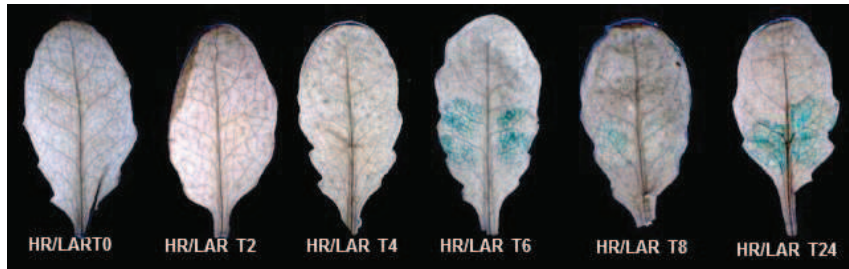


Figure 62: GUS staining of *Pto* DC3000 infected leaves from *Prom*_{CYP76C2}:*GUS* transformed plants: effect of priming with *P. syringae* DC3000 *avrRpm1*.

Plants were primed by syringe-infiltration of the avirulent bacteria and 24 h later inoculated by dipping the whole plant in a suspension with the virulent strain *Pto* DC3000. *CYP76C2* is induced in the HR zone, but not in the adjacent tissues (LAR). Mock-treated leaves and SAR leaves did not displayed any significant coloration and are not presented.

Conclusion of the *CYP76C2* expression monitored via GUS activity

The results showed here confirmed, as in qRT-PCR experiment, that *CYP76C2* is induced after *B. cinerea* infection. This experiment also enriched the previous information by showing that the induction is localized in a ring of cells (“halo”) surrounding the lesion that do not spray beyond (Figure 57). This halo, as it was described before (Figure 57 and 58), corresponds to a group of cells coursing HR and accumulating SA synthesized via PAL. Moreover, at a glance, this halo quite resembles the pattern of camalexin production (localized cell death/HR). This was an important observation to do since the [transcriptomic data](#) had suggested co-expression of *CYP76C2* with *PAD3* (took >24 HPI).

CYP76C2 also showed localized responses facing another necrotroph: *A. brassicicola* (Figure 59). This interaction is incompatible and also implies cell death, but with limited lesion development. The use of this pathogen was not intended for this thesis or even considered as an objective itself, but at the moment of GUS experiments was used with the aim of shortly analyzing or illustrate *CYP76C2* induction in other cell death scenario. Later in this thesis will also be discussed preliminary data of this gene on *Hyaloperonospora arabidopsidis* infection, other pathogen that was tested beyond the scopus of this work with the aim of enlarge the possible scenarios in which *CYP76C2* could be responsive.

Additionally GUS activity confirmed that *CYP76C2* was induced under virulent and avirulent interaction with *Pto* DC3000 from 8 to 96 HPI. The pattern of gene expression on *Prom*_{CYP76C2}: *GUS* lines mostly confirmed the data obtained in the qRT-PCR experiment and provided precise information about the

pattern of localization of gene expression *in planta*. This experiment was particularly important to analyze LAR and SAR responses. It was confirmed that *CYP76C2* is not induced in LAR zone and showed that, in spite of the fact that *CYP76C2* displayed some gene induction in SAR zone evidenced by the qRT-PCR experiment (Figure 55), here in this experiment there was no GUS activity detected in systemic tissues (Figure 61). Furthermore this experiment confirmed the responses of *CYP76C2* in HR zone and showed that these responses are not related to wounding effects as evidenced by the lack of responses in mock-treated leaves (Figures 60, 61 and 62).

To confirm the results obtained in LAR and SAR zones, plant leaves were primed by syringe-infiltration of the avirulent strain followed by dipping with the virulent one (Figure 62). Yet again no responses were observed in LAR and SAR tissues but in HR zone.

CYP76C2: Phenotyping in response to pathogens

In order to tackle the question of *CYP76C2* playing a role in defense responses, knock-out and overexpressing lines of *A. thaliana* were analyzed after infection with:

- *Pto* DC3000
- *Pto* DC3000 *avrRpm1*
- *B. cinerea*

The T-DNA insertion and the overexpression lines, already available at host lab, were first genotyped. Insertion of T-DNA was confirmed by amplification of the insertion borders and qRT-PCR. Additionally, the levels of transcripts present in the overexpression line was checked by means of qRT-PCR. Information is available in [appendix](#) and has been published in Höfer *et al.*, (2014).

Virulent infection with *Pto* DC3000

A. thaliana Col-0 and *CYP76C2* mutants, 4-5 weeks old, were infected by dipping the whole areal part of the plant in a suspension containing MgCl₂ (mock) or *Pto* DC3000 at a titer of 5 x10⁷ CFU/ml.

The colonization of plant tissues by bacterial pathogen was quantified in each sample by qPCR on genomic DNA from mock and infected plant according to Boachon *et al.*, (2014). Samples were collected at the moment of infection and 72 HPI, called T0 and T3 hereafter. In [appendix](#) section can be found information about standard/calibration curves and melting curves analysis of primers.

qPCR results for the pathogen quantification were expressed as logarithm of the ratio: copy numbers of the pathogen gene per copy numbers of the plant gene. Three technical triplicates and five biological replicates were used for each treatment. Experiment was repeated twice with similar results.

As is shown in Figure 63, there were no statistical differences between the Col-0, *cyp76c2* and *35S:CYP76C2* after infection with the virulent strain *Pto* DC3000. The three genotypes supported the same level of bacterial growth at 72 HPI. The differences between mock and infected plants between T0 and T3 as expected reflected pathogen multiplication. A slight variation was observed at T0 and T3 among genotypes for the mock samples (within time), but not reaching statistical significance in most of cases.

The levels of infection achieved were optimal as it was confirmed not only by qPCR estimation of the pathogen biomass through the ratio copy numbers pathogen gene /copy numbers plant gene, but also by visual inspection of diseased plants and by comparison with publications on the subject (Figure 64).

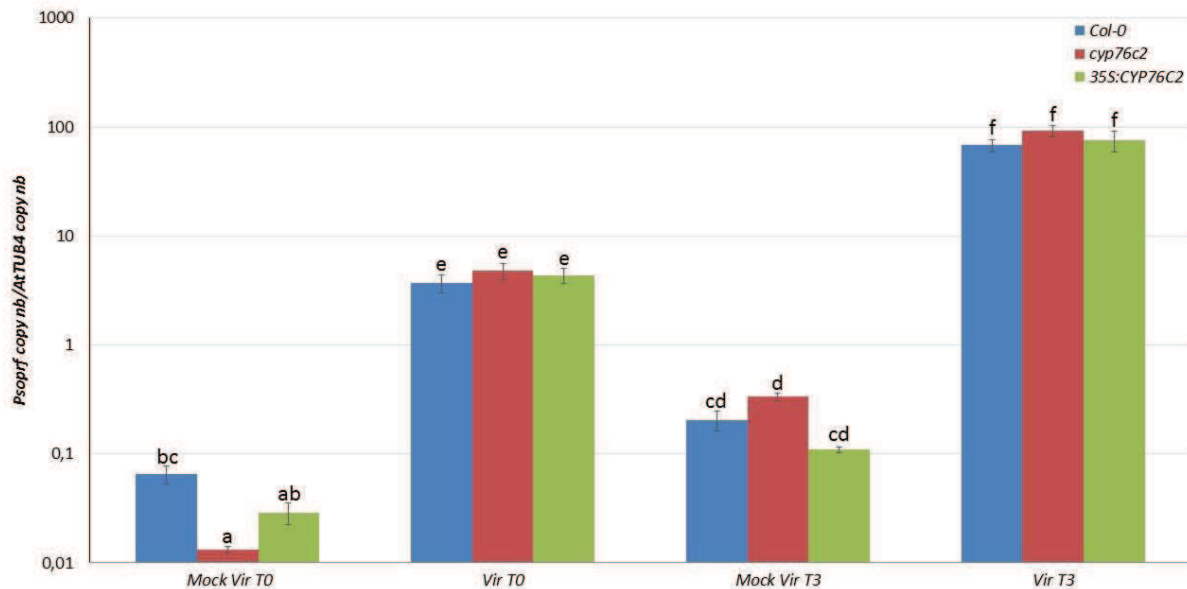


Figure 63: qPCR quantification of the *Pto* DC3000 infection on *A. thaliana* leaves of Col-0, *cyp76c2* and 35S:CYP76C2 mutant lines.

Plants were infected by dipping the whole areal part of the plant in a suspension containing $MgCl_2$ (mock) or *Pto* DC3000 at a concentration of 5×10^7 CFU/ml. Data are means of three technical and five biological replicates. Errors bars represent the standard error of the mean. Letters show statistically significant differences calculated by Tuckey's test at a probability level of 5%.

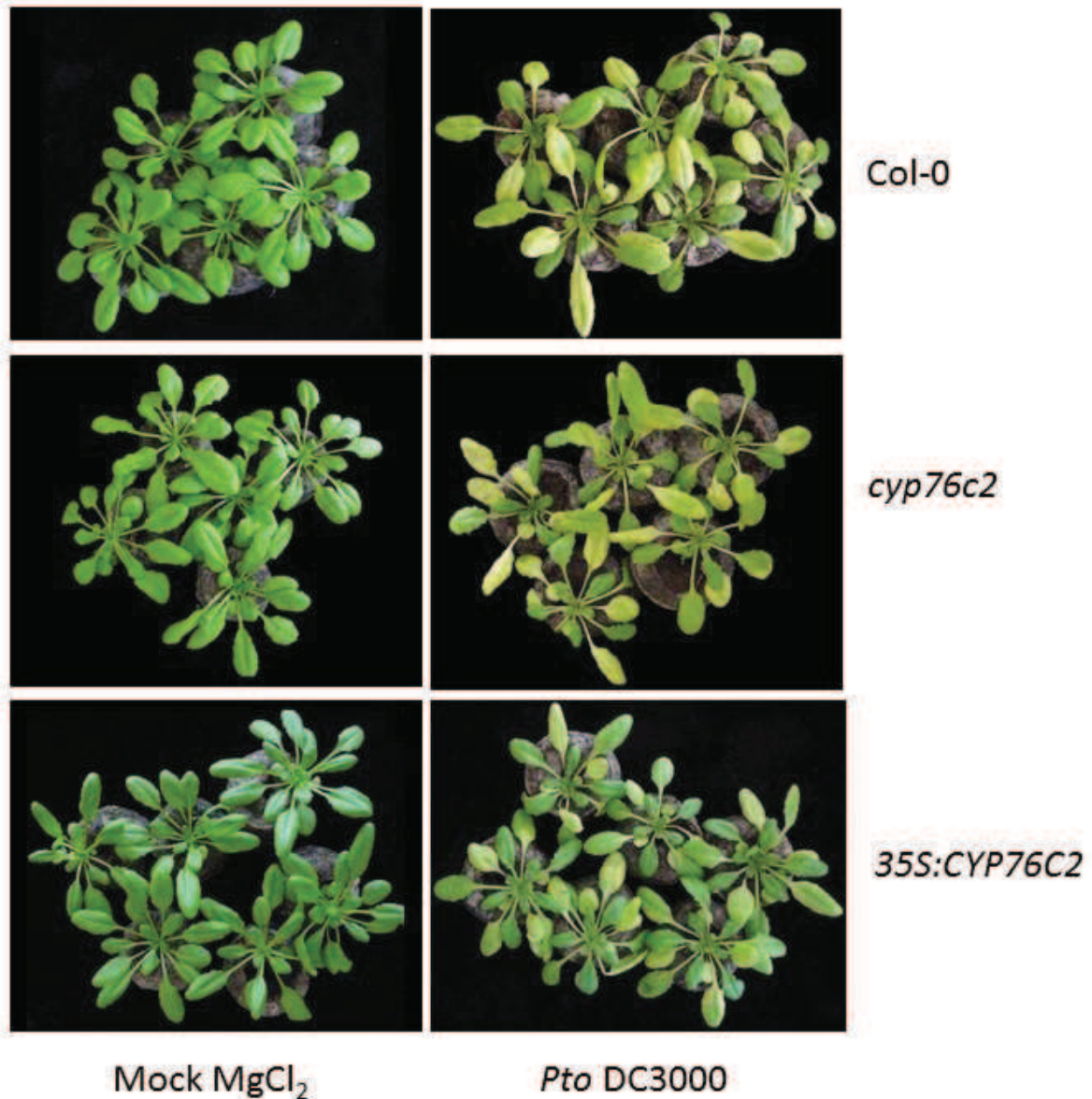


Figure 64: Disease symptoms at 72 HPI in *A. thaliana* leaves of Col-0, *cyp76c2* and *35S:CYP76C2* lines infected with the virulent strain *Pto* DC3000.

Plants were dipped in a solution containing only MgCl_2 (mock) or *Pto* DC3000 at a concentration of 5×10^7 CFU/ml in 10 mM MgCl_2 and 0.03% (v/v) Silwet L-77. Water soaked lesions and chlorosis can be observed in the infected plants, while mock treated plants do not develop any symptoms.

Temporal analysis of symptoms development after *Pto DC3000* infection

When plants were infected and evaluated at 72 HPI, no evident difference was observed in the infection development and plant stress between the different lines (Figure 63). This result was surprising given the significant increase in *CYP76C2* transcripts (Figure 54) and GUS activation (Figure 60) observed in plants challenged with *Pto DC3000*.

In order to detect a possibly transient impact on infection development, a second experiment was planned to study the onset of symptoms in a time series. A statistical significant difference was found at 24 HPI among the infected plants, where *cyp76c2* bacterial growth was slightly higher than in Col-0 and *35S:CYP76C2* plants. Whereas this was however a very minor effect, it would be in agreement with *CYP76C2* being significant induced at 24 HPI (also at 4-48 HPI) in the gene expression experiment (Figure 54). The same trend was observed at 48 HPI but not considered as statistically significant. *35S:CYP76C2* plants did not behave as more (or slightly more) resistant than Col-0 across the time course, instead was faintly more affected. On the other hand, the lack of significant effect at 72 HPI confirms the results obtained in the previous experiment (Figure 63). The slight difference in bacterial growth at 24 HPI by qPCR analysis did not result in any difference detectable by human eye (Figure 65 and 66).

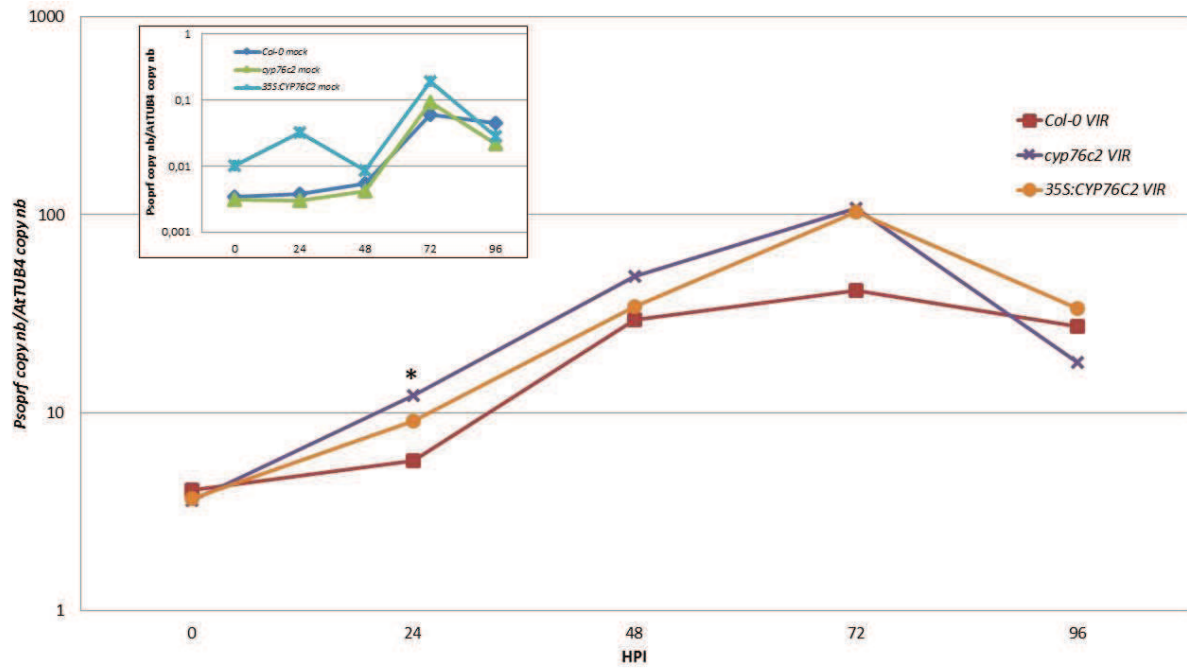


Figure 65: Time course qPCR quantification of the progress of *Pto* DC3000 infection in Col-0, *cyp76c2* and 35S:CYP76C2 lines.

Data represent means of three technical replicates and five biological ones. Errors bars are not shown to avoid blurring information (see [Appendix](#)). A detail of mock treatment is displayed in the frame. Asterisk shows statistically significant differences calculated by Tuckey's test at a probability level of 5%.

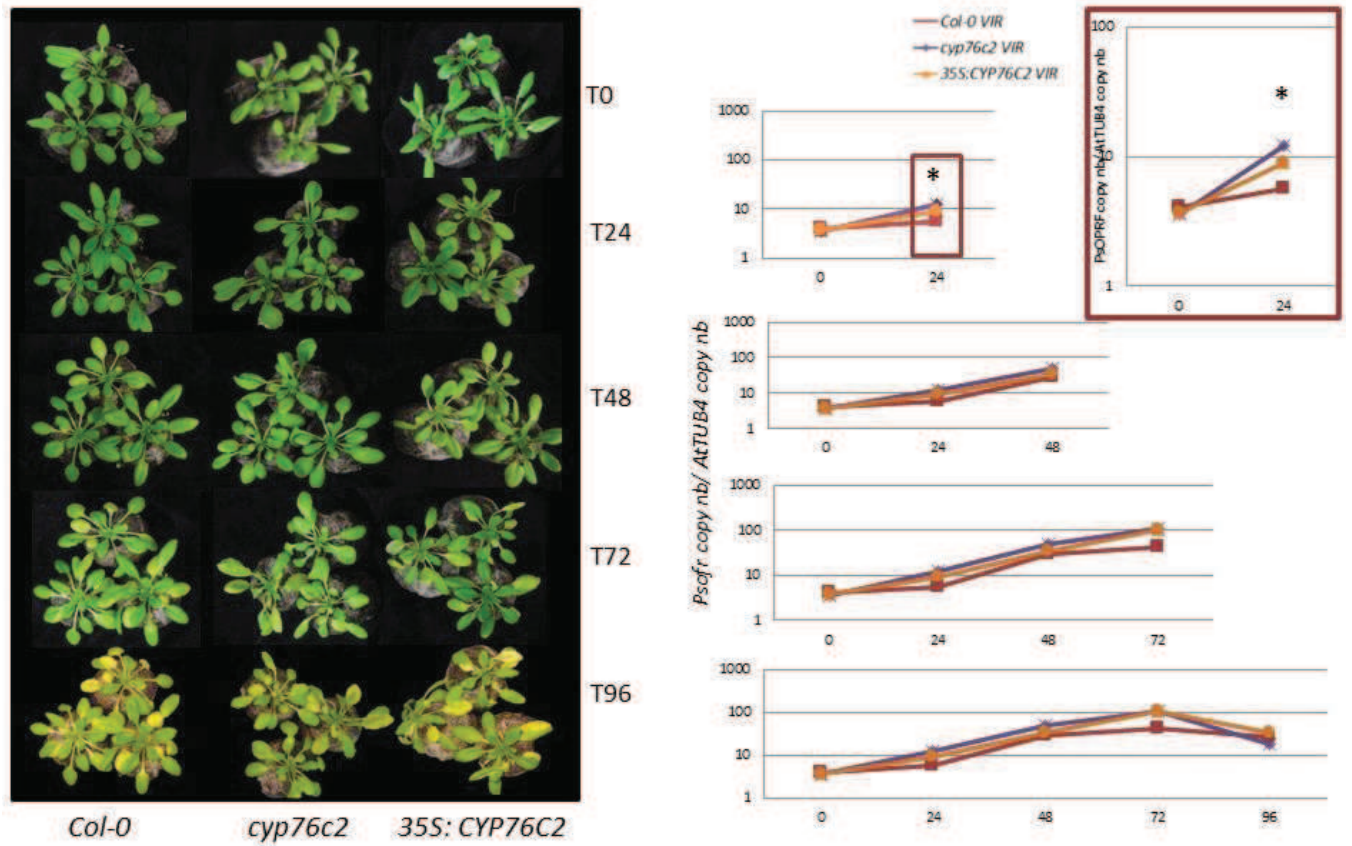


Figure 66: qPCR quantification of time course infections of *Pto* DC3000 on Col-0, *cyp76c2* and *35S:CYP76C2* lines showing infected plants at the left and charts at the right.

Plants were dipped in a solution containing $MgCl_2$ (mock) or *Pto* DC3000 at a concentration of 5×10^7 CFU/ml. Only data corresponding to infected plants is displayed in the charts (right side of the figure). Data represent means of three technical replicates and five biological ones. Errors bars are not shown to avoid blurring information. Asterisk shows statistically significant differences calculated by Tuckey's test at a probability level of 5%.

Infection with *Pto* DC3000 *avrRpm1*: HR, LAR and SAR responses

HR

A. thaliana Col-0 and *CYP76C2* mutants, 4-5 weeks old, were syringe infiltrated with a suspension containing MgCl₂ (mock) or *Pto* DC3000 *avrRpm1* at 5 x10⁶ CFU/ml.

The colonization of plant tissues by bacterial pathogen was quantified in each sample by qPCR on genomic DNA from mock and infected plant as described before for virulent infections. Three technical triplicates and five biological replicates were used for each treatment.

The quantification of pathogen growth in the HR zone did not reveal any significant difference among the different lines (Figure 67). Col-0 and *cyp76c2* showed similar bacterial titer between HR at T0 and T3 illustrating in some way how PCD stops pathogen growth. The *35S:CYP76C2* mutant line instead showed a difference between the titer in HR at T0 and T3 possibly reflecting a subtle lack of HR.

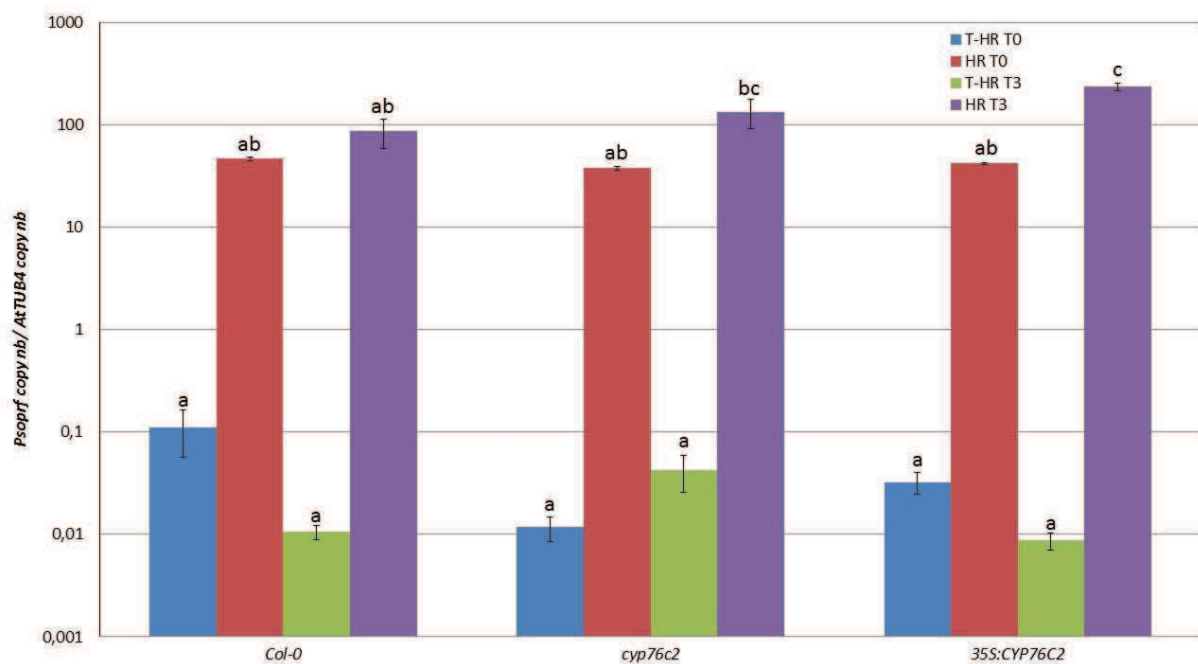


Figure 67: qPCR quantification of *Pto* DC3000 *avrRpm1* infection on Col-0, *cyp76c2* and *35S:CYP76C2* mutant lines (HR response).

Plants were syringe-infiltrated with MgCl_2 (mock) or *Pto* DC3000 *avrRpm1* at a titer of 5×10^6 . Data corresponds to the mean of three technical and five biological replicates. Errors bars represent the standard error of the mean. Different letters shows statistically significant differences calculated by Tuckey's test at a probability level of 5%.

LAR and SAR responses

Avirulent infections for better assessment of LAR and SAR responses were carried out by priming the plant by syringe- infiltration with the avirulent bacteria (5×10^6 CFU/ml) followed 24 h later by dipping the whole plant with the virulent strain (5×10^7 CFU/ml) as stated for virulent infections (more details in materials and methods, Figure 49). For mock treatment, plants were syringe infiltrated with MgCl_2 and 24 h later dipped in a suspension of the virulent strain.

qPCR quantification of pathogen growth was performed in the same way as for virulent infections. Plant material from T-LAR (mock), LAR, T-SAR (mock) and SAR areas (Figure 68, 69, 70) were frozen in liquid nitrogen for total genomic DNA extraction. Three technical replicates and five biological replicates were analyzed for each treatment. One plant was considered one experimental unit. Statistical differences ($p < 0.05$) were represented by different letters. Experiment was repeated twice with similar results.

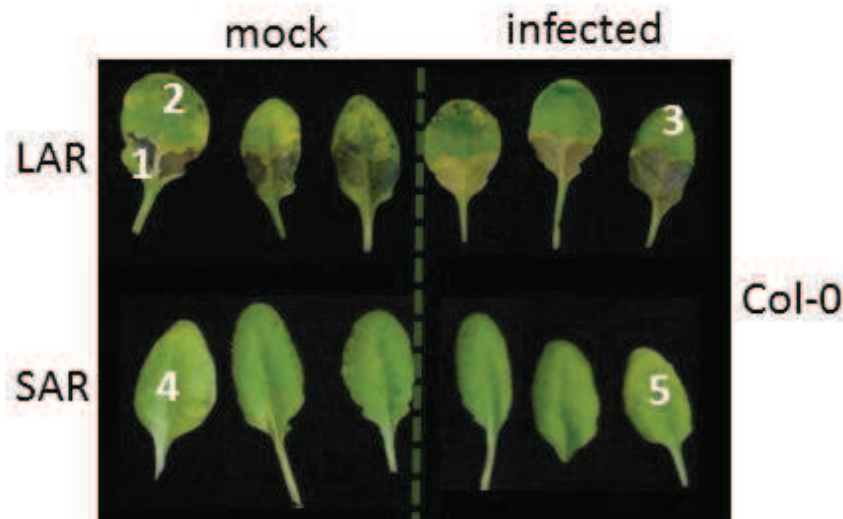


Figure 68: Disease symptoms, LAR and SAR responses at 72 HPI in Col-0 plants.

Mocks plants were syringe-infiltrated with $MgCl_2$ in **1)** and 24 hours later dipped in *Pto* DC3000 suspension.

Infected plants (right panel) were first syringe-infiltrated with the avirulent strain in **1)** and 24 later dipped in the virulent strain. SAR responses in **4)** and **5)**.

References: **1)** infiltration HR zone, **2)** LAR zone: in the mock shows no LAR but symptoms of virulent infection, **3)** LAR zone in the infected plants: shows LAR responses (no virulent symptoms), **4)** SAR zone in the mock: shows symptoms of virulent infection (note: the quality of the picture/impression does not allowed a good image), **5)** SAR zone in the infected plants: shows SAR responses. Significant HR and necrosis are visible in **1)**. Mock infiltrated plants show significant water soaked lesions and chlorosis in zone **2)**.

Results presented in Figure 69, showed a LAR response at 72 HPI but only statistically significant for Col-0 plants which validates the experimental procedure and qPCR analyses. Surprisingly, *35S:CYP76C2* showed a LAR response that was not significant. Conversely, *cyp76c2* did not show any LAR responses in the two repetitions of the experiment.

It is interesting how *CYP76C2* again shows restrained responses but still presents and how the knock-out mutant *cyp76c2* behaves somewhat different from wild-type and *35S:CYP76C2*.

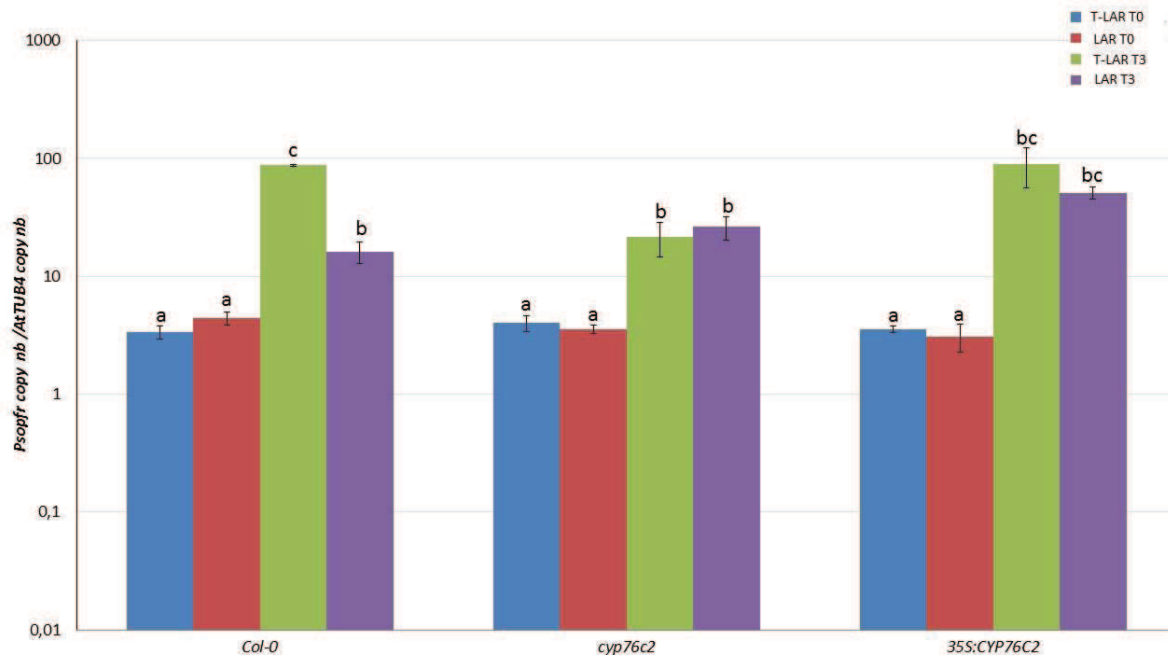


Figure 69: qPCR quantification of *Pto* DC3000 infection on *A. thaliana* leaves of Col-0, *cyp76c2* and *35S:CYP76C2* mutant lines primed with *Pto* DC3000 *avrRpm1* and showing LAR responses.

Data come from the average mean of three technical and five biological replicates. Errors bars represent the standard error of the mean. Letters shows statistically significant differences calculated by Tuckey's test at a probability level of 5%.

The Figure 70 illustrates SAR responses. No significant SAR is observed for any of the genotypes tested but instead there was significant effects at T0 between mock and infected plants of Col-0. In Col-0 and *cyp76c2* plants there was some tendency indicative of SAR that was not significant, but *35S:CYP76C2* plants showed no SAR at all (as observed in GUS experiment).

The first possible explanation would be that priming by virulent infection through dipping could have failed priming the response. Leaves of the SAR zone of mock-infiltrated plants are supposed to show the same levels of infection as a virulent infection. However when the LAR data is observed the levels of virulent infection observed in T-LAR T3 are correct and very similar to a typical virulent infection. On the other hand, observing the data it is obvious that if dipping failed to show SAR it should fail to show/to prime LAR, and that was not the case since LAR responses are present (both samples came from same plant).

In the same line, LAR responses were present but no so relevant in the mutants of *CYP76C2*. However Col-0 plants (wild-type check) showed relevant and significant LAR responses without SAR. Then the idea of low-quality of priming by the virulent infection does not to seem very plausible. The only probable argument is that SAR responses are probably displayed later and with this experiment closed at 72 HPI, SAR responses were not displayed. In fact, dipping infection are always more retarded in the response effect than the infiltration technique because constitutive barriers are not bypassed. Nevertheless in the [GUS](#) experiment at 96 HPI there was no SAR responses either.

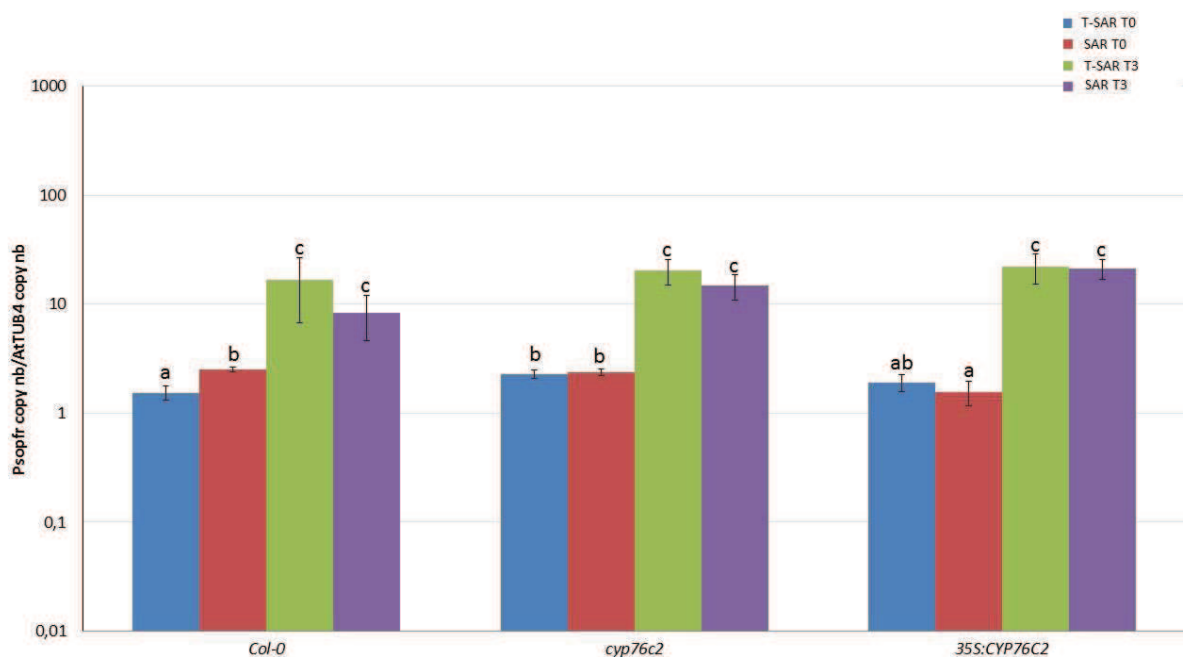


Figure 70: qPCR quantification of *Pto* DC3000 infection on *A. thaliana* leaves of Col-0, *cyp76c2* and *35S:CYP76C2* mutant lines primed with *Pto* DC3000 *avrRpm1* and showing SAR responses.

Data come from the average mean of three technical and five biological replicates. Errors bars represent the standard error of the mean. Letters shows statistically significant differences calculated by Tuckey's test at a probability level of 5%.

Temporal analysis of symptoms development after *Pto* DC3000 *avrRpm1* infections

As in the case of virulent infections, no definitive phenotype was found in incompatible interaction with the avirulent bacteria. Subsequently a similar type of experiment was planned to study the onset of symptoms in a time series for avirulent infections. Whole leaves were syringe-infiltrated with the *Pto* DC3000 *avrRpm1* or MgCl_2 (mock) and evaluated at 0-24-48-72 HPI. The idea was to focus on responses to avirulent interaction analyzing whole leaves not taking into account LAR and SAR spatial responses and using the infiltration technique to obtain a stronger response.

Interestingly, *35S:CYP76C2* showed a significant different response at 24-48 HPI by comparison to Col-0 and *cyp76c2* plants. Contrary to what was observed in virulent interaction, *35S:CYP76C2* was more affected than the other two genotypes. Moreover, this “susceptible” behavior of *35S:CYP76C2* was sustained from 24 HPI to 72 HPI. Conversely, *cyp76c2* plant were less affected than Col-0 at 48 HPI, thus showing a contrasting effect of both mutants.

This seems to indicate a possible difference in the role of *CYP76C2* facing compatible vs incompatible interactions. Somehow this experiment also shows how *CYP76C2* behaves in cell death scenarios, something that was also observed in HR in the relative gene induction and in the necrotic lesions of *B. cinerea*, and something also established in some other publications ([Hypothesis](#)) (Godiard *et al.*, 1998).

A characteristic feature of the avirulent infections is the oxidative burst produced in the HR ([Figure 27](#)). The transitory and subtle susceptibility of *35S:CYP76C2* mutants (transitory increase in susceptibility) suggest some intricate relationship between *CYP76C2* and ROS. Probably *CYP76C2* is contributing to enhance ROS generation, instead of helping in detoxification or ROS scavenging. Another possibility would be that *CYP76C2* catalyzes a poorly coupled reaction and thus directly generates ROS. Nevertheless, Millet (2009) demonstrated with paraquat treatments, that *CYP76C2* had a weak antioxidant effect.

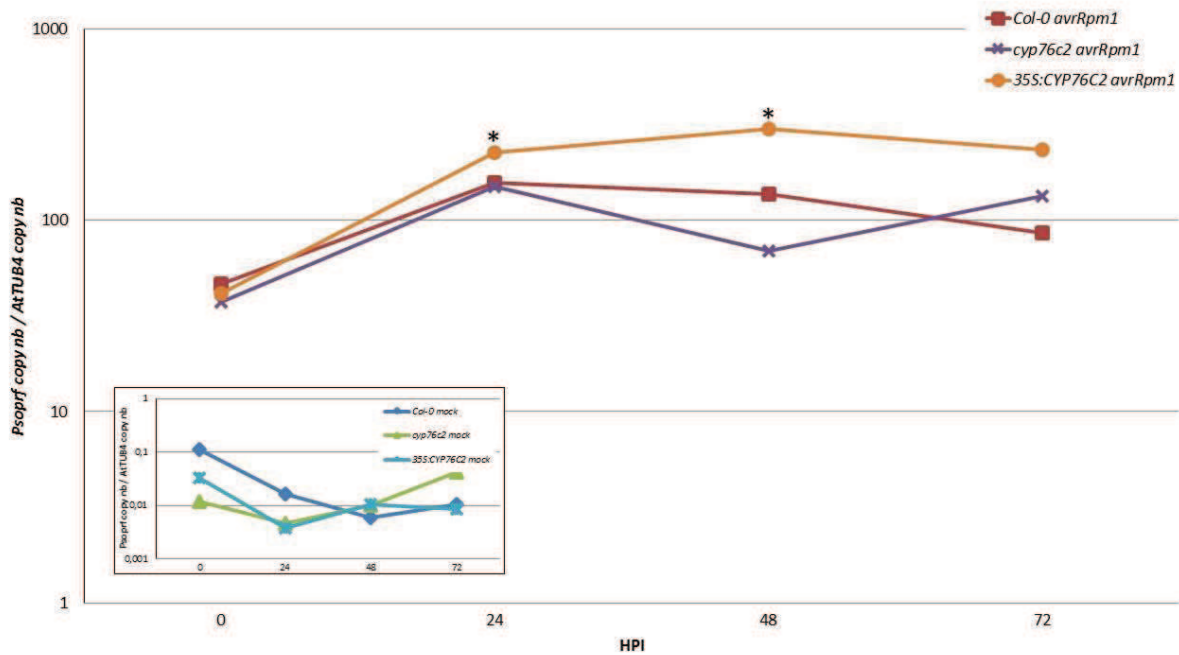


Figure 71: Time course qPCR quantification of the progress of the *Pto* DC3000 *avrRpm1* avirulent infection in the Col-0, *cyp76c2* and *35S:CYP76C2* lines.

Data are mean of three technical replicates and five biological replicates. Mock treatment are displayed in the frame. Errors bars represent the standard error of the mean. Letters shows statistically significant differences calculated by Tuckey's test between non-infected and infected plants at T0 and T3, at a probability level of 5%.

***Botrytis cinerea* Infection**

For *B. cinerea* infections, 8-10 plants per treatment were used and 5-7 leaves of each plant were inoculated with a 5 μ L droplet containing 1×10^5 conidia/ml in potato dextrose broth. Plants were 4-5 weeks old.

The macroscopic estimation of *B. cinerea* growth was done by measuring the diameter of necrotic lesions 4 days post inoculation. One plant was considered as one experimental unit and a replicate. Results were expressed as necrosis size in square millimeters. Experiment was repeated several times. One-way ANOVA on ranks Kruskal-Wallis (Balzarini *et al.*, 2008) was performed since the data did not fulfilled a normal distribution.

Both the insertion and overexpressing lines appeared slightly more susceptible than the wild-type, but difference was not statistically significant (Figure 72).

Good levels of infections were obtained by comparison with published data. Some variation between independent experiments was observed, never reaching statistical significance, denoting some degree of stochastic effects. This was not unexpected and has been reported elsewhere (Rowe and Kliebenstein, 2008; Buxdorf *et al.*, 2013). Buxdorf *et al.*, (2013) have suggested that the cause could be the unequal distribution of glucosinolates in the leaves (Stroff *et al.*, 2008 cited in Buxdorf *et al.*, 2013).

Experiments with different isolates were carried out with the aim of detecting a possible combination that would allow to better discriminate a phenotype since different sensitivity to glucosinolates or derivatives have been observed among different strains (Kliebenstein *et al.*, 2005; Buxdorf *et al.*, 2013). We did not observed significant differences in the infection using these different isolates (data not shown).

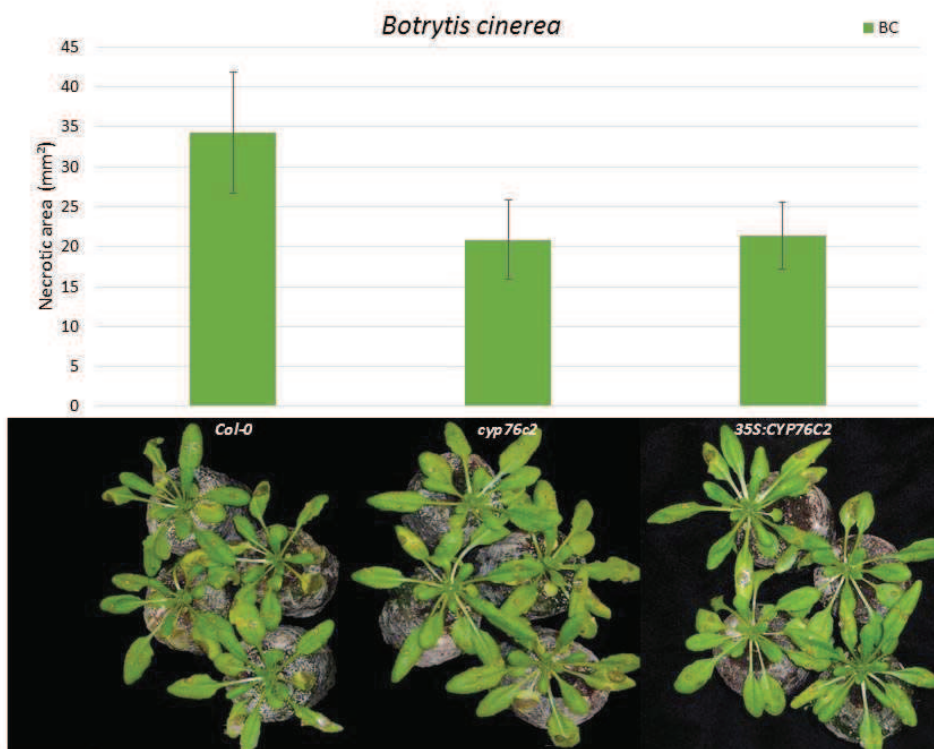


Figure 72: Visual assessment of disease development in *Arabidopsis thaliana* Col-0, *cyp76c2* and 35S:YP76C2 plants infected with *B. cinerea* at 72 HPI.

Each value correspond to the average area and standard error of 8-10 plants and 5-7 leaves per plant, inoculated with a 5 μ L droplet containing 1×10^5 conidia/ml. Average areas are expressed in mm^2 . Estimation of necrotic areas were done at 72 HPI. Statistically differences were calculated through the Kruskal-Wallis test ($\alpha=0.05$). Not statistical differences were found among the tested genotypes.

Temporal analysis of symptoms development after *Botrytis cinerea* infections

Considering the lack of phenotype observed at 72 HPI, another experiment was planned in order to test the hypothesis of a transient impact on the timing of symptoms development.

The time course of necrosis development can be seen in Figure 73. Only minor differences can be detected mainly at very late stages of the lesion development, 80 HPI (*cyp76c2* and *35S:CYP76C2* higher than Col-0) and at 96 HPI (Col-0 higher than *cyp76c2* and *35S:CYP76C2*). Lesion progression in the *cyp76c2* line strictly parallels that in *35S:CYP76C2* plants. *CYP76C2* presence and expression thus does not seem to have any impact on the progress of *Botrytis* infection.

An increase in the accumulation of *CYP76C2* transcripts in the qRT-PCR experiments, was observed during the early stages of the infection (8-24-48 HPI), but the first symptoms did not appear before 48 HPI, so that any earlier effect cannot be detected. In any case, those would not significantly affect the overall disease development.

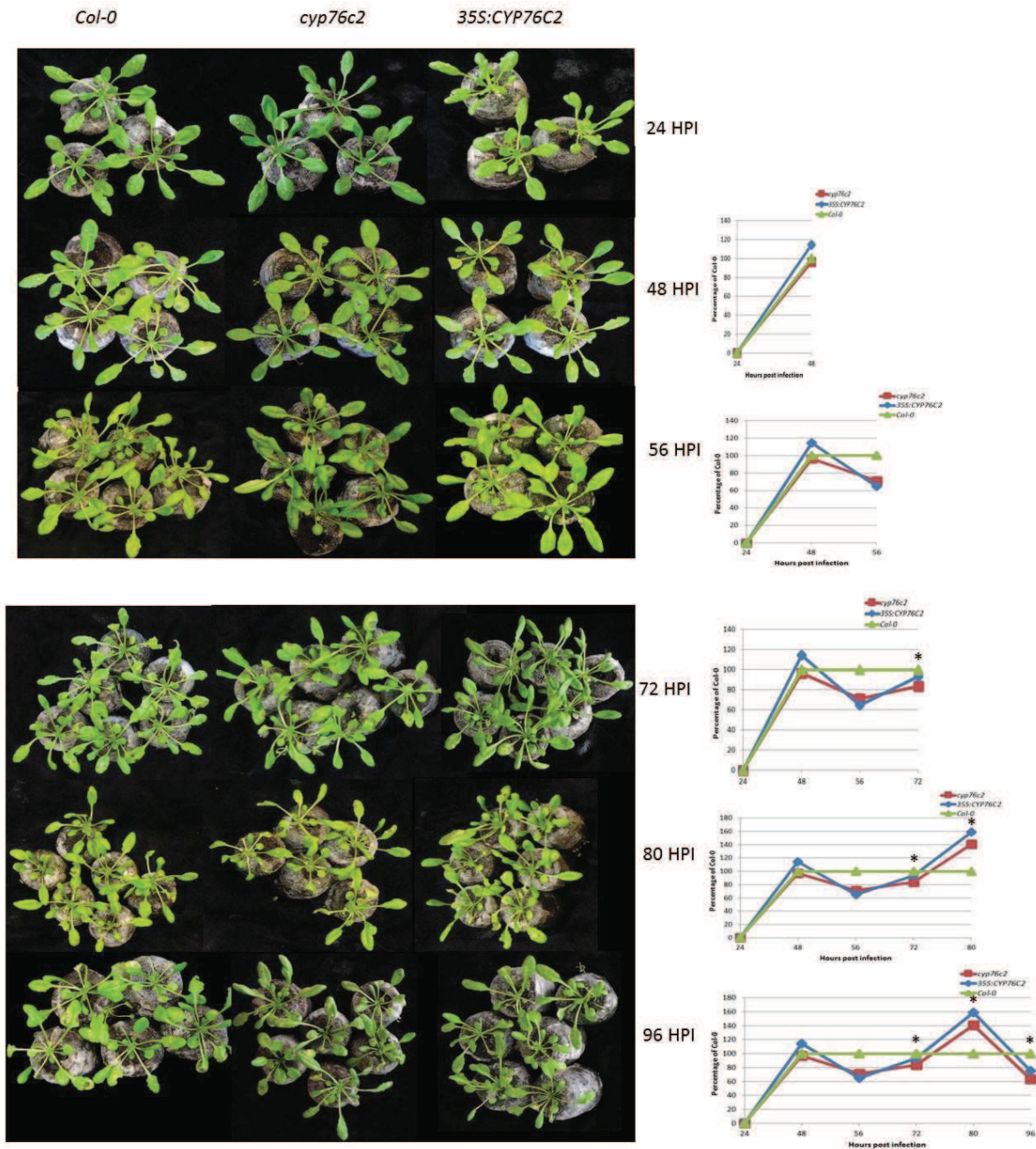


Figure 73: Quantification of disease development in *Arabidopsis thaliana* Col-0, *cyp76c2* and 35S:CYP76C2 plants infected with *B. cinerea*.

Each value corresponds to the average area and standard error of 8-10 plants and 5-7 leaves per plant, inoculated with a 5 μ L droplet containing 1×10^5 conidia/ml. Average areas were calculated in mm^2 and expressed as the relative percentage of Col-0 plants at each time point. Statistically significant differences were calculated using the Kruskal-Wallis test ($\alpha=0.05$) and are indicated by an asterisk. Errors bars are not presented for space constrains, but can be seen in Table 24 and [appendix](#).

Table24: Mean value of necrotic lesion expressed as the relative percentage of Col-0 plants at 48-56-72-80-96 HPI.

H*: Statistic of Kruskal Wallis. Different letter within time point and among genotypes represents statistical significances (P<0.05).

HPI	Genotype	Means%	±EE	H*
48	<i>Col-0</i>	100	9,83	a
48	<i>cyp76c2</i>	96,6	9,57	a
48	<i>35S:CYP76C2</i>	114,4	9,98	a
56	<i>Col-0</i>	100	11,88	a
56	<i>cyp76c2</i>	71,3	9,23	a
56	<i>35S:CYP76C2</i>	64,8	4,84	a
72	<i>Col-0</i>	100	9,20	b
72	<i>cyp76c2</i>	83,5	14,62	a
72	<i>35S:CYP76C2</i>	93,4	21,07	a
80	<i>Col-0</i>	100	20,52	a
80	<i>cyp76c2</i>	140,9	17,52	b
80	<i>35S:CYP76C2</i>	158,8	20,58	b
96	<i>Col-0</i>	100	9,87	b
96	<i>cyp76c2</i>	63,9	7,55	ab
96	<i>35S:CYP76C2</i>	75,3	12,67	a

Conclusion of the experiments of phenotyping of the *CYP76C2* impact on pathogens resistance

The *CYP76C2* gene being responsive to pathogens, we postulated that it might have role in disease resistance. The experiments implemented to evaluate how *CYP76C2* may affect disease resistance or susceptibility in the mutant lines of *CYP76C2* seem to indicate that *CYP76C2* only has a very minor and subtle or transient impact on the development of the infection, if any. One of the most interesting responses of gene induction was obtained in the experiment of *B. cinerea* (Figure 52) and for which no effect on necrosis progression was found. This might be to some extent due to some functional redundancy with other members of the family, although the radically different profiles of gene expression do not seem to support this hypothesis. Redundancy with another, unrelated, gene however cannot be excluded.

On the other hand, it is also possible that the main function of *CYP76C2* is the detoxification of a plant defense molecule or the production of antioxidants, thus contributing to the protection of intact plant tissues. In the latter case, many other genes would be also expected to contribute to the buffering of ROS generated upon pathogens attack, and the specific part of *CYP76C2* might be only revealed upon

multiple gene inactivation. The latter scenario would be plausible considering that *CYP76C2* was found activated in many circumstance associated with ROS production.

Metabolomics Analysis

CYP76C2 was clearly responsive to pathogen infection, but its impact on the development of the disease symptoms triggered by the tested pathogens was transitory or very subtle. In order to understand the role of this gene in defenses responses and to detect a potential metabolic phenotype, extensive metabolic profiling was carried out before and after infection.

Analysis of P450 co-expression with terpene synthases and functional screening previously suggested that several members of the *CYP76C* family, including *CYP76C2*, might contribute to the metabolism of monoterpenols ([Hypothesis](#)). The lack of a clear-cut phenotype might thus result from functional redundancy, which could also prevent clear responses in metabolic profiling. For this reason, several approaches were planned.

The first approach more specifically targeted terpenoid metabolism. Both volatile and soluble terpenoids were investigated first by volatile collection and analysis, and second by targeted profiling of infected tissues in UPLC-3Q-MS/MS. In addition, a hormone profiling was also carried out focused on the main defense-related hormonal and signaling pathways. Camalexin analysis was included in the study. Finally, the investigation was completed with a non-targeted analysis in UPLC Orbitrap-MS.

The sole experiment that included all the pathogens tested was the volatile collection, after that experiment, the strategy was focused in avirulent interaction by syringe-infiltration of whole *A. thaliana* 4-5 weeks old plant leaves.

Headspace volatile analysis in GC-MS

A. thaliana wild-type and *CYP76C2* mutant plants were tested for volatile emission after pathogen infection with *Pto* DC3000, *Pto* DC3000 *avrRpm1* and *B. cinerea*. Infections were carried out as stated for phenotype assessment.

Plants were infected and 24 hours later the whole plant were subjected to volatile collection during 24 hours. Thus collection of volatiles was performed from 24 to 48 hours of symptoms development, time points at which *CYP76C2* was significantly induced and/or showed transitory phenotypes (previous section).

The experimental unit was composed of 3 plants/jar. Triplicates were made for each treatment (mock and infected) and the experiment was repeated twice with similar results.

The profiles of volatile emission obtained did not showed any differences between mock and infected plants upon *Pto* DC3000, *Pto* DC3000 *avrRpm1* or *B. cinerea* infections, whether in the profile of emitted volatile (presence vs absence) or in the magnitude of their emission.

In Figure 74, 76 and 77, can be seen the TIC (total ion current) scan profiles for each type of infection (only showing one replicate per mutant).

The detection of MeSA in *Pto* DC3000 virulent and avirulent infected plants confirmed the validity of experiment (Attaran *et al.*, 2009). Only MeSA emission after virulent infection is shown (Figure 75).

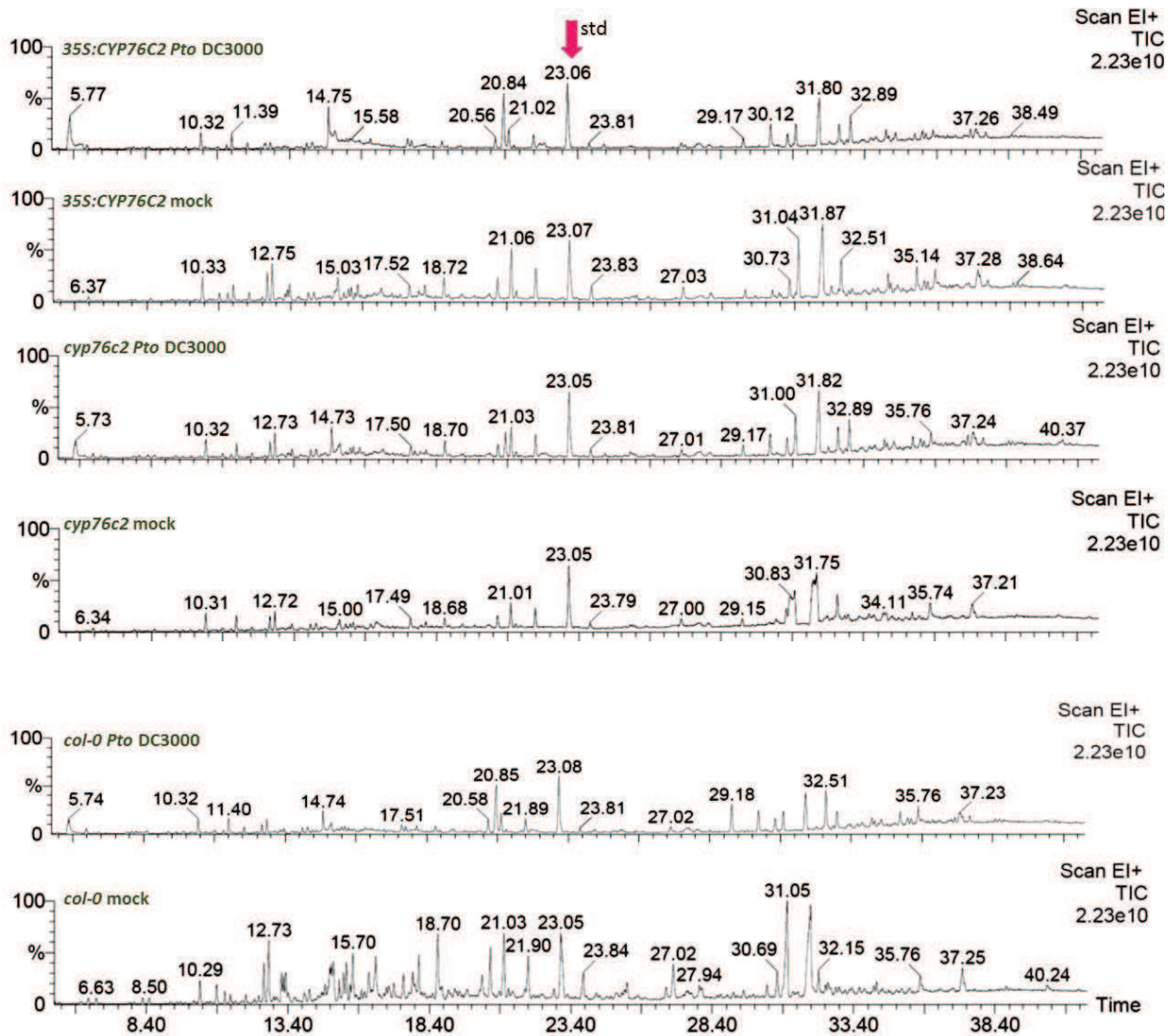


Figure 74: GC-MS chromatograms of the headspace volatiles collected from Col-0, *cyp76c2* and *35S:CYP76C2* plants of *A. thaliana* infected with *Pto* DC3000. The chromatogram shows at RT=23.05 the standard nonyl acetate. Y-axis: relative abundance (%) and x-axis: retention times.

Plants were dipped in a solution containing $MgCl_2$ (mock) or *Pto* DC3000 at a concentration of 5×10^7 CFU/ml and 24 hours later were subjected to volatile collection for 24 hours. The experimental unit was composed of 3 plants/jar. Triplicates were made for each treatment (mock and infected) and the experiment was repeated twice with similar results. Only one replicate per mutant is shown.

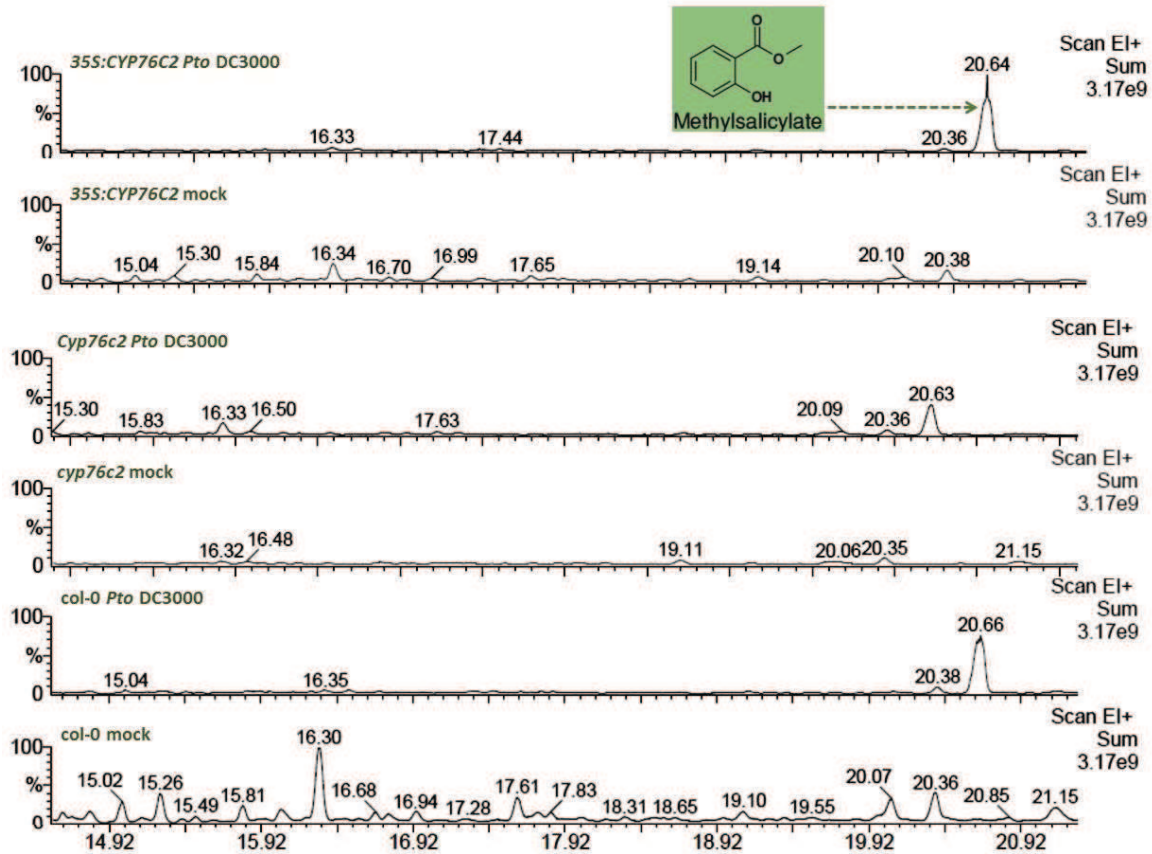


Figure 75: GC-MS chromatograms of the headspace volatiles collected from Col-0, *cyp76c2* and 35S:CYP76C2 plants of *A. thaliana* infected with *Pto* DC3000. The chromatogram shows at RT=20.64-20.66 strong emission of methyl salicylate. Y-axis: relative abundance (%) and x-axis: retention times.

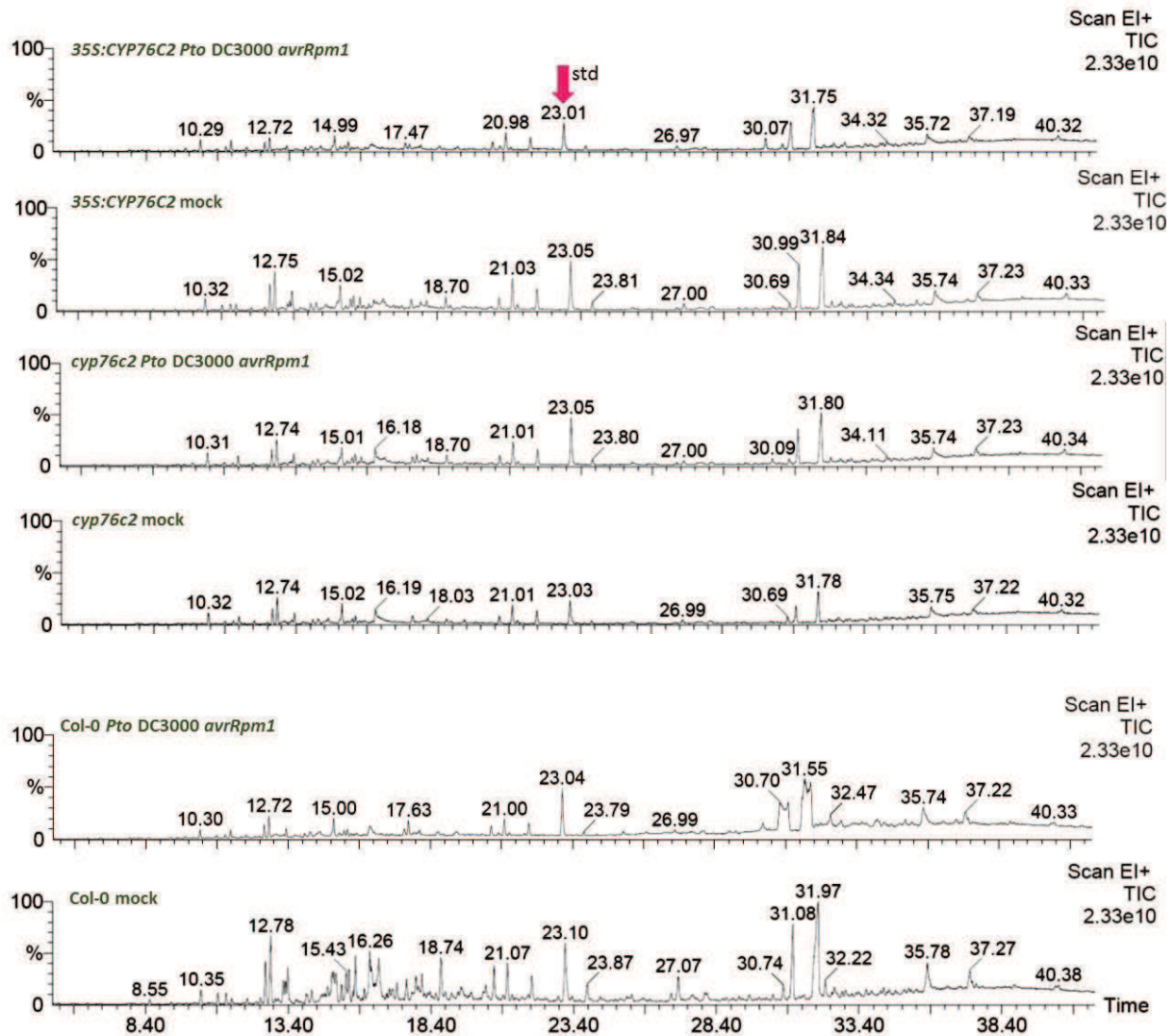


Figure 76: GC-MS chromatograms of the headspace volatiles collected from *Col-0*, *cyp76c2* and *35S:CYP76C2* plants of *A. thaliana* primed with *Pto DC3000 avrRpm1* and dipped with *Pto DC3000*. The chromatogram shows at RT=23.05 the standard nonyl acetate. Y-axis: relative abundance (%) and x-axis: retention times.

Plants were syringe-infiltrated with *Pto DC3000 avrRpm1* (5×10^6 CFU/ml) and 24 hours later dipped in a solution containing $MgCl_2$ (mock) or *Pto DC3000* at a concentration of 5×10^7 CFU/ml. Headspace volatiles were collected 24 hours later and for 24 hours. The experimental unit was composed of 3 plants/jar. Triplicates were made for each treatment (mock and infected) and the experiment was repeated twice with similar results.

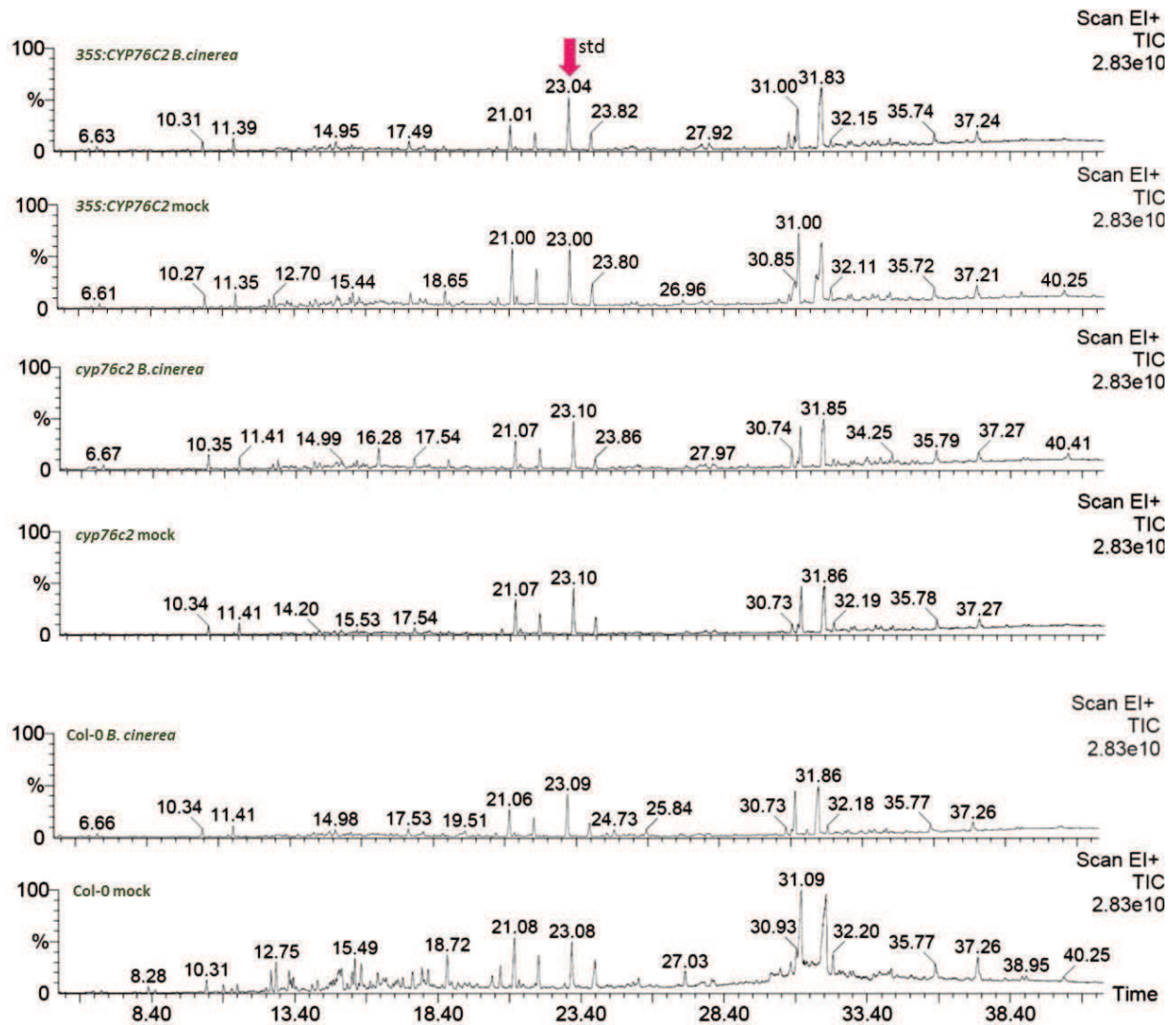


Figure 77: GC-MS chromatograms of the headspace volatiles collected from Col-0, *cyp76c2* and *35S:CYP76C2* plants of *A. thaliana* infected with *B. cinerea*. The chromatogram shows at RT=23.05 the standard nonyl acetate. Y-axis: relative abundance (%) and x-axis: retention times.

Plants were inoculated with a 5 μ L droplet containing 1×10^5 conidia/ml in potato dextrose broth and 24 hours later subjected to volatile collection during 24 hours. The experimental unit was composed of 3 plants/jar. Triplicates were made for each treatment (mock and infected) and the experiment was repeated twice with similar results.

Metabolic Profiling of Soluble Metabolites in UPLC-3Q-MS/MS

Targeted Analysis of Monoterpenoids: UPLC-3Q-MS/MS in MRM Mode

A. thaliana wild-type and *CYP76C2* mutant plants were syringe-infiltrated with *Pto* DC3000 *avrRpm1* at a concentration of 5×10^7 CFU/ml and analyzed 6 and 30 HPI for the accumulation of (soluble) free and conjugated monoterpenoids and derivatives, with main focus on linalool derivatives (See [Table 18](#)).

The experimental unit consisted in a bulk of infected and non-infected leaves coming from 3-5 plants. Triplicates were made for each treatment (mock and infected) and the experiment was repeated twice with similar results and confirmed in UPLC-Orbitrap.

The resulting (targeted) profiles did not showed any difference between mock and infected plants upon *Pto* DC3000 *avrRpm1* infections. Consequently an analysis considering all the compound peaks found from 100-450 m/z was done across mutants and treatments. Results can be found at Figure 78 and 79.

A total of 16 peaks differentially displayed between treatment (mock vs infected) or mutants were selected and analyzed. Figure 78 shows the RT and m/z information of all the 16 peaks selected.

Peaks of m/z **103** (RT 0.68), **166** (RT 1.52-1.56), **201** (RT 19.41-44), **393+433** (RT: 28.53, RT 28.86) were not significantly different between treatments or mutants. Statistical analysis founded significant differences between mock vs infected plants for m/z **130** (RT 1.46-1.56), **132** (RT1.12-1.15), **146** (8.97), **166** (RT 1.52-1.56), **197** (RT 9.72-9.75), **211** (RT 20.97), **277** (RT 4.04), **293** (RT 27.26) for all genotypes.

The m/z **239** (RT 22.54) (compound **9**) was absent in Col-0 and *cyp76c2* infected plants and highly accumulated in *35S:CYP76C2* but the lack of homogeneity among triplicates of this mutant made not possible to be sure about this result.

Moreover, a compound **393+433** m/z eluted at RT: 27.91 min, was significantly different between mock and infected plants of *cyp76c2* and *35S:CYP76C2* lines (named **14**) (interaction mutant x treatment statistically significant). Compound 14 was down-regulated in infected plants of *cyp76c2* and *35S:CYP76C2* infected plants compared to mock treatment, and less accumulated in both infected mutants compared to Col-0. The levels in mock and infected plants of Col-0 plants remained the same.

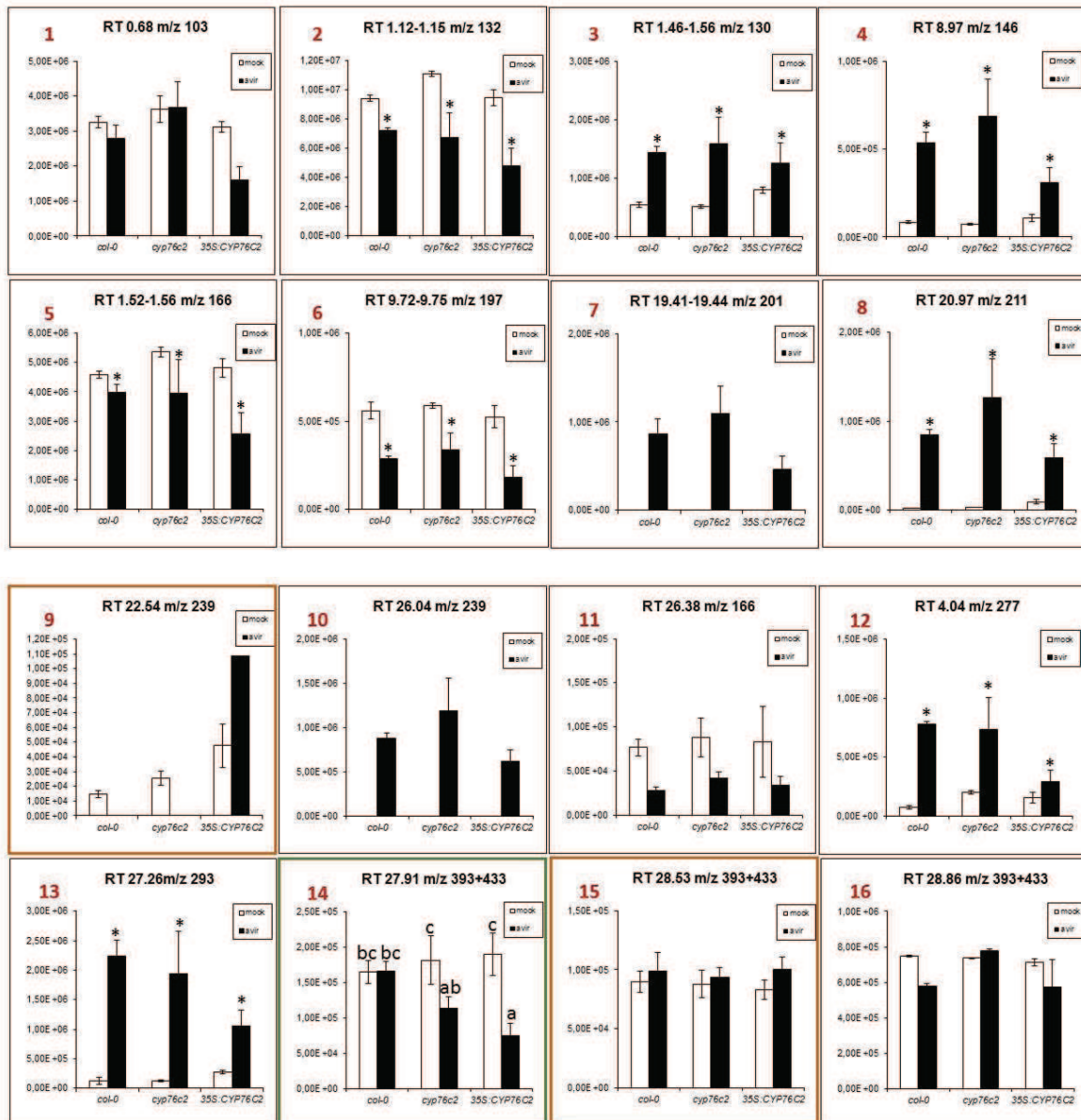


Figure 78: Targeted UPLC-3Q-MS/MS profiling of Col-0, *cyp76c2* and 35S:CYP76C2 plants infected with *Pto* DC3000 *avrRpm1*. A total of 16 peaks were selected for comparison between mock and infected genotypes.

Plants were syringe-infiltrated with a solution containing MgCl_2 (mock) or *Pto* DC3000 *avrRpm1* at a concentration of 5×10^7 CFU/ml. Data represent means of three replicates. Errors bars represent the standard error of the mean. Asterisk and letters shows statistically significant differences calculated by Tuckey's test at a probability level of 5%. In red the number of peak with information of RT and m/z.

Framed in orange peaks **9** and **15** which resulted relevant in CPA (see below Figure 79). **Framed in green** peak **14**, the only which showed positive interaction for the effect genotype x treatment.

In addition, a Principal Component Analysis (PCA) was run (Figure 79). The component 1 (67%) and 2 (24%) (CP1 and CP2 from now on) explained a 92% of observed variation (Table 25).

The bi-plot obtained with CP1 and CP2 grouped the mutants and peaks in three different clusters:

- 1) Group I:** mock treatments of all the three mutants associated to peaks 1, 2, 5, 6, 11, 14, 16.
- 2) Group II:** Col-0 and *cyp76c2* under avirulent infection treatment associated to peaks 3, 4, 7, 8, 10, 12 and 13.
- 3) Group III:** *35S:CYP76C2* infected associated to peaks 9 and 15.

The CP1 and CP3 (73.3%) grouped the mutants by treatment (mock vs infected), and the CP2 and CP3 (30%) did not showed any pattern of relevance (not shown).

Table 25: Principal component analysis summary of eigenvalues and proportion of variance explained.

Component	Eigenvalue	Proportion of variance	Accum. proportion
CP1	10.80	0.67	0.67
CP2	3.85	0.24	0.92
CP3	0.93	0.06	0.97

The CP1 horizontally differentiated between mock and infected plants by grouping mock lines with the peaks that were more accumulated in mock plants, and infected plants with peaks that were more accumulated in infected ones (Figure 78).

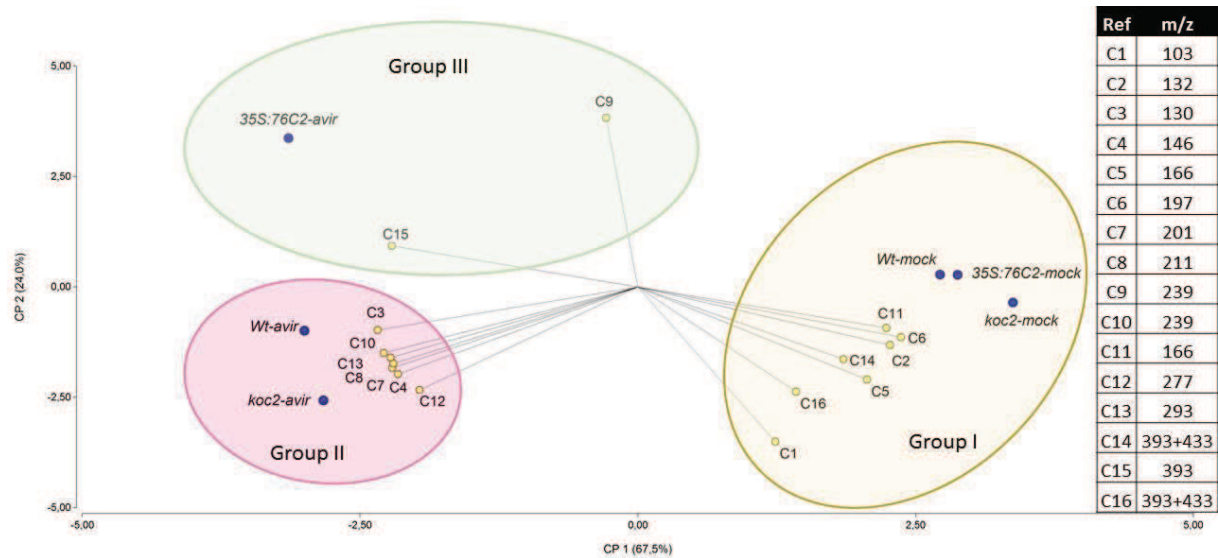


Figure 79: Bi-plot of PCA of the metabolic profiling of Col-0, *cyp76c2* and 35S: *CYP76C2* mock and infected plants with *Pto* DC3000 *avrRpm1*. The bi-plot displays three different clusters based on 16 peaks founds between 100-450 m/z.

Plants were syringe-infiltrated with a solution containing $MgCl_2$ (mock) or *Pto* DC3000 *avrRpm1* at a concentration of 5×10^7 CFU/ml. Data represent means of three replicates. CP1 and CP2 explained 92% of variances. In the right is the information about selected peaks m/z.

The peak **14** which was depicted as the one having relevance in infected *cyp76c2* and 35S:*CYP76C2* plants was grouped with mock plants (Group I) and not with group II or III, probably because the analysis weighted or balanced its value as more relevant for mock treated plants.

In addition, peaks **9** and **15** were the relevant ones for the group III. This result was expected for peak **9** but surprising for peak **15**. At the moment, and after analyzing the information and the model a plausible explanation is lacking for peak **15**, and its contribution for the grouping should be dismissed. In addition, the contribution of peak **9** must be cautiously considered since some inconsistencies among triplicates of 35S:*CYP76C2* infected plants were noticed.

PCA analysis ran without these two peaks showed that groups I and II stayed the same, as expected, but surprisingly let 35S:*CYP76C2* infected plants out of any cluster, *in extenso* I and II (bi-plot can be seen in [appendix](#)).

As a final point, tentative identification by using Massbank or Metlin databases unfortunately did not reach any putative compound or pathway.

Hormone profiling

Profiling of benzoates and derivatives at 24 HPI

A preliminary analysis on hormones at 24 HPI was performed. The initial idea was to set the method and conditions to realize broader analysis later. Surprisingly unexpected and relevant data on DHBA was obtained that prompt us to dig into this data and compounds by UPLC-3Q-MS/MS analysis and UPLC Orbitrap, before continuing with all the time points planned (T0-24-48-72) to complete the hormone profiling (see below).

UPLC-3Q-MS/MS analysis

A profiling of hormones performed at 0 and 24 HPI revealed the differential accumulation of putative benzoates in mutants of *CYP76C2*. This profiling mainly indicated a differential accumulation of 2,5 DHBA in the mock treated and infected plants of *35S:CYP76C2* (Figure 80 and 82). Four peaks were detected by means of MRM analysis in UPLC-3Q-MS, corresponding to putative 2,5 DHBA free or conjugated, hereafter called gentisic acid 1 to 4 (Figure 80 and 81).

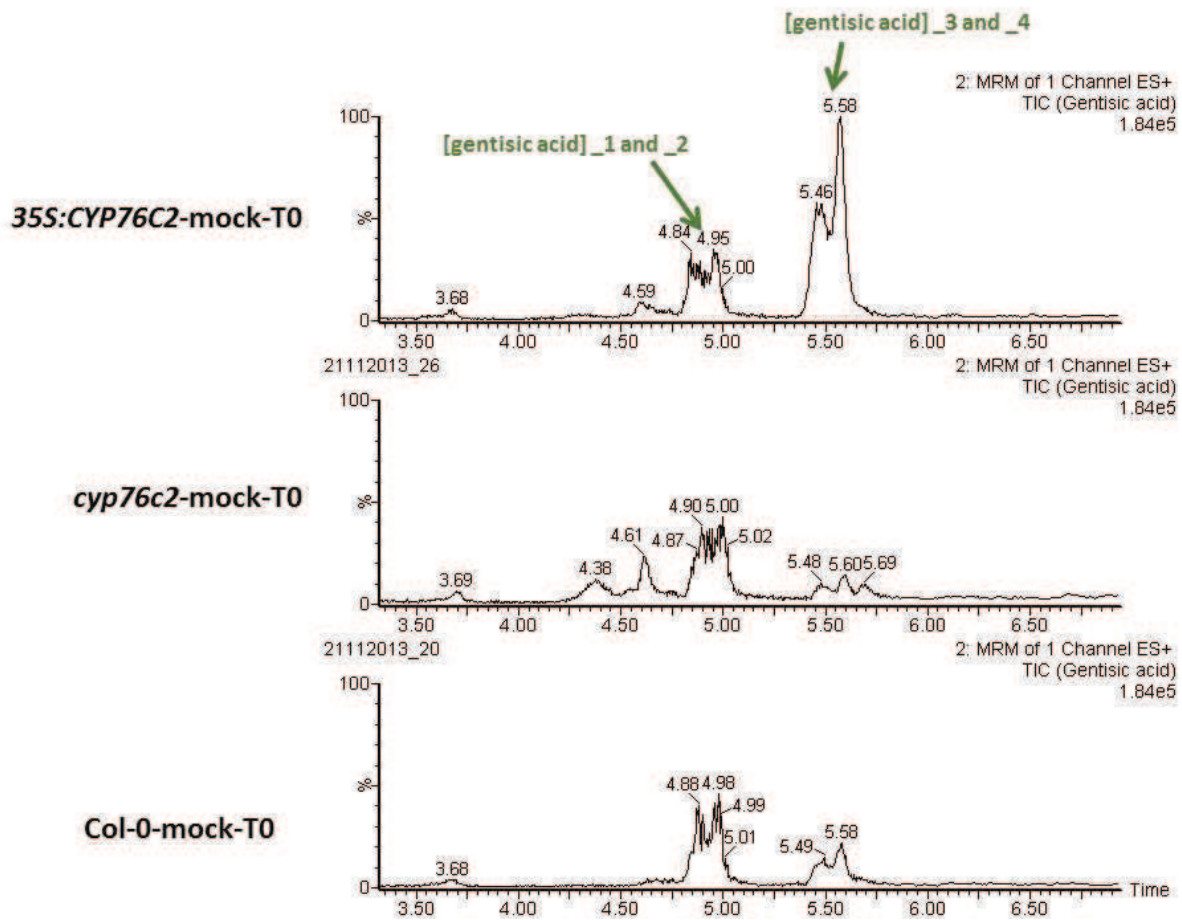


Figure 80: UPLC-3Q-MS/MS chromatograms of methanol extract of col-0, *cyp76c2* and *35S:CYP76C2* mock treated plants at T0. The chromatogram shows the elution of four putative compounds related to 2,5 DHBA (gentisic acid) at 4.84, 4.95, 5.46, 5.58 minutes. Y-axis: relative abundance (%) and x-axis: retention times.

At first, this outcome was unexpected since 2,5 DHBA has been found to accumulate (and conjugated to a xylose) in non-necrotizing and systemic infections unrelated to HR (Bellés *et al.*, 1999; 2006; Fayos *et al.*, 2006) and/or also described as antifungal (Lattanzio *et al.*, 1994, cited in Dean and Delaney, 2008). In a context of avirulent infection and HR, like the one of this experiment, it would be rather anticipated to find 2,3 DHBA and its xylose conjugate instead (Bartsch *et al.*, 2010, Zhang *et al.*, 2013).

Unaware of this possibility and following previously published data, 2,5 DHBA was also used in the mix of internal standards, to relate their signal to SA and 2,3 DHBA identification. This involuntary “mistake” led the experiment to intricate and inconclusive analyses of the putative peaks.

In Figure 81 it can be seen how these peaks were shown to elute after the standard 2,5 DHBA and even after SAG which made challenging the idea of being a pentose/hexose conjugate of the DHBA. Yet still gentisic 3-4 (RT \approx 5.47) showed unequivocal ions related to pentosyl-gentisic acid (m/z 309 and 155) but no gentisic 1 and 2 (RT \approx 4.72). Gentisic 1 and 2 showed same elution time and fragments in ESI+ that the standard but when results were analyzed in ESI- identification was less evident (see **red box** in Figure 81).

The most interesting peaks, gentisic acid 3 and 4 (Figure 81 and 82), were unknown compounds detected with the same MS/MS transition 154.8>137 as 2,5 DHBA.

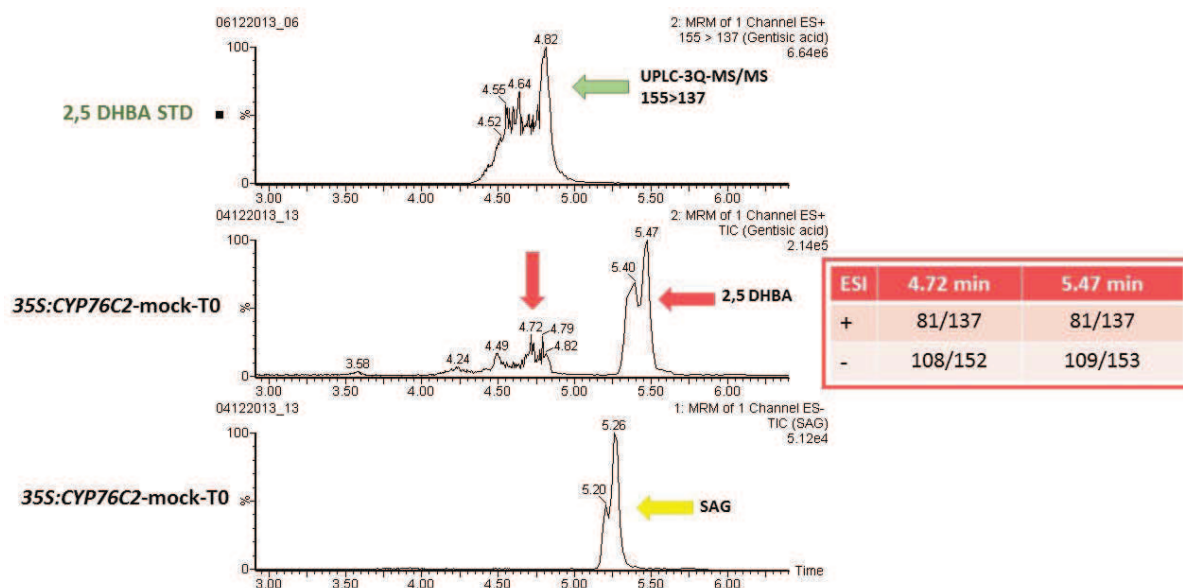


Figure 81: UPLC-3Q-MS/MS chromatograms of 2,5 DHBA standard and methanol extract of 35S:CYP76C2 mock treated plants at T0. Y-axis: relative abundance (%) and x-axis: retention times.

The chromatogram shows the elution of standard of 2,5 DHBA at 4.8 min (similar to gentisic 1 and 2). The putative gentisic 3 and 4 (RT= 5.40 and 5.47) are eluting later than the standard and SAG. In the box are presented daughter ion results in ESI positive and negative mode.

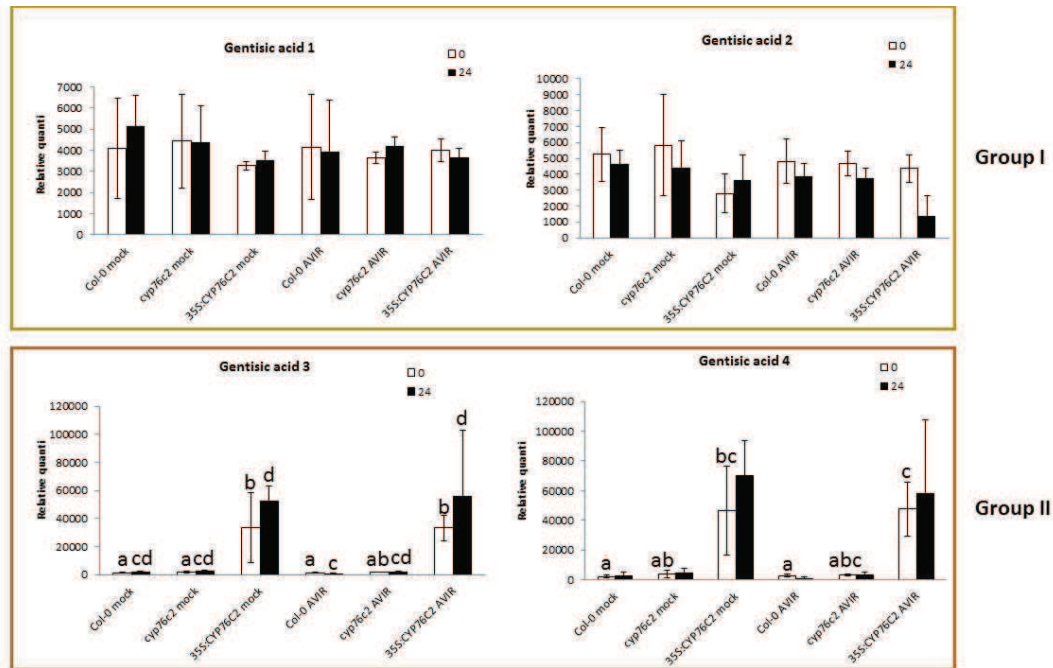


Figure 82: Pattern of accumulation of four potential compounds related to 2,5 DHBA in Col-0, *cyp76c2* and *35S:CYP76C2* lines at T0 and T24 HPI.

Plants were syringe-infiltrated with a solution containing $MgCl_2$ (mock) or *Pto* DC3000 *avrRpm1* at a concentration of 5×10^7 CFU/ml. Data are means of three replicates. Errors bars represent the standard error of the mean. Different letters represent statistical differences calculated by Kruskal-Wallis ($p < 0.05$). **Group I** and **II** depicted in the chart correspond to the groups obtained in the bi-plot of PCA (Figure 84, below).

Additionally, it was observed the presence of SA and putative SAG, ABA, JA-Ile and the clearance forms JA-Ile-OH and JA-Ile-COOH, TA and TAG. Putative OPDA accumulation was no informative. JA information was mislaid owing to technical reasons (Figure 83).

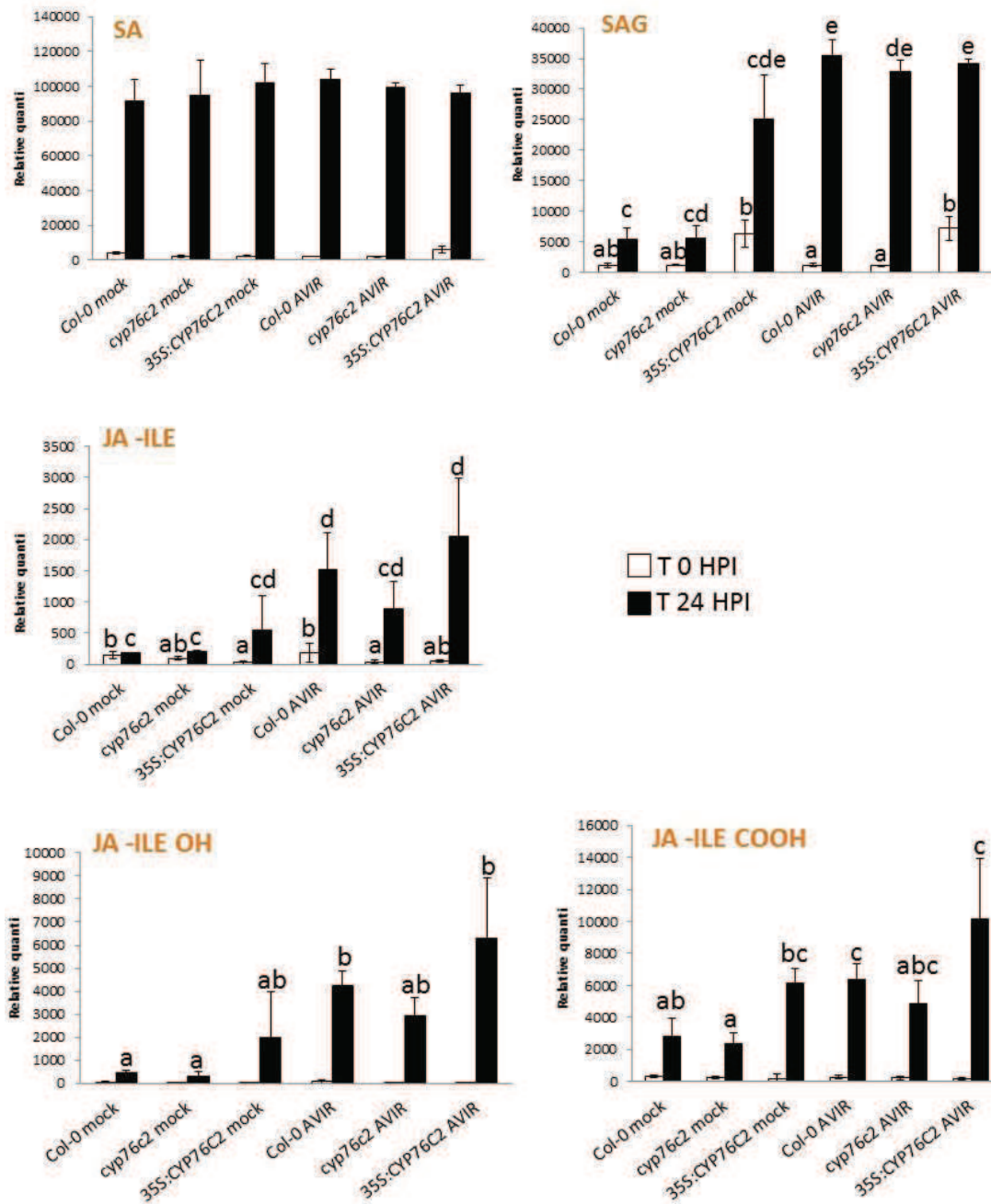


Figure 83: Hormone profiling of SA, SAG, JA-Ile, JA-Ile-OH, JA-Ile-COOH in Col-0, *cyp76c2* and *35S:CYP76C2* mock and infected plants at T0 and T24 HPI.

Plants were syringe-infiltrated with a solution containing $MgCl_2$ (mock) or *Pto* DC3000 *avrRpm1* at a concentration of 5×10^7 CFU/ml. Data are means of three replicates. Error bars represent the standard error of the mean. Different letter represent statistical differences calculated by Kruskal-Wallis ($p < 0.05$). These hormones were grouped in III and IV in the PCA (see below Figure 84).

In addition to the differential accumulation of gentisic 3 and 4 (Figure 82), the overexpressor mutant also showed increased SAG basal levels at T0 (Figure 83). A tendency to higher accumulation of JAs related compounds after infection was also observed in this mutant and was later confirmed in following experiences (Figure 90 and 91).

In the PCA, CP1 and CP2 explained 87% of observed variation (Table 26). The bi-plot obtained at 24 HPI grouped the mutants and peaks in four different clusters (Figure 84):

- 1) **Group I:** mock treated plants of Col-0 and *cyp76c2* associated to gentisic 1 and 2.
- 2) **Group II:** mock treated plants of *35S:CYP76C2* associated to gentisic 3 and 4.
- 3) **Group III:** Col-0 and *35S:CYP76C2* infected plants associated to JAs, ABA and SAG. This cluster showed some overlap with cluster **IV**.
- 4) **Group IV:** Col-0 and *cyp76c2* infected plants in closely association with SA accumulation, but also in proximity to TA, SAG, ABA, JA-Ile and JA-Ile-OH overlapping Group **III**.

Group **III** and **IV** revealed the closest association of *35S:CYP76C2* to JA-Ile and the clearance forms, mostly JA-Ile-COOH (see experiment below Figure 90) and also TAG (TAG results also confirmed later Figure 91). On the contrary Col-0 and *cyp76c2* infected plants were grouped in closer proximity to SA and TA (also confirmed below in Figure 88 and 91).

Table 26: Principal component analysis summary of eigenvalues and proportion of variance explained.

Component	Eigenvalues	Proportion of variance	Accum. proportion
CP1	8.64	0.72	0.72
CP2	1.86	0.15	0.87
CP3	1.31	0.11	0.98

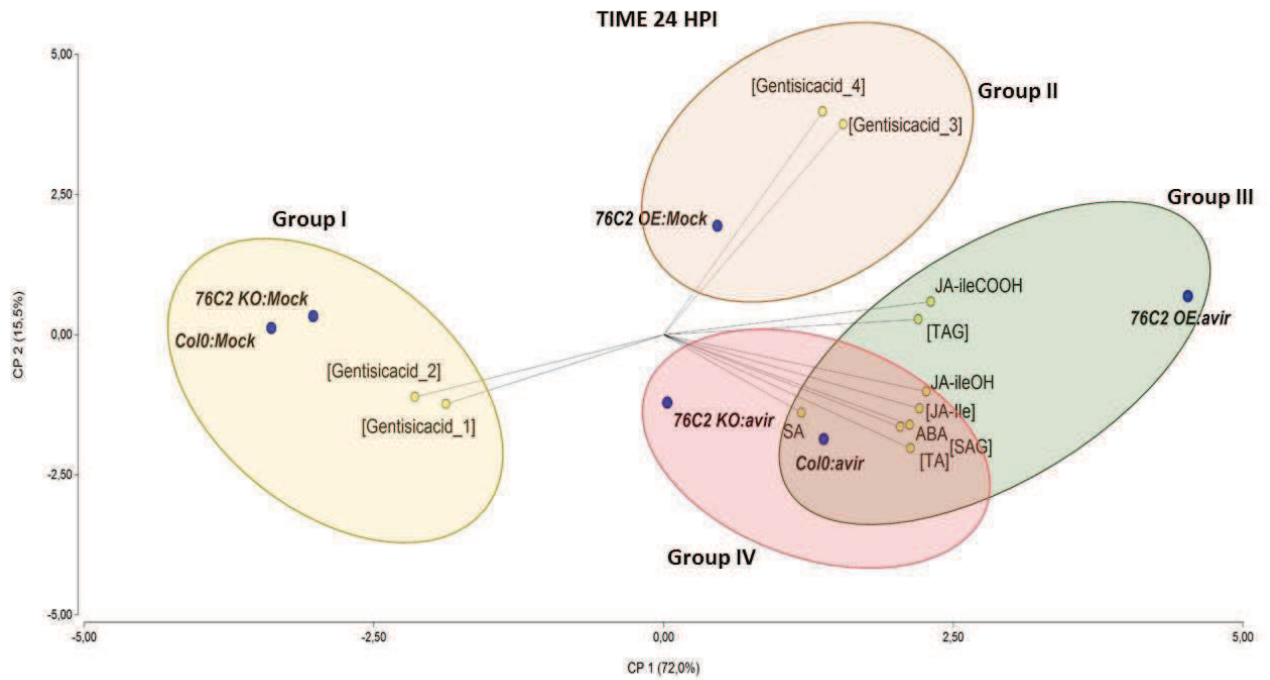


Figure 84: Bi-plot of PCA of the hormone profiling of Col-0, *cyp76c2* and *35S:CYP76C2* mock and infected plants with *Pto* DC3000 *avrRpm1* at 24 HPI. The bi-plot displays four different clusters.

UPLC-ORBITRAP-MS/MS analysis

In parallel, more analyses were carried out using UPLC-Orbitrap-MS with new samples containing no standard related to the 2,5 DHBA. SA derivatives, with special emphasis in DHBA and its glycosylated forms were analyzed. Results can be seen in Figures 85 and 86.

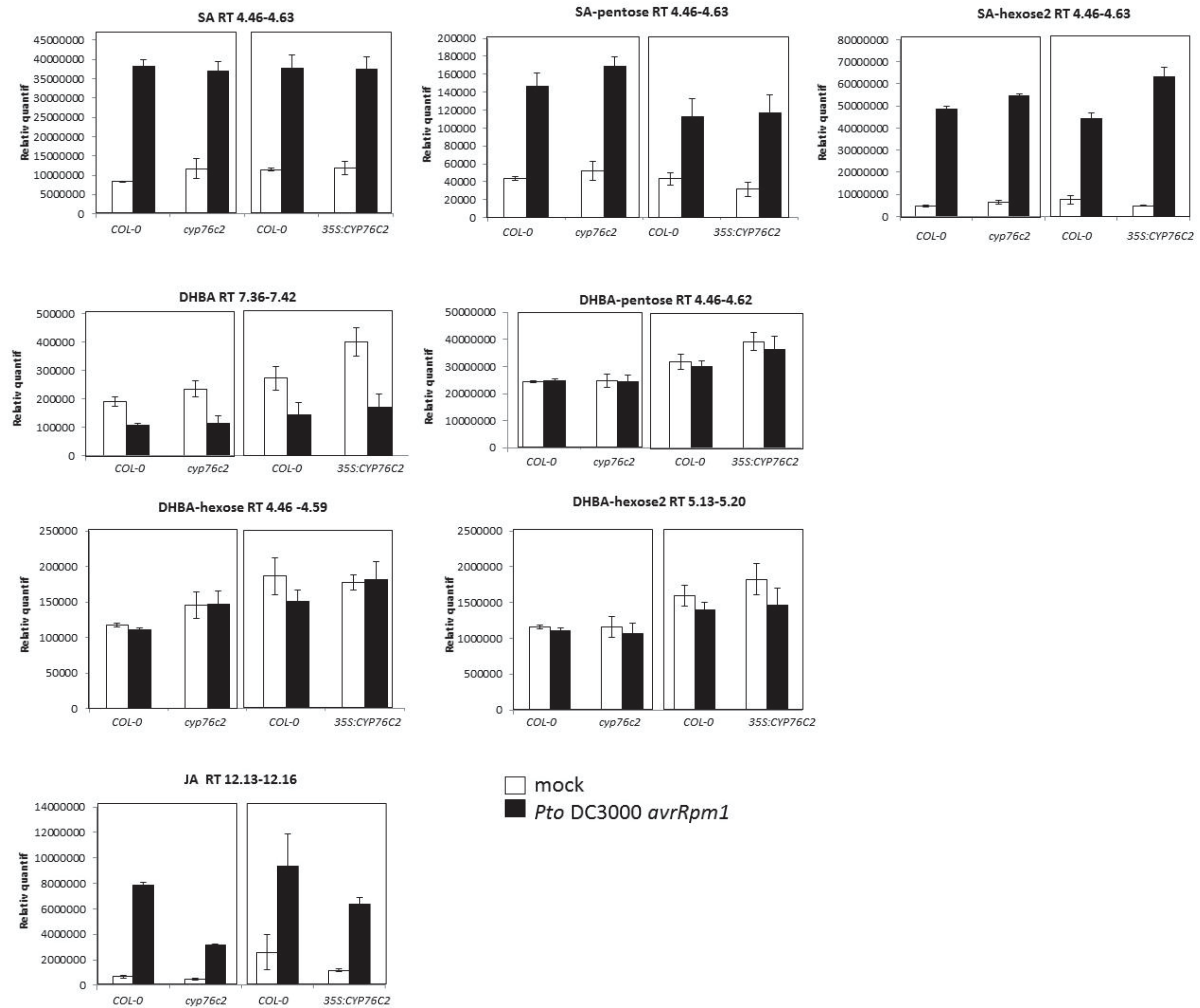


Figure 85: Quantification of compounds potentially related to 2,5 DHBA and conjugated forms via UPLC-Orbitrap-MS analysis in Col-0, *cyp76c2* and *35S:CYP76C2* at T0 and T24 HPI.

Plants were syringe-infiltrated with a solution containing $MgCl_2$ (mock) or *Pto DC3000 avrRpm1* at a concentration of 5×10^7 CFU/ml. Data represent means of three replicates. Errors bars represent the standard error of the mean. Experiment design in this case corresponded to a design in paired block in which the wild type was paired to each mutant by rack, as a way to get information on the variability existing. This matched pairs design is a special case of a randomized block design that was exceptionally used in this experiment.

The pattern of SA accumulation were similar to those observed before in this section and below (Figure 83 and 88), constant level for all genotypes at 24 HPI, which validates the experience. Two putative glycosylated forms: SA-pentose and SA-hexose were found, none of them showing disparity in their accumulation after 24 HPI.

DHBA and conjugated forms were also found, but again information obtained was entangled and puzzling. Several putative peaks related to DHBA conjugated to pentose (DHBA-PENT2 and 3) and hexoses (DHBA-HEX3) at different elution times were discarded for inconsistencies.

In the PCA, PC1 and PC2 explained 92% of the observed variation (Table 27).

Table 27: Principal component analysis summary of eigenvalues and proportion of variance explained.

Component	Eigen value	Proportion of variance	Accum. proportion
CP1	4.93	0.62	0.62
CP2	2.40	0.30	0.92
CP3	0.51	0.06	98

The CP1 categorically differentiated mock from infected plants, while PC2 was associated to relative abundance values. The bi-plot obtained allowed the clustering of mutants and treatments into three groups (Figure 86):

- 1) **Group I:** mock treated plants of *35S:CYP76C2* associated to putative DHBA, and closely located to a DHBA-Hexose (dashed circle).
- 2) **Group II:** Col-0 and *cyp76c2* infected plants associated to SA-pentose.
- 3) **Group III:** Col-0 and *35S:CYP76C2* infected plants associated to JA, SA and their putative conjugated forms SA-pentose and SA-hexose.

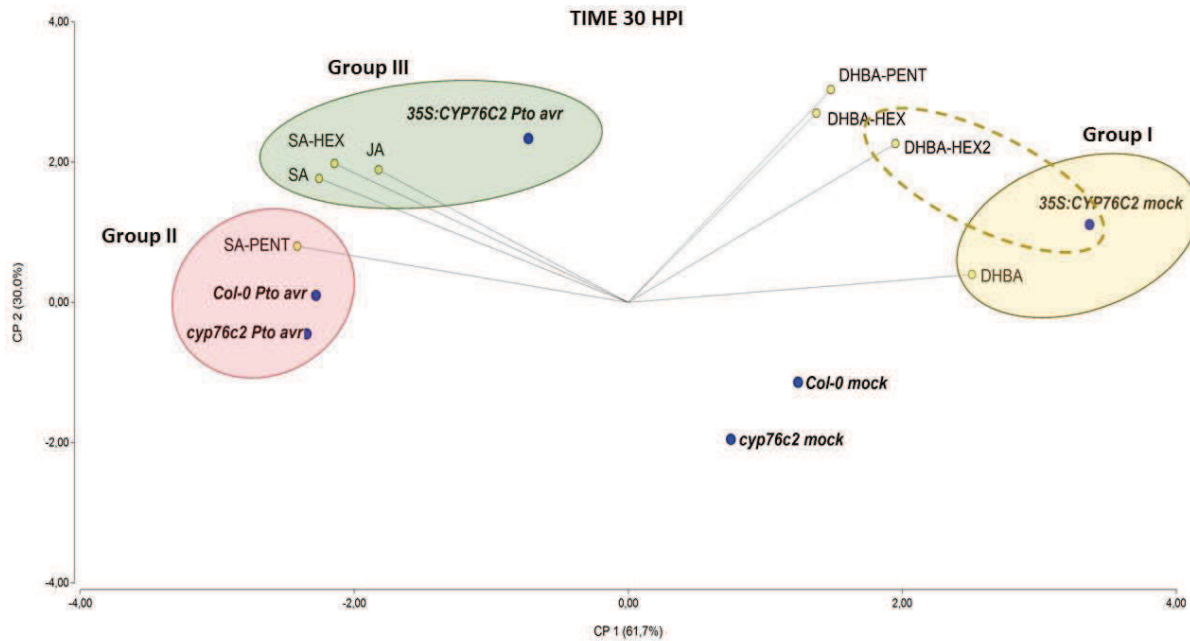


Figure 86: Bi-plot of PCA of the hormone profiling of Col-0, *cyp76c2* and *35S:CYP76C2* mock and infected plants with *Pto* DC3000 *avrRpm1* at 24 HPI. The bi-plot displays three different clusters.

The results obtained from the bi-plot support again a relation between the mock treated plants of *35S:CYP76C2* and DHBA (was before associated to putative gentisic 3 and 4, Figure 84). The mock-treated overexpressor cluster locates near to DHBA-pentose and hexose, by comparison to the other two genotypes, which was also informative. Col-0 and *cyp76c2* mock-treated plants did not grouped in any cluster (before was gentisic 1 and 2, Figure 84).

Furthermore, infected plants of *35S:CYP76C2* clustered again with JA (as in Figure 84) and additionally with SA and SA-hexose. At first this could seem contradictory to what it was shown in figure 84, in which the clustering indicate that SA was closely located to *cyp76c2* or/and Col-0. The proximity of SA to **Group II** in this clustering (here Figure 86) still suggest a proximity.

Additionally in this bi-plot was observed how Col-0 and *cyp76c2* infected plants were clustered with SA-pentose. This information is still surprising. Later analysis in a broader timeline will rather show a marked association of this two genotypes to SAG or SGE at 48 and 72 HPI (putative analysis, Figure 88). Moreover, β -xylosidase analysis would not show any aglycone (Figure 101).

What it was still undefined at this point was the “identity” of the putative DHBA. Is it hydroxylated in the position 2,3 or 2,5 of the ring? What is the kind of glycoside conjugate it has? As it was mentioned before expected candidates would be 2,3 DHBA conjugated to a xylose (DHAB-PENT outside of the cluster but still in proximity to mock *35S:CYP76C2*) or a 2,5 DHBA conjugated to a glucose in uninfected leaves (Bellés *et al.*, 1999, Bartsch *et al.*, 2010; Zhang *et al.*, 2013) (DHBA-HEX also outside of the cluster but in proximity to mock *35S:CYP76C2*).

This “exploratory” experiments so far seems to suggest an association of the *35S:CYP76C2* to at least some glycosylated and clearance forms of SA and JA respectively, likewise the association to DHBA that seems to be predominant in mock treated plants.

In order to address these questions new and wider hormone analysis and incubations *in vitro* were performed with relevant benzoic compounds. Moreover β -glycosidase and β -xylosidase hydrolysis were carried out.

Hormone Profiling: kinetics of accumulation in a timeline from 0 to 72 HPI

A. thaliana wild-type and *CYP76C2* mutant plants were syringe-infiltrated with MgCl_2 10mM (mock) or *Pto* DC3000 *avrRpm1* at a concentration of 5×10^7 CFU/ml and analyzed at 0, 24, 48 and 72 HPI. The experimental unit consisted in a pool of infected leaves collected from 3-5 plants. For each time point and treatment (mock vs infected) triplicates were collected. One-way ANOVA on ranks Kruskal-Wallis was performed ($p < 0.05$) (Table 28).

Figure 88 shows the profile of benzoic compounds obtained (BA, SA, SAG and SGE). BA levels in mock-treated plants of the three genotypes and in *35S:CYP76C2* infected plants were low at all the time points. Col-0 and *cyp76c2* showed an increment from 48-72 HPI that did not reach statistical significance but that still was informative.

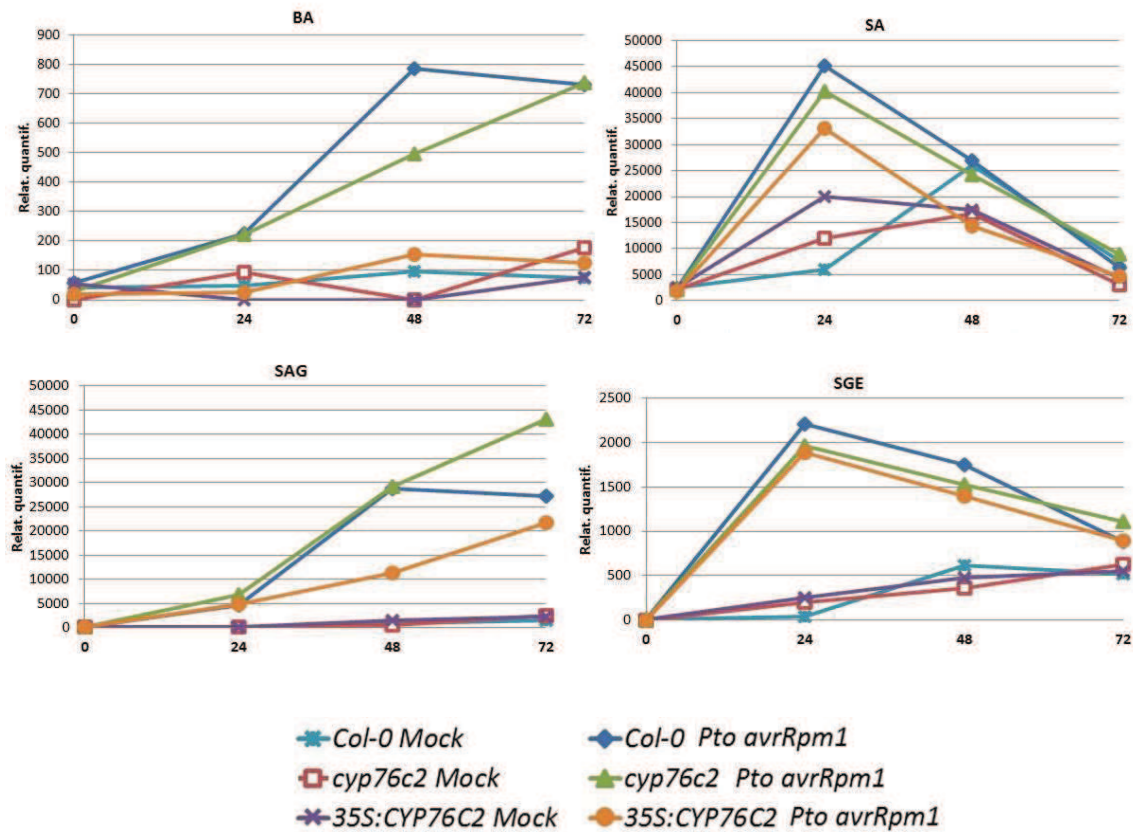


Figure 87: Hormone profiling of BA, SA, SAG and SGE upon *Pto* DC3000 *avrRpm1* infection.

Plants were syringe-infiltrated with a solution containing MgCl_2 (mock) or *Pto* DC3000 *avrRpm1* at a concentration of 5×10^7 CFU/ml. Data represent means of three replicates. Errors bars and statistically significant differences calculated by Kruskal- Wallis ($p < 0.05$) are not displayed here but can be seen in [appendix](#) and Table 28 below.

Col-0 infected plants showed high levels of SA accumulation at 24 HPI validating the experience. SA levels of 35S:CYP76C2 were lower than Col-0 and *cyp76c2* through all time points in infected plants. This could be linked to data presented in Figure 67 and 71 where 35S:CYP76C2 showed less HR and accumulated transiently (24-48 HPI) higher bacterial titer than Col-0 and *cyp76c2*. Differences between mock vs infected plant for col and *cyp76c2* were statistically relevant at 24 HPI. The *cyp76c2* SA levels were differentially accumulated in infected plants at 24 HPI and 72 HPI.

Overall levels of SA decreased after 24 HPI, from 48 to 72 HPI, when it can be metabolized into several storage forms before reaching cellular toxic levels (Table 4) (Dean Delaney, 2008; Wildermuth, 2006; Vlot *et al.*, 2009; Bartsch *et al.*, 2010; Zhang *et al.*, 2013).

The glycosylated forms of SA, SAG and SGE (putative identification) (Figure 88), showed opposite patterns of accumulation and contrasting relative amounts. SAG was highly accumulated by comparison to SGE (\approx 15 times less), and increased over the time course in infected plants. SAG accumulation was significant (statistically different from mock) in Col-0 and *cyp76c2* infected plants at 24, 48, and 72 HPI, but lower (and statistically not different from mock) in *35S:CYP76C2* infected plants.

The kinetic of accumulation observed for SAG seems to be in agreement with results obtained in SA: SAG levels increased from 48 to 72 HPI while SA decreased after 24 HPI. On the other hand SGE levels decreased from 24 HPI and, as showed in SAG, Col-0 and *cyp76c2* infected plants showed significant accumulation after being challenged with the avirulent pathogen while *35S:CYP76C2* showed a tendency but it was not significant. The mutants did not showed altered levels of SGE in comparison to Col-0.

Furthermore DHBA compounds were analyzed (Figure 89). Accurated methods and standards were used in this experiment, with the aim of clarifying all the remaining questions from previous experiments (previous section). Once again, it was hypothesized that 2,3 and 2,5 DHBA would show a pattern of induction or repression since they have been associated to pathogen responses and senescence (another scenario of cell death) (Bellés *et al.*, 2006; Bartsch *et al.*, 2010, Zhang *et al.*, 2013).

Surprisingly, as shown in Figure 89, no differences between mock and inoculated plants was observed for any of the analyzed lines at any time point. The levels of accumulated 2,3 DHBA were very low and the levels of 2,5 DHBA remained constant through all the time points. Additionally, two other hydroxylated forms of SA: 2,4 DHBA (β -resorcylic acid) and 3,4 DHBA (protocatechuic acid from green tea), were analyzed although no information on this compounds is available for *Arabidopsis* or diseased plants. 2,4 DHBA was significantly accumulated while 3,4 DHBA was not. Furthermore 2,4 DHBA reached higher levels in Col-0 infected plants at 72 HPI while in the mutants remained the same in mock and infected plants.

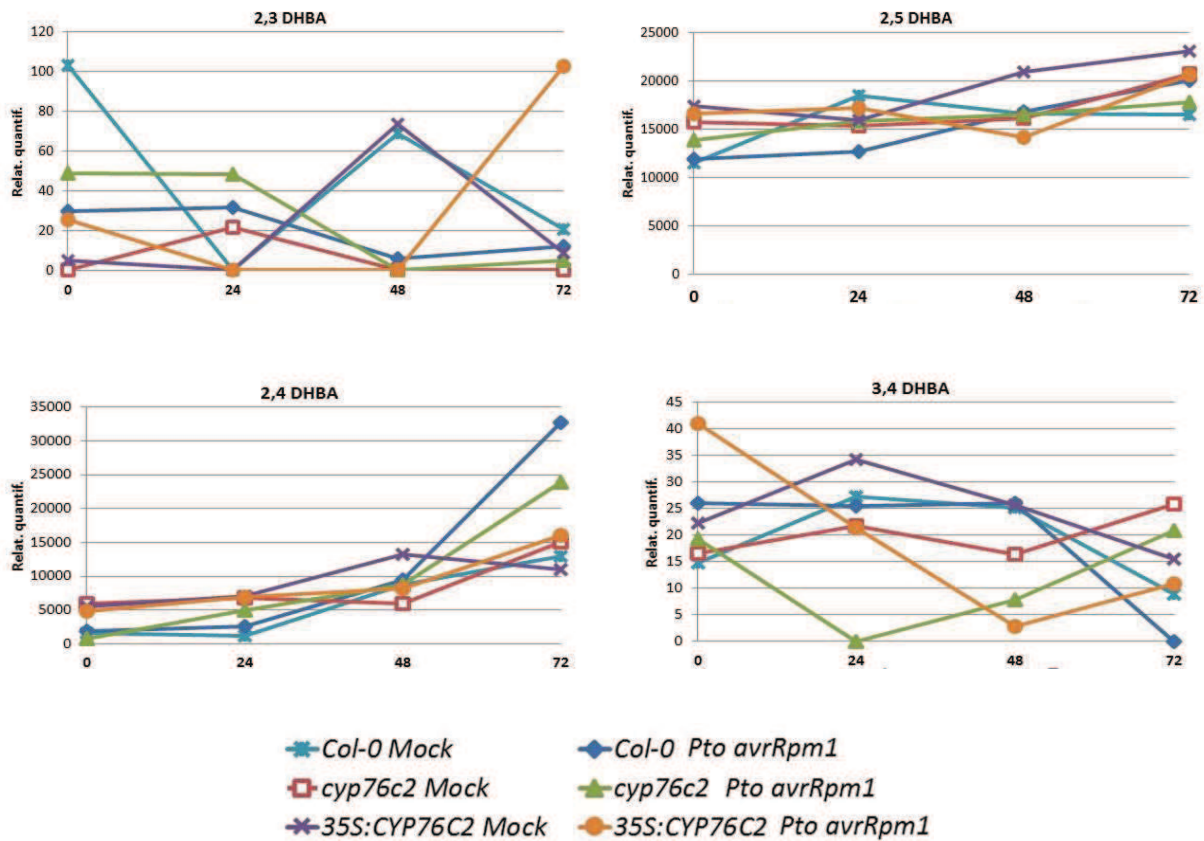


Figure 88: Hormone profiling of 2,3 , 2,5, 2,4 and 3,4 DHBA upon *Pto* DC3000 *avrRpm1* infection.

Plants were syringe-infiltrated with a solution containing MgCl_2 (mock) or *Pto* DC3000 *avrRpm1* at a concentration of 5×10^7 CFU/ml. Data represent means of three replicates. Errors bars and statistically significant differences calculated by Kruskal- Wallis ($p < 0.05$) are not displayed here but can be seen in [appendix](#) and Table 28 below.

The profile of JAs and its precursor OPDA can be seen in Figure 90 .The overexpression mutant consistently showed to be more associated to JA metabolism than to SA (as in Figure 84, 86). Even though this trend never reached statistical significance, it correlated well with SA/JA crosstalk.

OPDA levels showed the same trend (higher in 35S:CYP76C2) and were higher after infection, but the differences among lines did not reach statistical significance. Conversely, differences between mock and infected plants were always significant (exceptions: not significant for mutant lines at 24 HPI and not significant *cyp76c2* at 72 HPI). Notably, OPDA relative concentration values were higher than those of JA metabolites and maximum at 48 HPI.

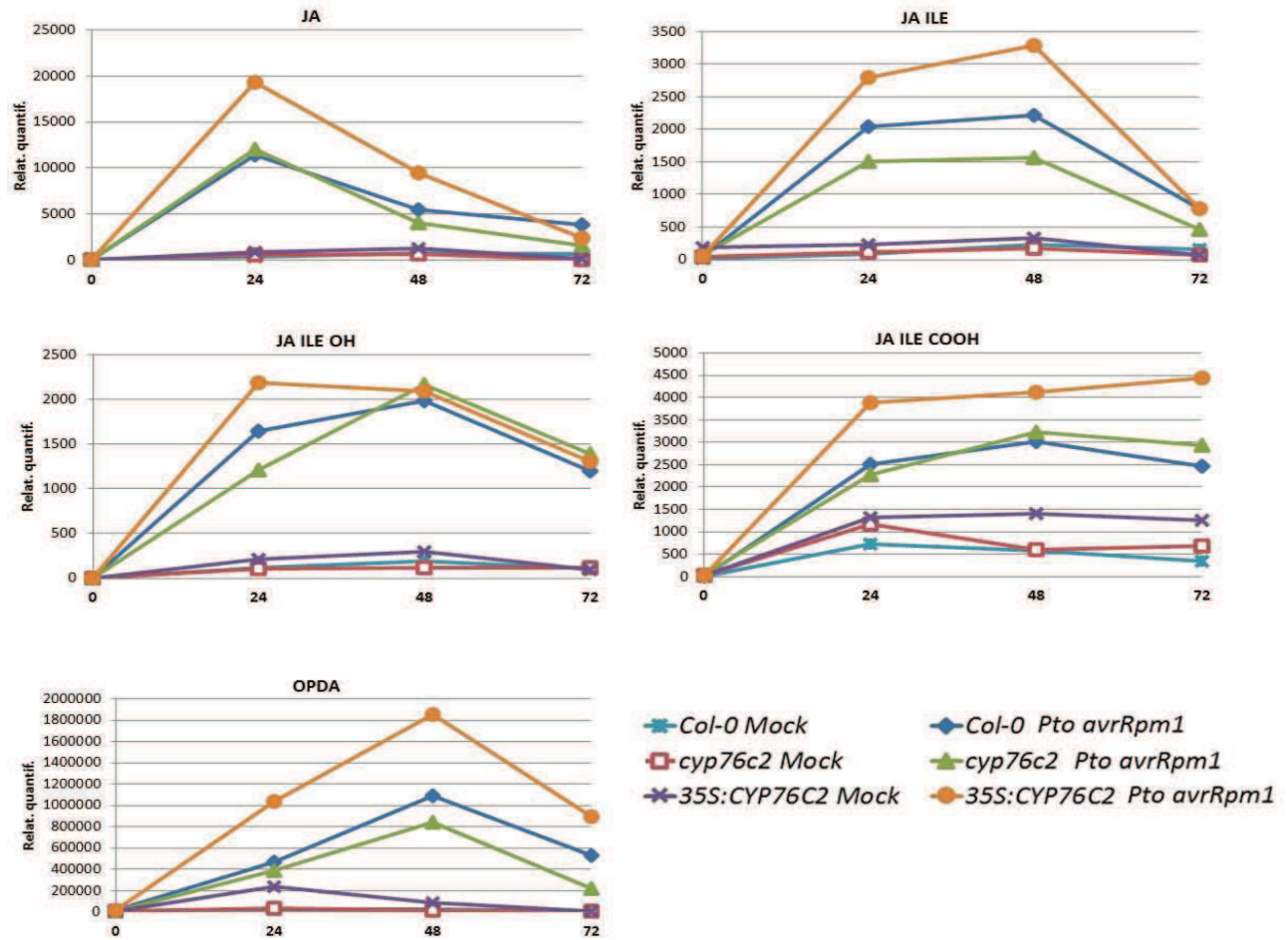


Figure 89: Hormone profiling of JAs upon *Pto* DC3000 *avrRpm1* infection.

Plants were syringe-infiltrated with a solution containing MgCl_2 (mock) or *Pto* DC3000 *avrRpm1* at a concentration of 5×10^7 CFU/ml. Data represent means of three replicates. Errors bars and statistically significant differences calculated by Kruskal- Wallis ($p < 0.05$) are not displayed here, but can be seen in [appendix](#) and Table 28 below.

Col-0 and 35S:CYP76C2 infected plants accumulated significantly higher levels of JA than mock infected plants from 24 to 72 HPI (a slightly different accumulation between mock Col-0 and 35S:CYP76C2 was observed at T0). The same trend was observed for *cyp76c2* infected plants. The overexpression mutant showed the tendency of major accumulation of JA (and several precursors and derivatives, see below) but was not statistically different from Col-0 or *cyp76c2* infected plants. This was for instance the case for JA-Ile, the biologically active form of JA. Its accumulation levels were higher at 24-48 HPI and decreased at 72 HPI.

The “clearance” forms of JA-Ile: JA-Ile-OH and JA-Ile-COOH, were also more relevant in *35S:CYP76C2* mutant (Figure 90). The accumulation of JA-Ile-COOH doubled JA-Ile-OH. In most of cases mock and infected plant for each mutants were significantly different, yet still no statistical difference within treatment and among mutants was found.

The accumulation of TA and its clearance forms can be seen in Figure 91. TA was high in comparison to the other JA metabolites, showing an 18000-fold increase upon infection vs 3000-fold in some other JAs. Overexpression mutant mock -treated plants were different from infected plants at 24-48 HPI and overall levels of TA accumulation for this mutant was higher than the two other lines. Surprisingly, at T0 infected plant of knock-out line showed higher levels of initial TA by comparison to Col-0. Across the following time-points *cyp76c2* mock and infected plants were significantly different. The glycosylated form of TA (TAG) instead was detected in very low amounts and little informative, it was only differentially accumulated between mock and infected plants in both mutants at 72 HPI (140-fold). Conversely, 12-OH-JA-sulfate, another clearance form of TA, was highly accumulated in *35S:CYP76C2* infected plants. Mock and infected plants of Col-0 and overexpression mutant were significantly different at each time course, but *cyp76c2* plants were not. In the knock-out mutant the levels of 12-OH-JA-Sulfate were similar (not statistically relevant) between mock vs infected plants.

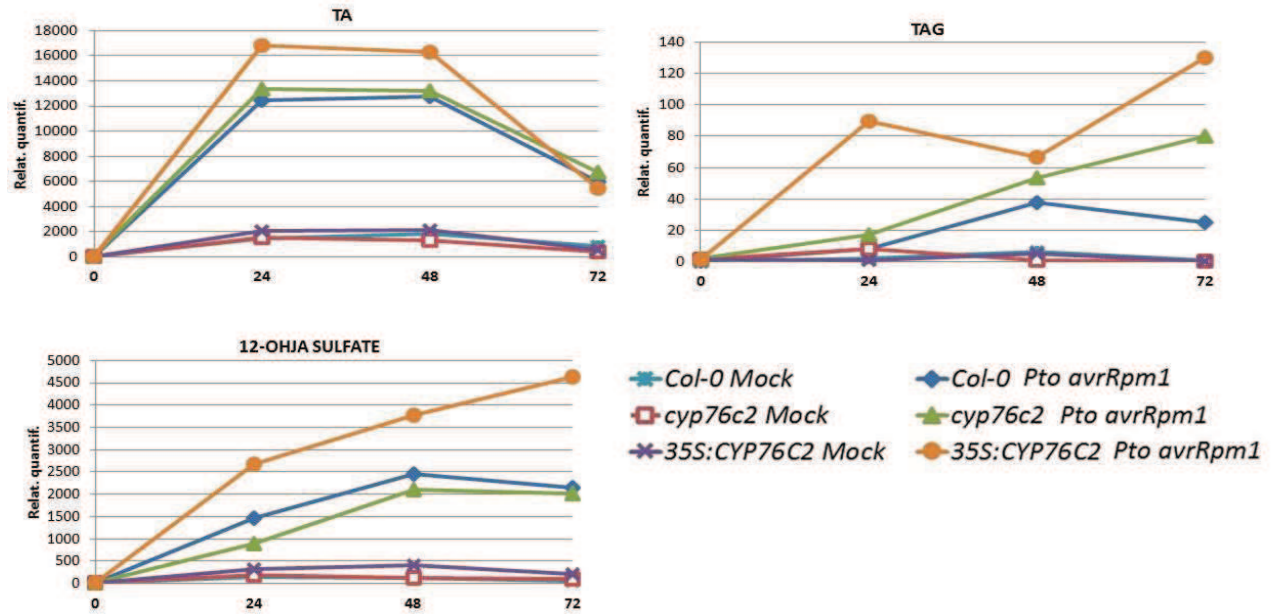


Figure 90: Hormone profiling of TA and its sulfated and glycosylated forms upon *Pto* DC3000 *avrRpm1* infection.

Plants were syringe-infiltrated with a solution containing $MgCl_2$ (mock) or *Pto* DC3000 *avrRpm1* at a concentration of 5×10^7 CFU/ml. Data represent means of three replicates. Errors bars and statistically significant differences calculated by Kruskal- Wallis ($p < 0.05$) are not displayed here but can be seen in [appendix](#) and Table 28 below.

Finally, ABA concentration values increased in infected plants but were significantly different between infected and mock-treated plants only for Col-0 and *cyp76c2*, but not for 35S:CYP76C2. ABA level were not significantly different among mutants in this experiment (Figure 92).

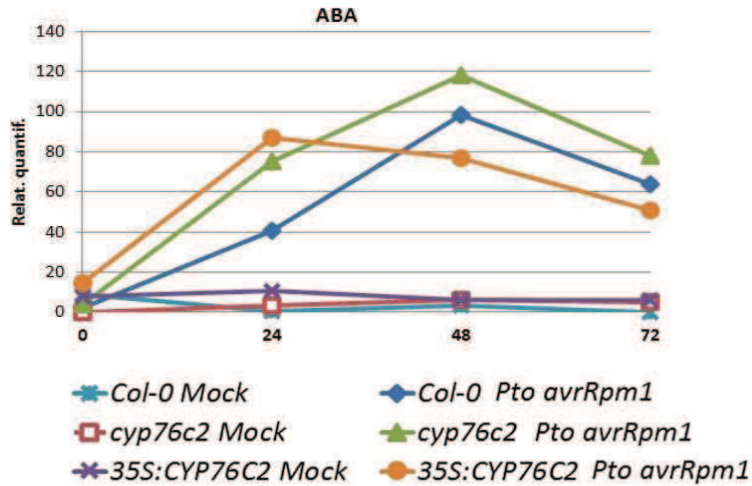


Figure 91: Profiling of ABA upon *Pto* DC3000 *avrRpm1* infection.

Plants were syringe-infiltrated with a solution containing MgCl_2 (mock) or *Pto* DC3000 *avrRpm1* at a concentration of 5×10^7 CFU/ml. Data represent means of three replicates. Errors bars and statistically significant differences calculated by Kruskal- Wallis ($p < 0.05$) are not displayed here but can be seen in [appendix](#) and Table 28 below.

Two compounds of relevance: Camalexin and Linalool accumulation in a timeline

Own to the relevance of this two molecules for this studio, they were included in the analyses.

Camalexin was highly accumulated in this experiment (Figure 93). Surprisingly *cyp76c2* infected plants showed highest accumulation among the tested lines. This difference did not reach statistical significance but was markedly different from mock inoculated plants all across the time line analyzed from time 0 to 72 HPI. This was in part unforeseen for an avirulent infection. On the other hand, it can be connected to the different behavior of *CYP76C2* by comparison to LAR zone, (for instance transcriptomic data showed *CYP76C2* highly co-expressed with *PAD3* at 6 HPI in LAR responses).

To close, Linalool and hydroxylated forms 1 and 2 were not relevant (Figure 94).

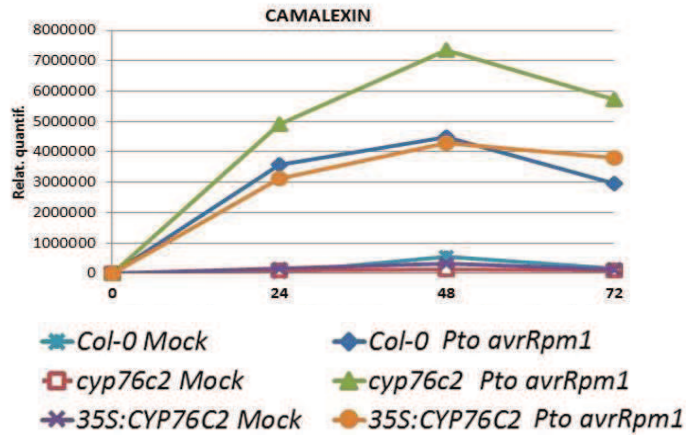


Figure 92: Profiling of camalexin upon *Pto* DC3000 *avrRpm1* infection.

Plants were syringe-infiltrated with a solution containing MgCl_2 (mock) or *Pto* DC3000 *avrRpm1* at a concentration of 5×10^7 CFU/ml. Data represent means of three replicates. Errors bars and statistically significant differences calculated by Kruskal- Wallis ($p < 0.05$) are not displayed here but can be seen in [appendix](#) and Table 28 below.

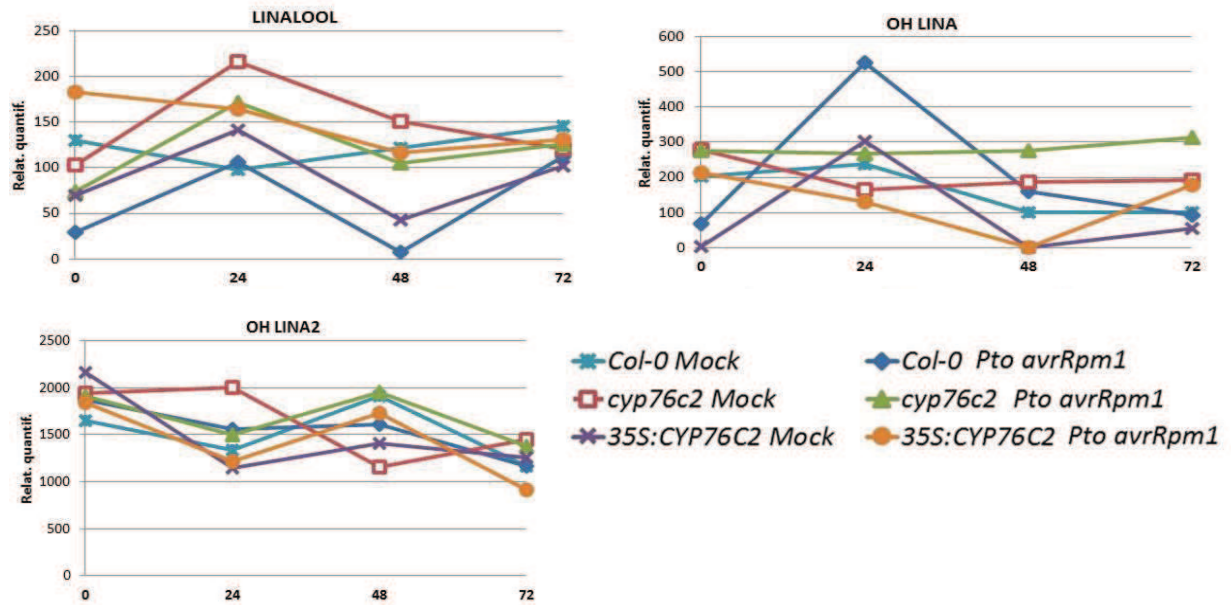


Figure 93: Profiling of Linalool and hydroxylated derivatives.

Plants were syringe-infiltrated with a solution containing MgCl_2 (mock) or *Pto* DC3000 *avrRpm1* at a concentration of 5×10^7 CFU/ml. Data represent means of three replicates. Errors bars and statistically significant differences calculated by Kruskal- Wallis ($p < 0.05$) are not displayed here but can be seen in [appendix](#) and Table 28 below.

Table 28: Kruskal Wallis test for mean comparison (p<0.05).

Genotype	HPI	Treat	BA	2,3 DHBA	2,5 DHBA	2,4 DHBA	3,4 DHBA	SA	[SAG]	[SGE]	JA	JA-Ile	JA-Ile-OH	JA-Ile-COOH	12-OHJA sulf	OPDA	TA	[TAG]	ABA	Camalex	Linalool	8OH-linal_1	8OH-linal_2
COL-0 <i>cyp76c2</i> 35S:CYP76C2	0	mock	-	-	-	-	-	c	abc	-	abc	-	-	-	-	-	ab	abc	-	-	a	-	-
COL-0 <i>cyp76c2</i> 35S:CYP76C2	0	avir	-	-	-	-	-	abc	ab	-	ab	-	-	-	-	-	a	bc	-	-	abc	-	-
COL-0 <i>cyp76c2</i> 35S:CYP76C2	24	mock	-	-	ab	-	-	a	ab	a	a	a	a	a	a	a	a	ab	-	a	a	-	-
COL-0 <i>cyp76c2</i> 35S:CYP76C2	24	avir	-	-	abc	-	-	c	bc	c	bc	bc	bc	bc	bc	bc	bc	abc	-	ab	bc	-	-
COL-0 <i>cyp76c2</i> 35S:CYP76C2	48	mock	-	-	a	-	-	c	a	abc	a	a	ab	a	a	ab	ab	ab	-	a	ab	-	-
COL-0 <i>cyp76c2</i> 35S:CYP76C2	48	avir	-	-	ab	-	-	c	b	d	bc	bc	bc	b	cd	cd	bcd	bcd	-	b	bc	-	-
COL-0 <i>cyp76c2</i> 35S:CYP76C2	72	mock	-	-	a	-	-	bc	a	a	abc	ab	a	a	a	a	abc	a	a	a	abc	-	-
COL-0 <i>cyp76c2</i> 35S:CYP76C2	72	avir	-	-	b	-	-	abc	bc	bc	d	bc	b	bc	bc	bc	c	ab	bc	bcd	-	-	

 Differences among mutants within treatment bc ≠ a
 Difference mock vs infected within mutant

Statistically significant differences in color. Violent for differences between mock vs infected plants within mutant. Others color for differences between mutants within treatment. Charts with errors bars and letters representing the statistical significance are presented in [appendix](#).

In order to complement the obtained information, a PCA analysis at each time point including all the analyzed hormones and camalexin was ran. In table 29 information about eigenvalues and proportion of variance explained, are presented. In figure 95, 96, 97 and 98 bi-plots are displayed for each time point. CP1 and CP2 resulted to be the most informative components for this analysis (variation explained up to 80%). CP1 allowed the discrimination of mock from infected plants. CP2 allowed the clustering between hormones and treated mutants and also the location according to relative concentration values.

Table 29: Principal component analysis summary of eigenvalues and proportion of variance explained.

T0	PC	Eigenvalue	Proportion Var.	Accum. proportion
	1	6.52	0.36	0.36
	2	4.87	0.27	0.63
	3	3.12	0.17	0.81
T24	PC	Eigenvalue	Proportion Var.	Accum. proportion
	1	11.89	0.66	0.66
	2	3.68	0.2	0.86
	3	1.24	0.07	0.93
T48	PC	Eigenvalue	Proportion Var.	Accum. proportion
	1	12.35	0.69	0.69
	2	2.85	0.16	0.84
	3	1.77	0.1	0.94
T72	PC	Eigenvalue	Proportion Var.	Accum. proportion
	1	11.49	0.64	0.64
	2	3.24	0.18	0.82
	3	1.7	0.09	0.91

At T0, no pattern of grouping was observed, which also explained the low percentage of variance explained by the components (63% see table 29) (Figure 95).

At time 24 HPI (Figure 96) three main groups were obtained by the combination of “hormones” (yellow vectors) and “mutant x treatment” (blue dots) factors.

1- **Group I:** constituted by the three mock-treated lines showing no-association to any vector and located in the opposite field of the bi-plot. This cluster will remain the same all across the time course.

2- **Group II:** comprising infected plants of Col-0 and *cyp76c2* plants, located in close association to SA and its glycosylated forms. Camalexin was also clustered in this group, since it was more accumulated in knock-out mutant and wild-type infected plants.

3- **Group III:** comprising only 35S: *CYP76C2* infected plants in proximity to JAs and ABA (which will switch at later time points)

In addition, BA and the different DHBA did not grouped with any cluster, since they were mostly not informative in this context at any time point (BA showed some tendency in relation to *35S:CYP76C2* infected plants that was very low) .

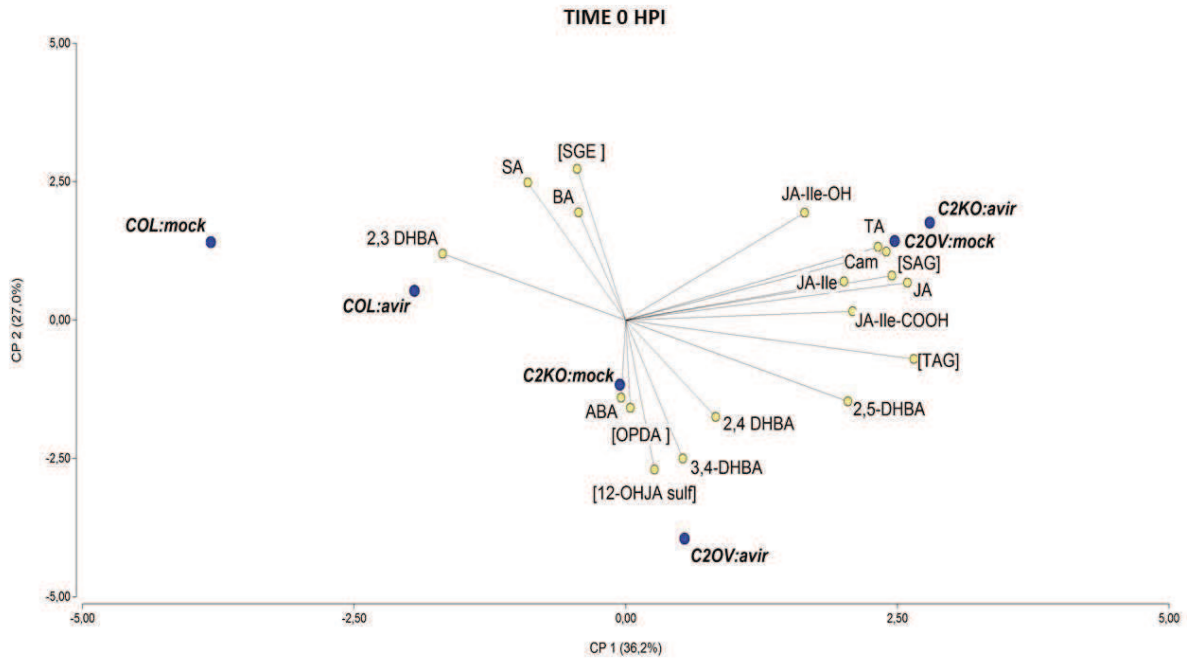


Figure 94: Bi-plot of PCA of the hormone profiling of Col-0, *cyp76c2* and *35S:CYP76C2* mock and infected plants with *Pto* DC3000 *avrRpm1* at the moment of infection at T0.

Plants were syringe-infiltrated with a solution containing $MgCl_2$ (mock) or *Pto* DC3000 *avrRpm1* at a concentration of 5×10^7 CFU/ml. Data represent means of three replicates. CP1 and CP2 explained 63% of observed variances.

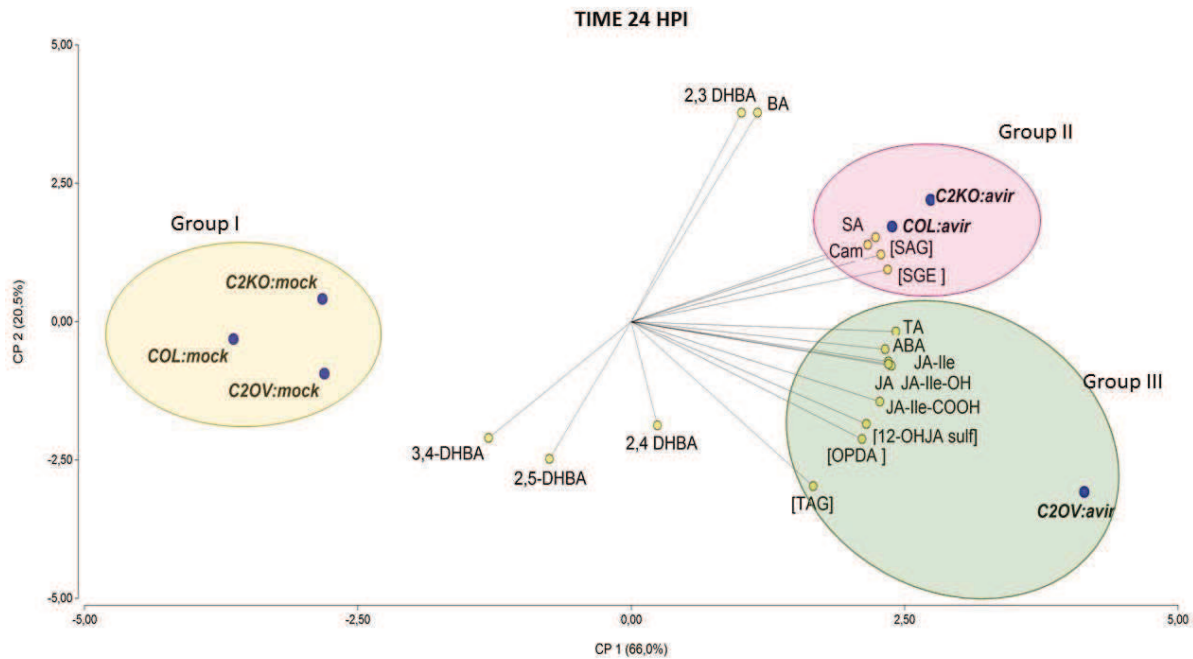


Figure 95: Bi-plot of PCA of the hormone profiling of Col-0, *cyp76c2* and *35S:CYP76C2* mock and infected plants with *Pto* DC3000 *avrRpm1* at 24 HPI.

Plants were syringe-infiltrated with a solution containing $MgCl_2$ (mock) or *Pto* DC3000 *avrRpm1* at a concentration of 5×10^7 CFU/ml. Data represent means of three replicates. CP1 and CP2 explained 86% of observed variances. The bi-plot displays three different clusters, highlighted in different colors.

At 48 HPI (Figure 97) the clustering of infected plants is less defined in its limits but still shows the same trend as that observed at 24 HPI with some minor changes. For instance some overlap between group II and III at JA-Ile-OH is observed (same concentration for all infected mutants). In addition, BA (no-significant effects) appears highly associated to group II and SA (the levels of which starts to decrease) appears out of the cluster grouped outside with the different DHBA, not associated to any mutants x treatment entry. Interestingly, ABA switched from Group II to Group III in close association to camalexin and SGE.

Finally, at 72 HPI (Figure 98) the clustering pattern remains the same with some changes in the patterns of JAs grouping. JA-Ile remained off the clusters. JA, JA-Ile-OH and TA were closely located to the group II (switched position). The location of groups II and III switched upside down own to a rise in concentration mostly owned to OPDA and 12-OH-JA-sulfate.

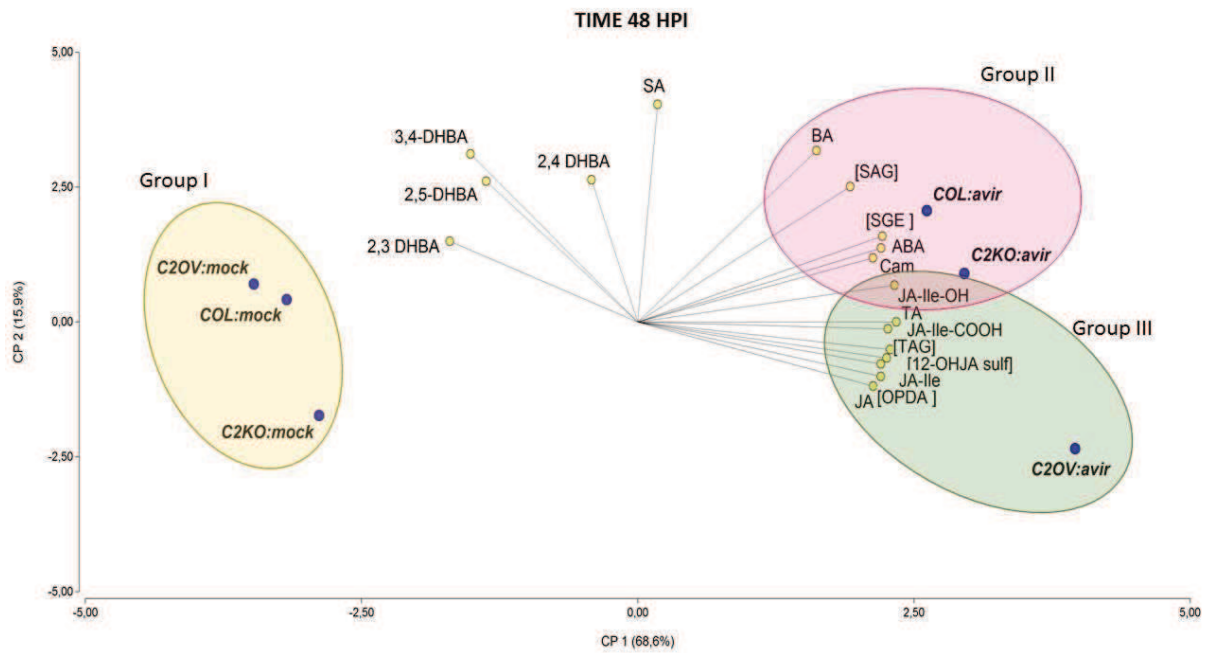


Figure 96: Bi-plot of PCA of the hormone profiling of Col-0, *cyp76c2* and *35S:CYP76C2* mock and infected plants with *Pto* DC3000 *avrRpm1* at 48 HPI.

Plants were syringe-infiltrated with a solution containing $MgCl_2$ (mock) or *Pto* DC3000 *avrRpm1* at a concentration of 5×10^7 CFU/ml. Data represent means of three replicates. CP1 and CP2 explained 84% of observed variances. The bi-plot displays three different clusters, highlighted in different colors.

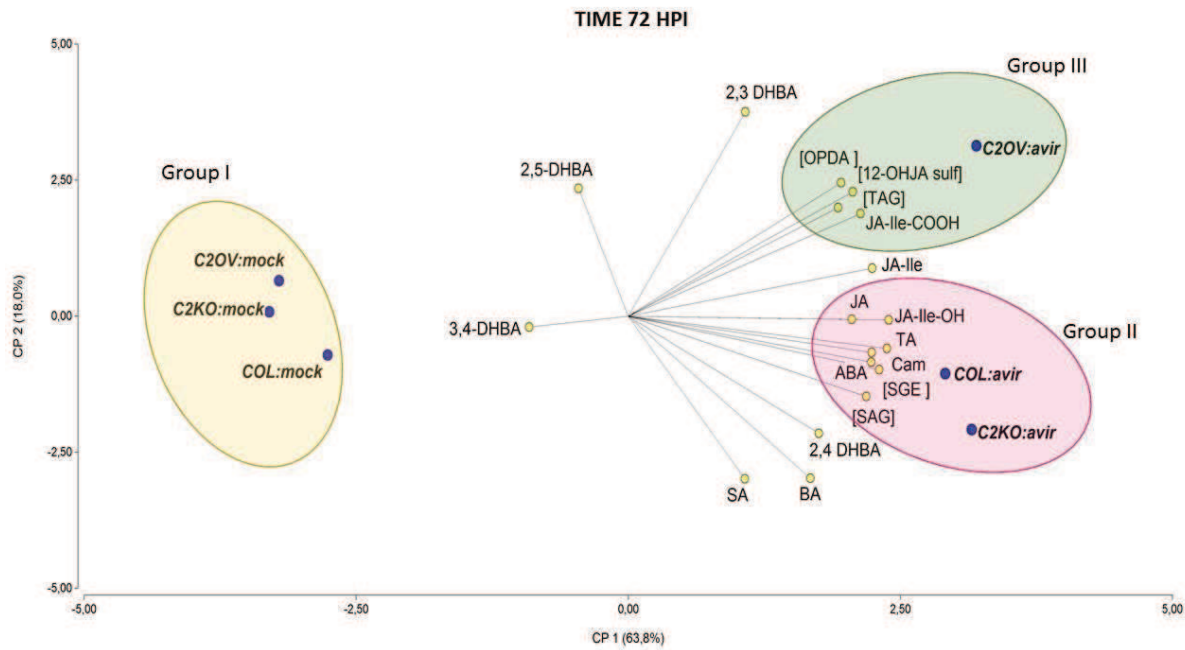


Figure 97: Bi-plot of PCA of the hormone profiling of Col-0, *cyp76c2* and *35S:CYP76C2* mock and infected plants with *Pto* DC3000 *avrRpm1* at 72 HPI.

Plants were syringe-infiltrated with a solution containing $MgCl_2$ (mock) or *Pto* DC3000 *avrRpm1* at a concentration of 5×10^7 CFU/ml. Data represent means of three replicates. CP1 and CP2 explained 82% of observed variances. The bi-plot displays three different clusters, highlighted in different colors.

Conclusions on hormone profiling and camalexin accumulation in a time line

The PCA thus helped clarifying the existing relationship between hormone profiles and genotypes through the different time points. Tendencies and grouping appeared more evident to the naked eye and the obtained groups displayed coherence.

The presented data on hormone profiling suggest a trend to prevalent accumulation of SA and its conjugated forms in the *cyp76c2* and an opposite behavior in the *35S:CYP76C2* line. This seems to be in agreement with symptoms phenotyping, in which it was observed that *35S:CYP76C2* had less important HR. Indeed SA is a key regulator of PCD. In addition, is not surprising the lack of statistical significance especially in JAs profiling since it was observed in several experiences that *CYP76C2* effects are mostly subtle or transitory.

Another important outcome of this profiling is camalexin. The *cyp76c2* mutant line not only showed significant accumulation of SA metabolites but also displayed a marked increase in camalexin accumulation upon infection. Nevertheless camalexin effect in avirulent interaction has been related more to antioxidant properties than defense (Simon *et al.*, 2010; Glazebrook and Ausubel, 1994). Overall, the profiling data are consistent with phenotyping and support a subtle role of *CYP76C2* in the defense process.

β -glycosidase/ β -xylosidase treatments

In order to elucidate the structure of DHBAs and sugar conjugates present in the samples corresponding to the avirulent infected plants of wild type and *35S:CYP76C2* line, an MRM method was developed and enzymatic hydrolysis of the samples were carried out (Figure 99).

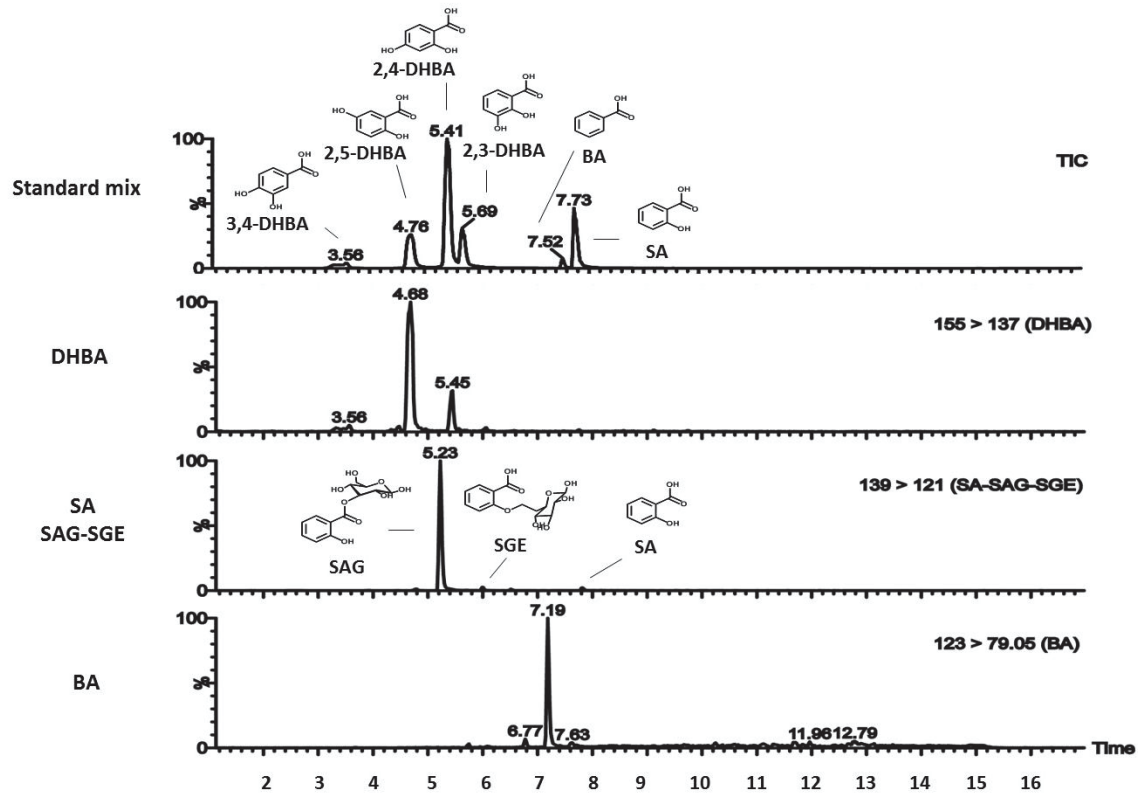


Figure 98: MRM methods in UHPL-3QP-MS/MS for BA, DHBA compounds (2,3, 2,5, 2,4, 3,4 DHBA) and SA, SAG, SGE. Information on transition ions is shown at each chromatogram. Courtesy of Dr. Boachon.

In Figure 100 A and B can be seen the analysis ran for BA.

The β -glycosidase treatment only released a small aglycone peak (named 1) which was slightly higher in *35S:CYP76C2*. In this profile, peak 2 might include the conjugated BA since a small decrease in its size was observed after the treatment. β -xylosidase treatment resulted in very similar profiles.

What was interesting to observe was the behavior of peak 3. Peak 3 was not present in Col-0 infected plants and only appeared after β -xylosidase treatment. Conversely, on *35S:CYP76C2* samples, this peak

was present in treated and non-treated extracts and showed a small decrease after the β -xylosidase treatment. This peak still remain unidentified but probably does not correspond to BA.

In the experiment of hormone profiling, the relative abundance of BA in the *35S:CYP76C2* infected line was lower than compared to Col-0 and *cyp76c2* infected plants (Figure 88) reaching values as low as in the mock treated plants.

Putting all this information together, it seems to suggest that BA in *35S:CYP76C2* was mainly conjugated and a recurrent link existing between this mutant line and conjugated/glycosylated forms in HR.

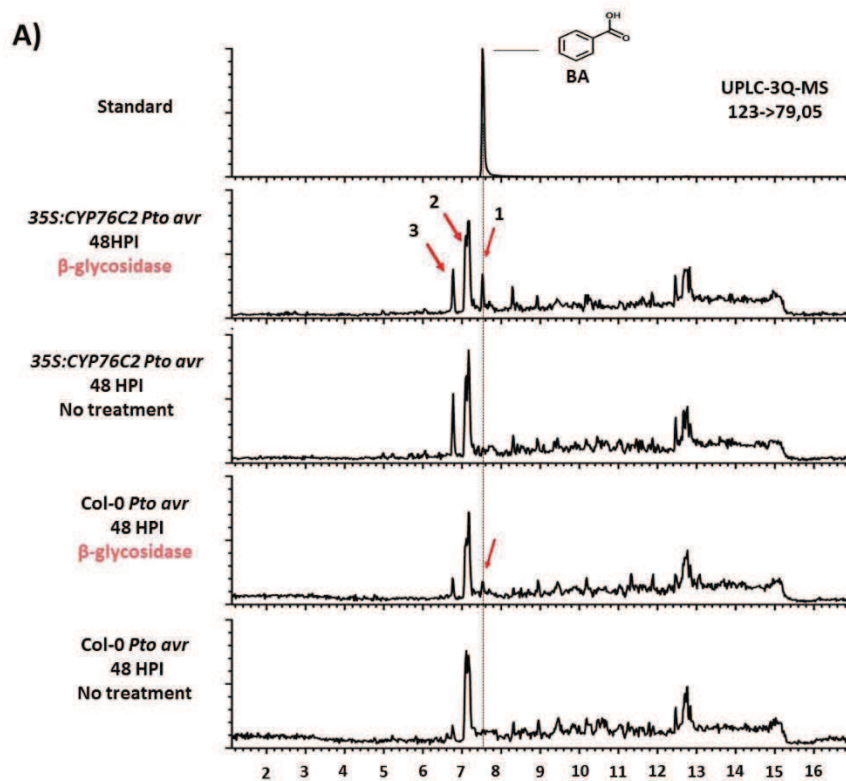


Figure 99A: Targeted UPLC profiling of BA and glycosylated forms in Col-0 and *35S:CYP76C2* infected plants with/without β -glycosidase treatment.

Plants were syringe-infiltrated with *Pto* DC3000 *avrRpm1* at a concentration of 5×10^7 CFU/ml and 48 HPI methanol-extracted for metabolomics analysis.

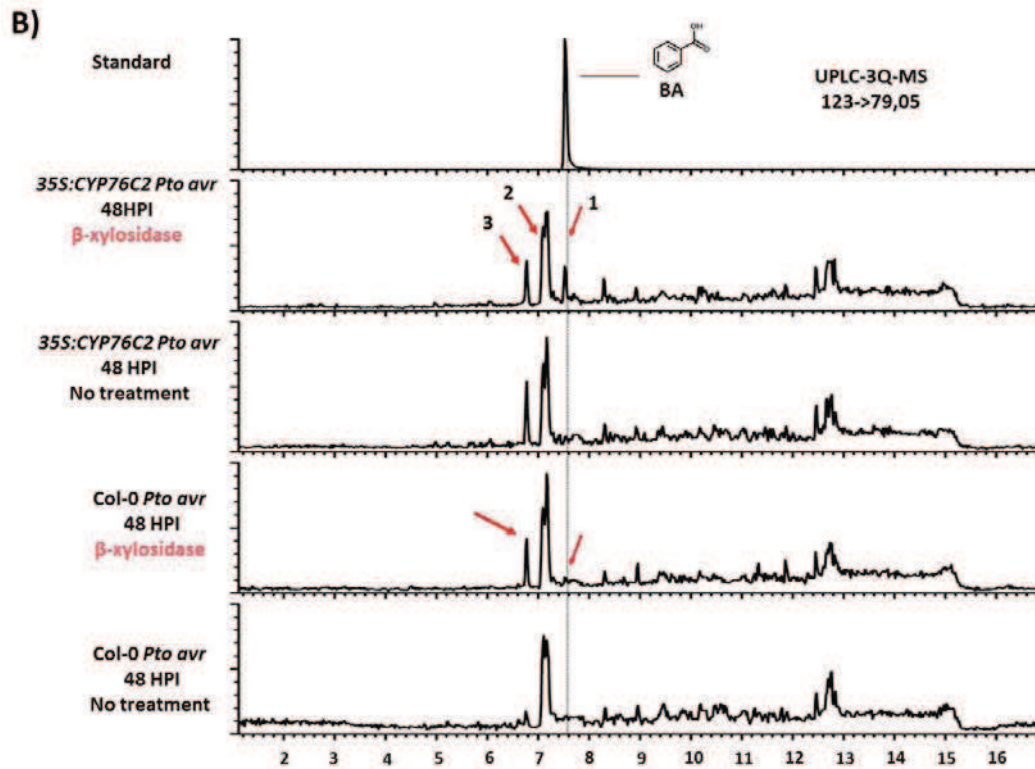


Figure 100B: Targeted UPLC profiling of BA and glycosylated forms in Col-0 and 35S:CYP76C2 infected plants with/without β -xylosidase treatment.

Plants were syringe-infiltrated with *Pto* DC3000 *avrRpm1* at a concentration of 5×10^7 CFU/ml and 48 HPI methanol-extracted for metabolomics analysis.

Analyses of SA with and without β -glycosidase treatment confirmed the presence of SAG in Col-0 infected plants but not in 35S:CYP76C2 (Figure 101A). This result might agree with the low levels of 35S:CYP76C2 found in SAG profiling, by comparison to Col-0 and *cyp76c2* infected plants (Figure 88 and 97). β -xylosidase treatment (Figure 101B) did not release any aglycone (or very minor amounts) which indicate that SA was not conjugated to a xylose in this experiment even though putative analysis indicated association of Col-0 infected plants to SA-pentose (Figure 86, UPLC Orbitrap).

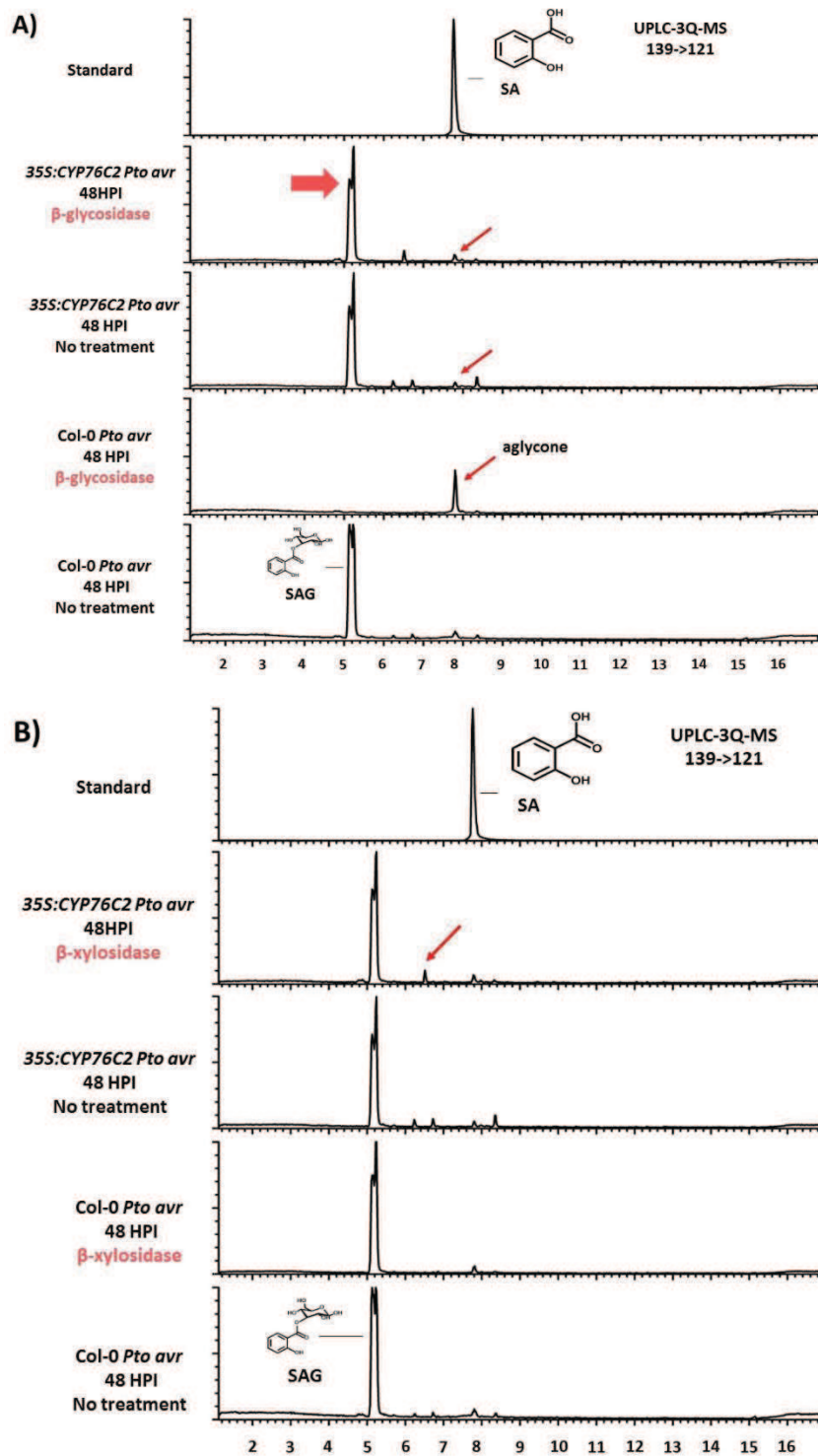


Figure 101: Targeted UPLC profiling of SA and glycosylated forms in Col-0 and 35S:CYP76C2 infected plants with/without β -glycosidase (A) and β -xylosidase (B) treatment.

Plants were syringe-infiltrated with *Pto* DC3000 *avrRpm1* at a concentration of 5×10^7 CFU/ml and 48 HPI methanol extracted for metabolomics analysis.

Finally, the analysis of DHBA permitted to detect the presence of compounds potentially matching 2,5 DHBA (relevant peak) and interestingly 2,4 DHBA in Col-0 and *35S:CYP76C2* infected plants (Figure 102 A and B).

β -glycosidase treatment resulted in a minor change in the profile of Col-0 samples, but in *35S:CYP76C2* where the three peaks disappeared suggesting that the conjugate differed between Col-0 and *35S:CYP76C2* infected plants. β -xylosidase treatment led to similar result but aglycone peaks were not detected. Although this might be due to the instability of the aglycone, it did not allow a definitive conclusion.

Although these data would require further confirmation to ascertain that detected compounds were DHBA derivatives they seem to suggest a presence of significant amounts 2,5 DHBA under the conditions of this experiment (HR), and of 2,4 DHBA (never described before) with significant differences in the compounds accumulated between *35S:CYP76C2* and Col-0 infected plants. Besides, it also seems to suggest an unexpected abundance of xylose-conjugated forms, something that has been described as prevalent in abiotic stresses and non-necrotizing infections (Bellés *et al.*, 1999; Fayos *et al.*, 2006).

In the context of previous/ subsequent results presented here this information would probably help to explain the association of mock infected plants of *35S:CYP76C2* to putative free forms of DHBA and to support the idea of the persistent association of *35S:CYP76C2* to clearance forms.

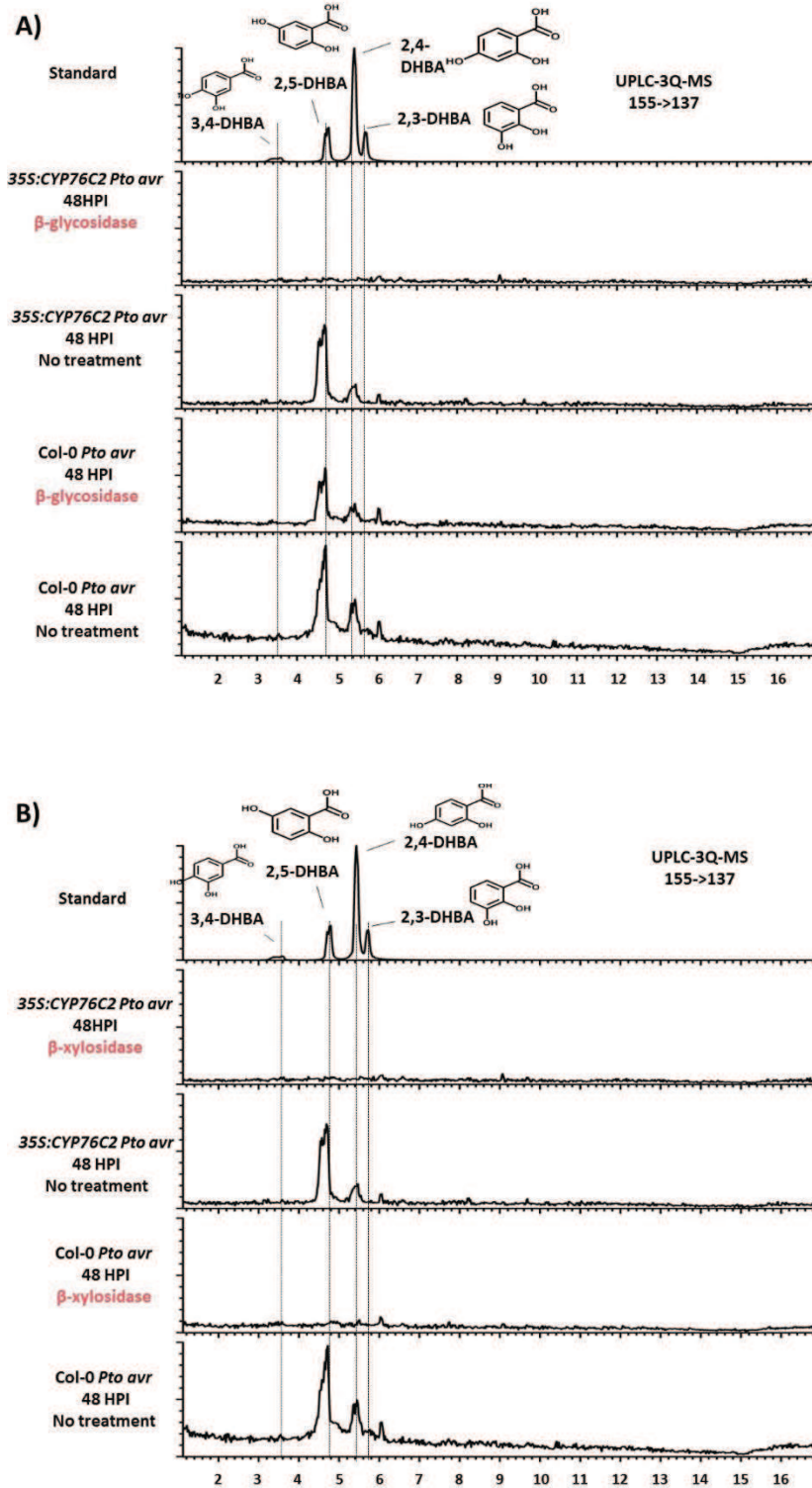


Figure 102: Targeted UPLC profiling of DHBA compounds and glycosylated forms in Col-0 and 35S:CYP76C2 infected plants with/without β -glycosidase (A) and β -xylosidase (B) treatment.

Plants were syringe-infiltrated with *Pto* DC3000 *avrRpm1* at a concentration of 5×10^7 CFU/ml and 48 HPI methanol extracted for metabolomics analysis.

Enzymatic Activities *in vitro* with Microsomal Fraction of Recombinant Yeast

Comparative profiling of BA and DHBA derivatives in the wild type and mutant lines led us to hypothesize that *CYP76C2* might contribute to metabolism of benzoic compounds. *CYP76C2* was cloned into the yeast expression vector *pYeDP60U2* and expressed in *Saccharomyces cerevisiae* WAT11 strain. The yeast microsomal fraction containing the recombinant protein was extracted and used for enzyme assays.

Incubations with candidate substrates were carried out at 20 min (Figure 103), 60 min and 120 min and analyzed in HPLC and UPLCMS/MS.

Unfortunately, no product was detected. Samples were incubated longer times and analyzed in UPLC-3Q-MS/MS obtaining the same results (not presented).

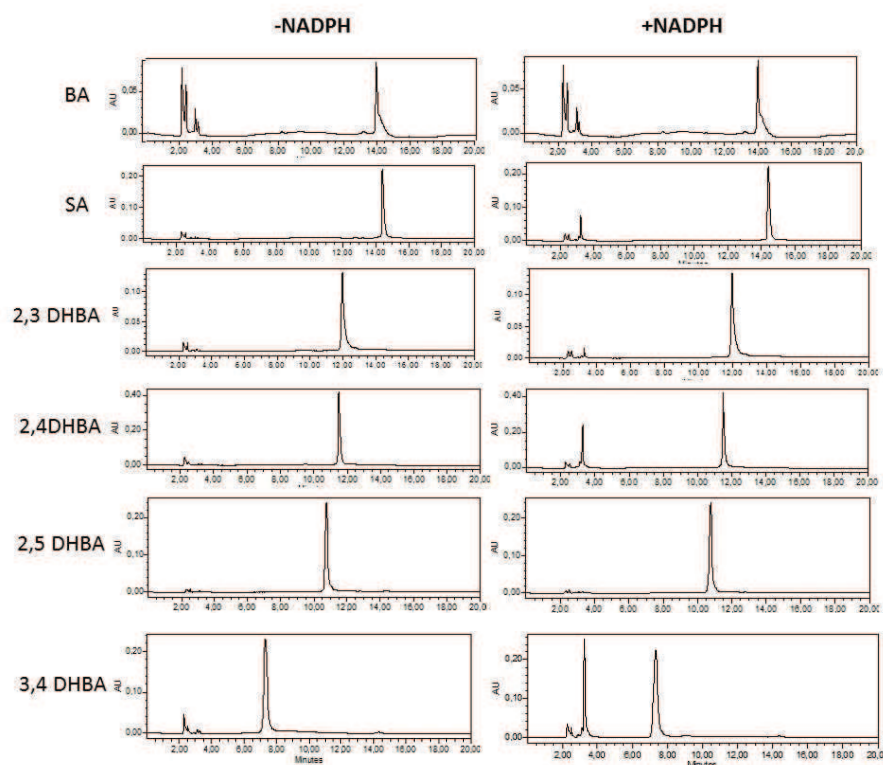


Figure 103: HPLC-photodiode array chromatogram of the products of *in vitro* conversion of potential substrates after 20 min incubation by yeast-expressed *CYP76C2* enzyme. Negative control without NADPH. AU: arbitrary unit.

Non-targeted analysis: Orbitrap UPLC-MS

A. thaliana wild-type and *CYP76C2* mutant plants were syringe-infiltrated with MgCl_2 (mock treated plants) or *Pto* DC3000 *avrRpm1* at a concentration of 5×10^7 CFU/ml, harvested and frozen in liquid nitrogen for non-targeted analysis. The experimental unit consisted in a pool of infected and/or non-infected leaves coming from 3-5 plants. Triplicates were made for each treatment. Results were confirmed in three independent experiences carried out at different time points under the same experimental conditions.

Samples were analyzed at 30 HPI, and a peak with a m/z 377.17813 in positive mode (compound 1) corresponding to a putative raw formula $\text{C}_{17}\text{H}_{27}\text{O}_9$, that can be plausible decomposed as $\text{C}_{11}\text{H}_{17}\text{O}_4 + \text{C}_6\text{H}_{10}\text{O}_5$, was identified as being down-regulated in *cyp76c2* infected plants (Figure 104). The levels of this ion accumulated in the wild type and remained ≈ 10 -fold lower in the knock-out line. No significant difference was found between Col-0 and *35S:CYP76C2* infected plants.

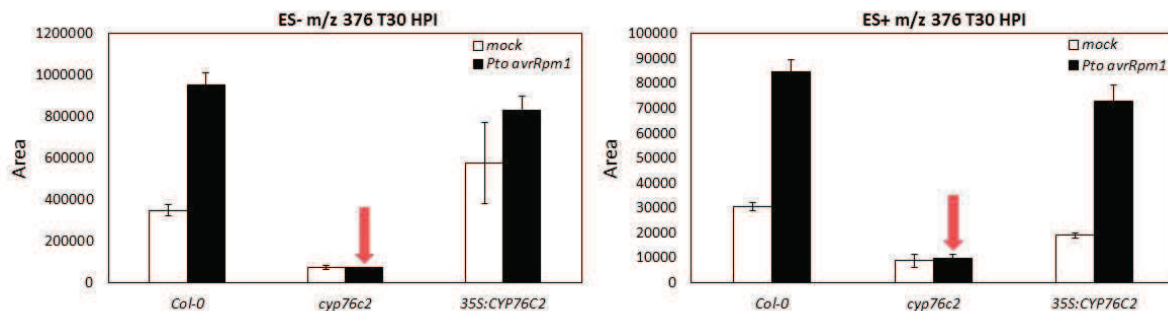


Figure 104: Area values of the peak corresponding to compound 1 obtained from Orbitrap UPLC-MS analysis of Col-0, *cyp76c2* and *35S:CYP76C2* mock and infected plants at T30 HPI. Results were confirmed in both modes: ESI negative (left) and ESI positive (right).

Plants were syringe-infiltrated with a solution containing MgCl_2 (mock) or *Pto* DC3000 *avrRpm1* at a concentration of 5×10^7 CFU/ml. Data represent means of three replicates. Errors bars represent the standard error of the mean.

Accurate mass data for the peak and proposed chemical formulae are presented in Table 30. These formulae were then used to search the identity of the conjugate or aglycone in known databases, however no identification was possible.

Table 30: Information on chemical formulae calculated with the m/z of compound 1

Mode ESI*	Formula	m/z	RT	RDB*	Delta ppm
+	C ₁₇ H ₂₉ O ₉	377.17813	6.87	3.5	-6.572
+	C ₁₁ H ₁₅ O ₄	215.12823	6.87	2.5	2.066
-	C ₁₇ H ₂₇ O ₉	375.16577	6.87	4.5	2.162
-	C ₁₁ H ₁₇ O ₄	213.11241	6.87	3.5	1.288

*RDB: ring plus double bond equivalent. ESI: electrospray ionization mode.

The kinetic of accumulation of this compound during the development of infection was then investigated, the same ion was analyzed in a timeline at T0-T24-T48-T72 HPI (Figure 105). Obtained results confirmed the same findings as on Figure 104.

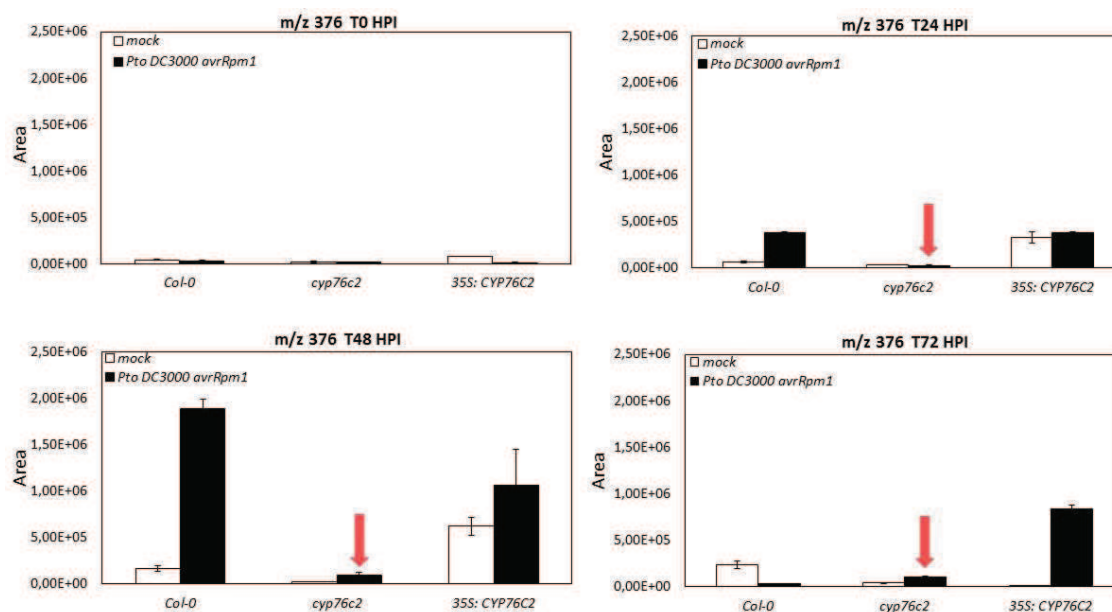


Figure 105: Area values of the peak corresponding to compound 1 obtained from Orbitrap UPLC-MS analysis of Col-0, *cyp76c2* and 35S:CYP76C2 mock and infected plants at T0-24-48-72 HPI. Red arrows are indicating the low values showed by *cyp76c2* at different time points.

Plants were syringe-infiltrated with a solution containing $MgCl_2$ (mock) or *Pto DC3000 avrRpm1* at a concentration of 5×10^7 CFU/ml. Data represent means of three replicates. Errors bars represent the standard error of the mean.

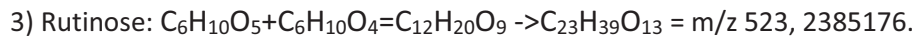
At T0, the levels of compound 1 were quite low in all three lines. In mock treated plants of the three lines it was slightly more abundant than in the infected plants. Infection induced a strong accumulation of compound 1 in Col-0 and 35S:CYP76C2 plants. The *cyp76c2* line only showed a very minor increase after infection at 48 and 72 HPI. A striking accumulation of compound 1 was detected in the 35S:CYP76C2 plants at 72 HPI. These data thus confirmed a suppression of the formation of compound 1 in the *cyp76c2* insertion mutant.

In the search for conjugate

The high number of oxygen atoms found in the putative formula $C_{17}H_{27}O_9 \rightarrow C_{11}H_{17}O_4 + C_6H_{10}O_5$ suggested that compound 1 was a conjugate.

In order to test whether the molecule was a glycoside, different ions were targeted. Figure 106 shows the relative areas (ESI+) of 377 m/z and 215 m/z in an experience carried at 6 HPI confirming the presence of the putative aglycone.

Unfortunately it was no possible to find any ion associated to a larger conjugate including for example:



At the moment, enzymatic hydrolysis studies are lacking, for instance treatment with β -glycosidase or β -xylosidase.

Additionally, studies on the fragmentation of the aglycone m/z 215, by water loss, were performed in ESI+ and can be seen in Figure 106 (information on formulae) and Figure 107 (spectrum).

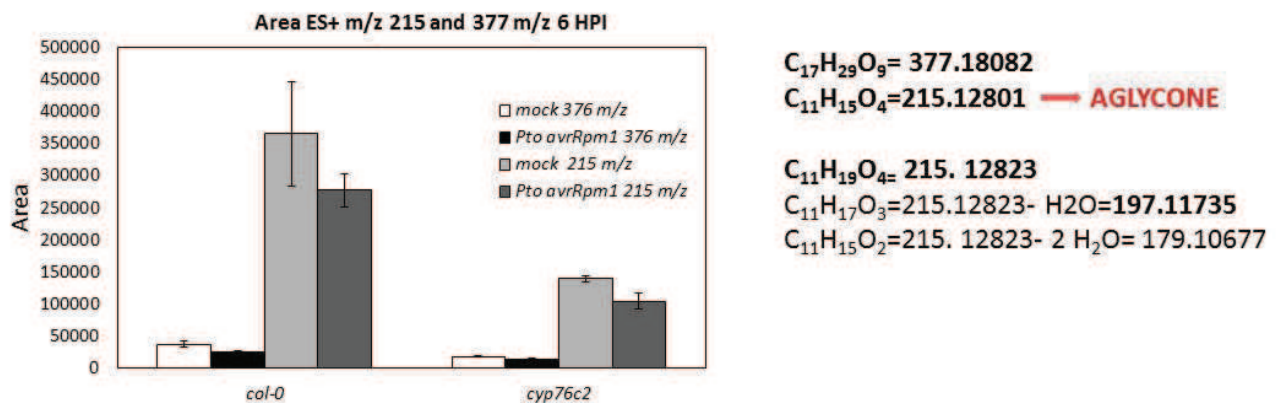


Figure 106: Peak area of the compounds of m/z 377 and 215 obtained from Orbitrap UPLC-MS analysis of Col-0 and *cyp76c2* mock and infected plants at T6 HPI. Information about formulae, m/z 215 fragments (water loss) is also displayed in the right side of panel.

Plants were syringe-infiltrated with a solution containing $MgCl_2$ (mock) or *Pto* DC3000 *avrRpm1* at a concentration of 5×10^7 CFU/ml. Data represent means of three replicates. Errors bars represent the standard error of the mean.

JL-POS1-5 #790-799 RT: 6.83-6.90 AV: 10 SB: 14 6.60-6.72 NL: 1.60E5
T: FTMS (1.1) + p ESI Full lock ms [110.00-900.00]

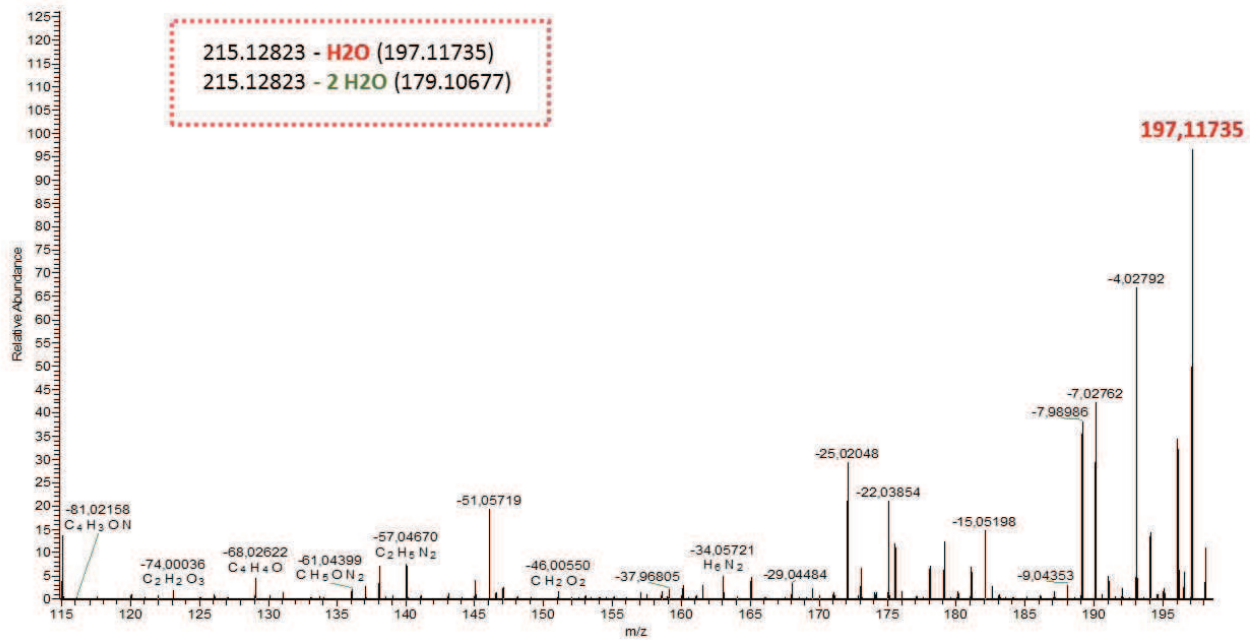


Figure 107: Mass spectrum of the [M - H₂O] ion 215 m/z, ESI positive.

Conclusion on Non-Targeted Profiling

The non-targeted profiling revealed the existence of a candidate compound that does not seem to accumulate in the knock-out *cyp76c2* line under infection with the avirulent *Pseudomonas*. This finding opens a new track for further investigation on the function of *CYP76C2*. Questions related to the structure and nature of this compound, the conjugated molecule and its role in disease and/or HR, more precisely, remain to be answered. NMR studies are required for structure elucidation of this compound, and more studies would be needed in order to understand its role in defense responses.

CONCLUSION AND PERSPECTIVES

Conclusion
and
Perspectives

CONCLUSION AND PERSPECTIVES

Previous transcriptome-based predictive analyses suggested a possible role of members of the CYP76 family of P450 enzymes in plant defense responses against pathogens in *Arabidopsis*. Especially *CYP76C2* showed a highly induced expression (≈ 50 fold) in response to biotic stress in the context of LAR responses (Kauffman, personal communication). In addition, *CYP76C2* has been mentioned elsewhere as differentially regulated in response to biotic and abiotic stress (Godiard *et al.*, 1998; Ehltling *et al.*, 2008; Höfer *et al.*, 2014) and glucosinolate metabolism (Rowe *et al.*, 2010).

Taking into account these previous results, a functional approach was carried out, with particular emphasis on the *CYP76* family and especially on *CYP76C2*, to identify P450 genes playing a key role in the development of defense mechanisms in *A. thaliana*.

The work of this thesis was focused on three main aspects:

- **Analysis of gene expression** of mock vs infected plants
- **Phenotyping of the mutants** of mock vs infected plants
- **Metabolic profiling** of mock vs infected plants

Results have revealed that within the *CYP76* family, *CYP76C2* displayed the most significant increase in transcript level in response to *B. cinerea* and *Pto* DC3000 infection. Responses to avirulent infection by *Pto* DC3000 *avrRpm1* were also significant in the HR zone and in the SAR zone, but the induction of this gene was negligible in the LAR zone.

Gene expression data obtained from qRT-PCR were refined *in planta* by using GUS staining of *Prom_{CYP76C2}:GUS* transformed *Arabidopsis* plants. Resulting information confirmed that *CYP76C2* is responsive to the virulent infection, avirulent infection (HR) and *B. cinerea*, and confirmed that no significant gene activation occurs in LAR and SAR tissues.

The information obtained from qRT-PCR and GUS was surprising since transcriptomic data predicted *CYP76C2* highly induced in LAR and down-regulated in the mutant *dth9* at 6 HPI. This mutant is incapable of mounting SAR, but is not affected in SA and camalexin accumulation. More information seems thus required about how previous experiments were conducted to be able to properly compare experiments and make a conclusion. For instance a down-regulation of *CYP76C2* in SAR, just as reported for *dth9* at 6 HPI, was also observed in our experiment from 0-6 HPI, until 8 HPI when gene induction reached an unexpected 10-fold increase.

HR is highly interconnected with LAR and is decisive for its development, however SAR is a phenomenon that not necessarily depends on HR for its progress (Dorey *et al.*, 1997; Costet *et al.*, 1999). Besides the relevance of *CYP76C2* in HR, evidently this effect was not of relevance for the activation of LAR and SAR responses in distant tissues. The *35S:CYP76C2* mutant showed less ability to mount SAR than the *cyp76c2*, conversely *cyp76c2* was impaired in mounting LAR. In this light, if *CYP76C2* has a role in HR, probably it has no relation with LAR or SAR signaling, but rather with the oxidative burst prevailing during HR (Lamb and Dixon, 1997, Torres *et al.*, 2002; 2006; Wang *et al.*, 2013).

It would be interesting to have a complete picture of *CYP76C2* in relation to the onset of HR and oxidative burst. It can be investigated in different ways, for instance monitoring gene expression or phenotyping of the mutants response to pathogens. As it was mentioned in the introduction, HR not only relies on cell death. Monitoring of HR marker and mutants would thus be required, including:

- Studies on *CYP76C2* expression/induction in *A. thaliana* mutants impaired in HR and/or oxidative burst, such as: *HSR3*, *HIN1*, *HSR203*, *LSD1* and/or *ACD2* (Greenberg *et al.*, 1994; Godiard *et al.*, 1998; Pontier *et al.*, 1999; Mur *et al.*, 2008; Coll *et al.*, 2011; Rossi *et al.*, 2011).
- Studies in mutant impaired in SAR like *dth9* (Mayda *et al.*, 2000).
- Studies with mutants related to oxidative burst like *Atrboh* (Torres and Dangl, 2005; Heller and Tduzynski, 2011; Suzuki *et al.*, 2011). The *AtrbohD* and/or *AtrbohF* genes are responsible for ROS production and oxidative burst in *A. thaliana* (Torres *et al.*, 2002; Chaouch *et al.*, 2012). Another option would be to work with a *cat2* mutant (Simon *et al.*, 2010) were ROS is up-regulated.

It would be also interesting to quantify cellular death in the HR of each genotype. A preliminary experiment performed in this thesis was performed using trypan blue and DAB (3,3'-diaminobenzidine), but did not reveal differences within the whole *CYP76* family, but it might be informative to repeat it, increasing the pathogen dose to maximize responses. Increasing pathogen pressure would also help to better analyse SAR response, which was not very well addressed in this thesis.

Concerning the other members of the *CYP76* family, none of them showed responses with relevance for the onset of defense. *CYP76C1*, the closest homologue to *CYP76C2* (Höfer *et al.*, 2014) behaved very differently and showed a unique pattern of down-regulation in response to all the infections

investigated. The expression pattern of *CYP76C5*, *CYP76C6* and *CYP76C7* after *B. cinerea* and *Pseudomonas* infections followed time courses very similar to those observed for *TPS10* and *TPS14*, suggesting a functional association of these members of the *CYP76* family with the monoterpenol metabolism, that was not anticipated.

In agreement with the moderate gene induction observed, the phenotype of infected *CYP76C2* mutants was not significantly different from wild-type upon treatment with any of the pathogen tested (*Pseudomonas* or *Botrytis*). *CYP76C2* expression only had only a subtle or transient impact on the development of the infection.

Initially, it was inferred that this might be due to functional redundancy with other members of the *CYP76* family (Millet, 2009). Nevertheless, the radically different profiles of gene expression obtained for the different genes of the family do not seem to support this hypothesis. Infection of the insertion and overexpression mutant lines of the other relevant members of the family was carried out for all the pathogens considered, without detecting any significant phenotype (*i.e.* *CYP76C3*, *CYP76C4*, *CYP76C7*, *CYP76G1*) (results not shown). However as double or triple mutants were not tested, redundancy with another *CYP76* member cannot be totally excluded. Redundancy with another, unrelated, gene(s) is also possible. For instance *CYP76C2* has been found co-regulated with two UDP-glucuronosyl/UDP-glucosyl (At3g46660 and At2g36770) and a dihydroorotate dehydrogenase/oxidase (At3g17810), both types of enzymes which could contribute to blur the response due to redundancy or conjugation of active compounds

From a metabolic point of view, the transitory and subtle susceptibility of *35S:CYP76C2* mutants to the avirulent infection (HR) suggests some relationship between *CYP76C2* and ROS. Possibly, *CYP76C2* is contributing to enhance ROS generation instead of helping in detoxification or ROS scavenging. Another possibility would be that *CYP76C2* catalyzes a poorly coupled reaction and thus directly generates ROS.

Transcriptomic data and co-expression analysis of P450 with terpene synthases have previously suggested that several members of the *CYP76C* subfamily might be involved in the biosynthesis of monoterpenoids (Ehlting *et al.*, 2008). *CYP76C1*, *CYP76C2* and *CYP76C4* were in addition shown to metabolize several monoterpenols like citronellol, linalool, geraniol and nerol *in vitro* (Höfer *et al.*, 2013; 2014; Ginglinger *et al.*, 2013) but there is no evidence to date for the involvement of *CYP76C2* or *CYP76C4* in monoterpenol metabolism *in vivo* and or under pathogen infection.

Pulling all these facts and evidences together, my working hypothesis for this work was:

“The members of the CYP76C family seem to be involved in defense responses, in particular CYP76C2 might be involved in LAR mediated responses and monoterpenol metabolism”.

Monoterpenoids had been described as having antioxidative capacity owing to their hydrogen donating or radical scavenging activities as well as their interaction with other antioxidants (Grabmann, 2005). Moreover, recently (*E*)- β -caryophyllene (sesquiterpene) has been linked to resistance to *Pseudomonas* infection in *A. thaliana* flowers (Huang *et al.*, 2012).

Consequently, profiling of volatile terpenoid emission upon *Pto* DC3000, *Pto* DC3000 *avrRpm1* and *B. cinerea* infections and of soluble free or conjugated monoterpenol derivatives in leaves was carried out. Results from both experiments indicated no difference in volatile or soluble terpenoids between mock and infected plants of *CYP76C2* mutants. Moreover, volatile profiles of other members of the CYP76 family were also analyzed with no conclusive results.

Subsequently, more targeted studies were performed in Orbitrap UPLC-MS focusing only on the comparison of mock treated and infected tissues of *CYP76C2* mutants, still not revealing any significant differences, challenging our initial hypothesis and almost excluding an oxidized monoterpenol derivative from the equation.

However, a non-targeted analysis ran in Orbitrap UPLC-MS put the idea of a terpenoid derivative back into the track since a compound with putative raw formula $C_{17}H_{27}O_9$ (*m/z* 376) probably corresponding to $C_{11}H_{17}O_4$ (*m/z* 215) + $C_6H_{10}O_5$ was found down-regulated in the knock-out mutant of *CYP76C2* infected with the avirulent *Pseudomonas*, in the HR zone.

At the moment, although this result has been confirmed at several time points and in several independent experiments, more studies are required for the elucidation of the structure of this compound as well as studies on its role in defense. The down-regulation of this molecule in the *cyp76c2* mock and infected mutant, together with the strong up-regulation in the *35S:CYP76C2* infected plants at 72 HPI clearly support a role of *CYP76C2* in its formation. However the low values of areas and intensities found all along the investigated time points suggest that the targeted compound must be present in low amounts. This may explain a low impact on diseased plants. Virulent infections would help to evaluate the relevance of this compound for resistance of diseased plants.

Though the presence of this compound is undeniable, it would be advisable to test other pathosystem and plant responses to insect attack. For instance a preliminary experiment was performed during this thesis with *Hyaloperonospora arabidopsidis*, an obligate biotroph (compatible interaction). It showed

a significantly increased susceptibility of the *cyp76c2* line (see [appendix](#)). It would be interesting to quantify this compound in plant tissues infected with this pathogen for which the role of *CYP76C2* seems more determinant for the final phenotype.

A main follow-up of this work would be the identification of this compound. Its structure and properties might provide some hint about its origin and role. It would be then possible to determine if it is differentially accumulated in local and distant tissues in comparison to ROS. It has been well established that the spatial distribution of some metabolites in avirulent interaction of *A. thaliana*-*Pto* DC3000 *avrRpm1* is influenced by ROS (Simon *et al.*, 2010).

The hormone profiling carried out upon avirulent infections revealed an unexpected trend to accumulation of SA and its conjugated forms (SAG and SGE) in the *cyp76c2* line and an opposite trend in the *35S:CYP76C2* plants, which would be in agreement with phenotyping of symptoms.

According to PCA analyses, the *35S:CYP76C2* mutant was mainly associated to the JA precursor OPDA and the clearance forms of JAs, but also associated to putative DHBA accumulation as evidenced by preliminary analyses carried out at 24 HPI in UPLC MS/MS and Orbitrap UPLC-MS. These analyses pointed out that mock treated plants of *35S:CYP76C2* were recurrently associated to a putative increase in 2,5 DHBA. Subsequently, the profiling of DHBA accumulation performed on a broader time line and including relevant standards did not show any differential accumulation of any DHBA between the wild type and the *CYP76C2* mutant genotypes. Furthermore no product was detected after incubation of the recombinant *CYP76C2* enzyme with DHBA.

At first all this information was suggesting no difference in the pattern of DHBA compounds accumulation in the overexpressor, including the 2,5 DHBA. However there was still a possibility to be explored that would help explain the intricate result. It was still plausible that the compounds were not free but conjugated. Thus enzymatic hydrolysis performed with β -glycosidase at 48 HPI evidenced the presence of several conjugated forms of DHBAs in the *35S:CYP76C2* infected mutant but not in the wild type. This was especially evident in the profile of 2,5 DHBA but was also supported by the profile of 2,4 DHBA, an unexplored compound about which not much is known to date, especially in relation to *Arabidopsis* and to defense responses.

The finding of 2,5 DHBA probably conjugated to a glucose in our infected plants was surprising because 2,5 DHBA has been found conjugated to xylose in non-necrotic lesions and to glucose in uninfected plants tissues (Bellés *et al.*, 2006; Tarraga *et al.*, 2010; Bartsch *et al.*, 2010; Campos *et al.*, 2014). 2,5

DHBA conjugated to xylose has been found in our experiment, but was also found in the wild-type plants with no differential induction/accumulation upon avirulent infection. To our knowledge 2,5 DHBA has never been related to a cell death scenario such as HR or senescence. It is also unknown in which amounts this compound is accumulated in HR or local tissues by comparison to systemic tissues. It would be expected to find it conjugated predominantly in areas adjacent to HR (Simon *et al.*, 2010).

The hypothetical presence of glycosylated 2,5 DHBA, also provides context to other information obtained in this profiling. For instance it could help to explain why no significant amount of SAG is found in the *35S:CYP76C2* mutant (very low in the profiling at 48 HPI). This could be an indication that clearance of SA (from 48 HPI to 72 HPI) of this mutants in HR tissues is rewiring the flow through 2,5 DHBA conjugates and not as expected to SAG (Tárraga *et al.*, 2010). In addition, SGE levels were low compared to SAG. SGE was negligible, and deglycosylation did not provide more information.

Moreover, the *35S:CYP76C2* mutant showed minimal levels of 2,3 DHBA, and in addition (and may be in consequence) conjugated forms of this compound were not detected. 2,3 DHBA accumulates in low levels (Bartsch *et al.*, 2010) however has been described as highly relevant in the interaction *Arabidopsis-Pseudomonas*, senescence and oxidative stress in general, mainly conjugated to xylose or glucose in uninfected tissues or viroid infected plants (Bellés *et al.*, 2006; Bartsch *et al.*, 2010; Lopez-Gresa *et al.*, 2010; Zhang *et al.*, 2013).

Another interesting molecule in *35S:CYP76C2* infected plants was BA. In the hormone profiling, the levels of BA in infected plants of the *35S:CYP76C2* mutant was as low as in the mock infected plants of the three genotypes, but after enzymatic hydrolysis of conjugates, the presence of the aglycone was observed.

Altogether these results suggest a preference for SA detoxification via glycosylated 2,5 DHBA or BA, and/or xylosylated BA instead of SAG in the *35S:CYP76C2* infected mutant. This could explain the results obtained for BA and DHBA in the profiling, but also association with JAs. Interestingly, it has been reported that, while SA induced a certain type of PR proteins, 2,5 DHBA induced other PRs (Bellés *et al.*, 1999, 2006, Lison *et al.*, 2013). Additionally, these results may explain co-regulation with UDP-glucuronosyl/UDP-glucosyl transferases (At3g46660 (UGT 76E12) and At2g36770).

Since BA and 2,5 DHBA have been described as very efficient antifungal compounds (Latanzio, 1994 cited in Dean and Delaney, 2008 and elsewhere), it would be interesting to test their accumulation in

the interaction of *CYP76C2* mutants with *B. cinerea*, which induces *PR1* and SA synthesis in the necrotic halo, and to determine the fate of SA in this interaction. In this thesis and in Millet (2009) it was observed that upon *B. cinerea* infection, *CYP76C2* was specifically activated in the necrotic area of *Botrytis*-induced lesions in which SA is synthesized via PAL (Govrin and Levine, 2002; Ferarri *et al.*, 2003, 2007; Rossi *et al.*, 2011) contrary to the SA present in HR, which is synthesized via isochorismate (Wildermuth *et al.* 2006; Dempsey *et al.*, 2011; Pieterse *et al.*, 2012, among others). This suggests that if *CYP76C2* is induced there, it might be somehow associated to the production of SA. Moreover, Kliebenstein *et al.*, (2005) have stated that *Botrytis* induces camalexin accumulation in necrotic areas. Camalexin usually accumulates upon HR and cell death, but the timing of gene induction in the necrotic zone was too delayed for contributing to phytoalexin synthesis (Dangl *et al.*, 1996; Mazid *et al.*, 2011; Gonzalez Lamothe *et al.*, 2009; Ahuja *et al.*, 2012; Jeandet *et al.*, 2014).

Another important outcome of this profiling was about the well documented phytoalexin camalexin. The *cyp76c2* mutant line not only showed significant accumulation of SA metabolites, but also displayed a noticeable increase in camalexin accumulation upon infection that was not observed in the overexpressor. Camalexin accumulation in the *cyp76c2* mutant might be related to active SA metabolism since the plant may direct the metabolic flux from tryptophan to camalexin instead of indole acetic acid to avoid auxin biosynthesis that would contribute helping bacteria to proliferate (Navarro *et al.*, 2006; Bari and Jones, 2009; Pieterse *et al.*, 2012, Xin and He, 2013). Increasing camalexin levels would mean in consequence less bacterial titer and a transitory phenotype as the one observed around 24-48 HPI. Camalexin effect in avirulent interaction has been related more to antioxidant properties than to defense (Simon *et al.*, 2010; Glazebrook and Ausubel, 1994) and here it seems to be the case since everything occurs in a context of HR and oxidative burst with no phenotype of resistance. ROS is important for camalexin production (Kliebenstein *et al.*, 2004; Persson *et al.*, 2009; Glawischig, 2007).

This work consisted in characterizing the role of *CYP76C2* in *A. thaliana* during biotic interactions with pathogens. Although we have been able to confirm that the gene is locally activated in response to biotic stress, the level of expression of *CYP76C2* does not seem to affect the plant resistance to the pathogens tested and probably is not directly implicated in responses to these pathogens. Its role might however be masked by functional redundancy that could only be revealed in multiple mutants.

Efforts to identify its substrates and products focused on the most probable pathways according to previous data were carried out. Although *CYP76C2* is biochemically active *in vitro* with linalool, citronellol, monoterpenol derivatives do not seem involved in the defense reactions.

Moreover, *CYP76C2* being SA-dependent (Millet, 2009), it was interesting to investigate its implications in the formation of SA derivatives. Despite of some interesting results, it was not possible to demonstrate a role of *CYP76C2* in SA metabolism.

The lines affected in the expression of *CYP76C2* showed no clear difference in their infection phenotype when compared to wild plants. This indicates that *CYP76C2* is probably not directly involved in the synthesis of vital molecule for the implementation of the process of defense, but more likely plays a secondary role related to biotic stress, maybe catabolism of a signal or defense molecules.

REFERENCES

References

- Abramoff M.D., Magalhaes P.J., Ram S.J. 2004. Image Processing with ImageJ. *Biophotonics International* 11 (7): 36-42.
- Acosta I.F. and Farmer E.E. 2010. Jasmonates. *The Arabidopsis Book* 8: e0129.
- Agrawal G.K., Tamogami S., Han O., Iwahashi H., and Rakwal R. 2004. Rice octadecanoid pathway. *Biochemical and Biophysical Research Communication* 317:1-15.
- Aharoni A. and Galili G. 2011. Metabolic engineering of the plant primary–secondary metabolism interface. *Current Opinion in Biotechnology* 22:239–244.
- Ahuja I., Kissen R., Bones A.M. 2012. Phytoalexins in defense against pathogens. *Trends in Plant Science* 17:2.
- Akatsuka T., Kodama O., Kato H., Kono Y., Takeuchi S. 1983. 3-Hydroxy-7-oxo-sandaracopimaradiene (Oryzalexin A), a new phytoalexin isolated from rice blast leaves. *Agricultural and Biological Chemistry* 47: 445-447.
- Alfano J. R., Charkowski A. O., Deng W. L., Petnicki T., van Dijk K., Collmer A.. 2000. The *Pseudomonas syringae* Hrp pathogenicity island has a tripartite mosaic structure comprised of a cluster of type III genes bounded by an exchangeable effector and conserved effector loci that contribute to parasitic fitness and pathogenicity in plants. *Proceedings of the National Academy of Sciences USA* 97:4856-4861.
- Alonso J. M., Stepanova A. N., Leisse T. J., Kim C. J., Chen H. M., Shinn P., Stevenson D. K., Zimmerman J., Barajas P., Cheuk R., Gadrinab C., Heller C., Jeske A., Koesema E., Meyers C. C., [...], Ecker J. R. 2003. Genome-wide insertional mutagenesis of *Arabidopsis thaliana*. *Science* 3016(1):653–657.
- Alvarez, M.E. 2000. Salicylic acid in the machinery of hypersensitive cell death and disease resistance. *Plant Molecular Biology* 44: 429–442.
- Amselem J., Cuomo C., Avan Kan J.A.L., Viaud M., Benito E.P., Couloux A., Coutinho P.M., de Vries R.P., Dyer P.S., Fillinger S., Fournier E., Gout L., Hahn M. [...], Dickman M. 2011. Genomic analysis of the necrotrophic fungal pathogens *Sclerotinia sclerotiorum* and *Botrytis cinerea*. *PLoS Genetics* 7(8) e1002230.
- Anderson J.P., Badruzsaufari E., Schenk P.M., Manners J.M., Desmond O.J., Ehlert C., Maclean D.J., Ebert P.R., Kazan K. 2004. Antagonistic interaction between abscisic acid and jasmonate-ethylene signaling pathways modulates defense gene expression and disease resistance in *Arabidopsis*. *The Plant Cell* 16:3460–79.
- Apel K. and Hirt H. 2004. Reactive oxygen species: metabolism, oxidative stress, and signal transduction. *Annual Review of Plant Biology* 55: 373–399.

- Arimura G., Ozawa R., Kugimiya S., Takabayashi J., Bohlmann J. 2004. Herbivore-induced defence response in a model legume: two spotted spider mites *Tetranychus urticae*, induce emission of (E)- β -ocimene synthase in *Lotus japonicas*. *Plant Physiology* 135:1976–1983.
- Ashour M., Wink M., Gershenzon J. 2010. Biochemistry of terpenoids: monoterpenes, sesquiterpenes and diterpenes. *Annual Plant Reviews* 40: 258–303.
- Attaran E., Rostás M., Zeier, J. 2008. *Pseudomonas syringae* elicits emission of the terpenoid (E,E)-4,8,12-trimethyl-1,3,7,11-tridecatetraene in *Arabidopsis* leaves via jasmonate signaling and expression of the terpene synthase TPS4. *Molecular Plant Microbe Interaction* 21: 1482–1497.
- Attaran E., Zeier T.E., Griebel T., Zeier, J. 2009. Methyl salicylate production and jasmonate signaling are not essential for systemic acquired resistance in *Arabidopsis*. *Plant Cell* 21: 954–971.
- Avanci N.C., Luche D.D., Goldman G.H., Goldman M.H.S. 2010. Jasmonates are phytohormones with multiple functions, including plant defense and reproduction. *Genetics and Molecular Research* 9 (1): 484-505.
- Aziz A., Poinssot B., Daire X., Adrian M., Bezier A., Lambert B., Joubert J.M., Pugin A. 2003. Laminarin elicits defense responses in grapevine and induces protection against *Botrytis cinerea* and *Plasmopara viticola*. *Molecular Plant-Microbe Interactions* 16: 1118-1128.
- Bak S. and Feyereisen R. 2001. The involvement of two p450 enzymes, *CYP83B1* and *CYP83A1*, in auxin homeostasis and glucosinolate biosynthesis. *Plant Physiology* 127(1):108-118.
- Bak S., Tax F.E., Feldmann K.A., Galbraith D.W. and Feyereisen R. 2001. *CYP83B1*, a cytochrome P450 at the metabolic branch point in auxin and indole glucosinolate biosynthesis in *Arabidopsis thaliana*. *The Plant Cell* 13(1):101-111.
- Bak S., Beisson F., Bishop G., Hamberger B., Höfer R., Paquette S., Werck-Reichhart D. 2011. Cytochromes P450. *Arabidopsis Book* 9: e0144.
- Balzarini M.G., Gonzalez L., Tablada M., Casanoves F., Di Rienzo J.A., Robledo C.W. 2008. Infostat. Manual del Usuario, Editorial Brujas, Córdoba, Argentina.
- Ballaré C.L. 2011. Jasmonate-induced defenses: a tale of intelligence, collaborators and rascals. *Trends in Plant Science* 16:249–57.
- Ballhorn D.J., Lieberei R. and Ganzhorn J.U. 2005. Plant cyanogenesis of *Phaseolus lunatus* and its relevance for herbivore-plant interaction: the importance of quantitative data. *Journal of Chemical Ecology* 31(7): 1445–73.
- Bannenberg G., Martinez M., Hamberg M., Castresana C. 2009. Diversity of the enzymatic activity in the lipoxygenase gene family of *Arabidopsis thaliana*. *Lipids* 44: 85–95.

- Barah P., Winge P., Kusnierczyk A., Tran D.H., Bones A.M. 2013. Molecular signatures in *Arabidopsis thaliana* in response to insect attack and bacterial infection. PLoS One 8(3): e58987.
- Bari R., Jones J.D.G. 2009. Role of plant hormones in plant defence responses. Plant Molecular Biology 69:473–488.
- Bartsch M., Bednarek P., Vivancos P.D., Schneider B., von Roepenack-Lahaye E., Foyer C.H., Kombrink E., Scheel D., Parker J.E. 2010. Accumulation of isochorismate-derived 2,3-dihydroxybenzoic 3-O- β -D-xyloside in *Arabidopsis* resistance to pathogens and ageing of leaves. Journal of Biological Chemistry 285: 25654-25665.
- Bate N.J., Sivasankar S., Moxon C., Riley J.M., Thompson J.E., Rothstein S.J. 1998. Molecular characterization of an *Arabidopsis* gene encoding hydroperoxide lyase, a cytochrome P-450 that is wound inducible. Plant Physiology 117(4):1393-1400.
- Beets C.A., Huang J.C., Madala N.E., Dubery I. 2012. Activation of camalexin biosynthesis in *Arabidopsis thaliana* in response to perception of bacterial lipopolysaccharides: a gene-to-metabolite study. Planta 236(1):261-72.
- Bednarek P., Schneider B., Svatoš A., Oldham N.J., Hahlbrock K. 2005. Structural complexity, differential response to infection, and tissue specificity of indolic and phenylpropanoid secondary metabolism in *Arabidopsis* roots. Plant Physiology 138(2): 1058–1070.
- Bednarek P., Pilewska-Bednarek M., Svatoš A., Schneider B., Doubsk J., Mansurova M., Humphry M., Consonni C., Panstruga R., Sanchez-Vallet A., Molina A., Schulze-Lefert P. 2009. Glucosinolate metabolism pathway in living plant cells mediates broad-spectrum antifungal defense. Science 323: 101 – 106.
- Belkhadira Y., Jaillais Y., Epplé P., Balsemão-Piresa E., Dangl J.L., Chorya J. 2011. Brassinosteroids modulate the efficiency of plant immune responses to microbe-associated molecular patterns. Proceeding of the National Academy of Sciences USA 109 (1): 297-302.
- Bellés J.M., Garro R., Pallás V., Fayos J., Rodrigo I., Conejero V. 2006. Accumulation of gentisic acid as associated with systemic infections but not with the hypersensitive response in plant-pathogen interactions. Planta 223: 500-511.
- Bent A.F., Mackey D. 2007. Elicitors, effectors, and R genes: the new paradigm and a lifetime supply of questions. Annual Review of Phytopathology 45:399-436.
- Berkey R., Bendigeri D., Xiao S. 2012. Sphingolipids and plant defense/disease: the “death” connection and beyond. Frontiers in Plant Science 3, article 68.
- Blee E. 2002. Impact of phyto-oxylipins in plant defense. Trends in Plant Science 7:315–22.

- Block A., Schmelz E., Jones J.B., Klee H.J. 2005. Coronatine and salicylic acid: the battle between *Arabidopsis* and *Pseudomonas* for phytohormone control. *Molecular Plant Pathology* 6(1):79-83.
- Block A., Guo M., Li G., Elowsky C., Clemente T.E., Alfano J.R. 2010. The *Pseudomonas syringae* type III effector HopG1 targets mitochondria, alters plant development and suppresses plant innate immunity. *Cell Microbiology* 12:318–30.
- Blum R., Beck A., Korte A., Stengel A., Letzel T., Lenzian K., Grill E. 2007. Function of phytochelatin synthase in catabolism of glutathione-conjugates. *Plant Journal* 49: 740–749.
- Boachon B., Gamir J., Pastor V., Erb M., Dean J.V., Flors V., Mauch-Mani B. 2014. Role of two UDP-Glycosyltransferases from the L group of *Arabidopsis* in resistance against *Pseudomonas syringae*. *European Journal of Plant Pathology* 139 (4): 707-720.
- Bohman S., Staal J., Thomma B.P., Wang M., Dixelius C. 2004. Characterisation of an *Arabidopsis-Leptosphaeria maculans* pathosystem: Resistance partially requires camalexin biosynthesis and is independent of salicylic acid, ethylene and jasmonic acid signalling. *Plant Journal* 37: 9–20.
- Bohlmann J. and Keeling C.I. 2008. Terpenoid biomaterials. *Plant Journal* 54:656–669.
- Böttcher C., Westphal L., Schmotz C., Prade E., Scheel D., Glawischnig E. 2009. The multifunctional enzyme *CYP71B15 (PHYTOALEXIN DEFICIENT3)* converts cysteine-indole-3-acetonitrile to camalexin in the indole-3-acetonitrile metabolic network of *Arabidopsis thaliana*. *Plant Cell* 21: 1830–1845.
- Böttcher C., Chapman A., Fellermeier F., Choudhary M., Scheel D., Glawischnig E. 2014. The Biosynthetic pathway of Indole-3-Carbaldehyde and Indole-3-Carboxylic Acid derivatives in *Arabidopsis*. *Plant Physiology* 165(2): 841-853.
- Bouizgarne B., El-Maarouf-Bouteau H., Frankart C., Reboutier D., Madiona K., Pennarun A.M., Monestiez M., Trouverie J., Amiar Z., Briand J., Brault M., Rona J.P., Ouhdouch Y., El Hadrami I., Bouteau F. 2006. Early physiological responses of *Arabidopsis thaliana* cells to fusaric acid: toxic and signalling effects. *New Phytologist* 169: 209–218.
- Van Breusegem F. and Dat J.F. 2006. Reactive oxygen species in plant cell death. *Plant Physiology* 141: 384-390.
- Brodersen P., Petersen M., Bjorn Nielsen H., Zhu S., Newman M.A., Shokat K.M., Rietz S., Parker J., Mundy J. 2006. *Arabidopsis* MAP kinase 4 regulates salicylic acid- and jasmonic acid/ethylene-dependent responses via EDS1 and PAD4. *Plant Journal* 47:532–46.
- Brooks D.M., Hernandez-Guzman G., Kloek A.P., Alarcon-Chaidez F., Sreedharan A., Rangaswamy V., Peñaloza-Vázquez A., Bender C.L., Kunkel B.N. 2004. Identification and

characterization of a well-defined series of coronatine biosynthetic mutants of *Pseudomonas syringae* pv. *tomato* DC3000. *Molecular Plant-Microbe Interaction* 17:162–74.

- Brouwer M., Lievens B., Van Hemelrijck W., Van den A.G., Cammue B.P., Thomma B.P. 2003. Quantification of disease progression of several microbial pathogens on *Arabidopsis thaliana* using real-time fluorescence PCR. *FEMS Microbiology Letters* 228:241–248.
- Browne L.M., Conn K.L., Ayer W.A., Tewari J.P. 1991. The camalexins: new phytoalexins produced in the leaves of *Camelina sativa* (*Cruciferae*). *Tetrahedron* 47: 3909–3914.
- Buell C.R., Joardar V., Lindeberg M., Selengut J., Paulsen I.T., Gwinn M.L., Dodson R.J., Deboy R.T., Durkin A.S., Kolonay J.F., Madupu R., Daugherty S., Brinkac L., Beanan M.J., Haft D.H., Nelson W.C., [...], Collmer A. 2003. The complete genome sequence of the *Arabidopsis* and tomato pathogen *Pseudomonas syringae* pv. *tomato* DC3000. *Proceeding of the National Academy of Science USA* 100:10181–86.
- Buxdorf K., Yaffe H., Barda O., Levy M. 2013. The effects of glucosinolates and their breakdown products on necrotrophic fungi. *PLoS One* 8(8):e70771.
- Callaway A., Liu W., Andrianov V., Stenzler L., Zhao J., Wettlaufer S., Jayakumar P., Howell S.H. 1996. Characterization of cauliflower mosaic virus (CaMV) resistance in virus-resistant ecotypes of *Arabidopsis*. *Molecular Plant Microbe Interaction* 9: 810–818.
- Campos L., Granell P., Tárraga S., López-Gresa P., Conejero V., Bellés J.M., Rodrigo I., Lisón P. 2014. Salicylic acid and gentisic acid induce RNA silencing-related genes and plant resistance to RNA pathogens. *Plant Physiology and Biochemistry* 77:35-43.
- Caputi L. and Aprea E. 2011. Use of terpenoids as natural flavouring compounds in food industry. *Recent Patents in Food, Nutrition and Agriculture* 3(1):9-16.
- Cartwright D.W., Langcake P., Pryce R.J., Leworthy D.P., Ride J.P. 1981. Isolation and characterization of two phytoalexins from rice as momilactones A and B. *Phytochemistry* 20: 535-537.
- Castresana J. 2000. Selection of conserved blocks from multiple alignments for their use in phylogenetic analysis. *Molecular Biology and Evolution* 17(4):540-52.
- Champigny M.J., Shearer H., Mohammad A., Haines K., Neumann M., Thilmony R., He S.Y., Fobert P., Dengler N., Cameron R.K. 2011. Localization of DIR1 at the tissue, cellular and subcellular levels during systemic acquired resistance in *Arabidopsis* using DIR1:GUS and DIR1:EGFP reporters. *BMC Plant Biology* 11: 125.
- Chanda B., Xia Y., Mandal M.K., Mandal M.K., Yu K., Sekine K.T., Gao Q.M., Selote D., Hu Y., Stromberg A., Navarre D., Kachroo A., Kachroo P. 2011. Glycerol-3-phosphate is a critical mobile inducer of systemic immunity in plants. *Nature Genetics* 43: 421–427.

- Chang X., Heene E., Qiao F., Nick P. 2011. The phytoalexin resveratrol regulates the initiation of hypersensitive cell death in *Vitis* cells. PLoS One 6 (10):e26405.
- Chaouch S., Queval G., Noctor G. 2012. AtRbohF is a crucial modulator of defence-associated metabolism and a key actor in the interplay between intracellular oxidative stress and pathogenesis responses in *Arabidopsis*. The Plant Journal 69: 613-627.
- Chapple, C., Shirley, B., Zook, M., Hammerschmidt, R., Somerville, S.1994. 36: Secondary Metabolism in *Arabidopsis*. Cold Spring Harbor Monograph Archive, North America, 27, Jan. 1994. Available at: <http://cshmonographs.org/index.php/monographs/article/view/3129>. Date accessed: sept. 2014.
- Chassot C., Buchala A., Schoonbeek H.J., Métraux J.P., Lamotte O.2008. Wounding of *Arabidopsis* leaves causes a powerful but transient protection against *Botrytis* infection. Plant Journal 55(4):555-67.
- Chaturvedi R., Krothapalli K., Makandar R., Nandi A., Sparks A.A., Roth M.R., Welti R., Shah J.2008. Plastid omega3-fatty acid desaturase-dependent accumulation of a systemic acquired resistance inducing activity in petiole exudates of *Arabidopsis thaliana* is independent of jasmonic acid. The Plant Journal 54 (1):106–117.
- Chaturvedi R., Venables B., Petros R.A., Nalam V., Li M., Wang X.,Takemoto L.J., Shah J. 2012. An abietane diterpenoid is a potent activator of systemic acquired resistance. Plant Journal 71: 161–172.
- Chen S.X., Glawischnig E., Jørgensen K., Naur P., JørgensenB, Olsen C.E., Hansen C.H., Rasmussen H., Pickett J.A.,Halkier B.A .2003. Cytochrome P450 *CYP79F1* and *CYP79F2* genes catalyse the first step in the biosynthesis of short-chain and long-chain aliphatic glucosinolates in *Arabidopsis*. Plant Journal 33:923–937.
- Chen H., Xue L.,Chintamanani S.,Germain H., Lin H., Cui H., Cai R., Zuo J., Tang X., Li X., Guo H., Zhou J.M. 2009. *ETHYLENEINSENSITIVE3* and *ETHYLENE INSENSITIVE3-LIKE1* repress *SALICYLIC ACID INDUCTION DEFICIENT2* expression to negatively regulate plant innate immunity in *Arabidopsis*. The Plant Cell 21:2527–40.
- Chen J., Vandelle E., Bellin D., Delledonne M.2014. Detection and function of nitric oxide during the hypersensitive response in *Arabidopsis thaliana*: where there's a will there's a way. Nitric Oxide 43:81-8.
- Cheng Y.T., Germain H., Wiermer M., Bi D., Xu F., García A.V., Wirthmueller L., Després C., Parker J.E., Zhang Y., Li X. 2009. Nuclear pore complex component MOS7/Nup88 is required for innate immunity and nuclear accumulation of defense regulators in *Arabidopsis*. The Plant Cell 21:2503–16.

- Chinchilla D., Zipfel C., Robatzek S., Kemmerling B., Nurnberger T., Jones J.D., Felix G., Boller T. 2007. A flagellin-induced complex of the receptor FLS2 and BAK1 initiates plant defence. *Nature*. 448:497–500.
- Chisholm S.T., Coaker G., Day B., Staskawicz B.J. 2006. Host-microbe interactions: shaping the evolution of the plant immune response. *Cell* 124: 803–814.
- Choi J., Huh S.U., Kojima M., Sakakibara H., Paek K.H., Hwang I. 2010. The cytokinin-activated transcription factor ARR2 promotes plant immunity via TGA3/NPR1-dependent salicylic acid signaling in *Arabidopsis*. *Developmental Cell* 19:284–95.
- Chong J., Baltz R., Schmitt C., Beffa R., Fritig B. and Saindrenan P. 2002. Downregulation of a pathogen-responsive tobacco UDP-GLC:phenylpropanoid glucosyltransferase reduces scopoletin glucoside accumulation, enhances oxidative stress, and weakens virus resistance. *The Plant Cell* 14 (5): 1093-1107.
- Choquer M., Fournier E., Kunz C., Levis C., Pradier J., Simon A., Viaud M. 2007. *Botrytis cinerea* virulence factors: New insights into a necrotrophic and polyphageous pathogen. *FEMS Microbiology Letters* 277: 1–10.
- Clay N. K., Adio A. M., Denoux C., Jander, G. and F. M. Ausubel .2009. Glucosinolate metabolites required for an *Arabidopsis* innate immune response. *Science* 323, 95-101.
- Clough S.J. and Bent A.F. 1998. Floral dip: A simplified method for *Agrobacterium*-mediated transformation of *Arabidopsis thaliana*. *Plant Journal* 16: 735–743.
- Coll N.S., Vercammen D., Smidler A., Clover C., Van Breusegem F., Dangl J.L., Epple P. 2010. *Arabidopsis* type I metacaspases control cell death. *Science* 3 (330):1393-7.
- Coll N.S., Eppel P., Dangl J.L. 2011. Programmed cell death in the plant immune system. *Cell Death and Differentiation* 18: 1247-1256.
- Coll N.S., Smidler A., Puigvert M., Popa C., Valls M., Dangl J.L. 2014. The plant metacaspase AtMC1 in pathogen-triggered programmed cell death and aging: functional linkage with autophagy. *Cell Death and Differentiation* 21: 1399-1408.
- Collier S.M. and Moffett P. 2009. NB-LRRs work a “bait and switch” on pathogens. *Trends in Plant Science* 14 (10):1360-1385.
- Cona A., Rea G., Angelini R., Federico R., Tavladoraki P. 2006. Functions of amine oxidases in plant development and defense. *Trends in Plant Science* 11(2): 80-88.
- Conover W. J. 1999. *Practical Nonparametric Statistics* (3rd ed.) New York: Wiley.
- Costet L, Cordelier S., Dorey S., Baillieul F., Fritig B., Kauffmann S. 1999. Relationship between localized acquired resistance (LAR) and the hypersensitive response (HR): HR is necessary for LAR to occur and salicylic acid is not sufficient to trigger LAR. *Molecular Plant-Microbe Interaction* 12(8): 655-662.

- Costet L., Fritig B., Kauffmann, S. 2002. Scopoletin expression in elicitor-treated and tobacco mosaic virus-infected tobacco plants. *Physiologia Plantarum* 115 (2):228-235.
- Croteau R., Ketchum R.E., Long R.M., Kaspera R., Wildung M.R. 2006. Taxol biosynthesis and molecular genetics. *Phytochemistry Reviews* 5:75–97.
- Cui J., Bahrami A.K., Pringle E.G., Hernandez-Guzman G., Bender C.L., Pierce N.E., Ausubel F.M. 2005. *Pseudomonas syringae* manipulates systemic plant defenses against pathogens and herbivores. *Proceedings of the National Academy of Sciences USA* 102:1791–1796
- Cutler S.R., Rodriguez P.L., Finkelstein R.R., Abrams S.R. 2010. Abscisic acid: emergence of a core signalling network. *Annual Review of Plant Biology* 61:651–679.
- Czechowski T., Stitt M., Altmann T., Udvardi M.K., Scheible, W.R. 2005. Genome-wide identification and testing of superior reference genes for transcript normalization in *Arabidopsis*. *Plant Physiology* 139: 5–17.
- D'Auria J.C. and Gershenzon J. 2005. The secondary metabolism of *Arabidopsis thaliana*: growing like a weed. *Current Opinion in Plant Biology*. 8: 308 – 316.
- Dangl J.L., Dietrich R.A., Richberg M.H. 1996. Death don't have no mercy: cell death's programs in plant -microbe interactions. *Plant Cell* 8: 1793-1807.
- Dangl J.L. and Jones J.D.G. 2001. Plant pathogens and integrated defence responses to infection. *Nature* 411: 826-833.
- Dangl J.L. and McDowell J.M. 2006. Two modes of pathogen recognition by plants. *Proceedings of the National Academy of Sciences USA* 103(23): 8575-8576.
- Davidson S.E., Elliott R.C., Helliwell C.A., Poole A.T., Reid, J.B. 2003. The pea gene NA encodes ent-kaurenoic acid oxidase. *Plant Physiology* 131:335–344.
- Davidson S.A., Reid, J.B., Helliwell, C.A. 2006. Cytochromes P450 in gibberellin biosynthesis. *Phytochemistry Review* 5:405–419.
- Davies T.G., Field L.M., Usherwood P.N. and Williamson M.S. 2007. DDT, pyrethrins, pyrethroids and insect sodium channels. *IUBMB Life* 59: 151–62.
- Dean J.V. and Delaney S.P. 2008. Metabolism of salicylic acid in wildtype, *ugt74f1* and *ugt74f2* glucosyltransferase mutants of *Arabidopsis thaliana*. *Physiologia Plantarum* 132: 417-425.
- De Cremer K., Mathys J., Vos C., Froenicke L., Michelmore R.W., Cammue B.P., De Coninck B. 2013. RNAseq-based transcriptome analysis of *Lactuca sativa* infected by the fungal necrotroph *Botrytis cinerea*. *Plant Cell and Environment* 36 (11): 1992-2007.
- de Torres-Zabala M., Truman W., Bennett M.H., Lafforgue G., Mansfield J.W., Rodriguez Egea P., Bögre L., Grant M. 2007. *Pseudomonas syringae* pv. *tomato* hijacks the *Arabidopsis* abscisic acid signaling pathway to cause disease. *EMBO journal* 26 (5): 1434-43.

- De Vos M., Van Zaanen W., Koornneef A., Korzelius J.P., Dicke M., Van Loon L.C., Pieterse C. M.J. 2006. Herbivore-induced resistance against microbial pathogens in *Arabidopsis*. *Plant Physiology* 142:352–63.
- De Vries S., Hoge H., Bisseling T. 1988. Isolation of total and polysomal RNA from plant tissues. In Gelvin SB, Schilperoot RA (eds) *Plant molecular biology*. Kluwer Academic Publishers, Dordrecht, Netherlands, B6: 1-13.
- Dean R., Van Kan J.A., Pretorius Z.A., Hammond-Kosack K.E., Di Pietro A., Spanu P.D., Rudd J.J., Dickman M., Kahmann R., Ellis J., Foster G.D. 2012. The Top 10 fungal pathogens in molecular plant pathology. *Molecular Plant Pathology* 13: 414–430.
- Deising H.B., Werner S., Wernitz M. 2000. The role of fungal appressoria in plant infection. *Microbes and infection* 2: 1631-1641.
- Dempsey D.A., Pathirana M.S, Wobbe., K.K., Klessig D.F. 1997. Identification of an *Arabidopsis* locus required for resistance to turnip crinkle virus. *Plant Journal* 11: 301–311.
- Dempsey D.A., Vlot A.C., Wildermuth M.C., Klessig, D.F. 2011. Salicylic acid biosynthesis and metabolism. *Arabidopsis Book* 9: e0156.
- Dempsey D.A. and Klessig D.F. 2012. SOS—too many signals for systemic acquired resistance? *Trends in Plant Science* 17: 538–545.
- Denancé N., Sánchez-Vallet A., Goffner D., Molina A. 2013. Disease resistance or growth: the role of plant hormones in balancing immune responses and fitness costs. *Frontiers in Plant Science* 4 (article 155):66-77.
- Denby K.J., Kumar P., Kliebenstein D.J. 2004. Identification of *Botrytis cinerea* susceptibility loci in *Arabidopsis thaliana*. *Plant Journal* 38: 473–478.
- Denoux C., Galletti R., Mammarella N., Gopalan S., Werck D., De Lorenzo G., Ferrari S., Ausubel F.M., Dewdney J. 2008. Activation of defense response pathways by OGs and Flg22 elicitors in *Arabidopsis* seedlings. *Molecular Plant* 1(3):423-45. (erratum 2009 2(4):838)
- Dereeper A., Guignon V., Blanc G., Audic S., Buffet S., Chevenet F., Dufayard J.F., Guindon S., Lefort V., Lescot M., Claverie J.M., Gascuel O. 2008. Phylogeny.fr: robust phylogenetic analysis for the non-specialist. *Nucleic Acids Research* 36 (Web Server issue):W465-9.
- Detzel A. and Wink M. 1993. Attraction, deterrence or intoxication of bees (*Apis mellifera*) by plant allelochemicals. *Chemoecology* 4:8–18.
- Dewick, P. M. 2002. The mevalonate and deoxyxylulose phosphate pathways: terpenoids and steroids. In: *Medicinal natural products: a biosynthetic approach*. 2nd ed. Wiley. pp 167.
- Didierlaurent, L. 2012. UGT76E12, UGT73B3 et UGT73B5, trois glycosyltransférases du métabolisme secondaire d'*Arabidopsis thaliana* impliquées dans les réponses de défense aux microorganismes pathogènes. PhD these. Univ. Paris Sud, Orsay, France.

- Di Rienzo J.A., Casanoves F., Balzarini M.G., Gonzalez L., Tablada M., Robledo C.W. 2010. InfoStat versión 2010. Grupo InfoStat, FCA, Universidad Nacional de Córdoba, Argentina.
- Dietrich R.A., Richberg M.H., Schmidt R., Dean C., Dangl J.L. 1997. A novel zinc-finger protein is encoded by the *Arabidopsis* *Isd1* gene and functions as a negative regulator of plant cell death. *Cell* 88: 685–694.
- Dixon R.A. 2001. Natural products and plant disease resistance. *Nature* 411: 843-847.
- Dixon R.A., Achnine L., Kota P., Liu C.J., Reddy S. and Wang L. 2002. The phenylpropanoid pathway and plant defence—a genomics perspective. *Molecular Plant Pathology* 3(5):371-390.
- Dodds P.N. and Rathjen J.P. 2010. Plant immunity: towards an integrated view of plant–pathogen interactions. *Nature Reviews* 11: 539-548.
- Dong X. 2004. NPR1, all things considered. *Current Opinion in Plant Biology* 7:547–52.
- Dorey S., Baillieul F., Pierrel M.-A., Saindrenan P., Fritig B., Kauffmann, S. 1997. Spatial and temporal induction of cell death, defense genes, and accumulation of salicylic acid in tobacco leaves reacting hypersensitively to a fungal glycoprotein elicitor. *Molecular Plant-Microbe Interaction* 10:646–655.
- Dorey S., Baillieul F., Saindrenan P., Fritig B., Kauffmann, S. 1998. Tobacco class I and II catalases are differentially expressed during elicitor-induced hypersensitive cell death and localized acquired resistance. *Molecular Plant-Microbe Interaction* 11: 1102–1109.
- Du Fall L.A. and Solomon P.S. 2011. Role of cereal secondary metabolites involved in mediating the outcome of plant-pathogen interactions. *Metabolites* 1: 64-78.
- Duan H. and Schuler M.A. 2005. Differential expression and evolution of the *Arabidopsis* *CYP86A* subfamily. *Plant Physiology* 137: 1067–1081.
- Durrant W.E. and Dong X. 2004. Systemic acquired resistance. *Annual Review of Phytopathology* 42: 185–209.
- Edgar R.C. 2004. MUSCLE: multiple sequence alignment with high accuracy and high throughput. *Nucleic Acids Research* 32(5):1792-7.
- Edwards K., Johnstone C., Thompson C. 1991. A simple and rapid method for the preparation of plant genomic DNA for PCR analysis. *Nucleic Acid Research* 19: 1349.
- Ehrling J., Sauveplane V., Olry A., Ginglinger J.F., Provart N.J., Werck-Reichhart D. 2008. An extensive (co-)expression analysis tool for the cytochrome P450 superfamily in *Arabidopsis thaliana*. *BMC Plant Biology* 8:47.
- Elad Y., Williamson B., Tudzynski P., Delen N. 2007. *Botrytis*: biology, pathology and control. Kluwer Academic Publishers. Dordrecht, The Netherlands. 428 p.
- Erb M., Glauser, G. 2010. Family business: Multiple members of major phytohormone classes orchestrate plant stress responses. *Chemistry A European Journal* 16: 10280-10289.

- Etalo D.W., Stulemeijer I.J., van Esse H.P., de Vos R.C., Bouwmeester H.J., Joosten M.H. 2013. System-wide hypersensitive response-associated transcriptome and metabolome reprogramming in tomato. *Plant Physiology* 162(3): 1599-617.
- FAO. 2009/2012. The voluntary guidelines on the responsible governance of tenure of land, fisheries and forests in the context of national food security. <http://www.fao.org/news/story/en/item/142587/icode/>. Accessed: 2014.
- Farmer E.E., Almeras E., Krisnamurthy V. 2003. Jasmonates and related oxylipins in plant responses to pathogenesis and herbivory. *Current Opinion in Plant Biology* 6:372–78.
- Faulkner C., and Robatzek S. 2012. Plants and pathogens: putting infection strategies and defence mechanisms on the map. *Current Opinion in Plant Biology* 15:699–707.
- Fayos J., Bellés J.M., López-Gresa M.P., Primo J., Conejero V. 2006. Induction of gentisic acid 5-O-beta-D-xylopyranoside in tomato and cucumber plants infected by different pathogens. *Phytochemistry* 67 (2):142-148.
- Feil H., Feil W.S., Chain P., Larimer F., DiBartolo G., Copeland A., Lykidis A., Trong S., Nolan M., Goltsman E., Thiel J., Malfatti S., Loper J.E., Lapidus A., Detter J.C., Land M., Richardson P.M., Kyrpides N.C., Ivanova N., Lindow S.E. 2005. Comparison of the complete genome sequences of *Pseudomonas syringae* pv. *syringae* B728a and pv. *tomato* DC3000. *Proceedings of the National Academy of Science USA* 102:11064–69.
- Fernie A.R. 2007. The future of metabolic phytochemistry: Large numbers or metabolites, higher resolution, greater understanding. *Phytochemistry* 68: 2861–2880.
- Ferrari S., Plotnikova J.M., De Lorenzo G., Ausubel F.M. 2003. *Arabidopsis* local resistance to *Botrytis cinerea* involves salicylic acid and camalexin and requires EDS4 and PAD2, but not SID2, EDS5 or PAD4. *Plant Journal* 35: 193–205.
- Ferrari S., Galletti R., Denoux C., De Lorenzo G., Ausubel F.M., Dewdney J. 2007. Resistance to *Botrytis cinerea* induced in *Arabidopsis* by elicitors is independent of salicylic acid, ethylene, or jasmonate signaling but requires PHYTOALEXIN DEFICIENT3. *Plant Physiology* 144 (1)367-379.
- Ferrari S., Savatin D.V., Sicilia F., Gramegna G., Cervone F., De Lorenzo J. 2013. Oligogalacturonides: plant damage- associated molecular patterns and regulators of growth and development. *Frontiers in Plant Science* 4, article 49: 1-9.
- Ferrier T., Matus J.T., Jin J., Riechmann J.L. 2011. *Arabidopsis* paves the way: genomic and network analyses in crops. *Current Opinion in Biotechnology* 22:260–270.
- Fiore A., Dall'Osto L., Cazzaniga S., Diretto G., Giuliano G., Bassi R. 2012. A quadruple mutant of *Arabidopsis* reveals a β -carotene hydroxylation activity for *LUT1/CYP97C1* and a regulatory role of xanthophylls on determination of the PSI/PSII ratio. *BMC Plant Biology* 18: 12:50.

- Flor H.H.1956. The complementary genic systems in flax and flax rust. *Advances in Genetics* 8:29-54.
- Flor H.H.1971. Current status of the gene-for-gene concept. *Annual Review of Phytopathology* 9: 275–296.
- Flors C. and Nonell S. 2006. Light and singlet oxygen in plant defense against pathogens: phototoxic phenalenone phytoalexins. *Accounts of chemical research* 39 (5): 293-300.
- Fonseca S., Chini A., Hamberg M., Adie B., Porzel A., Kramell R., Miersch O., Wasternack C., Solano R. 2009. (+)-7-iso-jasmonoyl-L-isoleucine is the endogenous bioactive jasmonate. *Natural Chemical Biology* 5:344–50.
- Foyer C. and Noctor G. 2005. Redox homeostasis and antioxidant signaling: a metabolic interface between stress perception and physiological responses. *Plant Cell* 17: 1866-1875.
- Freeman B.C. and Beattie G.A. 2008. An overview of plant defenses against pathogens and herbivores .*The Plant Health Instructor*. DOI: 10.1094/PHI-I-2008-0226-01. Data accessed: nov 2013/2014.
- Freeman B.C. and Beattie G.A. 2009. Bacterial growth restriction during host resistance to *Pseudomonas syringae* is associated with leaf water loss and localized cessation of vascular activity in *Arabidopsis thaliana*. *Molecular Plant-Microbe Interaction* 7:857-867.
- Fu Z.Q., Ya, S., Saleh A., Wang W., Ruble J., Oka N., Mohan R., Spoel S., Tada Y., Zheng N., Dong X. 2012. NPR3 and NPR4 are receptors for the immune signal salicylic acid in plants. *Nature* 486: 228–232.
- Fu Z. and Dong X. 2013. Systemic acquired resistance: turning local infection into global defense. *Annual Review of Plant Biology* 64: 839-863.
- Gachon C. and Saindrenan P. 2004. Real-time PCR monitoring of fungal development in *Arabidopsis thaliana* infected by *Alternaria brassicicola* and *Botrytis cinerea*. *Plant Physiology and Biochemistry* 42: 367-371.
- Gadjev I., Stone J. M., Gechev T.S. 2008. Programmed cell death in plants: new insights into redox regulation and the role of hydrogen peroxide. *International Review of Cell and Molecular Biology* 270: 87-143.
- García-Olmedo F., Molina A., Alamillo J.M., Rodríguez-Palenzuela P. 1998. Plant defense peptides. *Biopolymers* 47(6):479-91.
- Gauthier A., Trouvelot S., Kelloniemi J., Frettinger P., Wendehenne D., Daire X., Joubert J.M., Ferrarini A., Delledonne M., Flors V.,Poinso B. 2014. The sulfated laminarin triggers a stress transcriptome before priming the SA- and ROS-dependent defenses during grapevine's induced resistance against *Plasmopara viticola*.*Plos One* 9 (2) e88145.

- Geng X., Cheng J., Gangadharan A., Mackey D. 2012. The coronatine toxin of *Pseudomonas syringae* is a multifunctional suppressor of *Arabidopsis* defense. *The Plant Cell* 24:4763–74.
- Geu-Flores, F., Møldrup, M.E., Böttcher, C., Olsen, C.E., Scheel, D., Halkier, B.A. 2011. Cytosolic g-glutamyl peptidases process glutathione conjugates in the biosynthesis of glucosinolates and camalexin in *Arabidopsis*. *Plant Cell* 23: 2456–2469.
- Gietz R.D. and Schiestl R.H. 2007. High-efficiency yeast transformation using the LiAc/SS carrier DNA/PEG method. *Nature Protocols* 2: 31–34.
- Ginglinger J.F., Boachon B., Höfer R., Paetz C., Köllner T.G., Miesch L., Lugan R., Baltenweck R., Mutterer G., Ullmann P., Beran F., Claudel P., Verstappen F., Fischer M.J.C., Karst F., Bouwmeester H., Miesch M., Schneider B., Gershenzon J., Ehlting J., Werck-Reichhart D. 2013. Gene Coexpression Analysis Reveals Complex Metabolism of the Monoterpene Alcohol Linalool in *Arabidopsis* Flowers. *The Plant Cell* 25: 4640–4657.
- Glawischnig E., Hansen B.G., Olsen C.E., Halkier B.A. 2004. Camalexin is synthesized from indole-3-acetaldoxime, a key branching point between primary and secondary metabolism in *Arabidopsis*. *Proceedings of the National Academy of Sciences USA* 101: 8245–8250.
- Glawischnig E. 2006. The role of cytochrome P450 enzymes in the biosynthesis of camalexin. *Biochemical Society Transactions* 34(Pt 6):1206-8.
- Glawischnig, E. 2007. Camalexin. *Phytochemistry* 68: 401–406.
- Glazebrook, J. and Ausubel, F.M. 1994 Isolation of phytoalexin-deficient mutants of *Arabidopsis thaliana* and characterization of their interactions with bacterial pathogens. *Proceedings of the National Academy of Sciences USA* 91: 8955- 8959.
- Glazebrook J., Chen W., Estes B., Chang H.S., Nawrath C., Métraux J.P., Zhu T., Katagiri F. 2003. Topology of the network integrating salicylate and jasmonate signal transduction derived from global expression phenotyping. *Plant Journal* 34:217–28.
- Glazebrook, J. 2005. Contrasting mechanisms of defense against biotrophic and necrotrophic pathogens. *Annual Review of Phytopathology* 43: 205-227.
- Gleadow R.M., Woodrow I.E. 2002. Constraints on effectiveness of cyanogenic glycosides in herbivore defense. *Journal of Chemical Ecology* 28(7):1301-13.
- Godard S., Slacanin I., Viret O., Gindro K. 2009. Induction of defence mechanisms in grapevine leaves by emodin- and anthraquinone-rich plant extracts and their conferred resistance to downy mildew. *Plant Physiology and Biochemistry* 47(9):827-37.
- Godiard L., Sauviac L., Dalbin N., Liaubet L., Callard D., Czernic P., Marco Y. 1998. *CYP76C2*, an *Arabidopsis thaliana* cytochrome P450 gene expressed during hypersensitive and developmental cell death. *FEBS letters* 438(3):245-9.

- González Collado I., Macías Sánchez A.J., Hanson J.R. 2007. Fungal terpene metabolites: biosynthetic relationships and the control of the phytopathogenic fungus *Botrytis cinerea*. *Natural Products Reports* 24: 674-686.
- Gonzalez-Coloma A., Lopez-Balboa C., Santana O., Reina M., Fraga B. 2011. Triterpene-based plant defenses. *Phytochemistry Reviews* 10:245–260.
- González-Lamothe R., Mitchell G., Gattuso M., Diarra M.S., Malouin F., Bouarab K. 2009. Plant Antimicrobial Agents and Their Effects on Plant and Human Pathogens. *International Journal of Molecular Sciences* 10: 3400-3419.
- Goode M.J. and Sasser M. 1980. Prevention - The key to controlling bacterial spot and speck of tomato. *Plant Disease* 64:831-34.
- Govrin E.M., Levine A. 2000. The hypersensitive response facilitates plant infection by the necrotrophic pathogen *Botrytis cinerea*. *Current Biology* 10(13):751-7.
- Graßmann, J. 2005. Terpenoids as plant antioxidants. *Vitamins and Hormones* 72:505-534.
- Graham M.A., Silverstein K.A.T, VandenBosch K.A. 2008. Defensin-like genes: genomic perspectives on a diverse superfamily in plants. *Crop Science* 48:S3–S11.
- Grant M. and Lamb C. 2006. Systemic immunity. *Current Opinion in Plant Biology* 9:414–420.
- Grayer R.J. and Kokubun T. 2001. Plant-fungal interactions: the search for phytoalexins and other antifungal compounds from higher plants. *Phytochemistry* 56: 253-263.
- Griebel T. and Zeier J. 2008. Light regulation and daytime dependency of inducible plant defenses in *Arabidopsis*: phytochrome signaling controls systemic acquired resistance rather than local defense. *Plant Physiology* 147: 790-801.
- Guengerich F.P., Martin M.V., Sohl C.D., and Cheng Q. 2009. Measurement of cytochrome P450 and NADPH–cytochrome P450 reductase. *Nature Protocols* 4(9):1245-1251.
- Guest D. and Brown J. 1997. Plant defences against pathogens. In: *Plant Pathogens and Plant Diseases*. J.F. brown and H.J. Ogle eds., endorsed by the Australasian Plant Pathology Society Inc. Chapter 17, pp 263- 286. http://www.appsnet.org/Publications/Brown_Ogle/. Data accessed January 2015.
- Guindon S., Dufayard J.F., Lefort V., Anisimova M., Hordijk W., Gascuel O. 2010. New algorithms and methods to estimate maximum-likelihood phylogenies: assessing the performance of PhyML 3.0. *Systematic Biology* 59(3):307-21.
- Gupta V., Willits M.G., Glazebrook J. 2000. *Arabidopsis thaliana* EDS4 contributes to salicylic acid (SA)-dependent expression of defense responses: evidence for inhibition of jasmonic acid signaling by SA. *Molecular Plant Microbe Interaction* 13 (5):503-11.
- Gust A.A., Biswas R., Lenz H.D., Rauhut T., Ranf S., Kemmerling B., Götz F., Glawischnig E., Lee J., Felix G., Nürnberger, T. 2007. Bacteria-derived peptidoglycans constitute pathogen-

associated molecular patterns triggering innate immunity in *Arabidopsis*. *Journal of Biological Chemistry* 282: 32338–32348.

- Hagemeyer J., Schneider B., Oldham N.J., Hahlbrock K. 2001. Accumulation of soluble and wall-bound indolic metabolites in *Arabidopsis thaliana* leaves infected with virulent and avirulent *Pseudomonas syringae* pathovar *tomato* strains. *Proceedings of the National Academy of Sciences USA* 98: 753–758.
- Haldane J.B.S. 1949. Disease and Evolution. *La Ricerca Scientifica Suppl* A19: 68–76.
- Hammond-Kosack K.E. and Jones J.D.G. 1997. Plant disease resistance genes. *Annual Review of Plant Physiology and Plant Molecular Biology* 48:575–607.
- Hansen C.H., Wittstock U., Olsen C.E., Hick A.J., Pickett J.A., Halkier B.A. 2001. Cytochrome P450 *CYP79F1* from *Arabidopsis* catalyzes the conversion of dihomomethionine and trihomomethionine to the corresponding aldoximes in the biosynthesis of aliphatic glucosinolates. *The Journal of Biological Chemistry* 276:11078–11085.
- Hasegawa M., Mitsuhashi I., Seo S., Imai T., Koga J., Okada K., Yamane H., Ohashi Y. 2010. Phytoalexin accumulation in the interaction between rice and the blast fungus. *Molecular Plant-Microbe Interactions* 23: 1000–1011.
- Heath M.C. 2000. Hypersensitive response-related death. *Plant Molecular Biology* 44, 321–334.
- Heil M. 1999. Systemic acquired resistance: available information and open ecological questions. *Journal of Ecology* 87: 341-346.
- Heil, M. 2014. Herbivore-induced plant volatiles: targets, perception and unanswered questions. *New Phytologist* 204: 297-306.
- Heitz T., Widemann E., Lugan R., Miesch L., Ullmann P., Désaubry L., Holder E., Grausem B., Kandel S., Miesch M., Werck-Reichhart D., Pinot F. 2012. Cytochromes P450 *CYP94C1* and *CYP94B3* catalyze two successive oxidation steps of plant hormone Jasmonoyl-isoleucine for catabolic turnover. *The Journal of Biological Chemistry* 287(9):6296-6306.
- Heller J. and Tudzynski P. 2011. Reactive oxygen species in phytopathogenic fungi: signaling, development, and disease. *Annual Review of Phytopathology* 49: 16.1-16.22.
- Helliwell C.A., Sheldon C.C., Olive M.R., Walker A.R., Zeevaart, J.A., Peacock W.J., Dennis E.S. 1998. Cloning of the *Arabidopsis* ent-kaurene oxidase gene GA3. *Proceedings of the National Academy of Sciences USA* 95:9019–9024.
- Helliwell C.A., Sullivan J.A., Mould R.M., Gray J.C., Peacock W.J., Dennis E.S. 2001. A plastid envelope location of *Arabidopsis* ent-kaurene oxidase links the plastid and endoplasmic reticulum steps of the gibberellin biosynthesis pathway. *The Plant Journal* 28:201–208.

- Hemm M.R., Ruegger M.O., Chapple C. 2003. The *Arabidopsis ref2* mutant is defective in the gene encoding *CYP83A1* and shows both phenylpropanoid and glucosinolate phenotypes. *The Plant Cell* 15:179–194.
- Hemmerlin A., Harwood J.L., Bach T.J. 2012. A raison d'être for two distinct pathways in the early steps of plant isoprenoid biosynthesis? *Progress in Lipid Research* 51:95–148.
- Hiruma K., Fukunaga S., Bednarek P., Pislewska-Bednarek M., Watanabe S., Narusaka Y., Shirasu K., Takano Y. 2013. Glutathione and tryptophan metabolism are required for *Arabidopsis* immunity during the hypersensitive response to hemibiotrophs. *Proceedings of the National Academy of Sciences USA* 110(23) 9589-9594.
- Höfer R., Dong L., André F., Ginglinger J.F., Lugan R., Gavira C., Grec S., Lang G., Memelink J., Van Der Krol S., Bouwmeester H., Werck-Reichhart, D. 2013. Geraniol hydroxylase and hydroxygeraniol oxidase activities of the *CYP76* family of cytochrome P450 enzymes and potential for engineering the early steps of the (seco)iridoid pathway. *Metabolic Engineering* 20: 221–232.
- Höfer R., Boachon B., Renault H., Gavira C., Miesch L., Iglesias J., Ginglinger J.F., Allouche L., Miesch M., Grec S., Larbat R., Werck-Reichhart D. 2014. Dual function of the cytochrome P450 *CYP76* family from *Arabidopsis thaliana* in the metabolism of monoterpenols and phenylurea herbicides. *Plant Physiology* 66(3):1149-61.
- Holz G.; Coertze S., Williamsom B. 2007. The ecology of *Botrytis* on plant surfaces. In: *Botrytis: biology, pathology and control*, 9-27 (Chapter 2) .Elad et al. (eds.).
- Hopkins R.J., van Dam N.M., van Loon J.J.A. 2009. Role of glucosinolates in insect-plant relationships and multitrophic interactions. *Annual Review of Entomology* 54:57–83.
- Huang J., Cardoza Y. J., Schmelz E. A., Raina R., Engelberth J., Tumlinson J. H. 2003. Differential volatile emissions and salicylic acid levels from tobacco plants in response to different strains of *Pseudomonas syringae*. *Planta* 217:767-775.
- Huang J., Gu M., Lai Z., Fan B., Shi K., Zhou Y.H., Yu J.Q., Chen Z. 2010. Functional analysis of the *Arabidopsis* PAL gene family in plant growth, development, and response to environmental stress. *Plant Physiology* 153(4):1526-38.
- Huang T., Jander G., de Vos M. 2011. Non-protein amino acids in plant defense against insect herbivores: Representative cases and opportunities for further functional analysis. *Phytochemistry* 72 (13): 1531–1537.
- Huang M., Sanchez-Moreiras A.M., Abel C., Sohrabi R., Lee S., Gershenzon J., Tholl D. 2012. The major volatile organic compound emitted from *Arabidopsis thaliana* flowers, the sesquiterpene (E)- β -caryophyllene, is a defense against a bacterial pathogen. *New Phytologist* 193 (4):997-1008.

- Hull A.K., Vij R., Celenza J.L. 2000. *Arabidopsis* cytochrome P450s that catalyse the first step of tryptophan-dependent indole-3-acetic acid biosynthesis. *Proceeding of the National Academy of Sciences* 97:2379–2384.
- Janzen D.J., Allen L.J., MacGregor K.B. and Bown A.W. 2001. Cytosolic acidification and β -aminobutyric acid synthesis during the oxidative burst in isolated *Asparagus sprengeri* mesophyll cells. *Canadian Journal of Botany* 79: 438–43.
- Jeandet P., Hébrard C., Deville M.A., Cordelier S., Dorey S., Aziz A., Crouzet J. 2014. Deciphering the role of phytoalexins in plant-microorganism interactions and human health. *Molecules* 19: 18033-18056.
- Jefferson R.A., Kavanagh T.A., Bevan M.W. 1987. GUS fusions: Beta-glucuronidase as a sensitive and versatile gene fusion marker in higher plants. *EMBO Journal* 6: 3901–3907.
- Jelenska J., Yao N., Vinatzer B.A., Wright C.M., Brodsky J.L., Greenberg J.T. 2007. A J domain virulence effector of *Pseudomonas syringae* remodels host chloroplasts and suppresses defenses. *Current Biology* 17, 499–508.
- Jones J.D.G. and Dangl J.L. 2006. The plant immune system. *Nature* 444: 323-329.
- Jung H.W., Tschaplinski T.J., Wang L., Glazebrook J., Greenberg, J.T. 2009. Priming in systemic plant immunity. *Science* 324: 89–91.
- Kachroo A. and Kachroo P. 2009. Fatty Acid-derived signals in plant defense. *Annual Review of Phytopathology* 47:153-76.
- Kagan I.A., Hammerschmidt R. 2002. *Arabidopsis* ecotype variability in camalexin production and reaction to infection by *Alternaria brassicicola*. *Journal of Chemical Ecology* 28:2121–2140.
- Kangasjarvi S., Neukermans J., Li S., Aro E.M., Noctor G. 2012. Photosynthesis, photorespiration, and light signalling in defence responses. *Journal of Experimental Botany* 63 (4): 1619-1636.
- Katagiri, F. Thilmony, R., Heb, S.H. 2002. The *Arabidopsis Thaliana-Pseudomonas Syringae* Interaction. *The Arabidopsis Book* 20(1): 1.
- Katoh A., Ohki H., Inai K., Hashimoto T. 2005. Molecular regulation of nicotine biosynthesis. *Plant Biotechnology* 22:389–92.
- Katsir L., Schilmiller A.L., Staswick P.E., He S.Y., Howe G.A. 2008. COI1 is a critical component of a receptor for jasmonate and the bacterial virulence factor coronatine. *Proceedings of the Natural Academy of Science USA* 105:7100–5.
- Kim Y.M., Lee C.H., Kim H.G., Lee H.S. 2004. Anthraquinones isolated from *Cassia tora* (*Leguminosae*) seeds show an antifungal property against phytopathogenic fungi. *Journal of Agriculture and Food Chemistry* 52:6096–6100.

- Kim G.T., Fujioka S., Kozuka T., Tax F.E., Takatsuto S., Yoshida S., Tsukaya H. 2005. *CYP90C1* and *CYP90D1* are involved in different steps in the brassinosteroid biosynthesis pathway in *Arabidopsis thaliana*. *Plant Journal* 41:710–721.
- Kim M.G., da Cunha L., McFall A.J., Belkhadir Y., DebRoy S., Dangl J.L., Mackey D. 2005. Two *Pseudomonas syringae* typeIII effectors inhibit RIN4-regulated basal defense in *Arabidopsis*. *Cell* 121: 749–759.
- Kim J., DellaPenna D. 2006. Defining the primary route for lutein synthesis in plants: the role of *Arabidopsis* carotenoid beta-ring hydroxylase *CYP97A3*. *Proceedings of the National Academy of Sciences USA* 103:3474–3479.
- Kishimoto K., Matsui K., Ozawa R., Takabayashi J. 2006. Analysis of defensive responses activated by volatile allo-ocimene treatment in *Arabidopsis thaliana*. *Phytochemistry* 67:1520–1529.
- Kitaoka N., Matsubara T., Sato M., Takahashi K., Wakuta S., Kawaide H., Matsui H., Nabeta K. Matsuura H. 2011. *Arabidopsis CYP94B3* encodes jasmonoyl isoleucine 12-hydroxylase, a key enzyme in the oxidative catabolism of jasmonate. *Plant Cell and Physiology*: 52, 1757-1765.
- Klarzynski O., Descamps V., Plesse B., Yvin J.C., Kloareg B., Fritig B.2003. Sulfated fucan oligosaccharides elicit defense responses in tobacco and local and systemic resistance against tobacco mosaic virus. *Molecular Plant Microbe Interaction* 16(2):115-22.
- Klein A.P.,Anarat-Cappillino G., Sattely E.S. 2013. Minimum set of cytochromes P450 for reconstituting the biosynthesis of camalexin, a major *Arabidopsis* antibiotic. *Angewandte Chemie International Edition* 52 (51): 13625–13628.
- Kleinboelting N., Huep G., Kloetgen A., Viehoveer P., Weisshaar B. 2012. GABI-Kat Simple Search: new features of the *Arabidopsis thaliana* T-DNA mutant database. *Nucleic Acids Research* 40 (Database issue): D1211-1215.
- Kliebenstein D. 2004. Secondary metabolites and plant/environment interactions: a view through *Arabidopsis thaliana* tinted glasses. *Plant Cell and Environment* 27: 675–684.
- Kliebenstein D.J., Rowe H.C. and Denby K.J. 2005. Secondary metabolites influence *Arabidopsis/Botrytis* interactions: variation in host production and pathogen susceptibility. *Plant Journal* 44(1):25-36.
- Kliebenstein D.J. and Rowe H.C. 2008. Ecological costs of biotrophic versus necrotrophic pathogen resistance, the hypersensitive response and signal transduction. *Plant Science* 174(6)551-6.
- Klingenberg M. 1958. Pigments of rat liver microsomes. *Archives of biochemistry and biophysics* 75: 376-386.

- Köllner T.G., Lenk C., Schnee C., Köpke S., Lindemann P., Gershenzon J. and Degenhardt J. 2013. Localization of sesquiterpene formation and emission in maize leaves after herbivore damage. *BMC Plant Biology* 13:15.
- Koo A.J., Cooke T.F., Howe G.A. 2011. Cytochrome P450 *CYP94B3* mediates catabolism and inactivation of the plant hormone jasmonoyl-L-isoleucine. *Proceedings of the National Academy of Sciences USA* 108 (22):9298-303.
- Koornneef M. and Meinke D. 2010. The development of *Arabidopsis* as a model plant. *The Plant Journal* 61: 909-921.
- Kreis W. and Müller-Uri F. 2010. Biochemistry of sterols, cardiac glycosides, brassinosteroids, phytoecdysteroids and steroid saponins. *Annual Plant Reviews* 40: 304–363.
- Krings U. and Berger R.G. 2010. Terpene bioconversion: how does its future look? *Natural products communication* 5 (9): 1507-22.
- Kroymann, J. 2011. Natural diversity and adaptation in plant secondary metabolism. *Current Opinion in Plant Biology* 14:246–251.
- Kruskal W. H., Wallis W. A. 1952. Use of ranks in one-criterion variance analysis. *Journal of the American Statistics Association* 47: 583–621.
- Kushiro T., Okamoto M., Nakabayashi K., Yamagishi K., Kitamura S., Asami T., Hirai N., Koshiba T., Kamiya Y., Nambara E. 2004. The *Arabidopsis* cytochrome P450 *CYP707A* encodes ABA 8-hydroxylases: key enzymes in ABA catabolism. *EMBO Journal* 23:1647–1656.
- Kvitko B.H., Park D.H., Velasquez A.C., Wei C.F., Russell A.B., Martin G. B., Schneider D. J., Collmer A. 2009. Deletions in the repertoire of *Pseudomonas syringae* pv. *tomato* DC3000 type III secretion effector genes reveal functional overlap among effectors. *PLoS Pathogens* 5:e1000388.
- Lait C.G., Alborn H.T., Teal P.E.A., Tumlinson J.H. 2003 Rapid biosynthesis of N-linolenoyl-L-glutamine, an elicitor of plant volatiles, by membrane-associated enzyme(s) in *Manduca sexta*. *Proceedings of the National Academy of Sciences USA* 100 (12):7027–7032.
- Lamb C. and Dixon R.A. 1997. The oxidative burst in plant disease resistance. *Annual Review of Plant Physiology. Plant Molecular Biology* 48: 251–275.
- Langlois-Meurinne M., Gachon C.M.M., Saindrenan P. 2005. Pathogen-responsive expression of glycosyltransferase genes *UGT73B3* and *UGT73B5* is necessary for resistance to *Pseudomonas syringae* pv *tomato* in *Arabidopsis*. *Plant Physiology* 139(4): 1890–1901.
- Lapin D. and Van den Ackerveken G. 2013. Susceptibility to plant disease: more than a failure of host immunity. *Trends in Plant Science* 18 (10): 546-554.

- Lazniewska J., Macioszek V.K., Kononowicz A.K. 2012. Plant-fungus interface: the role of surface structures in plant resistance and susceptibility to pathogenic fungi. *Physiological and Molecular Plant Pathology* 78: 24e30.
- Laudert D., Pfannschmidt U., Lottspeich F., Hollander-Czytko H., Weiler E.W. 1996. Cloning, molecular and functional characterization of *Arabidopsis thaliana* allene oxide synthase (*CYP74*), the first enzyme of the octadecanoid pathway to jasmonates. *Plant Molecular Biology* 31:323–335.
- Lee A.H., Hurley B., Felsensteiner C., Yea C., Ckurshumova W., Bartetzko V., Wang P.W., Quach V., Lewis, J.D., Liu Y.C., Bo F., Angers S., Wilde A., Guttman D.S., Desveaux D. 2012. A bacterial acetyltransferase destroys plant microtubule networks and blocks secretion. *PLoS Pathogens* 8:e1002523.
- Leon-Reyes A., Spoel S.H., De Lange E.S., Abe H., Kobayashi M., Tsuda S., Millenaar F.F., Welschen R.A.M., Ritsema T., Pieterse C.M.J. 2009. Ethylene modulates the role of NONEXPRESSOR OF PATHOGENESIS-RELATED GENES1 in cross talk between salicylate and jasmonate signaling. *Plant Physiology* 149:1797–809.
- Lewis, D.F.V. 2002. Oxidative stress: the role of cytochromes P450 in oxygen activation. *Journal of Chemical Technology and Biotechnology* 77(10): 1095-1100.
- Li J., Brader G., Palva E.T. 2004. The WRKY70 transcription factor: a node of convergence for jasmonate-mediated and salicylate mediated signals in plant defence. *The Plant Cell* 16:319–331.
- Li L., Chang Z., Zhiqiang Pan Z., Fu Z.Q. and Wang X. 2008. Modes of heme binding and substrate access for cytochrome P450 *CYP74A* revealed by crystal structures of allene oxide synthase. *Proceeding of the National Academy of Sciences* 10 (37):13883-13888.
- Li-Beisson Y., Pollard M., Sauveplane, V., Pinot F., Ohlrogge, J. and Beisson, F. 2009. Nanoridges that characterize the surface morphology of flowers require the synthesis of cutin polyester. *Proceeding of the National Academy of Sciences USA* 106:22008.
- Lichtenthaler H.K. 2000. Non-mevalonate isoprenoid biosynthesis: enzymes, genes and inhibitors. *Biochemical Society Transactions* 28: 785–9.
- Lindeberg M., Cunnac S., Collmer A. 2012. *Pseudomonas syringae* type III effector repertoires: last words in endless arguments. *Trends in Microbiology* (4):199-208.
- Linstrom P.J. and Mallard W.G. 2014. NIST Chemistry WebBook, NIST Standard Reference Database Number 69, National Institute of Standards and Technology, Gaithersburg MD, 20899, retrieved from <http://webbook.nist.gov> data accessed: different dates.

- Lisón P., Tárraga S., López-Gresa P., Saurí A., Torres C., Campos L., Bellés J.M., Conejero V., Rodrigo I. 2013. A noncoding plant pathogen provokes both transcriptional and posttranscriptional alterations in tomato. *Proteomics* 13 (5): 833-844.
- Liu P.P., von Dahl C.C., Klessig, D.F. 2011. The extent to which methyl salicylate is required for signaling systemic acquired resistance is dependent on exposure to light after infection. *Plant Physiology* 157: 2216–2226.
- Lomáscolo S.B., Levey D.J., Kimball R.T., Bolker B.M., Alborn H.T. 2010. Dispersers shape fruit diversity in *Ficus* (*Moraceae*). *Proceeding of the National Academy of Sciences USA* 107: 14668–14672.
- López-Gresa M.P., Maltese F., Bellés J.M., Conejero V., Kim H.K., Choi Y.H., Verpoorte R. 2010. Metabolic response of tomato leaves upon different plant–pathogen interactions. *Phytochemical Analysis* 21:89–94.
- Lorenzo O., Solano R. 2005. Molecular players regulating the jasmonate signaling network. *Current Opinion in Plant Biology* 8:532–540.
- Lorrain S., Vaillieu F., Balague C., Roby D. 2003. Lesion mimic mutants: keys for deciphering cell death and defense pathways in plants? *Trends in Plant Science* 8: 263–271.
- Luna E. and Ton J. 2012. The epigenetic machinery controlling transgenerational systemic acquired resistance. *Plant Signal and Behaviour* 7: 615–618.
- Luna E., Bruce T.J.A., Roberts M.R., Flors V., Ton J. 2012. Next generation systemic acquired resistance. *Plant Physiology* 158: 844–853.
- Lv Q., Cheng R. and Shi T. 2014. Regulatory network rewiring for secondary metabolism in *Arabidopsis thaliana* under various conditions. *BMC Plant Biology* 14:180.
- Maffei M.E., Gertsch J., Appendino G. 2011. Plant volatiles: production, function and pharmacology. *Natural Product Reports* 28:1359–80.
- Mahibbur Rahman M. and Govindarajulu Z. 1997. A modification of the test of Shapiro and Wilk for normality. *Journal of Applied Statistics* 24 (2): 219-236.
- Maekawa T., Cheng W., Spiridon L.N., Töller A., Lukasik E., Saijo Y., Liu P., Shen Q.H., Micluta M.A., Somssich I.E., Takken F.L., Petrescu A.J., Chai J., Schulze-Lefert P. 2011. Coiled-coil domain-dependent homodimerization of intracellular MLA immune receptors defines a minimal functional module for triggering. *Cell Host Microbe* 17, 9(3):187-99.
- Manners J. M., Penninckx I. A., Vermaere K., Kazan K., Brown R. L., Morgan A., Maclean D. J., Curtis M. D., Cammue B. P., Broekaert W. F. 1998. The promoter of the plant defensin gene *PDF1.2* from *Arabidopsis* is systemically activated by fungal pathogens and responds to methyl jasmonate but not to salicylic acid. *Plant Molecular Biology* 38: 1071–1080.
- [Pubmed Abstract](#) | [Pubmed Full Text](#) | [CrossRef Full Text](#)

- Manosalva P.M., Park S.W., Forouhar F., Tong L., Fry W.E., Klessig D.F. 2010. Methyl Esterase 1 (StMES1) is required for systemic acquired resistance in potato. *Molecular Plant-Microbe Interaction* 23: 1151–1163.
- Martin J.J., Pitera D.J., Withers S.T., Newmann J.D., Keasling J.D. 2003. Engineering a mevalonate pathway in *Escherichia coli* for production of terpenoids. *Nature Biotechnology* 21:796–802.
- Massoud K., Barchietto T., Le Rudulier T., Pallandre L., Didierlaurent L., Garmier M., Ambard-Bretteville F., Seng J.M., Saindrenan P. 2012. Dissecting phosphite-induced priming in *Arabidopsis* infected with *Hyaloperonospora arabidopsidis*. *Plant Physiology* 159(1):286-98.
- Mauch F., Mauch-Mani B., Boller T.1988. Antifungal hydrolases in pea tissue II. Inhibition of fungal growth by combinations of chitinase and beta-1,3-glucanase. *Plant Physiology* 88: 936-942.
- Mauch-Mani B. and Slusarenko A. 1993. *Arabidopsis* as a model host for studying plant-pathogen interactions. *Chemical Review* 104(9):3947-80.
- Mauch-Mani B. and Slusarenko A. 1996. Production of salicylic acid precursors is a major function of phenylalanine ammonia-lyase in the resistance of *Arabidopsis* to *Peronospora parasitica*. *Plant cell* 8: 203-212.
- Mayda E., Mauch-Mani, B. Vera P. 2000. *Arabidopsis* dth9 mutation identifies a gene involved in regulating disease susceptibility without affecting salicylic acid–dependent responses. *The Plant Cell* 12: 2119-2128.
- Mazid M., Khan T.A., Mohammad F. 2011. Role of secondary metabolites in defense mechanism in plants. *Biology and medicine* 3 (2) special issue: 232:249.
- Melotto M., Underwood W., Koczan J., Nomura K., He S.Y.. 2006. Plant stomata function in innate immunity against bacterial invasion. *Cell* 126:969–80.
- Ménard R., Alban S., de Ruffray P., Jamois P., Franz G., Fritig B., Yvinc J.C. and Kauffmann S. 2004. β -1, 3 Glucan Sulfate, but Not β -1,3 Glucan, Induces the Salicylic Acid Signaling Pathway in Tobacco and *Arabidopsis*. *The Plant Cell* 16(11): 3020-3032.
- Méndez-Bravo A., Calderón-Vázquez C., Ibarra-Laclette E., Raya-González J., Ramírez-Chávez E., Molina-Torres J.,Guevara-García A.A., López-Bucio J. and Herrera-Estrella L. 2011. Alkamides activate jasmonic acid biosynthesis and signaling pathways and confer resistance to *Botrytis cinerea* in *Arabidopsis thaliana*. *PLoS One* 6(11): e27251.
- Mengiste T. 2012. Plant immunity to necrotrophs. *Annual Review of Phytopathology* 50:267-94.

- Mert-Türk F., Bennet M.H., Mansfield J.W., Holub E.B. 2003. Camalexin accumulation in *Arabidopsis thaliana* following abiotic elicitation or inoculation with virulent or avirulent *Hyaloperonospora parasitica*. *Physiological and Molecular Plant Pathology* 62: 137–145.
- Mert-Türk F. 2006. Saponins versus plant fungal pathogens. *Journal of Cell and Molecular Biology* 5: 13-17.
- Meunier B., de Visser S.P., Shaik S. 2004. Mechanism of oxidation reactions catalysed by cytochrome p450 enzymes. *Trends in Microbiology* 1: 265 - 270.
- Mezencev R., Mojzis J., Pilatova M., Kutschy P. 2003. Antiproliferative and cancer chemopreventive activity of phytoalexins: focus on indole phytoalexins from crucifers. *Neoplasma* 50: 239–245.
- Mezencev R., Galizzi M., Kutschy P., Docampo R. 2009. *Trypanosoma cruzi*: Antiproliferative effect of indole phytoalexins on intracellular amastigotes *in vitro*. *Experimental Parasitology* 122: 66-69.
- Mezencev R., Updegrove T., Kutschy P., Repovská M., McDonald J.F. 2011. Camalexin induces apoptosis in Jurkat T-leukemia cells by increased concentration of reactive oxygen species and activation of caspases-8 and -9. *Journal of Natural Medicine* 65(3-4): 488-499.
- Mierziak J., Kostyn K. and Kulma A. 2014. Flavonoids as Important Molecules of Plant Interactions with the Environment. *Molecules* 19: 16240-16265.
- Mikkelsen M.D., Hansen C.H., Wittstock U., Halkier B.A. 2000. Cytochrome *CYP79B2* from *Arabidopsis* catalyses the conversion of tryptophan to indole-3-acetaldoxime, a precursor of indole glucosinolates and indole-3-acetic acid. *Journal of Biological Chemistry* 275:33712–33717.
- Miller J.A., Thompson P.A., Hakin I.A., Sherry Chow H.H., Thomson C.A. 2011. D-Limonene: a bioactive food component from Citrus and evidence for a potential role in breast cancer prevention and treatment. *Oncology Review* 5:31–42.
- Millet Y.A., Danna C.H., Clay N.K., Songnuan W., Simon M.D., Werck-Reichhart D., Ausubel F.M. 2010. Innate immune responses activated in *Arabidopsis* roots by microbe-associated molecular patterns. *The Plant Cell* 22(3):973-90.
- Millet, Y.A. 2009. Suppression de la réponse immunitaire des racines d'*Arabidopsis thaliana* par la phytotoxine coronatine produite par *Pseudomonas syringae* and étude fonctionnelle du cytochrome P450 *CYP76C2* d'*Arabidopsis thaliana* impliqué dans la réponse aux pathogènes. Thèses de doctorat, Université de Strasbourg.
- Mithöfer A., Wanner G., Boland W. 2005. Effect of feeding *Spodoptera littoralis* on lima bean leaves: II. Continuous mechanical wounding resembling insect feeding is sufficient to elicit herbivory-related volatile emissions. *Plant Physiology* 137:1160–1168.

- Mithöfer A. and Boland W. 2012. Plant defense against herbivores: chemical aspects. *Annual Review of Plant Biology* 63:431-50.
- Mittler R., Vanderauwera S., Suzuki N., Miller G., Tognetti V.B., Vandepoele K., Gollery M., Shulaev V., Van Breusegem F. 2011. ROS signaling: the new wave? *Trends in Plant Science* 16 (6): 300-309.
- Miura K. and Tada Y. 2014. Regulation of water, salinity, and cold stress responses by salicylic acid. *Frontiers in Plant Science* 5, article 4, pp12.
- Mizutani M., Ward E., Ohta D. 1998. Cytochrome P450 superfamily in *Arabidopsis thaliana*: isolation of cDNAs, Differential Expression, and RFLP mapping of multiple cytochromes P450. *Plant Molecular Biology* 37: 39–52.
- Møldrup M.E., Geu-Flores F., Halkier B.A. 2013. Assigning gene function in biosynthetic pathways: camalexin and beyond. *Plant Cell* 25: 360-367.
- Monte I., Hamberg M., Chini A., Gimenez-Ibanez S., García-Casado G., Porzel A., Pazos F., Boter M., Solano R. 2014. Rational design of a ligand-based antagonist of jasmonate perception. *Nature Chemical Biology* 10(8):671-676.
- Moody C.J., Roffey J.R.A., Stephens M.A., Stratford I.J. 1997. Synthesis and cytotoxic activity of indole thiazoles. *Anticancer Drugs* 8: 489–499.
- Morant M., Bak S., Moller B. L., Werck-Reichhart D. 2003. Plant cytochromes P450: tools for pharmacology, plant protection and phytoremediation. *Current Opinion in Biotechnology* 14(2):151-62.
- Morel J.B. and Dangl J.L. 1997. The hypersensitive response and the induction of cell death in plants. *Cell Death and Differentiation* 4: 671-683.
- Muckenschnabel I., Williamson B., Goodman B.A., Lyon G.D., Stewart D., Deighton N. 2001. Markers for oxidative stress associated with soft rots in French beans (*Phaseolus vulgaris*) infected by *Botrytis cinerea*. *Planta* 212:376–381.
- Mulema J.M., Denby K.J. 2012. Spatial and temporal transcriptomic analysis of the *Arabidopsis thaliana*-*Botrytis cinerea* interaction. *Molecular Biology Reports* 39(4):4039-49.
- Müller, K.O. and Börger, H. 1940. Experimentelle Untersuchungen über die Phytophthora-Resistenz, Kartoffel. *Arbeiten aus der Biologischen Reichsanstalt für Land- und Forstwirtschaft* 23, 189-231.
- Munro A.W., Girvan H.M., Mason A.E., Dunford A.J., McLean K.J. 2013. What makes a P450 tick? *Trends in Biochemical Sciences* 38:140-150.
- Mur L.A.J., Kenton P., Atzorn R., Miersch O., Wasternack C. 2005. The outcomes of concentration-specific interactions between salicylate and jasmonate signaling include

- synergy, antagonism, and oxidative stress leading to cell death. *Plant Physiology* 140 (1):249-262.
- Mur L.A.J., Kenton P., Lloyd A.J., Ougham H., Prats E. 2008. The hypersensitive response; the centenary is upon us but how much do we know? *Journal of Experimental Botany* 59 (3): 501–520.
 - Nafisi M., Sønderbye I.E., Hansen B.G., Geu F., Eldin H.H.N., Nielsen M.H.N., Jensen N.B., Li J., Halkier B.A. 2006. Cytochromes P450 in the biosynthesis of glucosinolates and indole alkaloids. *Phytochemistry Reviews* 5 (2-3): 331-346.
 - Nafisi M., Goregaoker S., Botanga C.J., Glawischnig E., Olsen C.E., Halkier B.A., Glazebrook J. 2007. *Arabidopsis* cytochrome P450 monooxygenase 71A13 catalyzes the conversion of indole-3-acetaldoxime in camalexin synthesis. *Plant Cell* 19: 2039–2052.
 - Nakamura M., Satoh T., Tanaka S., Mochizuki N., Tokota T., Nagatani A. 2005. Activation of the cytochrome P450 gene, *CYP72C1*, reduces the levels of active brassinosteroids *in vivo*. *Journal of Experimental Botany* 56:833–840.
 - Narusaka Y, Narusaka M, Seki M, Umezawa T, Ishida J, Nakajima M, Enju A, Shinozaki K .2004. Crosstalk in the responses to abiotic and biotic stresses in *Arabidopsis*: analysis of gene expression in cytochrome P450 gene superfamily by cDNA microarray. *Plant Molecular Biology* 55: 327–342.
 - Naur P., Petersen B.L., Mikkelsen M.D., Bak S., Rasmussen H., Olsen C.E., Halkier BA .2003. *CYP83A1* and *CYP83B1*, two non-redundant cytochrome P450 enzymes metabolizing oximes in the biosynthesis of glucosinolates in *Arabidopsis*. *Plant Physiology* 133:63–72.
 - Návarová H., Bernsdorff F., Döring A.C., Zeier J. 2012. Pipecolic acid, an endogenous mediator of defense amplification and priming, is a critical regulator of inducible plant immunity. *Plant Cell* 24: 5123–5141.
 - Navarro L., Dunoyer P., Jay F., Arnold B., Dharmasiri N., Estelle M., Voinnet O., Jones J.D. 2006. A plant miRNA contributes to antibacterial resistance by repressing auxin signaling. *Science* 312:436–39.
 - Navarro L., Bari R., Achard P., Lison P., Nemri A., Harberd N.P., Jones J.D. 2008. DELLAs control plant immune responses by modulating the balance of jasmonic acid and salicylic acid signaling. *Current Biology* 18:650–55.
 - Nawrath C., Métraux J.P. 1999. Salicylic acid induction-deficient mutants of *Arabidopsis* express PR-2 and PR-5 and accumulate high levels of camalexin after pathogen inoculation. *The Plant Cell* 11: 1393-1404.

- Ndamukong I., Abdallat A.A., Thurow C., Fode B., Zander M., Weigel R., Gatz C. 2007. SA-inducible *Arabidopsis* glutaredoxin interacts with TGA factors and suppresses JA-responsive PDF1.2 transcription. *Plant Journal* 50:128–39.
- Nelson D. 2004. Cytochrome P450 nomenclature. *Methods in Molecular Biology* 320:1-10.
- Nelson D.R., Schuler M.A., Paquette S.M., Werck-Reichhart D. and Bak S. 2004. Comparative genomics of rice and *Arabidopsis*. Analysis of 727 cytochrome P450 genes and pseudogenes from a monocot and a dicot. *Plant Physiology* 135, 756–757.
- Nelson D. 2009. The Cytochrome P450 Homepage. *Human Genomics* 4: 59-65.
- Nelson D. and Werck-Reichhart D. 2011. A P450-centric view of plant evolution. *Plant Journal* 66(1):194-211.
- Nishida N., Tamotsu S., Nagata N., Saito C., Sakai A. 2005. Allelopathic effects of volatile monoterpenoids produced by *Salvia leucophylla*: inhibition of cell proliferation and DNA synthesis in the root apical meristem of *Brassica campestris* seedlings. *Journal of Chemical Ecology* 31:1187–1203.
- Norsworthy J.K., Malik M.S., Jha P. and Riley M.B. 2007. Suppression of *Digitaria sanguinalis* and *Amaranthus palmeri* using autumn-sown glucosinolate-producing cover crops in organically grown bell pepper. *Weed Research* 47: 425–32.
- Nour-Eldin H.H., Hansen B.G., Norholm M.H.H., Jensen J.K., Halkier B.A. 2006. Advancing uracil-excision based cloning towards an ideal technique for cloning PCR fragments. *Nucleic Acids Research* 34: 122.
- Omura T. and Sato R. 1964. Carbon monoxide binding pigment of liver microsomes. I. Evidence for its hemoprotein nature. *Journal of Biological Chemistry* 239: 2370-2378.
- Ohm R.O., Feau N., Henrissat B., Schoch C.L., Horwitz B.A., Barry K.W., Condon B.J., Copeland A.C., Dhillon B., Glaser F., Hesse C.N., Kosti I., LaButti K., [...], Grigoriev I.V. 2012. Diverse lifestyles and strategies of plant pathogenesis encoded in the genomes of eighteen dothideomycetes fungi. *PLoS Pathogens* 8 (12): e1003037.
- Ohnishi T., Godza B., Watanabe B., Fujioka S., Hategan L., Ide K., Shibata K., Yokota T., Szekeres M., Mizutani M. 2012. *CYP90A1/CPD*, a brassinosteroid biosynthetic cytochrome P450 of *Arabidopsis*, catalyses C-3 oxidation. *Journal of Biological Chemistry* 287:31551-31560.
- Okamoto M., Kuwahara A., Seo M., Kushiro T., Asami T., Hirai N., Kamiya Y., Koshihara T., and Nambara E. 2006. *CYP707A1 and CYP707A2*, Which Encode Abscisic Acid 8-Hydroxylases, Are Indispensable for Proper Control of Seed Dormancy and Germination in *Arabidopsis*. *Plant Physiology* 141: 97–107.

- Okamoto M., Tanaka Y., Abrams S.R., Kamiya Y., Seki M., Nambara E. 2009. High humidity induces abscisic acid 8'-hydroxylase in stomata and vasculature to regulate local and systemic abscisic acid responses in *Arabidopsis*. *Plant Physiology* 149:825-834.
- Okamoto M., Kushiro T., Jikumaru Y. Abrams S.R., Kamiya Y., Seki M., Nambara E. 2011. ABA 9'-hydroxylation is catalysed by *CYP707A* in *Arabidopsis*. *Phytochemistry* 72:717-722.
- Osborn R.W., Desamblanx G.W., Thevissen K., Goderis I., Torrekens S., Vanleuven F., Attenborough S., Rees S., and Broekaert W.F. 1995. Isolation and characterization of plant defensins from seeds of *Asteraceae*, *Fabaceae*, *Hippocastanaceae* and *Saxifragaceae*. *FEBS Letters* 368(2):257-262.
- Otah D. and Mizutani M. 1998. Plant geraniol 10-hydroxylase and DNA coding thereof. US patent 5,753, 507.
- Pandey S.P., Roccaro M., Schön M., Logemann E., Somssich I.E. 2010. Transcriptional reprogramming regulated by WRKY18 and WRKY40 facilitates powdery mildew infection of *Arabidopsis*. *Plant Journal* 64(6):912-23.
- Park J.H., Halitschke R., Kim H.B., Baldwin I.T., Feldmann K.A., Feyereisen R. 2002. A knock-out mutation in allene oxide synthase results in male sterility and defective wound signal transduction in *Arabidopsis* due to a block in jasmonic acid biosynthesis. *Plant Journal* 31:1-12.
- Park S.W., Kaimoyo E., Kumar D., Mosher S., Klessig, D.F. 2007. Methyl salicylate is a critical mobile signal for plant systemic acquired resistance. *Science* 318: 113–116.
- Pastor V., Vicent C., Cerezo M., Mauch-Mani B., Dean J., Flors V. 2012. Detection, characterization and quantification of salicylic acid conjugates in plant extracts by ESI tandem mass spectrometric techniques. *Plant Physiology and Biochemistry* 53: 19-26.
- Paxton J.D. 1981. Phytoalexins a working redefinition. *Phytopathology Z* 101:106-109.
- Pfaffl M.W. 2001. A new mathematical model for relative quantification in real-time RT-PCR. *Nucleic Acids Research* 29: e45.
- Papadopoulou K., Melton R. E., Leggett M., Daniels M. J., Osbourn A.E. 1999. Compromised disease resistance in saponin-deficient plants. *Proceeding of the National Academy of Sciences* 96 (22): 12923-12928.
- Pauwels L. and Goossens A. 2011. The JAZ Proteins: a crucial interface in the jasmonate signaling cascade. *The Plant Cell* 23 (9): 3089-3100.
- Pedras, M. S. C., Ahiahonu, P. W. K. 2002. Probing the phytopathogenic stem rot fungus with phytoalexins and analogs: unprecedented glucosylation of camalexin and 6-methoxycamalexin. *Bioorganic Medicinal Chemistry* 10: 3307-3312.

- Pedras, M. S. C., Jha, M., Okeola, O. G. 2005. Camalexin induces detoxification of the phytoalexin Brassinin in the plant pathogen *Leptosphaeria maculans*. *Phytochemistry* 66: 2609-2616.
- Pedras M.S., Hossain S., Snitynsky R.B. 2011. Detoxification of cruciferous phytoalexins in *Botrytis cinerea*: spontaneous dimerization of a camalexin metabolite. *Phytochemistry* 72 (2-3):199-206.
- Peters, R.J.2006. Uncovering the complex metabolic network underlying diterpenoid phytoalexin biosynthesis in rice and other cereal crop plants. *Phytochemistry* 67: 2307-2317.
- Persson M., Staal J., Oide S., Dixelius C. 2009. Layers of defense responses to *Leptosphaeria maculans* below the RLM1- and camalexin-dependent resistances. *New Phytologist* 182: 470-482.
- Petersen M., Brodersen P., Naested H., Andreasson E., Lindhart U., Johansen B., Nielsen H.B., Lacy M., Austin M.J., Parker J..E, Sharma S.B., Klessig D.F., Martienssen R., Mattsson O., Jensen A.B., Mundy J. 2000. *Arabidopsis* map kinase 4 negatively regulates systemic acquired resistance. *Cell* 103:1111–20.
- Pichersky E. and Gang D.R. 2000. Genetics and biochemistry of secondary metabolites in plants: an evolutionary perspective. *Trends in Plant Sciences* 5 (10): 439-445.
- Pichersky E. and Gershenzon J. 2002. The formation and function of plant volatiles: perfumes for pollinator attraction and defense. *Current Opinion in Plant Biology* 5: 237–243.
- Piesik D., Pańka D. ,Delaney K.J., Skoczek A., Lamparski R., Weaver D.K. 2011. Cereal crop volatile organic compound induction after mechanical injury, beetle herbivory (*Oulema* spp.), or fungal infection (*Fusarium* spp.). *Journal of Plant Physiology* 168: 878-886.
- Pieterse C.M.J., Leon-Reyes A., Van der Ent S., Van Wees S.C.M.2009. Networking by small-molecule hormones in plant immunity. *Nature Chemical Biology* 5: 308 – 316.
- Pieterse C.M.J., Van der Does D., Zamioudis C., Leon-Reyes A., Van Wees S. C.M. 2012. Hormonal modulation of plant immunity. *Annual Review of Cell and Developmental Biology* 28:489-521.
- Pinot F., Beisson F. 2011. Cytochrome P450 metabolizing fatty acids in plants: characterization and physiological roles. *FEBS Journal* 278(2):195-205.
- Polverari A., Molesini B., Pezzotti M., Buonauro R., Marte M., Delledonne M. 2003. Nitric oxide-mediated transcriptional changes in *Arabidopsis thaliana*. *Molecular Plant-Microbe Interaction* 16 (12): 1094–1105.
- Pompon D., Louerat B., Bronine A., Urban P. 1996. Yeast expression of animal and plant P450s in optimized redox environment. *Methods in Enzymology* 272:51–64.

- Powles S.B. and Yu, Q. 2010. Evolution in action: plants resistant to herbicides. *Annual Review of Plant Biology* 61:317-347.
- Pré M., Atallah M., Champion A., De Vos M., Pieterse C.M.J., Memelink J. 2008. The AP2/ERF domain transcription factor ORA59 integrates jasmonic acid and ethylene signals in plant defense. *Plant Physiology* 147:1347–57.
- Preston G. 2000. *Pseudomonas syringae* pv. *tomato*: the right pathogen, of the right plant, at the right time. *Molecular Plant Pathology* 11(1):263–275.
- Qutob D., Kemmerling B., Brunner F., Kufner I., Engelhardt S., Gust A., Luberacki B., Seitz H.-U., Stahl D., Rauhut T., Glawischnig E., Schweene G., Lacombe B., Watanabe P., Lam E., Schlichting R., Scheel D., Nau K., Dodt G., Hubert D., Gijzen M., Nürnberger T., 2006. Phytotoxicity and innate immune responses induced by Nep1-like proteins. *Plant Cell* 18(12): 3721–3744.
- Raacke I.C., Rad U., Mueller M.J., Berger S. 2006. Yeast increases resistance in *Arabidopsis* against *Pseudomonas syringae* and *Botrytis cinerea* by salicylic acid-dependent as well as - independent mechanisms. *Molecular Plant Microbe Interaction* 19: 1138–1146.
- Raffaele S., Rivas S., Roby D. 2006. An essential role for salicylic acid in *AtMYB30*-mediated control of the hypersensitive cell death program in *Arabidopsis*. *FEBS Letters* 580: 3498-3504.
- Ramel F., Birtic S., Ginies C., Soubigou-Taconnat L., Triantaphylidès C., Havaux M. 2012. Carotenoid oxidation products are stress signals that mediate gene responses to singlet oxygen in plants. *Proceedings of the National Academy of Sciences USA* 109(14):5535–5540.
- Rate D.N. and Greenberg J.T. 2001. The *Arabidopsis* aberrant growth and death2 mutant shows resistance to *Pseudomonas syringae* and reveals a role for NPR1 in suppressing hypersensitive cell death. *Plant Journal* 27:203–211.
- Razavi S.M. 2011. Plant Coumarins as Allelopathic Agents. *International Journal of Biological Chemistry* 5: 86-90.
- Reinhardt J.A., Baltrus D.A., Nishimura M.T., Jeck W.R., Jones C.D., Dangl J.L. 2009. De novo assembly using low-coverage short read sequence data from the rice pathogen *Pseudomonas syringae* pv. *oryzae*. *Genome Research* 19:294–305.
- Reintanz B., Lehnen M., Reichelt M., Gershenzon J., Kowalczyk M., Sandberg G., Godde M., Uhl R., Palme K. 2001 *Bus*, a bushy *Arabidopsis* *CYP79F1* knockout mutant with abolished synthesis of short-chain aliphatic glucosinolates. *The Plant Cell* 13:351–367.
- Renault H., Bassard J.E., Hamberger J., Werck-Reichhart D. 2014. Cytochrome P450-mediated metabolic engineering: current progress and future challenges. *Current Opinion in Plant Biology* 19:27-34.

- Rice-Evans C.A., Miller N.J., and Paganga G. 1997. Antioxidant properties of phenolic compounds. *Trends in Plant Science* 2: 152–159.
- Richfield, David. 2014. Medical gallery of David Richfield 2014. *Wikiversity Journal of Medicine* 1 (2). DOI:10.15347/wjm/2014.009. ISSN 2001-8762. - M.Sc. Thesis, David Richfield. Data accessed: July 2014.
- Robert-Seilaniantz A. Grant M., Jones J.D.G. 2011. Hormone crosstalk in plant disease and defense: more than just jasmonate -salicylate antagonism. *Annual Review of Phytopathology* 49:317–43.
- Rodríguez A., Shimada T., Cervera M., Alquézar B., Gadea J., Gómez-Cadenas A., De Ollas C.J., Rodrigo M.J., Zacarías L., Peña L. 2014. Terpene down-regulation triggers defense responses in transgenic orange leading to resistance against fungal pathogens. *Plant Physiology* 164: 321-339.
- Rodriguez-Herva J.J., Gonzalez-Melendi P., Cuartas-Lanza R., Antunez-Lamas M., Rio-Alvarez I., Li Z., López-Torrejón G., Díaz I., Del Pozo J.C., Chakravarthy S., Collmer A., Rodríguez-Palenzuela P., López-Solanilla E. 2012. A bacterial cysteine protease effector protein interferes with photosynthesis to suppress plant innate immune responses. *Cell Microbiology* 14:669–81.
- Roetschi A., Si-Ammour A., Belbahri L., Mauch F. Mauch-Mani B. 2001 .Characterization of an *Arabidopsis-Phytophthora* pathosystem: resistance requires a functional PAD2 gene and is independent of salicylic acid, ethylene and jasmonic acid signaling. *Plant Journal* 28:293–305.
- Rogers E.E, Glazebrook J., Ausubel F.M. 1996. Mode of action of the *Arabidopsis thaliana* phytoalexin camalexin and its role in *Arabidopsis*–pathogen interactions. *Molecular Plant Microbe Interaction* 9:748–757.
- Ross, A.F.1961.Systemic acquired resistance induced by localized virus infections in plants. *Virology* 14: 340-358.
- Rossi F.R., Gárriz A., Marina M., Romero F.M., Gonzalez M.E., Collado I.G., Pieckenstain F.L. 2011. The sesquiterpene botrydial produced by *Botrytis cinerea* induces the hypersensitive response on plant tissues and its action is modulated by salicylic acid and jasmonic acid signaling. *Molecular Plant Microbe Interaction* 24(8): 888-896.
- Rowe H.C. and Kliebenstein D.J. 2008. Complex genetics control natural variation in *Arabidopsis thaliana* resistance to *Botrytis cinerea*. *Genetics* 180, 2237–2250.
- Rowe H.C. Walley J.W., Corwin J.A., Chan E.K.F., Corwin,J.A., Dehesh K. Kliebenstein D.J. 2010. Deficiencies in JA-mediated plant defense reveal quantitative genetic variation in *Botrytis cinerea* pathogenesis. *PLoS Pathogens* 6(4):e1000861.

- Ruijter J.M., Ramakers C., Hoogaars W.M., Karlen Y., Bakker O., van den Hoff M.J., Moorman A.F. 2009. Amplification efficiency: linking baseline and bias in the analysis of quantitative PCR data. *Nucleic Acids Research* 37: e45.
- Ryals J., Uknes S., Ward E. 1994. Systemic Acquired Resistance. *Plant Physiology* 104: 1109-11112.
- Sacco M.A., Mansoor S., Moffett P. 2007. A RanGAP protein physically interacts with the NB-LRR protein Rx, and is required for Rx-mediated viral resistance. *Plant Journal* 52: 82–93.
- Sagor G.H.M., Cong R., Berberich T., Takahashi H. Takahashi Y. and Kusanoco T. 2009. Spermine signaling in defense reaction against avirulent viral pathogen in *Arabidopsis thaliana*. *Plant Signal and Behaviour* 4(4): 316–318.
- Saito S., Hirai N., Matsumoto C., Ohigashi H., Ohta D., Sakata K., Mizutani M. 2004. *Arabidopsis CYP707As* encode (+)-abscisic acid 8-hydroxylase, a key enzyme in the oxidative catabolism of abscisic acid. *Plant Physiology* 134:1439–1449.
- Sanchez-Vallet A, Ramos B., Bednarek P., López G., Piślewska-Bednarek M., Schulze-Lefert P., Molina A. 2010. Tryptophan-derived secondary metabolites in *Arabidopsis thaliana* confer non-host resistance to necrotrophic *Plectosphaerella cucumerina* fungi. *Plant Journal* 63:115-127.
- Sauveplane V., Kandel S., Kastner P.E., Ehling J., Compagnon V., Werck-Reichhart D., Pinot F. 2009. *Arabidopsis thaliana CYP77A4* is the first cytochrome P450 able to catalyze the epoxidation of free fatty acids in plants. *FEBS Journal* 276(3):719-35.
- Schenke D., Böttcher C., Scheel D. 2011. Crosstalk between abiotic ultraviolet-B stress and biotic (flg22) stress signalling in *Arabidopsis* prevents flavonol accumulation in favor of pathogen defence compound production. *Plant, Cell and Environment* 34: 1849-1864.
- Schlaeppli K., Abou-Mansour E., Buchala A., Mauch F. 2010. Disease resistance of *Arabidopsis* to *Phytophthora brassicae* is established by the sequential action of indole glucosinolates and camalexin. *Plant Journal* 62:840-851.
- Schnee C., Kollner T.G., Held M., Turling T.C.J., Gershenzon J., Degenhardt J. 2006. The products of a single maize sesquiterpene synthase form a volatile defense signal that attracts natural enemies of maize herbivores. *Proceeding of the National Academy of Sciences USA* 103:1129–1134.
- Schön M., Töller A., Diezel C., Roth C., Westphal L., Wiermer M., Somssich I.E. 2013. Analyses of *wrky18 wrky40* plants reveal critical roles of SA/EDS1 signaling and indole-glucosinolate biosynthesis for *Golovinomyces orontii* resistance and a loss-of resistance towards *Pseudomonas syringae* pv. *tomato AvrRPS4*. *Molecular Plant Microbe interaction* 7: 758-767.

- Schouten A., Tenberge K.B., Vermeer J., Stewart J., Wagemakers L., Williamson B., van Kan J.A.L. 2002. Functional analysis of an extracellular catalase of *Botrytis cinerea*. *Molecular Plant Pathology* 3: 227–238.
- Schuhegger R., Nafisi M., Mansourova M., Petersen B.L., Olsen C.E., Svatos A., Halkier B.A., Glawischnig E. 2006. *CYP71B15 (PAD3)* catalyzes the final step in camalexin biosynthesis. *Plant Physiology* 141:1248–1254.
- Schuhegger R., Rauhut T., Glawischnig E. 2007. Regulatory variability of camalexin biosynthesis. *Journal of Plant Physiology* 164:636-644.
- Schuler M.A. 1996. Plant cytochrome P450 monooxygenases. *Critical Reviews in Plant Science* 15:235–284.
- Schuler M.A., Werck-Reichhart D. 2003. Functional Genomics of P450s. *Annual Review of Plant Biology* 54: 629-667.
- Schuler M.A., Duan H., Bilgin M., Ali S. 2006. *Arabidopsis* cytochrome P450s through the looking glass: A window on plant biochemistry. *Phytochemistry Reviews* 5 (2-3): 205-237.
- Sellam A., Dongo A., Guillemette T., Hudhomme P., Simoneau P. 2007. Transcriptional responses to exposure to the *brassicaceous* defence metabolites camalexin and allyl-isothiocyanate in the necrotrophic fungus *Alternaria brassicicola*. *Molecular Plant Pathology* 8:195-208.
- Selmar D. 2011. Biosynthesis of cyanogenic glycosides, glucosinolates and non-protein amino acids. *Annual Plant Reviews* 40: 92–181.
- Seo H.S., Song J.T., Cheong J.J., Lee Y.H., Lee Y.W., Hwang I., Lee J.S., Choi Y.D. 2001. Jasmonic acid carboxyl methyltransferase: a key enzyme for jasmonate-regulated plant responses. *Proceeding of the Natural Academy of Sciences USA* 98:4788-4793.
- Shafiei R., Hang C., Kang J.-G., Loake, G.J. 2007. Identification of loci controlling non-host disease resistance in *Arabidopsis* against the leaf rust pathogen *Puccinia triticina*. *Molecular Plant Pathology* 8: 773–784.
- Shah, J. 2005. Lipids, lipases, and lipid-modifying enzymes in plant disease resistance. *Annual Review of Phytopathology* 43:229-260.
- Shah J. and Zeier J. 2013. Long-distance communication and signal amplification in systemic acquired resistance. *Frontiers in Plant Science* 4, article 30: 1-16
- Shah J., Chaturvedi R., Chowdhury Z., Venables B., Petros R.A. 2014. Signaling by small metabolites in systemic acquired resistance. *The Plant Journal* 79: 645–658.
- Shlezinger N., Minz A., Gur J., Hatam I., Dagdas Y.F., Talbot N. J., Sharon A. 2011. Anti-apoptotic machinery protects the necrotrophic fungus *Botrytis cinerea* from host-induced apoptotic-like cell death during plant infection. *PLoS Pathogens* 7(8): e1002185.

- Simon C., Langlois-Meurinne M., Bellvert F., Garmier M., Didierlaurent L., Massoud K., Chaouch S., Marie A., Bodo B., Kauffmann S., Noctor G., Saindrenan P. 2010. The differential spatial distribution of secondary metabolites in *Arabidopsis* leaves reacting hypersensitively to *Pseudomonas syringae* pv. *tomato* is dependent on the oxidative burst. *Journal of Experimental Botany* 61(12): 3355-3370.
- Simon C., Langlois-Meurinne M., Didierlaurent L., Chaouch S., Bellvert F., Massoud K., Garmier M., Thareau V., Comte G., Noctor G., Saindrenan P. 2014. The secondary metabolism glycosyltransferases *UGT73B3* and *UGT73B5* are components of redox status in resistance of *Arabidopsis* to *Pseudomonas syringae* pv. *tomato*. *Plant Cell and Environment* 37(5):1114-29.
- Singh B. and Sharma R.A. 2014. Plant terpenes: defense responses, phylogenetic analysis, regulation and clinical applications. 3 *Biotech Data* accessed online: June 2014.
- Skadhauge B., Thomsen K.K., Von Wettstein D. 1997. The role of the barley testa layer and its flavonoid content in resistance to *Fusarium* infections. *Hereditas* 126: 147-160.
- Slusarenko J. A. and Schlaich, N. L. 2003. Downy mildew of *Arabidopsis thaliana* caused by *Hyaloperonospora parasitica* (formerly *Peronospora parasitica*). *Molecular Plant Pathology* 4 (3):159-170.
- Smith C.J. 1996. Accumulation of phytoalexins: defence mechanism and stimulus response system. *New Phytologist* 132:1–45.
- Smith B.A., Neal C.L., Chetram M., Vo B., Mezencev R., Hinton C., Odero-Marah VA. 2013. The phytoalexin camalexin mediates cytotoxicity towards aggressive prostate cancer cells via reactive oxygen species. *Journal of Natural Medicine* 67 (3): 607-618.
- Smith B., Randle D., Mezencev R., Thomas L., Hinton C., Odero-Marah V. 2014. Camalexin-induced apoptosis in prostate cancer cells involves alterations of expression and activity of lysosomal protease cathepsin D. *Molecules* 19: 3988-4005.
- Snyder B.A. and Nicholson R.L. 1990. Synthesis of phytoalexins in sorghum as a site-specific response to fungal ingress. *Science* 248: 1637-1639.
- Song J.T., Koo Y.J., Seo H.S., Kim M.C., Choi Y.D., Kim J.H. 2008. Overexpression of AtSGT1, an *Arabidopsis* salicylic acid glucosyltransferase, leads to increased susceptibility to *Pseudomonas syringae*. *Phytochemistry* 69: 1128-1134.
- Spoel S.H., Koornneef A., Claessens S.M.C., Korzelius J.P., Van Pelt J.A., Martin J. Mueller, Buchala A.J., Métraux J.P., Brown R., Kazan K., Van Loon L.C., Dong X., Pieterse C.J.M. 2003. NPR1 modulates cross-talk between salicylate- and jasmonate-dependent defense pathways through a novel function in the cytosol. *The Plant Cell* 15:760–70.

- Spoel S.H., Johnson J.S., Dong X. 2007. Regulation of trade-offs between plant defenses against pathogens with different lifestyles. *Proceeding of the Natural Academy of Sciences USA* 104: 18842-18847.
- Spoel S.H. and Dong X. 2008. Making sense of hormone crosstalk during plant immune response. *Cell Host and Microbe* 3: 348-351.
- Spoel S.H., Mou Z., Tada Y., Spivey N.W., Genschik P., Dong X. 2009. Proteasome-mediated turnover of the transcription co-activator NPR1 plays dual roles in regulating plant immunity. *Cell* 137: 860-872.
- Spoel S.H. and Dong X. 2012. How do plants achieve immunity? Defence without specialized immune cells. *Nature Reviews Immunology* 12: 89-100.
- Staal J., Kaliff M., Bohman S., Dixelius C. 2006. Transgressive segregation reveals two *Arabidopsis* TIR-NB-LRR resistance genes effective against *Leptosphaeria maculans*, causal agent of blackleg disease. *Plant Journal* 46: 218–230.
- Stael S., Kmiciek P., Willems P., Van Der Kelen K., Coll N., Teige M., Van Breusegem F. 2015. Plant innate immunity - sunny side up? *Trends in Plant Science* 20(1):3-11.
- Staswick P.E. and Tiryaki I. 2004. The oxylipin signal jasmonic acid is activated by an enzyme that conjugates it to isoleucine in *Arabidopsis*. *Plant Cell* 16:2117-2127.
- Staswick P.E. 2009. The tryptophan conjugates of jasmonic and indole-3-acetic acids are endogenous auxin inhibitors. *Plant Physiology* 150: 1310–1321.
- Stintzi A. and Browse J. 2000. The *Arabidopsis* male-sterile mutant, opr3, lacks the 12-oxophytodienoic acid reductase required for jasmonate synthesis. *Proceedings of the National Academy of Sciences USA* 97:10625-10630.
- Stintzi A., Weber H., Reymond P., Browse J., Farmer E.E. 2001. Plant defense in the absence of jasmonic acid: the role of cyclopentenones. *Proceedings of the National Academy of Sciences USA* 98: 12837–12842.
- Stotz H.U., Sawada Y., Shimada Y., Hirai M.Y., Sasaki E., Krischke M., Brown P.D., Saito K., Kamiya Y. 2011. Role of camalexin, indole glucosinolates, and side chain modification of glucosinolate-derived isothiocyanates in defense of *Arabidopsis* against *Sclerotinia sclerotiorum*. *Plant Journal* 67:81-93.
- Stotz H.U., Waller F., and Wang K. 2013. Innate immunity in plants: The role of antimicrobial peptides. In: *Antimicrobial Peptides and Innate Immunity, Progress in Inflammation Research* P.S. Hiemstra and S.A.J. Zaat (eds.).
- Stuart L.M., Paquette N., Boyer L. 2013. Effector-triggered versus pattern triggered immunity: how animals sense pathogens. *Nature Reviews* 13:199-206.

- Su T., Xu J., Li Y., Lei L., Zhao L., Yang H., Feng J., Liu G., Ren D. 2011. Glutathione-indole-3-acetonitrile is required for camalexin biosynthesis in *Arabidopsis thaliana*. *Plant Cell* 23:364-380.
- Su T., Li Y., Yang H., Ren D. 2013. Reply: complexity in camalexin biosynthesis. *Plant Cell* 25: 367-370.
- Suarez M.B., Walsh K., Boonham N., O'Neill T., Pearson S., Barker I. 2005. Development of real-time PCR (TaqMan) assays for the detection and quantification of *Botrytis cinerea* in planta. *Plant Physiology and Biochemistry* 43(9):890-9.
- Suresh K. P. and Chandrashekara S. 2012. Sample size estimation and power analysis for clinical research studies. *Journal of Human Reproductive Sciences* 5:7-13.
- Suzuki N., Miller G., Morales J., Shulaev V., Torres M.A., Mittler R. 2011. Respiratory burst oxidases: the engines of ROS signaling. *Current Opinion in Plant Biology* 14: 691-699.
- Takahashi N., Nakazawa M., Shibata K., Takao Y., Akie I., Suzuki K., Kawashima M., Ichikawa T., Shimada H. y Matsui M. 2005. shk1-D, a dwarf *Arabidopsis* mutant caused by activation of the CYP72C1 gene, has altered brassinosteroid levels. *Plant Journal* 42:13-22.
- Tamura K., Stecher G., Peterson D., Filipski A., Kumar S. 2013. MEGA6: Molecular Evolutionary Genetics Analysis Version 6.0. *Molecular Biology and Evolution* 30: 2725-2729.
- Tao Y., Xie Z., Chen W., Glazebrook J., Chang H.S., Han B., Zhu T., Zou G., Katagiri F. 2003. Quantitative nature of *Arabidopsis* responses during compatible and incompatible interactions with the bacterial pathogen *Pseudomonas syringae*. *Plant Cell* 15(2): 317-330.
- Tárraga S., Lisón P., López-Gresa M. P., Torres C., Rodrigo I., Bellés J. M., Conejero V. 2010. Molecular cloning and characterization of a novel tomato xylosyltransferase specific for gentisic acid. *Journal of Experimental Botany* 61(15): 4325–4338.
- Tattersall D.B., Bak S., Jones P.R., Olsen C.E., Nielsen J.K., Hansen M.L., Høj P.B. and Møller B.L. 2001. Resistance to an herbivore through engineered cyanogenic glucoside synthesis. *Science* 293: 1826–8.
- The Arabidopsis Genome Initiative. 2000. Analysis of the genome sequence of the flowering plant *Arabidopsis thaliana*. *Nature* 408: 796–815. <http://www.arabidopsis.org/>
- Thomma B.P.H.J., Eggermont K., Penninckx IAMA, Mauch-Mani B., Vogelsang R., Cammue B.P.A, Broekaert W.F. 1998. Separate jasmonate-dependent and salicylate-dependent defense-response pathways in *Arabidopsis* are essential for resistance to distinct microbial pathogens. *Proceedings of the National Academy of Sciences USA* 95:15107–15111.
- Thomma B.P., Nelissen I., Eggermont K., Broekaert W.F. 1999. Deficiency in phytoalexin production causes enhanced susceptibility of *Arabidopsis thaliana* to the fungus *Alternaria brassicicola*. *Plant Journal* 19:163-171.

- Tholl D. and Lee S. 2011. Terpene specialized metabolism in *Arabidopsis thaliana*. The Arabidopsis Book 9: e0143.
- Thornton L.E., Rupasinghe S.G., Peng H., Schuler M.A., Neff M.M. 2010. *Arabidopsis CYP72C1* is an atypical cytochrome P450 that inactivates brassinosteroids. Plant Molecular Biology 74: 167–181.
- Tian L., Musetti V., Kim J., Magallanes-Lundback M., DellaPenna D. 2004. The *Arabidopsis LUT1* locus encodes a member of the cytochrome P450 family that is required for carotenoid e-ring hydroxylation activity. Proceeding of the Natural Academy of Sciences 101:402–407.
- Torres M.A., Dangl J.L., Jones J.D. 2002. *Arabidopsis gp91phox* homologues *AtrbohD* and *AtrbohF* are required for accumulation of reactive oxygen intermediates in the plant defense response. Proceeding of the National Academy of Sciences USA 99: 517–522.
- Torres M.A. and Dangl J.L. 2005. Functions of the respiratory burst oxidase in biotic interactions, abiotic stress and development. Current Opinion of Plant Biology 8: 397–403.
- Torres-Vera R., Garcia J.M., Pozo M.J. and López-Ráez J.A. 2014. Do strigolactones contribute to plant defence? Molecular Plant Pathology 15 (2): 11–216.
- Torres M.A., Jones J.D.G., Dangl J.L. 2006. Reactive oxygen species signaling in response to pathogens. Plant Physiology 141: 373-378.
- Tripathi, A.K., Upadhyay, S., Bhuiyan, M., Bhattacharya, P.R. 2009. A review on prospects of essential oils as biopesticides in insect-pest management. Journal of Pharmacology and Phytotherapy 1: 52-63.
- Truman W., Bennett M.H., Kubigsteltig I., Turnbull C., Grant M. 2007. *Arabidopsis* systemic immunity uses conserved defense signaling pathways and is mediated by jasmonates. Proceedings of the National Academy of Sciences USA 104: 1075–1080.
- Turk E.M., Fujioka S., Seto H., Shimada Y., Takatsuto S., Yoshida S., Denzel M.A., Torres Q.I., Neff M.M. 2003. *CYP72B1* inactivates brassinosteroid hormones: an intersection between photomorphogenesis and plant steroid signal transduction. Plant Physiology 133:1643–1653.
- Turk E.M., Fujioka S., Seto H., Shimada Y., Takatsuto S., Yoshida S., Wang H., Torres Q.I., Ward J.M., Murthy G., Zhang J., Walker J.C., Neff M.M. 2005. *BAS1* and *SOB7* act redundantly to modulate *Arabidopsis* photomorphogenesis via unique brassinosteroid inactivation mechanisms. Plant Journal 42(1):23-34.
- Turlings T.C.J., Tumlinson J.H. and Lewis W.J. 1990. Exploitation of herbivore-induced plant odors by host-seeking parasitic wasps. Science 250:1251–3.
- Turlings T.C.J., McCall P.J., Alborn H.T., Tumlinson J.H. 1993. An elicitor in caterpillar oral secretions that induces corn seedlings to emit chemical signals attractive to parasitic wasps. Journal of chemical ecology 19 (3): 411-425.

- Turlings T.C.J., Loughrin J.H., McCall P.J., Rose U.S.R., Lewis W.J. and Tumlinson J.H. 1995. How caterpillar-damaged plants protect themselves by attracting parasitic wasps. *Proceedings of the National Academy of Sciences USA* 92: 4169–74.
- Unsicker, S. B., Kunert, G., Gershenzon, J. 2009. Protective perfumes: the role of vegetative volatiles in plant defense against herbivores. *Current Opinion in Plant Biology* 12: 479-485.
- Urban P., Mignotte C., Kazmaier M., Delorme F., Pompon D. 1997. Cloning, yeast expression, and characterization of the coupling of two distantly related *Arabidopsis thaliana* NADPH-cytochrome P450 reductases with P450 *CYP73A5*. *Journal of Biological Chemistry* 272:19176–19186.
- Utsugi S., Sakamoto W., Murata M., Motoyoshi F. 1998. *Arabidopsis thaliana* vegetative storage protein (*VSP*) genes: gene organization and tissue-specific expression. *Plant Molecular Biology* 38(4): 565-576.
- van der Hoorn R. and Kamoun S. 2008. From guard to decoy: a new model for perception of plant pathogen effectors. *The Plant Cell* 20:2009-2017.
- Van der Biezen E.A. and Jones J.D.G. 1998. Plant disease resistance proteins and the gene-for-gene concept. *Trends in Plant Science* 23: 454–456.
- van Doorn W.G., Beers E.P., Dangl J.L., Franklin-Tong V.E., Gallois P., Hara-Nishimura I., Jones A.M., Kawai-Yamada M., Lam E., Mundy J., Mur L.A., Petersen M., Smertenko A., Taliansky M., Van Breusegem F., Wolpert T., Woltering E., Zhivotovsky B., Bozhkov P.V. 2011a. Morphological classification of plant cell deaths. *Cell Death and Differentiation* 18:1241-1246.
- Van Doorn W.G. 2011b. Classes of programmed cell death in plants, compared to those in animals. *Journal of Experimental Botany* 62 (14): 4749-4761.
- van Kan J.A.L 2006. Licensed to kill: the lifestyle of a necrotrophic plant pathogen. *Trends in Plant Science* 11:247–253.
- Van Etten H.D., Matthews D.E., Matthews P.S. 1989. Phytoalexin detoxification: importance for pathogenicity and practical implications. *Annual Review of Phytopathology* 27: 143-164.
- VanEtten, H.D., Mansfield, J.W., Bailey, J.A., Farmer E.E. 1994. Two classes of plant antibiotics: Phytoalexins versus phytoanticipins. *The Plant Cell* 6: 1191-1192.
- van Schie C.C., Takken F.L. 2014. Susceptibility genes 101: how to be a good host. *Annual Review of Phytopathology* 52:551-81.
- Velloso T., Vicente J., Kulasekaran S., Hamberg M., Castresana C. 2010. Emerging complexity in reactive oxygen species production and signaling during the response of plants to pathogens. *Plant Physiology* 154: 444-448.
- Vercammen D., van de Cotte B., De Jaeger G., Eeckhout D., Casteels P., Vandepoele K., Vandenberghe I., Van Beeumen J., Inzé D., Van Breusegem F. 2004. Type II metacaspases

Atmc4 and Atmc9 of *Arabidopsis thaliana* cleave substrates after arginine and lysine. Journal of Biological Chemistry 279:45329–45336.

- von Roepenack-Lahaye E., Degenkolb T., Zerjeski M., Franz M., Roth U., Wessjohann L., Schmidt J., Scheel D., Clemens S. 2004. Profiling of *Arabidopsis* Secondary Metabolites by Capillary Liquid Chromatography Coupled to Electrospray Ionization Quadrupole Time-of-Flight Mass Spectrometry. Plant Physiology 134(2): 548–559.
- Vlot A.C., Liu P.P., Cameron R.K., Park S.W., Yang Y., Kumar D., Zhou F., Padukkavidana T., Gustafsson C., Pichersky E., Klessig D.F. 2008. Identification of likely orthologs of tobacco salicylic acid-binding protein 2 and their role in systemic acquired resistance in *Arabidopsis thaliana*. Plant Journal 56 (3): 445-456.
- Vlot A.C., Dempsey D.A., Klessig D.F. 2009. Salicylic acid, a multifaceted hormone to combat disease. Annual Review of Phytopathology 47:177-206.
- Vourc'h G., De Garine-Wichatitsky M., Labbé A., Rosolowski D., Martin J.L., Fritz H. 2002. Monoterpene effect on feeding choice by deer. Journal of Chemical Ecology 28:2411–2427.
- Walters DR.2003. Polyamines and plant disease. Phytochemistry 64(1):97-107.
- Wang Y., Loake G.J., Chu C. 2013. Cross-talk of nitric oxide and reactive oxygen species in plant programmed cell death. Frontiers in Plants Sciences 4, article 314.
- Wang X., Sager R., Cui W., Zhang C., Lu H., Lee JY. 2013b. Salicylic acid regulates Plasmodesmata closure during innate immune responses in *Arabidopsis*. Plant Cell 25(6):2315-29.
- Wang C., El-Shetehy M., Shine M.B., Yu K., Navarre D., Wendehenne D., Kachroo A., Kachroo P.2014. Free radicals mediate systemic acquired resistance. Cell Reports 7(2): 348-55.
- Wasternack C. and Hause B. 2013. Jasmonates: biosynthesis, perception, signal transduction and action in plant stress response, growth and development. An update to the 2007 review in Annals of Botany. Annals of Botany 111: 1021–1058, 2013.
- Weigel, D. and Glazebrook, J. 2002. *Arabidopsis* A laboratory manual. Cold Spring Harbor Laboratory press, Cold Spring Harbor, New York, USA.
- Wellesen K., Durst F., Pinot F., Benveniste I., Nettesheim K., Wisman E., Steiner-Lange S., Saedler H., Yephremov A.2001. Functional analysis of the *LACERATA* gene of *Arabidopsis* provides evidence for different roles of fatty acid α -hydroxylation in development. Proceeding of the Natural Academy of Sciences 98:9694–9699.
- Werck-Reichhart D. and Feyereisen R. 2000. Cytochromes P450: a success story. Genome Biology 1:6.
- Wen L. 2013. Cell death in plant immune response to necrotrophs. Journal of Plant Biochemistry and Physiology 1 (1): e103.

- Whalen M.C., Innes R.W., Bent A.F., Staskawicz B.J. 1991. Identification of *Pseudomonas syringae* pathogens of *Arabidopsis* and a bacterial locus determining avirulence on both *Arabidopsis* and soybean. *The Plant Cell* 3(1):49-59.
- Widemann E., Miesch L., Lugan R., Holder E., Heinrich C., Aubert Y., Miesch M., Pinot F., Heitz T. 2013. The amido-hydrolases IAR3 and ILL6 contribute to jasmonoyl-isoleucine hormone turnover and generate 12-hydroxy-jasmonic acid upon wounding in *Arabidopsis* leaves. *The Journal of Biological Chemistry* 288: 31701-31714.
- Wildermuth M.C. 2006. Variations on a theme: synthesis and modification of plant benzoic acids. *Current Opinion in Plant Biology* 9: 288-296.
- Williams J.L., Eilers-Kirk C., Orth R.G., Gassmann A.J., Head G., Tabashnik B.E., Carrière Y. 2011. Fitness cost of resistance to Bt cotton linked with increased gossypol content in pink bollworm larvae. *Plos One* 6(6):e21863.
- Windram O., Madhou P., McHattie S., Hill C., Hickman R., Cooke E., Jenkins D.J., Penfold C.A., Baxter L., Breeze E., Kiddle S.J., Rhodes J., Atwell S., Kliebenstein D.J., Kim Y.S., Stegle O., Borgwardt K., Zhang C., Tabrett A., Legaie R., Moore J., Finkenstadt B., Wild D.L., Mead A., Rand D., Beynon J., Ott S., Buchanan-Wollaston V., Denby K.J. 2012. *Arabidopsis* defense against *Botrytis cinerea*: chronology and regulation deciphered by high-resolution temporal transcriptomic analysis. *The Plant Cell* 24 (9):3530-57.
- Wink, M. 1988. Plant breeding: importance of plant secondary metabolites for protection against pathogens and herbivores. *Theoretical and Applied Genetics* 75: 225-233.
- Wink, M. 2010. Introduction: biochemistry, physiology and ecological functions of secondary metabolites. *Annual Plant Reviews* 40: 1-19.
- Wink, M. 2011. Occurrence and function of natural products in plants. *Phytochemistry and Pharmacognosy* edited by J. M. Pezzuto and M.J. Kato, in *Encyclopedia of Life Support Systems (EOLSS)*, Developed under the Auspices of the UNESCO, Eolss Publishers, Paris, France, retrieved from <http://www.eolss.net>. Data accessed: October 2014.
- Wittstock U., Halkier B.A. 2000. Cytochrome P450 *CYP79A2* from *Arabidopsis thaliana* L. catalyzes the conversion of L-phenylalanine to phenylacetaldoxime in the biosynthesis of benzyl-glucosinolate. *Journal of Biological Chemistry* 275:14659–14666.
- Wittstock U. and Gershenzon J. 2002. Constitutive plant toxins and their role in defense against herbivores and pathogens. *Current Opinion in Plant Biology* 5(4):300-307.
- Wittstock U. and Burow M. 2010. Glucosinolate Breakdown in *Arabidopsis*: mechanism, regulation and biological significance. *Arabidopsis Book* 8: e0134.

- Xin X.F. and He S.Y. 2013. *Pseudomonas syringae* pv. *Tomato* DC3000: a model pathogen for probing disease susceptibility and hormone signaling in plants. *Annual Review of Phytopathology* 51: 473-498.
- Xiao F., Goodwin S.M., Xiao Y., Sun Z., Baker D., Tang X., Jenks M.A., Zhou J.M. 2004. *Arabidopsis* CYP86A2 represses *Pseudomonas syringae* type III genes and is required for cuticle development. *EMBO Journal* 23:2903–2913.
- Yan Y., Borrego E., Kolomiets M.V. 2013. Jasmonate Biosynthesis, Perception and Function in Plant Development and Stress Responses. In: *Lipid Metabolism*, Prof. Rodrigo Valenzuela Baez (Ed.), ISBN: 978-953-51-0944-0, InTech, DOI: 10.5772/52675. Available from: <http://www.intechopen.com/books/lipid-metabolism/jasmonate-biosynthesis-perception-and-function-in-plant-development-and-stress-responses>.
- Yasuda M., Ishikawa A., Jikumaru Y., Seki M., Umezawa T., Asami T., Maruyama-Nakashita A., Kudo T., Shinozaki K., Yoshida S., Nakashita H. 2008. Antagonistic interaction between systemic acquired resistance and the abscisic acid-mediated abiotic stress response in *Arabidopsis*. *The Plant Cell* 20:1678–1692.
- Yuan J.S., Reed A., Chen F., Stewart C.N. 2006. Statistical analysis of real-time PCR data. *BMS Bioinformatics* 7: 85.
- Zagrobelny M., Bak S., Ekstrøm C.T., Olsen C.E. and Møller B.L. 2007. The cyanogenic glucoside composition of *Zygaena filipendulae* (*Lepidoptera: Zygaenidae*) as effected by feeding on wild-type and transgenic lotus populations with variable cyanogenic glucoside profiles. *Insect Biochemistry and Molecular Biology* 37: 10–8.
- Zhao J., Williams C.C., Last R.L. 1998. Induction of *Arabidopsis* tryptophan pathway enzymes and camalexin by amino acid starvation, oxidative stress, and an abiotic elicitor. *Plant Cell* 10: 359–370.
- Zhang Y., Zhang B., Yan D., Dong W., Yang W., Li Q., Zeng L., Wang J., Wang L., Hicks L.M., He Z. 2011. Two *Arabidopsis* cytochrome P450 monooxygenases, *CYP714A1* and *CYP714A2*, function redundantly in plant development through gibberellin deactivation. *Plant Journal* 67(2):342-53.
- Zhang K., Halitschke R., Yin C., Liu C.J., Gan S.S. 2013. Salicylic acid 3-hydroxylase regulates *Arabidopsis* leaf longevity by mediating salicylic acid catabolism. *Proceeding of the National Academy of Sciences USA* 110(36):14807-12.
- Zhang C., Xie Q., Anderson R.G., Ng G., Seitz N., Peterson T., Robertson McClung C., McDowell J.M., Kong D., Kwak J.M., Lu H. 2013b. Crosstalk between the Circadian Clock and Innate Immunity in *Arabidopsis*. *PLOS pathogens* 9(6):e1003370.

- Zheng X., Weaver Spivey N., Zeng W., Liu P., Fu Q., Klessig D., He S., Dong X. 2012. Coronatine promotes *Pseudomonas syringae* virulence in plants by activating a signaling cascade that inhibits salicylic acid accumulation. *Cell Host Microbe* 11 (6):587-596.
- Zhou N., Tootle T.L., Glazebrook J. 1999. Arabidopsis *PAD3*, a gene required for camalexin biosynthesis, encodes a putative cytochrome P450 monooxygenase. *The Plant Cell* 11:2419–2428.
- Zhu J.W., and Park K.C. 2005. Methyl salicylate, a soybean aphid-induced plant volatile attractive to the predator *Coccinella septempunctata*. *Journal of Chemical Ecology* 31: 1733–1746.
- Zipfel C., Robatzek S., Navarro L., Oakeley E.J., Jones J.D., Felix G., Boller T. 2004. Bacterial disease resistance in *Arabidopsis* through flagellin perception. *Nature* 428(6984):764-7.
- Zipfel C. 2008. Pattern-recognition receptors in plant innate immunity. *Current opinion in Immunology* 20:10-16.

APPENDIX

Appendix

APPENDIX

List of P450 used in transcriptomic analysis made by Kauffmann (IBMP Strasbourg) for the trilateral project Génoplante SARA.

ACCESSION NUMBER	P450 GENE	ACCESSION NUMBER	P450 GENE
At2g45570	CYP76C2	At4g31950	CYP82C3
At3g26830	CYP71B15, PAD3	At5g05260	CYP79A2
At2g30770	CYP71A13	At5g08250	CYP86B2
At3g20110	CYP705A20	At5g57260	CYP71B10
At4g37430	CYP81F1	At4g31970	CYP82C2
At3g25180	CYP82G1	At2g23220	CYP81D6
At3g26150	CYP71B16	At3g01900	CYP94B2
At4g15350	CYP705A2	At3g14620	CYP72A8
At5g63450	CYP94B1	At3g14680	CYP72A14
At4g32170	CYP96A2	At3g61040	CYP76C7
At4g19230	CYP707A1	At2g46950	CYP709B2
At2g34500	CYP710A1	At5g42650	CYP74A, AOS
At4g39950	CYP79B2	At5g52400	CYP715A1
At5g06900	CYP93D1	At5g24910	CYP714A1
At3g44970	CYP708A4	At5g52320	CYP96A4
At3g53300	CYP71B31	At1g12740	CYP87A2
At1g11610	CYP71A18	At4g37410	CYP81F4
At4g31940	CYP82C4	At2g02580	CYP71B9
At2g30490	CYP73A5, C4H	At3g26270	CYP71B25
At3g48520	CYP94B3	At1g64950	CYP89A5
At1g64940	CYP89A6	At5g24900	CYP714A2
At2g46960	CYP709B1	At2g22330	CYP79B3
At2g30750	CYP71A12	At1g50560	CYP705A25
At4g37370	CYP81D8	At1g57750	CYP96A15
At2g27690	CYP94C1	At1g13140	CYP86C3
At4g15380	CYP705A4	At5g47990	CYP705A5
At3g28740	CYP81D11	At4g36220	CYP84A1, F5H, FAH1, CA5H
At3g03470	CYP89A9	At5g42590	CYP71A16
At3g26190	CYP71B21	At3g20940	CYP705A30
At3g20140	CYP705A23	At4g20240	CYP71A28
At5g36220	CYP81D1	At1g66030	CYP96A14P
At5g58860	CYP86A1	At2g27010	CYP705A9
At1g58260	CYP79C2	At4g15440	CYP74B2, HPL1
At4g39480	CYP96A9	At1g34540	CYP94D1
At1g65340	CYP96A3	At5g10610	CYP81K1
At4g15330	CYP705A1	At1g79370	CYP79C1
At1g64930	CYP89A7	At4g31500	CYP83B1, SUR2, RNT1, RED1, ATR4
At5g35920	CYP79A4P	At2g23180	CYP96A1
At4g12330	CYP706A7	At1g73340	CYP720A1

ACCESSION NUMBER	P450 GENE	ACCESSION NUMBER	P450 GENE
At3g10560	CYP77A7	At3g53290	CYP71B30P
At3g19270	CYP707A4	At5g25140	CYP71B13
At5g61320	CYP89A3	At5g25900	CYP701A3, GA3
At3g26290	CYP71B26	At4g39500	CYP96A11
At2g24180	CYP71B6	At1g66540	CYP81D10
At2g26170	CYP711A1, MAX1	At1g13070	CYP71B27
At5g04330	CYP84A4	At1g74110	CYP78A10
At3g14610	CYP72A7	At1g05160	CYP88A3, KAO1
At3g26210	CYP71B23	At1g33720	CYP76C6
At4g39490	CYP96A10	At2g25160	CYP82F1
At1g64900	CYP89A2	At1g19630	CYP722A1
At5g23190	CYP86B1	At2g42850	CYP718
At1g47630	CYP96A7	At2g12190	CYP89A4
At1g65670	CYP702A1	At1g67110	CYP735A2
			CYP72C1, SHK1, SOB7, CHI2
At4g37400	CYP81F3	At1g17060	
At3g20950	CYP705A32	At2g05180	CYP705A6
At5g09970	CYP78A7	At3g14640	CYP72A10
At1g11600	CYP77B1	At1g55940	CYP708A1
At2g17330	CYP51G2 (CYP51A1)	At1g75130	CYP721A1
At3g52970	CYP76G1	At3g26125	CYP86C2
At1g50520	CYP705A27	At4g13290	CYP71A19
At4g15310	CYP702A3	At3g14660	CYP72A13
At5g14400	CYP724A1	At3g26220	CYP71B3
At2g40890	CYP98A3, C3'H	At5g24950	CYP71A15
At5g44620	CYP706A3	At4g37360	CYP81D2
At2g45510	CYP704A2	At1g74550	CYP98A9
At5g38450	CYP735A1	At1g13710	CYP78A5
At3g20960	CYP705A33	At4g36380	CYP90C1, ROT3
At2g45580	CYP76C3	At5g36110	CYP716A1
At1g01190	CYP78A8	At1g24540	CYP86C1
At5g07990	CYP75B1, F3'H	At2g42250	CYP712A1
At4g37310	CYP81H1	At5g02900	CYP96A13
At2g27000	CYP705A8	At1g74540	CYP98A8
At4g15360	CYP705A3	At1g78490	CYP708A3
At3g26170	CYP71B19	At3g20080	CYP705A15
At3g20090	CYP705A18	At3g30290	CYP702A8
At5g04660	CYP77A4	At2g46660	CYP78A6
At3g14630	CYP72A9	At3g30180	CYP85A2, BR6OX2
At4g12300	CYP706A4	At5g04630	CYP77A9

ACCESSION NUMBER	P450 GENE	ACCESSION NUMBER	P450 GENE
At2g14100	CYP705A13	At2g45560	CYP76C1
At3g14690	CYP72A15	At1g13150	CYP86C4
At3g13730	CYP90D1	At2g32440	CYP88A4, KAO2
At3g44250	CYP71B38	At3g10570	CYP77A6
At1g01600	CYP86A4	At4g39510	CYP96A12
At1g11680	CYP51G1 (CYP51A2)	At4g13770	CYP83A1, REF2
At4g00360	CYP86A2	At4g22710	CYP706A2
At5g45340	CYP707A3	At5g38970	CYP85A1, BR6OX
At2g34490	CYP710A2	At3g26310	CYP71B35
At3g26230	CYP71B24	At5g36140	CYP716A2
At2g28850	CYP710A3	At5g25180	CYP71B14
At1g69500	CYP704B1	At1g28430	CYP705A24
At4g27710	CYP709B3	At5g48000	CYP708A2
At1g16410	CYP79F1, SPS, BUS1	At4g37330	CYP81D40
At3g26280	CYP71B4	At5g05690	CYP90A1, CPD
At1g13110	CYP71B7	At3g20100	CYP705A19
At4g37340	CYP81D3	At5g25130	CYP71B12
At1g13090	CYP71B28	At3g26300	CYP71B34
At4g15300	CYP702A2	At5g25120	CYP71B11
At3g56630	CYP94D2	At3g26330	CYP71B37
At1g01280	CYP703A2	At4g37320	CYP81D5
At5g57220	CYP81F2	At5g42580	CYP705A12
At4g15110	CYP97B3	At4g12310	CYP706A5
At1g13080	CYP71B2	At2g45970	CYP86A8, LCR
At3g53280	CYP71B5	At2g26710	CYP734A1, BAS1
At3g61880	CYP78A9	At2g21910	CYP96A5
At1g63710	CYP86A7	At3g26320	CYP71B36
At2g45550	CYP76C4	At1g13100	CYP71B29
At3g20130	CYP705A22		
At3g26200	CYP71B22		
At3g26160	CYP71B17		
At3g50660	CYP90B1, DWF4		
At1g47620	CYP96A8		
At3g20120	CYP705A21		
At5g51900	CYP96A6P		
At1g31800	CYP97A3, LUT5		
At3g14650	CYP72A11		
At3g53130	CYP97C1, LUT1		
At2g29090	CYP707A2		

The transcriptomic analysis was made from *A. thaliana* Col-0 plant infected with the avirulent strain of *P. syringae* pv. *tomato* DC3000 *avrRpm1*. Half of the leaves, in the apical zone opposite to the petiole, were syringe infiltrated with the bacteria at a concentration of 1×10^7 CFU/ml using MgCl_2 10 mM buffer as a mock treatment. The “LAR zone” of the leaf, opposite to the infected one, was collected at time intervals of 0, 6 and 16 HPI. Triplicates of approximately 50-75 mg fresh material were generated, coming from a pool of 10 plants with two leaves per plant.

Transcriptomic analysis was made by using ATH1 chip Affymetrix® containing about 22.500 genes and was performed by the Platform Génopole Alsace-Lorraine (Institute Genetics and Molecular and Cellular Biology, Illkirch, France; <http://www.microarrays.u-strasbg.fr/index.php>) following standard protocols from Affymetrix. A principal component analysis (PCA) was performed on the standardized data (software StatBox 6.40, <http://www.grimmersoft.com>) to confirm the reproducibility between the triplicates control/infected. The FiRe software was used to sort the data (<http://www.unifr.ch/plantbio/FiRe/main.html>). (Detailed information on experiments was extracted from Didierlaurent, Laure PhD thesis, 2012).

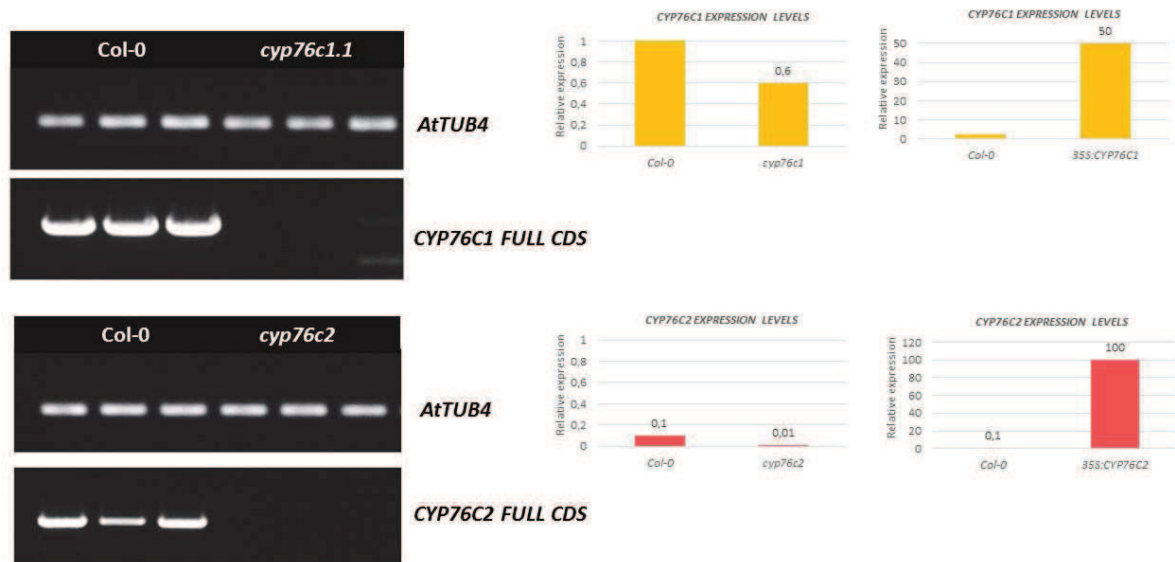
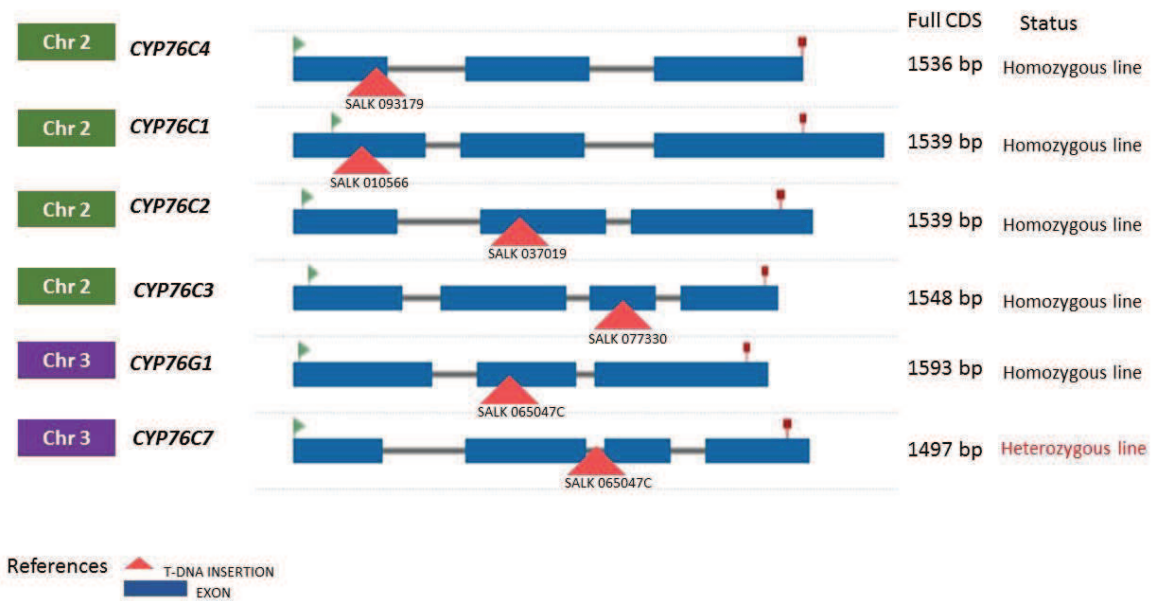
Genotyping of T-DNA insertion lines and overexpression lines used in this thesis

Overexpression lines for *CYP76C1*, *CYP76C2*, *CYP76C3*, *CYP76C4* and *PromCYP76C2:GUS* were obtained by Millet Y. and Höfer R., *CYP76C7* was obtained during this work.

Lines *cyp76c1* (SALK 010566), *cyp76c2* (SALK 037019), *cyp76c3* (SALK 077330), *cyp76c4* (SALK 093179), *cyp76c7* (GK-213C08-014134), *cyp76g1* (SALK 065047C) were obtained from the Nottingham European Arabidopsis Stock Centre (NASC, Alonso et al., 2003) and GABI KAT (Kleinboelting et al., 2012).

All lines were checked before use, by means of PCR and qPCR with specific primers (see below).

Figure 108: Schematic representation of T-DNA insertion in the lines used in this thesis.

Published in Höfer *et al.*, 2014Figure 109: Genotyping of T-DNA insertion and overexpression lines of *CYP76C1* and *CYP76C2* from leaves. Absence of transcripts in the T-DNA insertion lines were verified by qRT-PCR.

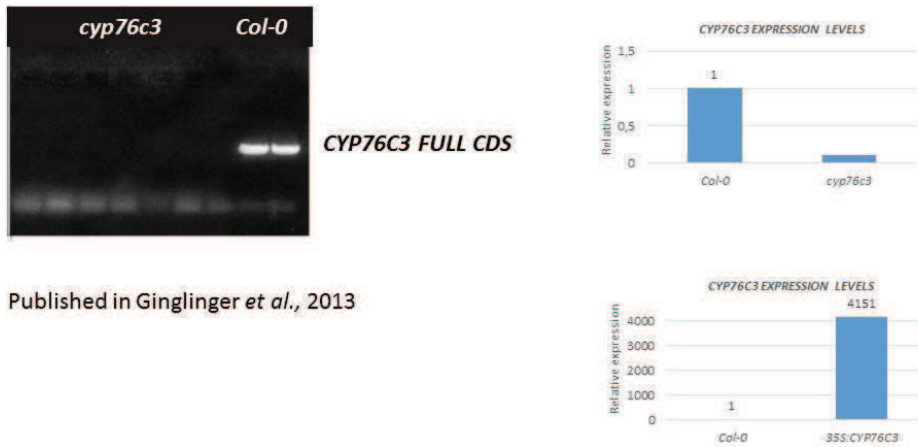


Figure 110: Genotyping of T-DNA insertion and overexpression lines of *CYP76C3* from flowers. Absence of transcripts in the T-DNA insertion lines were verified by qRT-PCR.

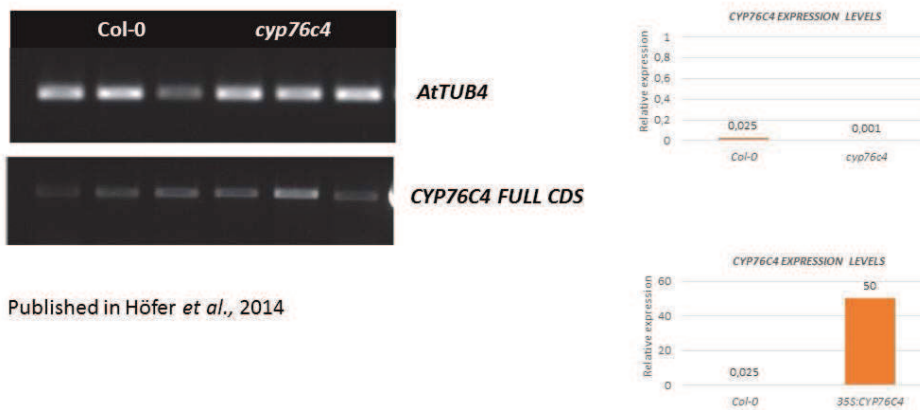


Figure 111: Genotyping of T-DNA insertion and overexpression lines of *CYP76C4* from roots. Absence of transcripts in the T-DNA insertion lines were verified by qRT-PCR.

Accession	Gene	Status
SALK010566	<i>cyp76c1</i>	homozygous
SALK037019	<i>cyp76c2</i>	homozygous
SALK077330	<i>cyp76c3</i>	homozygous
SALK093179	<i>cyp76c4</i>	homozygous
GK213C08-014134	<i>cyp76c7</i>	No line
SALK065047C	<i>cyp76g1</i>	homozygous
	<i>35S :CYP76C1</i>	ok
	<i>35S :CYP76C2</i>	ok
	<i>35S :CYP76C3</i>	ok
	<i>35S :CYP76C4</i>	ok
	<i>35S :CYP76C7</i>	ok
	<i>PromCYP76C2:GUS</i>	ok

Table 31: List of genetic material available and genetic status.

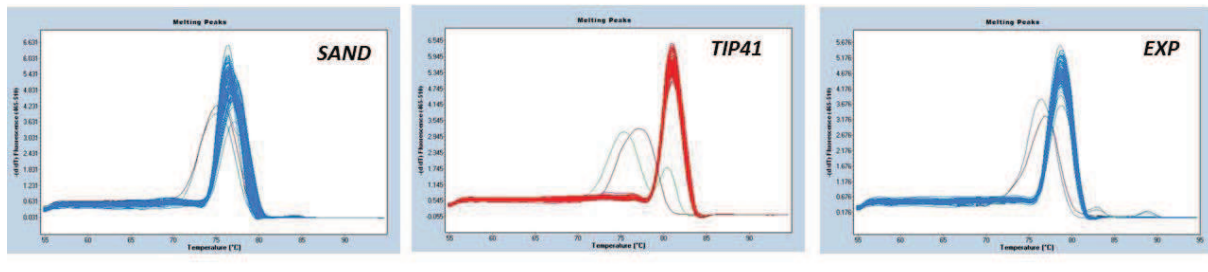
Melting curve analysis of primers used in qRT-PCR

Figure 112: Melting curve analysis of primers used in qRT-PCR of gene expression. Reference genes *SAND*, *TIP41*, *EXP*.

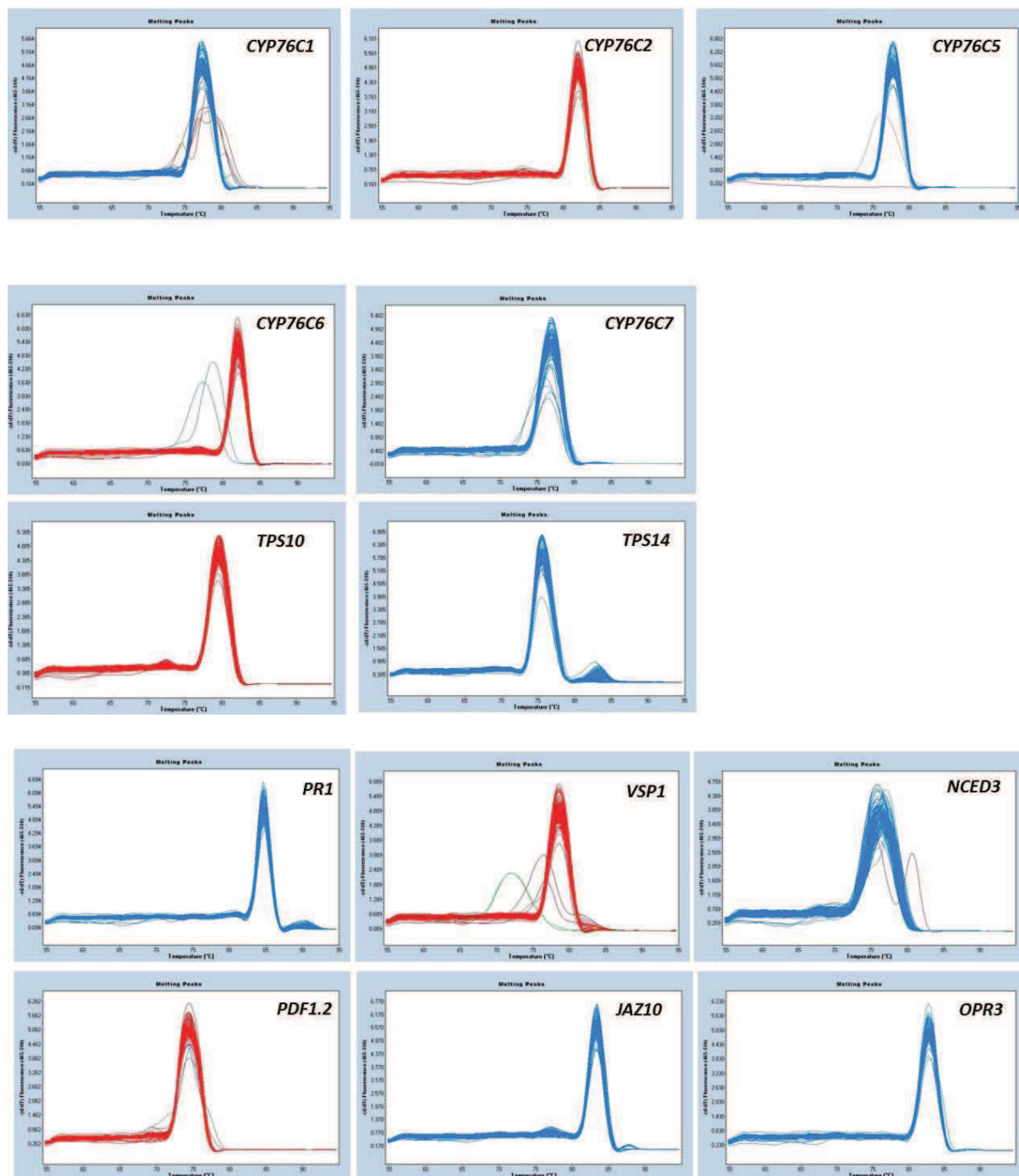


Figure 113: Melting curve analysis of primers used in qRT-PCR of gene expression. *CYP76C* family members, *TPS10*, *TPS14* and marker genes *PR1*, *VSP1*, *NCED3*, *PDF1.2*, *JAZ10*, *OPR3*.

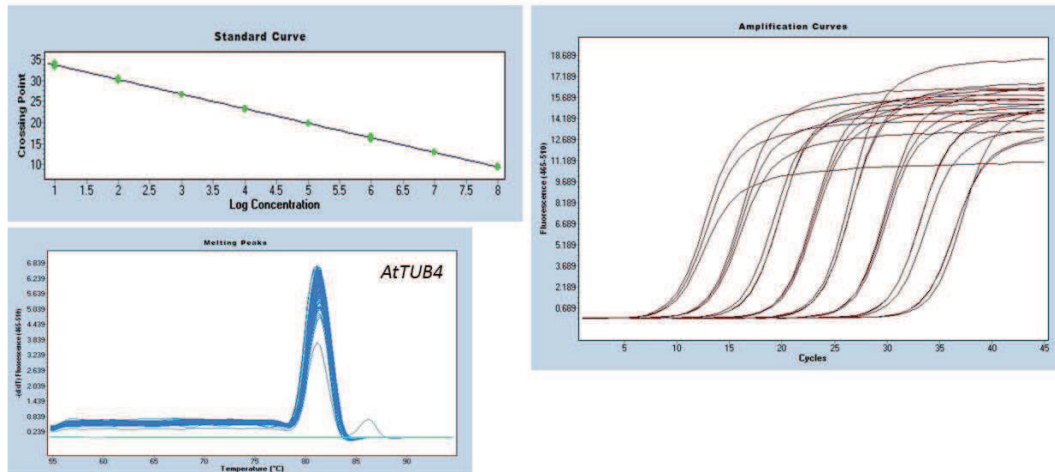
qPCR quantification of *Pseudomonas syringae* growth in planta

Figure 114: Standard curve constructed from a serial dilutions of plasmid containing the *AtTUB4* gene from *A. thaliana*.

Standard curve represents a lineal regression of the log of the concentration of the diluted clone vs CT. $Eff \approx 2$ was calculated from the slope of the curve. Each value corresponds to the average mean of three technical replicates. Below melting curve analysis of all qPCR products amplified with *AtTUB4* to verify primers specificity, from genomic DNA of *A. thaliana* infected with *Pto* DC3000.

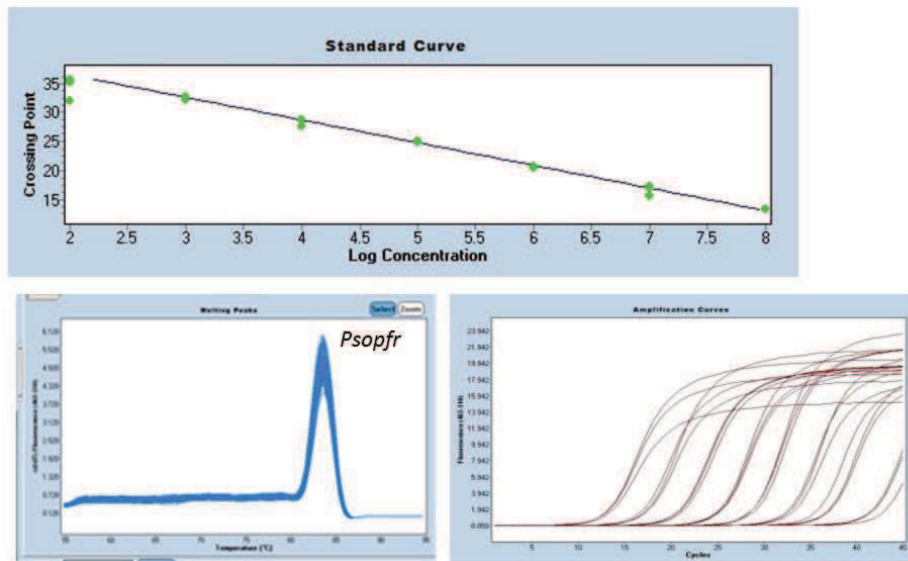


Figure 115: Standard curve constructed from a serial dilutions of plasmid containing the *Psofr* gene from *Pto* DC3000.

Standard curve represents the lineal regression of the log of the concentration of the diluted clone vs CT. $Eff \approx 2$ was calculated from the slope of the curve. Each value corresponds to the average mean of three technical replicates. Below melting curve analysis of all qPCR products amplified with *Psofr* to verify primers specificity, from genomic DNA of *A. thaliana* infected with *Pto* DC3000.

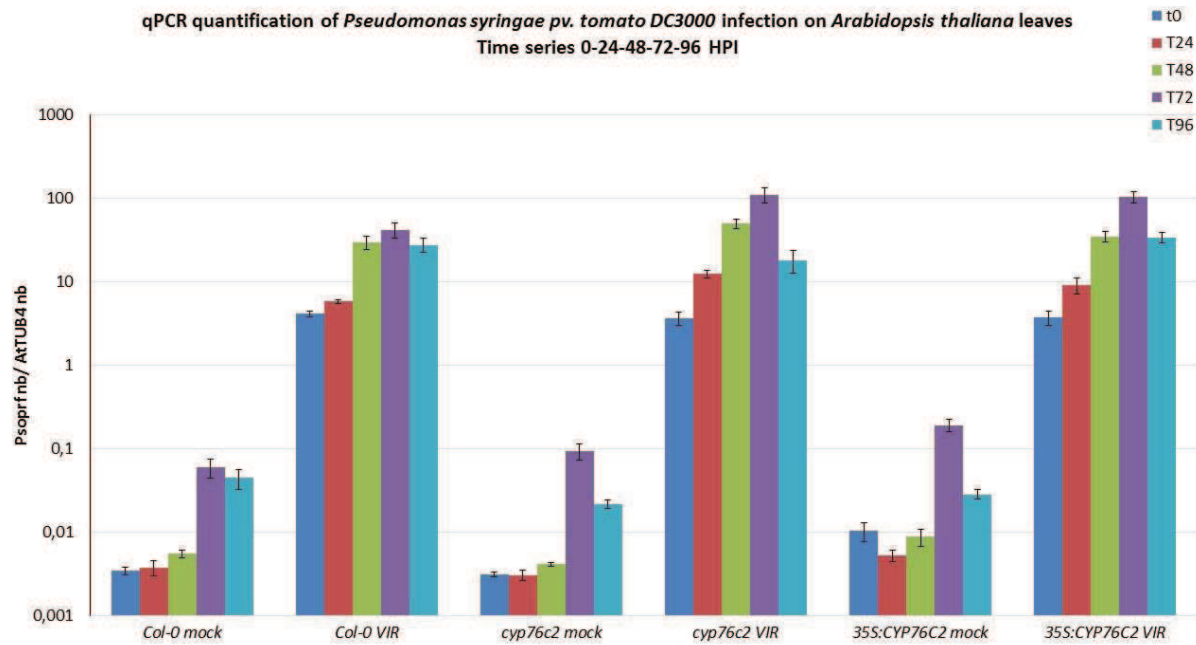
Temporal analysis of symptoms development after *Pto* DC3000 infections

Figure 116: qPCR quantification of time course infection *Pto* DC3000 on *A. thaliana* leaves displaying information about EE.

Data come from the average mean of three technical replicates and five biological ones. Errors bars correspond to errors standard of the mean that were not showed in the manuscript for space constraints.

Temporal analysis of symptoms development after *B. cinerea* infections

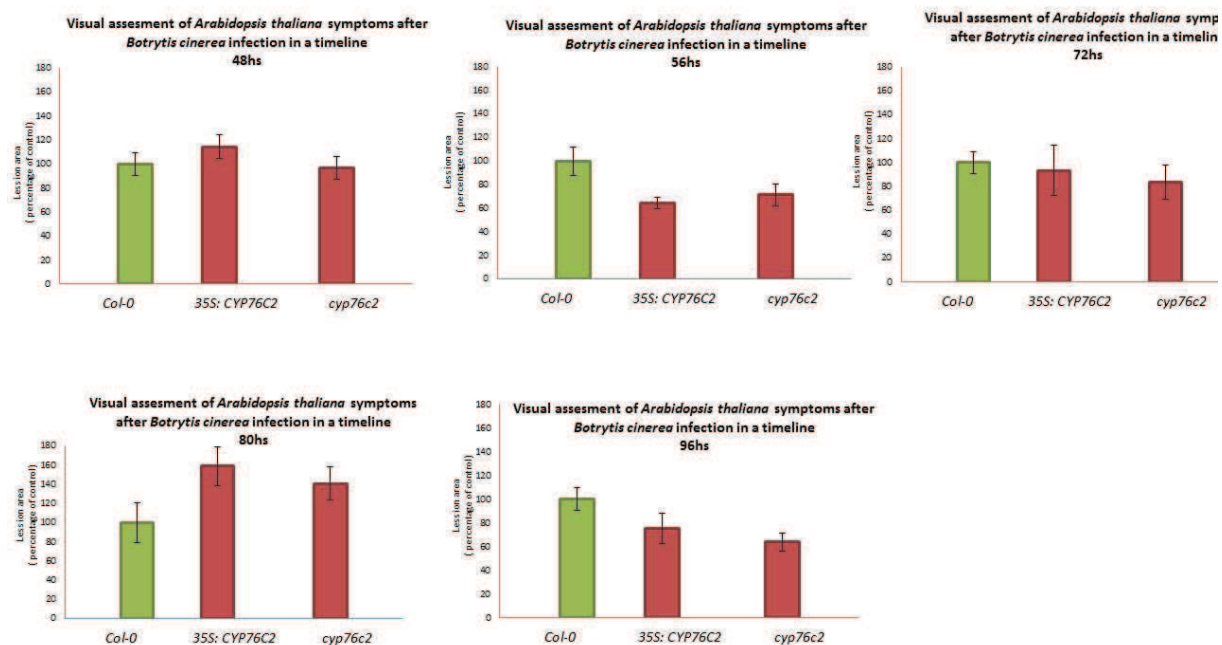


Figure 117: Quantification of disease development in *Arabidopsis thaliana* Col-0, *cyp76c2* and 35S:YFP76C2 plants infected with *B. cinerea* following a time series displaying EE.

Each value correspond to the average area and standard error of 8-10 plants and 5-7 leaves per plant, inoculated with a 5 μ L droplet containing 1×10^5 conidia/ml. Average areas were calculated in mm^2 and expressed as the relative percentage of Col-0 plants at each time point. Estimation of necrotic areas were done at 24-48-56-72-80-96 HPI. Statistically differences were calculated through the Kruskal-Wallis test ($\alpha=0.05$) and are indicated by an asterisk. Errors bars correspond to EE of the mean.

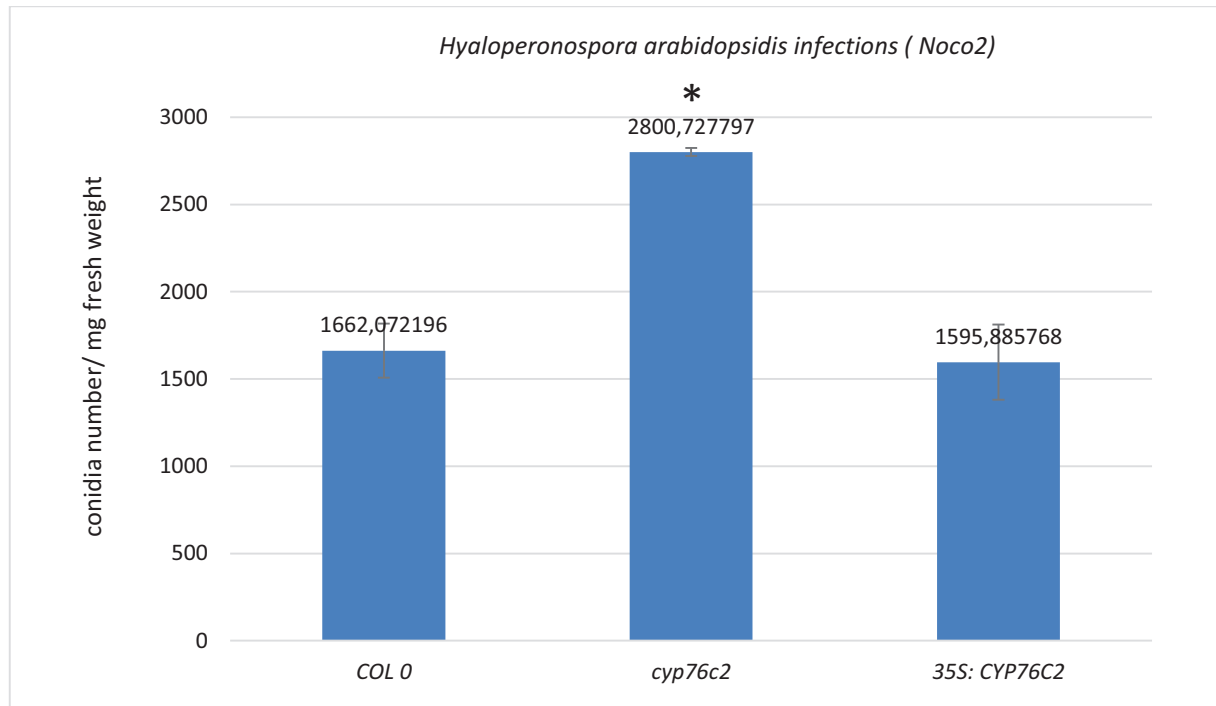
***Hyaloperonospora arabidopsidis* infection with strain Noco2.**

Figure 118: *Hyaloperonospora arabidopsidis* infection with strain Noco2 on *Arabidopsis thaliana* Col-0 wild-type and CYP76C2 mutant plants.

Conidia from Noco2 were quantified at 7 days post infection (DPI) on two pots of seedlings 2-week-old of each genotype (Col-0, *cyp76c2* and 35S:CYP76C2). Quantification on Nageotte chamber was done twice. Asterisk denotes statistically significant differences (Tuckey test at level of 5%). Errors bars represent EE.

Targeted analysis for (mono) terpenoids in UPLC-3Q-MS/MS

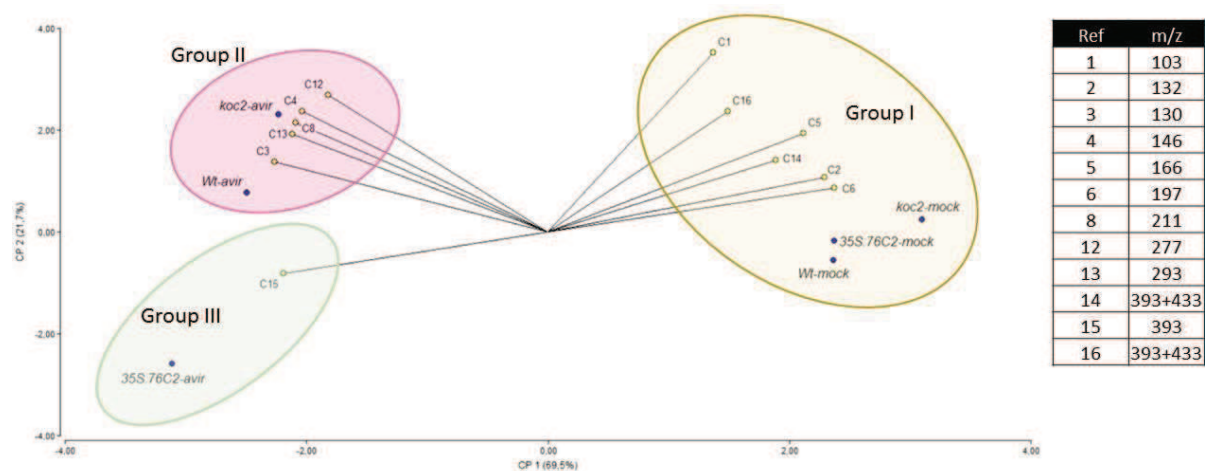


Figure 119: Bi-plot of PCA of the metabolic profiling of Col-0, *cyp76c2* and *35S: CYP76C2* mock and infected plants with *Pto* DC3000 *avrRpm1*. The bi-plot displays three different clusters based peaks founds between 100-450 m/z. Peaks 7-9-11 were eliminated for having variation among triplicates, results obtained by the grouping remained the same.

Plants were syringe-infiltrated with a solution containing $MgCl_2$ (mock) or *Pto* DC3000 *avrRpm1* at a concentration of 5×10^7 CFU/ml. Data represent means of three replicates. CP1 and CP2 explained 91% of variances. In the right is the information about selected peaks m/z.

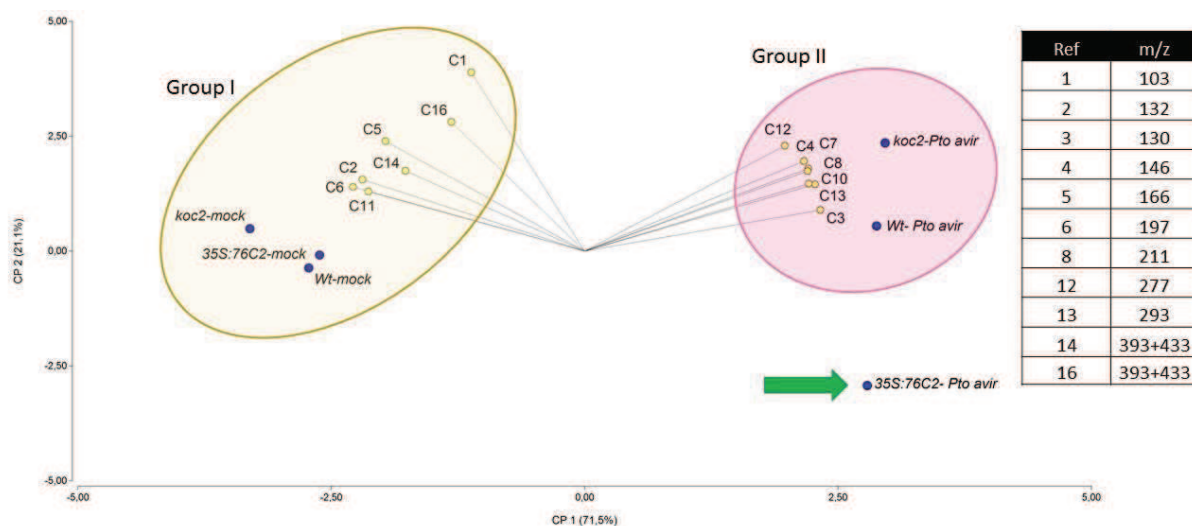


Figure 120: Bi-plot of PCA of the metabolic profiling of Col-0, *cyp76c2* and *35S: CYP76C2* mock and infected plants with *Pto* DC3000 *avrRpm1*. Peaks 9 and 15 were removed, results obtained by the grouping remained the same for clusters I and II, cluster III disappeared. The bi-plot displays two different clusters based in peaks founds between 100-450 m/z. The overexpression mutant does not group to any cluster.

Plants were syringe-infiltrated with a solution containing $MgCl_2$ (mock) or *Pto* DC3000 *avrRpm1* at a concentration of 5×10^7 CFU/ml. Data represent means of three replicates. CP1 and CP2 explained 91% of variances. In the right is the information about selected peaks m/z.

Hormone Profiling in a timeline

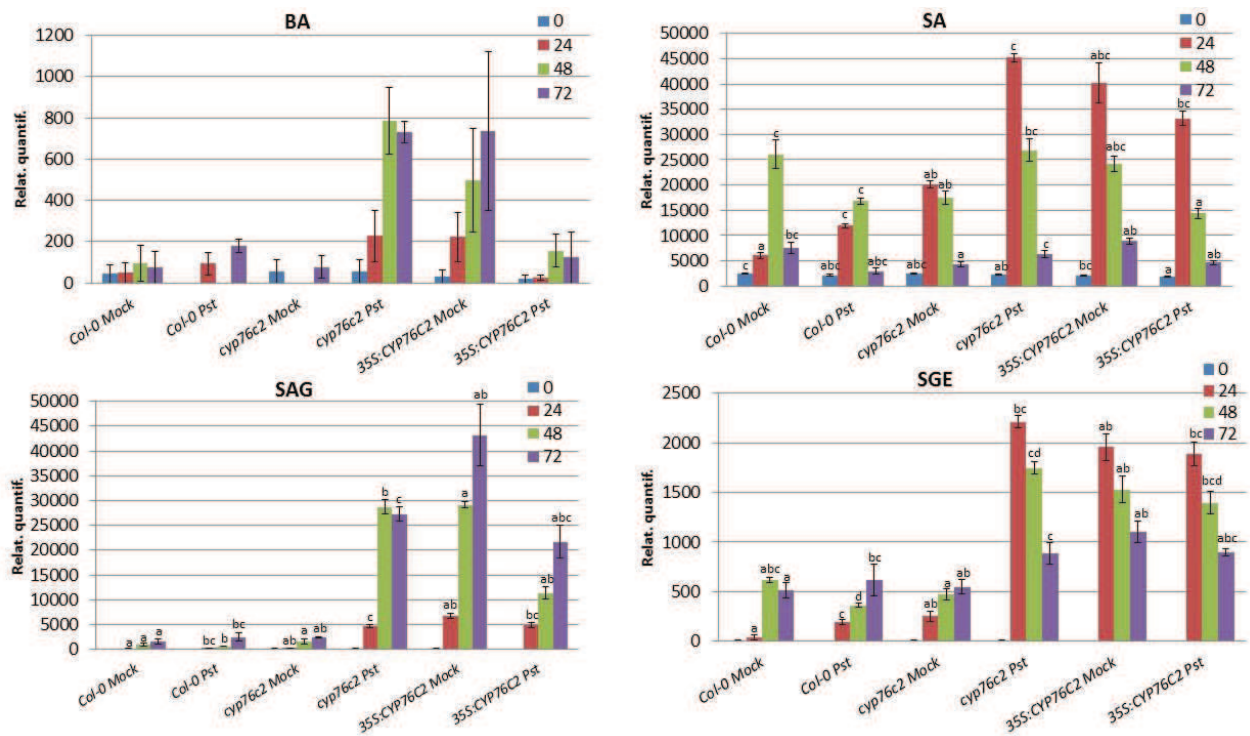


Figure 121: Hormone profiling of BA, SA, SAG and SEG upon *Pto* DC3000 *avrRpm1* infection at T0-24-48-72 HPI.

Plants were syringe-infiltrated with a solution containing $MgCl_2$ (mock) or *Pto* DC3000 *avrRpm1* at a concentration of 5×10^7 CFU/ml. Data represent means of three replicates. Error bars represent the standard error of the mean. Letters show statistically significant differences calculated by Kruskal-Wallis test ($p < 0.05$).

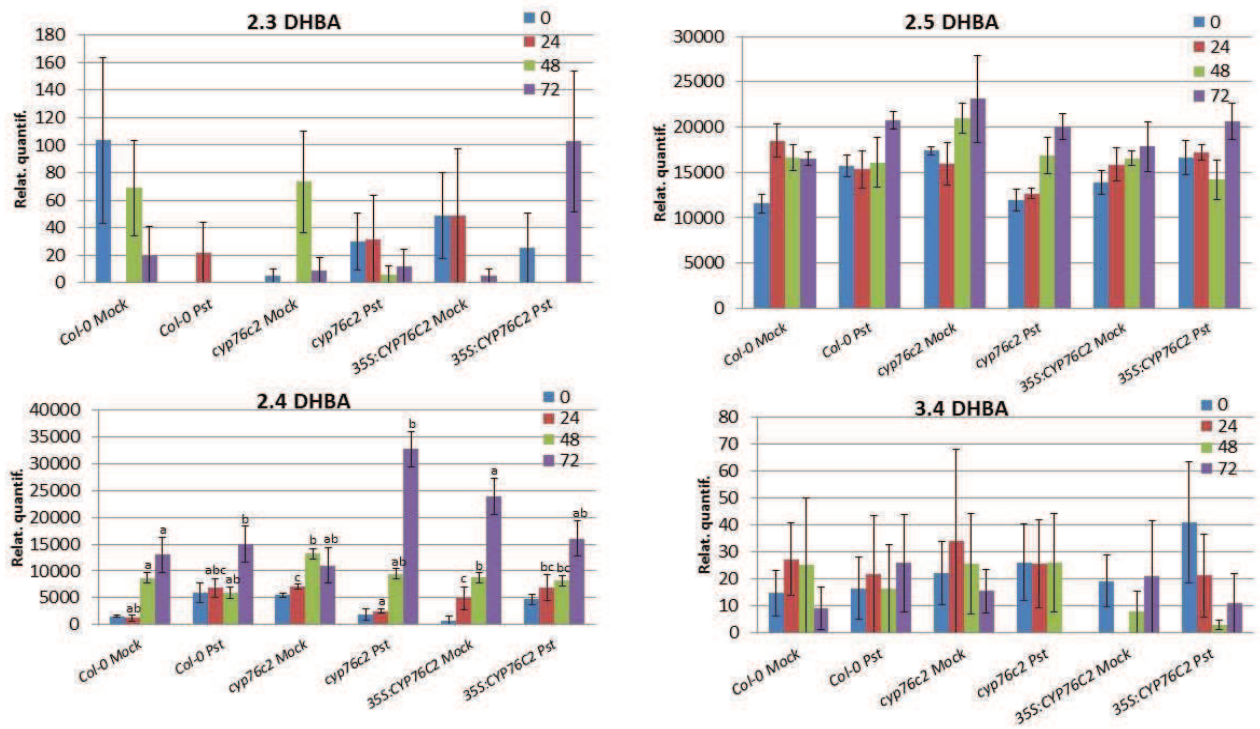


Figure 122: Hormone profiling of 2,3, 2,5, 2,4 and 3,4 DHBA upon *Pto DC3000 avrRpm1* infection at T0-24-48-72 HPI.

Plants were syringe-infiltrated with a solution containing $MgCl_2$ (mock) or *Pto DC3000 avrRpm1* at a concentration of 5×10^7 CFU/ml. Data represent means of three replicates. Error bars represent the standard error of the mean. Letters show statistically significant differences calculated by Kruskal-Wallis test ($p < 0.05$).

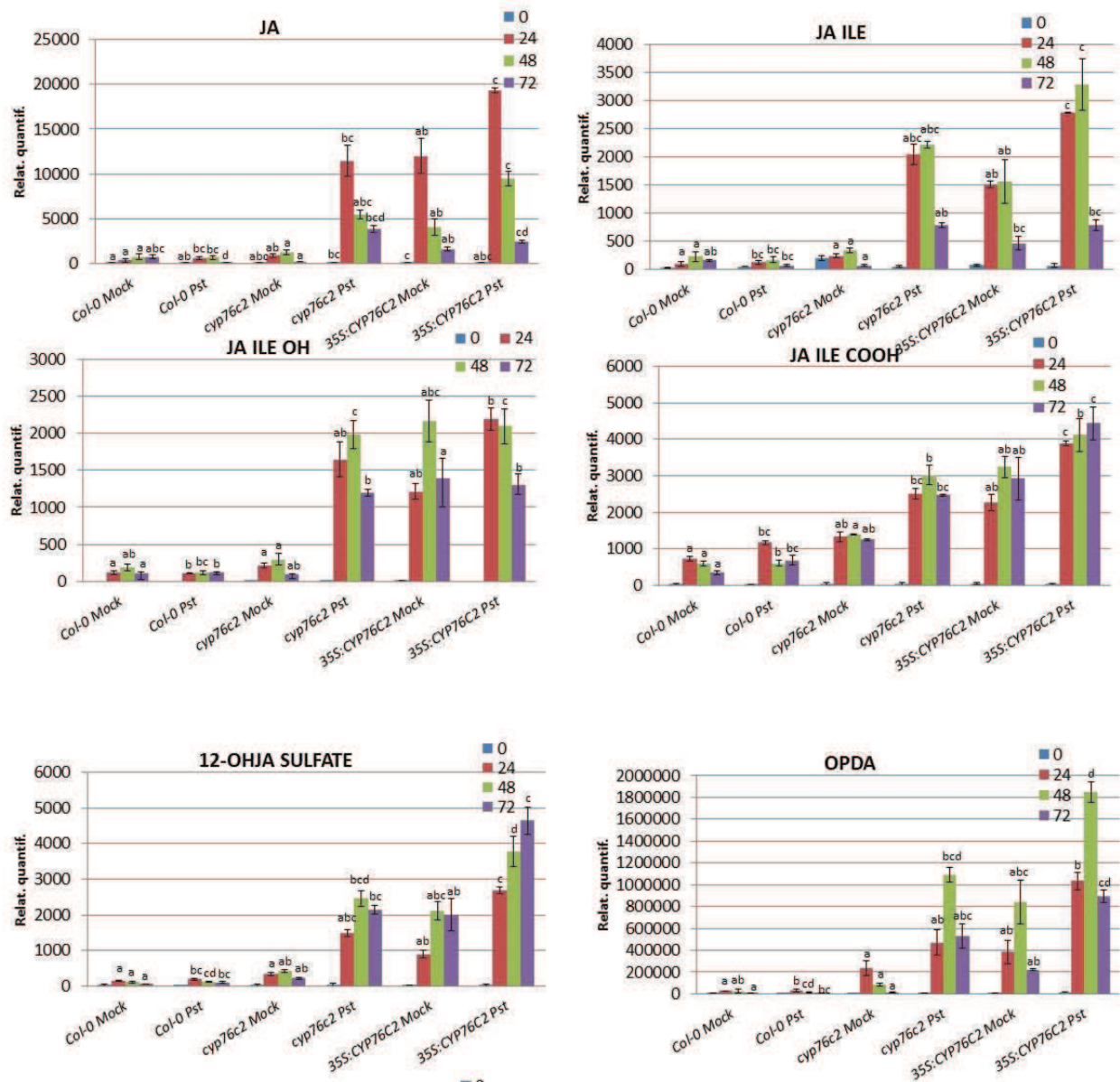


Figure 123: Hormone profiling of JAs upon *Pto* DC3000 *avrRpm1* infection at T0-24-48-72 HPI.

Plants were syringe-infiltrated with a solution containing $MgCl_2$ (mock) or *Pto* DC3000 *avrRpm1* at a concentration of 5×10^7 CFU/ml. Data represent means of three replicates. Errors bars represents the standard error of the mean. Letters shows statistically significant differences calculated by Kruskal-Wallis test ($p < 0.05$).

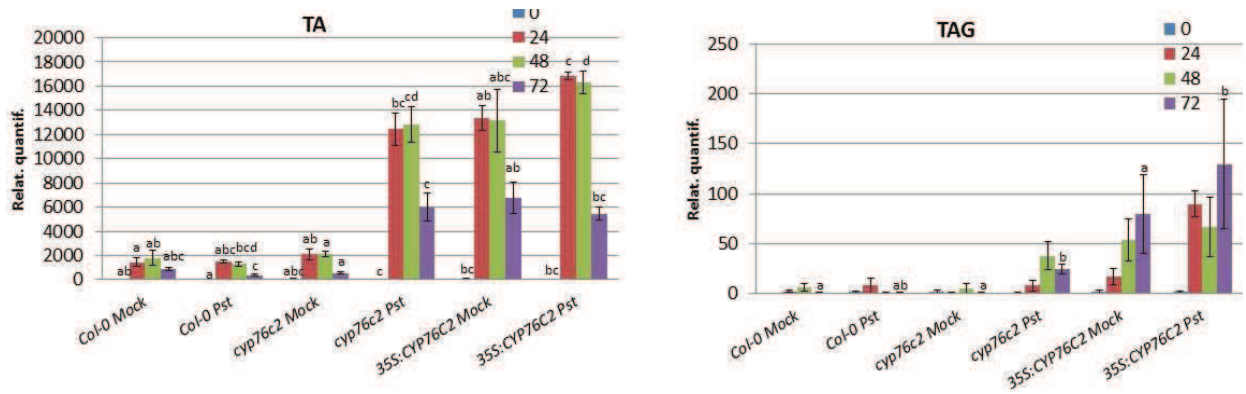


Figure 124: Hormone profiling of TA and its glycosylated form upon *Pto* DC3000 *avrRpm1* infection at T0-24-48-72 HPI.

Plants were syringe-infiltrated with a solution containing $MgCl_2$ (mock) or *Pto* DC3000 *avrRpm1* at a concentration of 5×10^7 CFU/ml. Data represent means of three replicates. Error bars represent the standard error of the mean. Letters show statistically significant differences calculated by Kruskal-Wallis test ($p < 0.05$).

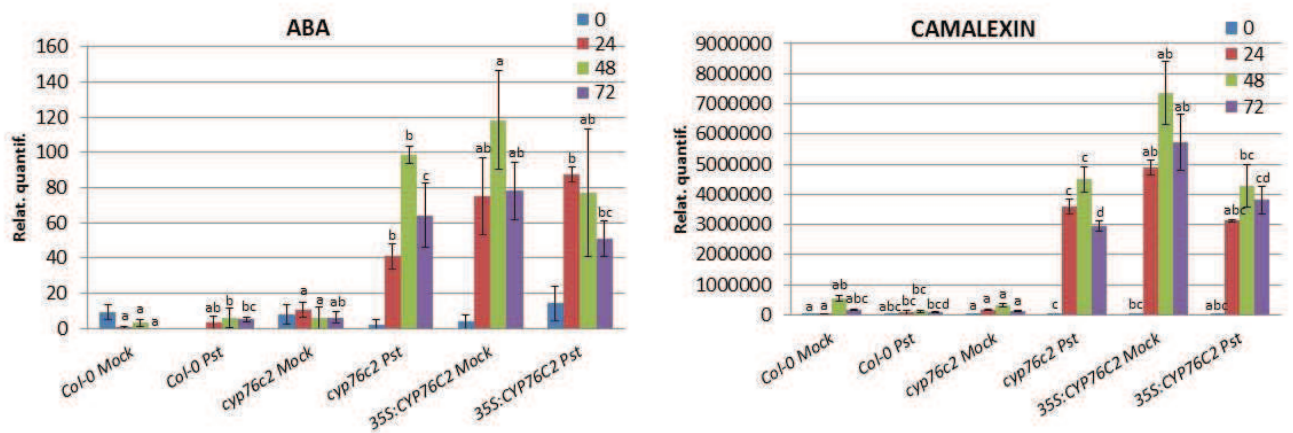


Figure 125: Profiling of ABA and camalexin upon *Pto* DC3000 *avrRpm1* infection at T0-24-48-72 HPI.

Plants were syringe-infiltrated with a solution containing $MgCl_2$ (mock) or *Pto* DC3000 *avrRpm1* at a concentration of 5×10^7 CFU/ml. Data represent means of three replicates. Error bars represent the standard error of the mean. Letters show statistically significant differences calculated by Kruskal-Wallis test ($p < 0.05$).

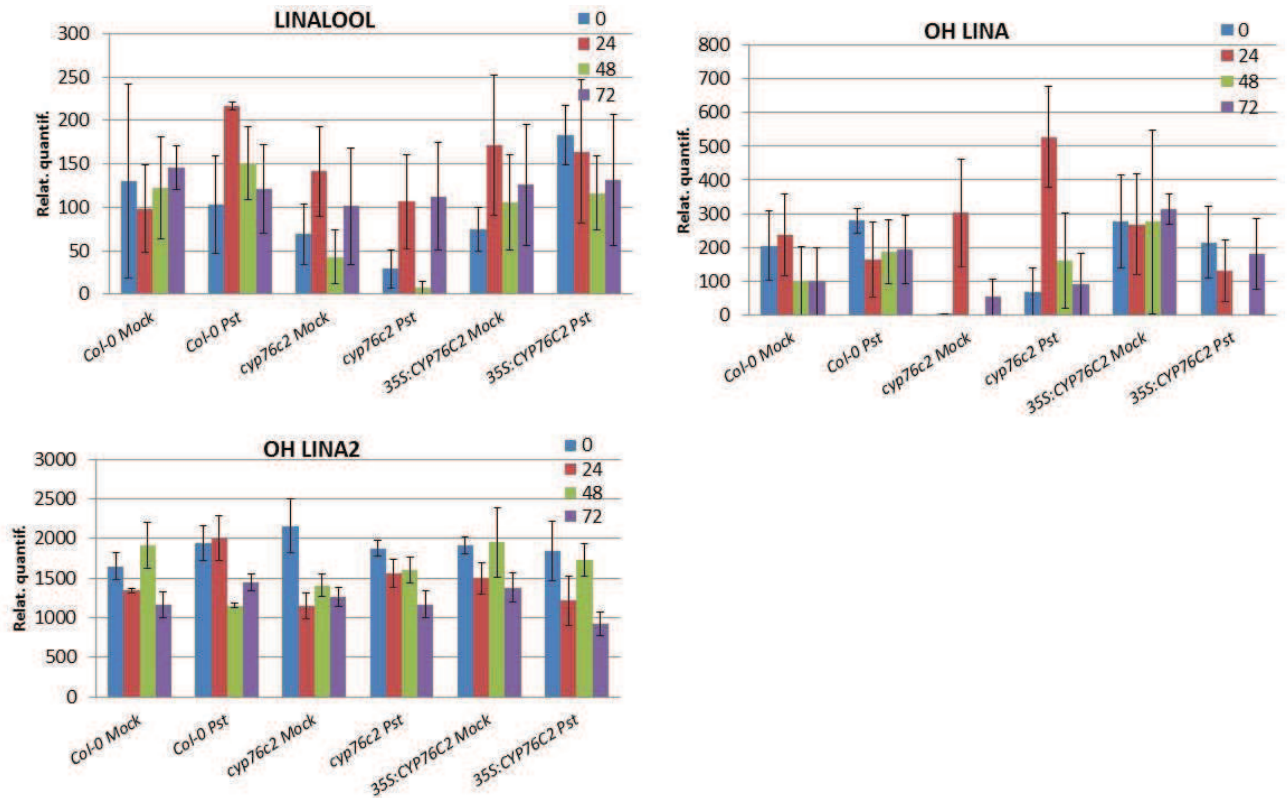
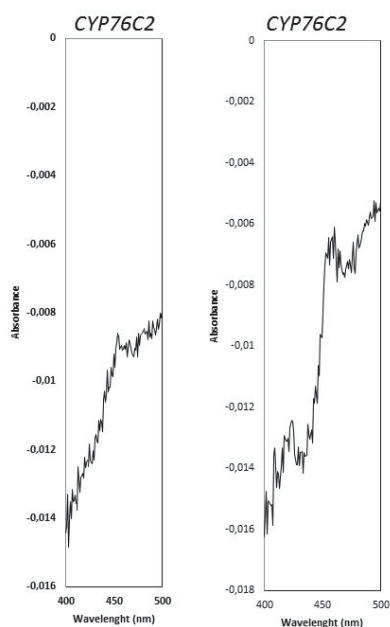


Figure 126: Profiling of Linalool and hydroxylated derivatives at T0-24-48-72 HPI.

Plants were syringe-infiltrated with a solution containing $MgCl_2$ (mock) or *Pto* DC3000 *avrRpm1* at a concentration of 5×10^7 CFU/ml. Data represent means of three replicates. Error bars represent the standard error of the mean. No statistically significant differences calculated by Kruskal-Wallis test ($p < 0.05$) were found.

Microsomes CYP76C2

a)



b)

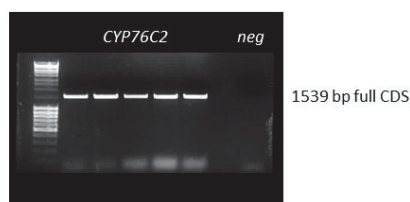


Figure 127: *CYP76C2* was cloned into the yeast expression vector *pYeDP60U2* and expressed in *Saccharomyces cerevisiae* *WAT11* strain.

The yeast microsomal fraction containing the recombinant protein was extracted and used for incubations. **a)** CO-induced difference spectrum of reduced yeast microsomes expressing *CYP76C2*. Microsomes diluted 10× in TG buffer and gassed with CO. Sodium dithionite was added to reduce the P450 and generate the difference spectrum. **b)** Confirmation of positive transformants by PCR with specific gene primers. PCR products on agarose gel 1X.

Résumé étendu en Français

Analyse fonctionnelle du rôle de *CYP76C2* dans les mécanismes de défense des plantes contre les agents pathogènes

Introduction

Les plantes disposent d'un système d'immunité innée pour combattre les agressions par des agents pathogènes. L'activation de cette immunité implique des réponses locales au niveau du site d'attaque, comme la réaction d'hypersensibilité (HR) caractérisée par la mort par suicide cellulaire des cellules percevant l'attaque, et des réponses à distance du site d'infection, comme la résistance locale acquise (LAR) et la résistance systémique acquise (SAR). Le phénomène LAR, qui implique de nombreuses reprogrammations géniques, participe au confinement de l'infection primaire. Le phénomène SAR équivaut à une « mise en éveil » de l'ensemble des tissus de la plante, permettant une réponse plus efficace dans le cas d'une éventuelle infection secondaire. L'efficacité de ces mécanismes de défense est directement liée à la production de signaux endogènes, synthétisés en réponse à un agresseur ; mais aussi à la capacité d'induction de ces signaux pour la production de protéines et de métabolites secondaires, contribuant ensemble à la résistance de la plante.

Une analyse transcriptomique d'*Arabidopsis thaliana* (*A. thaliana*) réalisée à l'IBMP par Serge Kaufmann (Project SARA Trilateral Genoplante « *Functional genomics of local and systemic acquired resistance in Arabidopsis*) sous différents stress biotiques a montré une activation des gènes codants pour des cytochromes P450 (P450), suggérant que certains membres de cette famille de protéines enzymatiques auraient un rôle dans l'efficacité des réponses de défense contre les agents pathogènes. En effet, plusieurs études ont pu montrer le rôle de certains P450 dans les mécanismes de défense chez *A. thaliana*, c'est par exemple le cas de *CYP71B15* (Schuhegger *et al.*, 2006), *CYP71A13* (Nafisi *et al.*, 2007) ou encore *CYP79B2/B3* (Hull *et al.*, 2000).

Cependant, le rôle et la fonction de la grande majorité des P450 identifiés par cette analyse transcriptomique sont encore mal compris ou méconnus. Les membres de la famille *CYP76*, et particulièrement *CYP76C2* montrant un fort taux d'expression suite à l'application d'un stress biotique (env. 50 fois supérieur), font parties des P450 dont la fonction et le rôle ne sont pas encore connus à ce jour.

La caractérisation fonctionnelle de la famille des *CYP76*, et plus particulièrement de *CYP76C2*, a donc fait l'objet de ce projet de thèse.

Afin d'étudier la fonction des différents membres de la famille des *CYP76*, mais aussi les voies métaboliques qu'ils font intervenir, plusieurs types de mutants d'*A. thaliana* ont été générés: des mutants de type « perte de fonction » pour lesquels l'expression du *CYP76* étudié est supprimée (appelés aussi mutants *cyp76c*) et à l'inverse, des mutants de surexpression du *CYP76* (*35S:CYP76C*), pour lesquels le gène *CYP76* étudié est mis sous contrôle du promoteur d'expression fort 35S du virus de la mosaïque du chou-fleur (CaMV). Le phénotype de ces mutants a été caractérisé sous différentes conditions d'infection: par deux souches de la bactérie hémibiotrophe *Pseudomonas syringae* (*P. syringae*): une souche virulente (*P. syringae* DC3000) et une souche avirulente porteuse du gène d'avirulence *AvrRpm1* (*P. syringae* DC3000 *AvrRpm1*); ainsi que par le champignon nécrotrophe *Botrytis cinerea* (*B. cinerea*). La voie métabolique faisant intervenir le CYP sélectionné a été étudiée par une approche de « profiling » métabolique ciblée et non ciblée en cherchant le(s) métabolite(s) potentiellement impliqué(s) dans les mécanismes de défense, ainsi que leurs/son rôle(s) potentiel(s) dans les processus de défense mis en place et qui participent à la résistance ou à la susceptibilité de la plante.

Objectifs de thèse

- Etudier l'expression des gènes de la famille de *CYP76* chez *Arabidopsis thaliana*, en réponse à une infection par des pathogènes ayant un mode vie Hémibiotrophe (*P. syringae* souche virulente ou avirulente) ou nécrotrophe (*B. cinerea*).
- Etudier l'impact des gènes de la famille des *CYP76* sur la défense des plantes.
- Comparer les profils métaboliques des différents mutants des P450 sélectionnés avec ceux des plantes de type sauvage, avant et après le déclenchement de l'infection.
- Associer ces différentes P450 aux voies métaboliques déjà caractérisées, ou potentiellement à de nouvelles voies de biosynthèse.
- Etudier le mode d'action de ces métabolites dans les mécanismes de défense des plantes.

Résultats obtenus

Analyses de l'expression des gènes de la famille CYP76 avant et après infection avec des organismes pathogènes et sélection des gènes candidats

Dans un premier temps, une analyse de l'expression des différents membres de la famille *CYP76* a été réalisée par RT-qPCR. Ces analyses ont été faites sur des feuilles d'*A. thaliana* var. *Col-0* avant et après infection par *P. syringae* (souche virulente et avirulente) et *B. cinerea*.

Afin de préciser la chronologie et la localisation de l'expression, du déclenchement de l'infection à l'établissement des symptômes, une courbe cinétique a été réalisée aux intervalles de 0-2-4-6-8-24-48-72 heures post-infection, selon le type de pathogène testé. Les infections ont été caractérisées aussi selon le type de réponse de défense engagé (LAR, SAR ou HR), et pourtant chaque région ayant été analysée de façon indépendante.

Les résultats obtenus ont montrés que seul le gène *CYP76C2* était fortement induit après infection (*P. syringae* virulent et *B. cinerea*) ou élicitation (*P. syringae* avirulent), et plus précisément au niveau des régions caractérisées pour la présence de mort cellulaire : HR (morte cellulaire comme manifestation de la résistance) et nécrose (morte cellulaire comme conséquence du maladie). *CYP76C2* a montré une activité maximale d'induction dès 6-8 h post-infection pour la souche avirulente de *P. syringae*, 4-6 h post-infection par la souche virulente de *P. syringae*, et 48 h post-infection par *B. cinerea*.

Aucun membre de la famille des *CYP76*, *CYP76C2* inclus, n'est exprimé à distance du site d'attaque, ce qui aurait été caractéristique de la mise en place d'une résistance locale acquise (LAR) et d'une résistance systémique acquise (SAR). Les mêmes observations ont été constatées au niveau des régions périphériques aux blessures causées par *B. cinerea*.

Cette réponse a été visualisée et confirmée par histochimie en exprimant le gène rapporteur *GUS* sous contrôle du promoteur de *CYP76C2* (*Prom_{CYP76C2}* : *GUS*).

Analyse phénotypique des mutants CYP72C2 après infection par des organismes pathogènes

Dans un deuxième temps, le phénotype des mutants de type « perte de fonction » ou « surexpression » du gène candidat *CYP76C2* a été caractérisé suite à une infection par *P. syringae* ou *B. cinerea*. Chacun des ces pathogènes représente, de façon simplifiée, une stratégie d'infection particulière pour se nourrir, coloniser, et se multiplier dans la plante. De même, pour chaque type de pathogène, les plantes adapteront leurs mécanismes de défense.

P. syringae est un parasite de type « hémibiotrophe » dont le cycle de vie se compose de deux étapes : une première étape, dite « biotrophe », durant laquelle le pathogène colonise les tissus végétaux sans tuer l'hôte ; et une seconde étape, dite « nécrotrophe », où le pathogène tue l'hôte afin de pouvoir se nourrir des cellules mortes. D'autre part, *B. cinerea* représente un style de parasitisme « nécrotrophe ». Ainsi, le phénotype des différents mutants d'*A. thaliana* a été caractérisé selon ces deux styles de parasitisme bien distincts dans leur mode de fonctionnement

Les analyses des mutants de *CYP76C2* n'ont révélées aucun impact sur la résistance des plantes face à ces deux agents pathogènes, à *contrario* de l'induction des gènes observée préalablement. Le phénotype n'est pas si fort que l'induction de gènes .

La famille des *CYP76*, dont fait partie *CYP76C2*, comporte en totalité 8 membres très proches les uns des autres. De ce fait, une redondance d'activité entre les différentes isoformes pourrait être envisagée pour expliquer l'absence de phénotype. Pour vérifier cette hypothèse, des cinétiques d'infection ont été réalisées au niveau des feuilles des différents mutants de *CYP76C2* (0, 24, 48, 72 et 96 h selon l'agent pathogène considéré), l'objectif étant de rechercher d'éventuels phénotypes transitoires, pouvant confirmer ou infirmer l'hypothèse de la redondance fonctionnelle au sein de la famille des *CYP76*. Ces analyses ont pu mettre en évidence deux résultats intéressants, selon le type d'interaction plante/pathogène considérée.

Premièrement, dans le cas d'une interaction compatible (souche virulente, *i.e* plante susceptible qui développe les symptômes de la maladie), les plantes *cyp76c2* ont été plus affectés que les mutants *35S:CYP76C2* ou les plantes sauvages, 24 H post-infection, période pendant laquelle les symptômes se développent. Durant cette période, l'absence de *CYP76C2* rend donc les plantes plus sensibles aux pathogènes. Néanmoins, 48-72-96 H post-infection, il n'y a pas de différences entre les différents mutants et les plantes sauvages, ce qui suggère un phénomène de redondance.

Deuxièmement, dans le cas d'une interaction compatible (souche avirulente, *i.e* la plante reconnaît le pathogène et met en place un mécanisme de défense de type HR), le mutant *35S:CYP76C2* est plus affecté entre 24 et 48H post-infection, en comparaison avec le mutant *cyp76c2* ou la plante sauvage.

Dans le cas d'une infection par *B. cinerea*, dès que les symptômes sont développés (72-80h post infection), les plantes sauvages sont plus affectées que les deux mutants *CYP76C2*. A l'étape finale de la maladie (96 post-infection), les plantes de type sauvage *Col-0* et le mutant *35S:CYP76C2* sont significativement plus affectés par la maladie que le mutant *cyp76c2*, montrant des lésions nécrotiques de tailles inférieures.

« Profiling » métabolique ciblé et non-ciblé des mutants des plantes infectées et non-infectées et
Identification des métabolites secondaires candidats

Sur la base d'analyses *in silico* de co-expression avec des monoterpènes synthases, couplées aux données de coexpression préexistantes, les gènes de la famille *CYP76* pourraient être impliqués dans la biosynthèse de monoterpénoïdes (Elthing *et al.*, 2008). Le rôle des terpènes volatiles, émis au niveau des fleurs ou des feuilles et servant de signaux à distance inter- ou intra- plante, a bien été décrit chez différents modèles végétaux et dans différentes conditions de développement ou de stress (plusieurs auteurs). Plus récemment, les monoterpènes et les sesquiterpènes ont été décrits comme étant des activateurs des mécanismes de défenses d'*A. thaliana* (Kishimoto *et al.*, 2006, Godard *et al.*, 2008, Huang *et al.*, 2011, Chaturvedi *et al.*, 2012). Afin de démontrer l'implication de *CYP76C2* dans la biosynthèse de monoterpènes et l'interaction plante/pathogène, l'émission de composés volatils a été analysée au niveau des feuilles d'*A. thaliana* var. Col-0 (type sauvage) et des deux types de mutants *CYP76C2* infectés par *P. syringae* (souche virulente et avirulente) ou *B. cinerea*. Les analyses métaboliques par GC-MS ont pu montrer une très forte émission de salicylate de méthyle dans le cas d'une infection par *Pseudomonas*. Cependant, aucun métabolite de la famille des terpénoïdes ou appartenant à d'autres familles de composés volatils n'a pu être détecté, cela malgré le fait que *CYP76C2* soit capable de métaboliser le linalol, le nérol et le citronellol *in vitro* (Höffer *et al.*, 2014).

Par la suite, un profilage métabolique ciblé et non ciblé par UPLC-MS a été effectué sur des feuilles des mutants *CYP76C2* infectés/non-infectés, dans le but d'identifier les composés non volatils impliqués dans la réponse immunitaire observée. A partir de ce moment les manipulations ont été concentrées sur la réaction de HR d'*Arabidopsis thaliana* à *P. syringae* DC3000 *AvrRpm1* ou l'expression de *CYP76C2* a été fortement induite (*i.e.* résistance et mise en place des mécanismes de défense par la plante).

Le profilage ciblé axé sur les conjugués terpéniques n'a pas permis d'identifier de métabolites secondaires intéressants. Cependant, l'analyse par stratégie non-ciblée a permis de détecter un métabolite secondaire que l'on ne retrouve pas chez les mutants *cyp76c2*. L'analyse de la masse précise a permis de déterminer une formule brute correspondante à ce métabolite: $C_{17}H_{28}O_9$, ce qui correspond à une quinzaine de métabolites candidats environ.

Afin de compléter cette stratégie de profilage métabolique, une analyse métabolique des hormones a été effectuée. L'induction de *CYP76C2* en situation de mort cellulaire suggère que ce gène pourrait être impliqué dans la synthèse d'un signal de défense ou dans la synthèse d'une molécule de défense. En effet, l'induction des mécanismes de défense des plantes met en jeu un réseau complexe de signaux endogènes orchestré par des hormones telles que l'acide salicylique (SA), le jasmonate (JA), l'éthylène (ET), l'acide abscissique (ABA), les gibbérellines (GB), les Auxines (AUX /IAA) ou encore les

cytokinines (CK). En outre, la réaction d'hypersensibilité (HR) implique une activation de la voie de signalisation de l'acide salicylique. Ce dernier joue un rôle primordial dans la défense contre les pathogènes biotrophes/ hemibiotrophes, en activant des gènes de défense (upstream: PAD4, EDS1, SAG101; downstream: NDR1, PR1, GST6, etc.), mais aussi pour son effet antagonique avec certaines hormones végétales comme le JA/ET ou encore les auxines et l'ABA.

Ainsi, l'accumulation des dérivés de la voie de biosynthèse du SA et JA (voir en bas le détail des composés analysés) de l'ABA et la phytoalexine d'*Arabidopsis*, la camalexine ont été analysés au niveau de feuilles infectées et non infectées, des différents mutants de *CYP76C2* aux intervalles de 0, 24, 48, 72 H post-infection.

Les résultats ont pu montrer qu'il y a un corrélat entre la cinétique des symptômes observés (*i.e.* *35S:CYP76C2* a montré plus de symptômes à 24-48 H post-infection) et les niveaux hormonaux observés. Les niveaux du SA et ses formes conjuguées, SAG et SEG, sont diminués dans le *35S:CYP76C2* pendant que la voie du JA est renforcée (OPDA, JA, JA-Ile et ses formes inactives, TA, TAG).

D'autre part les niveaux d'ABA et Camalexine sont plus élevés chez le mutant *cyp76c2* quasiment pendant tout le démarrage de la cinétique d'infection (24-48-72 H).

Malheureusement on n'a pas trouvé des résultats intéressants (et statistiquement significatifs) dans la plupart des dérivés benzoïques, exception faite pour le 2.4 DHBA (jamais décrit on plante) plus accrue 72 HPI dans le Col-0 et le *cyp76c2* (*35S:CYP76C2* est au même niveau que les plantes non infectées).

Conclusion

Ce travail de thèse a consisté à caractériser le rôle de *CYP76C2* chez *Arabidopsis thaliana* lors des interactions biotiques avec des organismes pathogènes. De manière paradoxale, bien que nous ayons pu confirmer que le gène *CYP76C2* est très fortement activé de manière locale en réponse à divers stress biotiques, le niveau d'expression de *CYP76C2* ne semble pas affecter la résistance de la plante aux pathogènes que nous avons testés. Ceci pose la question du rôle de *CYP76C2* chez la plante. Nous avons donc tenté de comprendre le rôle métabolique de *CYP76C2*. Les efforts consacrés à l'identification de ses substrats et produits se sont concentrés sur les voies métaboliques les plus probables compte tenu de son activité *in vitro* et de l'activité de ses plus proches homologues *in vivo*. En effet d'autres membres de la famille *CYP76C*, tel que *CYP76C1*, *CYP76C3* ont un rôle important dans la formation de dérivés oxydés du linalool dans la fleur. Bien que *CYP76C2* soit biochimiquement actif *in vitro* sur le linalool, les dérivés du linalool ne semblent pas impliqués dans les réactions de défense. Par ailleurs, *CYP76C2* étant SA-dépendant il était intéressant de rechercher ses implications dans la formation des dérivés du SA. Malheureusement, et malgré quelques résultats intéressants, il est difficile de conclure quant à l'activité de *CYP76C2*.

Les lignées affectées dans l'expression de CYP76C2 ne présentent pas de phénotypes clairement différents de ceux des plantes sauvages. Ils indiquent que CYP76C2 n'est probablement pas impliqué directement dans la synthèse d'une molécule cruciale pour la mise en place du processus de défense, mais plus certainement dans un rôle secondaire lié au stress biotique, peut-être le catabolisme d'un signal ou de molécules de défense.

CONCLUSION ET PERSPECTIVES (Version française)

Les analyses de données transcriptomiques précédentes ont suggéré un rôle possible des membres de la famille *CYP76* des enzymes P450 dans les réponses de défense des plantes contre les pathogènes chez *Arabidopsis*. Surtout *CYP76C2* a montré une expression très induite (≈ 50 fois) en réponse au stress biotique dans le contexte des réponses LAR (Kauffmann, communication personnelle). De surcroît, *CYP76C2* a été mentionné par ailleurs comme induit en réponse à des stress biotiques et abiotiques (Godiard *et al.*, 1998; Ehrling *et al.*, 2008; Höfer *et al.*, 2014) et putativement impliqué dans le métabolisme du glucosinolates (Rowe *et al.*, 2010).

Compte-tenu de ces résultats précédents, une approche de génomique fonctionnelle a été réalisée, avec un accent particulier sur la famille *CYP76* et surtout sur *CYP76C2*, pour identifier les gènes P450 jouant un rôle clé dans le développement des mécanismes de défense chez *A. thaliana*.

Ce travail a été axé sur trois aspects principaux:

- **Analyse de l'expression des gènes** de la famille de *CYP76* dans des plantes non-infectées et infectées ;
- **Phénotypage des mutants** de type « perte de fonction » ou « surexpression » des plantes non-infectées et infectées ;
- **Profilage métabolique** des différents mutants des P450 sélectionnés avec ceux des plantes de type sauvage, avant et après le déclenchement de l'infection.

Les résultats ont révélé que, dans la famille de *CYP76*, *CYP76C2* a montré le taux d'induction le plus important au niveau de la réponse à *B. cinerea* et l'infection avec *Pto DC3000*. Les réponses à l'infection avirulente par *Pto DC3000 avrRpm1* étaient également importantes dans la zone HR (*Hypersensitive Response*) et dans la zone SAR (*Systemic Acquired Resistance*), mais l'induction de ce gène a été négligeable dans la zone de LAR (*Local Acquired Resistance*).

Des données d'expression génique obtenues à partir de qRT-PCR ont été affinées dans la plante à l'aide de la coloration GUS de plantes transformées d'*Arabidopsis Prom_{CYP76C2}:GUS*. Cet ensemble de résultats a confirmé que *CYP76C2* est sensible à l'infection virulente, l'infection avirulente (HR) et *B. cinerea*, et a confirmé qu'aucune activation du gène importante ne se produit dans les tissus LAR et SAR.

L'information obtenue à partir de qRT-PCR et GUS était surprenante puisque les données transcriptomiques étaient initialement prévues *CYP76C2* comme fortement induites dans LAR et supprimées dans le mutant *dth9* à 6 HAI (Heures Après Infection). Ce mutant est incapable de monter

SAR, mais il n'est pas affectée dans la production du SA (*Salicylic Acid*) et l'accumulation de camalexine. Plus d'informations semble donc nécessaire sur la façon dont les expériences précédentes ont été réalisées pour être en mesure de bien comparer les expériences et d'aboutir à une conclusion. Par exemple, une suppression de *CYP76C2* dans SAR, comme signalé pour *dth9* à 6 HAI, a également été observée dans notre expérience de 0-6 HAI, jusqu'au 8 HAI lorsque l'induction du gène atteint une augmentation 10 fois plus importante que ce qui était prévu.

La HR est fortement interconnectée avec la LAR et est décisive pour son développement, cependant la SAR est un phénomène qui ne dépend pas nécessairement de la HR pour sa progression (Dorey *et al.*, 1997; Costet *et al.*, 1999).

Malgré la pertinence de *CYP76C2* dans la HR, cet effet n'est pas important pour l'activation de réponses LAR et SAR dans les tissus éloignés. Le mutant *35S:CYP76C2* a montré moins de capacité à monter SAR que le mutant de perdre de fonction *cyp76c2*. Inversement le mutant *cyp76c2* a été affaibli dans les réponses type LAR. Dans ce contexte, si *CYP76C2* a un rôle dans la HR, probablement il n'a aucun rapport avec la signalisation LAR ou SAR, mais plutôt avec le stress oxydatif au cours de la HR (Lamb and Dixon, 1997, Torres *et al.*, 2002; 2006; Wang *et al.*, 2013).

Il serait intéressant d'avoir une image complète de *CYP76C2* par rapport à l'apparition de la HR et du métabolisme oxydatif. Il peut être étudié de différentes manières, par exemple pour la surveillance de l'expression génique ou le phénotypage des mutants de réponse à des pathogènes. Comme il a été mentionné dans l'introduction, la HR repose non seulement sur la mort cellulaire. L'analyse de marqueurs et mutants affectés dans la HR serait donc nécessaire, y compris:

- études sur l'expression/induction du *CYP76C2* / dans des mutants de *A. thaliana* affectés dans la HR et/ou stress oxydatif, comme: HSR3, HIN1, HSR203, LSD1 et / ou ACD2 (Greenberg *et al.*, 1994; Godiard *et al.*, 1998; Pontier *et al.*, 1999; Mur *et al.*, 2008; Coll *et al.*, 2011; Rossi *et al.*, 2011) ;

- des études avec des mutant ayant une déficience dans SAR comme *dth9* (Mayda *et al.*, 2000) ;

- des études avec des mutants liés à stress oxydatif comme *Atrboh* (Torres et Dangl, 2005; Heller and Tduszynski, 2011; Suzuki *et al.*, 2011). Le gènes *AtrbohD* et *AtrbohF* sont responsables de la production de ROS (*Reactive Oxygen Species*) et stress oxydatif chez *A. thaliana* (Torres *et al.*, 2002; Chaouch *et al.*, 2012). Une autre option serait de travailler avec un mutant de *cat2* (Simon *et al.*, 2010) dans lequel ROS est régulé à la hausse.

Il serait également intéressant de quantifier la mort cellulaire dans la HR de chaque génotype. Une expérience préliminaire effectué dans cette thèse a été réalisée en utilisant la coloration du trypan

blue et DAB (3,3'-diaminobenzidine), mais cet expérience n'a pas révélé des différences au sein de toute la famille de *CYP76*. De toute façon il pourrait être instructif de répéter l'expérience avec une augmentation de la dose de l'agent pathogène pour maximiser les réponses. L'augmentation de la dose de l'agent pathogène permettrait également de mieux analyser les interventions SAR, qui n'a pas été très bien traitée dans cette thèse.

Concernant les autres membres de la famille de *CYP76*, aucun d'entre eux ont montré des réponses de l'intérêt pour l'apparition de la défense. *CYP76C1*, l'homologue le plus proche de *CYP76C2* (Höfer *et al.*, 2014) se comportait très différemment et a montré un modèle unique de régulation à la baisse en réponse à toutes les infections réalisées.

Le profil d'expression de *CYP76C5*, *CYP76C6* et *CYP76C7* après l'infection avec *B. cinerea* et *Pseudomonas* a suivi des cinétiques d'expression très similaires à ceux observés pour *TPS10* et *TPS14*, suggérant une association fonctionnelle de ces membres de la famille *CYP76* avec le métabolisme de monoterpenol, qui n'a pas été anticipé.

En accord avec l'induction modérée du gène qui a été observée, le phénotype des mutants de *CYP76C2* infectés n'a pas été significativement différent des plantes sauvages lors d'un traitement avec l'un des agents pathogènes testés (*Pseudomonas* ou *Botrytis*). L'expression du *CYP76C2* n'a eu qu'un impact subtil ou transitoire sur le développement de l'infection.

Initialement, il a été déduit que cela pourrait être dû à la redondance fonctionnelle avec les autres membres de la famille *CYP76* (Millet, 2009). Néanmoins, les profils radicalement différents de l'expression des gènes obtenus pour les différents gènes de la famille ne semblent pas appuyer cette hypothèse. Les infections des mutants de perte de fonction et surexpression des autres membres concernés de la famille a été effectuée pour tous les agents pathogènes considérés, sans détecter aucun phénotype significatif (*CYP76C3*, *CYP76C4*, *CYP76C7*, *CYP76G1*) (résultats non montrés). Cependant, comme les mutants doubles ou triples n'ont pas été testés, la redondance avec un autre membre de *CYP76* ne peut pas être totalement exclue. La redondance avec autre gène(s), non liée est également possible. Par exemple *CYP76C2* a été trouvé co-régulé avec deux UDP-glucuronosyl / UDP-glucosyl (At3g46660 et At2g36770) et un dihydroorotate déshydrogénase/oxydase (At3g17810), les deux types d'enzymes qui pourraient contribuer à brouiller la réponse due à la redondance ou la conjugaison des substances actives.

D'un point de vue métabolique, la susceptibilité transitoire et subtile de mutants *35S:CYP76C2* à l'infection avirulente (HR) suggère une certaine relation entre *CYP76C2* et le ROS. Peut-être, *CYP76C2* contribue à améliorer la production de ROS au lieu d'aider à la désintoxication. Une autre possibilité serait que *CYP76C2* catalyse une réaction mal couplé et donc génère directement ROS.

Données transcriptomiques et analyse de co-expression de P450 avec des terpènes synthases ont déjà suggéré que plusieurs membres de la sous-famille de *CYP76C* pourraient être impliqués dans la biosynthèse de monoterpénoïdes (Ehlting *et al.*, 2008). *CYP76C1*, *CYP76C2* et *CYP76C4* étaient en outre présentés pour métaboliser plusieurs monoterpénols comme citronellole, le linalool, le géraniol et le nerol *in vitro* (Höfer *et al.*, 2013; 2014; Ginglinger *et al.*, 2013) mais il n'y a aucune preuve à ce jour pour la participation de *CYP76C2* ou *CYP76C4* dans le métabolisme de monoterpénol *in vivo* et ou sous une infection pathogène.

L'ensemble de tous ces faits et preuves a permis d'élaborer l'hypothèse de ce travail de thèse, qui était:

"Les membres de la famille de CYP76C semblent être impliqués dans les réponses de la défense des plantes, en particulier CYP76C2 pourrait être impliqué dans les réponses du type LAR et le métabolisme du monoterpénol".

Des monoterpénoïdes avaient été décrits comme ayant des propriétés antioxydantes pour sa capacité comme donneur d'hydrogène ou des activités de piégeage des radicaux libres ainsi que leur interaction avec d'autres antioxydants (Grabmann, 2005). De plus, récemment (E) - β -caryophyllène (sesquiterpène) a été liée à la résistance à l'infection par *Pseudomonas* dans les fleurs chez *A. thaliana* (Huang *et al.*, 2012).

Par conséquent, un analyse du profilage de volatile terpenoïde émis d'après l'infection avec *Pto DC3000*, *DC3000 Pto avrRpm1* et *B. cinerea* et des dérivés solubles de monoterpénol libres ou conjugués dans les feuilles a été réalisée. Les résultats des expériences n'ont indiqué aucune différence dans les terpènes volatils ou solubles entre les plantes sauvages et les mutants de *CYP76C2*. En outre, les profils des volatils des autres membres de la famille *CYP76* ont également été analysés sans résultats concluants.

Par la suite, des études plus ciblées ont été effectuées dans UPLC-MS, en se concentrant uniquement sur des mutants *CYP76C2*, ne révélant pas encore de différences significatives, contestant notre hypothèse de départ et presque à l'exclusion d'un dérivé de monoterpénol oxydé de l'équation.

Cependant, une analyse non ciblée dans UPLC-MS Orbitrap a remis d'actualité l'idée d'un dérivé de terpenoïde après la découverte d'un composé qui a une formule brute $C_{17}H_{27}O_9$ (m/z 376) correspondant probablement à $C_{11}H_{17}O_4$ (m/z 215) + $C_6H_{10}O_5$, qui a été trouvé régulé à la baisse dans le mutant knock-out de *CYP76C2* infectés par le *Pseudomonas* avirulent, dans la zone de HR.

À l'heure actuelle, bien que ce résultat ait été confirmé à plusieurs points dans une cinétique temporelle et dans plusieurs expériences indépendantes, d'autres études sont nécessaires pour l'élucidation de la structure de ce composé ainsi que des études sur son rôle dans la défense. La régulation à la baisse de cette molécule dans le mutant de perte de fonction *cyp76c2* non infectée et infecté, avec la forte régulation à la hausse dans le mutant 35S:*CYP76C2* infecté à 72 HAI soutien

clairement un rôle de *CYP76C2* dans sa formation. Toutefois, les faibles valeurs des intensités trouvées suggèrent que le composé ciblé doit être présent en faibles quantités. Cela peut expliquer un faible impact sur les plantes malades. Des infections virulentes aideraient à évaluer la pertinence de ce composé pour la résistance des plantes malades.

Bien que la présence de ce composé soit indéniable, il serait souhaitable de tester d'autres pathosystèmes et réponses aux attaques d'insectes. Par exemple, une expérience préliminaire a été effectuée au cours de cette thèse avec *Hyaloperonospora arabidopsidis*, un biotroph obligatoire. Cela montrait une sensibilité accrue de manière significative de la ligne *cyp76c2* (voir annexe). Il serait intéressant de quantifier ce composé dans les tissus végétaux infectés par ce pathogène pour lequel le rôle de *CYP76C2* semble plus déterminant pour le phénotype final.

Un principal suivi de ce travail serait l'identification de ce composé. Sa structure et ses propriétés pourraient fournir quelques indices sur son origine et son rôle. Il serait alors possible de déterminer s'il est accumulé de manière différentielle dans des tissus locaux et distants par rapport à ROS et stress oxydative. Il a été bien constaté que la distribution spatiale de certains métabolites dans l'interaction avirulente *A. thaliana*-*Pto DC3000 avrRpm1* est influencée par les ROS (Simon *et al.*, 2010).

Le profilage hormonal effectué sur des infections virulentes a révélé une tendance inattendue à l'accumulation de SA et de ses formes conjuguées (SAG et SGE) dans la ligne *cyp76c2* et une tendance inverse dans les plantes *35S:CYP76C2*, ce qui serait en accord avec le phénotype des symptômes.

Selon une analyse PCA (*Principal Component Analysis*), les plantes *35S:CYP76C2* ont été principalement associées au précurseur du JA (*Jasmonic Acid*), le OPDA, et ses formes conjuguées, mais aussi associées de façon récurrente à l'accumulation putative du DHBA (*Dihydroxybenzoic acid*) comme en témoignent les analyses préliminaires effectuées à 24 HAI en UPLC MS/MS et Orbitrap. Ces analyses ont souligné que les plantes traitées *35S:CYP76C2* ont été associées à une augmentation du 2,5 DHBA. Par la suite, le profilage de l'accumulation DHBA effectuée sur une cinétique du temps plus large ne montre aucune accumulation différentielle de tous les DHBA testées entre le type sauvage et les mutants du *CYP76C2*. En outre, aucun produit n'a été détecté après incubation avec DHBA de l'enzyme recombinant *CYP76C2*.

Dans un premier temps toutes ces informations ne suggéraient pas de différence dans l'accumulation des composés DHBA dans l'overexpressor, y compris le 2,5 DHBA. Cependant il y avait encore une possibilité à explorer qui aiderait à expliquer le résultat complexe. Il était encore plausible que les composés ne sont pas libres mais conjugués. Ainsi une hydrolyse enzymatique a été effectuée avec β -glycosidase/xylosidase à 48 HAI en témoignant la présence de plusieurs formes conjuguées de DHBA dans les *35S:CYP76C2* infectés mais pas dans le type sauvage. Cela a été particulièrement évident dans

le profil de 2,5 DHBA mais a également été soutenue par le profil de 2,4 DHBA, un composé inexploré que l'on ne connaît pas trop à ce jour, en particulier par rapport à *Arabidopsis* et réactions de défense. Le constat de 2,5 DHBA probablement conjugué à un glucose dans nos plantes infectées était surprenant parce 2,5 DHBA a été trouvé conjugué à xylose dans les lésions non-nécrotiques et conjugué à glucose dans les tissus de plantes non infectées (Bellés *et al.*, 2006; Tarraga *et al.*, 2010; Bartsch *et al.*, 2010; Campos *et al.*, 2014). Le 2,5 DHBA conjugué à xylose a été trouvé dans notre expérience, mais a également été trouvé dans les plantes de type sauvage avec aucune induction/accumulation différentielle lors de l'infection avirulente. À notre connaissance 2,5 DHBA n'a jamais été liée à un scénario de la mort cellulaire comme la HR ou la sénescence. Il est également inconnu comment ce composé est accumulée dans HR ou les tissus locaux par rapport aux tissus systémiques. On se serait attendu à trouver le composé conjugué principalement dans les zones adjacentes au HR (Simon *et al.*, 2010).

La présence hypothétique de 2,5 DHBA glycosylée, fournit aussi un contexte pour mieux comprendre d'autres informations obtenues dans ce profilage. Par exemple, il pourrait aider à expliquer pourquoi il n'y a pas de quantité significative de SAG dans le mutant *35S:CYP76C2* (très faible dans le profilage à 48 HAI). Ce pourrait être une indication que la clairance de SA (à partir de 48 à 72 HAI) de ce mutant dans les tissus des HR est dirigé à travers le 2,5 DHBA conjugués et non comme prévu au SAG (Tarraga *et al.*, 2010). En outre, les niveaux SGE étaient faibles par rapport à la SAG. SGE était négligeable, et les analyses avec des glycosydases n'ont pas fourni de plus amples informations.

En outre, le mutant *35S:CYP76C2* a montré des niveaux minimaux de 2,3 DHBA, et en plus (et peut-être de ce fait) des formes conjuguées de ce composé n'ont pas été détectés. Le 2,3 DHBA s'accumule à des niveaux faibles (Bartsch *et al.*, 2010) bien qu'il ait été décrit comme très pertinent dans l'interaction *Arabidopsis-Pseudomonas*, la sénescence et le stress oxydatif en général, principalement conjugué à xylose ou du glucose dans les tissus non infectés ou infectés par virus (Bellés *et al.*, 2006; Bartsch *et al.*, 2010; Lopez-Gresa *et al.*, 2010; Zhang *et al.*, 2013).

Une autre molécule intéressante dans des plantes *35S:CYP76C2* infectées était BA (*Benzoic acid*). Dans le profilage de l'hormone, les niveaux de BA dans les plantes infectées de *35S:CYP76C2* étaient aussi bas que dans les plantes non infectées des trois génotypes, mais après hydrolyse enzymatique des conjugués, la présence de l'aglycone a été observée.

Au total, ces résultats suggèrent une préférence pour la désintoxication du SA via la forme glycosylée du 2,5 DHBA ou BA/BA conjugué au xylose au lieu du SAG dans le mutant *35S:CYP76C2* infecté. Cela pourrait expliquer les résultats obtenus pour BA et DHBA dans le profilage, mais aussi l'association avec JAs. Fait intéressant, il a été rapporté que, bien que SA ait induit un certain type de protéines PR, 2,5 DHBA en induit d'autres PRs (Bellés *et al.*, 1999, 2006, Lison *et al.*, 2013). En outre, ces résultats

peuvent expliquer la co-régulation avec UDP-glucuronosyl / UDP-glucosyl transférase (At3g46660 (UGT 76E12) et At2g36770).

En plus, BA et 2,5 DHBA ont été décrits comme des composés antifongiques très efficaces (Latanzio, 1994 cité dans Dean et Delaney, 2008 et ailleurs). Il serait intéressant de tester leur accumulation dans des différents mutants du *CYP76C2* après l'infection avec *B. cinerea*, ce qui induit la synthèse du *PR1* et SA dans le halo nécrotique, et de déterminer le sort de SA dans cette interaction. Dans ce mémoire et dans Millet (2009), il a été observé que lors de l'infection avec *B. cinerea*, *CYP76C2* a été spécifiquement activé dans la zone nécrotique de lésions induites par *Botrytis* où SA est synthétisé via PAL (Govrin and Levine, 2002; Ferarri *et al.*, 2003, 2007; Rossi *et al.*, 2011) contrairement à la SA présente dans la HR, qui est synthétisée par l'intermédiaire isochorismate (Wildermuth *et al.*, 2006; Dempsey *et al.*, 2011; Pieterse *et al.*, 2012, entre autres). Cela donne à penser que, si *CYP76C2* y est induite, il pourrait être d'une certaine manière liée à la production de SA. En outre, Kliebenstein *et al.*, (2005) ont indiqué que *Botrytis* induit l'accumulation de la camalexine dans des zones nécrotiques. La camalexine s'accumule habituellement sur la HR et la mort cellulaire, mais le moment de l'induction du gène dans la zone nécrotique a été trop retardée pour contribuer à la synthèse de phytoalexin (Dangl *et al.*, 1996; Mazid *et al.*, 2011; Gonzalez Lamothe *et al.*, 2009; Ahuja *et al.*, 2012; Jeandet *et al.*, 2014).

Un autre résultat important de ce profilage était sur la camalexine, un phytoalexin bien documenté chez *Arabidopsis*. La lignée mutante *cyp76c2* a non seulement montré une accumulation significative de métabolites du SA, mais aussi affichée une augmentation notable de l'accumulation de la camalexine lors de l'infection avirulente, qui n'a pas été observée dans le mutant overexpressor.

L'accumulation de camalexin dans le mutant *cyp76c2* pourrait être liée au métabolisme du SA. La plante peut diriger le flux métabolique à partir du tryptophane à camalexine, au lieu de l'acide indole acétique (IAA) pour éviter une biosynthèse d'auxines qui contribuerait en aidant les bactéries à proliférer (Navarro *et al.*, 2006; Bari et Jones, 2009; Pieterse *et al.*, 2012, Xin *et al.*, 2013). L'augmentation des niveaux de camalexine signifierait en conséquence moins de titre bactérien et un phénotype transitoire que celui observé autour de 24-48 HAI. En effet la camalexine en interaction avirulente a été davantage liée à des propriétés antioxydantes plus qu'à la défense (Simon *et al.*, 2010; Glazebrook and Ausubel, 1994) et ici, cela semble être le cas, puisque tout se passe dans un contexte de HR sans phénotype de résistance. En plus, le ROS est important pour la production de camalexine (Kliebenstein *et al.*, 2004; Persson *et al.*, 2009; Glawischig, 2007).

Ce travail a consisté à caractériser le rôle de *CYP76C2* chez *A. thaliana* lors des interactions biotiques avec des agents pathogènes. Bien que nous ayons été en mesure de confirmer que le gène est activé

localement en réponse au stress biotique, le niveau d'expression de *CYP76C2* ne semble pas affecter la résistance des plantes aux agents pathogènes testés et probablement ne sont pas directement impliqués dans les réponses de ces pathogènes. Ce rôle pourrait toutefois être masqué par une redondance fonctionnelle.

Les efforts visant à identifier ses substrats et produits axés sur les voies les plus probables selon les données précédentes ont été réalisés. Bien que *CYP76C2* soit biochimiquement active *in vitro* avec le linalool et le citronellole, les dérivés de monoterpène ne semblent pas impliqués dans les réactions de défense.

En outre, *CYP76C2* étant SA dépendant (Millet, 2009), il était intéressant d'étudier ses implications dans la formation de dérivés du SA. Malgré quelques résultats intéressants, il n'a pas été possible de démontrer un rôle dans le métabolisme de SA.

Les lignées affectées dans l'expression de *CYP76C2* n'ont montré aucune différence claire dans leur phénotype d'infection par rapport aux plantes sauvages. Cela indique que *CYP76C2* est probablement pas directement impliqué dans la synthèse de la molécule vitale pour la mise en œuvre du processus de défense, mais plus probablement joue un rôle secondaire liée au stress biotique, peut-être le catabolisme d'un signal ou la molécule de défense dans *Arabidopsis*.

Dual Function of the Cytochrome P450 CYP76 Family from *Arabidopsis thaliana* in the Metabolism of Monoterpenols and Phenylurea Herbicides^{1[W][OPEN]}

René Höfer^{2,3}, Benoît Boachon², Hugues Renault, Carole Gavira⁴, Laurence Miesch, Juliana Iglesias, Jean-François Ginglinger⁴, Lionel Allouche, Michel Miesch, Sebastien Grec, Romain Larbat, and Danièle Werck-Reichhart*

Institute of Plant Molecular Biology, Centre National de la Recherche Scientifique Unité Propre de Recherche 2357 (R.H., B.B., H.R., C.G., J.I., J.-F.G., D.W.-R.), Institute for Advanced Study (H.R., D.W.-R.), Laboratoire de Chimie Organique Synthétique, Institut de Chimie, Centre National de la Recherche Scientifique Unité Mixte de Recherche 7177 (L.M., M.M.), and Plateforme d'Analyses pour la Chimie (L.A.), University of Strasbourg, 67000 Strasbourg, France; Freiburg Institute for Advanced Studies, University of Freiburg, D-79104 Freiburg, Germany (H.R., D.W.-R.); Instituto Nacional de Tecnología Agropecuaria, C1033AAE Pergamino, Argentina (J.I.); Fibres Végétales Unité Mixte de Recherche, Institut National de la Recherche Agronomique/USTL 1281 Stress Abiotiques et Différenciation des Végétaux Cultivés, Université de Lille 1, 59655 Villeneuve d'Ascq cedex, France (S.G.); and Institut National de la Recherche Agronomique-Université de Lorraine Unité Mixte de Recherche 1121 "Agronomie and Environnement" Nancy-Colmar, 54518 Vandoeuvre cedex, France (R.L.)

ORCID ID: 0000-0002-0871-9912 (H.R.).

Comparative genomics analysis unravels lineage-specific bursts of gene duplications related to the emergence of specialized pathways. The CYP76C subfamily of cytochrome P450 enzymes is specific to Brassicaceae. Two of its members were recently associated with monoterpene metabolism. This prompted us to investigate the CYP76C subfamily genetic and functional diversification. Our study revealed high rates of CYP76C gene duplication and loss in Brassicaceae, suggesting the association of the CYP76C subfamily with species-specific adaptive functions. Gene differential expression and enzyme functional specialization in *Arabidopsis thaliana*, including metabolism of different monoterpenols and formation of different products, support this hypothesis. In addition to linalool metabolism, CYP76C1, CYP76C2, and CYP76C4 metabolized herbicides belonging to the class of phenylurea. Their ectopic expression in the whole plant conferred herbicide tolerance. CYP76Cs from *A. thaliana* thus provide a first example of promiscuous cytochrome P450 enzymes endowing effective metabolism of both natural and xenobiotic compounds. Our data also suggest that the CYP76C gene family provides a suitable genetic background for a quick evolution of herbicide resistance.

¹ This work was supported by the European Commission Seventh Framework Programme for Research and Technological Development Framework (grant no. KBBE-2007-3-1-01 to the SMARTCELL project), the Centre National de la Recherche Scientifique and the Région Alsace (Bourse de doctorat pour ingénieur to J.-F.G.), the European Fund for Regional Development in the INTERREG IVA Broad Region EU Invests in Your Future programme (to B.B.), the Agence Nationale de la Recherche (grant no. ANR-10-BLAN-1528 to H.R. and D.W.-R. for the PHENOWALL project), and the University of Strasbourg Institute for Advanced Study and the Freiburg Institute for Advanced Studies (funding for the METABEVO project).

² These authors contributed equally to the article.

³ Present address: Department of Plant Systems Biology, Vlaams Instituut voor Biotechnologie, Technologiepark 927, B-9052 Ghent, Belgium.

⁴ Present address: Plant Advanced Technologies, 13 rue du Bois de la Champelle, 54500 Vandoeuvre-lès-Nancy, France.

* Address correspondence to werck@unistra.fr.

The author responsible for distribution of materials integral to the findings presented in this article in accordance with the policy described in the Instructions for Authors (www.plantphysiol.org) is: Danièle Werck-Reichhart (werck@unistra.fr).

[W] The online version of this article contains Web-only data.

[OPEN] Articles can be viewed online without a subscription.

www.plantphysiol.org/cgi/doi/10.1104/pp.114.244814

Although extensive monoterpene (especially linalool) oxidative metabolism has been described in many plant species, leading to fragrant and bioactive compounds as diverse as alcohols, aldehydes, acids, and epoxides (Williams et al., 1982; Matich et al., 2003, 2011; Luan et al., 2005, 2006; Ginglinger et al., 2013), pyranoid or furanoid linalool derivatives (Pichersky et al., 1994; Raguso and Pichersky, 1999), and geraniol-derived iridoids and secoiridoids (Dinda et al., 2007a, 2007b, 2011; Tundis et al., 2008), limited information is available on the enzymes generating these oxygenated compounds. Involvement of a cytochrome P450 (P450) enzyme extracted from *Vinca rosea* (now renamed *Catharanthus roseus*) in the hydroxylation of geraniol and nerol was suggested as early as 1976 (Madyastha et al., 1976). The first plant P450 gene to be isolated, CYP71A1 from avocado (*Persea americana*) fruit, was later shown to encode an enzyme with geraniol/nerol epoxidase activity (Hallahan et al., 1992, 1994). To our knowledge, a connection with compounds formed in the fruit has not yet been established. The geraniol 8-hydroxylase (often named geraniol 10-hydroxylase) CYP76B6, involved in the biosynthesis of secoiridoids and monoterpene indole alkaloid anticancer

drugs in *C. roseus*, was found to belong to the CYP76 family in 2001 (Collu et al., 2001). The catalytic function of this enzyme was recently revised, and was shown to include a second oxidation activity, the conversion of 8-hydroxygeraniol into 8-oxogeraniol (Höfer et al., 2013). The same work also revealed a geraniol 8- and 9-hydroxylase activity of CYP76C4 from *Arabidopsis thaliana*. More recently, another CYP76 enzyme (CYP76A226) from *C. roseus* was found to metabolize oxidized geraniol derivatives and to have an iridoid oxidase activity, catalyzing the triple oxygenation of cis-trans-nepetalactol into 7-deoxyloganetic acid for the biosynthesis of secoiridoids and terpene indole alkaloids (Miettinen et al., 2014; Salim et al., 2014). Not all CYP76 enzymes seem to be devoted to the metabolism of monoterpenols. In most cases, however, CYP76s seem to be involved in terpenoid metabolism. CYP76Ms from monocots were found to metabolize diterpenoids for the synthesis of antifungal phytocassanes (Swaminathan et al., 2009; Wang et al., 2012; Wu et al., 2013), CYP76AH1 from *Salvia miltiorrhiza* and its ortholog CYP76AH4 from rosemary (*Rosmarinus officinalis*) were shown to hydroxylate the norditerpene abietatriene in the pathway to labdane-related compounds (Zi and Peters, 2013), whereas CYP76Fs from sandalwood (*Santalum album*) were found to hydroxylate the sesquiterpenes santalene and bergamotene (Diaz-Chavez et al., 2013). CYP76B1 from *Helianthus tuberosus* was, however, found to metabolize herbicides belonging to the class of phenylurea (Robineau et al., 1998; Didierjean et al., 2002), but its physiological function was not reported. Other P450s from soybean (*Glycine max*; CYP71A10; Siminszky et al., 1999) or tobacco (*Nicotiana tabacum*; CYP71A11 and CYP81B1; Yamada et al., 2000) were also reported to metabolize phenylurea, but their physiological function was not investigated.

A. thaliana ecotype Columbia-0 (Col-0) emits no geraniol and only tiny amounts of linalool, and extensive volatile profiling of different tissues detected only minor amounts of lilac aldehydes (oxygenated linalool derivatives; Rohloff and Bones, 2005). However, ectopic expression of a linalool/nerolidol synthase of strawberry (*Fragaria × ananassa* cv Elsanta) revealed a potentially efficient oxidative linalool metabolism in *A. thaliana* rosette leaves (Aharoni et al., 2003). Only recent work started to explore linalool metabolism in *A. thaliana*, which was found mainly localized in the flowers (Ginglinger et al., 2013). This work demonstrated the existence of two linalool synthases producing different enantiomers, and the concomitant involvement of two P450 enzymes, CYP76C3 and CYP71B31, with predominance of CYP76C3, in linalool oxidation. It also suggested the presence of partially redundant enzymes that may contribute to floral linalool metabolism.

A family of eight CYP76 genes is detected in the *A. thaliana* genome. We report here an evolutionary and functional analysis of this family. We show that members of the CYP76C subfamily, when successfully expressed in yeast (*Saccharomyces cerevisiae*), all metabolize monoterpenols with different substrate specificities. Although CYP76Cs seem specific to Brassicaceae,

they share common functions with CYP76s from other plants, such as CYP76B1 from *H. tuberosus* and CYP76B6 from *C. roseus*. These functions include not only monoterpenol oxidation, but also metabolism and detoxification of herbicides belonging to the class of phenylurea. Because of this property, CYP76Cs can be used simultaneously for monoterpenol oxidation and as selectable markers for plant transformation.

RESULTS

CYP76C Is a Recent P450 Subfamily Specific to Brassicaceae

Eight CYP76 genes have been annotated in the *A. thaliana* genome (<http://www.p450.kvl.dk/p450.shtml>). One member belongs to the CYP76G subfamily (CYP76G1), and the seven others fall into the CYP76C subfamily. A BLAST search in other fully sequenced plant genomes (<http://www.phytozome.net>) indicates that CYP76G1 orthologs are found usually as single copies in dicots (e.g. tomato [*Solanum lycopersicum*], eucalyptus [*Eucalyptus grandis*], and papaya [*Carica papaya*]; Fig. 1A), which suggests that duplicate copies of CYP76G are rapidly purged from the genome. The gene phylogeny (Fig. 1A) shows that CYP76C genes are expanded within Brassicaceae. The timing of this expansion is coincident with the diversification of the family, but did not occur before, because we found no CYP76C copies in *Carica papaya*, which is representative of an early diverging lineage within the order Brassicales, nor did we find copies in earlier diverging species (i.e. *Gossypium raimondii* or *Theobroma cacao*). Thus, the expansion of CYP76C occurred at least 50 million years ago (Beilstein et al., 2010).

The *A. thaliana* CYP76C genes and a pseudogene (CYP76C8p) are organized in three genomic clusters: CYP76C7 and CYP76C8p on chromosome 3; CYP76C3, CYP76C2, CYP76C1, and CYP76C4 on chromosome 2; and CYP76C5 and CYP76C6 on chromosome 1 (Supplemental Fig. S1A). CYP76C7 and CYP76C3 belong to the same clade and share three common introns, whereas CYP76C8, CYP76C2, CYP76C1, and CYP76C4 belong to a different clade and show only two common introns (Fig. 1, A and B). Based on phylogeny and intron-exon organization, the cluster on chromosome 2 thus most likely derives from a segmental duplication of the cluster formed by CYP76C7 and CYP76C8, possibly as a result of the *A. thaliana* α whole-genome duplication that occurred during early evolution of Brassicaceae (Bowers et al., 2003), followed by further amplification of the ancestral copy of CYP76C8 to generate CYP76C1, CYP76C2, and CYP76C4 (Fig. 1C). Support for this hypothesis is provided by the analysis of the locus structure in *A. lyrata* and other Brassicaceae where a copy of the *WD-40 repeat family* gene is found on the right border and a copy of the *PEROXIN11* gene on the left border of both clusters formed by CYP76C7 and CYP76C8 as well as CYP76C3, CYP76C2, CYP76C1, and CYP76C4 (Supplemental Fig. S1B). Loss of CYP76C8 as a pseudogene is recent and only observed in *A. thaliana* for which no

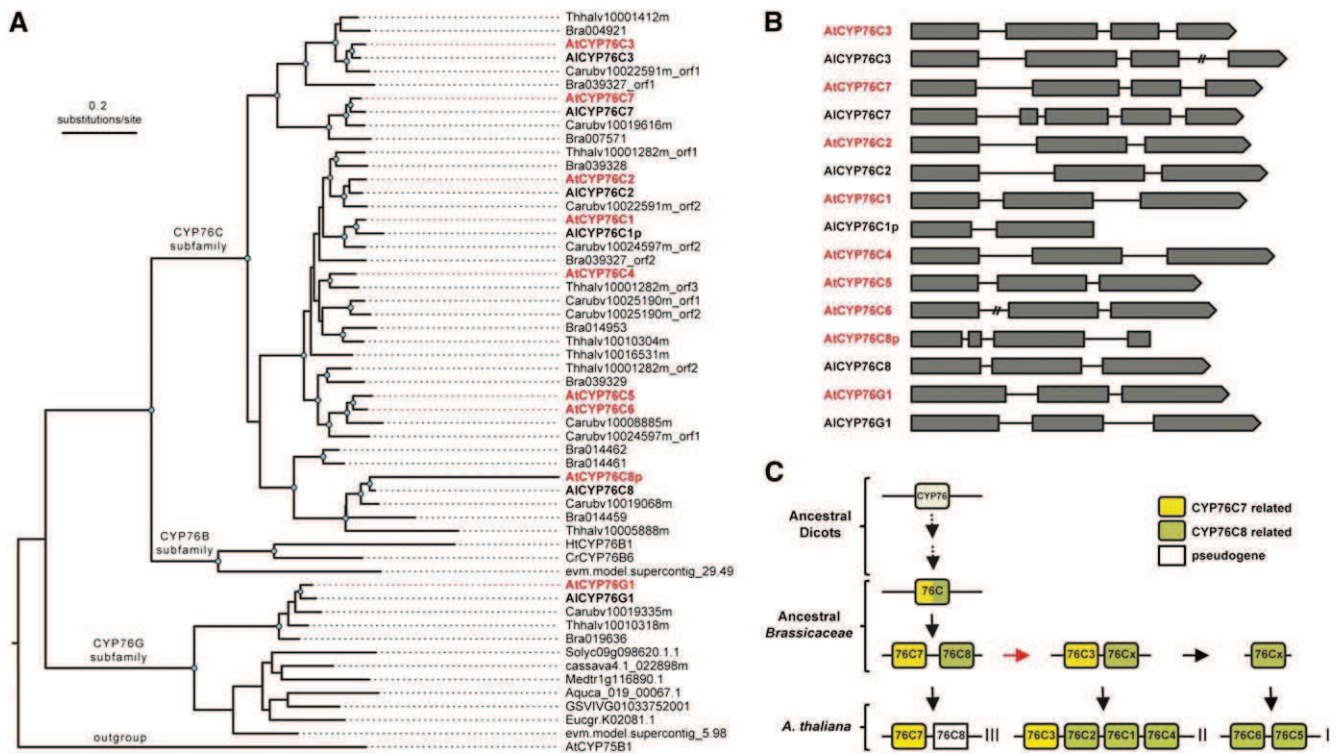


Figure 1. Phylogeny, gene structure, and history of the CYP76 family in Brassicaceae. A, Phylogeny of the CYP76 genes in Brassicaceae. *A. thaliana* and *Arabidopsis lyrata* genes are highlighted in bold red and black, respectively. Note that contiguous loci were found, in which cases individual open reading frames (orf) were arbitrarily separated and labeled with the orf tag. Nodes supported with bootstrap values $\geq 85\%$ are marked with blue dots. The tree was rooted with At-CYP75B1. B, Intron-exon map of the CYP76 genes in *A. thaliana* (red) and *A. lyrata* (black). C, The likely sequence of duplication events that led to the CYP76C genes found in *A. thaliana*. The red arrow indicates segmental duplication. Roman numerals indicate the chromosomal location of each gene. Al, *A. lyrata*; Aquca, *Aquilegia coerulea*; At, *A. thaliana*; Bra, *Brassica rapa*; Carub, *Capsella rubella*; Cassava, *Manihot esculenta*; Cr, *C. roseus*; Eucgr, *Eucalyptus grandis*; evm.model, *Carica papaya*; GSVIV, *Vitis vinifera*; Ht, *H. tuberosus*; Medtr, *Medicago truncatula*; Solyc, *Solanum lycopersicum*; Thhal, *Eutrema salsugineum*.

ESTs are reported, and a stop codon is present at position 341 of the protein (i.e. before the heme anchoring Cys in the active site), whereas CYP76C1 is present as a pseudogene in *A. lyrata* (Supplemental Fig. S1B). The CYP76C5-CYP76C6 tandem present in *A. thaliana* seems to derive from the dispersion of a tandem duplicate of CYP76C8, followed by a recent duplication event, because only a single homolog is found in other Brassicaceae, associated with the cluster formed by CYP76C3, CYP76C2, CYP76C1, and CYP76C4 (Supplemental Fig. S1B). Overall synteny analysis of the corresponding CYP76 loci in different Brassicaceae (Supplemental Fig. S1B) indicates complex genomic rearrangements with frequent gene duplications and losses or pseudogenizations. The CYP76C subfamily thus radiated in Brassicaceae and shows very high versatility, most likely associated with adaptive functions.

Expression Pattern of the CYP76 Genes in *A. thaliana* Suggests Limited Functional Redundancy

To evaluate functional specialization of the different members of the CYP76 family in *A. thaliana*, a quantitative real-time (qRT)-PCR analysis of their expression levels in

different organs and floral stages was carried out (Fig. 2). CYP76C1, CYP76C2, and CYP76C3 were mainly expressed in flowers upon anthesis as already reported for CYP76C3 (Ginglinger et al., 2013). CYP76C1 and CYP76C2 were also expressed in siliques as well as at low levels in healthy leaves for CYP76C1, but the expression of CYP76C2 was at least 10 times lower than that of CYP76C1 or CYP76C3. Siliques were the main site of expression of CYP76C5 and CYP76C7, with the expression of the latter being extremely low and thus most likely restricted to very specific tissues. The expression of CYP76C4 was essentially restricted to roots, and was very low. CYP76C6 expression was mainly restricted to the leaves. CYP76C8 expression was investigated in *A. lyrata* and was the highest in flowers (carpels; Supplemental Fig. S2). CYP76G1 was expressed at very low levels in siliques and roots. Limited functional redundancy of the CYP76 genes is thus expected, except in flowers and siliques.

CYP76C Enzymes Are Versatile Monoterpenol Oxidases

CYP76C3 and CYP76C4 were recently shown to metabolize linalool and geraniol, respectively (Ginglinger

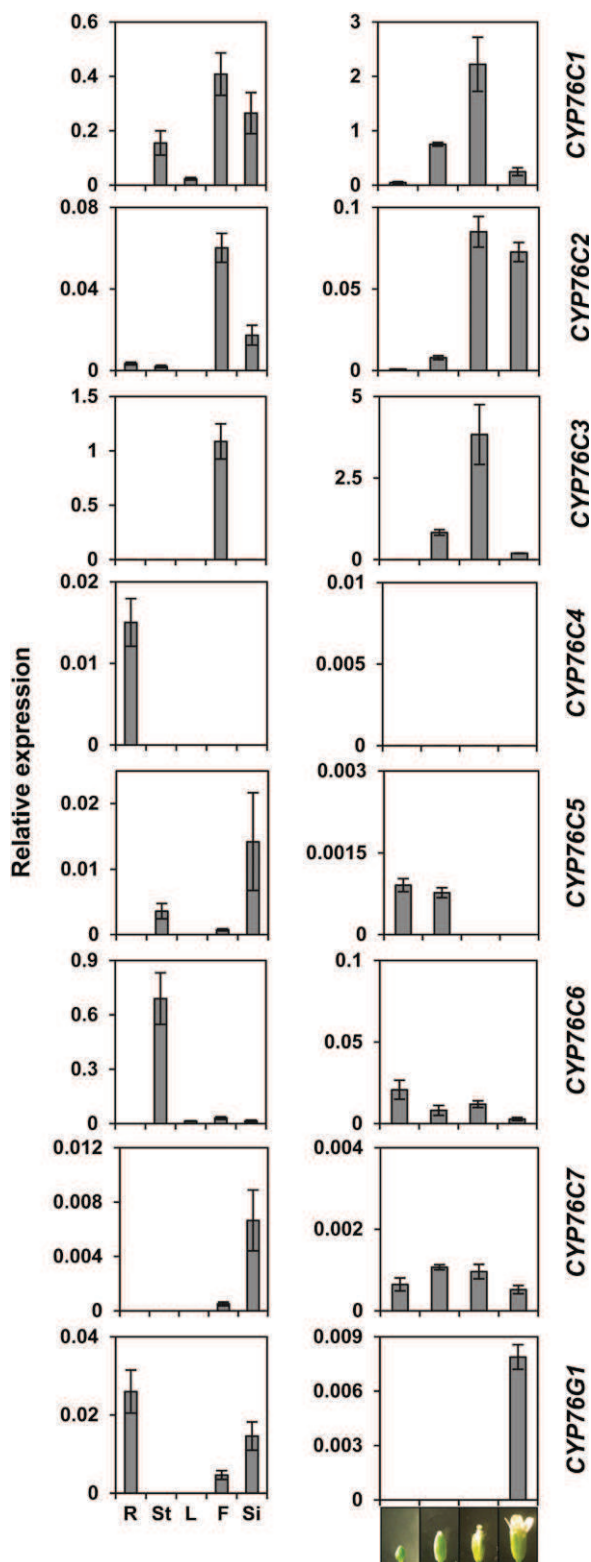


Figure 2. Relative *CYP76* gene transcripts levels in different plant organs and during flower development in *A. thaliana*. Evaluation of gene expression in different organs (left) and at different floral stages (right) was carried out by qRT-PCR. The cycle threshold (Ct) values were normalized to the Ct values obtained for four reference genes whose

et al., 2013; Höfer et al., 2013). To determine whether monoterpenol hydroxylation is a common property of the members of the *CYP76* family, a set of monoterpenols and monoterpenes was tested for conversion by *CYP76Cs* and *CYP76G1* enzymes expressed in yeast, and their activities were compared with those of *CYP76B6*, the geraniol oxidase of the iridoid and terpenoid indole alkaloid pathways of *C. roseus* (Collu et al., 2001; Höfer et al., 2013), and of *CYP76B1* of *H. tuberosus* (Robineau et al., 1998), the physiological function of which is still unknown. As previously reported (Höfer et al., 2013), expression levels of the *A. thaliana CYP76s* were low when evaluated from carbon monoxide-bound absorption spectra of the reduced enzymes (Supplemental Fig. S3). They were considered to be significant only for *CYP76C1*, *CYP76C2*, and *CYP76C4*, and were very low and close to the detection limit for *CYP76C6*, *CYP76C7*, and *CYP76G1*. Microsomes prepared from yeast transformed with each of them were tested for activity on 200 μM of five different monoterpenols and four monoterpene olefins (Fig. 3; Table I). No activity was detected with microsomes from yeast expressing *CYP76C3*, *CYP76C5*, *CYP76C6*, *CYP76C7*, and *CYP76G1*. Metabolism of geraniol was observed only with *CYP76C4* and *CYP76B6*, confirming previous results (Höfer et al., 2013), and only *CYP76B6* further oxidized metabolized 8-hydroxygeraniol. However, nerol was converted by *CYP76C2*, *CYP76C4*, *CYP76B1*, and *CYP76B6* into the same major product, most likely 8-hydroxyneryl (Fig. 3A; electron-ionization mass spectrum [EI-MS] in Supplemental Fig. S4) and different minor products. Based on mass spectra and data previously reported for geraniol (Höfer et al., 2013), the minor product is expected to be 9-hydroxyneryl for *CYP76C2* and *CYP76C4* (Fig. 3A; EI-MS in Supplemental Fig. S5), and 8-oxoneryl for *CYP76B6* (Fig. 3A; EI-MS in Supplemental Fig. S6).

Linalool was found to be metabolized by *CYP76C1*, *CYP76C2*, *CYP76C4*, and *CYP76B6* (Fig. 3, B and C). The same products, 8-hydroxylinalool (main) and 9-hydroxylinalool (minor), were obtained from linalool, based on a comparison of retention times and mass spectra with authentic standards and/or NMR validation of the products extracted from upscaled reactions (Fig. 3B; EI-MS in Supplemental Figs. S7 and S8, respectively, and NMR in Supplemental Fig. S9, A and B). *CYP76C4* and *CYP76C2* additionally formed 1,2-epoxylinalool (Fig. 3B; EI-MS in Supplemental Fig. S10). Metabolism of citronellol by the different enzymes led to several different products (Fig. 3C). In the absence of authentic standards, product structures were assigned by NMR analysis of the products extracted from upscaled reactions (Supplemental

stable expression in *A. thaliana* tissues is known (Czechowski et al., 2005) and relative expression was calculated with the specific efficiency of each primer pair using the $\Delta\Delta\text{Ct}$ method. Results represent the mean \pm SE of two technical repetitions and five biological replicates for organs, and three for flower stages. F, Flower; L, leaf; R, root; Si, silique; St, stem.

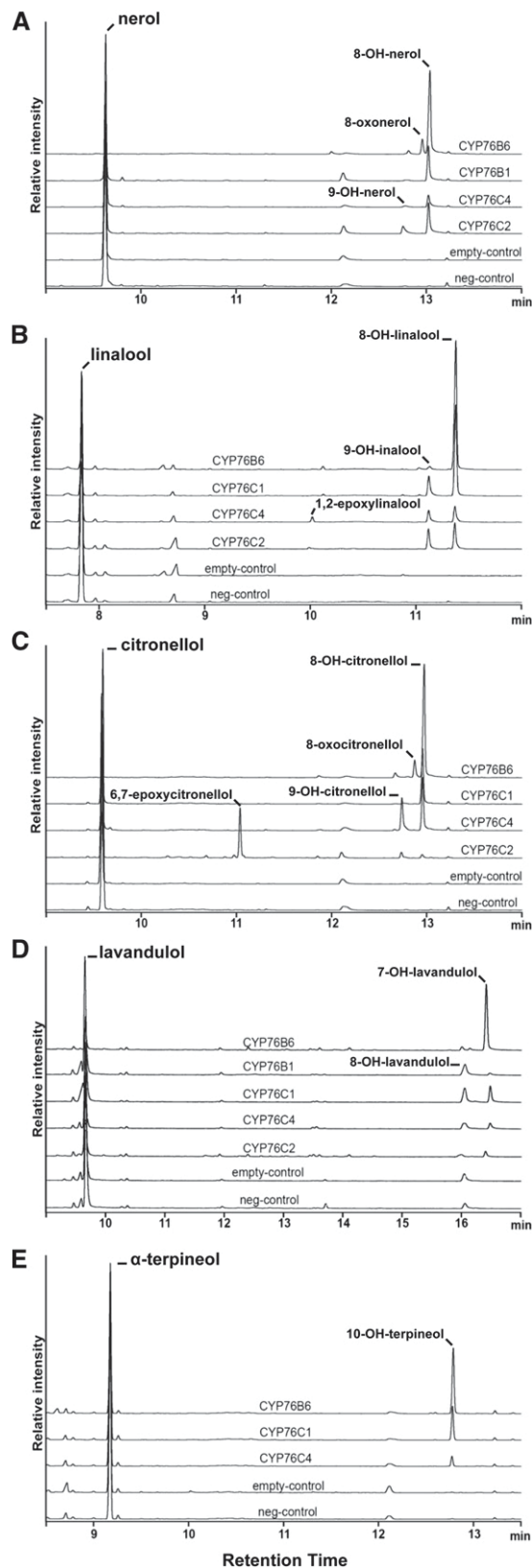


Figure 3. GC-FID chromatograms of the reaction products resulting from the conversion of monoterpenols by the yeast-expressed CYP76C1, CYP76C2, CYP76C4, CYP76B1, and CYP76B6 enzymes. Microsomal

Fig. S9, C–E). 8-Hydroxycitronellol (Fig. 3C; EI-MS in Supplemental Fig. S11) appeared as the major product for CYP76C1, CYP76C4, and CYP76B6 and as the sole product for CYP76C1. CYP76C4 also generated 9-hydroxycitronellol as the minor product (Fig. 3C; EI-MS in Supplemental Fig. S12), whereas CYP76B6 rather generated a compound assumed to be 8-oxocitronellol as the minor product (Fig. 3C; EI-MS in Supplemental Fig. S13). CYP76C2, however, catalyzed the formation of a completely different major product (Fig. 3C; EI-MS in Supplemental Fig. S14) with a shorter retention time, which was identified by NMR as 6,7-epoxycitronellol (Supplemental Fig. S9E), and generated very minor amounts of 8- and 9-hydroxylated products. Lavandulol was converted by CYP76B6 into one major product (Fig. 3D), most likely 7-hydroxylavandulol (Fig. 3D; EI-MS in Supplemental Fig. S15), with one minor side product, presumably 8-hydroxylavandulol (Fig. 3D; EI-MS in Supplemental Fig. S16). It was, however, a poor substrate for CYP76C1, CYP76C2, and CYP76C4, which catalyzed the formation of the same two products, most likely 7- and 8-hydroxylavandulol in equal amounts, and for CYP76B1, which formed mostly 7-hydroxylavandulol. The cyclic monoterpene, α -terpineol, was converted by CYP76B6, CYP76C1, and CYP76C4 into a single product, 10-hydroxy- α -terpineol (Fig. 3E; NMR and EI-MS in Supplemental Figs. S9F and S17, respectively).

Olefinic monoterpenes were very poor substrates and only traces of oxygenated products were obtained with CYP76C4, CYP76B1, or CYP76B6 (Table I). The capacity to oxidize monoterpenols is thus shared by a large number of quite divergent members of the CYP76 family (Fig. 4). Most of them are promiscuous enzymes with regard to monoterpenols, but do not metabolize olefins.

Comparison of the Efficiency of Linalool Metabolism by CYP76Cs from *A. thaliana*

Evaluation of the catalytic parameters was focused on linalool (Supplemental Fig. S18), the most relevant substrate in *A. thaliana*. It was carried out using short incubation times and low enzyme concentrations to minimize further conversion of primary products. The catalytic parameters for the different enzymes are summarized in Supplemental Figure S18 and indicate that CYP76C1 is likely to be the most effective linalool oxygenase in *A. thaliana*.

membranes from recombinant yeast transformed with the *P450* expression vectors or with the empty vector (empty-control) were incubated with 200 μ M of substrate for 20 min in the presence of NADPH. No NADPH was added to the negative control (neg-control). Samples corresponding to the major peaks (except for lavandulol and nerol) were analyzed by NMR for compound identification (Supplemental Fig. S9). Identified compounds were then assigned based on their retention time and EI-MS. Mass spectra of the products and references are available in Supplemental Figs. S4 to S17.

Table I. Monoterpenoid metabolism by yeast-expressed CYP76 enzymes

Microsomal membranes from recombinant yeasts were incubated with 200 μM of substrate for 20 min in the presence of NADPH. Minus signs indicate not metabolized, whereas plus signs indicate formation of minor products that were not quantified. Data are means \pm SD of three replicates.

Substrate	Enzyme Activity				
	CYP76C1	CYP76C2	CYP76C4	CYP76B1	CYP76B6
	pmol product/min per pmol P450				
8-OH-geraniol	–	–	–	–	75.9 \pm 1.5
Nerol	–	22.4 \pm 1.3	6.3 \pm 0.5	11.7 \pm 0.3	52.0 \pm 1.8
Linalool	211.7 \pm 7.3	19.9 \pm 0.6	6.9 \pm 0.1	–	35.5 \pm 1.1
Citronellol	147.7 \pm 11.2	53.4 \pm 2.2	18.8 \pm 1.1	–	63.0 \pm 0.6
α -Terpineol	95.2 \pm 5.7	–	1.8 \pm 0.1	–	22.5 \pm 1.6
Lavandulol	7.5 \pm 0.1	4.5 \pm 0.2	2.4 \pm 0.1	3.7 \pm 0.2	118.5 \pm 0.3
Limonene	–	–	+	+	+
<i>p</i> -Cymene	–	–	+	+	+
Camphene	–	–	+	–	–
α -Phellandrene	–	–	–	+	+

CYP76Cs Also Metabolize Herbicides Belonging to the Class of Phenylurea

CYP76B1 from *H. tuberosus* was previously reported (Robineau et al., 1998) to metabolize the PSII inhibitors phenylurea, leading to nonphytotoxic products. As a result, its ectopic expression confers phenylurea resistance and was shown to be effective as a selectable marker for plant transformation (Didierjean et al., 2002). The yeast-expressed CYP76s (all except CYP76C5 and CYP76C6) were thus screened for herbicide metabolism (Supplemental Table S1). The *A. thaliana* CYP76C enzymes active in vitro on monoterpenols (i.e. CYP76C1, CYP76C2, and CYP76C4) all metabolized a large subset of phenylurea (Supplemental Table S1). CYP76C1 and CYP76C2 metabolized a larger set of compounds. We focused on chlorotoluron and isoproturon, metabolized by all three enzymes, for product determination (Fig. 5). CYP76C1 was the most active, and converted chlorotoluron into ring-methyl-hydroxychlorotoluron as the main product and also produced minor amounts of *N*-demethyl-chlorotoluron (Fig. 5A; Supplemental Table S2). Isoproturon was similarly converted into isoproturon hydroxylated on the isopropyl side chain and *N*-demethyl-isoproturon (Fig. 5A; Supplemental Table S2). CYP76C2 and CYP76C4 generated the same compounds in lower amounts (Fig. 5, B and C). Table II compares the catalytic parameters determined with CYP76C1, CYP76C2, and CYP76C4 and shows that the most efficient metabolism was obtained with CYP76C1 and occurs via hydroxylation leading to nonphytotoxic products.

Conversely, no metabolism of phenylurea was detected with CYP76B6 from *C. roseus*, which is the most promiscuous enzyme with monoterpenols. There is thus no systematic correlation of monoterpenols and phenylurea metabolism.

Ectopic Expression of CYP76Cs Confers Resistance to Phenylurea

Considering the low and spatially restricted expression of *A. thaliana* CYP76Cs in roots and leaves,

we did not anticipate a significant impact of their current natural expression on plant tolerance to phenylurea. To confirm this hypothesis and to test the influence of gene-increased expression on herbicide resistance, insertion mutants and overexpression lines were isolated for CYP76C1, CYP76C2, and CYP76C4 (Supplemental Fig. S19). Their herbicide tolerance was compared with the wild type. Figure 6 illustrates isoproturon and chlorotoluron tolerance of CYP76C1 insertion and overexpression lines. As anticipated, no significant effect of gene inactivation on herbicide tolerance was observed, independent of the herbicide concentration added to the growth medium. Ectopic overexpression, however, led to a significant gain in herbicide tolerance, the most significant being for isoproturon with all three enzymes (Fig. 6; Supplemental Fig. S20).

DISCUSSION

The CYP76 family of P450 enzymes arose with the emergence of seed plants (Nelson and Werck-Reichhart, 2011) and shows an extensive diversification in monocots and dicots (<http://drnelson.uthsc.edu/CytochromeP450.html>) with 34 subfamilies named thus far. Based on currently available plant genomes, homologs of the CYP76Cs from *A. thaliana* are found only in Brassicaceae, but not in papaya. Together with the high frequency of gene duplication and loss observed within Brassicaceae CYP76Cs, this suggests a high versatility, and a role in fast lineage-specific adaptation and plant-herbivore or plant-microbe interaction. A similar trend to high gene duplication is observed in rice (*Oryza sativa*), in which 29 CYP76 genes were annotated in six subfamilies (Nelson and Werck-Reichhart, 2011). Thus far, the function of only one of these subfamilies is described, being the formation of antifungal diterpenoids phytocassanes (Swaminathan et al., 2009; Wang et al., 2012; Wu et al., 2013). This raises the question of the functional divergence(s) associated with the CYP76 subfamily burst and CYP76Cs duplications in Brassicaceae.

For tandem duplicated genes, the divergence of the expression profile usually occurs at or shortly after gene duplication (Ganko et al., 2007). Clear expression

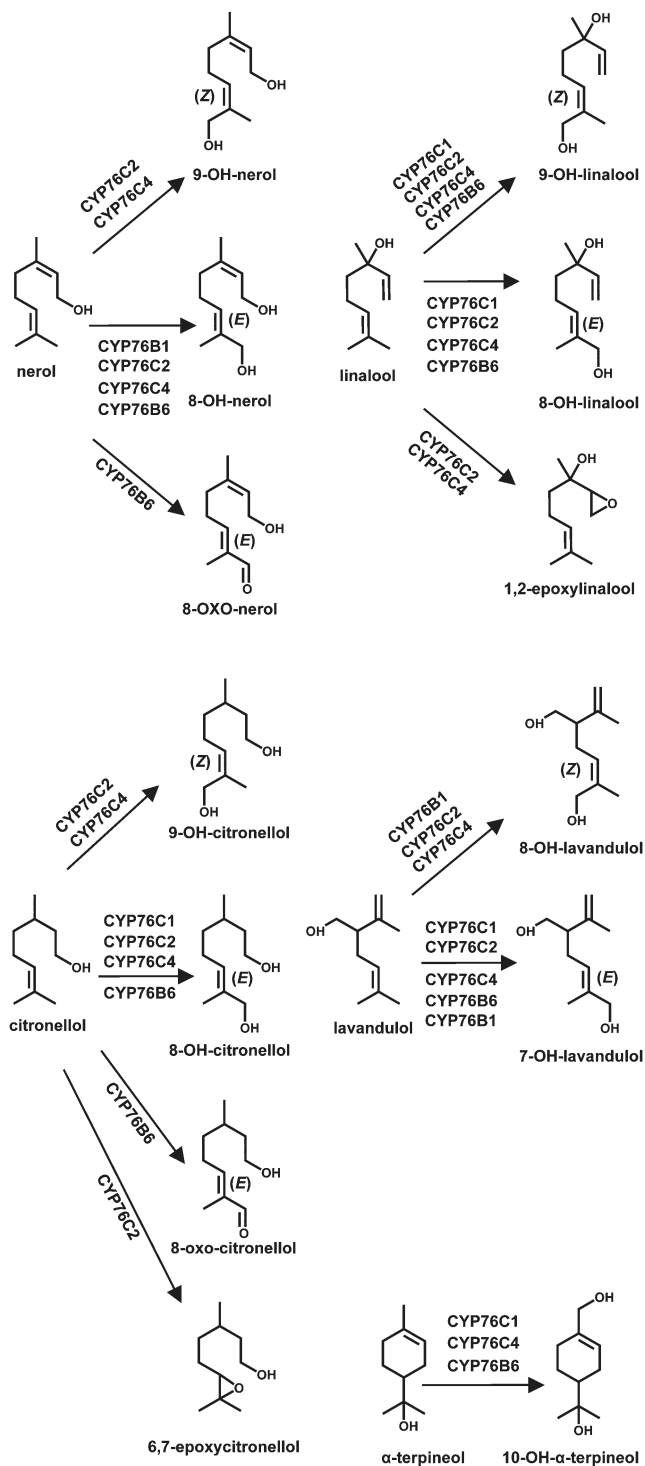


Figure 4. Summary of the reactions catalyzed by CYP76 enzymes on monoterpenols.

divergences were observed among duplicates such as *CYP76C7* (mainly expressed in siliques) and *CYP76C3* (flowers), or *CYP76C5* (roots), and *CYP76C6* (leaves). Large differences were also observed between their respective expression levels, with much higher expression

of *CYP76C3* and *CYP76C6* than of *CYP76C7* and *CYP76C5*. Divergence is even stronger between *CYP76C8* and the three duplicates *CYP76C1*, *CYP76C2*, and *CYP76C4*. Whereas *CYP76C8* turned into a pseudogene in *A. thaliana* (but is expressed in flower carpels in *A. lyrata*), *CYP76C1* is the most highly expressed gene of the tandem repeats in chromosome 2, especially in flowers, and *CYP76C4* is expressed only at low levels in roots. Overall, expression patterns indicate functional specialization of the different paralogs in *A. thaliana*, although not excluding some redundancy (e.g. between *CYP76C3* and *CYP76C1*). The very low expression of some of them, such as *CYP76C7*, *CYP76C5*, or *CYP76C4*, possibly results from a restricted expression in specific tissues. Considering the high versatility and propensity to gene loss of *CYP76Cs*, it may also be indicative of ongoing pseudogenization.

If divergence in spatiotemporal expression is a factor that favors gene retention at or just after duplication, it is often followed by a further divergence in expression and in protein sequence and function. We recently reported the activity of *CYP76C4* and *CYP76C3* in monoterpenol oxidation, the first catalyzing geraniol 8- and 9-hydroxylation (Höfer et al., 2013), and the second the oxygenation of both (3*R*)- and (3*S*)-linalool, mainly into 4- and 5-hydroxylinalool, with 8- and 9-hydroxylinalool as minor products (Ginglinger et al., 2013). To further investigate their capacity for monoterpenol oxidation, the whole set of eight *CYP76* genes from *A. thaliana* was expressed in yeast. For most of them, the expression was low if any, possibly reflecting either toxicity for the host or low intrinsic protein stability. However, the three best expressed *CYP76Cs* (*CYP76C1*, *CYP76C2*, and *CYP76C4*), as well as *CYP76B1* from *H. tuberosus* and *CYP76B6* from *C. roseus*, were all found to metabolize several monoterpenols with different substrate preferences and different efficiencies, and sometimes forming different products. Olefinic monoterpenes were poor substrates for all of them. The activities detected with *CYP76C2*, *CYP76C4*, and *CYP76B1* were low; however, this might be related to their low levels of expression. Expression of *CYP76C2* was previously reported to be strongly activated by bacterial pathogens and in senescent tissues (Godiard et al., 1998). Production of monoterpenols and their oxides is thus far not reported in infected or senescent tissues. However, monoterpenols and their oxides are described for antimicrobial activity (Junker and Tholl, 2013; Radulović et al., 2013). Conversely, *CYP76C1* and *CYP76B6* very actively catalyzed the oxidation of several tested compounds. *CYP76C1* was the most active with linalool, the only monoterpenol for which oxidation products were thus far reported to be emitted by *A. thaliana* (Rohloff and Bones, 2005) and detected as soluble conjugates (Aharoni et al., 2003; Ginglinger et al., 2013). Moreover, linalool synthases were previously shown to be essentially expressed in *A. thaliana* flowers, the main site of expression of *CYP76C1* (Ginglinger et al., 2013). *CYP76C1* therefore appears as a prime candidate to play a significant role in floral linalool metabolism in *A. thaliana*, which is under current investigation. *CYP76C1* also very

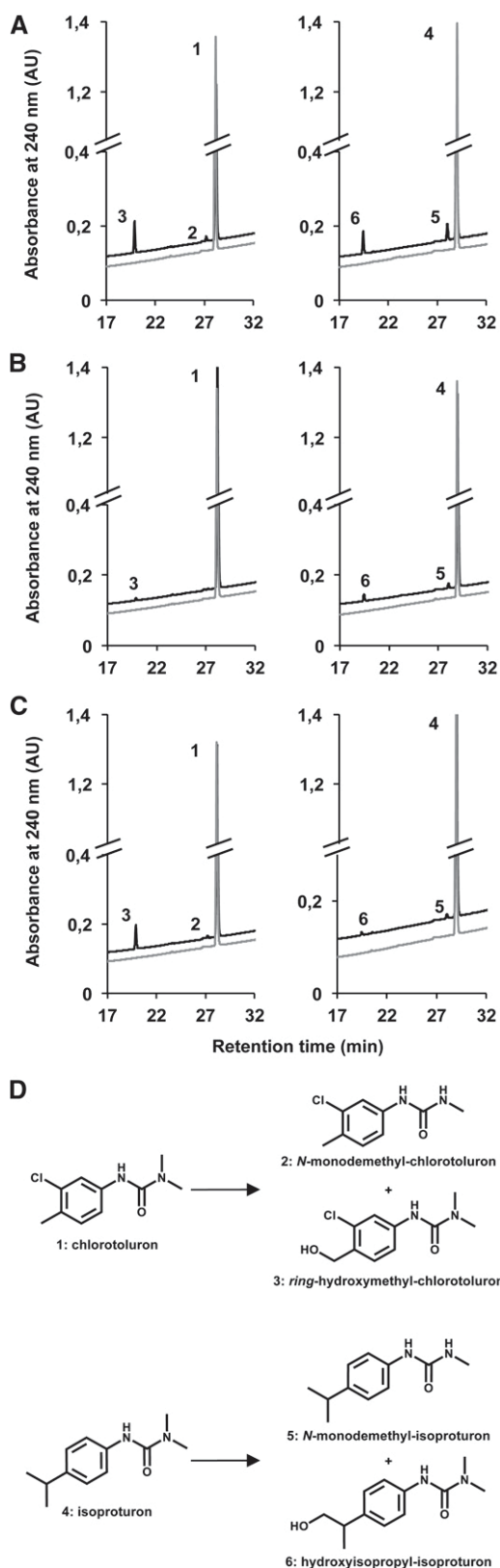


Figure 5. HPLC-photodiode array chromatograms and phenylurea conversion products of yeast-expressed CYP76C enzymes. Microsomal membranes from recombinant yeasts were incubated with herbicide

actively metabolized citronellol and α -terpineol, the latter of which was also detected after volatile profiling of *A. thaliana* plants (Rohloff and Bones, 2005).

Our preliminary data (Ginglinger et al., 2013; B. Boachon and J. Iglesias, unpublished data) indicate that gene suppression or overexpression of CYP76Cs does not lead to any growth or fertility phenotype. It is thus expected that they play a role in the synthesis of allelochemicals involved in plant-microbe or plant-insect interaction. Identification of the final products resulting from the CYP76C-mediated monoterpene oxidation is expected to be challenging, because the expression of most of them is low or restricted to very specific tissues available in very small amounts and some of them may use the same substrate (Ginglinger et al., 2013). The primary oxygenated monoterpenols are unlikely to be the final products in the plant and these products, as well as their final degree of oxidation/glycosylation and physico-chemical properties, cannot be predicted from published data. However, the differential expression of the CYP76C genes in Brassicaceae predicts that they are unlikely to catalyze successive oxidation steps in a same pathway.

It is interesting to note that the ability to metabolize monoterpenols is not restricted to CYP76Cs from Brassicaceae, but extends to enzymes classified as CYP76Bs from Compositae and Apocynaceae. CYP76A26 from *C. roseus* has also been reported to be active with monoterpenols, although its main activity was in iridoid metabolism (Miettinen et al., 2014). Monoterpene metabolism is thus expected to be a quite common feature of the CYP76 family in dicots. Unexpectedly, CYP76B6, thought to be a specific geraniol oxidase dedicated to the secoiridoid/TIA pathway (Höfer et al., 2013), emerged from the screening as the most promiscuous enzyme with regard to monoterpenols, efficiently metabolizing geraniol, nerol, linalool, citronellol, and lavandulol. CYP76B6 promiscuity thus points to the critical importance of the geraniol synthase for producing the relevant substrate for iridoid and terpene indole alkaloid production (Miettinen et al., 2014) and to the capacity of CYP76B6 and resulting duplicates for evolving multiple functions in different monoterpene-derived pathways in the plant. In contrast with CYP76Cs from *A. thaliana*, CYP76B6 essentially formed with all monoterpenols a single hydroxylated derivative and its further oxidation product. The second 9-hydroxylation product observed with the *A. thaliana* enzymes was

(400 μ M) for 20 min in the presence of NADPH (black), or without NADPH (gray) for negative controls. Products were identified by comparison of retention times and mass spectra with authentic standards. Reference MS data are provided in Supplemental Table S2. A, CYP76C1 + chlorotoluron (left) or isoproturon (right). B, CYP76C2 + chlorotoluron (left) or isoproturon (right). C, CYP76C4 + chlorotoluron (left) or isoproturon (right). D, Phenylurea conversion products of CYP76C1, CYP76C2, and CYP76C4. 1, Chlorotoluron; 2, *N*-monodemethyl-chlorotoluron; 3, ring-hydroxymethyl-chlorotoluron; 4, isoproturon; 5, *N*-monodemethyl-isoproturon; 6, hydroxyisopropyl-isoproturon; AU, arbitrary unit.

Table II. Catalytic parameters of phenylurea metabolism by *A. thaliana* CYP76C enzymes

Kinetic assays were carried out in a final volume of 200 μL for 20 min in the presence of 1 mM NADPH, 7 pmol of P450, and variable substrate concentrations. Kinetic parameters were deduced from Michaelis-Menten representation. dM-CTU: monodemethyl-chlorotoluron; dM-IPU: monodemethyl-isoproturon; OH-CTU: *ring*-hydroxymethyl-chlorotoluron; OH-IPU: hydroxyisopropyl-isoproturon. Data are means \pm SD of three determinations. Units for catalytic parameters are as follows: K_m (μM), k_{cat} (min^{-1}), and k_{cat}/K_m ($\mu\text{M}^{-1} \text{min}^{-1}$). Dash indicates product not formed or in amounts too low for quantification.

Product	Catalytic Parameter	CYP76C1	CYP76C2	CYP76C4
OH-CTU	K_m	589 \pm 190	249 \pm 28	96 \pm 14
	k_{cat}	61 \pm 10	1.4 \pm 0.2	15 \pm 3
	k_{cat}/K_m	0.1	0.006	0.16
dM-CTU	K_m	135 \pm 52	—	—
	k_{cat}	4 \pm 0.8	—	—
	k_{cat}/K_m	0.03	—	—
OH-IPU	K_m	595 \pm 98	63 \pm 4	3.8 \pm 2
	k_{cat}	38 \pm 5	2.4 \pm 0.9	0.9 \pm 0.1
	k_{cat}/K_m	0.06	0.04	0.2
dM-IPU	K_m	165 \pm 67	196 \pm 112	—
	k_{cat}	12 \pm 2	1.4 \pm 0.7	—
	k_{cat}/K_m	0.07	0.007	—

not obtained or in tiny amounts. Surprisingly, whereas CYP76B6 acquired an extended capacity to regioselectively metabolize a large set of monoterpenols, it is completely unable to metabolize phenylurea, which are substrates of the *A. thaliana* and *H. tuberosus* enzymes.

Herbicide resistance is a major challenge for modern agriculture (Powles and Yu, 2010). It can result from a mutation at the level of the herbicide target site, from increased metabolism, or from reduced translocation (Powles and Yu, 2010). P450s most often catalyze primary herbicide metabolism and activation, before further processing by conjugation enzymes and storage in the vacuole. Their role in the acquisition of insecticide resistance in insect pests is quite well documented (Ffrench-Constant, 2013), but their part in endowing herbicide resistance and the mechanisms of acquisition of this resistance in weeds are still poorly understood. P450-dependent herbicide metabolism is usually thought to result from the serendipitous docking of herbicides in the active site involved in physiological processes (Powles and Yu, 2010). To our knowledge, CYP76s constitute the first example providing a potential link between the metabolism of physiologically relevant compounds and the metabolism of herbicides and herbicide tolerance. The fast evolution and versatility of the CYP76 family, together with the herbicide tolerance of CYP76C overexpression lines, illustrate how herbicide resistance can be acquired either via gene activation or via gene duplication when those lead to extended or increased gene expression.

CYP76C1, CYP76C2, and CYP76C4, like CYP76B1, metabolize a quite broad set of phenylurea compounds, forming both *N*-demethylated and *ring*-methyl(isopropyl)-hydroxylated products. CYP76Cs thus allow herbicide

docking in two opposite orientations. Irreversible herbicide detoxification requires either *ring*-hydroxylation or a double *N*-dealkylation. Hydroxylation is thus expected to constitute the main CYP76C-dependent detoxification process. In spite of relatively low herbicide turnovers measured *in vitro*, particularly in the case of CYP76C2, a significant effect on herbicide detoxification is confirmed by the increased herbicide tolerance of overexpressors of all three CYP76C1, CYP76C2, and CYP76C4 enzymes. Natural CYP76C expression of *A. thaliana* Col-0 does not significantly affect herbicide tolerance. This is not surprising given the restricted tissue-specific expression of each; the amount of enzyme(s) currently present in the wild-type plant is not sufficient to support herbicide resistance. Our data, however, demonstrate the possibility of using the CYP76Cs from *A. thaliana* to engineer herbicide tolerance. These findings raise the interesting possibility of using genes of the plant's specialized metabolism as selectable markers for plant transformation. In some cases, the selectable marker and metabolic function could be conveyed by the same gene. These results also point to a potential complex interplay of the metabolism of herbicides with that of specialized plant compounds, and to a possible effect of herbicide treatment and

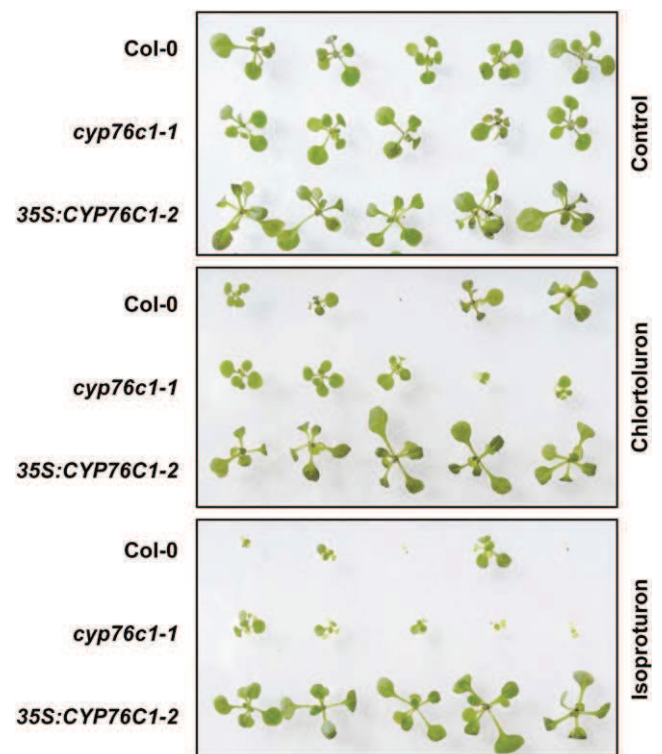


Figure 6. CYP76C1 overexpression confers herbicide tolerance to *A. thaliana* Col-0, *cyp76c1* insertion, or *Cauliflower mosaic virus 35S* (35S) promoter-driven overexpression lines were grown on Murashige and Skoog medium for 14 d in the presence or absence of 1 μM of chlorotoluron or isoproturon.

detoxification on plant-insect or plant-pathogen interaction.

MATERIALS AND METHODS

CYP76C Subfamily History and Phylogeny

CYP76 coding sequences from various species were retrieved from Phytozome (<http://www.phytozome.org>) and GenBank (<https://www.ncbi.nlm.nih.gov/genbank/>) databases. Coding sequences were translated into amino acid sequences and aligned with MUSCLE (Edgar, 2004) prior to determination of Gblocks (Castresana, 2000) using the SeaView software (<http://pbil.univ-lyon1.fr/>; Gouy et al., 2010). The corresponding nucleotides Gblocks alignment (Supplemental Data Set S1) was subsequently used for phylogeny reconstruction by maximum likelihood analysis with PhyML 3.0 (Guindon et al., 2010) using the generalized time reversible model (default settings except that the proportion of invariable sites was estimated). Phylogeny consistency was tested by performing 100 bootstrap iterations. The output tree was shaped using the FigTree software (<http://tree.bio.ed.ac.uk/software/figtree/>). Organization of *CYP76C* genes in the *Arabidopsis thaliana* genome was realized according to the chromosome map tool from The Arabidopsis Information Resource (<http://www.arabidopsis.org/jsp/ChromosomeMap/tool.jsp>). Synteny analysis of the *CYP76C3* and *CYP76C7* loci was realized with the help of the synteny tool on the Phytozome Web site (<http://www.phytozome.net/>).

Plant Growth

Seeds of *A. thaliana* Col-0 and *Arabidopsis lyrata* strain MN47 (Hu et al., 2011) were sown on a standard soil compost mixture. Plants were grown individually in 7-cm pots in growth chambers at 22°C during the 12-h-day period and 19°C during the 12-h-night period under white fluorescent lamps with a photon fluency of 60 $\mu\text{mol m}^{-2} \text{s}^{-1}$ (rosette leaves) to 90 $\mu\text{mol m}^{-2} \text{s}^{-1}$ (flower stage). *A. lyrata* plants were grown individually in 7-cm pots for 5 weeks, before transfer to 12-cm pots containing a standard soil compost mixture completed at 50% (v/v) with sand, and were grown in greenhouses at 24°C during the 16-h-day period and 20°C during the 8-h-night period under a sodium-vapor lamp with a photon fluency of 100 $\mu\text{mol m}^{-2} \text{s}^{-1}$ to 150 $\mu\text{mol m}^{-2} \text{s}^{-1}$.

Quantification of Gene Expression

Quantification of gene expression was carried out by qRT-PCR as previously described (Ginglinger et al., 2013). The different organs of *A. thaliana* and *A. lyrata* were harvested from five different plants at the flowering stage and were immediately frozen in liquid nitrogen. For the normalization of gene expression in *A. lyrata*, the orthologs of *A. thaliana* *SAND-like* (gene 481666) and *TIP41-like* (gene 491240) were used after their stable expression was validated among four putative reference genes by the GeNorm (Vandesompele et al., 2002) and NormFinder (Andersen et al., 2004) algorithms and GenEx 4 software (<http://genex.gene-quantification.info/>). Oligonucleotides used for each gene are provided in Supplemental Table S3. Relative expression was calculated with the specific efficiency of each primer pair using the $\Delta\Delta\text{Ct}$ method (Pfaffl, 2001). For *A. thaliana*, five biological replicates were used for the organs and three were used for the floral stages. For *A. lyrata*, five biological replicates were used for each tissue.

Generation of Expression Vectors

The generation of the *CYP76B1* construct is described in Didierjean et al. (2002). All other constructs are described in Höfer et al. (2013). The yeast (*Saccharomyces cerevisiae*) and plant expression constructs were generated by PCR amplification from complementary DNA prepared from tissues in which each gene was found to be the most highly expressed. The PCR fragments of *CYP76C1*, *CYP76C2*, *CYP76C5*, *CYP76C7*, and *CYP76B1* were integrated into the yeast expression vector pYeDP60. The constructs for *CYP76C3*, *CYP76C4*, *CYP76C6*, and *CYP76B6* were prepared using the Uracl-Specific Excision Reagent (New England Biolabs) cloning technique according to Nour-Eldin et al. (2006) and the PCR fragments were integrated into the yeast expression plasmid pYeDP60u2. For plant expression constructs, *CYP76C1* was cloned similarly and integrated in the plant expression vector pCAMBIA2300u. Complementary DNA from *CYP76C2* and *CYP76C4* was amplified by PCR

using specific primers tailed for Gateway cloning technology (Invitrogen) and successively cloned in pDONR 201 and the plant expression vector pB7WG2 (Karimi et al., 2002). Constructs were confirmed by sequencing at each step. Primers used for cloning are provided in Supplemental Table S3.

Heterologous Expression in Yeast

The WAT11 yeast strain was transformed with pYeDP60u2 containing the different P450 sequences as described in Gietz and Schiestl (2007). Yeast cultures were grown and P450 expression was induced as described in Pompon et al. (1996). Cells were harvested by centrifugation and manually broken with glass beads (0.45 mm in diameter) in 50 mM Tris-HCl buffer, pH 7.5, containing 1 mM EDTA and 600 mM sorbitol. The homogenate was centrifuged for 10 min at 10,000g and the resulting supernatant was centrifuged for 1 h at 100,000g. The pellet consisting of microsomal membranes was resuspended in 50 mM Tris-HCl, pH 7.4, 1 mM EDTA, and 30% (v/v) glycerol and stored at -20°C . P450 content of the microsomal preparations was measured by differential spectrophotometry according to Omura and Sato (1964).

Assays for Monoterpenoid Metabolism

A standard enzyme assay using the monoterpenols as substrates was carried out in 100 μL of 20 mM sodium phosphate buffer, pH 7.4, containing varying concentrations of substrate, 600 μM NADPH, and adjusted amounts of P450 enzyme. After addition of NADPH, samples were incubated at 28°C and the reaction was stopped with 10 μL of 1 M HCl and 500 μL of ethyl acetate. Samples were vortexed for 10 s and centrifuged at 4,000g for 2 min. The ethyl acetate phase was transferred to a new vial and the extraction was repeated once. The combined organic phase was dried over anhydrous Na_2SO_4 (Sigma-Aldrich), concentrated under argon and analyzed by gas chromatography (GC-flame ionization detection (FID) and GC-mass spectrometry (MS). For the determination of the kinetic parameters of *A. thaliana* CYP76Cs on linalool, assays were scaled up to a final volume of 400 μL , using R-linalool concentrations ranging from 5 μM to 600 μM , 1 mM NADPH, and about 50 nM P450s. Formation of products was quantified after 4 min of incubation. Kinetic parameters were deduced from Michaelis-Menten representation.

Olefin substrates were incubated in closed 2-mL glass vials for 20 min at 28°C using a thermomixer (Eppendorf) under constant shaking. In a reaction volume of 300 μL , 10% (v/v) of yeast microsomes were diluted in phosphate citrate buffer in the presence of 200 μM of olefin monoterpenes (dissolved in 0.8% [v/v] ethanol) and 1 mM of NADPH. The reaction was quenched on ice and products were extracted with 500 μL of pentane in a thermomixer during 5 min at 20°C. The solvent layer was recovered after centrifugation and analyzed by GC-FID and GC-MS.

GC-FID and GC-MS Analysis

Capillary GC was performed on a Varian 3900 gas chromatograph (Agilent Technologies) equipped with a flame ionization detector and a DB-5 column (30 m, 0.25 mm, and 0.25 μm ; Agilent Technologies) with splitless injection at a 250°C injector temperature, and a temperature program of 0.5 min at 50°C, 10°C/min to 320°C, and 5 min at 320°C. Terpenoids were identified based on their retention time and electron-ionization mass spectra (70 eV and mass-to-charge ratio of 50–600) with a PerkinElmer Clarus 680 gas chromatograph coupled to a PerkinElmer Clarus 600T mass spectrometer. Capillary GC-MS was performed as described above. Reference standards of 8-hydroxylinalool was synthesized as previously described (Ginglinger et al., 2013). 1,2-Epoxy linalool was kindly provided by Adam J. Mathich (New Zealand Institute for Plant and Food Research Limited).

NMR Characterization of Products

To generate amounts of products large enough for NMR analysis, the standard enzyme assay was scaled up to a volume of 10 mL containing 400 μM of substrate. After a first incubation for 15 min at 28°C, a second aliquot of P450 enzyme was added and incubated for another 15 min. The reaction was stopped by adding 1 mL of 1 M HCl, vortexing, and cooling on ice. Several upscaled assays were pooled to ensure proper NMR detection of the products. For the extraction of the products, solid-phase extraction columns (Oasis HLB extraction cartridges; Waters) were equilibrated with chloroform, methanol, and water prior to gradual extraction of up to 15 mL of combined samples.

After drying, the columns were eluted with CDCl_3 and the combined organic phase was dried over anhydrous Na_2SO_4 and concentrated under argon prior to NMR analysis.

NMR was conducted on a 500-MHz Bruker Avance II spectrometer equipped with a 5-mm dual ^{13}C and ^1H cryoprobe with a z-gradient operating at 500.13 MHz for ^1H and 125.758 MHz for ^{13}C . A number of different spectra including one-dimensional ^1H , ^1H to ^1H correlation spectroscopy, edited ^1H to ^{13}C heteronuclear single-quantum correlation, and ^1H to ^{13}C heteronuclear multiple bond correlation were recorded for each sample, adding ^1H to ^1H nuclear overhauser effect spectroscopy and one-dimensional ^{13}C when required. Pulse sequences were taken from the Bruker library. All experiments were acquired at 293 K with a minimal relaxation delay of 2 s and a mixing time of 600 or 800 ms for nuclear overhauser effect spectroscopy experiments. Coupling constants were assumed to be around 145 Hz and 8 Hz for $^1\text{J}(^{13}\text{C}-^1\text{H})$ and $^n\text{J}(^{13}\text{C}-^1\text{H})$, respectively. Acquisition parameters were adjusted when necessary but typically spectral windows were set to 7 kHz for ^1H and 27 or 31 kHz for ^{13}C . For two-dimensional spectra, the data size was at least 2,048 points in the direct dimension and varied between 128 and 256 points in the indirect dimension according to the required resolution.

Assays for Herbicide Metabolism

Screening for herbicide metabolism was carried out in a final volume of 200 μL of 0.1 M sodium phosphate buffer, pH 7.0, containing 400 μM of herbicide in the presence of 1 mM NADPH or without NADPH (control). The assay mixture was equilibrated for 2 min at 27°C before starting the reaction by the addition of microsomal membranes prepared from yeast expressing the different CYP76 genes. After 2 h at 27°C, the reaction was terminated by adding 50 μL of acetonitrile:HCl (99:1), and the reaction medium was analyzed by reverse-phase HPLC on a Purospher 5- μm , 4 \times 125-mm endcapped column (Merck). The column was equilibrated in water:acetic acid:acetonitrile (98:1:1) at a flow rate of 0.7 mL/min, and eluted with diode array detection (220–400 nm) using a convex gradient of acetonitrile:methanol (1:1) from 1% to 95% for 32 min, followed by 99% acetonitrile:methanol (1:1) for an additional 6 min. Kinetic assays were conducted in a final volume of 200 μL for 20 min in 0.1 M sodium phosphate, pH 7, containing 1 mM NADPH, 7 pmol of P450, and varying the concentration of substrate. Kinetic parameters were deduced from Michaelis-Menten representation.

Products were characterized by HPLC-MS. The system consisted in a binary solvent delivery pump (SurveyorMS; Thermo-Finnigan) connected to a diode array detector (Surveyor PDA plus; Thermo-Finnigan) and an LTQ mass spectrometer (Thermo Scientific), equipped with an atmospheric pressure ionization interface operated in electrospray ionization (ESI) negative and positive ion modes (ESI^- and ESI^+ , respectively). MS conditions were as follows for ESI^+ mode: spray voltage was set at 5 kV; source gases were set (in arbitrary units min^{-1}) for sheath gas, auxiliary gas, and sweep gas at 50, 10, and 10, respectively; capillary temperature was set at 300°C; capillary voltage at 0 V; and tube lens, split lens, and front lens voltages at 60 V, -46 V, and -5.75 V, respectively. For ESI^- mode, MS conditions were unchanged except ion optics parameters, which were automatically adapted as follows: capillary voltage at -48 V, and tube lens, split lens, and front lens voltages at -120 V, 34 V, and 4.25 V, respectively. The data were processed using the XCALIBUR software program.

Isolation of Null Mutant and Overexpression Lines

Insertion mutants were selected from SALK lines for CYP76C1 (SALK_010566: *cyp76c1-1*), CYP76C2 (SALK_037019: *cyp76c2-1*), and CYP76C4 (SALK_093179: *cyp76c4-1*) and obtained from the Nottingham Arabidopsis Stock Center (Alonso et al., 2003). Homozygous mutant lines were selected by PCR genotyping on genomic DNA extracted from young leaves using the primers provided in Supplemental Table S3. Absence of transcripts in the insertion lines was assessed by semi-qRT-PCR amplifying the full coding sequence. To generate *A. thaliana* lines overexpressing CYP76C1, CYP76C2, and CYP76C4, the plant expression vectors harboring each gene were used to transform the *Agrobacterium* GV3101 strain before transformation of Col-0 plants by floral dip (Clough and Bent, 1998). T1 progeny was screened by germination on glufosinate (BASTA). For each enzyme, two independent T1 BASTA-resistant lines were brought to T3 stable progeny by germination on BASTA to obtain homozygous stable lines. P450 expression was analyzed on T3 lines by qRT-PCR in leaves for CYP76C1 and CYP76C2-overexpressing lines as described above. A primers list is provided in Supplemental Table S3.

Resistance Test to Herbicides

Seeds of Col-0 and of the insertion and overexpression lines of CYP76C1, CYP76C2, and CYP76C4 were sterilized in open 1.5-mL tubes in a glass bottle containing a beaker with 20 mL of bleach (sodium hypochlorite solution). Two mL of 37% fuming HCl was added to the bleach and seeds were sterilized for 4 h. Sterilized seeds were sown on 2.2 g L^{-1} of Murashige and Skoog medium (Sigma-Aldrich) containing 0.7% agar and 15 g L^{-1} Suc, adjusted to pH 5.7. After 2 d of stratification at 4°C, plants were grown at 22°C during a 16-h-day period under 70 to 90 $\mu\text{mol m}^{-2} \text{s}^{-1}$ light and at 20°C during an 8-h-night period. Isoproturon or chlorotoluron was added to the medium at different concentrations for preliminary tests of tolerance. A concentration leading to a clear-cut difference in tolerance is shown.

Sequence data from this article can be found in the Arabidopsis Genome Initiative, GenBank/EMBL, or Phytozome databases under the following accession numbers: At-SAND-like (At2g28390), Al-SAND-like (gene 481666), At-TIP41-like (At4g34270), Al-TIP41-like (491240), At-PP2AA2 (At1g13320), Al-PP2AA2 (gene 936261), At-EXP (At4g26410), At-TUB4 (At5g44340), Al-ACT2 (gene 342019), At-CYP75B1 (At5g07990); At-CYP76C1 (At2g45560), Al-CYP76C1p (gene 871078), At-CYP76C2 (At2g45570), Al-CYP76C2 (gene 346366), At-CYP76C3 (At2g45580), Al-CYP76C3 (gene 322211), At-CYP76C4 (At2g45550), At-CYP76C5 (At1g33730), At-CYP76C6 (At1g33720), At-CYP76C7 (At3g61040), Al-CYP76C7 (gene 486570); At-CYP76C8p (At3g61035), Al-CYP76C8 (gene 867547), At-CYP76G1 (At3g52970), Al-CYP76G1 (gene 348388), Cr-CYP76B6 (AJ251269), and Ht-CYP76B1 (Y10098).

Supplemental Data

The following materials are available in the online version of this article.

Supplemental Figure S1. Structure of CYP76C loci in *Arabidopsis* spp. and other Brassicaceae.

Supplemental Figure S2. Expression of the CYP76C paralogs in different organs and floral stages in *A. lyrata*.

Supplemental Figure S3. Differential carbon monoxide-reduced versus reduced UV-visible absorption spectra of the microsomal membranes prepared from yeasts expressing the CYP76 genes.

Supplemental Figure S4. EI-MS of 8-hydroxynerol.

Supplemental Figure S5. EI-MS of 9-hydroxynerol.

Supplemental Figure S6. EI-MS of 8-oxonerol.

Supplemental Figure S7. EI-MS of 8-hydroxylinalool.

Supplemental Figure S8. EI-MS of 9-hydroxylinalool.

Supplemental Figure S9. NMR characterization of monoterpene products formed by CYP76C enzymes.

Supplemental Figure S10. EI-MS of 1,2-epoxylinalool.

Supplemental Figure S11. EI-MS of 8-hydroxycitronellol.

Supplemental Figure S12. EI-MS of 9-hydroxycitronellol.

Supplemental Figure S13. EI-MS of 8-oxocitronellol.

Supplemental Figure S14. EI-MS of 6,7-epoxycitronellol.

Supplemental Figure S15. EI-MS of 7-hydroxylavandulol.

Supplemental Figure S16. EI-MS of 8-hydroxylavandulol.

Supplemental Figure S17. EI-MS of 10-hydroxy- α -terpineol.

Supplemental Figure S18. Determination of the catalytic parameters of linalool conversion by CYP76C1, CYP76C2, and CYP76C4.

Supplemental Figure S19. Genotyping of insertion and overexpression lines.

Supplemental Figure S20. CYP76C1, CYP76C2, or CYP76C4 overexpression confers herbicide tolerance to *Arabidopsis* spp.

Supplemental Table S1. Screening for herbicide metabolism by CYP76 enzymes.

Supplemental Table S2. Retention time, mass, and tandem MS fragmentation patterns for chlorotoluron and isoproturon CYP76C1-dependent products.

Supplemental Table S3. PCR primer list.

Supplemental Data Set S1. Alignment used to generate the tree in Figure 1A.

ACKNOWLEDGMENTS

We thank Mark Beilstein (University of Arizona) for critical reading of the article.

Received June 10, 2014; accepted July 31, 2014; published July 31, 2014.

LITERATURE CITED

- Aharoni A, Giri AP, Deuerlein S, Griepink F, de Kogel WJ, Verstappen FWA, Verhoeven HA, Jongma MA, Schwab W, Bouwmeester HJ (2003) Terpenoid metabolism in wild-type and transgenic *Arabidopsis* plants. *Plant Cell* **15**: 2866–2884
- Alonso JM, Stepanova AN, Leisse TJ, Kim CJ, Chen H, Shinn P, Stevenson DK, Zimmerman J, Barajas P, Cheuk R, et al (2003) Genome-wide insertional mutagenesis of *Arabidopsis thaliana*. *Science* **301**: 653–657
- Andersen CL, Jensen JL, Ørntoft TF (2004) Normalization of real-time quantitative reverse transcription-PCR data: a model-based variance estimation approach to identify genes suited for normalization, applied to bladder and colon cancer data sets. *Cancer Res* **64**: 5245–5250
- Beilstein MA, Nagalingum NS, Clements MD, Manchester SR, Mathews S (2010) Dated molecular phylogenies indicate a Miocene origin for *Arabidopsis thaliana*. *Proc Natl Acad Sci USA* **107**: 18724–18728
- Bowers JE, Chapman BA, Rong J, Paterson AH (2003) Unravelling angiosperm genome evolution by phylogenetic analysis of chromosomal duplication events. *Nature* **422**: 433–438
- Castresana J (2000) Selection of conserved blocks from multiple alignments for their use in phylogenetic analysis. *Mol Biol Evol* **17**: 540–552
- Clough SJ, Bent AF (1998) Floral dip: a simplified method for *Agrobacterium*-mediated transformation of *Arabidopsis thaliana*. *Plant J* **16**: 735–743
- Collu G, Unver N, Peltenburg-Looman AMG, van der Heijden R, Verpoorte R, Memelink J (2001) Geraniol 10-hydroxylase, a cytochrome P450 enzyme involved in terpenoid indole alkaloid biosynthesis. *FEBS Lett* **508**: 215–220
- Czechowski T, Stitt M, Altmann T, Udvardi MK, Scheible WR (2005) Genome-wide identification and testing of superior reference genes for transcript normalization in *Arabidopsis*. *Plant Physiol* **139**: 5–17
- Diaz-Chavez ML, Moniodis J, Madilao LL, Jancsik S, Keeling CI, Barbour EL, Ghisalberti EL, Plummer JA, Jones CG, Bohlmann J (2013) Biosynthesis of sandalwood oil: *Santalum album* CYP76F cytochromes P450 produce santalols and bergamotol. *PLoS ONE* **8**: e75053
- Didierjean L, Gondet L, Perkins R, Lau SMC, Schaller H, O'Keefe DP, Werck-Reichhart D (2002) Engineering herbicide metabolism in tobacco and *Arabidopsis* with CYP76B1, a cytochrome P450 enzyme from Jerusalem artichoke. *Plant Physiol* **130**: 179–189
- Dinda B, Debnath S, Banik R (2011) Naturally occurring iridoids and secoiridoids. An updated review, part 4. *Chem Pharm Bull (Tokyo)* **59**: 803–833
- Dinda B, Debnath S, Harigaya Y (2007a) Naturally occurring iridoids. A review, part 1. *Chem Pharm Bull (Tokyo)* **55**: 159–222
- Dinda B, Debnath S, Harigaya Y (2007b) Naturally occurring secoiridoids and bioactivity of naturally occurring iridoids and secoiridoids. A review, part 2. *Chem Pharm Bull (Tokyo)* **55**: 689–728
- Edgar RC (2004) MUSCLE: multiple sequence alignment with high accuracy and high throughput. *Nucleic Acids Res* **32**: 1792–1797
- Ffrench-Constant RH (2013) The molecular genetics of insecticide resistance. *Genetics* **194**: 807–815
- Ganko EW, Meyers BC, Vision TJ (2007) Divergence in expression between duplicated genes in *Arabidopsis*. *Mol Biol Evol* **24**: 2298–2309
- Gietz RD, Schiestl RH (2007) High-efficiency yeast transformation using the LiAc/SS carrier DNA/PEG method. *Nat Protoc* **2**: 31–34
- Ginglinger JF, Boachon B, Höfer R, Paetz C, Köllner TG, Miesch L, Lugan R, Baltenweck R, Mutterer J, Ullmann P, et al (2013) Gene coexpression analysis reveals complex metabolism of the monoterpene alcohol linalool in *Arabidopsis* flowers. *Plant Cell* **25**: 4640–4657
- Godiard L, Sauviac D, Dalbin N, Liaubet L, Callard D, Czernic P, Marco Y (1998) CYP76C2, an *Arabidopsis thaliana* cytochrome P450 gene expressed during hypersensitive and developmental cell death. *FEBS Lett* **438**: 245–249
- Gouy M, Guindon S, Gascuel O (2010) SeaView version 4: a multiplatform graphical user interface for sequence alignment and phylogenetic tree building. *Mol Biol Evol* **27**: 221–224
- Guindon S, Dufayard JF, Lefort V, Anisimova M, Hordijk W, Gascuel O (2010) New algorithms and methods to estimate maximum likelihood phylogenies: assessing the performance of PhyML 3.0. *Syst Biol* **59**: 307–321
- Hallahan DL, Lau SMC, Harder PA, Smiley DWM, Dawson GW, Pickett JA, Christoffersen RE, O'Keefe DP (1994) Cytochrome P-450-catalysed monoterpene oxidation in catmint (*Nepeta racemosa*) and avocado (*Persea americana*); evidence for related enzymes with different activities. *Biochim Biophys Acta* **1201**: 94–100
- Hallahan DL, Nugent JHA, Hallahan BJ, Dawson GW, Smiley DW, West JM, Wallsgrove RM (1992) Interactions of avocado (*Persea americana*) cytochrome P-450 with monoterpenoids. *Plant Physiol* **98**: 1290–1297
- Höfer R, Dong L, André F, Ginglinger JF, Lugan R, Gavira C, Grec S, Lang G, Memelink J, Van der Krol S, et al (2013) Geraniol hydroxylase and hydroxygeraniol oxidase activities of the CYP76 family of cytochrome P450 enzymes and potential for engineering the early steps of the (seco)iridoid pathway. *Metab Eng* **20**: 221–232
- Hu TT, Pattyn P, Bakker EG, Cao J, Cheng JF, Clark RM, Fahlgren N, Fawcett JA, Grimwood J, Gundlach H, et al (2011) The *Arabidopsis lyrata* genome sequence and the basis of rapid genome size change. *Nat Genet* **43**: 476–481
- Junker RR, Tholl D (2013) Volatile organic compound mediated interactions at the plant-microbe interface. *J Chem Ecol* **39**: 810–825
- Karimi M, Inzé D, Depicker A (2002) GATEWAY vectors for *Agrobacterium*-mediated plant transformation. *Trends Plant Sci* **7**: 193–195
- Luan F, Mosandl A, Degenhardt A, Gubesch M, Wüst M (2006) Metabolism of linalool and substrate analogs in grape berry mesocarp of *Vitis vinifera* L. cv. Morio Muscat: demonstration of stereoselective oxygenation and glycosylation. *Anal Chim Acta* **563**: 353–364
- Luan F, Mosandl A, Münch A, Wüst M (2005) Metabolism of geraniol in grape berry mesocarp of *Vitis vinifera* L. cv. Scheurebe: demonstration of stereoselective reduction, E/Z-isomerization, oxidation and glycosylation. *Phytochemistry* **66**: 295–303
- Madyastha KM, Meehan TD, Coscia CJ (1976) Characterization of a cytochrome P-450 dependent monoterpene hydroxylase from the higher plant *Vinca rosea*. *Biochemistry* **15**: 1097–1102
- Matich AJ, Comeskey DJ, Bunn BJ, Hunt MB, Rowan DD (2011) Biosynthesis and enantioselectivity in the production of the lilac compounds in *Actinidia arguta* flowers. *Phytochemistry* **72**: 579–586
- Matich AJ, Young H, Allen JM, Wang MY, Fielder S, McNeillage MA, MacRae EA (2003) *Actinidia arguta*: volatile compounds in fruit and flowers. *Phytochemistry* **63**: 285–301
- Miettinen K, Dong L, Navrot N, Schneider T, Burlat V, Pollier J, Woittiez L, van der Krol S, Lugan R, Ilc T, et al (2014) The seco-iridoid pathway from *Catharanthus roseus*. *Nat Commun* **5**: 3606
- Nelson D, Werck-Reichhart D (2011) A P450-centric view of plant evolution. *Plant J* **66**: 194–211
- Nour-Eldin HH, Hansen BG, Nørholm MHH, Jensen JK, Halkier BA (2006) Advancing uracil-excision based cloning towards an ideal technique for cloning PCR fragments. *Nucleic Acids Res* **34**: e122
- Omura T, Sato R (1964) The carbon monoxide-binding pigment of liver microsomes. I. Evidence for its hemoprotein nature. *J Biol Chem* **239**: 2370–2378
- Pfaffl MW (2001) A new mathematical model for relative quantification in real-time RT-PCR. *Nucleic Acids Res* **29**: e45
- Pichersky E, Raguso RA, Lewinsohn E, Croteau R (1994) Floral scent production in *Clarkia* (Onagraceae). I. Localization and developmental modulation of monoterpene emission and linalool synthase activity. *Plant Physiol* **106**: 1533–1540
- Pompon D, Louerat B, Bronine A, Urban P (1996) Yeast expression of animal and plant P450s in optimized redox environments. *Methods Enzymol* **272**: 51–64
- Powles SB, Yu Q (2010) Evolution in action: plants resistant to herbicides. *Annu Rev Plant Biol* **61**: 317–347
- Radulović NS, Blagojević PD, Stojanović-Radić ZZ, Stojanović NM (2013) Antimicrobial plant metabolites: structural diversity and mechanism of action. *Curr Med Chem* **20**: 932–952
- Raguso RA, Pichersky E (1999) New perspectives in pollination biology: floral fragrances. A day in the life of a linalool molecule: chemical communication in a plant-pollinator system. Part 1: linalool biosynthesis in flowering plants. *Plant Species Biol* **14**: 95–120

- Robineau T, Batard Y, Nedelkina S, Cabello-Hurtado F, LeRet M, Sorokine O, Didierjean L, Werck-Reichhart D** (1998) The chemically inducible plant cytochrome P450 CYP76B1 actively metabolizes phenylureas and other xenobiotics. *Plant Physiol* **118**: 1049–1056
- Rohloff J, Bones AM** (2005) Volatile profiling of *Arabidopsis thaliana* - putative olfactory compounds in plant communication. *Phytochemistry* **66**: 1941–1955
- Salim V, Wiens B, Masada-Atsumi S, Yu F, De Luca V** (2014) 7-deoxyloganetic acid synthase catalyzes a key 3 step oxidation to form 7-deoxyloganetic acid in *Catharanthus roseus* iridoid biosynthesis. *Phytochemistry* **101**: 23–31
- Siminszky B, Corbin FT, Ward ER, Fleischmann TJ, Dewey RE** (1999) Expression of a soybean cytochrome P450 monooxygenase cDNA in yeast and tobacco enhances the metabolism of phenylurea herbicides. *Proc Natl Acad Sci USA* **96**: 1750–1755
- Swaminathan S, Morrone D, Wang Q, Fulton DB, Peters RJ** (2009) CYP76M7 is an *ent*-cassadiene C11 α -hydroxylase defining a second multifunctional diterpenoid biosynthetic gene cluster in rice. *Plant Cell* **21**: 3315–3325
- Tundis R, Loizzo MR, Menichini F, Statti GA, Menichini F** (2008) Biological and pharmacological activities of iridoids: recent developments. *Mini Rev Med Chem* **8**: 399–420
- Vandesompele J, De Preter K, Pattyn F, Poppe B, Van Roy N, De Paepe A, Speleman F** (2002) Accurate normalization of real-time quantitative RT-PCR data by geometric averaging of multiple internal control genes. *Genome Biol* **3**: H0034
- Wang Q, Hillwig ML, Okada K, Yamazaki K, Wu Y, Swaminathan S, Yamane H, Peters RJ** (2012) Characterization of CYP76M5-8 indicates metabolic plasticity within a plant biosynthetic gene cluster. *J Biol Chem* **287**: 6159–6168
- Williams PJ, Strauss CR, Wilson B, Massy-Westropp RA** (1982) Studies on the hydrolysis of *Vitis vinifera* monoterpene precursor compounds and model monoterpene β -D-glucosides rationalizing the monoterpene composition of grapes. *J Agric Food Chem* **30**: 1219–1223
- Wu Y, Wang Q, Hillwig ML, Peters RJ** (2013) Picking sides: distinct roles for CYP76M6 and CYP76M8 in rice oryzalexin biosynthesis. *Biochem J* **454**: 209–216
- Yamada T, Kambara Y, Imaishi H, Ohkawa H** (2000) Molecular cloning of novel cytochrome P450 species induced by chemical treatments in cultured tobacco cells. *Pestic Biochem Physiol* **68**: 11–25
- Zi J, Peters RJ** (2013) Characterization of CYP76AH4 clarifies phenolic diterpenoid biosynthesis in the Lamiaceae. *Org Biomol Chem* **11**: 7650–7652

ANALYSE FONCTIONNELLE DU ROLE DE CYP76C2 DANS LES MECANISMES DE DEFENSE DES PLANTES CONTRE LES AGENTS PATHOGENES

Une analyse du transcriptome d'*Arabidopsis thaliana* soumis à différents stress biotiques a révélé l'activation de certains membres de la famille CYP76, particulièrement celle de CYP76C2 (≈ 50 fois). La caractérisation fonctionnelle de la famille CYP76, et plus particulièrement celle de CYP76C2 a donc fait l'objet de cette thèse. Après confirmation de l'activation sélective de CYP76C2 en réponse aux pathogènes par qRT-PCR, le phénotype de ses mutants d'insertion et de surexpression a été caractérisé sous différentes conditions d'infection par: *Pseudomonas syringae* pv. *tomato* DC3000, *P. syringae* pv. *tomato* DC3000 *avrRpm1* et par *Botrytis cinerea*. Afin d'identifier la voie métabolique faisant intervenir CYP76C2, un profilage métabolique ciblé et non ciblé a été entrepris, centré sur le(s) métabolite(s) différenciellement accumulés dans les différents mutants en condition d'infection. Alors que des différences subtiles de sensibilité des mutants de CYP76C2 aux pathogènes semblent confirmer son rôle dans la réponse aux pathogènes, les lignées affectées dans son expression ne présentent pas de phénotypes clairement différents de ceux des plantes sauvages. Une analyse non-ciblée en UPLC-MS (Orbitrap) a permis d'identifier un composé absent dans le mutant *cyp76c2* qui pourrait correspondre à un dérivé conjugué en C11, sans que sa structure ne puisse pour l'instant être identifiée (formule brute $C_{17}H_{28}O_9$). CYP76C2 ne semble pas impliqué directement dans la synthèse d'une molécule cruciale pour la mise en place du processus de défense, mais exerce plus probablement une fonction spécialisée ou partiellement redondante de défense ou de détoxification.

FUNCTIONAL ANALYSIS OF CYP76C2 IN PLANT DEFENSE MECHANISMS AGAINST PATHOGENS

A transcriptome analysis of *Arabidopsis thaliana* subjected to biotic stresses has revealed the activation of members of the CYP76 family, especially of CYP76C2 (≈ 50 times). The functional characterization of CYP76C2, has been the objective of this thesis. After confirmation of the selective activation of CYP76C2 by pathogens, the phenotype of its insertion and overexpressor mutants was characterized under infection by *Pseudomonas syringae* pv. *tomato* DC3000, *P. syringae* pv. *tomato* DC3000 *avrRpm1* and *Botrytis cinerea*. In order to identify the metabolic pathway involving CYP76C2, targeted and non-targeted metabolic profiling was focused on differentially accumulated compounds in the different mutants after infection. Whereas subtle differences of response of the CYP76C2 mutant lines in response to pathogens seemed to confirm its involvement in response to biotic stress, phenotypes strikingly different from those of wild-type plants were not observed. A non-targeted analysis by UPLC-MS (Orbitrap) identified a compound absent in the *cyp76c2* line that may correspond to an oxygenated C11 conjugate (raw formula $C_{17}H_{28}O_9$), but its structure was not identified. CYP76C2 thus does not seem directly involved in the synthesis of a molecule crucial for defense responses, but more likely has a role in the synthesis of a potentially redundant specialized defense compound or in a detoxification process.